GEOLOGY AND PALEOTECTONIC HISTORY OF THE TALLY POND GROUP, DUNNAGE ZONE, NEWFOUNDLAND APPALACHIANS: AN INTEGRATED GEOCHEMICAL, GEOCHRONOLOGICAL, METALLOGENIC AND ISOTOPIC STUDY OF A CAMBRIAN ISLAND ARC ALONG THE PERI-GONDWANAN MARGIN OF IAPETUS

JEFFREY CHARLES POLLOCK

Memorial
University of Newfoundland

Geology and paleotectonic history of the Tally Pond Group, Dunnage Zone, Newfoundland Appalachians: an integrated geochemical, geochronological, metallogenic and isotopic study of a Cambrian island arc along the peri-Gondwanan margin of Iapetus

By:

Jeffrey Charles Pollock, B.Sc. (Hons.), P. Geo.

A thesis submitted to the school of Graduate Studies in partial fulfilment of the requirements for the degree of

Master of Science

Department of Earth Sciences
Memorial University of Newfoundland
St. John's, Newfoundland
January 2004

0-612-99106-7

Frontispiece
View looking southwest over Lake Ambrose from the summit of Harpoon Hill

"The important thing in science is not so much to obtain new facts as to discover new ways of thinking about them."

-Sir William Bragg

Abstract

The Cambro-Ordovician Victoria Lake Supergroup lies within the Exploits Subzone of the Newfoundland Appalachians and consists of felsic volcanic rocks with lesser amounts of mafic pillow lava, mafic and felsic pyroclastic rocks, chert, greywacke and shale. The group is a composite and structurally complex assemblage of volcanic, volcaniclastic, and epiclastic rocks which formed in a variety of island-arc, rifted arc, back-arc and mature-arc settings. It is divisible into several separate volcanic terranes that include the Tulks and Tally Pond belts.

The Tally Pond Group comprises Cambrian island-arc felsic pyroclastic rocks with intercalated mafic volcanic rocks and epiclastic volcanic and sedimentary rocks. The group hosts numerous volcanogenic massive sulphide deposits including the Duck Pond and Boundary deposits, the largest undeveloped VMS deposits in the Victoria Lake Supergroup. In the area of the Duck Pond deposit these rocks form two structurally juxtaposed sequences, the Upper block and the Mineralized block which form a structural window through an overthrust package of Ordovician sedimentary rocks.

1:50 000 scale mapping and geochemical studies in the Tally Pond area have resulted in new interpretations of the local geology and a redefinition of the Tally Pond belt. The Tally Pond belt is now elevated to group status, composed of four distinct rock formations comprising Cambrian island arc felsic pyroclastic rocks with intercalated mafic volcanic rocks and epiclastic volcanic and sedimentary rocks.

The oldest rocks in the study area are arc plutonic rocks of the Cripplebeck Lake Quartz Monzonite which forms the original basement to theTally Pond Group. The Lake Ambrose Formation is a sequence of dominantly mafic volcanic rocks comprised of vesicular and amygdaloidal, generally pillowed, flows and mafic to andesitic tuff, agglomerate and breccia that were unconformably deposited upon the Cripplebeck Lake Quartz Monzonite. The mafic volcanic rocks are intercalated with felsic volcanic rocks of the Boundary Brook Formation that consist of flow banded and massive rhyolite, felsic breccia, lapilli tuffs and quartz porphyry. Both of these rock units were intruded by small stocks and dykes of quartz porphyritic rhyodacite that may be coeval with the volcanic rocks in places.

An extensive unit of black shale mélange is in tectonic contact with the volcanic rocks of the Tally Pond Group. The mélange consists of volcanic and sedimentary clasts set in a matrix of fine-grained black shale. The mélange unit is also in contact with a volcaniclastic and epiclastic sequence of sedimentary rocks, the Burnt Pond Formation. This unit is dominated by greywacke and conglomerate containing volcanic detritus interpreted to be derived from the adjacent and underlying volcanic rocks. Dykes, stocks, and small plutons of medium-grained gabbroic-dioritic rocks intrude all of the rocks of the Tally Pond Group.

The youngest rocks in the study area are conglomerates and coarse-grained sandstones of the Rogerson Lake Conglomerate. The unit was deposited during the Silurian and contains volcanic clasts from the underlying volcanic sequences of the Tulks belt and Tally Pond Group.

Geochemical analysis indicates that the volcanic rocks of the Tally Pond belt are bimodal, with geochemical affinities consistent with a volcanic arc paleotectonic environment. Mafic rocks vary from sub-alkalic basalts to basaltic-andesites, consistently exhibit an arc signature, and are depleted arc tholeiites with moderate LREE enrichments. The felsic rocks are rhyolite to rhyodacite, are variably LREE-enriched island arc rocks, and are tholeiitic in nature; however, some have transitional to slight calc-alkaline affinities. Subalkalic gabbro and diorite intrusions are transitional in nature and exhibit LREE enrichment relative to the MREE and HREE. The altered footwall felsic rocks that lie beneath the Duck Pond VMS deposit exhibit REE depletions of different magnitudes; Eu being depleted in all of the altered samples to varying degrees. The hanging wall felsic rocks do not define a fractionation trend with the mafic varieties and the two sequences are not genetically related.

The U-Pb geochronological data for a quartz crystal tuff indicate that the volcanic succession of the Boundary Brook Formation is confined to an age of 509 Ma. These data coupled with field relationships, confirm that the main episode of felsic volcanism in the Tally Pond Group is Middle Cambrian. The 465 Ma age for the Harpoon Gabbro indicates that the mafic intrusions in the Tally Pond Group are Ordovician and therefore much older than previously thought, as they were considered to be Silurian-Devonian. This Ordovician age represents the youngest magmatism recognized in the Tally Pond Group and is comparable to similar Arenig-Llanvirn ages from the Red Indian Lake area. The age of the Harpoon Gabbro temporally correlates with other Early and Mid-Ordovician arc sequences in the Exploits Subzone, namely the Wild Bight and Exploits groups.

Chemical compositions of the alteration minerals chlorite, sericite and carbonate are quite variable in the samples analyzed from the Duck Pond deposit. Chlorites from the Duck Pond deposit contain a broad range of Fe/(Fe+Mg) ratios and atomic Si concentrations. Those from the chaotic carbonate alteration zone have a restricted Si content and have Fe/(Fe+Mg) ratios typical of high Mg chlorites. Chlorites from the feeder pipe to the Duck Pond deposit contain the highest atomic Si amounts and have intermediate Fe and Mg contents. The most ferroan-rich chlorites are those from the altered rhyolite rocks of the hanging-wall to the Duck Pond deposit. Sericites from the Duck Pond deposit are all classified as muscovite with little variation in composition. Carbonates from the Duck Pond deposit are dominantly dolomite with small compositional variations between the samples from the different alteration zones.

Geochronological data from the Rogerson Lake Conglomerate indicate that the age spectra in these rocks is dominated by Paleozoic zircons with minor Mesoproterozoic input. A large majority (~50%) of zircons from samples of the Rogerson Lake Conglomerate have Paleozoic ages of between 420 and 550 Ma; however the majority of these grains have ages in the 490-540 Ma range. These ages correspond well with the ages of Exploits arc/backarc volcanic sequences in the Victoria Lake Supergroup that are unconformably beneath the Rogerson Lake Conglomerate. The conglomerate detritus also contains zircon populations that are Ordovician, approximately 440-480 Ma. The source of these grains is most likely the adjacent rocks of the Notre Dame arc.

A minor quantity of zircons from Laurentian basement were identified in the Rogerson Lake Conglomerate. Neoproterozoic age groups (890, 1030 and 1250 Ma) correspond with rocks of the Grenville Orogen, while the Middle Mesoproterozoic ages (ca. 1500) are correlated with basement gneisses of the Grenville Orogen that are currently exposed in western Newfoundland. The high proportion of Paleozoic zircons relative to Proterozoic grains is presumably the result of Middle Ordovician exhumation of the Notre Dame arc and its subsequent collision and accretion to Laurentia.

Lead isotope data from the Tally Pond belt show a very small variation in $^{206}Pb/^{204}$ Pb ratios and are relatively more radiogenic than other VMS deposits in Newfoundland. The lead isotope data for the Tally Pond belt define three groups, 1) a primitive group; 2) a slightly more radiogenic group; and 3) a much more radiogenic group. The relatively more radiogenic lead ratios are found in the deep sections of the Upper Duck lens and may indicate the influence of a continental lead source in the initial hydrothermal ore system, followed by introduction of more mantle-derived lead when the fluid system became better developed. The high levels of the Upper Duck lens contain less radiogenic lead, which is almost certainly derived from a mantle source. Comparison with VMS deposits elsewhere in the Dunnage Zone indicate that there are two general groups of deposits: a primitive group in the Notre Dame Subzone, and a relatively more radiogenic group represented by deposits in the Exploits Subzone. Deposits in the Notre Dame Subzone were influenced by lead that evolved from the Laurentian margin while those in the Exploits Subzone appear to have been influenced by Gondwanan continental crust.

Sulphides for the Tally Pond belt in the area surrounding the Duck Pond and Boundary deposits are characterized by a wide range of $\delta^{34}S$ values (-17 to +13), representing sulphur from a variety of potential sources. Sulphide minerals hosted by mafic volcanic rocks from the Upper block of the Duck Pond Deposit, from the South Moose Pond zone, and from a mafic intrusion in the Upper block contain sulphur isotope values that fall within the range of igneous rocks with a mantle origin. This suggests that the sulphides in the mafic volcanic rocks were derived from reduced sulphur from a deep-seated magmatic source.

Sulphide minerals from the Mineralized block of the Duck Pond Deposit consist of pyrite, chalcopyrite, and sphalerite and are hosted by altered rhyodacitic flows, intensely chlorite altered feeder zones, and the massive sulphide lens. The felsic ash-tuff hosted Boundary Deposit has sulphur isotope ratios (+10 to +13) that are slightly higher than those of the Duck Pond Deposit (+5 to +11). Both the Duck Pond and Boundary deposits have sulphur isotope ratios that are higher than the normal mantle value for igneous rocks and show a shift towards a seawater sulphate value. The sulphur in these deposits is most likely derived from inorganic high-temperature reduction of seawater sulphate.

The lowest $\delta^{34}S$ values (-17 to -13) are from sediment-hosted pyrite in the Upper block of the Duck Pond Deposit, while slightly higher $\delta^{34}S$ values of -7 and -8‰ are from the North Moose Pond area, located northeast of the Duck Pond Deposit. The sulphur in these sedimentary-hosted samples are interpreted to result from biogenic reduction of seawater sulphate.

Acknowledgements

The production and completion of this thesis would not have been possible without the assistance and support of a number of people. Firstly, I would like to thank my supervisor, Dr. Derek Wilton, for his academic support and help during the course of this study. I am grateful to Derek for allowing me the opportunity to study in Newfoundland and for helping me stay on course and focus on this study during the many times that I delved into other projects. Derek is truly a great mentor and teacher and his easy going nature and willingness to allow me to try new ideas and methods is deeply appreciated. Derek, you will always be a "*sharp dressed man!*"

Dr. Cees van Staal of the Geological Survey of Canada acted as my co-supervisor and has been a constant source of help and encouragement during this study. Cees' willingness to discuss his comprehensive and wide-ranging knowledge of Newfoundland and Appalachian geology and world tectonics was truly an educational and enlightening experience. He taught me the importance of high-quality field work and that "*good geology always starts with good fieldwork*".

My colleagues at the Geological Survey of Newfoundland and Labrador are thanked for the numerous times I called upon their particular expertise. Dick Wardle is acknowledged for his help in suggesting the thesis topic and for his support during the completion of this project. Greg Stapleton is thanked for the numerous discussions over the years and for responding quickly when I required his assistance. Bruce Ryan, Sean O'Brien, Brian O'Brien, Baxter Kean, Lawson Dickson, Don James, Ian Knight and Steve Colman-Sadd were always willing to help and I express thanks for many thought-provoking discussions. Larry Nolan, Andrea Bassan and Gerry Kilfoil were always available when I encountered computer problems and were quick to help find a solution. The assistance of the cartography staff – Dave Leonard, Tony Paltanavage and Terry Sears – is acknowledged for their assistance in producing many of the high-quality figures and maps for this project.

I am grateful to numerous individuals at the Geological Survey of Canada, in particular Neil Rogers, Vicki McNicoll and Pablo Valverde-Vaquero. Thanks for the

wide ranging discussion in the field and for offering invaluable suggestions towards this project. Their willingness to share their vast geological knowledge and technical assistance during my trips to Ottawa is appreciated.

The technical staff at the Department of Earth Sciences, MUN provided excellent data, in particular Mike Tubrett (ICP-MS), Pam King (XRF), Mike Shaffer (electron microprobe), Rick Soper (lapidary) and Allison Pye (IR-MS). TI-MS geochronology was performed at the Geological Survey of Canada with the support of Vicki McNicoll and Julie Peressini. Their assistance and timely completion of analysis are greatly appreciated. Dr. Richard Cox is acknowledged for introducing me to the particulars of detrital zircon geochronology. Lead isotope analyses were provided by Clement Gariépy (UQAM).

Gerry Squires, Terry Brace and Andrew Hussey of Thundermin Resources provided accommodation while in the field and each openly shared their geological knowledge. Industry geologists Charlie Dearin, Phil Saunders and Dave Barbour are thanked for many informative discussions. Altius Minerals Corp., Thundermin Resources and Buchans River Corp. are acknowledged for allowing me access to unpublished geochemical data. Excellent and efficient helicopter support was provided by Derek Newhook and Canadian Helicopters.

I wish to extend my thanks to my fellow students and friends who have been willing to discuss academics and for the good times over past pasty couple of years. I have been fortunate to share my office first with Darrell Hyde and later with Kerri Riggs. Thanks for understanding my ways and for putting up with me. I would also like to thank Kerri for helping me when I needed a field assistant and for showing me how to relax and have fun outside of school. I am grateful to Patrick, Chris, Mark and Billy – *The Rams* – for many memorable Wednesday nights, great music, and teaching me the finer 'pints' of life.

Financial support for this study was provided by the Mineral Deposits Section of the Geological Survey of Newfoundland and Labrador and by the Geological Survey of Canada as part of the Targeted Geoscience Initiative project on the geology of the Red Indian Line. The Buchans Scholarship of ASARCO Inc. and the Special Scholarship for

natural resource development from Memorial University of Newfoundland are gratefully acknowledged.

Finally, I would like to thank Hank Williams for all of the support, geological and not so geological, that he has given me over the years since I started studying geology. Hank's extensive knowledge and his eagerness to talk to me at anytime has been a source of inspiration and encouragement. His memorable field excursions are experiences that opened my mind, always made me think outside of the norm and made me appreciate the wonders of Newfoundland geology.

TABLE OF CONTENTS

CHAPTER 5
HYDROTHERMAL ALTERATION GEOCHEMISTRY

CHAPTER 6
RADIOGENIC ISOTOPE GEOCHEMISTRY AND GEOCHRONOLOGY

CHAPTER 7
SULPHUR ISOTOPE GEOCHEMISTRY

LIST OF FIGURES

LIST OF PLATES

LIST OF TABLES

CHAPTER 1

INTRODUCTION

1.1 Preamble

The Dunnage Zone of Newfoundland has played an integral role in understanding the development of the Appalachian Orogen for over the past four decades (Williams, 1964; Dewey and Bird, 1971; Williams, 1979). Since the recognition that the Dunnage Zone is divisible into two separate and unique subzones (Williams *et al.*, 1988) most geological work has been concentrated on the Notre Dame Subzone (e.g. Swinden *et al.*, 1997). The Exploits Subzone has received far less attention yet its tectonic message is just as profound.

Volcanogenic massive sulphide deposits occur throughout the Victoria Lake Supergroup and have been the focus of intense interest from exploration and mining companies since the past century. The stratigraphic, tectonic, metallogenic and structural relationship between the various subgroups of the Victoria Lake Supergroup are poorly known and their temporal and spatial relationship to other units in the Exploits Subzone are ambiguous. Therefore, in 2000 the Geological Survey of Canada, in conjunction with the Geological Survey of Newfoundland and Memorial University of Newfoundland, commenced the Red Indian Line-Targeted Geoscience Initiative to address these questions and to resolve the myriad of internal problems that exist throughout the area.

1.2 Location and Access

The Victoria Lake-Burnt Pond study area (Figure 1.1) is located in central Newfoundland, and covers portions of NTS 1:50 000 map sheets 12A/4, 5, 7, 9, 10, 11, 15 and 16 and 2D/13. The area is bounded by geographical coordinates 48^{O} 30' and 48^{O} 45' north latitude and 56^{O} 15' and 57^{O} 00' east longitude. The study area encompassing the Tally Pond Group is located in the northeastern section of the map area, and forms a northeast-trending linear belt centred approximately 20 km south of the community of Millertown. Access to the area is excellent, as a series of logging roads that are owned and operated by Abitibi-Consolidated cover most of the map area. Outcrops that are exposed along the ridges and in some localities to the south are best reached by helicopter.

1.3 Physiography

The Victoria Lake–Red Indian Lake area of central Newfoundland is characterized by a gently undulating and hummocky heavily forested landscape with an elevation that varies between 150 to 300 m altitude. The southern part of the area consists of extensive bogs with numerous small rivers and ponds and a rugged topography dominated by deep glacial valleys and ridges ranging between 300 and 400 m in elevation (Plate 1.1). To the north, small brooks and ponds are scattered throughout the area where the topography is generally flat lying consisting of low rolling hills with isolated peaks that reach up to 400 m (Plate 1.2). Extensive areas of glacial till result in generally poor bedrock exposure except along the linear, northeast-trending locally barren ridges. The majority of the valleys in the area are

forested by spruce, fir and birch, however, extensive logging during the past century have resulted in large areas of immature growth and open cutover.

Three prominent glacial striae directions are present in the area (Evans and Kean, 2002). Glaciation during the Early Wisconsin (Twenhofel and MacClintock, 1940) produced a southward flow that was centered located northwest of Red Indian Lake. This was followed during the Late Wisconsin by southwest and northeasterly-directed flows which inturn were followed by a southwestward directed flow from a centre northeast of Buchans.

1.4 Previous work and history of exploration

The earliest geological survey in the Red Indian Lake area (Figure 1.2), central Newfoundland, was conducted by Alexander Murray in 1871 for the Geological Survey of Newfoundland (Murray, 1872). Murray's successor, J.P. Howley, conducted two separate geological expeditions through the area in 1875 and 1888 that focused on exploring the lower Exploits, Lloyds, and Victoria rivers along with parts of Noel Paul's Brook (Howley, 1917). At the beginning of the 20th century much of the land in the Red Indian Lake area was part of a long-term charter granted to the Anglo-Newfoundland Development Company (A.N.D.Co.). Prospectors working for the A.N.D.Co. discovered the Buchans River and the Victoria Mine prospects in 1905. In 1926 the A.N.D.Co. entered into a formal agreement with ASARCO to mine the Buchans River orebody and within six months a number of new orebodies in the Buchans area were discovered. These and later discovered orebodies were mined until 1984, at which time all known ore reserves were exhausted (Thurlow and Swanson, 1981).

The first detailed geological investigations of the present Victoria Lake Supergroup were conducted as part of a series of academic studies sponsored by ASARCO. Brown (1952) mapped the southeastern part of the Lake Ambrose area as part of an M.Sc. thesis at McGill University and Mullins (1961) mapped the area south of Lake Ambrose to Noel Paul's Steady for an M.Sc. study at Memorial University of Newfoundland.

The Geological Survey of Canada conducted regional (1: 250 000) scale mapping of the Red Indian Lake map area (NTS 12/A) in 1965 and 1966 (Williams, 1970). In 1975, the Newfoundland Department of Mines and Energy began a regional geological mapping survey of the Victoria Lake-Red Indian Lake area (Kean, 1977, 1979; Kean and Jayasinghe, 1980, 1982). A regional metallogenic study of the Victoria Lake Group was started in 1984 as part of the Canada-Newfoundland Mineral Development Agreement (Kean, 1985; Evans and Kean, 2002). This program consisted of detailed mapping and geochemical sampling (Evans *et al.*, 1990) coupled with an extensive regional gold sampling program (Evans and Wilson, 1994; Evans, 1996) and detailed deposit level studies (Evans, 1986; Evans and Wilton, 1995).

In the mid-1970s, Noranda began mineral exploration in the Tally Pond volcanic belt, which led to the discovery of the Burnt Pond Cu–Zn prospect in 1974. This was followed by a five-year period of intense exploration involving the diamond drilling of airborne geophysical anomalies and discovery of numerous geochemical anomalies, massive sulphide float, and outcrops of mineralized felsic volcanic rocks. In 1979, Noranda entered into a joint venture agreement with Abitibi-Price Corp. (later assumed by BP-Selco) who owned the mineral rights to the Tally Pond volcanics to the southeast of Tally Pond.

An extensive series of ground geophysical surveys were followed up by a diamond drilling program which led to the discovery of the Boundary Deposit in 1981. Over the next six years, diamond drilling to the south of the Boundary Deposit intersected abundant pyrite mineralization, altered felsic volcanic rocks, and lithogeochemical anomalies which culminated in the spring of 1987 with the intersection of 55 m of massive sulphide. This intersection included over 20 m of ore grade sulphide which contained over 2% Cu and 10% Zn in what was to be called the Upper Duck lens. Further drilling led to the discovery of the Lower Duck and Sleeper lenses, which were collectively called the Duck Pond Deposit. In 1998, Thundermin Resources Inc. entered into an agreement with Noranda to acquire a 100 percent interest in the Duck Pond/Boundary base metal property. Thundermin subsequently formed a 50/50 joint venture with Queenston Mining Corp. and undertook a diamond-drilling program aimed at delineating portions of the Duck Pond and Boundary deposits. This work added to the economic and geological reserves at the Duck Pond deposit. Feasibility studies have been conducted, with a view to possible development.

1.5 Purpose and Scope

This project was conducted at Memorial University of Newfoundland in conjunction with the Geological Survey of Newfoundland and Labrador and is part of the larger Geological Survey of Canada-Targeted Geoscience Initiative project entitled '*Geology of the Iapetus Suture Zone, Red Indian Line, Newfoundland*'. The purpose of this research is to define the extent, paleotectonic setting and age of the newly-defined Victoria Lake Supergroup and to complete a detailed examination of the geology, geochemistry, geochronology, and metallogeny of the Tally Pond Group. The last government funded

geological survey in the Victoria Lake Supergroup was conducted over 15 years ago but was mainly concentrated on rocks of the Tulks belt. Interest in the area was sparked by the discovery in the mid-1980's of volcanogenic sulphide mineralization in felsic volcanic rocks of the Tally Pond Group. Previous detailed work on the Tally Pond Group was mainly conducted as part of these industry exploration surveys, however, these surveys were mainly conducted on selected areas throughout the group and there has been no study of the group as a whole. As such, the main goals of this project involve: 1) detailed mapping and subdivision of rocks of the Tally Pond Group to understand its relationship to adjoining rock sequences; 2) U-Pb zircon geochronology to determine the age of magmatism and VMS mineralization; 3) Pb and S isotopic studies to compare sulphide occurrences to others in the Dunnage Zone; 4) detrital zircon U-Pb geochronology to define the source and provenance of overlying rock sequences; and 5) integration of all data to develop a tectonic model that explains the geologic relationships and origin of the various rocks units of the Tally Pond Group.

The significance of this research is that it aims to define the age and paleotectonic setting of the Tally Pond Group in the Exploits Subzone of central Newfoundland. The definition of the Tally Pond Group as a separate and distinct island arc terrane has implications for the regional paleotectonic setting of island arc systems in the Dunnage Zone of the entire Appalachian Orogen.

1.6 Methods of Research

Fieldwork for this study was carried out in during the summers of 2000 and 2001. During the summer of 2000 fieldwork was concentrated on the area surrounding Tally Pond and extending northeastward to Noel Paul's Brook; the summer of 2001 was spent examining

the area to the south, from Lake Ambrose to Rogerson Lake. Fieldwork was based out of a camp located 3 km northwest of Tally Pond operated by Thundermin Resources Inc. Parts of the 2001 fieldwork were conducted from a Geological Survey of Canada field camp located in Harbour Round, Red Indian Lake.

Mapping of the Tally Pond Group was carried out through the use of topographic maps on a scale of 1: 50 000. Detailed (1: 10 000 and 1: 5 000) maps from industry surveys were used in some areas to locate outcrops. The majority of mapping was conducted by ground traverses from the numerous logging roads. Outcrops along the ridges and along the southern shore of Rogerson Lake were accessed by helicopter. The scarcity of outcrop in the area necessitated the use of the extensive drill core collection from industry diamond drilling activities. The majority of this drill core is stored at Thundermin Resources' Tally Pond camp; diamond drill core housed in the provincial government's drill core library in Buchans was also examined.

The Duck Pond volcanogenic sulphide deposit was studied in more detail than other volcanogenic sulphide occurrences in the group due to the abundant number of diamond drill holes present in the Tally Pond area. Rocks containing and surrounding the deposit were studied in detail such that all rock types, mineralization, alteration and structures were closely examined. Information obtained from the detailed mapping in the Tally Pond area was used to extrapolate structures and outcrop patterns into less exposed adjoining areas and for re-interpretation of pre-existing maps.

Rock samples were collected for petrographical, petrological, geochemical, and geochronological studies. In addition sulphide samples were collected from sulphide occurrences for isotopic studies. Sample selection was conducted such that a representative

sample from each of the rock types of the Tally Pond Group was obtained and submitted for geochemistry. Samples obtained for U-Pb zircon geochronology were selected to determine the age of deposition of the Tally Pond Group, the age of mineralization of the Duck Pond and Boundary deposits, timing of mafic intrusive events and the sediment provenance of the Rogerson Lake Conglomerate.

Major and trace element analyses were conducted using a number of different analytical methods on samples collected geographically and stratigraphically throughout the Tally Pond Group. A collection of 48 whole rock samples were analyzed for major and trace elements by X-Ray Fluorescence spectrometry at Memorial University of Newfoundland using a Fisons/ARL model 8420 + sequential wavelength-dispersive X-Ray spectrometer. Rare Earth Elements and other trace elements were obtained on a subset of 15 samples by Inductively Coupled Plasma-Mass Spectrometry at Memorial University of Newfoundland using a Hewlett Packard 4500 + inductively coupled plasma-mass spectrometer.

Fifteen galena samples selected from VMS occurrences in the Tally Pond Group were analyzed for Pb isotopes by MC-ICP-MS at the GEOTOP Laboratory, Université du Québec á Montréal. Sulphur isotope analyses were conducted on 39 samples at Memorial University of Newfoundland using a Finnigan MAT 252 mass spectrometer. Chemical analyses of alteration minerals were analyzed at Memorial University of Newfoundland using a Cameca SX50 electron microprobe equipped with SAMx-XMAS software.

Two rock samples were submitted for U-Pb zircon geochronology at the Geochronology laboratory at the Geological Survey of Canada in Ottawa, Ontario. The samples were analyzed for U and Pb isotopes using a Finnigan MAT 251 thermal ionization mass spectrometer. Two conglomerate samples were analyzed for detrital zircon U-Pb

geochronology at Memorial University of Newfoundland by Laser Ablation Microprobe ICP-MS using a custom built ultraviolet laser coupled to a VG PlasmaQuad II S+ inductively coupled plasma-mass spectrometer.

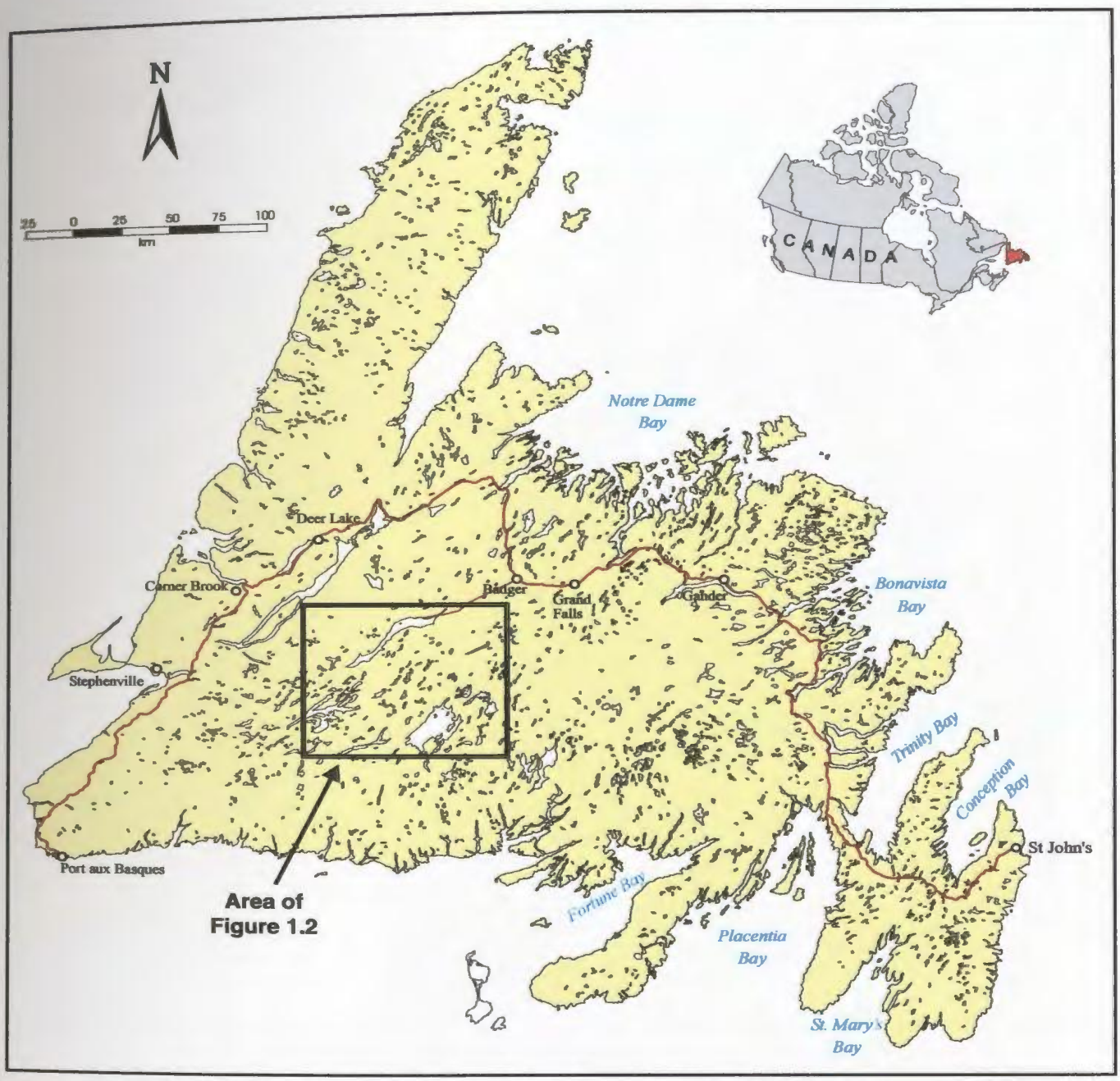

Figure 1.1 *Map of the island of Newfoundland showing the location of the study area shown in Figure 1.2..*

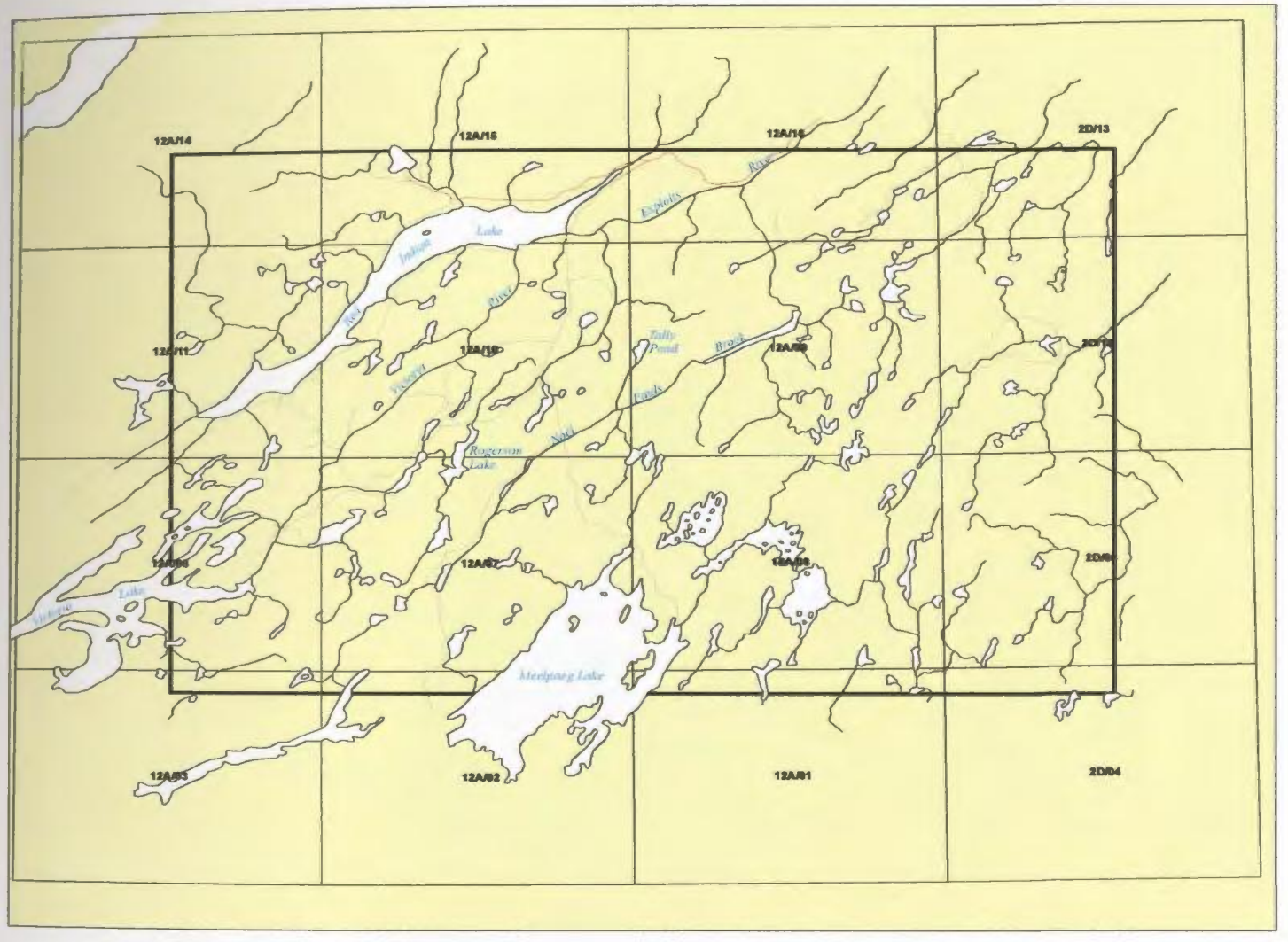

Figure 1.2 *Location of the Victoria Lake-Red Indian lake study area in parts of NTS areas 12A/06, 12A/07, 12A/08, 12A/09, 12A/10 and 12A/11.*

Plate 1.1 *Rugged topography of the Lloyds River valley and Annieopsquotch Mountains.*

Plate 1.2 *Looking northwest over flat lying, low rolling topography from the summit of Harpoon Hill.*

CHAPTER 2

REGIONAL GEOLOGY

2.1 Appalachian Tectonics

The Appalachian Orogen represents a Paleozoic mountain belt formed by the closing of the Iapetus Ocean. The orogen was segmented by the Mesozoic opening of the North Atlantic Ocean and now occurs on three continents (Figure 2.1). The Canadian segment is exposed in Newfoundland, Nova Scotia, New Brunswick and parts of southern Quebec. From Canada, the Appalachians extend southwestward through the eastern United States to the Pacific margin of Mexico. On the eastern side of the Atlantic Ocean, Appalachian remnants are found in Ireland and the British Isles, East Greenland, Scandinavia, and France (Caledonides), Northwest Africa (Mauritanides and Variscides), and the Iberian Peninsula (Hesperides) (Williams *et al.*, 1999).

Newfoundland is located in a central position of the orogen linking the northern Appalachians and British Caledonides. Post-Ordovician cover sequences are least extensive in Newfoundland and thus the geology provides important constraints upon tectonic modeling of the whole Appalachian-Caledonian Orogen (van Staal *et al.*, 1998).

The Newfoundland Appalachians are divided into four northeast-trending tectonostratigraphic zones, based on stratigraphic and structural contrasts between

constituent lower Paleozoic and older rocks (Figure 2.2). From west to east the zones are the Humber, Dunnage, Gander and Avalon (Williams, 1979). Rocks of these zones display the sharpest contrast in lithology, stratigraphy and thickness across the orogen. The zones also exhibit structural, faunal, geophysical, isotopic, plutonic and metallogenic contrasts, thereby enhancing their individuality. Selected areas of the orogen were subject to a variety of deformational events including the Early and Middle Ordovician Taconic Orogeny that affected the Humber Zone and western parts of the Dunnage Zone and portions of the Gander and eastern Dunnage zones. The Siluro-Devonian Acadian Orogen affected the entire orogen, except for parts of the Newfoundland Avalon Zone. The Carboniferous-Permian Alleghanian Orogeney dominantly affected the Humber and Dunnage zone boundary in Newfoundland (Williams, 1995).

The various tectonic zones each have a separate and distinct stratigraphic and tectonic history and represent changes in depositional environments and tectonic settings, that collectively record events in the rifting, opening, and eventual destruction of the Paleozoic Iapetus Ocean by collision of the opposing Laurentian and Gondwanan continental margins. The Humber Zone records the development and destruction of an Atlantic-type passive margin, the ancient continental margin of Laurentia. Parts of the Dunnage Zone represent vestiges of Iapetus with volcanic sequences and mélanges built upon oceanic crust. The Gander Zone represents the eastern margin of Iapetus; and the Avalon Zone is a sampling of tectonic elements that lay outboard or on the opposing Gondwanan side of Iapetus (Williams, 1979).

All of the zone boundaries are tectonic as the rocks that define the zones were widely separated during deposition and are now telescoped into a mountain belt. The

western boundary of the Humber Zone is defined by the limit of Appalachian deformation (Logan's Line) which separates deformed orogenic rocks from undeformed rocks of the St. Lawrence Platform (Williams, 1995). Its eastern margin is the Baie Verte-Brompton Line (Williams and St. Julien, 1982), a steep structural belt marked by ophiolite occurrences that separate polydeformed rocks of the Humber Zone to the west from less deformed volcanic sequences of the Dunnage Zone to the east. The Dunnage-Gander boundary is tectonic wherein Dunnage Zone ophiolitic rocks of the Gander River Complex are juxtaposed against sedimentary rocks of the Gander Zone and where Gander Zone rocks are present as structural windows beneath Dunnage Zone sequences. The Gander-Avalon zone boundary is an abrupt tectonic junction marked by two major faults, the Dover and Hermitage Bay faults. These faults separate Precambrian volcanic and granitic rocks of the Avalon Zone from Paleozoic gneisses and granites of the Gander Zone.

2.2 Dunnage Zone

2.2.1 History of Geological Thought of the Dunnage Zone

The central region of the Newfoundland Appalachians, the Dunnage Zone of Newfoundland, was regarded as being geologically distinct from other areas of Newfoundland since the first regional syntheses of Murray (1872) and Howley (1917). Snelgrove (1928) recognized the abundant base metal occurrences hosted by mafic volcanic sequences and referred to the area as the Central Mineral Belt. In triparte divisions of the Newfoundland Appalachians, the region, combined with the Gander Zone and parts of the Humber Zone, was termed the Central Paleozoic Mobile Belt

(Williams, 1964) and the Central Volcanic Belt (Kay and Colbert, 1965). In plate tectonic analyses the Dunnage Zone included parts of Williams *et al.* (1972, 1974) C, D, E, and F zones. It was later defined as the Dunnage Zone by Williams (1976) and extrapolated throughout the entire Appalachian-Caledonian Orogen (Williams, 1978, 1979; Kennedy, 1979).

The earliest tectonic models for the rocks that are presently described as part of the Dunnage Zone were those of Schuchert (1923) and Schuchert and Dunbar (1934). The Dunnage (and Gander) zones are equivalent to the general region of their New Brunswick Geanticline, a contrived land barrier that supposedly separated the contrasting Cambrian trilobite faunas of the St. Lawrence Geosyncline to the west, and the eastern Acadian Geosyncline. This unrealistic notion of a landmass was eventually replaced by the more realistic concept of a deep ocean basin that separated two sedimentary prisms deposited along the margins of opposing platforms (Williams, 1964). Since the advent of plate tectonics in the late 1960's-early 1970's, Dunnage Zone ophiolitic rocks have been interpreted to be oceanic crust and mantle (Dewey and Bird, 1971), mélanges as vestiges of subduction zones (Kay, 1976) or major back-arc olistostromes (Hibbard and Williams, 1979), and volcanic rocks as island arcs and oceanic islands (Williams, 1979). The Dunnage Zone is presently considered to be a suspect terrane (Williams and Hatcher, 1982), or more precisely a composite suspect terrane (Williams and Hatcher, 1983).

2.2.2 Geology of the Dunnage Zone

The Dunnage Zone is distinguished by its lower Paleozoic, dominantly mafic, volcanic rocks, ophiolitic suites, and mélanges. Sedimentary rocks include greywacke,

slate, chert, epiclastic volcanic rocks, and minor limestone, all of marine deposition (Figure 2.3). Some of these marine rocks rest on an ophiolitic substrate; others have stratigraphic relationships with rocks of the Gander Zone. Stratigraphic sequences are variable and formations are commonly discontinuous. Most rocks are Late Cambrian to Middle Ordovician age (Williams, 1995).

The Dunnage Zone is widest (150 km), and its rocks best preserved in northeast Newfoundland at the matching Newfoundland and Hermitage reentrants, where sublime wave-washed exposures are present across islands and headlands. The zone is traceable across most of Newfoundland although it is narrow and disappears southwestward near Cape Ray at the matching St. Lawrence and Cabot promontories.

The geological development of the Dunnage Zone is recorded in four very broad geological environments:

1) Cambro-Ordovician ophiolitic rocks, which are interpreted as remnants of oceanic crust.
2) Thick sequences of Cambrian and Ordovician volcanic and subvolcanic rocks and related volcaniclastic rocks, generally interpreted to represent the remains of island-arc and back-arc basins.
3) Middle Ordovician shale and chert, and Late Ordovician to Early Silurian flychsoid sequences of argillite, greywacke and conglomerate that commonly lie conformably upon the underlying volcanic and ophiolitic rocks.
4) Subaerial, mainly felsic, volcanic rocks and terrestrial-fluviatile sedimentary rocks of Silurian age interpreted to have been deposited in troughs and basins.

2.2.2.1 Subdivisions of the Dunnage Zone

The Dunnage Zone of Newfoundland has been subdivided into two major subzones, and several smaller ones based on the marked Lower to Middle Ordovician stratigraphic, faunal, geochemical, and isotopic differences (Williams *et al.*, 1988). The two major divisions are the Notre Dame Subzone, with Arenig Laurentian, low-latitude fauna in the northwest, and the Exploits Subzone, with an Arenig high-latitude, peri-Gondwanan fauna in the southeast (Figure 2.4) . Rocks of three smaller divisions are assigned to the Twillingate and Indian Bay subzones in the northeast and the Dashwoods Subzone in the southwest (Williams, 1995).

Rocks of the *Notre Dame Subzone* are mainly Lower Ordovician, thick, marine sequences dominated by mafic volcanic rocks; Late Cambrian to middle Ordovician trondjemites are common throughout the subzone. Exposures are best along the coast of the Baie Verte Peninsula and Notre Dame Bay; rock exposures decrease inland but are traceable to Red Indian Lake and the south end of Grand Lake.

Major structural zones bound the Notre Dame Subzone to the west and east. The western boundary between ophiolitic rocks of the Notre Dame Subzone and metaclastic rocks of the Humber Zone is the Baie Verte Line (Williams and St. Julien, 1978). This tectonic contact is present as a steep structural zone that is everywhere overprinted and rendered confusing by later structures and intrusions, and in places is present beneath continental cover sequences. Seismic reflection studies indicate that the entire Notre Dame Subzone is allochthonous, underlain by the eastward-dipping extension of the Humber Zone (Hall *et al.*, 1998).

Ophiolitic rocks of the Notre Dame Subzone are subdivided into a western and eastern belt based on the age and characteristics of the ophiolites (Colman-Sadd *et al.*, 1992). The western ophiolite belt consists of the St. Anthony, Lushs Bight, Betts Cove, and Grand Lake complexes that are dominantly Upper Cambrian to Tremadoc (505-489 Ma) in age (van Staal *et al.*, 1998). These assemblages are overlain by Arenig to Llanvirn calc-alkaline volcanic rocks and are intruded by Lower to Upper Ordovician (488-456 Ma) magmatic arc tonalite and granite plutons of the Notre Dame Arc.

The eastern ophiolite belt is composed of younger Arenig (481-478 Ma), fault-bounded ophiolite fragments, the King George IV, Annieopsquotch and Star Lake, Skidder and Mansfield Cove complexes. These ophiolite complexes are spatially associated with upper Tremadoc to upper Arenig (484-473 Ma) calc-alkaline volcanic and arc tholeiitic rocks of the Buchans, Roberts Arm, Cottrell's Cove and Chanceport groups. The original relationships between the younger volcanic arc rocks and older ophiolite rocks, however, are poorly defined. Both the ophiolitic rocks and volcanic arc sequences of the Notre Dame Subzone are unconformably overlain by extensive continental volcanic rocks and associated continental to shallow marine clastic sedimentary sequences of the Springdale Belt. Lithic similarities coupled with isotopic studies and regional correlations among rocks throughout the belt, suggest that most of the constituent rocks are Silurian.

The eastern boundary of the Notre Dame Subzone with the Exploits Subzone is the Red Indian Line, an extensive fault system traceable across Newfoundland. The Red Indian Line is commonly regarded as the main Iapetan suture in Newfoundland. As shown by van Staal *et al.* (1996), however, Iapetus contained several different basins and

arc systems and the notion of a single suture zone in an ocean system as complex as Iapetus is not logical. The Red Indian Line coincides with the Lukes Arm and Sops Head Faults on the northeast coast. Inland, to the southwest, the Red Indian Line coincides with faults along Red Indian Lake, Lloyds Valley, and the northwest side of Victoria Lake to Burgeo Road. These faults had a complex and protracted history of movements ranging from thrusting to strike slip. Therefore, the Red Indian Line is not a single, continuous fault but a fundamental tectonic boundary comprised of a collection of faults that collectively formed a complex movement zone that was continuously activated and re-activated during the closure of Iapetus.

The *Exploits Subzone* is a composite and structurally complex collection of rocks that are mainly Lower to Middle Ordovician with sedimentary rocks and mélanges more abundant than in the Notre Dame Subzone. Cambrian volcanic and Precambrian granitic rocks are present in places. In the northeast Exploits Subzone, Upper Ordovician and Silurian marine greywackes and conglomerates conformably overlie Caradocian black shale which are conformable on underlying Ordovician volcanic rocks. In places, sub-Middle Ordovician and sub-Silurian unconformities are present (Williams, 1995). Ordovician and younger mélanges are present throughout the northeast Dunnage Zone and of these Silurian olistostromes and mélanges are special rock types unique to the Exploits Subzone. Volcanic rocks of the Exploits Subzone are mainly mafic and marine along the north coastline and mainly felsic marine and partly subaerial inland to the south. All of the volcanic sequences are interlayed with, or laterally grade into, clastic sedimentary, dominantly tubiditic, rocks that contain abundant volcanic detritus.

Small bodies of mafic and ultramafic rocks belonging to the Gander River Complex (O'Neill and Blackwood, 1989) resemble incomplete ophiolite sequences and are present along the eastern margin of the Exploits Subzone extending along strike inland toward Bay d'Espoir. Large and more complete ophiolite complexes (Pipestone Pond, Coy Pond and Great Bend complexes) occur inland and surround inliers of Gander Zone rocks. All of these complexes consist dominantly of ultramafic rocks and gabbros, however, some examples contain diabase and pillow lavas. The ophiolite complexes are overlain by Ordovician volcanic and sedimentary rocks (Colman-Sadd and Swinden, 1984).

Mélanges occur all across the northeast Exploits Subzone. The Dunnage Mélange (Hibbard and Williams, 1979) is one of the most extensive and best known mélanges of the entire Appalachian Orogen. Other examples include the Joey's Cove, Dog Bay Point and Carmanville mélanges. All of these mélanges contain similar rock types with blocks of clastic sedimentary and mafic volcanic rocks enveloped in black shaly matrices, and all contain associated dark grey shales with thin coticule layers and nodules (Williams, 1995). The presence of numerous mélanges in the northeast Exploits Subzone implies continuity of a coastal lithic belt that extended for at least 50 km.

The thickest and best known mafic volcanic sequence of the Exploits Subzone is the Wild Bight Group (Dean, 1978; Swinden, 1987) which underlies a significant area of the northern Exploits Subzone. The group is dominated by Early to Middle Ordovician, coarse mafic agglomerates and tuffs, thick pillow lava sequences, and well-bedded units of tuff, chert, tuffaceous sandstone and greywacke. Felsic volcanic and pyroclastic rocks are rare (Williams, 1995). The Wild Bight Group has been previously correlated with the

Exploits Group to the east (O'Brien, 1997) as the Exploits Group contains volcanic and sedimentary rocks similar to those of the Wild Bight Group. Both groups grade conformably up into grey chert, black shale and greywacke of the Caradocian Shoal Arm Formation (MacLachlan *et al.*, 2001).

Inland, to the southwest, the Victoria Lake Group (Kean, 1977) is correlated with the Wild Bight and Exploits groups. The Victoria Lake Group consists of mafic pillow lava, mafic and felsic pyroclastic rocks, chert, greywacke and shale. One prominent feature of the group are laterally continuous belts of felsic pyroclastic rocks. Like the Wild Bight and Exploits groups, the Victoria Lake Group is overlain along the northeastern margin by Caradocian black shales.

The eastern part of the Exploits Subzone is characterized by sedimentary rocks with smaller amounts of mafic volcanic rocks. The sedimentary rocks include shale, conglomerate, sandstone and greywacke which constitute the Davidsville Group in the north, whereas in the south they are classified as the Baie d'Espoir Group. Both groups are considered to be Late Arenig to Caradoc based on fossil evidence (Colman-Sadd, 1990; Boyce *et al.*, 1988).

2.2.2.2 Middle Paleozoic Rocks

The Caradocian shale sequence of the Exploits Subzone is conformably overlain by an Upper Ordovician and Silurian turbiditic sequence of greywackes and conglomerate of the Badger Belt. The greywackes (Sansom Formation) and conglomerates (Goldson Formation) reach combined thicknesses of 3000 m and constitute a continuous conformable sequence that bridges the Ordovician-Silurian

boundary. Silurian mélanges, locally with fossiliferous shale matrices and containing Ordovician volcanic, limestone, and black argillite blocks, are present in upper parts of stratigraphic sections (Williams, 1995).

The Botwood Belt is the largest single area of uninterrupted Middle Paleozoic rocks in Newfoundland and overlies sedimentary, volcanic, and plutonic rocks of the Exploits Subzone. All of its rocks are Silurian, with the exception of marine greywackes and conglomerates that are correlatives of those in the Badger Belt. The belt is dominated by Silurian subaerial volcanic flows and pyroclastic rocks which are overlain by red and grey sandstones with local conglomerate at their bases. Boundaries of the Botwood Belt with the underlying rocks of the Exploits Subzone are marked by steep faults along its northwest and southwest margins; however, unconformable relationships between Silurian conglomerates and Cambro-Ordovician rocks of the Victoria Lake Group and Precambrian plutons are present inland to the south (Williams, 1995).

The eastern boundary of the Botwood Belt is marked by the Dog Bay Line, a major structural junction that separates different Silurian lithological units (Williams, 1993). Rocks of the Botwood Belt lie northeast of the Dog Bay Line while rocks southeast of the line are assigned to the Indian Islands Belt, a shallow marine sedimentary sequences that pass upwards into terrigenous redbeds all of Silurian age.

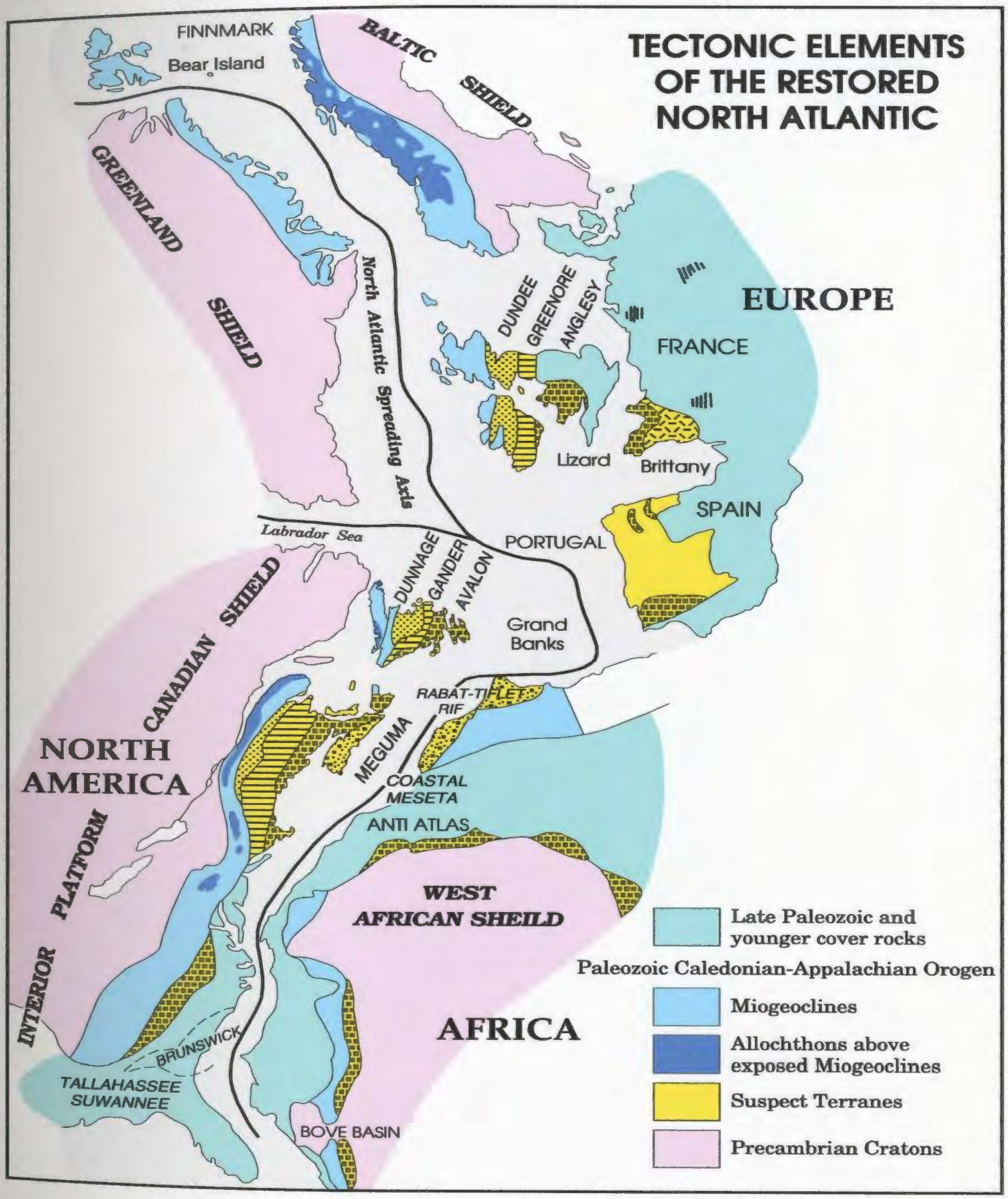

Figure 2.1 *Miogeoclines and suspect terranes of the Appalachian-Caledonian Orogen (Williams, 1984).*

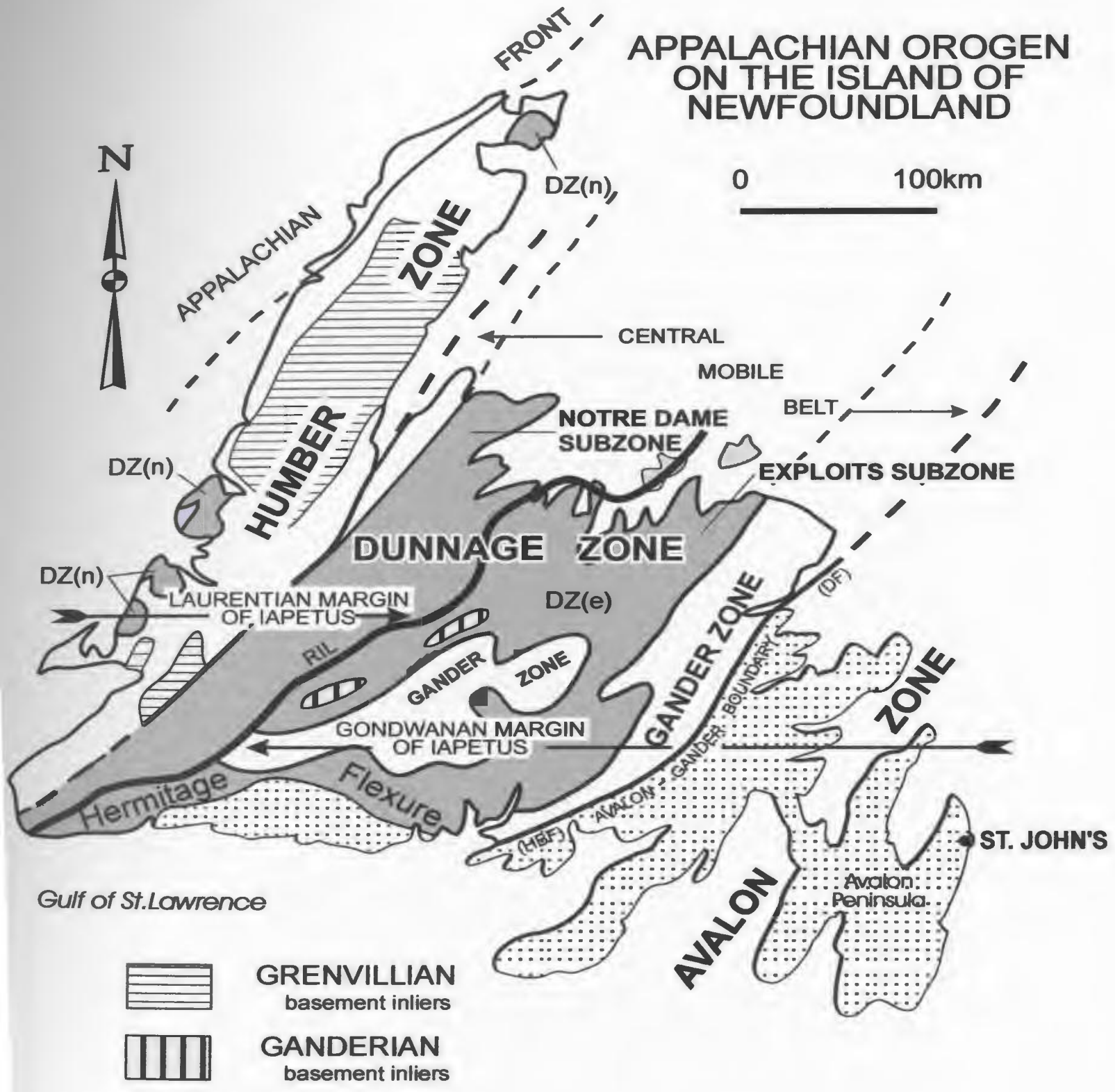

Figure 2.2 *Tectonostratigraphic subdivision of the Newfoundland Appalachians. DZ(e)= Dunnage Zone; Exploits subzone; DZ(n)= Dunnage Zone; Notre Dame subzone; GZ= Gander ZoNE; HBF= Hermitage Bay Fault; DF= Dover Fault; RIL= Red Indian Line (from O'Brien et. al.* 1996)

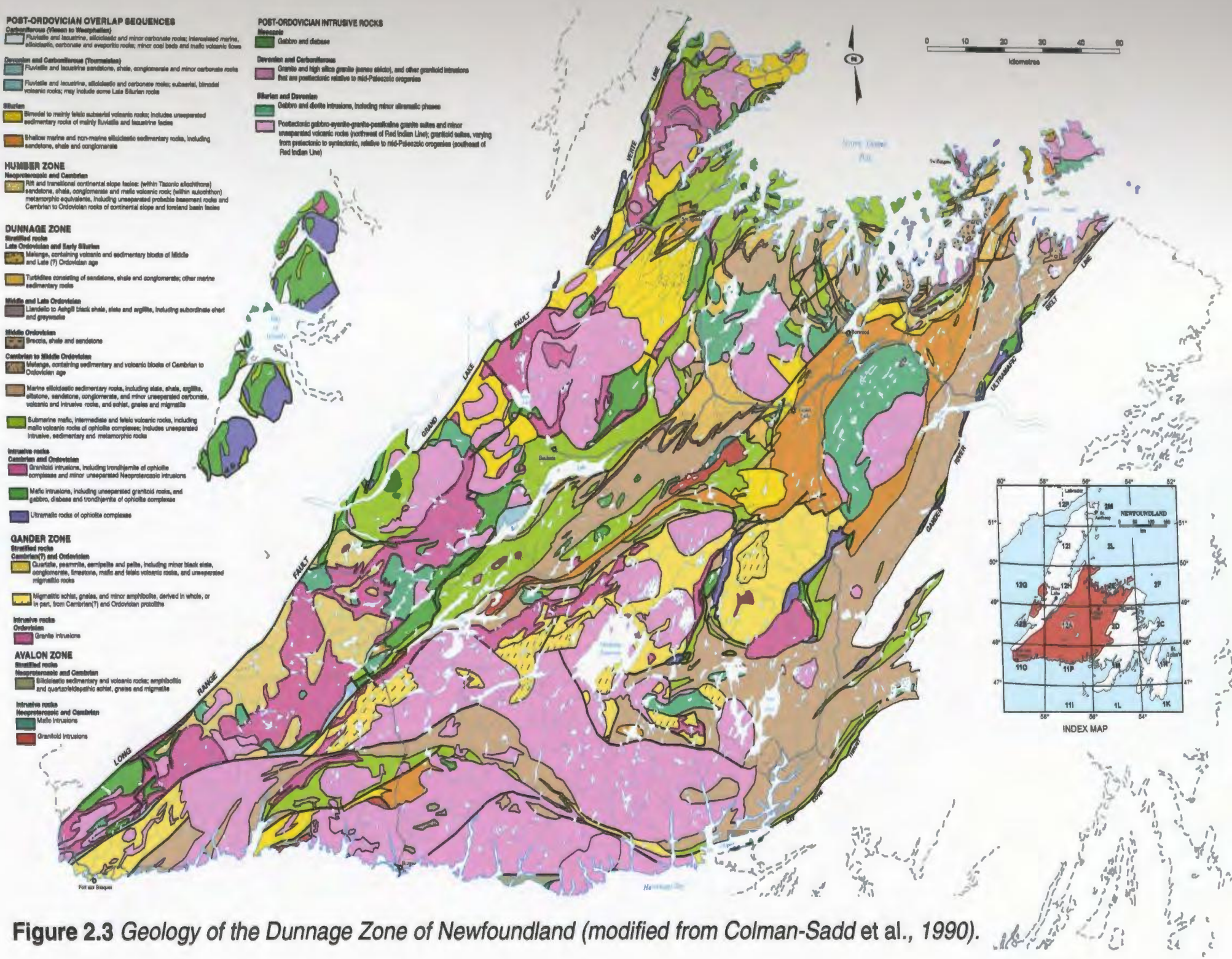

Figure 2.3 *Geology of the Dunnage Zone of Newfoundland (modified from Colman-Sadd* et al., *1990).*

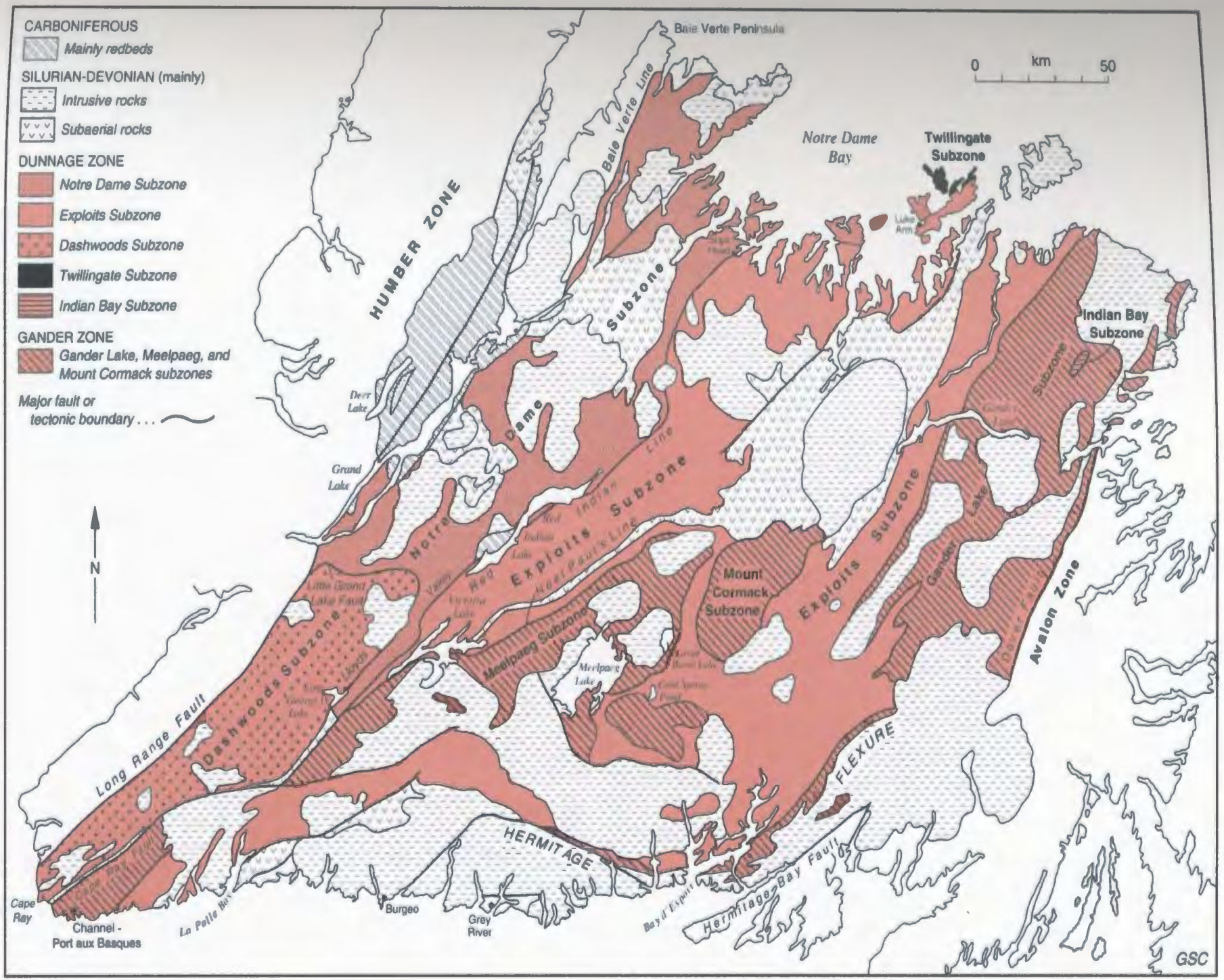

Figure 2.4 *Zonal subdivision of the Newfoundland Dunnage Zone. Modified from Williams* et al. *(1988) and Williams (1995).*

CHAPTER 3

GEOLOGY OF THE TALLY POND GROUP AND SURROUNDING ROCKS

3.1 Preamble

The Tally Pond volcanic belt and adjacent arc-related volcanic and volcaniclastic rocks of the Victoria Lake Group comprise one of the many Ordovician accreted oceanic terranes comprising the Exploits Subzone of the Newfoundland Appalachians. Previous workers (Kean, 1977, 1982; Kean and Jayasinghe, 1980; Dean, 1978) interpreted the Tally Pond volcanic belt to be equivalent to other pre-Caradocian volcanic sequences (e.g., Tulks belt) in the Victoria Lake Group. Subsequent work (Kean, 1985; Kean and Evans, 1986, 1988; Dunning *et al.*, 1987, 1991) however has shown that the Victoria Lake Group, as originally defined, does not adequately encompass the composite nature and wide range of temporal, spatial and geochemical assemblages present in these rocks.

Detailed 1:50 000 mapping for this study (Figure 3.4; Map 1) has shown that the Tally Pond volcanic belt is geologically and structurally distinct from other volcanic sequences of the Victoria Lake Group. Pb isotope data (Chapter 6) from volcanogenic massive sulphide occurrences suggest different sources of mineralizing fluids. Furthermore, geochemical (Chapter 4) and geochronological data (Chapter 6) indicate that the Tally Pond Group volcanic sequences are temporally and genetically distinct

from others in the Victoria Lake Group. Thus, following the suggestions of Evans and Kean (2002) and Rogers and van Staal (2002) the Victoria Lake Group has been elevated to supergroup status.

In the following section the geology of the proposed Victoria Lake Supergroup is described first as it was originally defined for the Victoria Lake Group by Kean (1977) and subsequently redefined and updated by Kean (1985), Kean and Evans (1988), Evans and Kean (1990) and Evans *et al.* (1990). Next the proposed revision and elevation to supergroup status is defined and described, and finally the geology of the Tally Pond Group is proposed and defined.

3.2 Geology of the Victoria Lake Group

The Victoria Lake Group as defined by Kean (1977) is a complex package of volcanic, volcaniclastic, and epiclastic rocks with varied age and geochemical affinities representing different tectonic environments (Figure 3.1). It comprises mafic pillow lava, mafic and felsic pyroclastic rocks, chert, greywacke and shale which were deposited in a variety of island-arc, rifted arc, back-arc and mature-arc settings. The original definition of the Victoria Lake Group included all pre-Caradocian rocks between Grand Falls in the northeast to King George IV Lake in the southwest, and from Red Indian Lake in the north to Noel Paul's Brook in the south (Kean, 1977; Kean and Jayasinghe, 1980).

In the northeast, the Victoria Lake Group is conformably overlain by Llandelio-Caradocian black shales and cherts, which in turn are conformably overlain by Middle Ordovician to Early Silurian flysch, argillite and conglomerate (Evans and Kean, 1987). Along its southeastern contact, the group is unconformably overlain by the Rogerson Lake Conglomerate, although this contact is generally sheared and faulted. The linear,

narrow outcrop pattern of the conglomerate and local clast provenance suggest that it is a fault-scarp, molasse-type deposit and thus the original southeastern margin of the Victoria Lake Group was probably fault bounded (Kean and Evans, 1988).

The Victoria Lake Group exhibits an inhomogeneously developed, regional, penetrative foliation, defined by chlorite, sericite, flattened clasts and crystal augen, which increase in intensity to the southwest. This foliation is subparallel to bedding and axial planar in tight to isoclinal folds. Rocks of the Victoria Lake Group are generally at lower greenschist facies, however, middle greenschist to lower amphibolite facies rocks are present along the southern margin (Evans *et al.*, 1990).

The Victoria Lake Group occupies a regional northeast-trending anticlinorium, termed the Victoria Anticlinorium (Kean, 1985). Regionally, the sequence youngs northwesterly on the north limb and southeasterly on the south limb; however, there are numerous smaller scale, first-order and second-order folds which result in variable facing directions. The lack of outcrop in the area has to date precluded detailed structural interpretation (Kean and Evans, 1988).

Regionally, the Victoria Lake Group has been divided into two major lithofacies (Kean and Jayasinghe, 1980, 1982): 1) volcanic rocks comprising two linear belts, the Tally Pond belt in the northeast and the Tulks belt in the southwest; and 2) an unnamed laterally equivalent, volcanically derived sedimentary belt in the northeast (Figure 3.2).

The Tally Pond belt refers to the sequence of volcanic, volcaniclastic and sedimentary rocks which extends from Victoria Lake northeastwards to the Diversion Lake area (Kean and Jayasinghe, 1980). The sequence contains volcanic rocks of the Tally Pond volcanics and Diversion Lake Formation, which are intercalated with

epiclastic volcanic and sedimentary rocks of the Burnt Pond and Stanley Waters sediments. The Tally Pond belt also contains the Valentine Lake plutonic suite and the Cripplebeck Lake quartz monzonite, considered to be in fault contact with the surrounding volcanic and sedimentary rocks.

The Tally Pond volcanics are exposed in a linear belt which consists of dominantly felsic pyroclastic rocks with intercalated mafic volcanic. The mafic volcanic rocks within the unit form two distinct volcanic sequences which are referred to as the Lake Ambrose basalts and the Sandy Lake basalts (Dunning *et al.*, 1991). Zircons from porphyritic rhyolite in the areas northeast of Tally Pond and east of Rogerson Lake have yielded identical U-Pb ages of 513 ± 2 Ma (Dunning *et al.*, 1991) making the Tally Pond volcanics one of the oldest well dated Iapetan island-arc sequence in the Appalachian Orogen.

3.3 Revised geology of the Victoria Lake Supergroup

The name Victoria Lake Supergroup was formally proposed by Evans and Kean (2002) for the collection of pre-Caradocian rocks termed the Victoria Lake Group. A provisional stratigraphy for these rocks was proposed by Rogers and van Staal (2002) who defined at least three distinct Ordovician and older units within the Victoria Lake Supergroup. The stratigraphic relationships between these units are at present inadequately defined and therefore internal subdivisions within the Victoria Lake Supergroup are informally classified as assemblages (Figure 3.3).

The Victoria Lake Supergroup consists of two volcanic dominated assemblages (Tally Pond and Tulks Hill) separated by one or more sequences of clastic sedimentary

rocks. Additionally, the Sutherlands Pond and Harbour Round assemblages may also constitute part of the Victoria Lake Supergroup, however, the present lack of detailed geochemical and geochronological data preclude their incorporation into the supergroup.

The Tally Pond assemblage (Rogers and van Staal, 2002) is a collection of volcanic and sedimentary rocks that extend from Victoria Lake northward to the Diversion Lake area (Figure 3.3). The Tally Pond assemblage is fault bounded to the west by a zone of black shale mélange and to the east by the overlying Rogerson Lake Conglomerate.

The Tally Pond assemblage is dominated by volcanic rocks of the Lake Ambrose volcanic belt (Dunning *et al.*, 1991) also known as the Lake Ambrose sequence (Rogers and van Staal, 2002). This sequence is characterized by a linear belt of predominantly felsic volcanic rocks consisting of pyroclastic rocks, volcanic breccia, agglomerate, breccia, tuff, crystal-tuff and flow-banded rhyolite. These rocks are intercalated with basalts (Lake Ambrose basalts of Evans *et al.*, 1990) which consist of pillowed to massive, amygdaloidal, tholeiitic flows.

The Tally Pond assemblage also includes the Sandy Lake sequence, which was originally defined by Evans *et al.* (1990) as a collection of chemically distinct basaltic rocks that are exposed northeast of the Lake Ambrose sequence in the area surrounding Sandy Lake. However, Rogers and van Staal (2002) expanded the definition of the Sandy Lake sequence to include not only the Sandy Lake basalts but also the bimodal volcanic rocks that are in fault contact with them.

The Lake Ambrose and Sandy Lake sequences of the Tally Pond assemblage are bounded by and locally intercalated with several packages of sedimentary and epiclastic

rocks. These rocks include sandstone with interbedded siltstone, greywacke, shale, argillite, conglomerate, minor tuff, and rare limestone.

The Tulks Hill assemblage (Rogers and van Staal, 2002) consists of two sequences of bimodal volcanic and minor clastic sedimentary rocks, termed the Tulks and Long Lake sequences. The Tulks Hill assemblage is separated from the Sutherlands Pond and Harbour Round assemblages to the northeast by a narrow zone of black shale mélange that represents the northwestern limit of the Victoria Lake Supergroup as defined by Rogers and van Staal (2002).

3.4 Local Geological Setting

3.4.1 Tally Pond Group

The Tally Pond Group can be divided into at least four separate rock formations that collectively are both temporally and structurally distinct from the remaining rocks of the Victoria Lake Supergroup. Thus, following the suggestion of Evans and Kean (2002) that the Victoria Lake Group be elevated to supergroup status, it is proposed that the geology of the Tally Pond volcanic belt be redefined and elevated to group status.

The name Tally Pond Group is hereby proposed for the sequence of volcanic, volcaniclastic and sedimentary rocks which extend from Burnt Pond southwestwards to the Victoria Lake area (Figure 3.4). It includes the rocks of the Tally Pond volcanics of Kean and Jayasinghe (1980), the Lake Ambrose volcanic belt of Dunning *et al.* (1991) and the Stanley Waters and Burnt Pond sediments of Evans and Kean (2002). The Sandy Lake sequence is considered to represent a separate package of volcanic rocks distinct from the Tally Pond Group and as such is excluded from the new definition. The

northwestern margin of the Tally Pond Group is defined by an extensive unit of black graphitic shale mélange which extends from Victoria Lake north to Burnt Pond area and is in tectonic contact with the adjacent volcanic rocks. The southern margin of the group is marked by the Rogerson Lake Conglomerate, a regionally extensive unit that unconformably overlies the Tally Pond Group and extends for at least 125 km from the Burgeo Highway north to the Cripplebeck Lake area. The base of the Tally Pond Group is not exposed but the Cripplebeck Lake Quartz Monzonite is considered to represent the Neoproterozoic Ganderian basement (van Staal *et al.*, 2002) upon which the Tally Pond Group was deposited.

The rocks of the Tally Pond Group are subdivided into five major units (Figure 3.4). The lack of structural data and precise geochronological age dates however, have made it difficult to constrain the temporal, stratigraphic and spatial relationships between the different rocks units.

3.4.1.1 Lake Ambrose Formation

The Lake Ambrose Formation is equivalent to the Lake Ambrose basalts (Evans *et al.*, 1990), unit 6b of Kean and Jayasinghe (1980) and part of the Lake Ambrose volcanic belt (Dunning *et al.*, 1991). These rocks form a discontinuous sequence of dominantly mafic volcanic rocks disposed in a northeasterly-trending, approximately 50 km long belt from Rogerson Lake north to the Steady Pond – Burnt Pond area. The formation is dominated by vesicular and amygdaloidal, generally pillowed, mafic flows and mafic to andesitic tuff, agglomerate and breccia.

Mafic flows consist dominantly of fine- to medium-grained, amygdaloidal basalt. The thickness of these mafic units varies from a few metres to tens of metres for both massive and pillowed flows. The pillowed flows (Plate 3.1) consist of dark green to grey, 5 to 10 % amygdaloidal basalt. The amygdules are commonly 1-4 mm in diameter and consist of quartz, calcite, carbonate, chlorite, pyrite and rare jasper. They are present in quantities of approximately 5 % in the pillow centers and increase in abundance to 10-15 % at the outer pillow margins. The pillows are generally small, with a maximum diameter of 50 centimetres (Plate 3.2) and moderate to strongly chloritized pillow rims. In places, pillow rims are extensively mineralized with pyrite.

In thin section the mafic volcanic rocks are comprised of 80 % plagioclase, 10 % augite and up 10 % magnetite and pyrite (Plate 3.3). The rock displays a seriate texture with micro phenocrysts of plagioclase. Generally, the small amygdules contain quartz while the larger ones consist of calcite with small quartz rims. Interpillow material is common throughout the formation and consists of mafic tuff, green chert and minor graphitic shale. Carbonate alteration is common throughout the mafic volcanic rocks and ranges from carbonate veins and spots, to pervasive carbonatization (Plate 3.4) of the primary mineral assemblage. The calcite is present as pseudomorphs in the groundmass after plagioclase and as a network of veins throughout the rock. The intensity of carbonate alteration is proportional to the proximity to the Duck Pond Boundary deposit as the level of alteration increases towards the deposit.

The mafic breccias consist of mafic volcanic rock fragments that range from 5 to 20 centimetres in diameter. Some breccias, containing pillow fragments are intimately associated with pillow basalts. Locally, minor hyaloclastite is present.

[redacted].2 *Boundary Brook Formation*

The name Boundary Brook Formation is proposed for the felsic volcanic rocks that crop out in the Rogerson Lake, Tally Pond and East Pond area. The name is derived from rock exposures in Boundary Brook, where it flows into East Pond. The rocks are felsic breccia, lapilli tuffs, quartz porphyry, crystal tuff, and flow banded rhyolite, rhyodacite, and rhyolite breccia. The breccias contain angular felsic volcanic fragments ranging from 5 to 50 cm in diameter within a fine- to medium-grained tuffaceous matrix (Plate 3.5). Tuffisitic gas breccias are present and consist of flow-aligned, in situ brecciated clasts in an aphanitic to vitric, siliceous matrix. The lapilli tuff (Plate 3.6) consists of dacite and rhyolite clasts, locally flow banded, in a fine-grained to locally vitric tuffaceous matrix. The rhyolite fragments are typically subrounded to subangular and measure 5 to 20 mm in diameter. The rhyolite (Plate 3.7) is generally a thick sequence of massive to locally flow banded, aphyric to quartz and/or feldspar porphyritic flows, commonly autobrecciated. These are mostly rhyolitic, but locally grade into dacitic compositions. Many of the felsic volcanic rocks contain a network of quartz and calcite veins (Plate 3.8) and disseminated pyrite in quantities of 1-2 %.

The Boundary Brook Formation hosts numerous volcanogenic massive sulphide occurrences including the Duck Pond and Boundary deposits. These are the largest known VMS occurrences in the Victoria Lake Supergroup and contain a combined resource of 6 350 000 tonnes grading 6.3% Zn, 3.29% Cu, 1.0% Pb, 63.5 g/t Ag and 0.82 g/t Au (Squires *et al.*, 2001). The mineralization is largely restricted to the felsic volcanic rocks and comprises disseminated, stockwork, massive, and transported sulphides.

The felsic volcanic rocks are commonly altered; alteration varies from weak phengite replacement to intense chloritization in "feeder-pipe" alteration zones (Plate 3.9). The best examples of alteration occur around the Duck Pond deposit, and consist of weak to strong vein chlorite with local zones of strong silicification, carbonatization, and sericitization.

4.1.3 Burnt Pond Formation

An extensive unit of epiclastic sedimentary rocks is exposed in a broad northeast-southwest trending belt, to the east of Burnt Pond-Tally Pond and north of Lake Ambrose and Barren Lake. The sedimentary rocks consist of greywacke, conglomerate, argillite, siltstone and minor chert. This unit, herein termed the Burnt Pond Formation, corresponds with units 7b, c and d of Kean and Jayasinghe (1980) and the Burnt Pond Sediments of Evans and Kean (2002).

The formation is dominated by medium-grained, light grey to buff-weathering greywacke. Bedding thickness ranges from a few centimetres up to a maximum of three metres and these rocks are generally more thickly bedded than the other rock types. The greywacke (Plate 3.10) consists of poorly sorted quartz, feldspar and rock fragments set in a matrix of weakly altered detrital silt. The relatively high proportion of matrix material (40 %) relative to clasts and the poorly sorted nature of the clasts, indicate that the greywackes are proximal sediments. Pebble conglomerate, argillite, siltstone and minor black shale beds are interbedded with the greywacke. Bedding planes are sharp and show no gradation between neighboring fine- and coarse-grained beds; however, the greywacke beds contain siltstone rip-ups. The conglomerate beds range in thickness from

less than one metre up to a maximum of a few metres. Volcanic clasts are dominant in the conglomerate and consist of quartz-feldspar porphyritic rhyolite and felsic tuff; siltstone and black shale clasts are also present, albeit in smaller amounts. The clasts in the conglomerate are matrix-supported, and the matrix is composed of fine-grained, weakly altered detrital silt. The clasts in both the conglomerate and greywacke were most likely derived from the adjacent volcanic rocks of the Tally Pond Group.

The formation also includes siltstone and minor chert. The siltstone is grey to green on fresh surfaces and devoid of primary sedimentary features. Beds are commonly 0.5 to 2.5 cm thick, however in places they are thicker and massive. The siltstones are locally interbedded with green to grey massive chert beds (Kean and Jayasinghe, 1980).

3.4.1.4 Black Shale Mélange

The volcanic and sedimentary rocks of the Tally Pond Group are bounded on their northwestern side by an extensive unit of black shale mélange. The unit extends for over 50 km from the north shore of Quinn Lake, in the southern end of the Tally Pond Group, northward to the Burnt Pond area, where the unit is apparently folded and in contact with the volcanic rocks along the southeastern edge of the group. The unit is best exposed in the area northeast of Gills Pond where it outcrops along the sides of brooks and logging roads (Plate 3.11). The unit is poorly exposed in other areas; however, its location can be inferred from airborne electromagnetic data (Figure 3.6).

The unit consists of pebble size black shale, rhyolite, greywacke, siltstone, and pyrite clasts set in a matrix of black shale that commonly contains graphite-rich sections (Plate 3.12). Most of the clasts comprise felsic volcanic rocks and exhibit an angular

morphology, but subrounded ones are present in minor amounts. The clasts are distributed randomly throughout the shale matrix and the elongate ones lie with their long axis at low angles to or in the plane of a moderate tectonic foliation in the matrix. The clasts are in various stages of disruption and consist of those that are fully intact to clasts that are completely fractured and separated by matrix material. In many places the clasts are in an intermediate stage of disruption and contain numerous veins of matrix material filling fractures and joints in the clasts. Secondary pyrite is present and overprints the foliation.

The matrix consists of fine-grained black shale with minor patches of dark grey siltstone (Plate 3.13). The dark material most likely consists of fine-grained sericite and clay minerals. Graphite rich areas are common. Primary sedimentary structures are completely destroyed due to the moderate to locally intense tectonic disruption of the rock.

3.4.1.5 Quartz-Porphyritic Rhyolite

Small discrete bodies of quartz and/or feldspar porphyritic rhyolite were previously interpreted (Dunning *et al.*, 1991; Evans and Kean, 2002) to intrude the volcanic rocks of the Tally Pond Group. Contacts in the Duck Pond area are generally sharp and well defined (Plate 3.14); however, in other places intrusive relationships are unclear and the quartz porphyry may be comagmatic with the Boundary Brook Formation. The rhyolite is a light green to grey, medium-grained, massive and commonly glassy porphyritic rock. It contains up to ten percent prismatic feldspar phenocrysts that are commonly 1-4 mm in diameter (Plate 3.15), but locally reach lengths of up to 20 mm.

Quartz phenocrysts locally comprise 5 to 10 percent of the rock, and consist of 1-3 mm subhedral crystals set in a fine-to medium-grained quartz and feldspar groundmass (Plate 3.16). The rock is generally massive, but in places exhibits evidence of flow banding. Alteration ranges from networks of chlorite and carbonate veins, to spotty iron carbonate alteration, to pervasive but light green phengite alteration. Disseminated pyrite forms cubes and stringer veins.

Two samples of the quartz-porphyritic rhyolite have been dated (U-Pb zircon) by Dunning *et al.* (1991) at 513 ± 2 Ma, and were interpreted as a suite of intrusive rocks. Whole rock lithogeochemical data (Chapter 4) for the quartz-porphyritic rhyolite indicate that these rocks have the same geochemical signature as the felsic volcanic rocks of the Boundary Brook Formation and that they correspond to volcanic arc granites with tholeiitic affinities. The Boundary Brook Formation has been dated at 509 ± 1Ma (Chapter 6), indicating that the quartz and/or feldspar porphyritic rhyolite rocks are not intrusions. They are now considered to represent episodes of coeval volcanism with, and thus comprise part of, the Boundary Brook Formation.

3.5 Intrusive Rocks within the Tally Pond Group

3.5.1 Harpoon Gabbro

The term Harpoon Gabbro is used for the package of gabbroic and dioritic rocks that intrudes the Tally Pond Group and surrounding rocks. It is equivalent to unit 13a of Kean and Jayasinghe (1980). Gabbro is the dominant rock type with minor occurrences of diorite north of the Tally Pond area, and within some of the larger gabbro bodies in the Harpoon Hill area. The unit is best-exposed along the top of Harpoon Hill, where it is a

light brown weathering, light to dark grey gabbro (Plate 3.17) with fine-to medium-grained grain size. Local coarse to pegmatitic phases are present at outcrops along the Harpoon Steady dam. Quartz is present as interstitial grains to the plagioclase and pyroxene and constitutes less than 10% of the rock. The most common accessory minerals include magnetite and ilmenite. Primary plagioclase is altered to a mixture of calcite and sericite; and pyroxene crystals are altered to green amphibole and epidote (Plate 3.18). Hornblende crystals are typically altered to chlorite along grain boundaries. Interstitial leucoxene is present in minor amounts and is interpreted to result from ilmenite alteration. In all locations, the Harpoon Gabbro is unfoliated and lies with its long axis of outcrop either parallel or subparallel to the trend of the adjacent country rocks.

Diorite intrusions in the Tally Pond area are generally medium to coarse-grained and green to brown in colour (Plate 3.19). The rock consists of plagioclase, clinopyroxene and hornblende with minor amounts of apatite and ilmenite as accessory minerals. Interstitial quartz is present in amounts ranging between five and ten percent. Alteration in the diorites is similar to that of the corresponding gabbro; plagioclase and pyroxene are altered to calcite/sericite and amphibole/epidote respectively. Hornblende is altered to a combination of chlorite and sericite and illmentite is partially altered to leucoxene. Carbonate and quartz occur as veins in abundances of approximately five percent and trace amounts of pyrite are present along minor fracture zones. Pegmatitic phases of the gabbro are exposed in Harpoon Brook at the Harpoon Steady dam (Plate 3.20). Diorite dykes intruding Tally Pond Group volcanic rocks commonly have chilled margins and are typically 50 to 100 metres thick.

3.6 Rocks in Contact with the Tally Pond Group

3.6.1 Crippleback Lake Quartz Monzonite

The Crippleback Lake Quartz Monzonite (Kean and Jayasinghe, 1980) is an elongate body that extends from Noel Paul's Brook northeastward through Crippleback Lake to West Lake. The rocks are in fault contact with volcanic rocks of the Tally Pond Group and subsequently nonconformably overlain by the Rogerson Lake Conglomerate.

The pluton includes a felsic phase dominated by quartz monzonite and granodiorite which extends for 25 km and a mafic phase of gabbro and diorite that forms a thin unit on the northern margin of the body. The contact between the two phases is not exposed; however, they are considered to be genetically related (Kean and Jayasinghe, 1982).

The felsic phase consists of pale grey to red quartz monzonite with minor granite and pale grey granodiorite (Plate 3.21). These are typically medium-grained, equigranular and do not contain a penetrative mineral alignment. They consist of quartz, plagioclase, potassium feldspar, with accessory biotite and amphibole that is generally chloritized. Locally, the quartz monzonite is porphyritic with 0.5 cm plagioclase phenocrysts that are set in fine-grained matrix.

The less extensive mafic phase of the Crippleback Lake Quartz Monzonite is mostly a dark grey, medium-grained, equigranular gabbro that consists of subhedral plagioclase and augite, with a subophitic texture. The diorite is medium grained,

equigranular, gray, locally cleaved and consists of plagioclase and amphibole. Both the gabbro and diorite contain finely disseminated pyrite throughout.

The Cripplebeck Lake Quartz Monzonite has yielded a U-Pb zircon age of 565 +4/-3 Ma (Evans *et al.*, 1990). A 561 Ma age obtained from titanite from the same sample overlaps with the age of crystallization.

3.6.2 Rogerson Lake Conglomerate

The Rogerson Lake Conglomerate is a northeast-trending unit that extends for over 100 km from the Burgeo Road to Sandy Lake. The conglomerate unconformably overlies the Tally Pond Group and is in nonconformable contact with the Cripplebeck Lake Quartz Monzonite. The unit consists of conglomerate, sandstone, siltstone and shale (Kean and Jayasinghe, 1980). Conglomerate is dominant in the Tally Pond area, and is grey to red to purple, with pebble-sized clasts in a matrix of grey to red sandy material (Plate 3.22). The matrix consists of quartz, feldspar, muscovite and chlorite with hematite and carbonate cement. The varied clast population includes subrounded to rounded clasts of red siltstone, sandstone and shale; mafic flows and porphyritic rhyolite clasts are abundant. Sedimentary structures are rare and grain size variations between silt and sand layers are sharp and well defined.

3.7 Structure

Rocks of the Victoria Lake Supergroup occupy a northeast-trending anticlinorium, termed the Victoria Anticlinorium (Kean, 1985). Regionally, the sequence youngs northwesterly on the north limb and southeasterly on the south limb; however,

there are numerous smaller scale, first-order and second-order folds that result in variable facing directions. The lack of outcrop in the area generally precludes detailed structural interpretation (Kean and Evans, 1988).

The Tally Pond Group displays evidence of folding, normal faulting and thrust faulting. The folds are a series of broad, open synclines and anticlines that trend and gently plunge to the northeast. These folds are associated with a penetrative axial planar cleavage and a locally developed penetrative foliation defined by chlorite and phengite. Regionally, the cleavage and main foliation in rocks of the Tally Pond Group lie in, or at low angles to, the axial fold plane, suggesting that the strain accumulated in the rocks and folding are related to the same deformational event. Sedimentary rocks locally contain subhorizontal to gently plunging open folds that are interpreted to result from gravity-driven orogen collapse. In the Tally Pond area, these folds are commonly asymmetrical, open to close folds with gently dipping axial planar surfaces and fold axes that plunge 24° to the southwest (Plate 3.23). These fold structures are recognized throughout the whole Victoria Lake Supergroup and the entire Appalachian Orogen (van Staal, personal comm., 2002).

These features are cut by a series of northeast-trending, northwest dipping thrust faults that are represented by zones of highly strained and intensely deformed mélanges. The mélanges are characterized by a steeply dipping S_1 foliation contained in the black shale matrix and a stretching lineation (L_S) defined by the long dimension of volcanic clasts in the mélange. The thrust faults are interpreted to have emplaced rock units in a southeasterly direction, locally placing the sedimentary rocks over the volcanic rocks, and producing the broad anticlinal fold structures in the Tally Pond Group.

A series of northeast-trending linear structures (Figure 3.5), that are in part coincident with the known thrust faults, have been identified by regional studies of colour infrared aerial photography, gradiometer data and Synthetic Aperture Radar (Evans *et al.*, 1990). These features seem to separate the various rock units of the Tally Pond Group and most likely represent a continuation of identified thrust faults.

Kean and Evans (1988) presented ^{40}Ar-^{39}Ar age dates for sericite obtained from massive sulphide and gold mineralization alteration zones associated with the northeast trending linears. They reported Middle Devonian ages (395-380 Ma) that indicate either the age of metamorphism or the latest movement along these fault zones.

The folds and thrust faults of the Tally Pond Group are crosscut by normal faults that strike northwest to west and appear to displace the felsic volcanic units by up to several hundred metres. Northwest trending linear structures (Figure 3.5) have also been identified by remote sensing techniques (Evans *et al.*, 1990) and are probably brittle structures which exhibit little displacement.

3.8 Interpretation of Magnetic Anomalies

Interpretation of the geology of the Tally Pond area suffers from the extensive glacial cover and paucity of outcrop, which hinders any attempt to successfully correlate units across the entire map area. To combat this problem, a total-field vertical gradient magnetic anomaly map (Figure 3.6) was produced from the regional geophysical compilation of Oneschuk *et al.* (2001). Interpretation of this map was conducted by mapping structural trends as lineations in the magnetic contours. The lineations are interpreted to reflect the strike lines of elongated intrusive features or the surfaces of

large faults. In an area such as Tally Pond, where high density field observations were not possible, the magnetic data are used to interpolate the broadly spaced field localities.

To increase the visual contrast, the magnetic anomaly map has been shaded from an azimuth of 315° (northwest) at an inclination of -45°. The red end of the spectrum represents positive magnetic anomalies, whereas the blue end of the spectrum corresponds to negative magnetic anomalies.

The majority of the positive magnetic anomalies occur as elongate linear features that trend northeast-southwest, equivalent to the regional structural trend. The exceptions to this are the two large positive anomalies in the area immediately east of Lake Ambrose and in the area surrounding Noel Paul's Brook, north of Caribou Lake. These features are marked by anomalies 1 and 4 and correspond to igneous plutonic rocks. The Harpoon Gabbro intrusion is exposed at anomaly 1 and shows a distinct positive anomaly which corresponds to areas underlain by mafic gabbroic rocks. The Harpoon Gabbro also exhibit positive anomalies at anomalies 2 and 3. Anomaly 2 is immediately west of Rogerson Lake whereas anomaly 3 is located west of Barren Lake. The large prominent positive anomaly marked by anomaly 4 corresponds with the Cripplebeck Lake Quartz Monzonite. The area is underlain by porphyritic monzonite that represents the felsic phase of the pluton.

Line 5 displays a significant magnetic high to the north of Rogerson Lake which trends northeast and separates the volcanic rocks of the Tally Pond Group from adjacent sedimentary rocks. The trace of the line coincides with the black shale mélange unit as mapped in the field. The relatively large positive magnetic anomalies associated with this unit are due to the significant amounts of graphite present in the mélange. The field

mapping of the mélange unit is hindered by the paucity of outcrop and therefore the extensions of the mélange unit along the northern margin of the Tally Pond Group are defined using the commonly associated positive magnetic anomalies. Anomaly 6 is located along strike to the northeast of anomaly 5 running from the northwest edge of Rogerson Lake northeastward towards the southern end of Harpoon Steady, and represents the continuation of the black shale mélange. This unit is also present as a linear northeast trending positive anomaly that tracks along the eastern edge of East Pond and continues northeast to the Burnt Pond area. This feature is marked as anomaly 7.

Other positive anomalies interpreted to be associated with the black shale mélange include 8 and 9. Anomaly 8 is located 1 km east of East Pond and consists of an approximately 7 km long, northeast-trending anomaly that terminates at the southern end of Burnt Pond. Anomaly 9 is located 3 km east of anomaly 8 and trends northeast for approximately 2 km where it pinches out south of Burnt Pond.

Small stocks and plugs of the quartz-porphyritic rhyolite exhibit discrete magnetic highs that are scattered throughout the Tally Pond area. The most obvious of these is marked by anomaly 10, located east of Rogerson Lake. Other positive anomalies that correspond to the quartz porphyritic rhyodacite include anomalies 11, located southeast of anomaly 10, and anomaly 12, situated approximately 1 km northeast of Tally Pond. A series of several small magnetic highs, located less than 1 km west of Tally Pond area, are labeled as anomaly 13 and are interpreted to be the result of Duck Pond volcanogenic massive sulphide deposit. Alternatively, theses anomalies may result from several small subterranean intrusions of the quartz porphyritic rhyodacite.

A significant magnetic low runs along the southern margin of the Tally Pond Group and is designated as line 14. This negative anomaly corresponds to the relatively non-magnetic sedimentary rocks of the Rogerson Lake Conglomerate. It extends for over 75 km from the Shoulder Blade Pond area southwards to the area south of Quinn Lake where this magnetic low thins out and is bound on both sides by significant positive anomalies, designated 15 and 16. Anomaly 15 coincides with volcaniclastic rocks adjacent to the Tally Pond Group and is interpreted result from disseminated sulphides interlayed throughout dark grey shales. Whereas anomaly 16 overlaps with black pelitic rocks that contain abundant graphite which is inferred to cause the distinct magnetic high.

3.9 Relative Ages and Relationships Between Lithostratigraphic and Lithodemic Units

The overall scarcity of outcrop in the Tally Pond-Lake Ambrose area, coupled with the paucity of geochronological data, makes it difficult to determine the stratigraphic, structural and temporal relationships between units within the Tally Pond Group. Most relationships are based upon information from drilling and regional geophysical surveys. These data are by no means complete, and a number of critical relationships remain uncertain, and must therefore be inferred.

The oldest rocks in the study area are the 565 +4/-3 Ma arc plutonic rocks of the Cripplebeck Lake Quartz Monzonite (CLQM). These rocks are interpreted to represent a suite of Late Neoproterozoic-Early Cambrian plutonic arc rocks that form the basement to the Gander Zone or the micro-continent of Ganderia (van Staal *et al.*, 2002). The mafic volcanic rocks of the Lake Ambrose formation are separated from the Cripplebeck Lake Quartz monzonite (CLQM) by an extensional fault presently exposed in Noel Paul's

Brook. Previous workers (Evans *et al.*, 1990) interpreted this contact as structural and suggested that the CLQM was either thrust into contact with the volcanic rocks or emplaced along a transcurrent fault system.

The felsic volcanic rocks of the Boundary Brook Formation are interpreted to have been deposited synchronously with the mafic rocks of the Lake Ambrose Formation. The contact between the volcanic units is exposed at numerous locations throughout the area, and in drill core, where mafic and felsic flows are intricately intermingled and interlayered. No geochronological data currently exists for Lake Ambrose Formation mafic rocks, however, an ash tuff unit of the Boundary Brook Formation, that stratigraphically overlies the Boundary Deposit yielded numerous euhedral zircons, which are dated at 509 ± 1 Ma (Chapter 6).

The Lake Ambrose and Boundary Brook formations were previously interpreted to be intruded by small stocks and dykes of quartz porphyry rhyolite. These contacts are best exposed in drill core where the dykes are tens of metres wide and display chilled margins. Locally, however, intrusive relationships are unclear and the quartz-porphryritic rhyolite may be related to main episode of felsic volcanism in the Boundary Brook Formation. Two samples of the quartz-porphyritic rhyolite, one from the southern end of the group east of Rogerson Lake, and another from north of Tally Pond, yield identical 513 ± 2 Ma ages (Dunning *et al.*, 1991). This age has important consequences as it indicates that the rocks of the Lake Ambrose and Boundary Brook formations are broadly contemporaneous with the rhyolite, and may be co-magmatic.

A clastic sedimentary sequence, the Burnt Pond Formation, is present along both the north and southern margins of the volcanic rocks of the Tally Pond Group. The

sequence contains dominantly volcanic detritus, and the amount of pyroclastic material and the clast size increase to the southeast towards the volcanic rocks. Kean (1985) suggested that the clastic sedimentary rocks were derived from the adjacent volcanic rocks. The Burnt Pond Formation is very rarely in direct contact with these volcanic rocks, as they are usually separated by an extensive black shale mélange unit. The mélange is exposed as a collection of narrow, sub-parallel outcrops that trend northeasterly along the edge of the Tally Pond volcanic rocks. Examination of drillcore, coupled with outcrop data, indicates that the black shale mélanges are preserved along a series of related thrust faults that dip to the northwest. Evans *et al.* (1990) suggest that the shales were once part of an extensive shale sequence that covered the sedimentary rocks of the Victoria Lake Supergroup. These rocks were subsequently thrust over the volcanic rocks of the Tally Pond Group along the black shale mélange unit and the volcanic rocks are presently exposed as a tectonic window through the sedimentary rocks.

The age of the black shale mélange sequence is unknown but is believed to be Middle Ordovician on the basis of correlation with extensive Caradocian black shale in Newfoundland. Williams (1988) reported that deformed graptolites from drill core south of Millertown were Middle Ordovician, and he also collected Middle Ordovician graptolites from an outcrop of black shale 2 km northeast of Tally Pond (G. Squires, personal com., 2001). However, minor black shale layers are interfingered within the volcanic rocks of the Lake Ambrose and Boundary Brook formations. Thus, the possibility exists that the black shale mélange unit is, at least in part, Cambrian.

Fine to medium grained gabbro and diorite intrude the Tally Pond Group as small dykes, stocks and larger plutonic bodies of the Harpoon Gabbro. The gabbro cross-cuts

the mafic and felsic volcanic units as well as the clastic sedimentary and black shale sequences. It contains no penetrative foliation and is undeformed. Kean and Jayasinghe (1980) suggested that the gabbro bodies could be Ordovician to Devonian based on inferred comagmatic relationships and comparison to other gabbros in the Newfoundland Dunnage Zone. In the Tally Pond area, the Harpoon Gabbro clearly intrudes the volcanic rocks, and is not comagmatic with them. Geochronology (Chapter 6) indicates that the Harpoon Gabbro is Mid-Ordovician.

The youngest rocks in the study area are those of the Rogerson Lake Conglomerate. This unit unconformably overlies the Tally Pond Group and sits nonconformably upon the Cripplebeck Lake Quartz Monzonite. Kean and Jayasinghe (1980) suggested that the Rogerson Lake Conglomerate is Middle Ordovician or younger as it contains volcanic and sedimentary clasts interpreted to be derived from the underlying Victoria Lake Supergroup. Williams (1970) correlated the conglomerate with sedimentary rocks of the Botwood Group to the northeast, thus implying a Silurian age. A U-Pb detrital zircon study (Chapter 6) of the Rogerson Lake Conglomerate illustrates that the volcanic clasts in the conglomerate were derived from the underlying volcanic sequences of the Tulks belt and Tally Pond Group, with a minor Grenvillian component.

3.10 Volcanogenic Sulphide Mineralization in the Tally Pond Group

Mineralization within the Victoria Lake Supergroup is divided into two distinct subgroups: volcanogenic massive sulphide (VMS) mineralization, and epigenetic gold mineralization. The epigenetic gold mineralization is normally associated with quartz veins in high alumina and potassium alteration systems with trace amounts of base

metals. The epigenetic gold mineralization was not studied in this research project and is not discussed further in this report.

The Victoria Lake Supergroup hosts approximately 130 mineral occurrences that are distributed throughout the unit; of these occurrences, 40 are significant VMS deposits, prospects, and showings (Figure 3.7) and together total over 20 million tonnes of combined ore. The majority of these significant occurrences, 21 in total, are hosted by the Tulks Hill assemblage and include the Tulks Hill, Tulks East, Jacks Pond, Daniel's Pond, Victoria Mine, Long Lake and Hoffe's Pond. The Tally Pond Group hosts two major deposits (Duck Pond and Boundary), four prospects (Rogerson Lake, Lemarchant, Moose Pond and Burnt Pond) and two significant showings (Old Sandy Road and East Pond). The mineralization is largely restricted to the felsic volcanic belts and comprises disseminated, stockwork, massive, and transported sulphides that are generally coeval with the enclosing felsic volcanic rocks. There are at least three phases of VMS mineralization present within the Victoria Lake Supergroup. There are two periods of mineralization recorded in the Tulks Hill assemblage, and geochronology and metallogenic differences between the Tulks East, Victoria Mine and Daniels Pond deposits indicate that mineralization occurred as numerous separate events over an extended time period extending from the Late Cambrian to the Llanvirn. Mineralization in the Tally Pond Group, mainly the Duck Pond and Boundary deposits, is constrained to the Middle Cambrian by a 509 ±1 Ma and 513 ±2 Ma ages from enclosing volcanic rocks. Other occurrences in the group (e.g. the Lemarchant and Burnt Pond prospects) have not been directly dated, however they are lithologically and metallogenically similar

to the Duck Pond and Boundary deposits and are considered to have formed during the Middle Cambrian.

3.10.1 Duck Pond Deposit

The Duck Pond deposit is located approximately 70 km southwest of the community of Grand Falls in central Newfoundland. The deposit is accessible by a series of logging roads that lead from the community of Millertown, 18 km south-southeast to the Tally Pond area.

Rocks of the Tally Pond Group (Figure 3.8) in the area of the Duck Pond deposit consist of felsic volcanic rocks of the Boundary Brook Formation, mafic volcanic varieties of the Lake Ambrose Formation and volcaniclastic, sedimentary, and intrusive rocks of the Tally Pond Group. In the immediate area of the Duck Pond deposit, these formations define two structurally juxtaposed sequences, informally named the Upper block and the Mineralized block (Figure 3.9), which form a structural window beneath an overthrust package of Ordovician sedimentary rocks (Squires *et al.*, 1990). A series of moderately to steeply dipping thrust and wrench faults complicate the stratigraphy, with displacements ranging from 500 m to 1 km.

The Upper block is in excess of 1000 m thick and comprises cycles of shallow-dipping, deep submarine, massive to pillowed (Plate 3.24) and brecciated mafic and felsic flows and pyroclastic rocks intercalated locally with graphitic sediments and reworked tuffs (Squires *et al.*, 2000). Gabbroic (Plate 3.25) and K-feldspar porphyritic dykes and sills (Plate 3.26) intruded the sequence along a number of reverse faults. Alteration and mineralization within the block are rare. The base of the block is delineated by the 45°

south-dipping Duck Pond thrust, which is marked by zones of mylonite and fault gouge, that juxtapose the Upper block upon the Mineralized block. Essentially the Upper block represents the unmineralized hanging wall material to VMS mineralization and the Mineralized block represents the mineralized footwall.

The Mineralized block comprises a greater than 900 m thick sequence of highly altered and deformed, flat-lying aphyric felsic flows and autobreccias (Plate 3.27), with minor amounts of mafic flows and mafic and felsic dykes with minor deep water graphitic argillite muds that locally contain base-metal bearing sulphide debris flow beds. The block is interpreted to be wedge-shaped due to the convergence of its bounding faults. Alteration is variable and comprises chloritization, sericitization, silicification, carbonitization (Plate 3.28) and pervasive pyrite. Deformation within the block is extensive and is dominated by moderately south-dipping, sub-parallel thrust faults which disrupt both the stratigraphy and mineralization.

The two juxtaposed blocks were subsequently disrupted by an episode of southwest-directed thrusting along the north-dipping Terminator thrust. This thrust cuts the Duck Pond deposit and is interpreted to be responsible for the offset between the Upper and Lower Duck zones. A series of northwest–southeast-trending wrench faults termed the Cove, Garage, Old Camp, and Loop Road faults offset the stratigraphy of the two blocks both vertically and laterally by up to 500 m (Squires *et al.*, 1990).

The Duck Pond deposit specifically refers to the collection of three massive sulphide lenses, the Upper Duck, Lower Duck and Sleeper Zone (Figure 3.10). The Upper Duck lens occurs at depths ranging from 250 to 500 m and measures approximately 400 m wide by 500 m in length. The lens averages 20 m in thickness and

consists of base metal-rich massive sulphides (Plate 3.29); however, semi-continuous massive sulphides of up to 120 m thick occur in places. The core of the lens is mantled by massive pyrite which grades into stringer pyrite that is, in turn surrounded by a halo of disseminated pyrite (Plate 3.30). The pyrite constitutes over 60% of the entire sulphide deposit. The Upper Duck lens is estimated to contain over 16 million tonnes of massive sulphides, of which 3.88 million tonnes is considered ore at an average grade of 6.7% Zn, 3.8% Cu, 1.1% Pb, 71.0 g/t Ag and 1.1 g/t Au (Thundermin Resources, 1999).

The Sleeper Zone consists of four small, 20 m thick, semi-massive and massive sulphide lenses that occur 50 to 100 m beneath the Upper Duck lens. Total sulphides in the Sleeper Zone is estimated at 500,000 tonnes grading 8.7% Zn, 1.7 % Cu, 1.2% Pb, 62.5 g/t Ag and 0.5 g/t Au (Thundermin Resources, 1999).

The Lower Duck lens is interpreted to be a faulted offset extension of the Upper Duck lens that is present as a structural boudin entrained within a segment of the Duck Pond thrust zone (Squires *et al.*, 1990). The lens measures 800 m in length, reaches 300 m wide and ranges from 5 to 15 m in thickness and contains an estimated 1.5 million tonnes of massive sulphide grading 5.0% Zn, 2.8% Cu, 1.4% Pb, 32.5 g/t Ag and 0.6 g/t Au.

An extensive zone of hydrothermal alteration is associated with massive sulphides of the Duck Pond deposit. In the area of the Upper Duck lens this alteration zone consists of an approximately 100 m wide region that surrounds the massive sulphide body and is dominated by pervasive chlorite and coarse grained disseminated and stringer pyrite. This alteration zone extends laterally for several hundred metres and is up to 75 thick in the footwall and 25 m thick in the hangingwall of the Upper Duck lens (Squires *et al.*, 2001),

where it consists of widespread silica, sericite, phengite and carbonate alteration. Where intense chlorite alteration is present near the Upper Duck lens, a distinct carbonate alteration, referred to as 'chaotic carbonate' (Squires *et al.*, op. cit), is developed (Plate 3.31). It consists of contorted dolomite and minor fluorite veins that are intimately associated with the intense chlorite alteration and replace the strongly chloritized mafic volcanic rocks. Feeder pipe alteration zones are present in the footwall to the Upper Duck lens and consist of several 100 m thick tabular zones of intense chlorite (25-100%) altered volcanic rocks. These zones are believed to represent conduits developed within steep syn-volcanic fault zones that served as a pathway to the seafloor surface for the metal-bearing saline solutions.

The present spatial distribution of the Upper Duck, Sleeper Zone, and Lower Duck lenses is the result of post mineralization deformation related to juxtaposition of the Upper and Lower structural blocks in the Duck Pond area. The east and south margins of the Upper Duck lens are strongly deformed and the massive sulphide bodies exhibit ductile deformation and mylonitic fabrics where they are truncated by faults. The offset segments of the Upper Duck lens are interpreted to constitute the Sleeper Zone and Lower Duck lenses, which were displaced along fault zones that cut the southern periphery of the Upper Duck lens (Squires *et al.*, 2001). Displaced segments along the eastern margin of the Upper Duck lens have not been identified as this margin is cut by the Duck Pond thrust zone.

3.10.2 Boundary Deposit

The Boundary deposit is located 4 km northeast of the Duck Pond deposit and is hosted by the same bimodal volcanic and sedimentary sequence as the Duck Pond deposit. The deposit occurs as three discrete sulphide lenses, called the North, South and Southeast zones (Figure 3.11). These three zones in total contain approximately 1 million tonnes of sulphide of which roughly 0.446 million tonnes are considered ore at an average grade of 3.5 % Cu, 3.5 % Zn, 0.5 % Pb and 22.8 g/t Ag (Thundermin Resources, 1999).

The Boundary deposit is underlain by a footwall consisting of massive to locally flow banded, light grey to green aphyric rhyolite flows and lapilli tuffs that reach 500 m in thickness (Plate 3.32). Lesser amounts massive quartz-feldspar porphyritic rhoydacite are present and range in thickness from several metres up to 80 m. These rocks are distinguished by the presence of 2-5 mm quartz and/or feldspar phenocrysts set in a fine grained siliceous matrix.

The rocks are overlain by a sequence pyroclastic autobreccias that reaches up to 175 m in thickness and consists of subangular to angular clasts of flow-banded and massive rhyolite that comprise 85 % of the fragments in the unit. Other fragments consist of felsic quartz porphyry, black argillite and graphitic shale, tuff, chloritized rhyolite and rare massive sulphide. The fragments range from 5 mm to >12 cm in size and constitute over 90 % of the rock. The fragments are contained in a fine-grained grey to black matrix that is typically altered to chlorite, sericite, phengite and minor carbonate. Chlorite alteration dominates immediately adjacent to the deposit and the alteration decreases with increasing distance from the deposit. Grain size and degree of sorting are variable and the

relationship between them is inversely proportional: fine-grained rocks are well sorted, whereas coarser-grained varieties are poorly-sorted.

The hangingwall to the Boundary deposit consists of fine-grained felsic crystal tuff, lapilli tuff (Plate 3.33) and rhyodacite that directly overly the sulphide lenses. The crystal tuff is medium to dark green-grey, becoming lighter up-section away from the sulphides. It is massive with 5 % subhedral 2-4 mm quartz and feldspar crystals in a fine-grained groundmass of quartz and k-feldspar. The lapilli tuff unit contain angular to sub-angular fragments that measure 3mm up to 8 cm set in a fine-grained quartz and k-feldspar matrix. The feldspar contained in the matrix of both the crystal tuff and lapilli tuff units is moderately altered to chlorite, sericite and phengite. Chlorite alteration increases in intensity towards the sulphide bodies, with sericite alteration dominant at stratigraphically higher levels.

The mineralization in all three sulphide lenses is dominated by fine-to medium-grained pyrite. The base metal-bearing minerals are fine-grained chalcopyrite, covellite, sphalerite, and minor galena (Plate 3.34). Jambor (1984) identified traces amounts of pyrrhotite, arsenopyrite and various tellurides including altaite (PbTe), hessite (Ag_2Te) and a bismuth telluride that all occur as laths and blebs in galena and sphalerite and chalcopyrite. Thin banding is present in all lenses and are defined by intercalated layers of massive pyrite and sphalerite with galena and small detrital grains of sulphide. The South Zone exhibits granular textured massive sulphide that is interpreted to be the result of sulphide recrystallization from migrating hydrothermal fluids (McKenzie, 1988).

The North Zone lens dips 25-35 northwards and is 250 m in length, up to 50 m wide and between 15 to 25 m thick. Metal zoning in the lens consists of a zinc- and

copper-rich core that is concentrated on its western half and a copper-rich envelope present in its eastern portion. The South Zone lens dips shallowly to the southeast and consists of an oblong shaped lens 120 m long and 70 wide with a thickness of 15 to 20 m. The northern section of the South Zone is characterized by high Cu/Zn ratios, whereas the remainder of the lens contains copper and zinc in equal quantities. The Southeast Zone is interpreted to be a portion of the South Zone that is present in the limb of a fold (Squires *et al.*, 2001). The Southeast Zone consists of a 65 m by 50 m lens that averages 15 m thick and dips gently to the northwest. Metal zoning in the Southeast Zone consists of the same copper-rich northern segment with the remainder being copper-zinc rich.

Alteration in the footwall of each of the three zones consists of variably intense chloritization, sericite and phengite alteration accompanied by veinlets, blebs and disseminations of pyrite and minor chalcopyrite that extend laterally up to several hundred metres from the deposit. Silicification and carbonate alteration are present in the footwall but are not as extensively developed as the chlorite and sericite/phengite alteration zones. The chlorite is black and usually occurs as matrix replacement in the tuff unit and as veins and blebs and varies from tabular to pipe-like. The thickness and degree of permeability of the footwall lithologies is considered the controlling factor in the size and shape of the chlorite feeder pipes. Migration of the hydrothermal fluids is believed to have formed in fracture systems that developed synchronously with the surrounding volcanic rocks.

3.10.3 Burnt Pond Prospect

The Burnt Pond prospect t is located approximately 20 km southeast of the community of Millertown and 10 km northeast of the Boundary deposit. The prospect (Figure 3.12) is underlain by a sequence of mafic and intercalated felsic volcanic rocks that grade upward into a transitional sequence of thinly bedded graphitic argillaceous sediment and interbedded felsic tuff (Collins, 1992). The volcanic sequence becomes carbonaceous near the contact with the argillites and was interpreted by Dimmell (1986) to indicate a cessation of volcanism coinciding with increased deep water sedimentation. These units are overlain by a fine-grained, grey-green tuff siltstone that are in-turn overlain by deep-water marine sediments and minor intercalated mafic volcanic rocks marked at the base by a distinctive red siltstone. The contacts between these units are generally sheared and faulted, however, Collins (1992) interprets these rocks as forming a continuous sequence.

Sulphide mineralization consists of narrow bands (< 50cm wide) of stratiform massive sulphides (sphalerite, galena, and minor chalcopyrite) hosted by the graphitic argillaceous sedimentary rocks, and as stringer, fracture-fill and disseminated sulphides developed in sericitized to locally chloritized felsic volcanic rocks (Dimmell, 1986; Collins, 1992). Dimmell (1986) suggested that the mineralization was associated with late-stage hydrothermal activity during the waning stages of island-arc volcanism.

3.10.4 Lemarchant Prospect

The Lemarchant prospect is located 20 km southwest of the Duck Pond deposit and approximately 1 km east of Rogerson Lake. Massive sulphide mineralization is situated along an inferred (Collins, 1992) conformable contact between aphyric felsic

volcanic flows and fragmental rocks and mafic flows. These rocks strike north-south and dip gently to the east. The felsic-mafic contact is locally marked by graphitic argillite and banded pyritic argillaceous sedimentary rocks. The mineralization consists of stringer to disseminated sulphides, chalcopyrite, sphalerite, pyrite and minor galena, with accompanying barite alteration. The felsic volcanic rocks occurring beneath the mineralized horizon are variably altered with widespread sericitization and local intense chloritization (Collins, 1992).

3.10.5 Other Volcanogenic Sulphide Occurrences

The Tally Pond Group is host to numerous other minor massive sulphide occurrences. These include the East Pond occurrence which consists of massive sulphide fragments (sphalerite, pyrite, galena) in felsic pyroclastics rocks; North and South Moose Pond showings, comprised of disseminated pyrite, chalcopyrite, sphalerite and galena hosted by altered felsic volcanics; and the Old Sandy Road showing, in which mafic volcanic rocks contain 20 to 30 per cent disseminated pyrite and trace pyrrhotite and chalcopyrite.

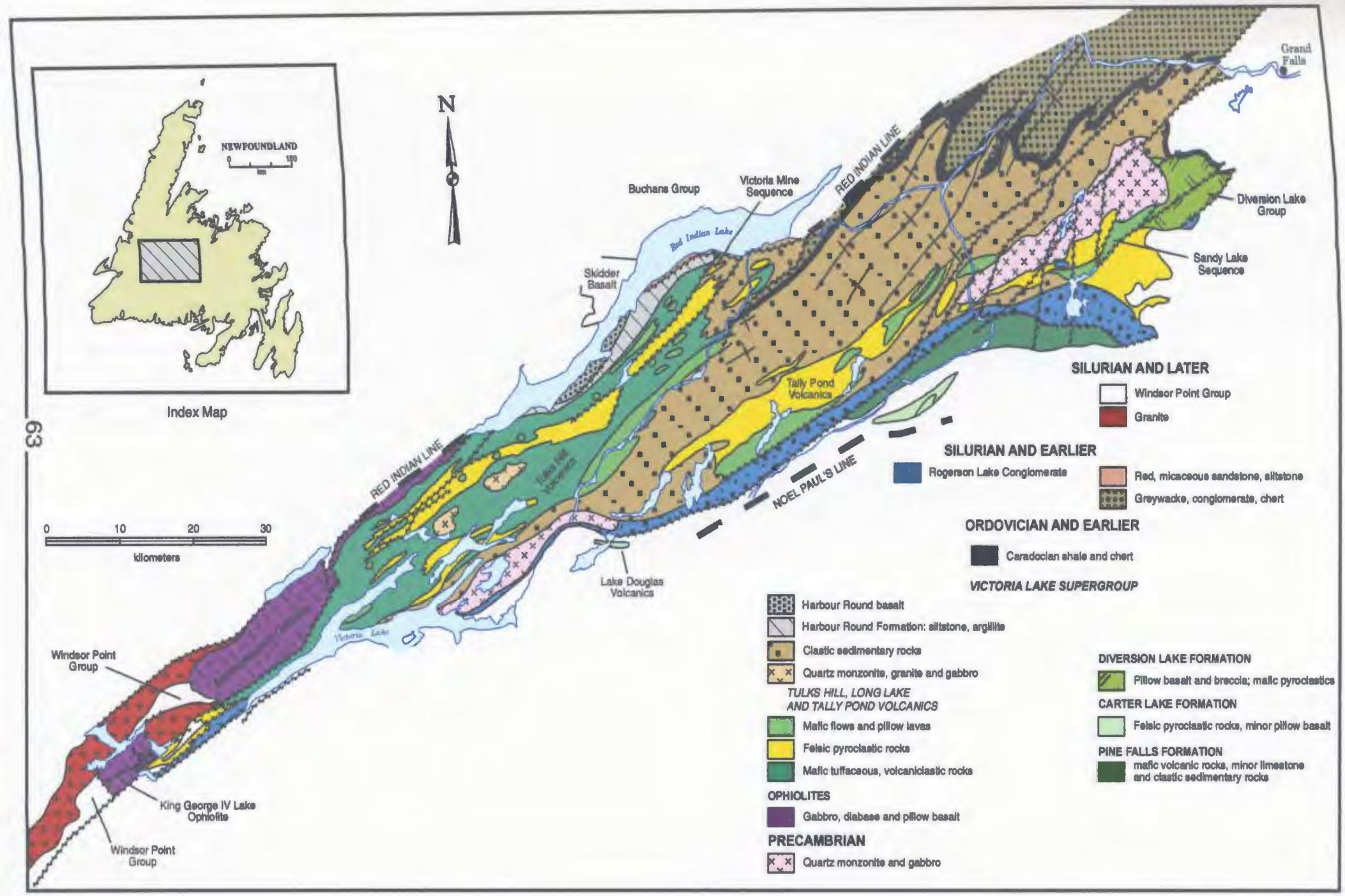

Figure 3.1 *Simplified geology (Kean, 1977) of the Victoria Lake-Red Indian Lake area.*

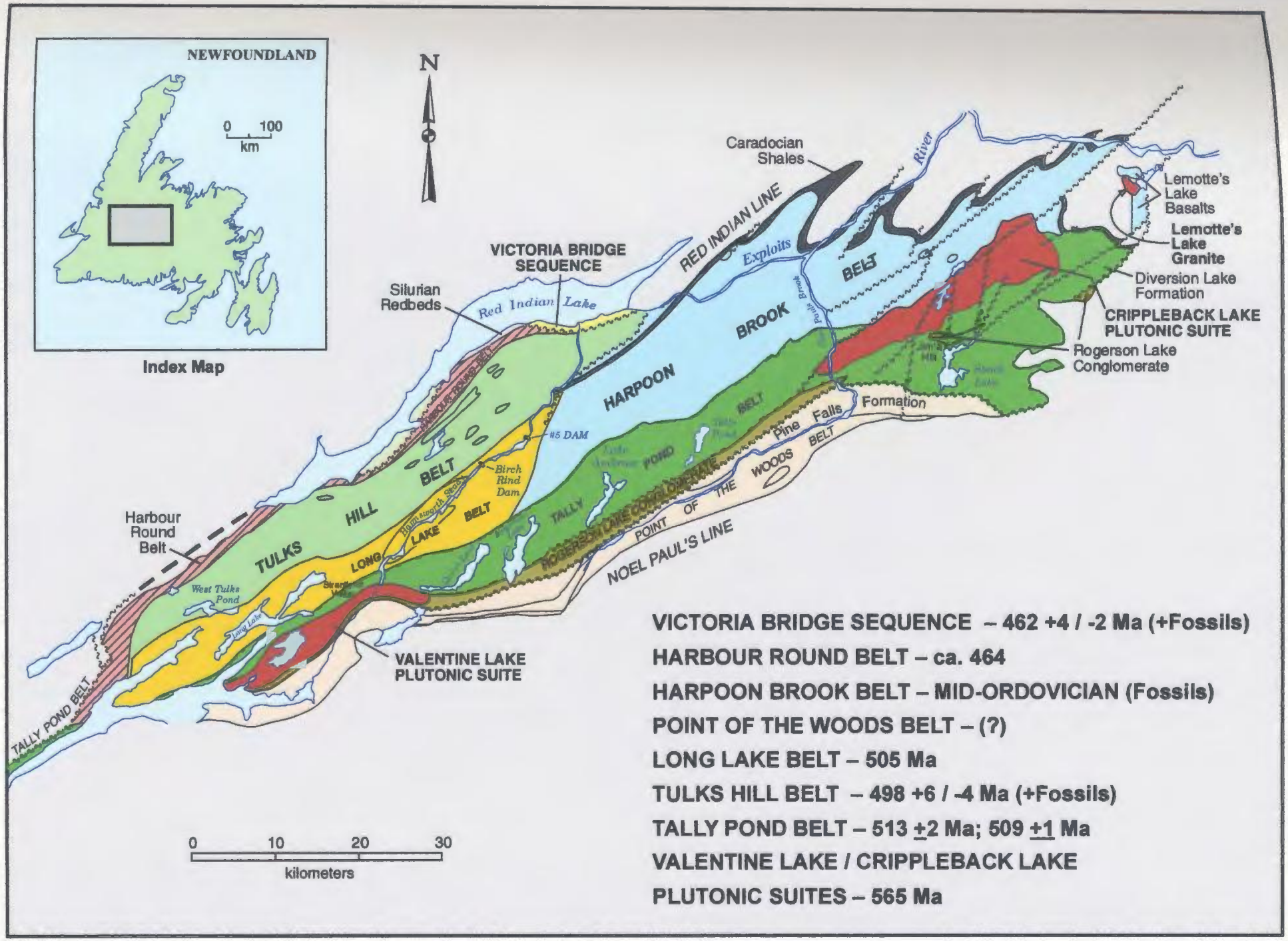

Figure 3.2 *Distribution of volcanic and sedimentary belts within the Victoria Lake Supergroup. Modified from Evans and Kean (2002).*

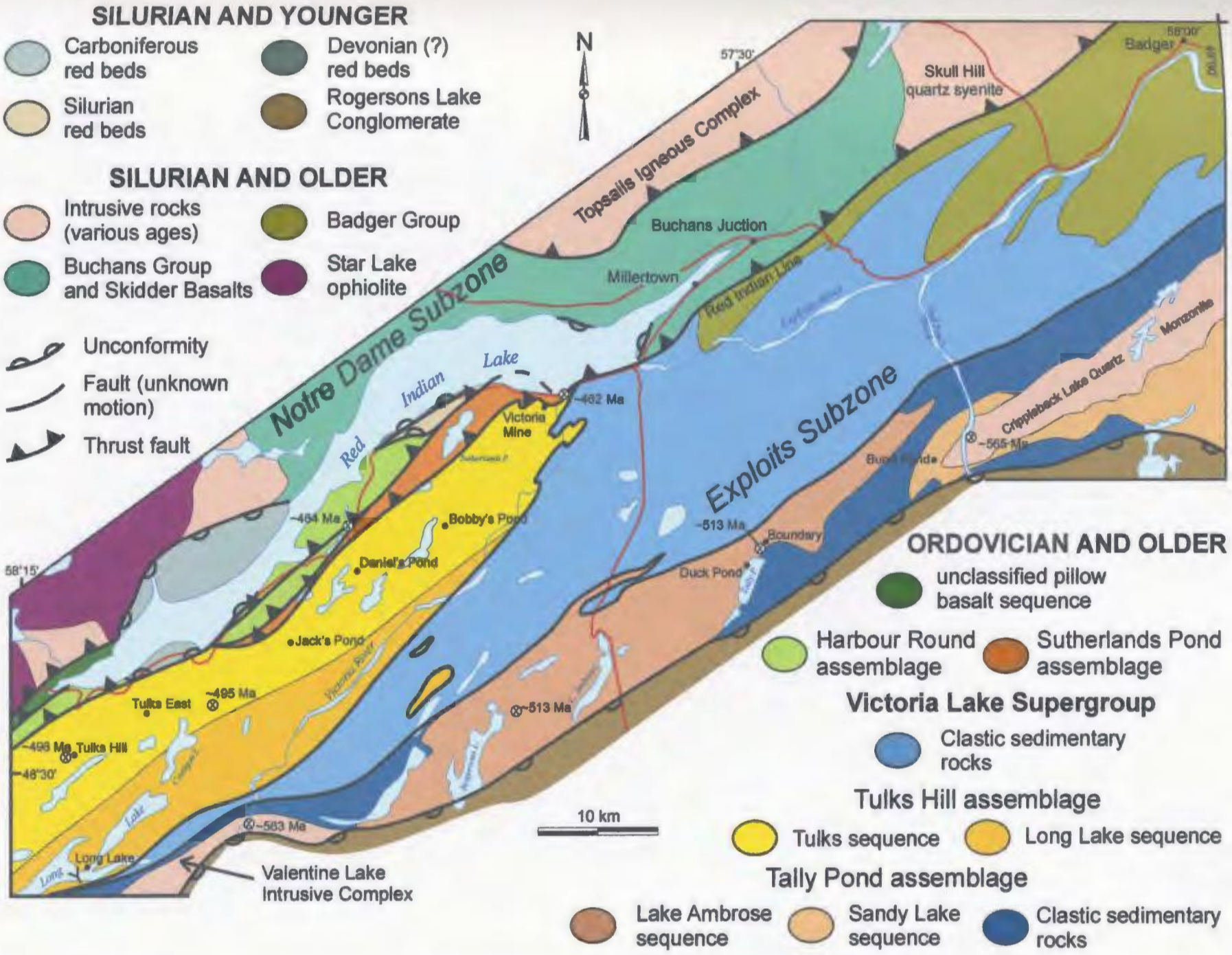

Figure 3.3 *Simplified geology of the Tally Pond-Red Indian Lake area (from Rogers and van Staal, 2002).*

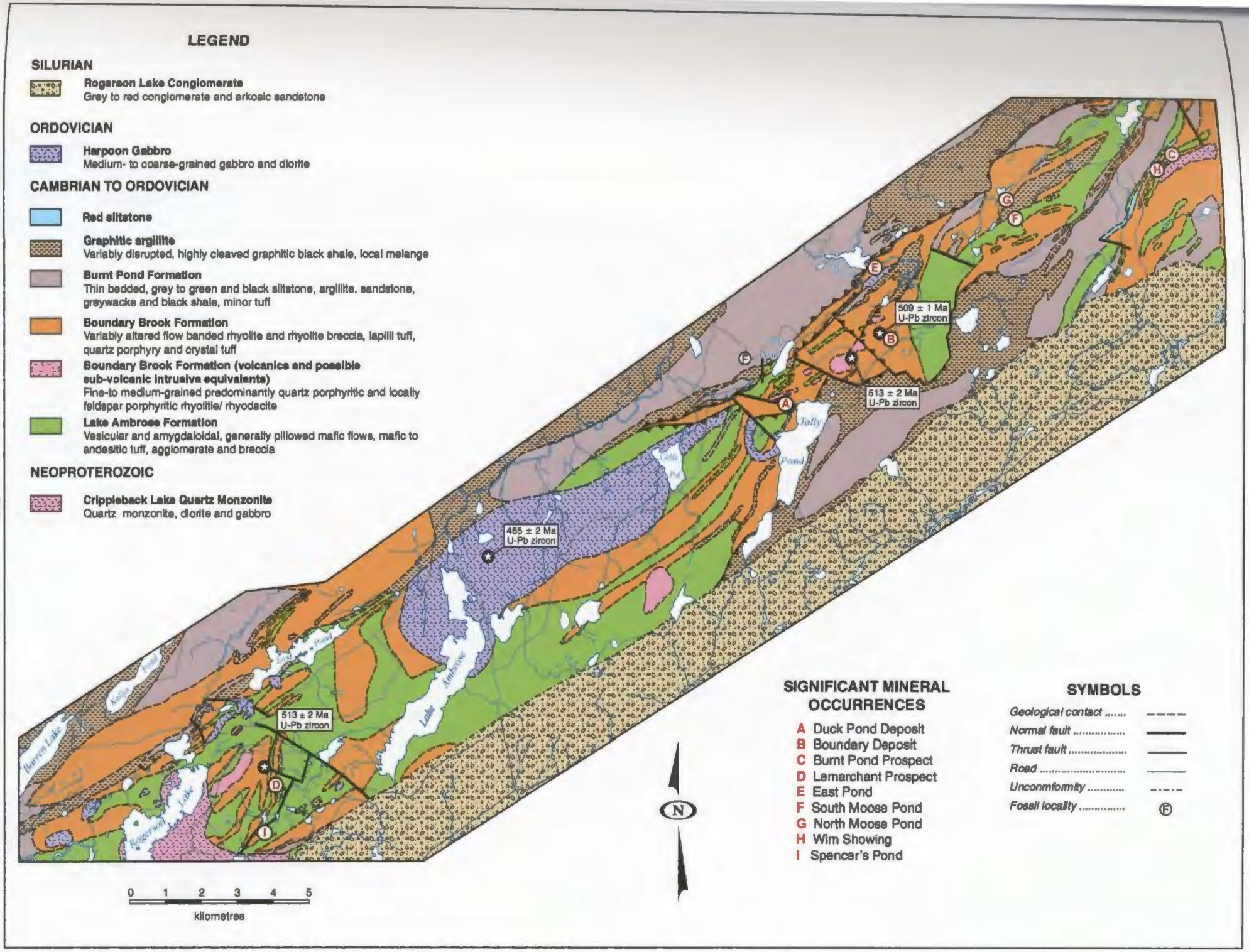

Figure 3.4 *Geology of the Tally Pond Group and surrounding rock units.*

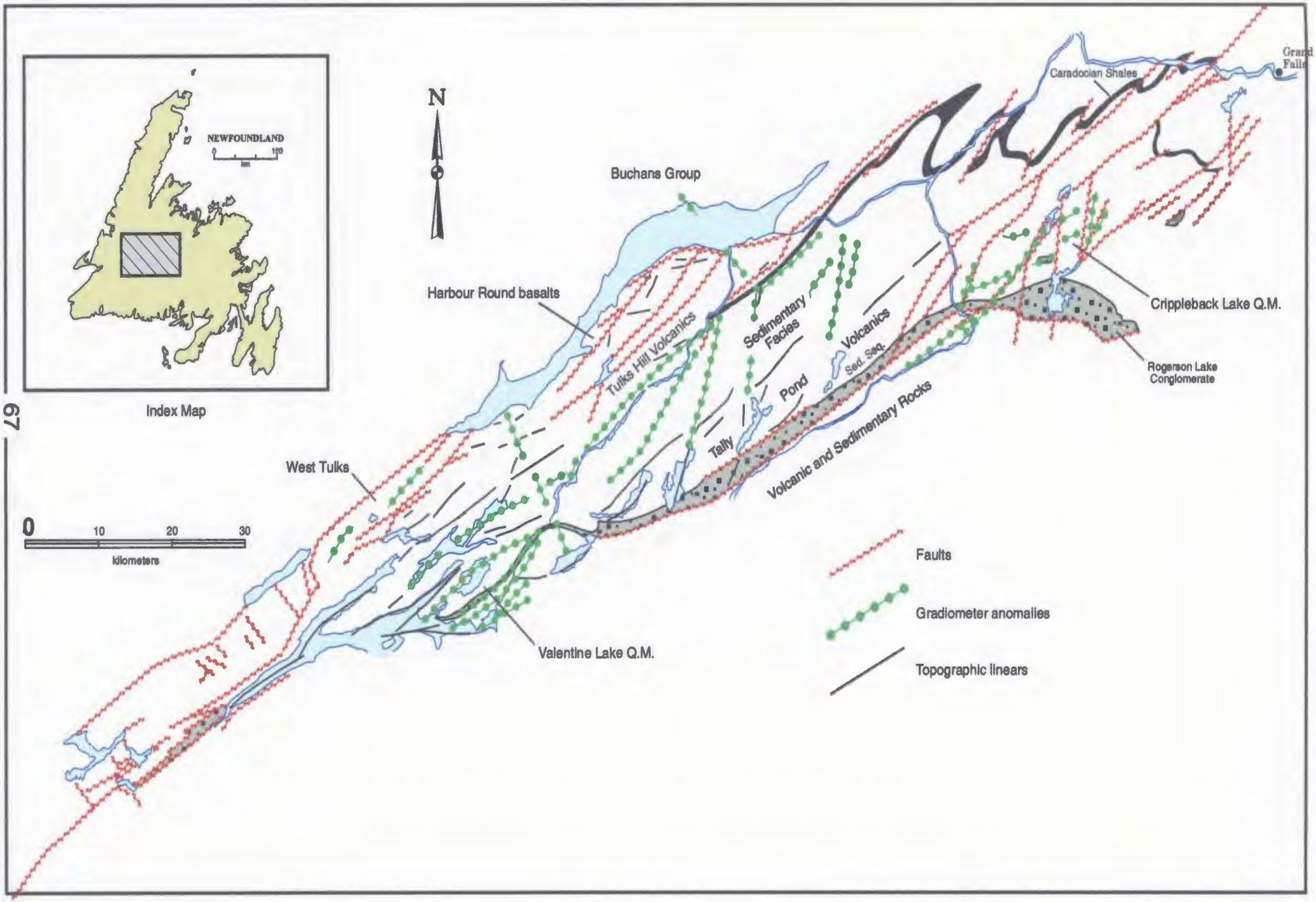

Figure 3.5 *Topographic, vertical gradient linears and faults within the Victoria Lake Supergroup (modified after Evans* et al., *1990).*

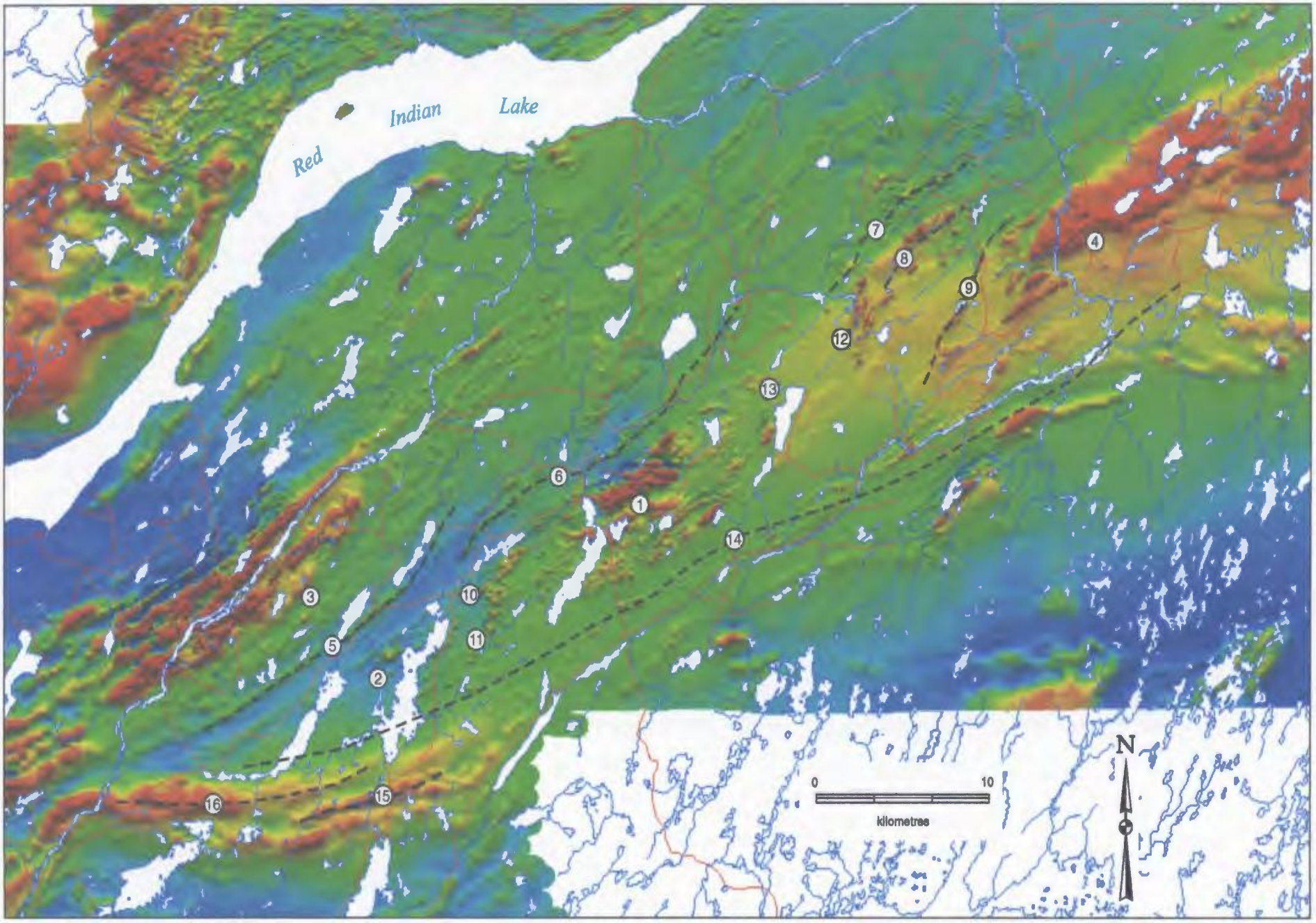

Figure 3.6 *Total-field vertical gradient aeromagnetic anomaly map of the Tally Pond study area. Numbers refering to specific geological features are described in the text (section 3.8).*

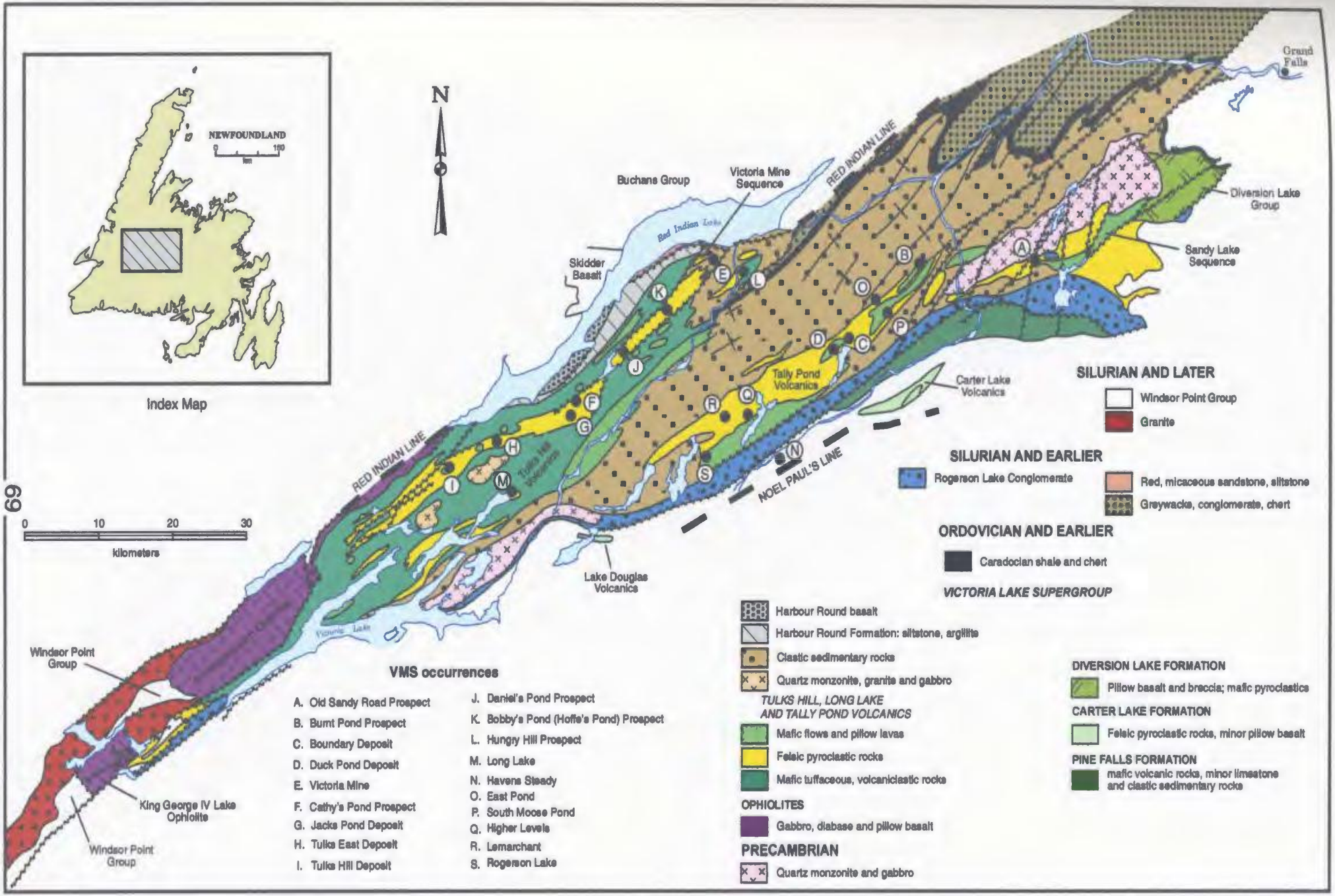

Figure 3.7 *Simplified geology of the Victoria Lake Supergroup and associated volcanogenic massive sulphide occurrences.*

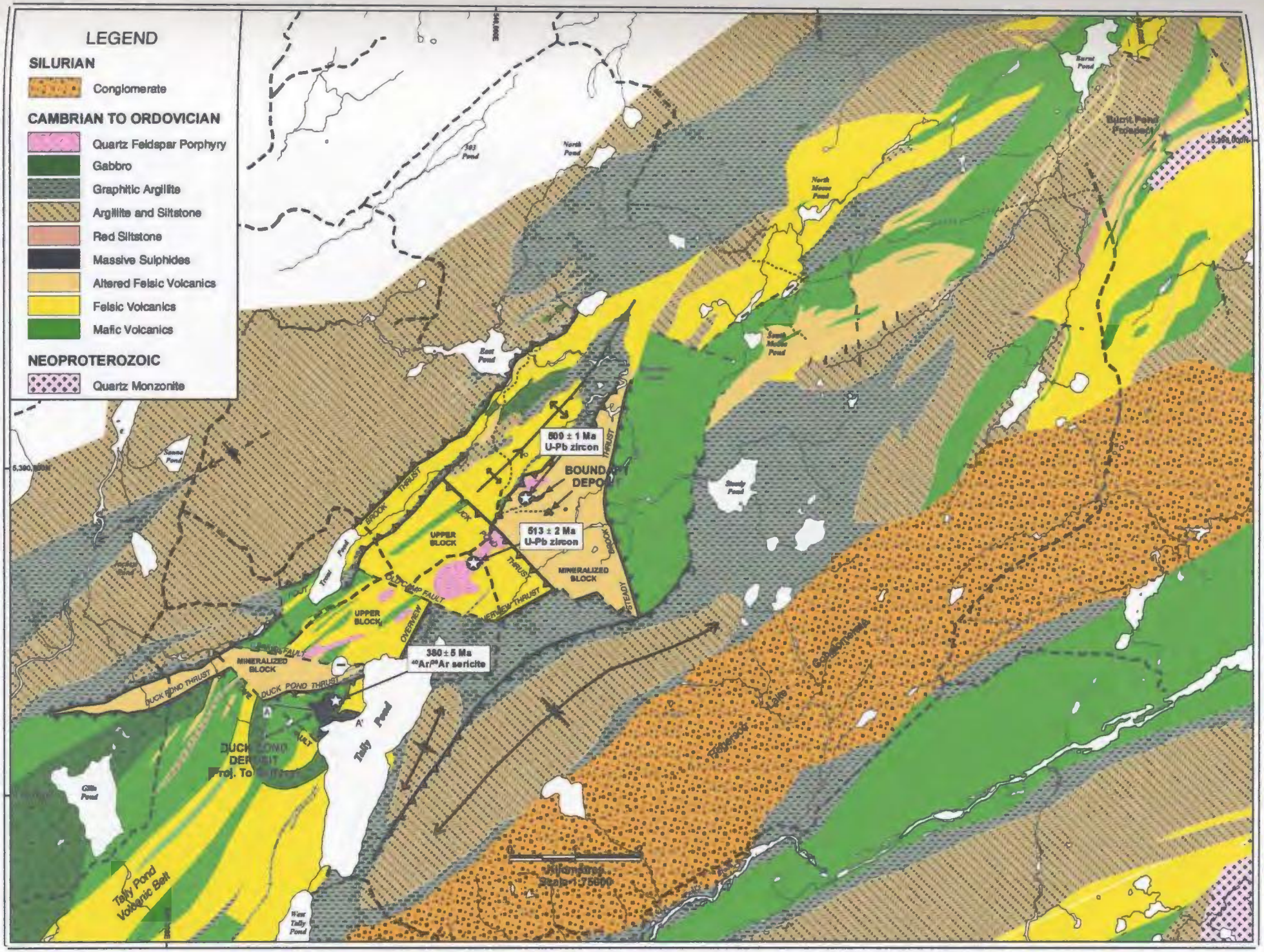

Figure 3.8 *Geological map of the Tally Pond Group in the Tally Pond-Burnt Pond area (modified from Squires* et al.*, 2000).*

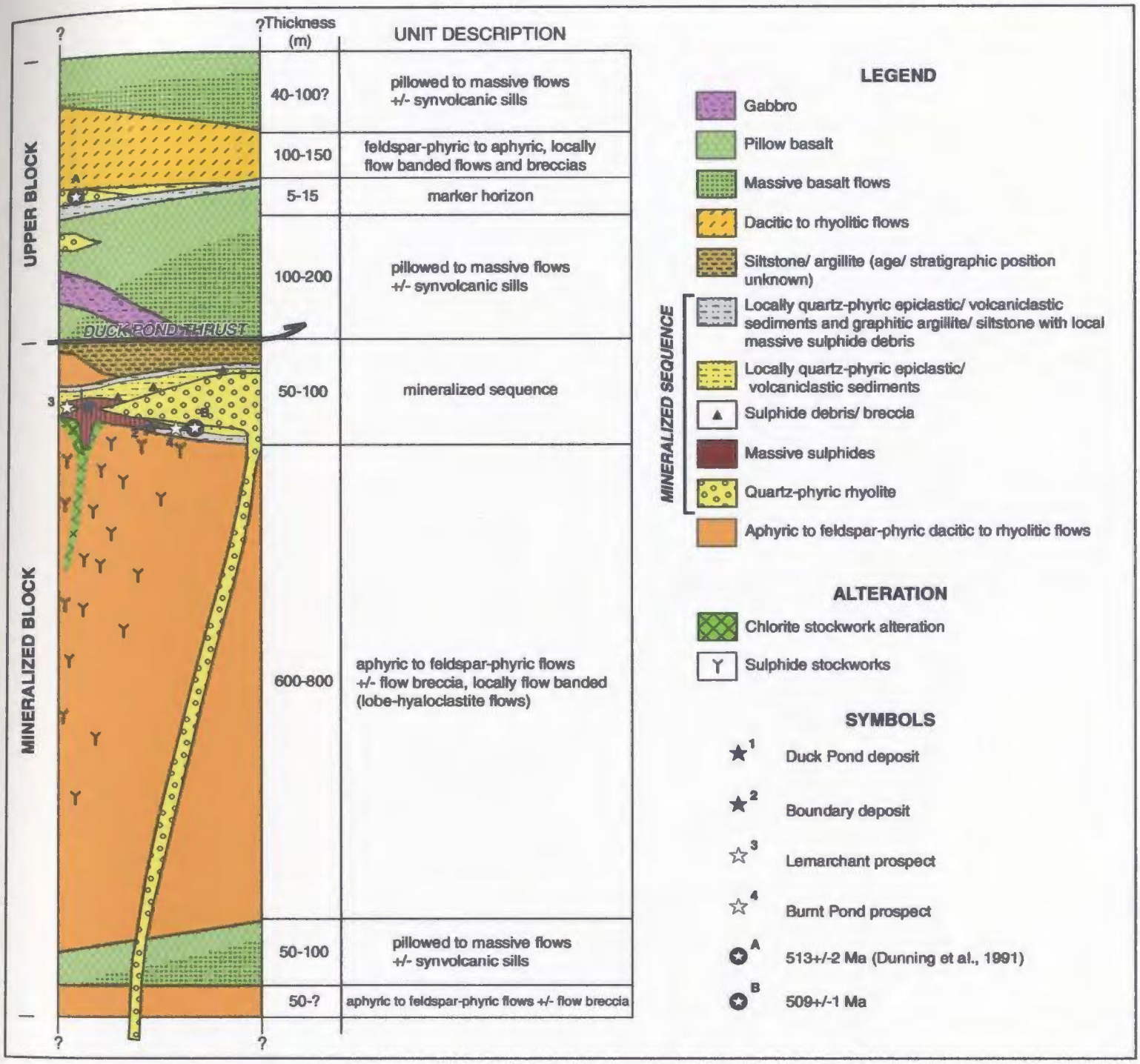

Figure 3.9 *Schematic stratigraphic column through the Tally Pond Group in the Tally Pond area. Modified from Moore (2003).*

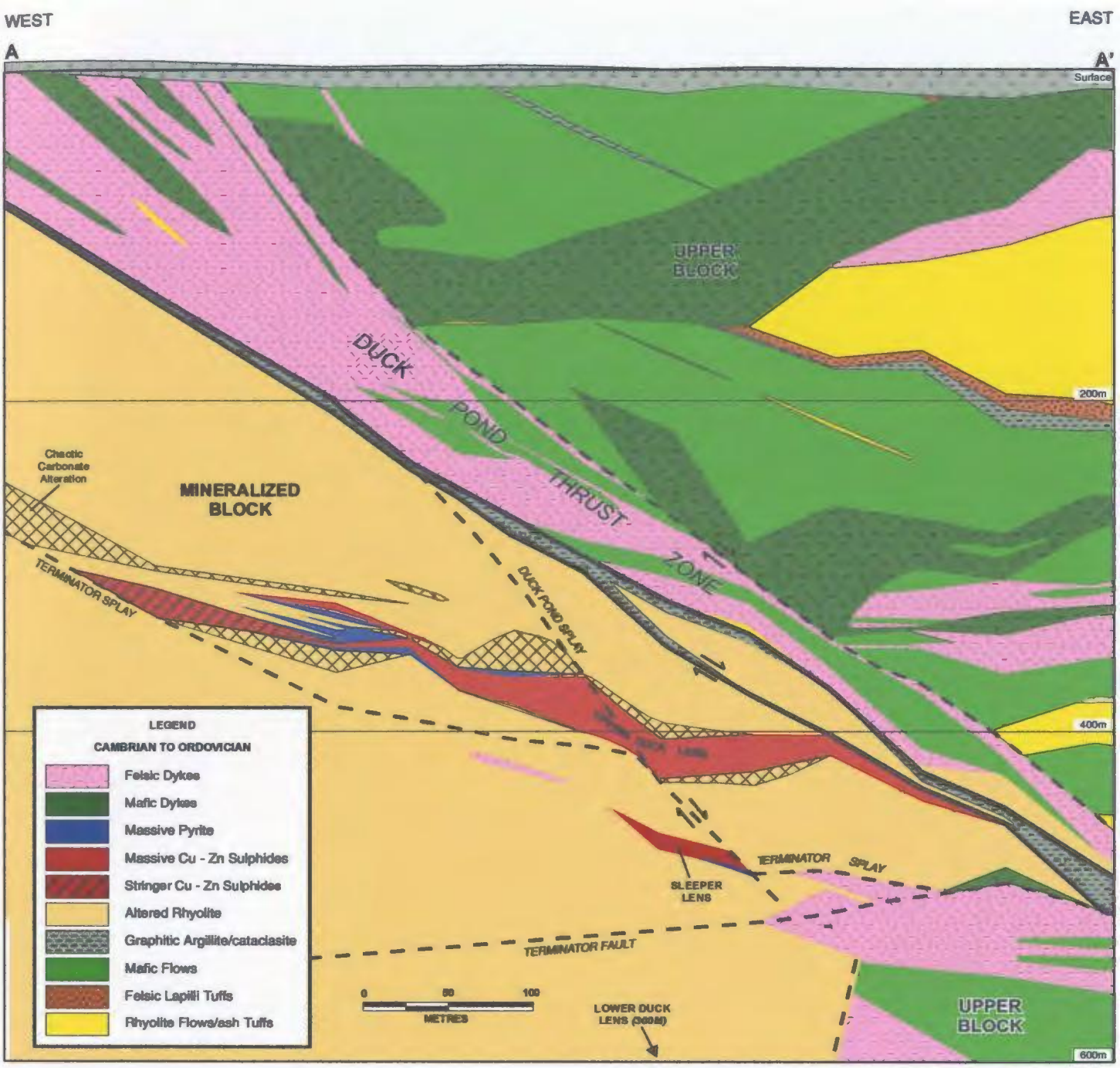

Figure 3.10 *Geological cross section through the Duck Pond deposit along line A-A'. Modified from Squires* et al. *(2000).*

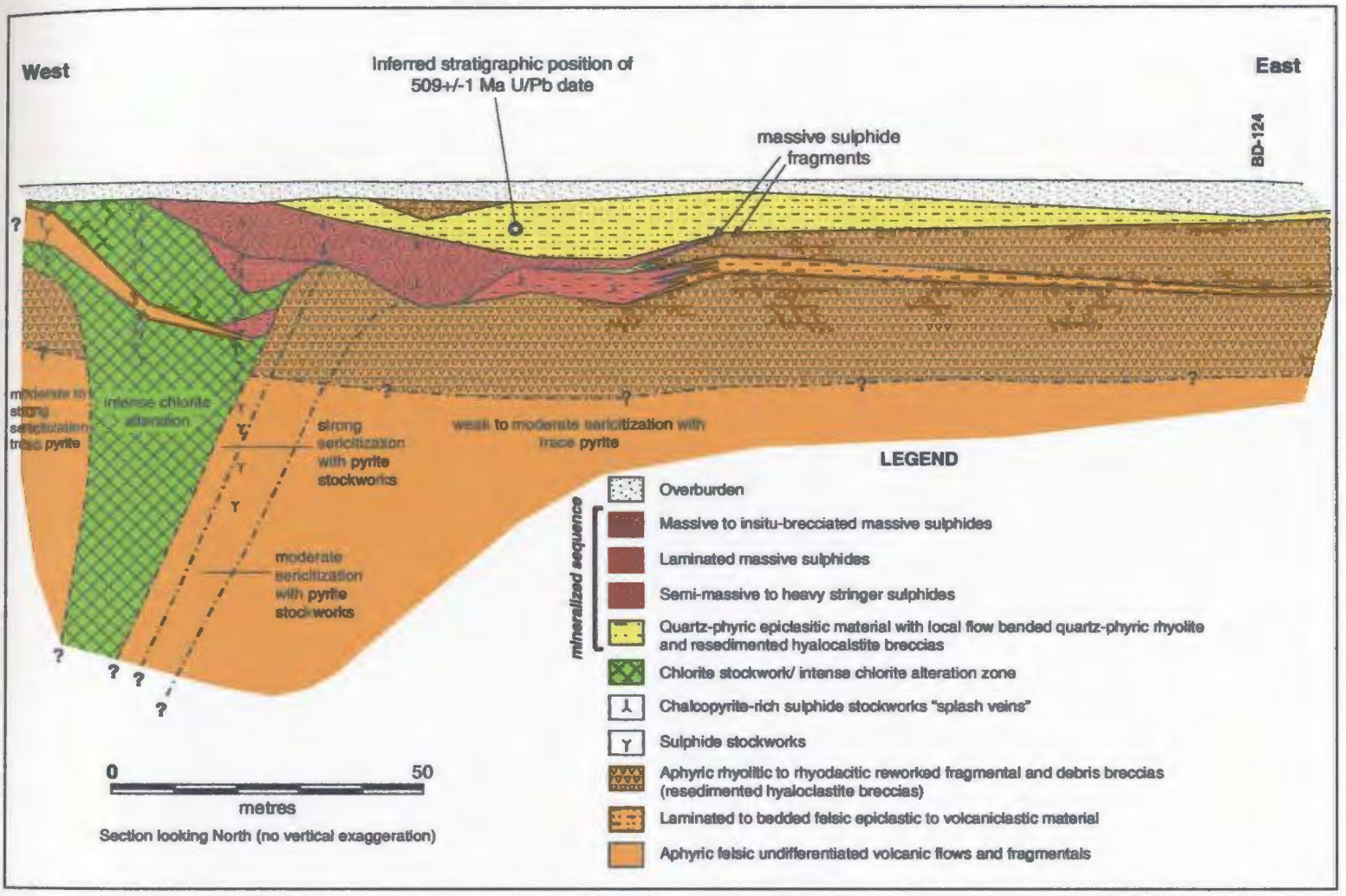

Figure 3.11 *Geological cross section through the Boundary Deposit (South Zone). Modified from Moore (2003).*

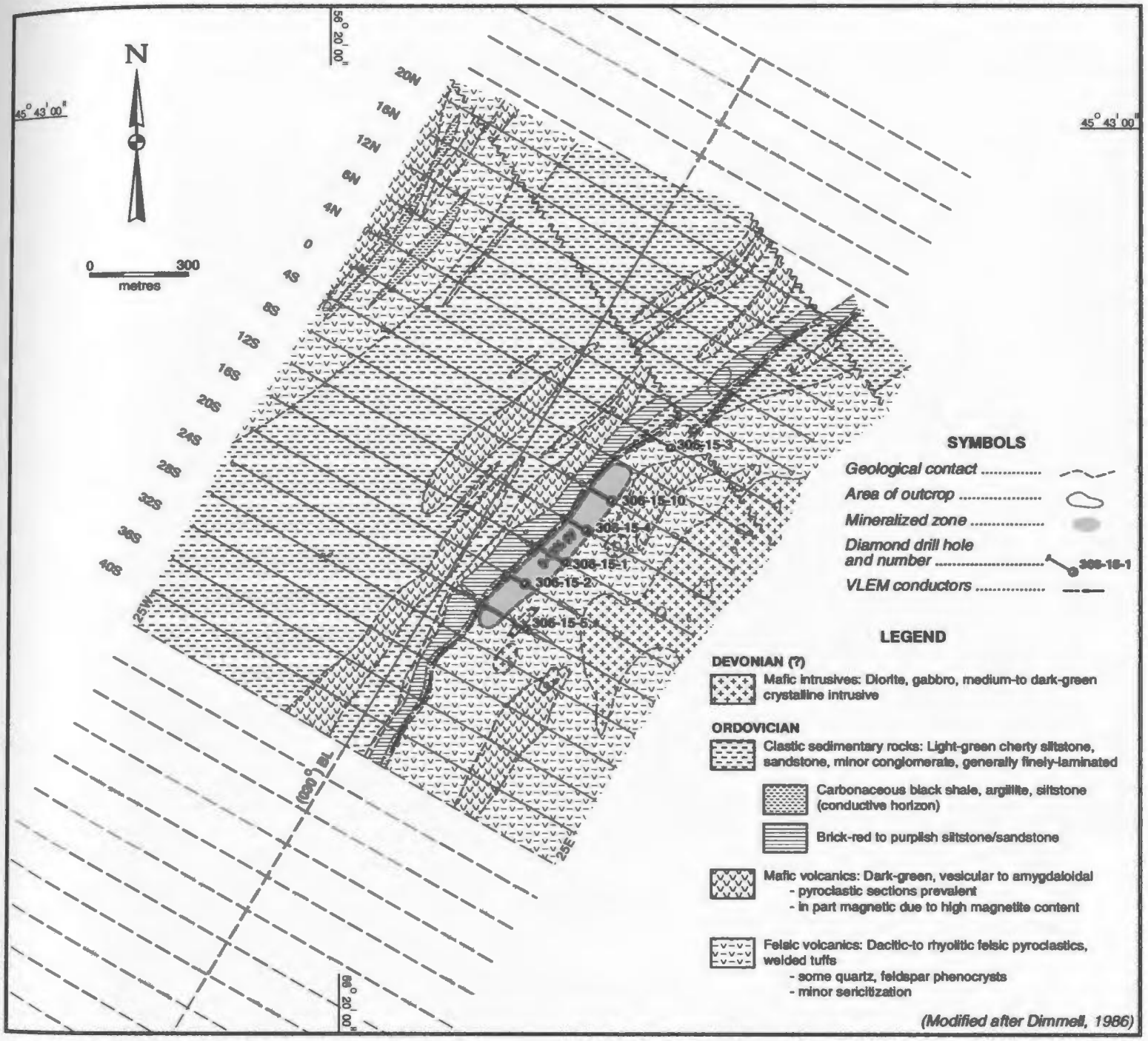

Figure 3.12 *Geological map of the Burnt Pond prospect.*

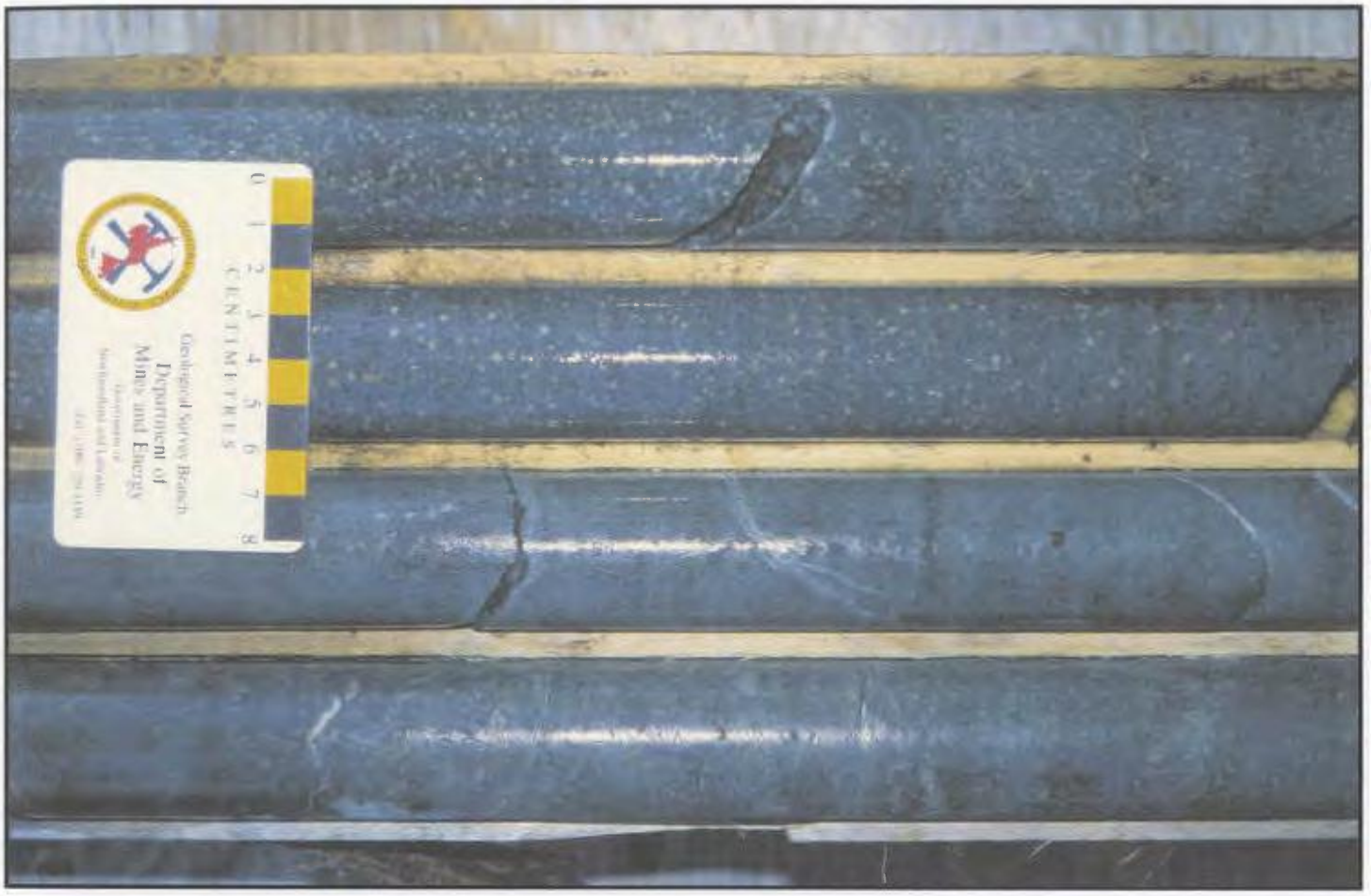

Plate 3.1 *Mafic volcanic rocks of the Lake Ambrose Formation.*

Plate 3.2 *Mafic volcanic pillowed basalt of the Lake Ambrose Formation. Note the abundant pyrite mineralization and sulphide staining along the pillow margins.*

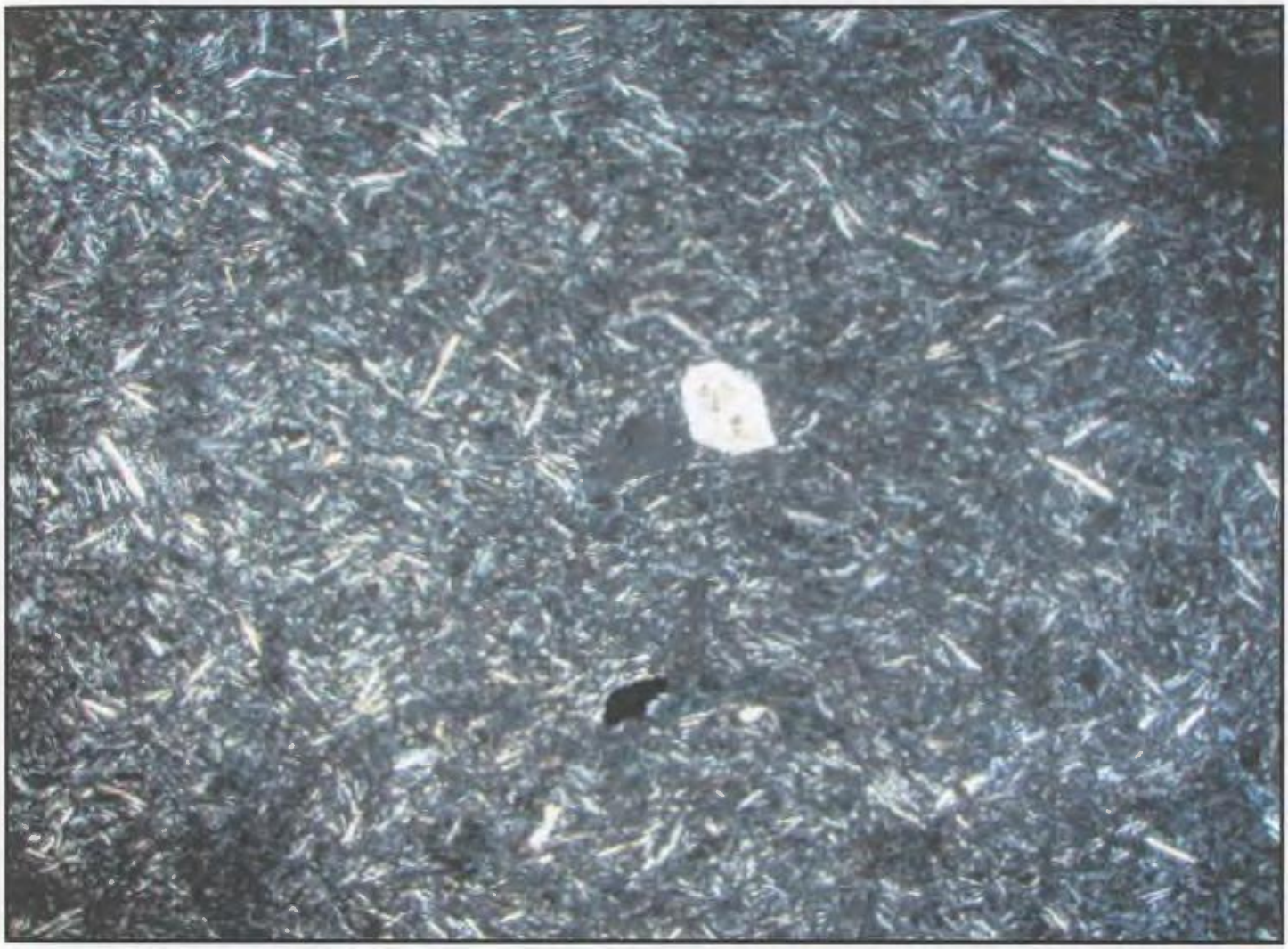

Plate 3.3 *Photomicrograph of mafic volcanic basalt of the Lake Ambrose Formation. Note the quartz filled amygdule in centre of photograph. Crossed polars, x 2.5*

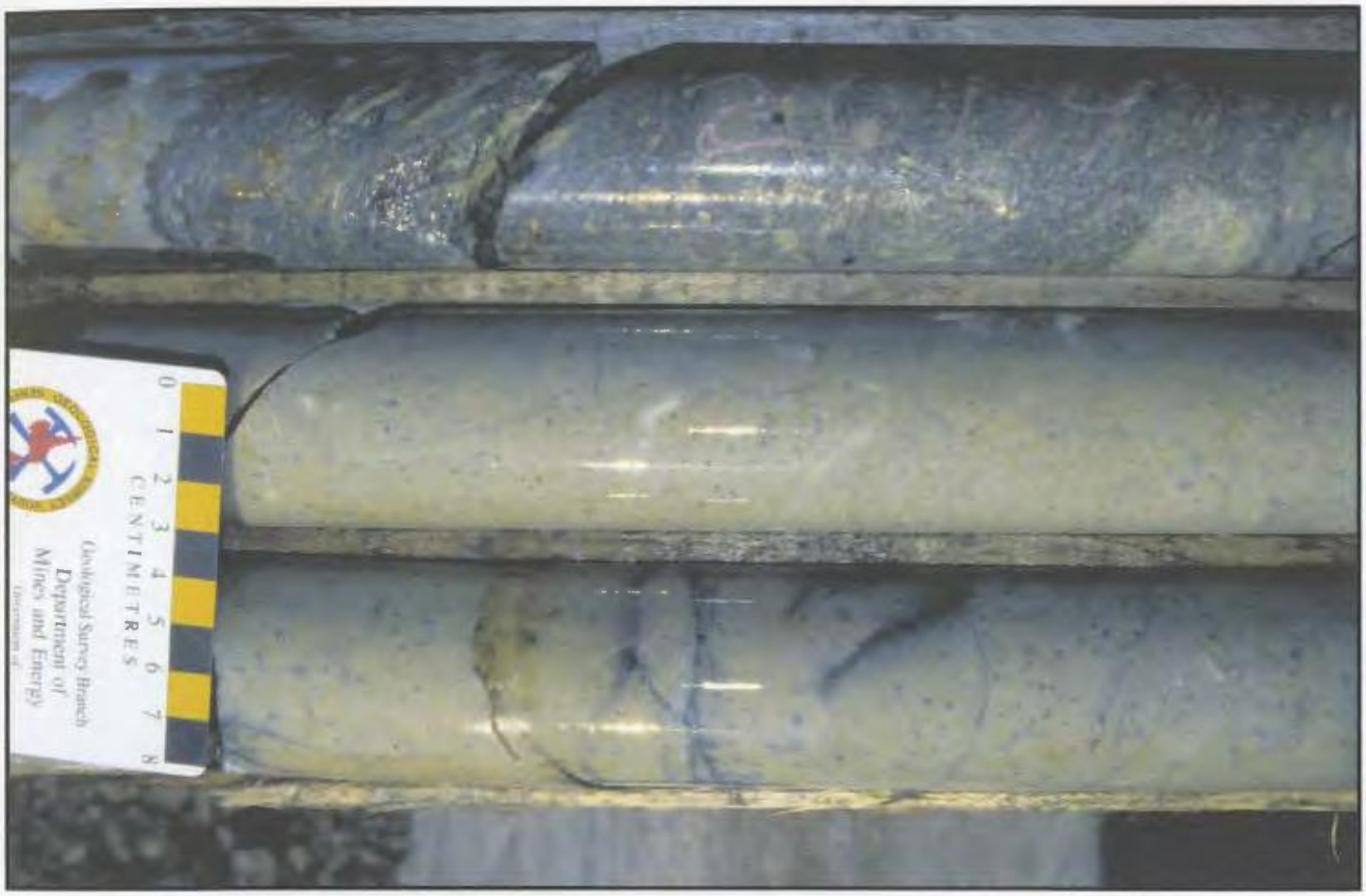

Plate 3.4 *Pervasive carbonate and sericite alteration with minor chlorite veins developed in a mafic volcanic protolith.*

Plate 3.5 *Felsic volcanic rhyolite breccia with minor sulphide staining.*

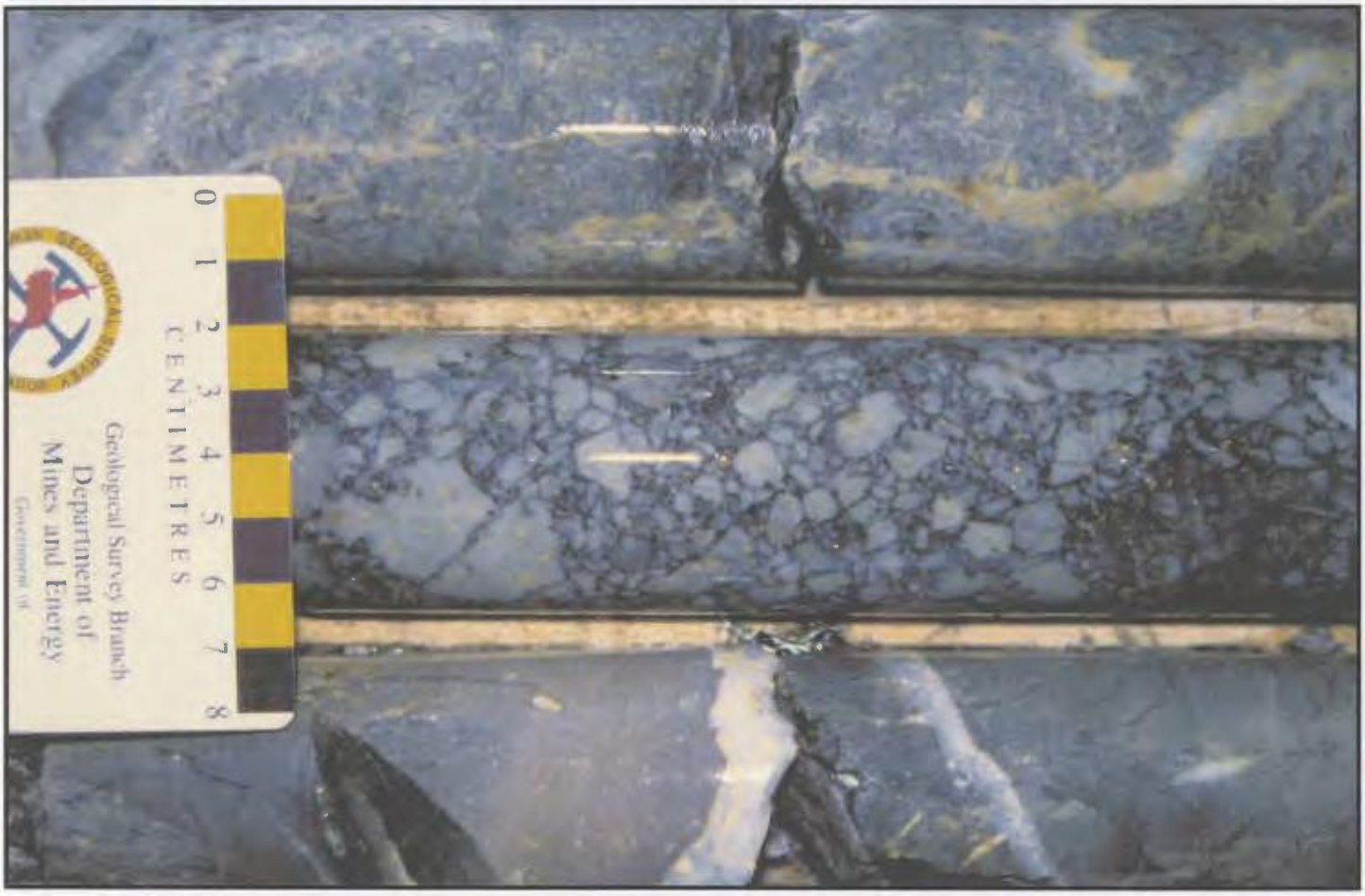

Plate 3.6 *Felsic lapilli tuff with a weakly chlorite altered matrix containing disseminated pyrite.*

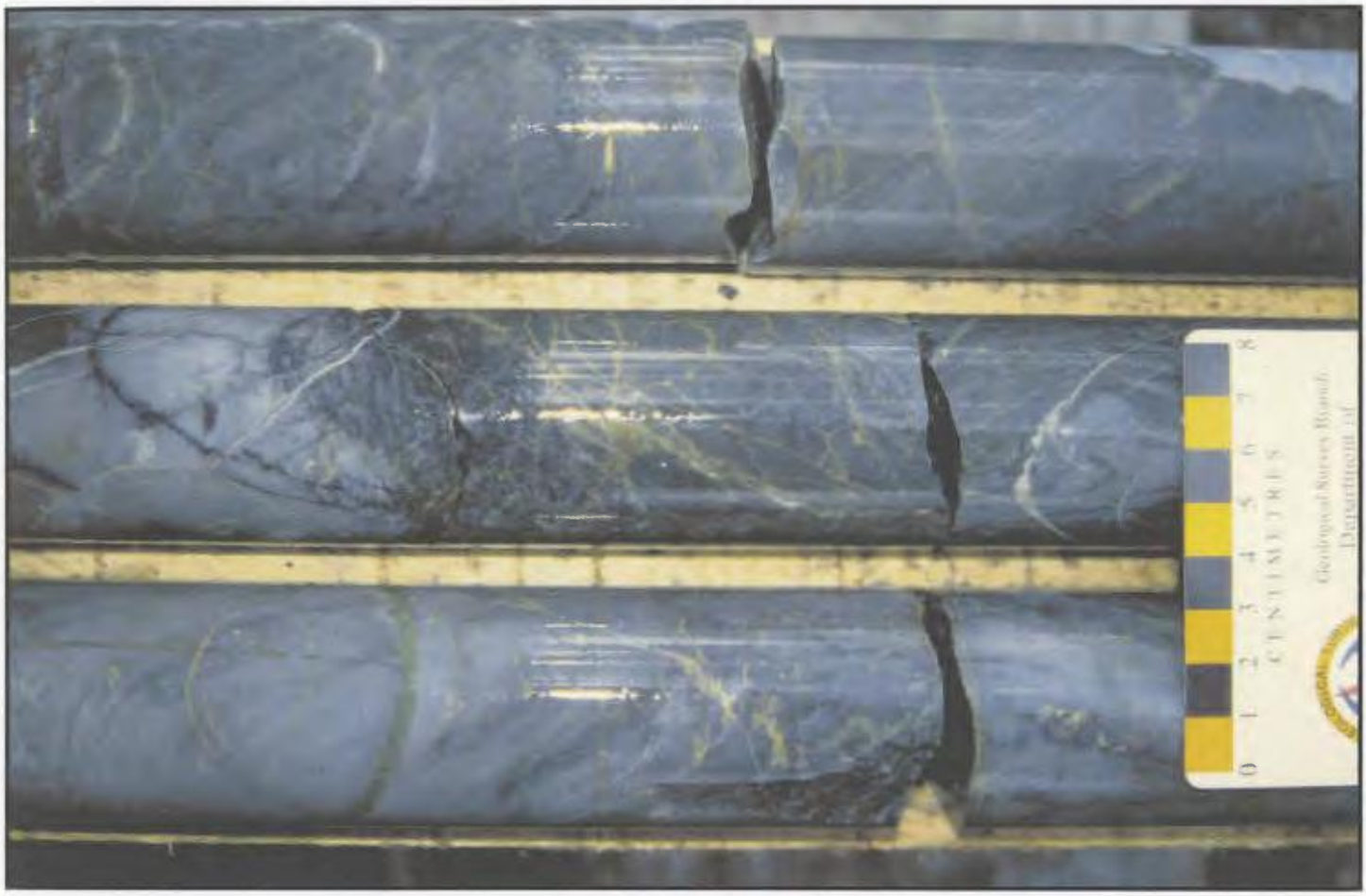

Plate 3.7 *Weakly chlorite altered fine gained rhyolite with sericite veins from the Mineralized block of the Duck Pond deposit.*

Plate 3.8 *Photomicrograph of fine-grained felsic volcanic rhyolite with secondary quartz veins. Crossed polars (x 2.5)*

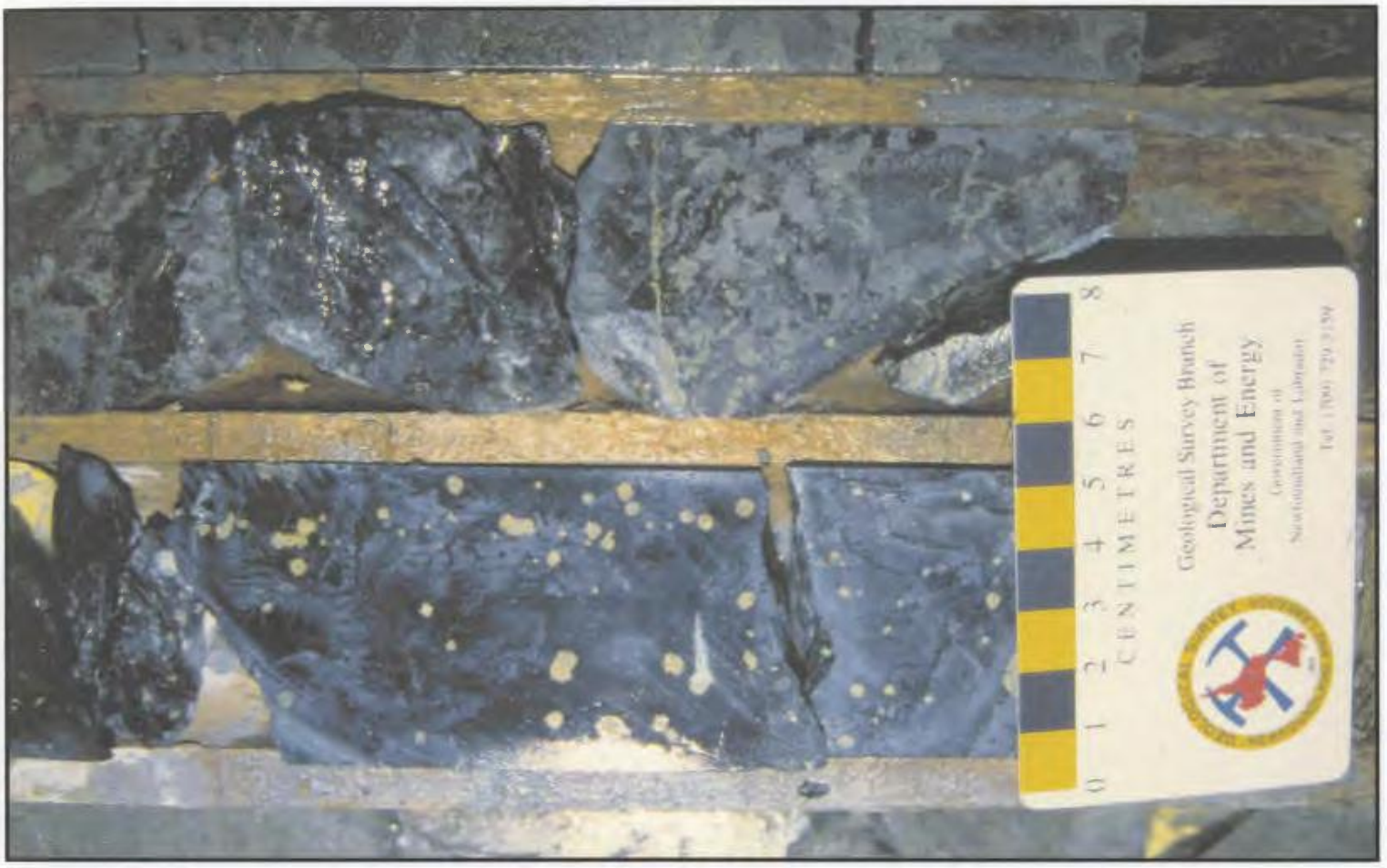

Plate 3.9 *Intense chlorite alteration from beneath the Duck Pond deposit interpreted as a feeder pipe zone to the massive sulphide deposit. Note the secondary carbonate alteration spots throughout the rock.*

Plate 3.10 *Weakly deformed, fine-to medium-grained light grey greywacke of the Burnt Pond Formation.*

Plate 3.11 *Intensely deformed black shale interpreted as melange that formed along thrust zones that form the contact between the Tally Pond Group and surrounding rocks units.*

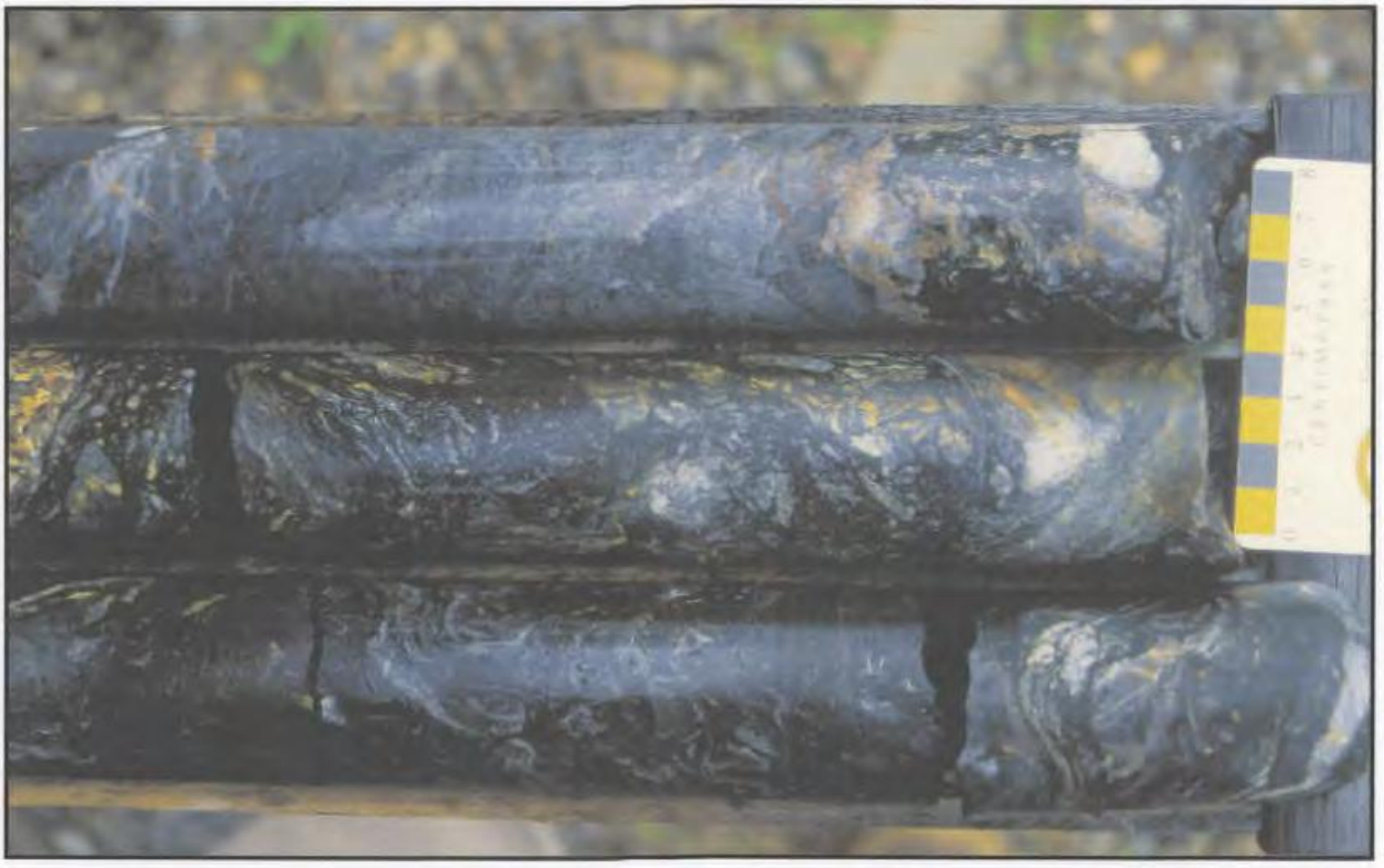

Plate 3.12 *Variably disrupted melange containing deformed pebble-size clasts set in a matrix of black shale.*

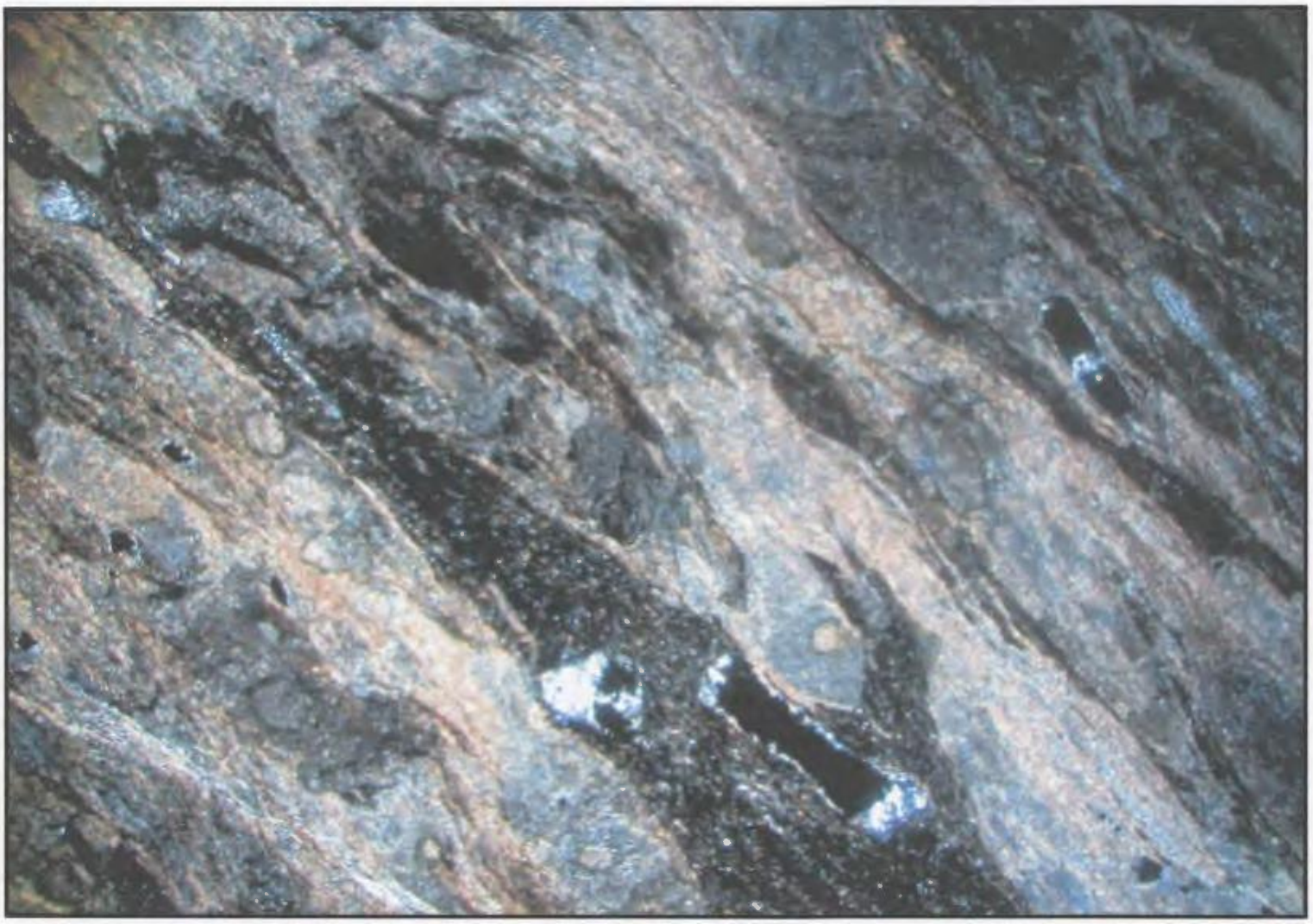

Plate 3.13 *Photomicrograph of enlongate felsic volcanic clasts set in a black shale matrix interpreted to be a tectonic melange. Crossed polars (x 2.5)*

Plate 3.14 *Sharp contact between quartz-porphyritic rhyolite on the left and rhyolite tuff on the right.*

Plate 3.15 *Pink medium-grained, massive K-feldspar phenocrysts set in a matrix of fine-grained grey rhyolite.*

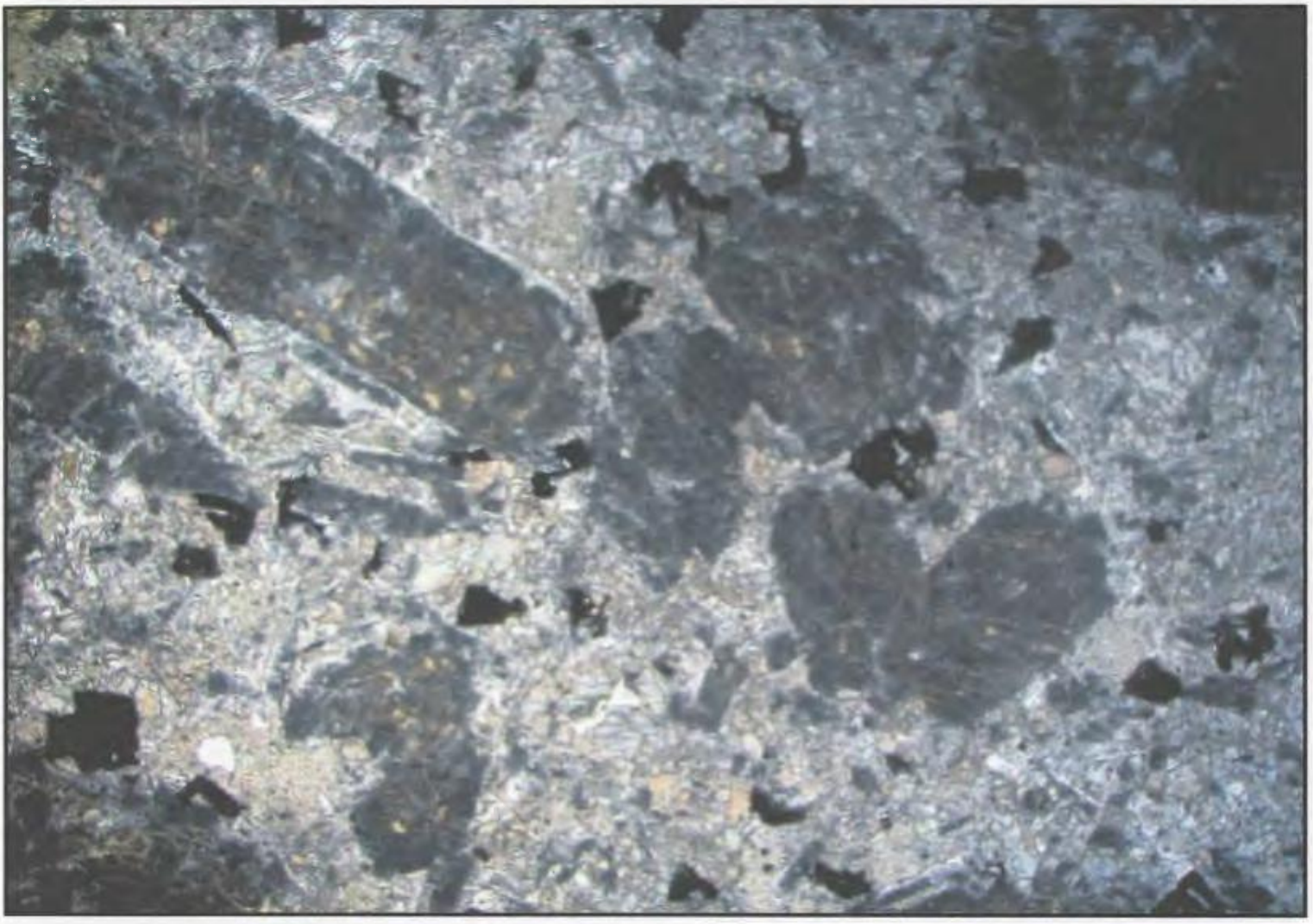

Plate 3.16 *Photomicrograph of K-feldspar phenocrysts set in a matrix of fine-grained felsic volcanic groundmass. Crossed polars (x 2.5)*

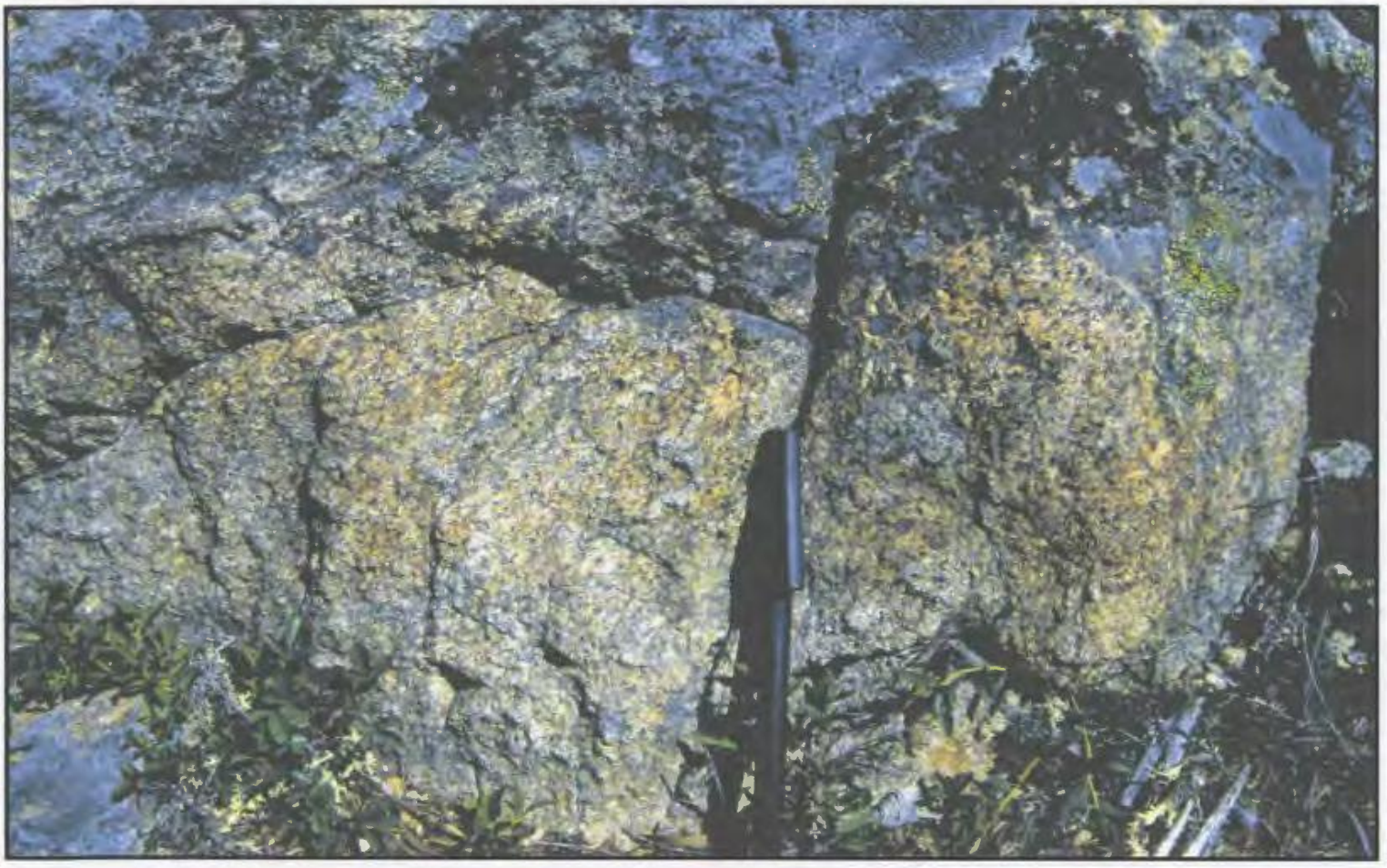

Plate 3.17 *Light brown-weathering, light to dark grey, medium grained gabbro located on the summit of Harpoon Hill.*

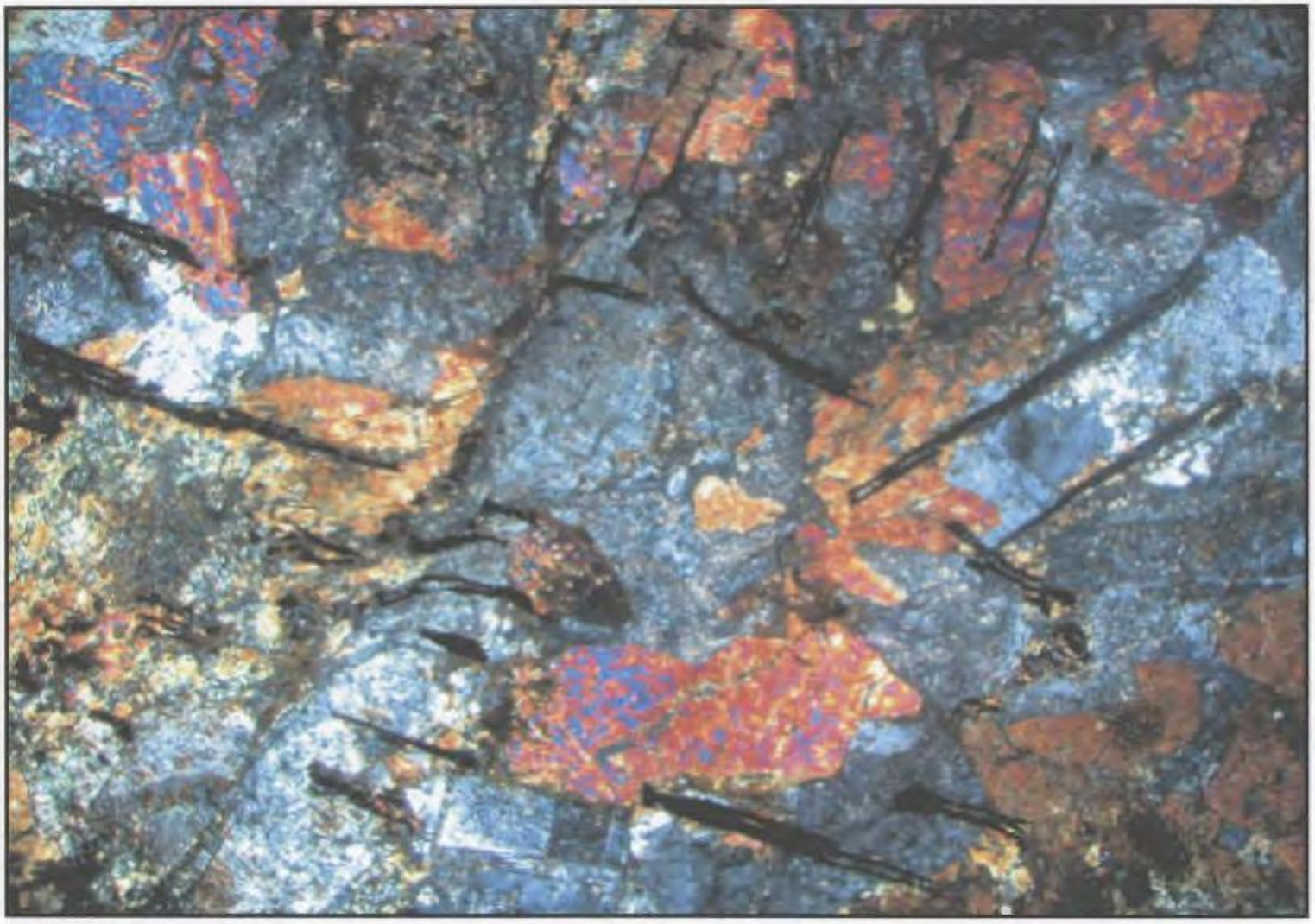

Plate 3.18 *Photomicrograph of coarse-grained gabbro. Note the altered plagioclase crystals and accessory magnetite and ilmenite. Crossed polars (x 2.5)*

Plate 3.19 *Medium-grained equigranular gabbro from the Upper block of the Duck Pond deposit.*

Plate 3.20 *Coarse-grained to pegmatitic gabbro located in Harpoon Brook north of the Harpoon Steady dam.*

Plate 3.21 *Dark grey medium-grained granodiorite of the Cripplebeck Lake quartz monzonite located southeast of Burnt Pond.*

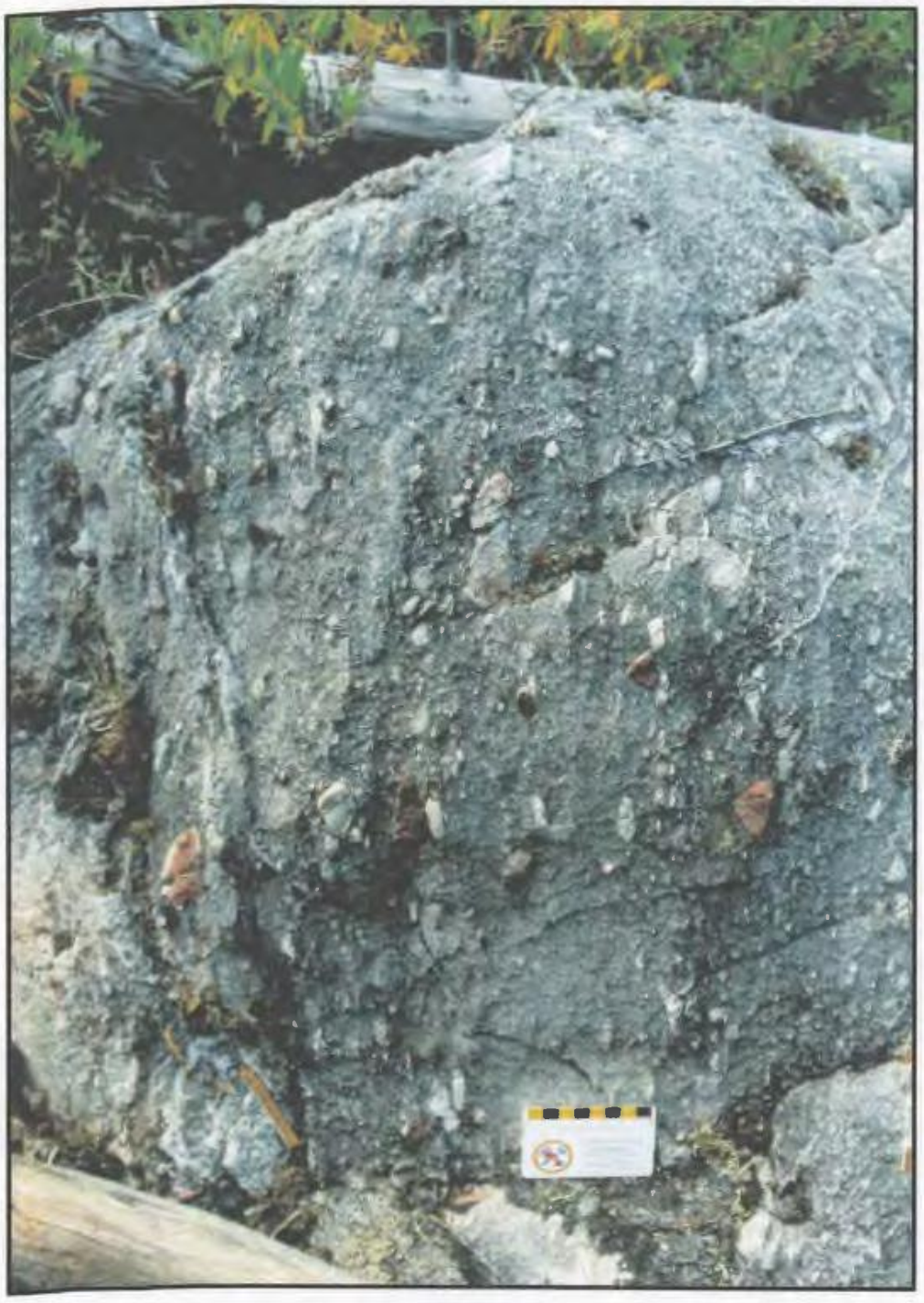

Plate 3.22 *Polymictic Rogerson Lake Conglomerate from the type area along the southern shore of Rogerson Lake.*

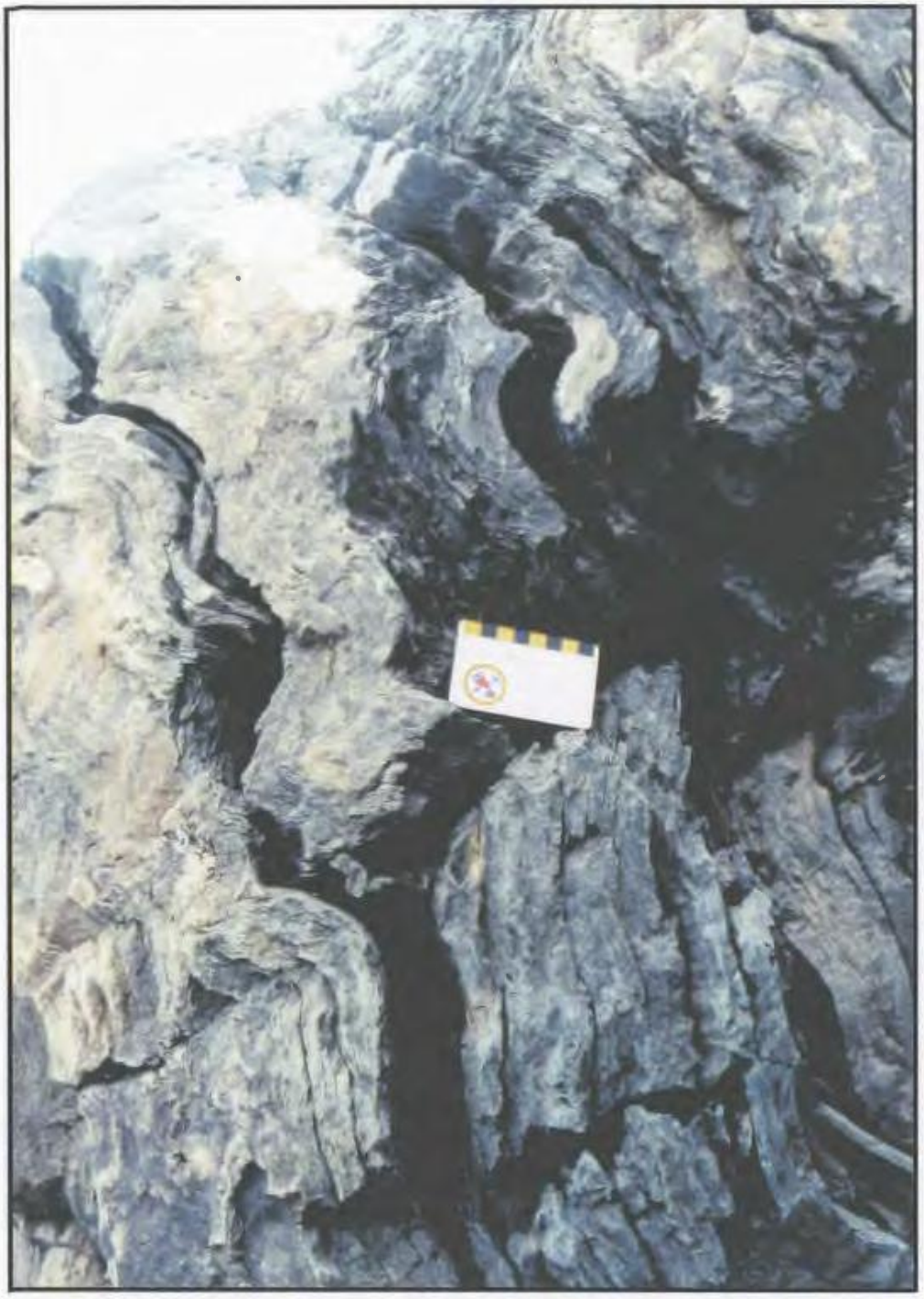

Plate 3.23 *Asymetrical, open to close folds with gently dipping axial planar surfaces and fold axes in fine-grained volcaniclastic greywackes.*

Plate 3.24 *Mineralized mafic pillow lava from the Upper block of the Duck Pond deposit.*

Plate 3.25 *Weakly altered fine-grained gabbroic to dioritic dyke intruding altered rhyolite in the Upper block of the Duck Pond deposit.*

Plate 3.26 *K-feldspar porphyritic dyke from the Upper block of the Duck Pond deposit.*

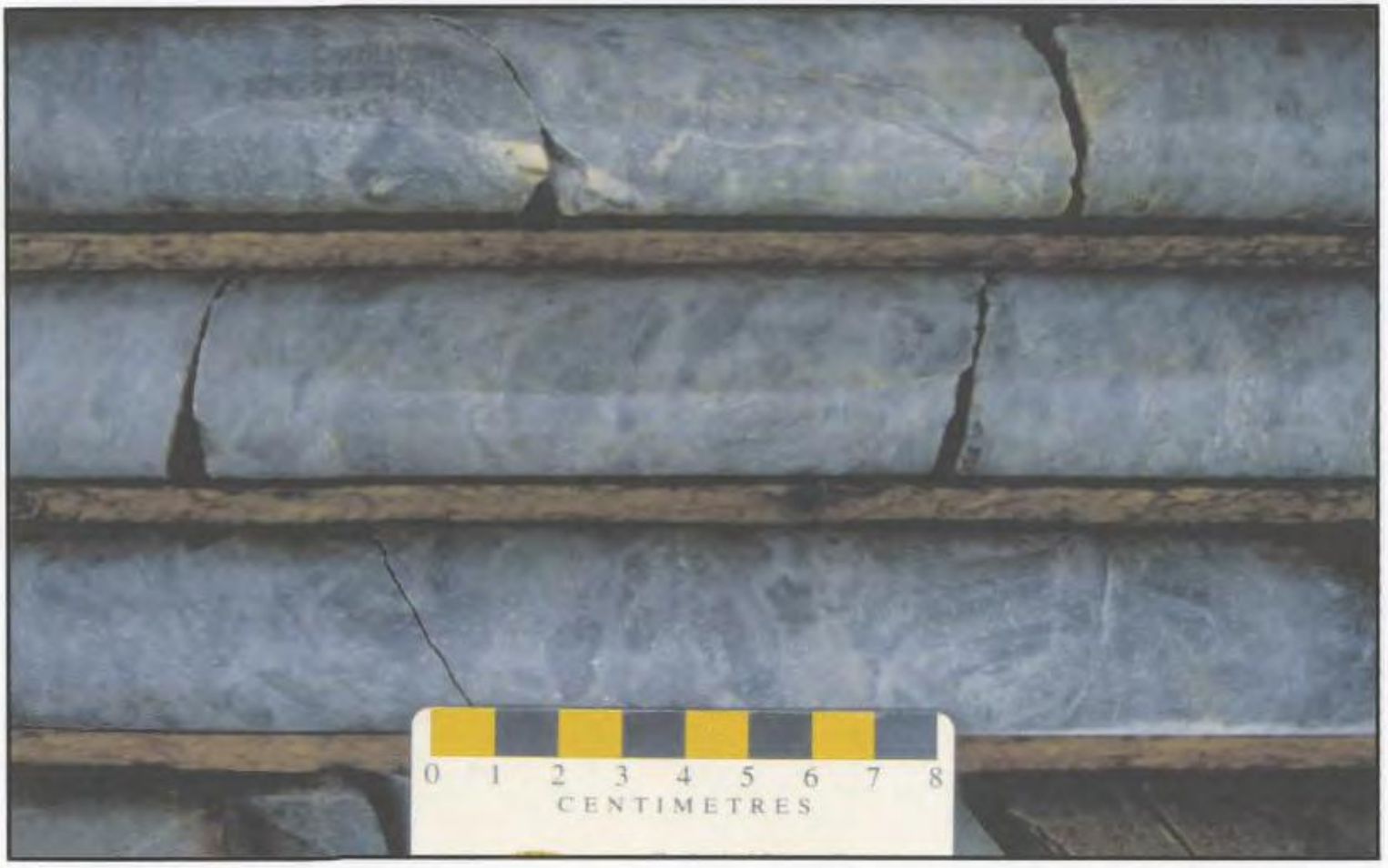

Plate 3.27 *Weakly carbonate/chlorite altered rhyolite autobreccia from the Mineralized block of the Duck Pond deposit.*

Plate 3.28 *Carbonate and sericite altered rhyolite from the Mineralized block of the Duck Pond deposit.*

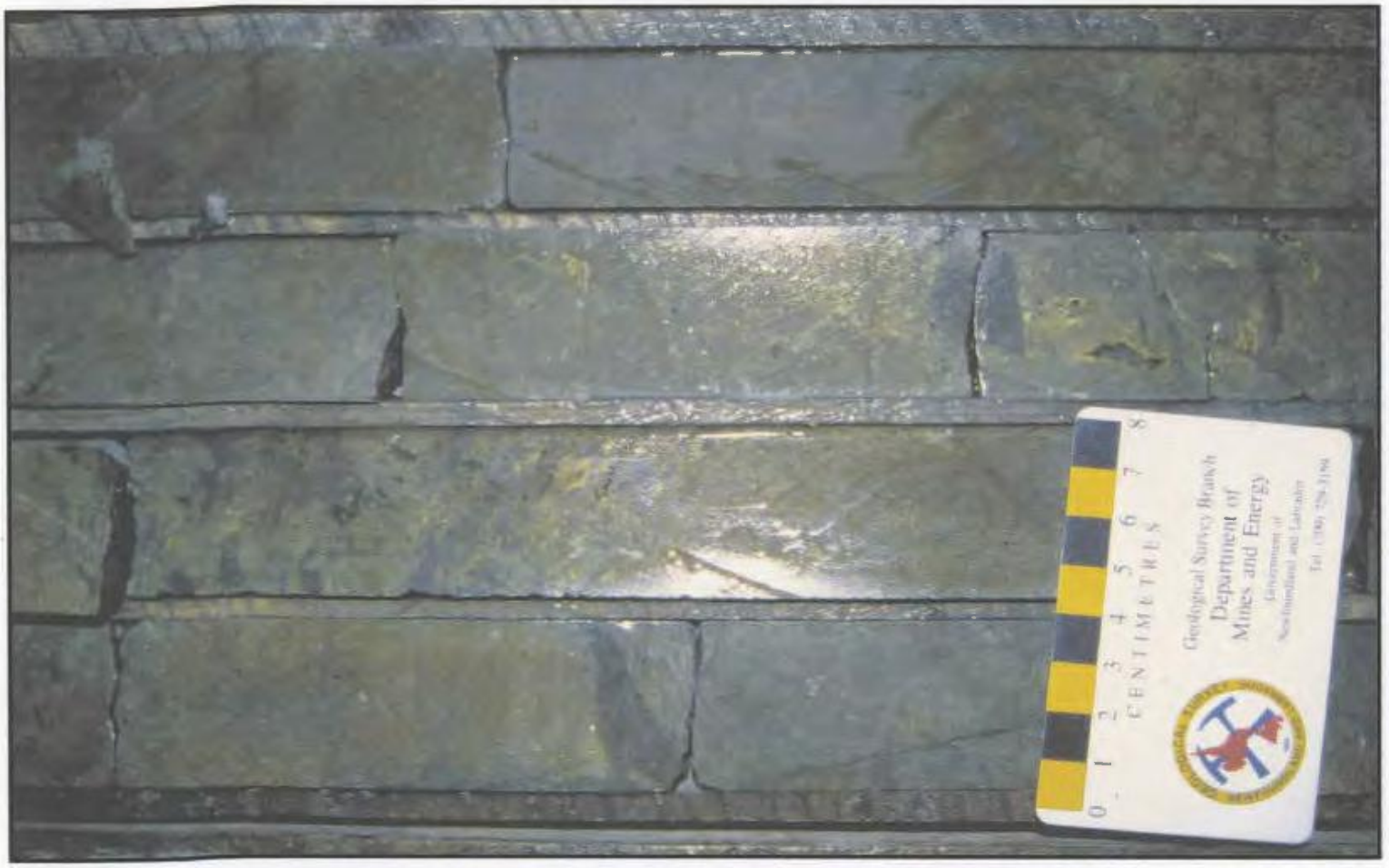

Plate 3.29 *Massive pyrite and chalcopyrite with minor sphalerite from the upper Duck lens.*

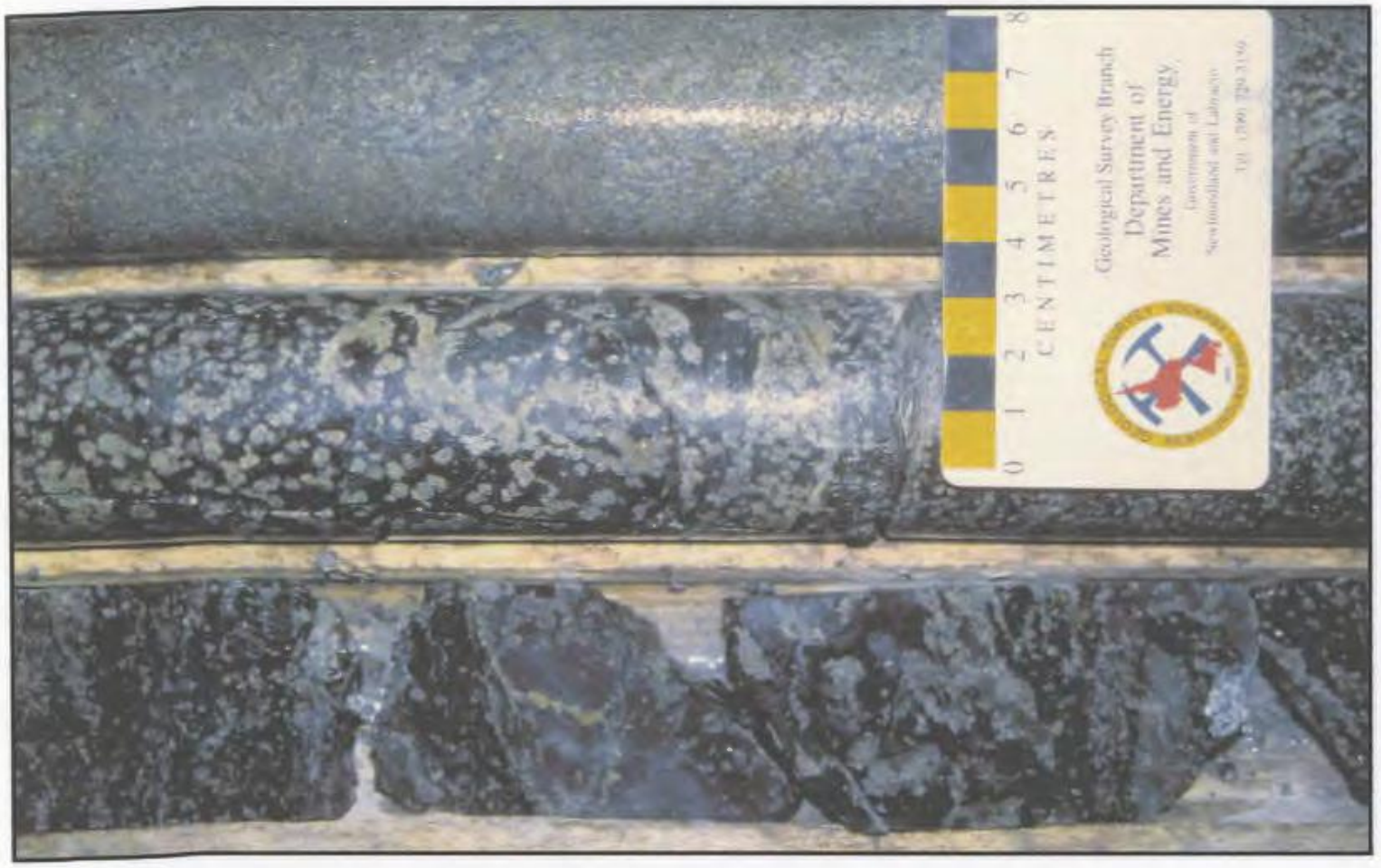

Plate 3.30 *Coarse-grained disseminated pyrite in chlorite from beneath the Upper Duck lens of the Duck Pond deposit.*

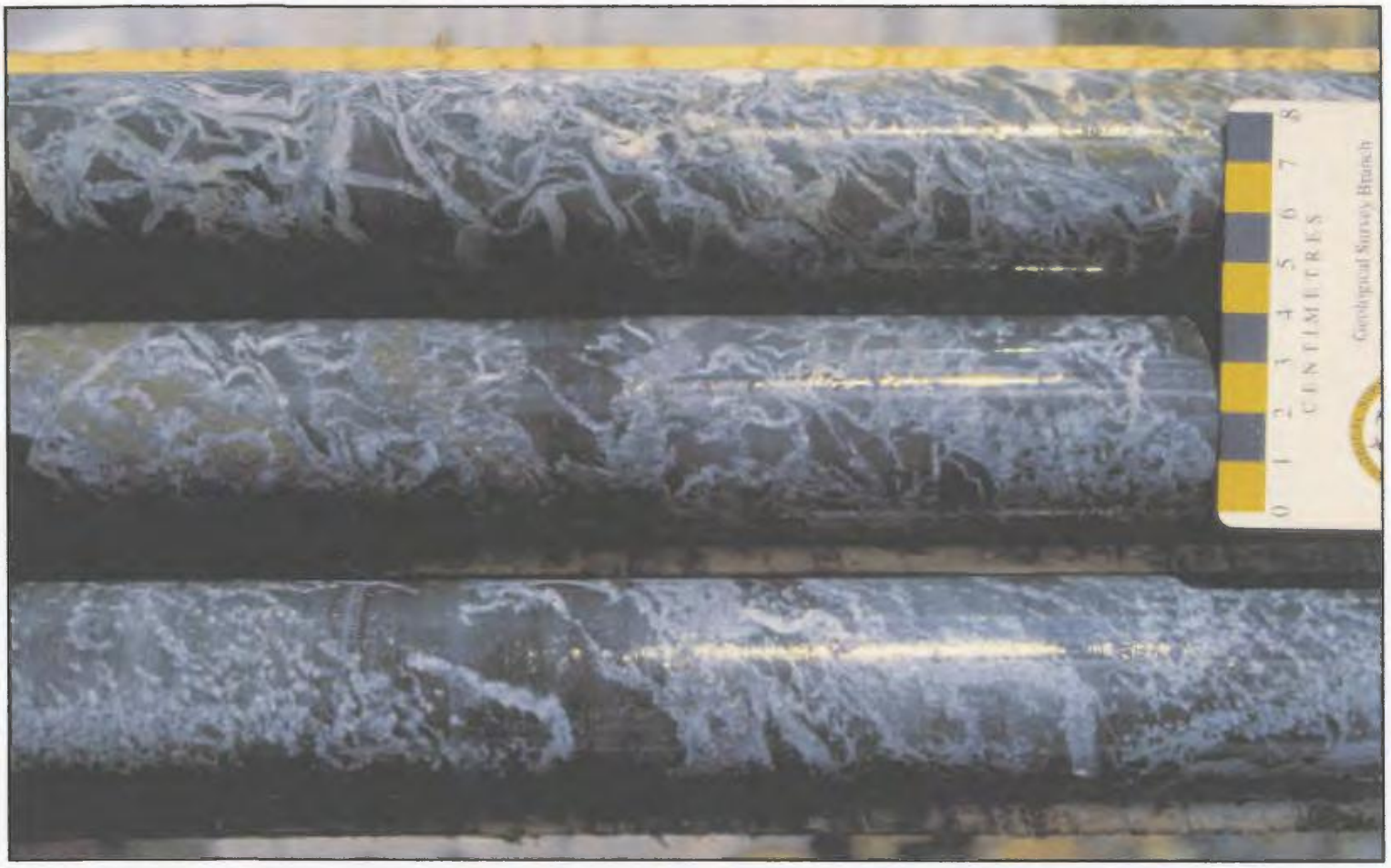

Plate 3.31 *Chaotic carbonate and chlorite from the periphery of the Upper Duck lens.*

Plate 3.32 *Weakly mineralized lapilli tuff exposed near the Boundary deposit.*

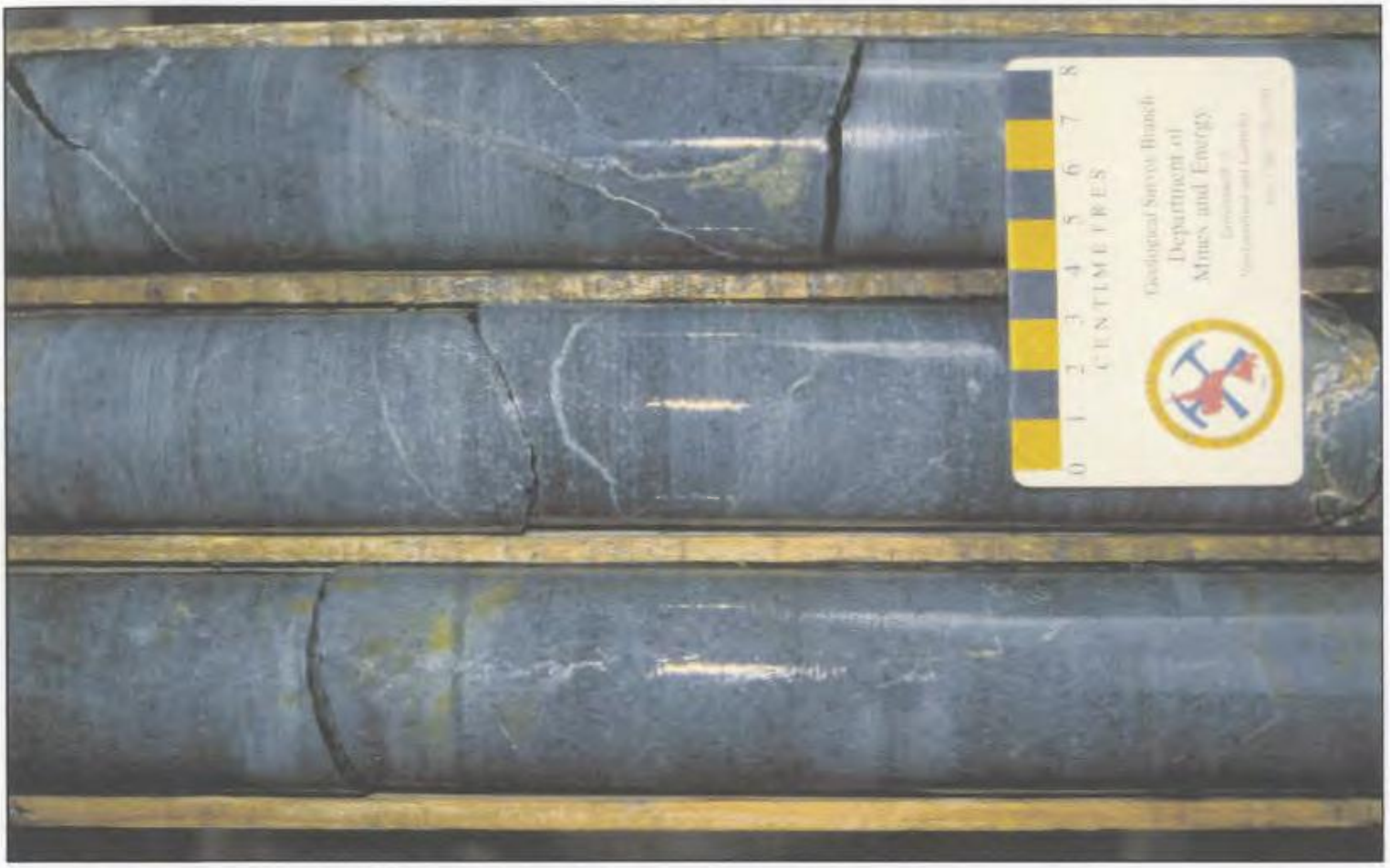

Plate 3.33 *Fine-grained rhyolite from the footwall of the Boundary deposit. Note the disseminated pyrite and weakly quartz/carbonate veins.*

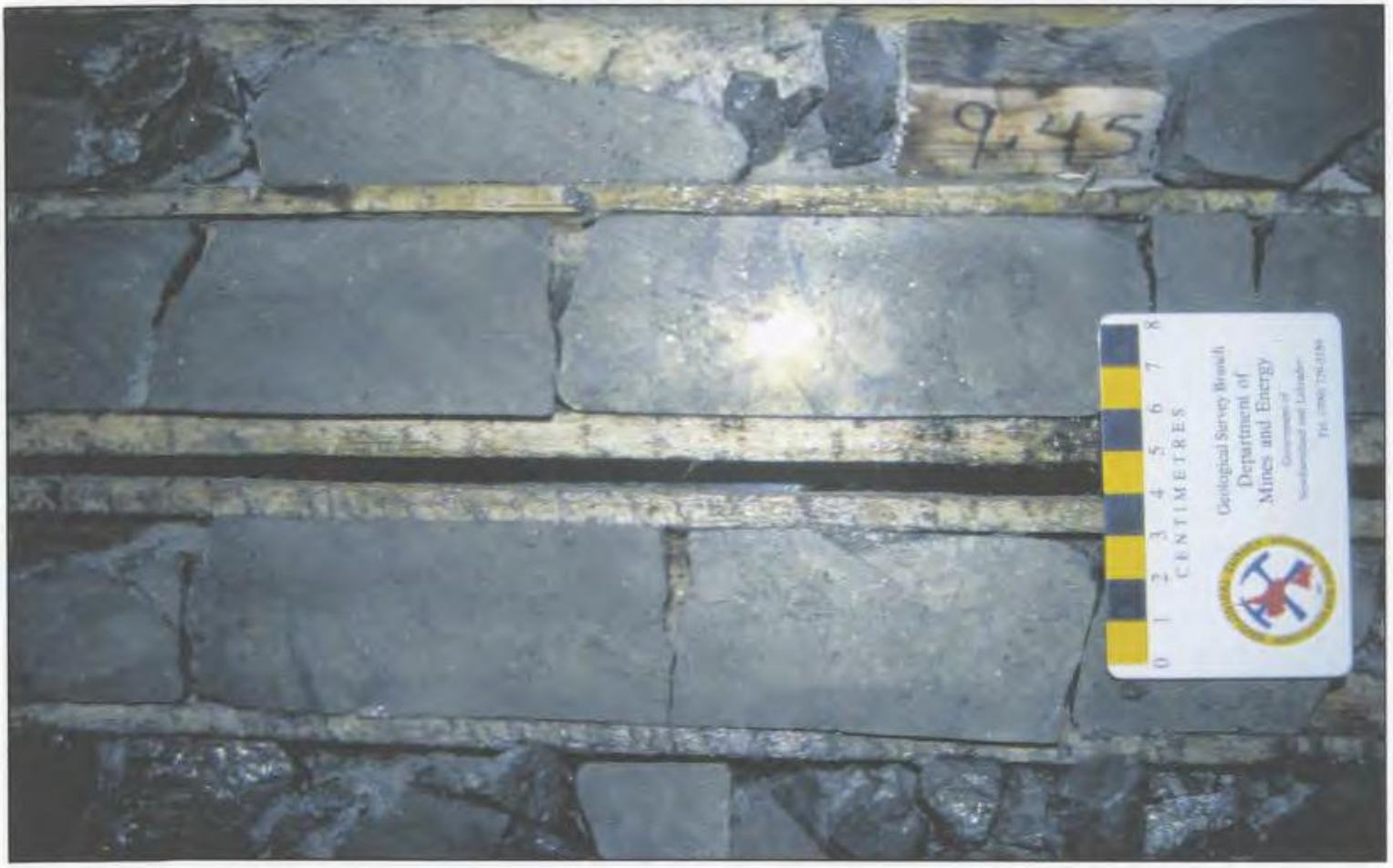

Plate 3.34 *Massive sulphides from the Boundary deposit, Southeast zone consisting of dominantly pyrite with minor chalcopyrite.*

CHAPTER 4

TRACE AND RARE EARTH ELEMENT GEOCHEMISTRY OF VOLCANIC, SUBVOLCANIC AND INTRUSIVE ROCKS

4.1 Preamble

The analysis of trace and rare earth element geochemical data is a valuable tool in understanding and interpreting the petrology and petrogenesis of igneous rocks. Trace elements are more capable of discriminating between petrological processes than the major elements and are used to assess the validity of petrogenetic and tectonic models. Trace elements are often classified and studied in groups and deviations or systematic changes from, and within, group behavior are used to indicate varying petrological processes. The value of trace element data for igneous geochemistry lies in the inherent nature of some trace elements to resist hydrothermal and metamorphic alteration and remain immobile in the rock.

This chapter discusses the trace element and rare earth element (REE) geochemistry of the representative lithologies of the Tally Pond Group including: 1) mafic volcanic rocks of the Lake Ambrose Formation; 2) felsic volcanic rocks of the Boundary Brook Formation; 3) felsic quartz-feldspar porphyritic rocks; and 4) mafic intrusive rocks of the Harpoon Gabbro. The purpose of this geochemical investigation is

primarily directed toward solving petrogenetic and tectonic, rather than alteration-related, problems. First, each of the different exploration zones and mineral occurrences will be described independently. The data will be used to categorize and classify lithologies based on composition and alkalinity. Second, the nature of the various paleotectonic environments that are represented by these volcanic rocks is discussed. Finally, rocks of the Tally Pond Group will be compared to other volcanic sequences in the Victoria Lake Supergroup and Newfoundland Dunnage Zone.

The samples submitted for geochemistry were collected throughout the Tally Pond Group with a particular emphasis in the Tally Pond area due to the extensive coverage of diamond drilling. Their selection was based on the need to provide a wide geochemical coverage for the various rock units in the Tally Pond area. Where possible, samples were collected from the interior of pillows and high level intrusions; samples showing excessive alteration, veining, or weathering were discarded. The samples include mafic flows and pillow lavas, gabbroic to dioritic intrusions, rhyolite and dacite from the Upper block, rhyolite and dacite from the Mineralized block, quartz porphyritic rhyolite and mafic dykes. The results are presented in Table A.1.

All geochemical analyses were performed at the Department of Earth Sciences, Memorial University of Newfoundland. Major-element oxides and selected trace element analyses were performed on pressed powder pellets using X-Ray Fluorescence (XRF) spectrometry, following the procedures of Longerich (1995). The REE were analyzed by inductively-coupled plasma mass-spectrometry (ICP-MS) following the $HF\text{-}HNO_3$ and Na_2O_2 preparation methods of Longerich *et al.* (1990) and Jenner *et al.* (1990). Details

regarding these analytical techniques, sampling protocol, elements analyzed, analytical methods, precision and accuracy of each method are outlined in appendices A and B.

In addition, geochemical data from exploration company archives has been added to this study for comparison and to provide a better spatial coverage throughout the Tally Pond Group. Geochemical data, from the southwestern end of the Tally Pond Group including the Lemarchant, Higher Levels, Beaver Pond, Spencer's Pond and Rogerson Lake prospects, were obtained from the Noranda Exploration archives. The data from Spencer's Pond and Rogerson Lake along with the South Tally Pond prospect were supplemented by more recent geochemical data derived by Altius Minerals Corporation. Data from the northeastern section of the Tally Pond Group, and the West Tally Pond area were supplied by Buchans River Ltd. It should be noted that the geochemical data from these companies is incomplete compared to the data analyzed for this study and as such not all of the exploration company data is used in the analysis.

In the following discussion, the data are separated into seven geographically separate mineralized zones that each contain several mineral occurrences (Figure 4.1). The Duck Pond zone encompasses the area between Tally Pond northward to Moose Pond and includes the Duck Pond Deposit, Boundary Deposit, East Pond and the North and South Moose Pond prospects. The Lemarchant-Spencer's Pond zone is located to the East of Rogerson Lake and includes the Lemarchant prospect and Spencer's Pond showing. The Higher Levels zone consists of a series of exploration grids that is located south of Lost Pond and east of Lake Ambrose. The Rogerson Lake-Beaver Pond zone occurs to the east of Rogerson Lake and extends northeast to the Beaver (Lost) Pond area. The South Tally zone occurs southeast of Lake Ambrose extending towards Rogerson

Lake while the West Tally Pond zone is located between West Tally Pond and Gills Pond.

4.2 Geochemical Nomenclature

The use of geochemical data to interpret the magmatic, petrogenetic, and tectonic history of volcanic rocks is based on the assumption that all or some of the original geochemical characteristics of the rocks have been preserved since their formation. Field evidence indicates that all of the rocks in the Tally Pond area, however, are weakly metamorphosed to lower greenschist facies, and several have undergone periods of intense hydrothermal alteration. Therefore, in this study, reliance is placed on elements that are perceived to have been immobile during alteration and metamorphism at low water/rock ratios. These include the major elements TiO_2 and P_2O_5, the high field strength elements (HFSE): Ti, Zr, Hf, Nb, Ta, Y and P; and the rare earth elements (REE): La to Lu. The REE can be further subdivided into light REE (LREE): La, Ce, Nd, and Sm; middle REE (MREE): Gd, Tb, Dy, and Ho; and heavy REE (HREE): Er, Th, Yb, and Lu. Most low field strength elements (LFSE): e.g. U, Rb, Sr, and Cs, are too mobile to be useful in altered rocks. Th, although by definition a LFSE, is however considered to be immobile during alteration and greenschist facies metamorphism (Jenner, 1996).

There are substantial variations in the geochemical signatures of magmatic rocks from oceanic and continental environments, signatures that reflect variations in source characteristics and magmatic differentiation processes, such as partial melting, fractional crystallization, assimilation, and contamination. In the following chapter, the distinction between arc volcanic rocks and nonarc volcanic rocks is based on geochemistry

following the suggestions of Wood *et al.* (1979), Sun (1982), and Swinden *et al.* (1989, 1997). Within these environments, a number of distinct petrochemical subtypes are recognized and allow for greater understanding of the finer structures of the tectonic settings.

Nonarc oceanic volcanic rocks are derived from heterogeneous mantle sources in which there are neither anomalous enrichments nor depletions in elements of similar geochemical character. Swinden *et al.* (1997) recognized three principal magmatic types of nonarc volcanic rocks based primarily on the behavior of the most incompatible elements. Normal mid-ocean ridge basalts (N-MORB) are depleted in the most incompatible elements and represent tholeiitic, mafic volcanism from segments of spreading ridges in major oceans or back arc basins. Ocean island basalts (OIB) are characterized by enrichment in the most incompatible elements and correspond to tholeiitic to alkalic volcanism related to hotspot or mantle plume activity. Enriched mid-ocean ridge basalts (E-MORB) represent tholeiitic volcanism from segments of spreading ridges affected by hotspot or plume activity, and have incompatible element patterns intermediate between those of N-MORB and OIB.

Oceanic volcanic rocks resulting from magmatism influenced by subduction are considered to exhibit an enrichment in LFSE (represented in altered rocks by Th) relative to the most incompatible HFSE (Nb and/or Ta), and a depletion in Nb relative to La. There are five distinct magmatic types recognized in arc volcanic rocks (Swinden *et al.*, 1997). Boninites (BON) are intraoceanic subduction zone volcanics that display a strong depletion in incompatible elements. Island arc tholeiities (IAT) represent partial melting of a mantle source that has been contaminated by mass transfer from a subducting slab

and are characterized by depletion of the most incompatible elements and a negative Nb anomaly. Transitional island arc tholeiites (TIAT) form in back arc basins, have geochemical characteristics transitional between N-MORB and IAT with depletion of the most incompatible elements and a weakly developed arc signature. Calc-alkalic basalts (CAB) represent partial melts of subduction-contaminated mantle sources and are enriched in the highly incompatible elements with strong negative Nb anomalies. High-magnesian andesites (HIMAG) are andesites characterized by high MgO, Cr, Ni and have HFSE, LFSE, and REE abundances that are more typical of CAB than BON. HIMAG are interpreted to represent hydrous partial melting of subduction contaminated mantle sources in island arc settings (Swinden *et al.*, 1997).

Two mobile elements that are commonly used in basalt petrogenesis are iron and magnesium as the fractionation between these elements is commonly defined as a differentiation index (Coish, 1977). In this study, the atomic [100 x Mg]/[Mg + Fe] ratio is used and referred to as the magnesium number (Mg#). Experimental studies (Ellis, 1968; Bischoff and Dickson, 1975), coupled with studies of ancient pillow lavas (Cann, 1971; Coish, 1977; Humphris and Thompson, 1978) and modern seafloor basalts (Alt and Emmermann, 1985) demonstrate that Mg is a major reactant in the hydrothermal alteration of basalts. Mg from seawater is taken up by basalt during chlorite-forming reactions whereas total iron is essentially conserved. The most important factor relating to the amount of Mg uptake during basalt alteration is the effective water/rock ratio of the system, as the amount of Mg-addition is proportional to the water/rock ratio (Seyfried *et al.*, 1978; Mottl and Seyfried, 1980; Mottl, 1983). These chemical changes during hydrothermal alteration are considered to be less intense in pillow cores rather than the

rims because the cores are altered at lower water/rock ratios and the cores contain more crystalline material from which elements are less easily mobilized than the glassy material at the rims (Coish, 1977).

Previous studies (Alt and Emmermann, 1985; Seyfried *et al.*, 1978) show that in rock altered at low water/rock ratios, changes in the Mg# are considered to be small to negligible. The Mg# exhibits consistent linear relationships with the immobile elements in petrogenetically related rock suites in the Tally Pond Group suggesting that alteration has not substantially affected the Mg# of these rocks. Consequently, the Mg# and FeO/MgO ratio are used in this study as indices of fractionation (cf. Swinden, 1987; Swinden *et al.*, 1990; Dunning *et al.*, 1991) because ferromagnesian minerals that crystallize at high temperatures are more magnesian than those that crystallize at lower temperatures. As a result, the Fe/Mg ratio of residual magma increases in the early and middle stages of fractional crystallization in practically all igneous rock suites. Consequently, this ratio may be used to represent the degree of fractional crystallization as rocks with low Fe/Mg ratios (high Mg#'s) are considered to have formed at higher temperatures and to be more primitive than those rocks with high Fe/Mg ratios (low Mg#'s).

4.3 Trace element discrimination diagrams for rock classification

4.3.1 Introduction

Before attempting to interpret the geochemical and tectonic significance of the volcanic rocks in the Tally Pond Group, it is necessary to subdivide them into geologically meaningful groups. As a first pass in understanding the geochemical

signatures, the samples are plotted on a discrimination diagram which distinguishes the various volcanic rock type differentiates and magma series. The bivariate, log-log scale plot of Nb/Y vs. Zr/TiO_2 (Winchester and Floyd, 1977) is used to distinguish the various rock types in metamorphosed and altered volcanic rocks. The Zr/TiO_2 ratio is taken as a measure of fractional crystallization, as this ratio tends to increase with increasing fractional crystallization since Ti is an incompatible element during basalt fractionation but the subsequent crystallization of an oxide (such as magnetite) causes Ti to become compatible. The Nb/Y ratio varies little with fractionation and this ratio is taken to correspond to parental controls and degree of alkalinity of the source (Barrett and MacLean, 1994) as Nb increases from tholeiitic to alkalic compositions.

4.3.2 Results

On the plot of Nb/Y vs. Zr/TiO_2 (Figure 4.2a) the volcanic and intrusive rocks within the Duck Pond zone define a bimodal distribution with three well defined groups. Mafic volcanic rock of the Lake Ambrose Formation have Zr/TiO_2 ratios ranging from 0.003 to 0.1 and Nb/Y ratios that vary between 0.006 and 0.2 and span the compositional range of sub-alkalic basalt or basaltic-andesite with one sample plotting in andesite field. Harpoon Gabbro intrusive rocks have approximately the same Zr/TiO_2 ratios but exhibit higher Nb/Y ratios of 0.3 to 0.5 and are restricted to the field of subalkaline basalt with minor overlap into the andesite field.

The felsic rocks of the Boundary Brook Formation of the Duck Pond zone are classified as largely rhyolite with some samples falling in the rhyodacite field. The rocks are divisible into three sub-fields. The majority of felsic volcanic rocks contain Zr/TiO_2

ratios of 0.1 to 0.3, Nb/Y ratios of 0.1 to 0.5 and comprise felsic volcanic and subvolcanic rocks from the East Pond and South Moose Pond showings and from the hangingwall of the Duck Pond and Boundary deposits. Rocks from the footwall sequence from both the Duck Pond and Boundary deposits form another sub-group that lie in the rhyolite field and contain approximately the same Zr/TiO_2 ratios but have higher Nb/Y ratios that vary between 0.2 and 0.5. Included in this group is one quartz-feldspar rhyolite porphyry sample from the Duck Pond deposit. Two samples from the North Moose Pond showing lie in the rhyodacite/dacite field and contain the lowest Nb/Y ratios of approximately 0.7.

Data from the West Tally Pond zone (Figure 4.2b) display three distinctive groupings. The Lake Ambrose Formation rocks are classified as andesite-basalt with limited variations in both Nb/Y and Zr/TiO_2 ratios. Rocks of the Boundary Brook Formation are intermediate in composition and contain Nb/Y ratios of 0.07-0.2 and Zr/TiO_2 ratios that vary between 0.02 and 0.04. These samples plot mainly as andesite with a select number of samples falling in the rhyodacite/dacite field. The felsic Boundary Brook Formation rocks from the West Tally Pond zone are rhyodacite and rhyolite. The samples display a wide range of Nb/Y ratios that vary between 0.1 and 0.4 with one sample containing an anomalously high value of 0.9. Zr/TiO_2 ratios fall in the range of 0.05-0.2; one sample exhibits a ratio of 0.3 and plots outside the field defined by the other felsic rocks.

The South Tally Pond zone Lake Ambrose Formation volcanic rocks (Figure 4.2c) are subalkaline basalts grading into andesitic basalts. Four samples contain lower Nb/Y ratios (<0.1) and plot as andesitic basalt, and one sample contains a higher Nb/Y

ratio and lies in the alkaline basalt field. An intermediate group of volcanic rocks generally falls into the andesite field with some extension into the dacite field. Nb/Y ratios for the mafic and intermediate rocks are fairly consistent and have values between 0.1 and 0.3. The Boundary Brook Formation volcanic rocks have Nb/Y (0.2-0.8) ratios that are slightly higher than those of the mafic and intermediate rocks. Zr/TiO_2 ratios are tightly constrained between 0.6 and 1.5; thus these rocks are classified as rhyolite and rhyodacite with some samples bordering the trachyte/andesite field. Two samples contain anomalously low Nb/Y ratios (<0.1) and plot away from the other felsic samples.

Data from the Higher Levels zone (Figure 4.2d) are separable into three groups. Mafic volcanic rocks of the Lake Ambrose Formation contain Zr/TiO_2 ratios between 0.05 and 0.2 and typically have high Nb/Y ratios of 0.7-2. These rocks are classified as alkaline basalt; however, two samples have lower Nb/Y ratios of 0.5 and are subalkaline basalt. Intermediate rocks are generally dacitic with minor andesite and trachyte samples present. Boundary Brook Formation volcanic rocks from the Higher Levels zone are subdivided into two sub-groups: an alkaline trachytic-andesite group and a rhyodacite to rhyolite assemblage. The trachyte/andesite samples have Nb/Y ratios of ~1 and Zr/TiO_2 ratios between 0.7 and 1.5 while the rhyodacite and rhyolite group have Zr/TiO_2 ratios the vary between 0.8 and 2 and Nb/Y ratios of 0.1-0.4.

Samples from the Rogerson Lake-Beaver Pond area (Figure 4.2e) consist of a triparte subdivision, similar to samples from the Higher Levels zone. Lake Ambrose Formation rocks have a wide range of Nb/Y values (0.2-2) and vary from alkaline basalt to andesitic basalt to subalkaline basalt. Intermediate rocks have similar Nb/Y values to the mafic rocks but contain higher Zr/TiO_2 ratios of 0.1 to 0.5 and are classified as

andesite and dacite with two samples being more alkaline and falling in the trachytic andesite field. Boundary Brook Formation volcanic rocks have fairly restricted Zr/TiO_2 ratios (0.07-0.2) and a large variation in the Nb/Y ratio which varies from a low of 0.08 to a high of 1.7. These rocks are mostly rhyolite with some samples overlapping into the rhyodacite field and others having the composition of trachyte/andesite.

The Lemarchant-Spencers Pond zone (Figure 4.2f) Lake Ambrose Formation volcanic rocks are alkaline basalt, Nb/Y ratios >0.7, with one sample having a Nb/Y ratio of 0.5 and classified as a subalkaline basalt. The intermediate rocks generally fall into the lower dacite/rhyodacite field but several samples fall into the trachyte/andesite and andesite field. Felsic rocks of the Boundary Brook Formation are similar to those from the Rogerson Lake-Beaver Pond zone, they have small variations in the Zr/TiO_2 ratios (0.08-0.27) and a large variation in the Nb/Y ratio (0.1-3). However, unlike the Rogerson Lake-Beaver Pond felsic rocks, the Lemarchant-Spencers Pond zone felsic volcanic rocks are dominantly trachytic andesite with minor rhyolite samples.

4.4 Normalized Rare Earth Element Geochemistry

4.4.1 Introduction

The rare earth element geochemical data for volcanic rocks of the Tally Pond Group is utilized to interpret the magmatic affinity and tectonic setting of the various rock types. The main elements used in these diagrams are the HFSE and the REE and Th. Th is a LFSE, but unlike other elements in the group, is resistant to alteration and metamorphic effects, and therefore provides the only opportunity to compare the primary behavior of these two different groups of elements in altered volcanic rocks. This is

important because the geochemical behaviour of the LFSE and HFSE is known to reflect the geological processes that are specific to differing tectonic environments. To compare the behavior of these different elements, they are plotted according to their bulk distribution coefficients with the most incompatible elements on the left increasing to the right in compatibility during partial melting of a peridotitic mantle that gives rise to a normal mid-ocean ridge basalt. The elements are normalized relative to the abundances in the primitive mantle (Wood, 1979), the hypothetical reservoir that existed after core separation, but prior to crust/mantle differentiation. There are other possibilities for normalizing factors available, e.g., Mid-ocean ridge basalt (MORB) and chondrite. Although the primitive mantle is a hypothetical reservoir, its composition is tightly constrained (Jenner, 1996). A customized primitive mantle normalized plot is used in this study, similar to those of Swinden *et al.* (1989, 1990) and Dunning *et al.* (1991), in which only those elements resistant to alteration are plotted.

4.4.1 Results

The geochemical REE-data for the Duck Pond zone are presented in appendix B.1 and graphically as Figures 4.3 to 4.7. In this section the mafic volcanic and intrusive rocks are discussed first, followed by an examination of the felsic volcanic rocks from the hangingwall and footwall of the Duck Pond deposit.

Mafic pillow lavas of the Lake Ambrose Formation from the Duck Pond zone are characterized by moderate LREE enrichment (La/Yb = ~2) with flat gently sloping extended REE patterns (Figure 4.3). The samples range between 2 to 11x primitive mantle values for the LREE and 4 to 5x for the HREE. They display prominent negative

Nb and Ta anomalies and positive Th anomalies with respect to La and Ce which is typical of island-arc, subduction related lavas (Swinden *et al.*, 1989). These samples also have prominent negative Zr and Hf anomalies with respect to the adjacent REE and less obvious to no negative Ti and Y anomalies of varying magnitude.

Extended REE patterns for the Harpoon Gabbro mafic intrusive rocks are illustrated in Figure 4.4. The rocks are enriched in the incompatible elements and are characterized by steep, relatively flat extended REE patterns (La/Yb = 3.5 to 4.9). Both samples are slightly enriched in Zr, Hf, and Ti relative to bordering REE. The prominent negative Ta anomaly in sample 284 is likely due to incomplete dissolution during the sodium peroxide sinter digestion method used to analyze the sample, and does not represent an actual depletion in Ta. The internal check of Zr and Hf analyzed by ICP-MS and XRF indicates that there are no further dissolution problems with the REE. Both samples have anomalously high Ti concentrations that are not present in corresponding V anomalies (section 4.52, Figure 4.10), thereby signifying that the anomalies are not the result of iron oxide crystallization. The most likely source of these anomalies is the presence of leucoxene, rutile or another Ti-rich phase related to alteration. The mafic intrusive rocks are enriched in the LREE, MREE, HREE and Th relative to the mafic volcanic rocks.

The extended REE plots (Figures 4.5, 4.6) for the Boundary Brook Formation felsic volcanic rocks from the hanging wall of the Duck Pond deposit are characterized by enrichment of the LREE relative to the HREE (La/Yb = ~3.7) and slightly concave upward patterns consistent with depletion in the MREE and HREE suggesting a control by amphibole fractionation (unlike the mafic samples). The samples range between 10 to

80x primitive mantle values for the LREE and approximately 10x primitive mantle for the HREE. Two samples of flow banded rhyolite (Figure 4.5) and two samples of porphyritic rhyolite (Figure 4.6) contain strong positive Th, and negative Ta, Nb anomalies, indicative of island-arc volcanism, along with prominent negative Ti and Eu anomalies. All four samples are slightly depleted in Y, strongly depleted in Nb. Compared to trace elements of similar compatibility the samples are variably enriched in Zr and Hf. Samples 208 and 212 both exhibit positive Zr and Hf anomalies relative to Nd and Sm; positive Hf and Zr anomalies are also present in sample 182. Three of the four felsic samples contain anomalously low Zr concentrations, in terms of ppm abundances, which is attributed to the lack of zircon; this was confirmed by petrography in the felsic volcanic rocks of the Tally Pond Group. The relatively low HREE concentrations also results from the absence of zircon, as zircon has a relatively large partition coefficient for the HREE. One of the porphyritic rhyolite samples (212) shows a relative depletion in the LREE when compared to the other samples. This sample contains a network of chlorite veins and has undergone at least one episode of alteration that is considered to have been responsible for the LREE depletion.

Four samples of rhyolitic flows from the footwall are the most LREE enriched felsic rocks; 80-90x primitive mantle (Figure 4.7). They have steep (La/Yb = 3.8 to 4.2) negatively sloping REE patterns, that indicate fractionation of the most incompatible elements, and all have distinctive negative Ti, Eu, Ta and Nb anomalies and positive Th anomalies. All of the samples contain small negative Y anomalies with respect to adjacent REE. Sample 288 is overall less enriched compared to the remaining three and displays a marked negative Nd anomaly along with severe depletion in the LREE relative

to the MREE and HREE. This sample is a highly altered and weakly mineralized rhyodacite that occurs immediately beneath the Duck Pond deposit. There appears to be a minor amount of mass gain in the rock and the alteration seems to have preferentially stripped the rock of LREE-La, Ce and Nd.

4.5 Tectono-magmatic discrimination diagrams

4.5.1 Introduction

Previous studies (Pearce and Cann, 1971, 1973; Pearce, 1982; Shervais, 1982; Meschede, 1986) have shown the applicability of using trace element geochemical data to discriminate between magmas produced in different tectonic settings. The relatively simple approach of using a few readily determined trace elements and the wide applicability of this technique have led to the publication of numerous papers describing the trace element signatures of the various tectonic environments. By comparing the trace element compositions of ancient volcanic rocks to their modern day counterparts, the paleotectonic environment of rocks whose state of preservation and/or poor exposure had previously precluded their identification, meant that their paleotectonic setting could now be determined.

Discrimination diagrams rarely provide indisputable proof of a former tectonic environment, however and at best the diagrams should be used only to suggest a relationship. To enhance their applicability and usefulness, numerous discrimination diagrams that incorporate various trace elements should be used to complement one another. It should be noted that with increasing ages of rocks used, the diagrams move

further away from the control set of samples used in the construction of the diagram and therefore there is a greater degree of ambiguity involved.

4.5.2 Results

The Ti/Y ratio is used in the triangular diagram, Ti-Zr-Y (Pearce and Cann, 1973) to identify rocks that have within plate basalt signatures. The characteristics include the enrichment in Th, Nb, Ce (and other LREE and P), Zr (and Hf), and Ti with respect to N-MORB and similar values in Y and HREE as N-MORB. Due to the fact that the absolute levels of the enriched elements vary with fractional crystallization, the ratio of enriched to unenriched elements is used to distinguish WPB magmas when compared to N-MORB. Of the enriched elements, Th can also be enriched in IAT whereas Th plus Nb and Zr are enriched in E-MORB. Therefore, because Ti is not significantly affected by these processes, WPB magmas may be best identified by high values of the Ti/Y ratio (Pearce, 1982; Pearce, 1996). Using this ratio alone does not enable the distinction between MORB and IAT magmas. However, by adding Zr to the diagram, the separation of MORB and IAT is possible.

The mafic rocks of the Lake Ambrose Formation are divisible into two distinctive groups. Volcanic rocks of the Duck Pond zone (Figure 4.8a) plot in fields A and B, indicative of island arc basalt, whereas mafic intrusive dykes and plutonic rocks of the Harpoon Gabbro contain lower Y concentrations and fall into the field of within-plate basalts with minor overlap into the calc-alkaline field. Rocks from the West Tally, Lemarchant-Spencers Pond, Rogerson Lake-Beaver Pond and Higher Levels zones (Figure 4.8b) plot mainly into fields A and B as island arc basalts. However, six samples

fall into the within-plate basalt field – D and two samples plot as calc-alkaline basalts in field C.

To distinguish IAT from other magma types, particularly MORB, their characteristics must be identified and utilized; these are the selective enrichment of Th relative to other elements (particularly the MREE and HREE) and the relative depletion of Ti and Y, and sometimes Zr (and Hf) and Nb (or Ta), relative to N-MORB. In IAT, Th enrichment is not accompanied by the simultaneous enrichment in Nb, Zr and Ti as it is in WPB or Nb in E-MORB (Pearce, 1996). Therefore, IAT may be characterized by higher Th/Ta ratios. With the addition of Hf to produce a Hf/3-Th-Ta diagram (Wood *et al.*, 1979), IAT and the different types of MORB can be distinguished. N-MORB occupies a field closest to the Hf apex while E-MORB and WPB plot with lower Hf/Ta ratio. The IAT field can be subdivided based on the Hf/Th ratio. Mantle enrichment/depletion and melting events above subduction zones are affected by the selective enrichment of the mantle in subducted Th and consequently cause the source composition to move toward the Th apex of the triangle. Therefore volcanic rocks that experienced high degrees of subduction zone enrichment are represented by lower (< 3) Hf/Th ratios (Pearce, 1996; Rollinson, 1993).

Mafic volcanic rocks of the Boundary Brook Formation (Figure 4.9) are characterized by low Ta contents, and Hf/Th ratios that vary between 0.6 and 2.2 with an average value of 1.3. All of these rocks plot in the island arc tholeiite field. The one sample from the Harpoon Gabbro has a higher Ta content and a slightly higher Hf/Th ratio of 2.3. This sample falls in the E-MORB/WPB field on the Hf/3-Th-Ta diagram.

The other unique feature of IAT, the depletion of Ti and Y, can be used to construct a discrimination diagram that separates IAT from MORB and WPB. Because evolved IAT can contain the same Ti contents as MORB or WPB due to the effects of crystal fractionation, Ti must be plotted against a compatible index of fractionation. V is used as this index and is plotted against Ti/1000 to distinguish between volcanic-arc tholeiites, MORB and alkali basalts (Shervais, 1982). The different fields are subdivided using their Ti/V ratios. IAT plot between a Ti/V ratio of 10 and 20, MORB and continental flood basalt (CFB) plots between Ti/V ratios of 20 and 50, OIB have Ti/V ratios of 50 to 100 and CAB plot between Ti/V ratios of 15 and 50 in a near vertical trend. It should be noted that there are several fields of overlap between the various groups.

The majority of mafic volcanic rocks from the Tally Pond Group show a minimal Ti spread with varying amounts of V, have Ti/V ratios less than 20, and plot in the field for island-arc tholeiites (Figure 4.10). A few samples contain higher Ti contents and have Ti/V ratios slightly greater than 20 and exhibit MORB characteristics. The mafic intrusive rocks, gabbro intrusions and diorite dykes, exhibit a slight V spread but display a large variation in Ti content. Ti/V ratios vary from a low of approximately 20 to a high of slightly greater than 50. The rocks plot in the field of CFB/ MORB and in the OIB and alkaline basalt fields. Several samples have anomalously high Ti/V ratios and plot outside of the defined geochemical fields. This discrepancy is attributed to excess cumulate magnetite that is now altered to leucoxene, and therefore is not a true primary liquid composition. This excess magnetite would have little to no dilution effect on the abundances of other incompatible trace elements.

Continental IAT differ from oceanic IAT in their higher Ta, Nb, Zr and Hf concentrations, therefore ratios such as Zr/Y and Nb/Y are used as to distinguish between oceanic and continental IAT. A logarithmic Zr–Zr/Y diagram (Pearce and Norry, 1979) is used to for this purpose and discriminates between basalts from volcanic island arcs, MORB and WPB. By plotting the Zr/Y ratio against the fractionation index Zr, volcanic arc basalts plot in fields A and D, MORB in fields B and D, and WPB in field C. This diagram (Figure 4.11) can also be used to subdivide the mafic rocks of Lake Ambrose Formation of the Tally Pond Group into those belonging to oceanic arcs, where only oceanic crust is used in arc construction, and arcs developed at continental margins. The fields are separated on the basis of a Zr/Y ratio of 3. Oceanic arcs plot in the field with Zr/Y ratios less than 3, while continental arcs plot with higher Zr/Y values and Zr contents.

Lake Ambrose Formation volcanic rocks from the Duck Pond and West Tally Pond zones (Figure 4.11a) contain Zr contents that vary from a low of 30 to a high of 70 ppm. The majority of samples plot in field B with overlap into field C, the fields defined by island-arc basalts and MORB. Zr/Y ratios have values between 2 and 5 and most samples fall in the field of ambiguity between continental and oceanic arcs. Harpoon Gabbro intrusive rocks from the Duck Pond zone are characterized by higher Zr contents (10 to 250 ppm) and higher Zr/Y ratios of between 5 and 6. These samples consistently plot into field A, that of within-plate basalts. Data for the Lemarchant, Higher Levels and Rogerson Lake-Beaver Pond zones exhibit the same general Zr contents; however, some samples have higher Zr/Y and plot outside the defined geochemical fields. Most samples show a continental influence as Zr/Y ratios are greater than 3.

Figure 4.12 is a binary diagram from Swinden *et al.* (1989) where Y is plotted against the Nb/Th ratio. The Nb/Th ratio is a measure of the extent of Nb depletion and Th enrichment in the magma source in that it separates arc signatures with a low Nb/Th ratio from non-arc signatures with higher Nb/Th ratios. Y provides an indicator of the relative incompatible element depletion in the magma as very low Y concentrations indicate highly depleted rocks that may constitute second stage melts. The stippled field of overlap between fields is due to the gradational nature of the geochemical boundaries between the differing rock types and from the uncertainties in the analytical techniques utilized (Swinden *et al.*, *op. cit.*).

Data from the Duck Pond and West Tally Pond zones are characterized by extremely low Nb/Th ratios. All of the samples contain Nb/Th ratios of less than 2.5, except for one anomalous sample that has a value of approximately 6. The mafic volcanic rocks of the Lake Ambrose Formation lie in the field of normal arc magmatism, with one mafic intrusive sample falling in the field of overlap between the normal arc and non-arc signatures. This diorite dyke has a Nb/Th ratio that is over three times a high as the volcanic rocks and is considered to have a non-arc signature. There is a wide range of Y values in these rocks, from a low of 11 to a high of almost 50. This may result from differences in the source reservoirs and/or the various degrees of fractionation between the different rocks; with the more differentiated rocks having lower Y contents. Alternatively, mass changes and Y mobility due to hydrothermal alteration may be responsible.

The linear bivariate plot of Zr and Ti (Pearce and Cann, 1973) is used to subdivide the mafic rocks into four separate geochemical fields. Fields A, C, and D are

outlined for IAT, CAB and MORB respectively while field B contains all three magma varieties. Pearce (1982) developed a modified version of the Zr-Ti plot by using a Logarithm scale rather than a linear scale. This version is extended in magma composition to include within-plate basalts.

The mafic rocks of the Lake Ambrose Formation have Ti contents less than 10 000 ppm and Zr concentrations of less than 100 ppm. As a result, the bulk of mafic volcanic rocks from the Duck Pond and Rogerson Lake-Beaver Pond zones (Figure 4.13a) plot in fields A and B. These signatures are typical of island-arc tholeiites, with possible MORB and/or CAB characteristics. Some samples from the Lemarchant, Higher Levels and South and West Tally zones (Figure 4.13b) contain elevated Zr contents and plot in field C, the area defined by calk-alkaline basalts. The samples that plot in field D are the mafic intrusions. Diorite dykes from the Duck Pond zone and gabbro plutons from the Rogerson Lake-Beaver Pond zone and Duck Pond deposit contain higher Ti and Zr contents and exhibit geochemical signatures consistent with MORB.

Using the logarithm plot of Zr vs. Ti (Figure 4.14), the greater part of mafic volcanic rocks plot in the volcanic-arc field. There are however, a considerable number of samples that overlap with the field defined by MORB. The mafic intrusive rocks of the Tally Pond Group exhibit within-plate basalts signatures with a few samples falling in the MORB field of overlap. The apparent scattered nature of the samples on both the linear and logarithmic Zr-Ti plots may in part result from mass changes due to hydrothermal alteration. Alternatively, the presence of any minerals (iron-titanium oxides or apatite) that contain the elements being used may cause the samples to plot erroneously and be misclassified.

A bivariate logarithm plot of Y vs. Nb (Figure 4.15) is used to subdivide the felsic rocks of the Boundary Brook Formation of Tally Pond Group. The HFSE elements Nb and Y are chosen because they are at both ends of the enrichment spectrum, the Nb/Y ratio varies little with fractionation, Nb increases from tholeiitic to alkalic compositions and therefore this ratio is taken to correspond to parental controls and degree of alkalinity of the source magma. The felsic rocks from the Duck Pond deposit plot (Figure 4.15a) as two groups that both lie in the volcanic-arc granite/syn-collisional granite field. One sample from the hanging wall displays an ocean ridge granite signature. The 17 samples from the hanging wall show a moderate Nb spread (1 to 10 ppm) and a large variation in Y (20 to 50 ppm), while the 11 samples from the footwall have a minimal variation in Nb (6-9 ppm) with a larger disparity in Y (9-40 ppm). It is interesting to note that the two samples of the quartz porphyritic rhyolite that occur in the hanging wall plot with the samples from the footwall.

Data from the West Tally Pond zone (Figure 4.15b) are characterized by Y concentrations between 10 and 50 ppm and Nb contents of 2 to 10 ppm. All of the samples fall in, or just outside of, the field for volcanic arc granites. Felsic volcanic rocks from the Lemarchant-Spencers Pond zone contain the same Y amounts but are slightly more enriched in Nb (3-15 ppm). These rocks, like those from the West Tally Pond zone, all plot in or near the volcanic arc granite region.

4.6 Trace elements for volcanic affinity

4.6.1 Introduction

Previous studies (Barrett and MacLean, 1994, 1999; MacLean and Barrett, 1993) have shown the applicability in using trace and rare earth elements to arrange samples into groups of differing chemical affinity. Trace element data from mafic and felsic volcanic rocks from the Tally Pond Group are used to compare different rock suites and to sort these rocks into tholeiitic, calc-alkaline, and transitional groups and to illustrate genetic relationships and possible petrogenetic controls on rocks genesis and tectonic environment of formation.

The methodology in using trace elements to infer genetic relationships is in the premise that incompatible and immobile HFSE data for a suite of volcanic rocks should produce linear enrichment trends from the mafic to felsic compositions. Petrogenetically related volcanic rock suites should exhibit and maintain constant HFSE ratios and thus plot as a linear line that intersects the origin. Additional, the REE can be used along with the HFSE as indicators of magmatic affinity, because the HREE are geochemically similar to Y and are less incompatible than LREE and Zr, Nb, Hf and Th. Therefore, the ratios of LREE/HREE and Zr/Y are usually higher in calc-alkaline suites than in tholeiitic rocks.

4.6.2 Results

The volcanic rocks are plotted on a Zr–Y diagram (Figure 4.16a-f) of Barrett and MacLean (1994) to subdivide them on the basis of volcanic affinity. The HFSE are highly incompatible in most mafic rocks and in intermediate to felsic suites of tholeiitic affinity. Some ratios between HFSE, which are usually immobile, change with rock affinity and can therefore be used as a discriminant that is unaffected by alteration. This

change is best exhibited in the Zr/Y ratios, and range from ~3 to 5 for tholeiites, to ~7 to 30 for calc-alkaline rocks. Those rocks with intermediate Zr/Y ratios of ~5 to 7 are considered to be transitional.

The data from the Duck Pond zone (Figure 4.16a) plot as two distinct trends. The upper trend represents the pillow lavas and rhyolitic rocks from the hanging wall of the Duck Pond Deposit and defines a linear trend with an average Zr/Y ratio of 4.3 that plots in the tholeiitic field. The lower trend represents the rhyodacite from the footwall of the deposit and the porphyritic rhyolites from the hanging wall and gabbro-diorite dykes from both the footwall and hanging wall. This group has a Zr/Y ratio of 6.1 and plots in the transition field, indicating that the rocks have both tholeiitic and calc-alkaline affinities.

Rocks from the West Tally Pond zone (Figure 4.16b) are similar to those from the Duck Pond zone as they are divisible into two separate data sets. The bulk of the samples have Zr contents of 10 to 200 ppm and Y concentrations of between 10 and 50 ppm. They plot as a linear trend that has a Zr/Y ratio less than five and fall in the tholeiitic field. A smaller second set of samples contain higher Zr contents (100-1800 ppm) and a very restricted Y concentration of between 15 and 30 ppm. These rocks are mainly transitional in nature with one sample plotting in the tholeiite field and four samples falling in the calc-alkaline field.

Data from the South Tally Pond zone (Figure 4.16c) of the Tally Pond Group are separable into two distinct groups, one that is tholeiitic and the other, calc-alkaline in nature. The tholeiitic group has Zr concentrations of 30-200 ppm and Y values of 15 to 50 ppm and most samples have Zr/Y ratios of less than five. However, some samples

contain slightly higher Zr/Y ratios and plot along the margin of the transitional field. The calc-alkaline group has higher Zr contents that vary from a low of 75 ppm to a high of 275 ppm and lower Y contents between 10-30 ppm. The samples exhibit a weak linear trend and all of them have Zr/Y ratios greater than 7.

Rocks from the Higher Levels zone (Figure 4.16d) exhibit highly variable Zr (40-220 ppm) and Y (10-85 ppm) contents and are not divisible into distinct linear trends. The samples predominantly contain Zr/Y ratios less than five, with an average value of 3.6 and plot in the tholeiitic field. Seven samples contain Zr/Y ratios between five and seven, and have an average Zr/Y value of 5.9. These samples are therefore considered to be transitional between tholeiitic and calc-alkaline. Four samples from the Higher Levels zone have Zr/Y ratios between 8.3 and 13.6 with an average Zr/Y ratio of 10.5, consistent with a calk-alkaline affinity.

Rogerson Lake-Beaver Pond zone (Figure 4.16e) rocks are similar to those from the Higher Levels zone in that they contain highly variable Zr (20-300 ppm) and Y (10-69 ppm) contents, exhibit considerable scatter and do not define clear linear trends. The bulk of the samples plot in the tholeiitic field and have Zr/Y ratios between 1.0 and 4.9 with an average Zr/Y ratio of 3.1. An additional eight rocks contain Zr/Y ratios between 5.0 and 6.9 (average 6.0) and lie in the transitional field. A further seven samples from the Rogerson Lake-Beaver Pond zone have higher Zr/Y ratios of 7.0 to 21.4 with an average value of 10.2 and are indicative of calc-alkaline magmatism.

To distinguish tholeiitic from calc-alkaline rocks in orogenic environments, Gill (1981) used the initial Fe/Mg ratio and the rate of change of this ratio with increasing SiO_2 content. However, SiO_2, FeO and MgO are not used directly in this study because

these elements are mobile during alteration and their use is not always practical in ancient volcanic rocks. Consequently, TiO_2 and V are utilized because they vary proportionally with FeO in the non-alkaline series (Miyashiro, 1974, Shervais, 1982). TiO_2 contents typically increase with differentiation for tholeiitic rocks, while TiO_2 decreases during fractionation in calc-alkaline magmatism. V concentrations generally follow those of Ti and as a result, increasing or decreasing TiO_2 and V with fractionation (represented by the FeO/MgO ratio and Mg#) can be used as an indicator for tholeiitic and calc-alkaline magmas, respectively.

The plot of TiO_2 versus Mg# (Figures 4.17a-e) for mafic rocks of the Lake Ambrose Formation of the Tally Pond Group highlight the range of rock varieties present and illustrate geochemical relationships within the group. Mg#'s range from 50 to 80 in the West Tally Pond, Duck Pond, Rogerson Lake-Beaver Pond zones, to 40 to 60 in the Higher Levels zone while the South Tally Pond zone has Mg#'s that range from 10 to 70 with the majority having Mg#'s between 30 and 60. TiO_2 data appear to increase with decreasing Mg# in the Duck Pond, West Tally Pond, Rogerson Lake-Beaver Pond and Higher Levels zones; the data suggest a weak correlation as the samples at low TiO_2 concentrations span a range of Mg# and permit different correlation trends to be drawn. There is considerable scatter in the samples from the South Tally Pond zone samples and no trends are present in MG# between 15 and 55; some samples with the highest Mg#, however, generally have lower TiO_2 and are considered to be tholeiitic.

Some of the rocks of intermediate composition from the South Tally and West Tally Pond zones exhibit flatter TiO_2 enrichment trends with decreasing Mg#. These

samples show little or no increase in TiO_2 with differentiation, indicating that these rocks are in all probability transitional between tholeiitic and calc-alkaline magma series.

Vanadium concentrations (Figure 4.18a-e) typically parallel those of TiO_2 increasing with decreasing Mg#. Data from the West Tally Pond, Rogerson Lake-Beaver Pond, and Duck Pond zones show subtle enrichment trends. However, these trends are not as obvious as those for TiO_2. Samples from the South Tally Pond zone display extensive scatter and linear enrichment trends are not obvious. V contents from the Higher Levels zone are dichotomous and display two possible trends. The lower trend consists of six samples that show a marked increase in V with decreasing Mg#. The upper trend of five samples displays the opposite and indicates a decrease in V with fractional crystallization. There is no obvious process to account for these trends. Nonetheless, a weak relationship between V and Mg# in these rocks is increasing V content with decreasing Mg# which, like TiO_2, indicates that the Tally Pond Group rocks are tholeiitic.

4.7 Discussion

The Tally Pond Group comprises a mixed volcanic assemblage dominated by felsic pyroclastic rocks with lesser mafic flows and intrusions. The assemblage ranges from depleted arc tholeiitic basalt to moderately LREE-enriched rhyolites with tholeiitic affinities and transitional to slightly calc-alkaline, variably LREE-enriched rhyolite. The basaltic rocks consistently exhibit an arc signature based on their negative Nb anomalies on extended REE plots and their Zr–Zr/Y ratios and high V contents relative to Ti. They are actually depleted arc tholeiites with moderate LREE enrichments. The felsic rocks range from rhyolite to rhyodacite and display a volcanic arc signature due to their high

Y/Nb ratios. These rocks are variably LREE-enriched island arc volcanic rocks that are mainly tholeiitic in nature with some of the samples having transitional to slight calc-alkaline affinities. Gabbro and diorite intrusions into the mafic and felsic rocks are subalkalic basalt in composition, transitional in nature, and exhibit LREE enrichment relative to the MREE and HREE. The altered felsic rocks that lie beneath the Duck Pond VMS deposit exhibit REE depletions of different magnitudes. Europium is depleted in all of the samples to varying degrees and the most heavily altered and weakly mineralized samples have the largest negative Eu anomalies in addition to severe depletion in the LREE-La, Ce, and Nd.

Although there may be minor natural variations in the total REE contents between the samples, these large differences in REE concentrations, seen in the felsic volcanic rocks, are considered to result from mass changes induced by hydrothermal alteration. The anomalously low Ti contents (reflected by negative Ti anomalies) in the felsic volcanic and subvolcanic rocks, in all probability results from the absence of TiO_2, which would initially be incompatible in the mafic composition of the parental magma. Ti concentrations initially increase with silica contents in a fractionating tholeiitic basalt magma, and reach a maxima between 50 % and 57 % SiO_2, thereafter decreasing.

The weak to moderate negative Eu anomalies in all the felsic volcanic samples may be due to a couple of factors. Eu anomalies in felsic magmas are predominantly governed by feldspars (Philpotts, 1990). One cause of Eu depleted magmas may involve plagioclase fractionation. Eu is significantly more compatible than all the rest of the REE with respect to plagioclase and thus plagioclase always has a positive Eu anomaly. Therefore, the removal of feldspar from a felsic melt by crystal fractionation or the partial

melting of a rock in which feldspar is retained in the source will produce a negative Eu anomaly in the melt. Alternatively, the relative Eu depletion in the felsic rocks may be the result of the breakdown and destruction of plagioclase during intense episodes of hydrothermal alteration.

The mafic volcanic rocks of the Tally Pond Group consistently display an enrichment of approximately 10 times for the MREE and HREE relative to primitive mantle, and are slightly more enriched in the LREE. This pattern is typical of island arc basalts and could result from high degrees of fractional crystallization from a MORB or OIB source, but the high Mg#s and particularly consistent REE patterns between the mafic rocks are evidence against such an origin. Instead, the high LREE contents are interpreted to result from varying degrees of partial melting in the source region that requires the addition of a component rich in the LREE (Hanson, 1978; Philpotts, 1990). This component is in all probability a hydrous fluid or water-saturated silicate melt that is derived from the subducted oceanic slab and added to the sub-arc mantle wedge. To generate REE patterns with the prominent negative Nb anomaly, characteristic of island arc volcanism as exhibited by mafic volcanic rocks, the subduction zone fluids must be strongly depleted in Nb, which when superimposed upon the Nb-enriched mantle source component would produce arc basalts with a negative Nb anomaly (Wilson, 1989). A Nb deficient hydrous fluid could be produced during subduction if Ta and Nb are retained in a titaniferous mineral phase such as ilmenite or titanite within the subducted oceanic crust (Saunders *et al.*, 1980).

The variations in REE patterns between the mafic and felsic volcanic rocks are possibly the result of fractionation differences between the mafic and felsic endmembers.

The felsic volcanic and subvolcanic rocks of the Tally Pond Group are 50 to 80x enriched in the LREE, relative to primitive mantle, and 5 to 8x more enriched in the LREE when compared to the mafic rocks. This variability between the mafic and felsic endmembers results from the LREE being the most incompatible of the REE and therefore remaining in the melt phase until the final stages of fractionation. The slightly concave-upward extended REE patterns exhibited by some of the felsic rocks results from the relative depletion of the MREE with respect to the LREE and HREE. The MREE are more compatible than the LREE and the depletion in the felsic rocks is attributed to fractionation from an amphibolite-facies source region (Dunning *et al.*, 1991; Swinden, 1987). Amphibolite facies rocks are characterized by hornblende, plagioclase and sphene, of which hornblende is the most geochemically important. Hornblende has a large partition coefficient for the MREE and differentiation of a magma in which hornblende remains in the source will result in a liquid that is depleted in the MREE. Such a source could be generated at the base of the continental crust in an island arc setting (constrained by the negative Nb and Ta anomalies) by the partial melting of an ocean floor MORB in the subducting lithosphere, producing an eclogitic residue. Alternatively, differentiation of basalts derived from partial melting of the mantle wedge above the subducting oceanic crust may also generate such a source. If the felsic rocks are derived by partial melting of basalt that had been converted to eclogite in the subducting ocean crust, they should be severely depleted (<2 or 3x primitive mantle) in the MREE and HREE. However, the MREE and HREE for the felsic rocks of the Tally Pond Group are approximately 10x primitive mantle and hence argue against such an origin. Therefore, the alternative interpretation of the felsic rocks being derived from differentiation of a mantle-sourced

basalt is favored. A felsic rock produced from such a source will display a rather flat REE pattern that is slightly enriched in the LREE and will also contain a prominent negative Eu anomaly, both of which are characteristic of the Tally Pond Group, Boundary Brook Formation rocks.

The felsic volcanic rocks of the hanging wall and footwall of the Duck Pond deposit show some slight differences. The two rock groups have the same general Nb-Y ratios but differ in the variation of each element; hanging wall rocks contain a large variation in Y and moderate variations in Nb, whereas the footwall rocks exhibit minor variations in both elements. Zr-Y ratios demonstrate that the hanging wall volcanic rocks have tholeiitic affinities, whereas felsic rocks from the footwall are transitional to somewhat calc-alkaline in nature. Comparison of the HFSE and REE elements from the hanging wall and footwall also illustrate that there are minor differences between the two rocks groups. Both rock groups have relatively flat to slightly concave-upwards patterns and are depleted in the MREE and HREE. All of the rocks exhibit prominent negative Ta, Nb and Ti anomalies. The differences in the hanging wall and footwall felsic volcanic rocks are in the degrees of LREE-enrichment; the footwall rocks are slightly more enriched in the LREE than those of the hanging wall.

Overall the felsic rocks of the Boundary Brook Formation do not appear to define a fractionation trend with the mafic varieties of the Lake Ambrose based on their Zr/Y ratios. The mafic rocks in the hangingwall of the Duck pond deposit, however, lie on the same trend as the hangingwall felsic rocks. Genetically related volcanic rock suites exhibit consistent Zr and Y enrichment from basalt to rhyolite and plot as clearly defined linear trends for those rocks with a tholeiitic affinity (MacLean and Barrett, 1993). The

data points do not plot as a continuous gradational overlap as would be excepted if a petrogenetic relationship were present between the two rock types. The data, however, do not preclude a relationship between the mafic and felsic rocks in the hangingwall of the Duck Pond deposit. Such trends are not readily visible in the Tally Pond Group rocks implying that the mafic and felsic endmembers are not genetically related. This hypothesis is further supported by the REE data. The REE concentrations for the felsic volcanic rocks do not parallel those of the mafic rocks and the overall abundances of the mafic volcanic rocks are less than those of the felsic rocks.

The general trend of increasing TiO_2 concentration with decreasing Mg# suggests that the Tally Pond volcanic rocks may result from fractional crystallization. If the mafic and felsic rocks were related by fractional crystallization, then the incompatible and compatible elements should co-vary over a range of bulk compositions. The trace element data for the Tally Pond Group do not co-vary, indicating that the mafic and felsic rocks are separate petrologically unrelated rock suites. Volcanic arc environments are notoriously complex geochemically and the disparity in the trace element abundances between the mafic and felsic rocks of the Tally Pond Group is considered to reflect variations in the source characteristics coupled with differences in the degree of partial melting, contamination and accumulation of minor phases.

Geochemical variations in Ti-Zr-Y ratios of the Tally Pond volcanic rocks are best explained by differing degrees of partial melting and enrichment in the source rocks. The differences in MORB and WPB are explained by plotting petrogenetic vectors using rocks with average N-MORB mantle compositions. These models indicate that low degrees of partial melting and enrichment events in garnet lherzolite facies move

compositions away from the Y apex and into the field of WPB. In contrast, shallow melting and enrichment in spinel lherzolite facies causes an increase in Zr concentration in the N-MORB composition as Zr becomes the most incompatible element (Pearce, 1996).

The highly depleted mantle sources and high degrees of melting that are characteristic of most island arcs are the two processes that best explain the partial discrimination of IAT from N-MORB compositions (Pearce, 1996; Pearce and Peate, 1995). The depletion of the mantle source may take place in the back-arc as the mantle advects into the mantle wedge. The high degrees of melting in island arcs are due to the combination of water in the mantle and decompression beneath the arc. Both of these processes cause N-MORB compositions to move away from Zr, that is toward the IAT field. The discrimination of calc-alkaline basalts is best explained by assimilation of the upper crust which incorporates Zr-rich material into the N-MORB magma and moves compositions of continental arcs toward upper crust composition (Pearce, 1996).

Petrogenetic models can also be used on a Th-Ta-Hf diagram as an indicator of subduction zone affinity. As with the Ti-Zr-Y diagram, mantle enrichment and depletion coupled with melting events will cause the magma compositions to move away from the average N-MORB composition. Rocks with this average N-MORB mantle composition plot in field A and mantle depletion or high degrees of partial melting will cause the resulting magma to be enriched in Hf. Conversely, mantle enrichment or low degrees of partial melting will result in magma compositions that move away from the Hf apex. Melting above subduction zones also tends to move compositions away from Hf, however, in this setting the selective enrichment of subducted Th in the mantle causes the

source composition to trend towards the Th apex and into the IAT field (Dudás, 1992; Pearce, 1996).

There are, however, ambiguities involved in these interpretations as the position of average upper crust lies in the calc-alkaline end of the IAT field which suggests the importance of continental contamination in magmas erupted in attenuated continental settings. The continental tholeiitic rocks of the Tally Pond Group that plot in the IAT field with Hf/Th ratios less than three are considered to have assimilated a Th-rich crustal material, which displaces the magma away from the tholeiitic IAT or MORB fields (Dudás, 1992; Pearce, 1987; Pearce, 1996). Naturally, this raises the question as to whether the Th enrichment represents a true subduction component (i.e. an island arc setting) or is the result of assimilation of continental crust. The easiest way to resolve this ambiguity is to use the Th-Ta-Hf diagram in conjunction with a projection that does not rely on elements that are strongly enriched in the crust such as Ti and V. These elements are less sensitive to magma-crust interaction and therefore actual IAT should plot in the IAT field on both diagrams. On the other hand, basalts that have been contaminated with crustal material usually plot in the IAT field of the Th-Ta-Hf projection and the MORB field of the Ti-V plot.

The geochemical data indicate that the volcanic rocks of the Tally Pond Group are viewed as broadly bimodal, with geochemical affinities to two tectonic environments. The mafic and felsic volcanic rocks have characteristics of island arc magmatism in their HFSE and REE elements and plot in plate marginal fields on the Ti-Zr-Y diagram. All of the rocks exhibit distinctive positive Th and negative Ta and Nb anomalies which indicate that magmatism was influenced by a subducting slab (Swinden *et al.*, 1989).

The mafic intrusive rocks of the Harpoon Gabbro exhibit no geochemical island arc affinities and plot in the within plate basalt field on the Ti-Zr-Y diagram. The distinctively high Ti/V and Zr/Ti ratios coupled with the obvious lack of a negative Nb anomaly in the REE patterns for the mafic intrusive rocks are characteristic of boninites and may result from a subduction component derived from partial melting of the subducting slab (Pearce *et al.*, 1992). The relatively high Ti/Sc values for these rocks coupled with less incompatible elements (Zr and Y), however, suggest partial contamination by crustal material in a non-subduction related environment. This interpretation is supported by the positive Nb anomaly and overall REE patterns which are similar to calc-alkaline rocks. These rocks are considered to be generated from partial melts of mantle sources with assimilation of continent (or continent derived) crustal component that are not contaminated by a subduction-derived component.

4.7.1 Relationship to other volcanic sequences in the Victoria Lake Supergroup

The Victoria Lake Supergroup comprises the volcanic sequences of the Tulks Hill assemblage and Tally Pond Group and one or more sequences of clastic sedimentary rocks (Evans and Kean, 2002; Rogers and van Staal, 2002). Felsic volcanic rocks are the principal volcanic rocks in the Victoria Lake Supergroup and for the most part consist of low-K rhyolite and rhyodacite (Evans, 1993). Mafic volcanic rocks represent less than half of the total volcanic rocks in the Victoria Lake Supergroup (Figure 4.19), however, the majority of geochemical data exist for these rocks. Evans and Kean (2002) recognized four diverse geochemical groups of mafic volcanic rocks of arc and non-arc signatures,

and they interpreted these differences to represent different paleotectonic environments of formation (Figure 4.20).

The primitive island-arc volcanic rocks are represented by the mafic volcanic rocks of the Cambrian Tally Pond Group, presented in the preceding discussion. The Sandy Lake basalts exhibit a similar island-arc signature as the Tally Pond mafic rocks, however, the REE concentrations are much more depleted than in the Tally Pond rocks (Rogers and van Staal, 2002) and thus the Sandy Lake basalts may have chemical affinities to boninites (Swinden *et al.*, 1989; Evans *et al.*, 1990). The Tulks Hill, Baxter's Pond, and Beatons Pond basalts, exhibit mildly to highly depleted, relatively flat to slightly concave profiles on primitive-mantle normalized multi-element diagrams. The basaltic rocks of the Long Lake sequence (Rogers and van Staal, 2002) are arc-like and exhibit large Nb depletions with slight LREE-enrichment. These sequences are also products of volcanism in a primitive arc setting, but are considered to have been formed during younger volcanic events, Late Cambrian, ca. 505 Ma, for the Long Lake sequence (Rogers *et al.*, 2003) and Tremadocian for the Tulks Hill, Baxter's Pond, and Beatons Pond basalts (Evans *et al.*, 1990).

Basaltic rocks interpreted to be rifted-arc sequences belong to the undated Upper basalts of the Tulks Hill assemblage, Carter Lake formation basalts, and Lemotte's Ridge basalts, all of which are thought to overlie the Tremadocian Tulks Hill sequence. Each of these rocks contain LREE-enriched, convex patterns on primitive mantle normalized multi-element plots. The distinct Nb depletions, indicative of arc volcanism are absent from each of these sequences and thus these rocks are interpreted to represent an arc-rift

tectonic setting which encompasses the transition from island-arc volcanism to a rifted arc setting (Evans and Kean, 2002).

Volcanic rocks with a back-arc signature are present in the Pine Falls formation to the east of the Tally Pond Group. REE patterns for the basalts are convex and slightly LREE depleted and may represent REE-enriched MORB (Evans and Kean, 2002). No age data exist for these rocks.

Mature arc sequences exhibit fairly steep REE patterns and have strong positive Th and negative Nb and Ti anomalies and plot on the calc-alkaline field on the Ti-Zr-Y diagram and outside of the island-arc filed on the Ti-V diagram. Such rocks are comprised of the Victoria Bridge basalts, Henry Waters and Number 5 Dam basalt breccias, Valley Brook Basalts, Diversion Lake group and Lake Douglas basalts (Evans and Kean, 2002; Rogers and van Staal, 2002).

The detailed geochemical studies of mafic and felsic volcanic sequences coupled with precise U-Pb geochronology clearly indicate the composite nature of the Victoria Lake Supergroup. There is a geochemical progression upward through the stratigraphy from island-arc volcanism to arc rifting and back-arc spreading. The volcanic and intrusive sequences in the Victoria Lake Supergroup span an age range of over 50 Ma from Mid-Cambrian to Mid-Ordovician. This time span is comparable to the entire history of Iapetus as recorded in central Newfoundland. This implies that the entire Victoria Lake Supergroup consists of several temporally distinct island-arc, rifted-arc and non-arc events that occurred more than once rather than representing the older and younger parts of a single, long lived arc system.

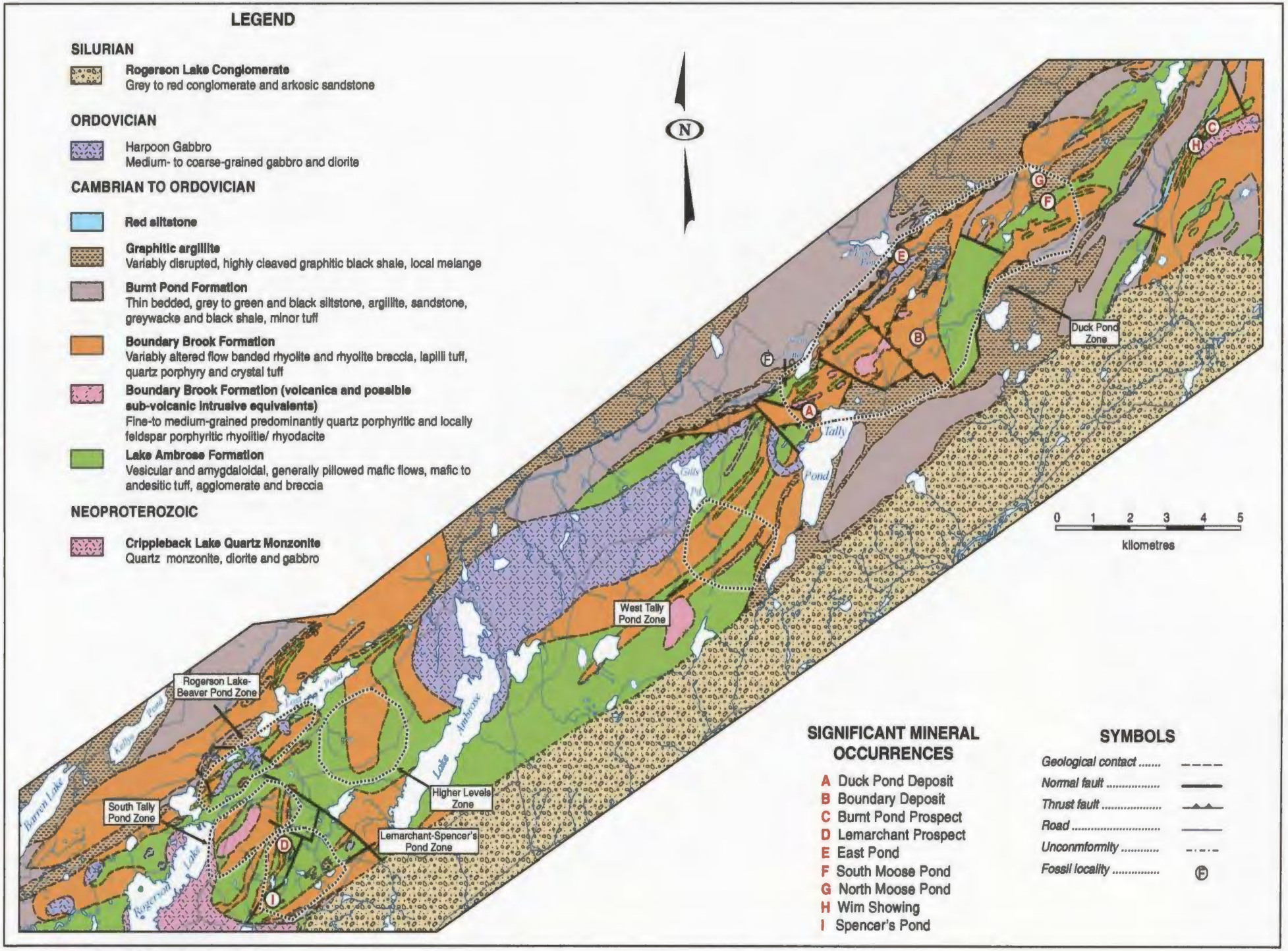

Figure 4.1 *Location of mineralized zones of the Tally Pond Group discussed in text.*

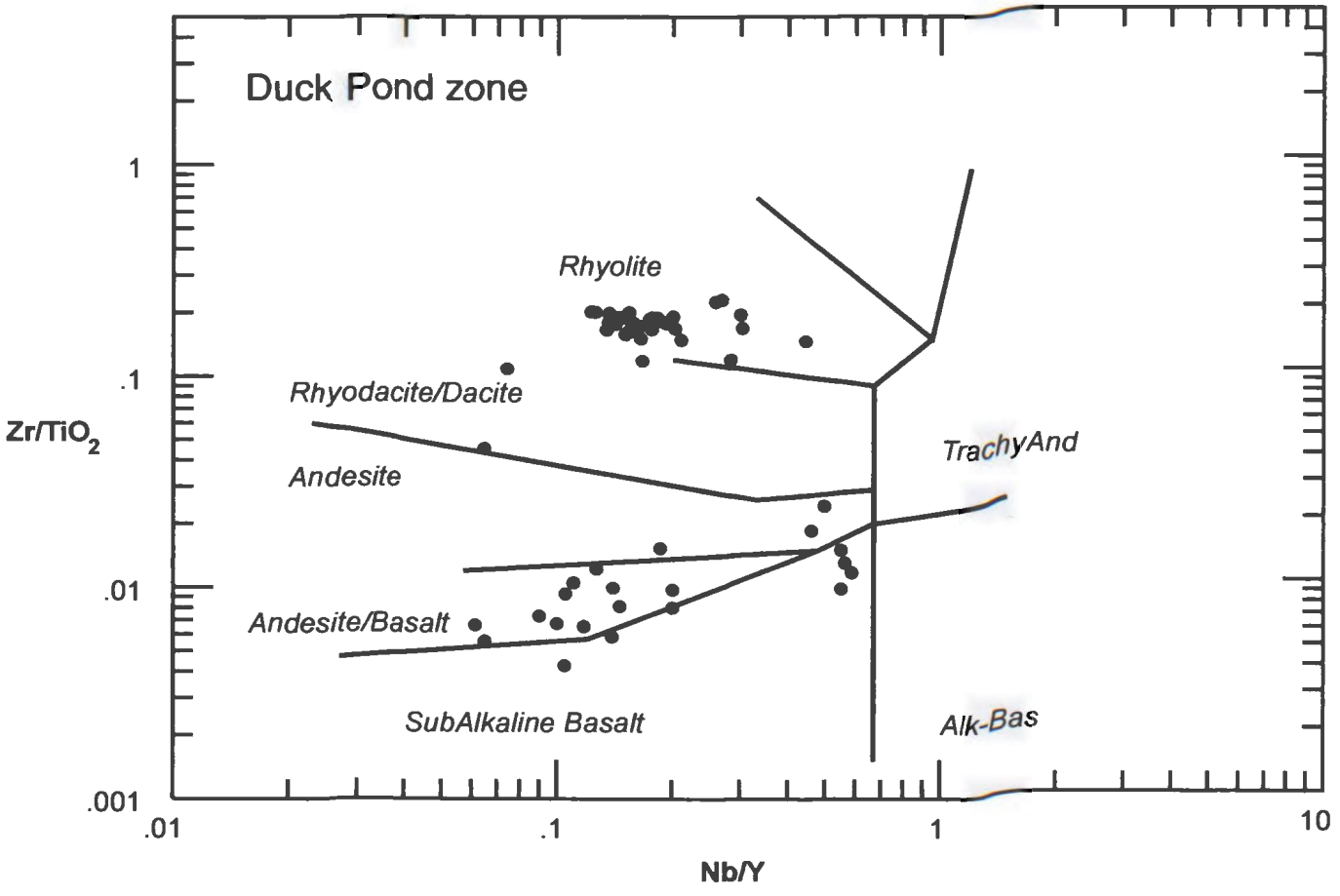

Figure 4.2(a) *Nb/Y vs. Zr/Ti discrimination diagram for identifying rock type (Winchester and Floyd, 1977).*

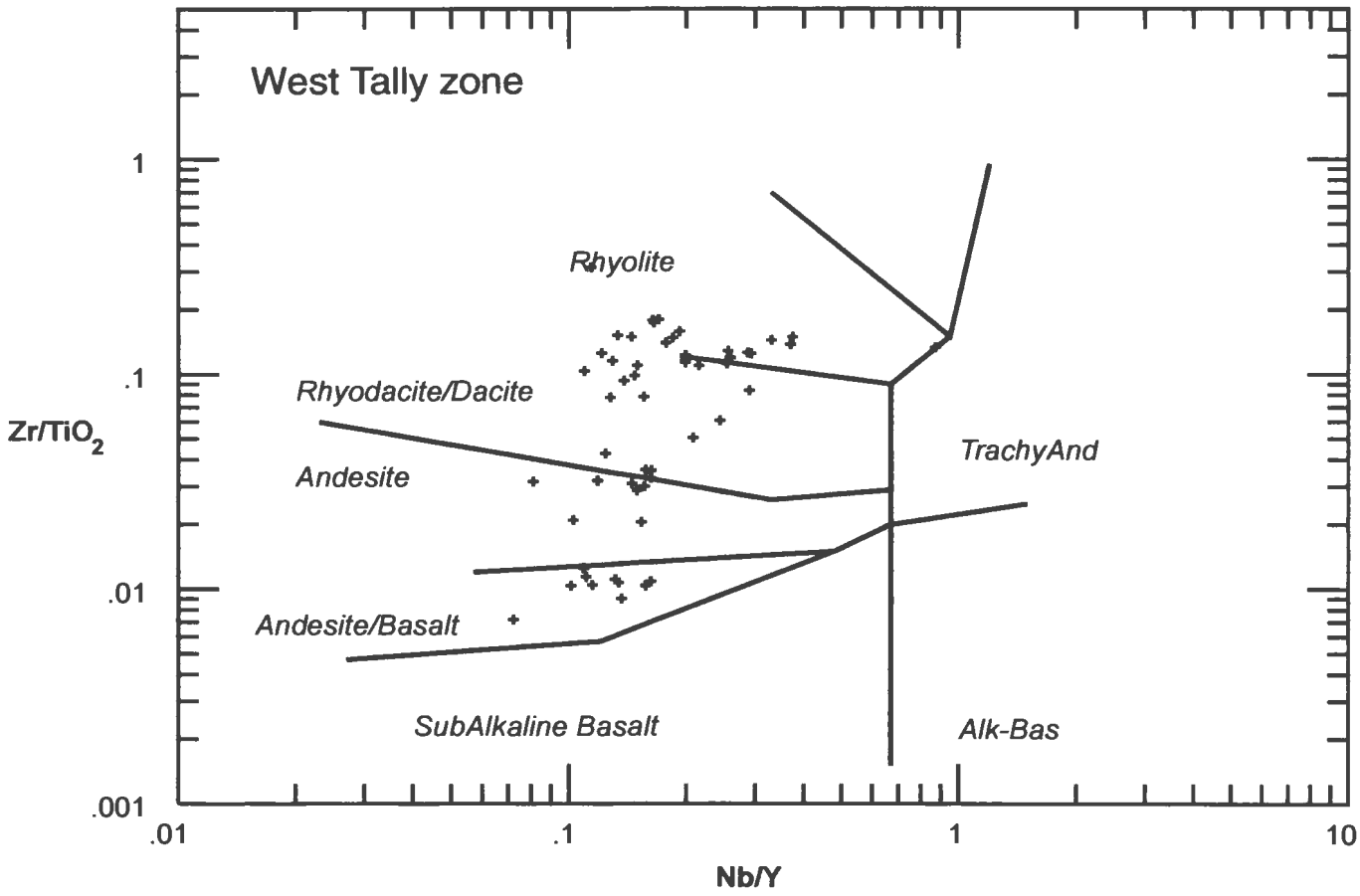

Figure 4.2(b) *Nb/Y vs. Zr/Ti discrimination diagram for identifying rock type (Winchester and Floyd, 1977).*

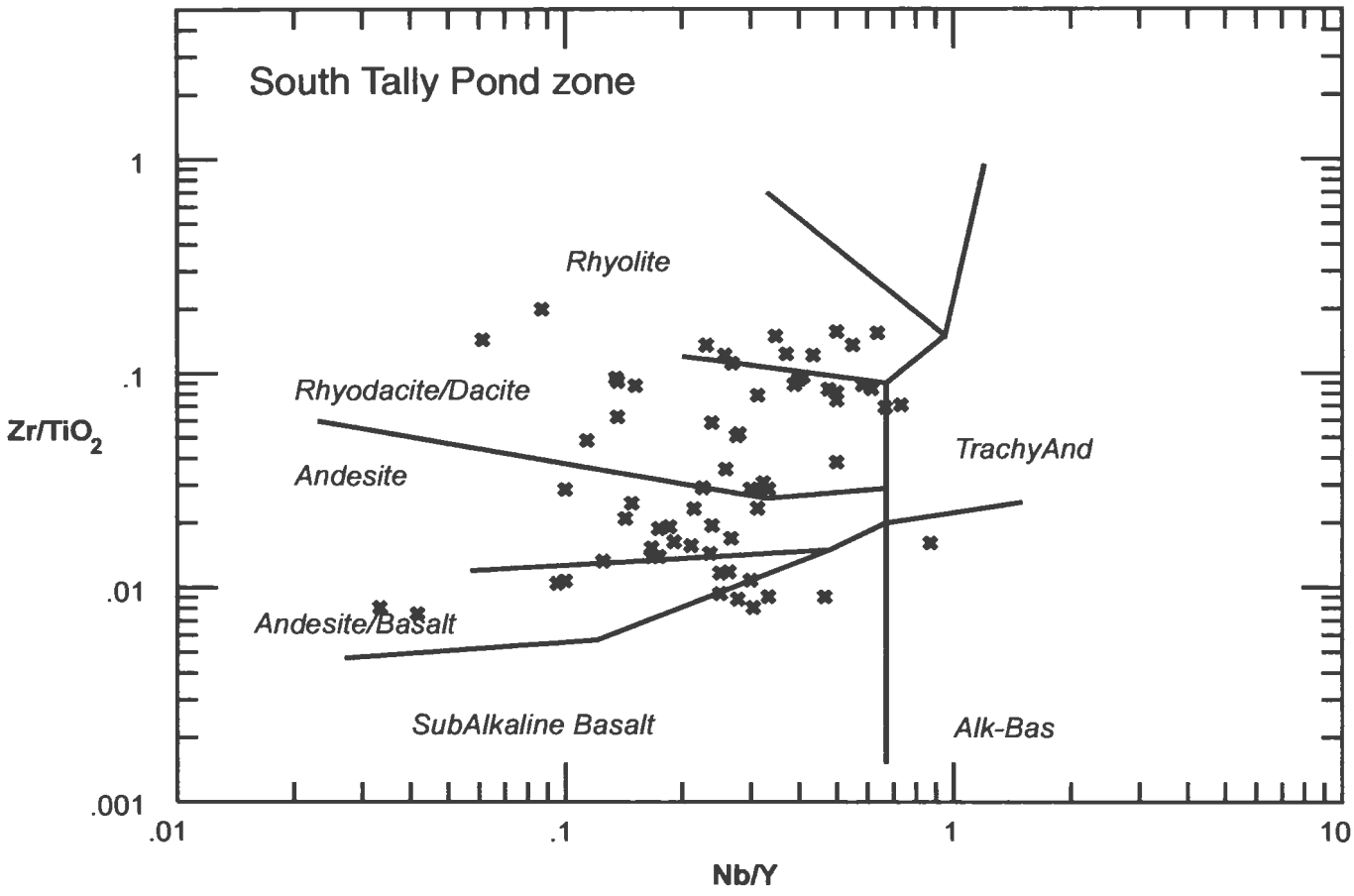

Figure 4.2(c) *Nb/Y vs. Zr/Ti discrimination diagram for identifying rock type (Winchester and Floyd, 1977).*

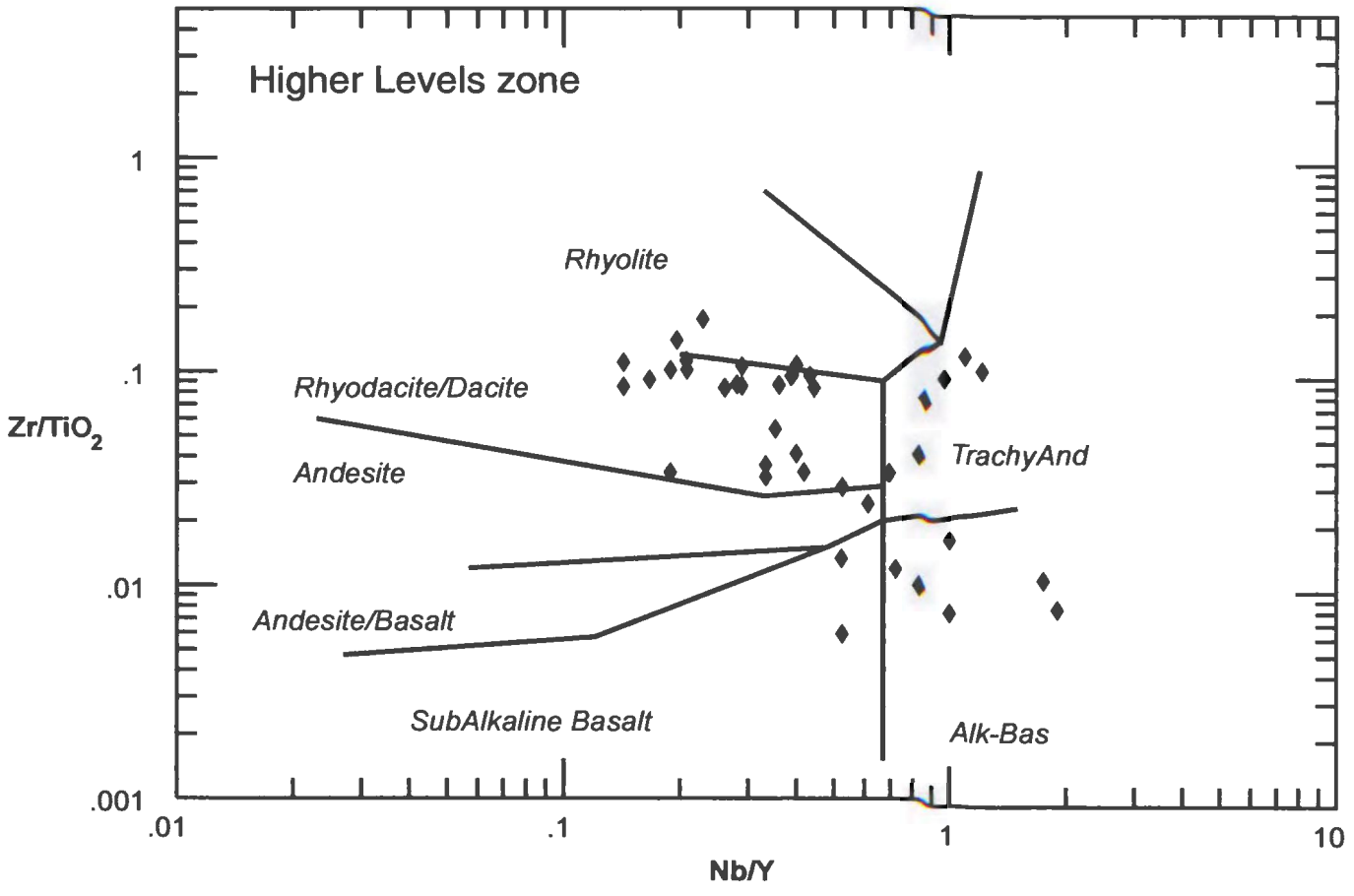

Figure 4.2(d) *Nb/Y vs. Zr/Ti discrimination diagram for identifying rock type (Winchester and Floyd, 1977).*

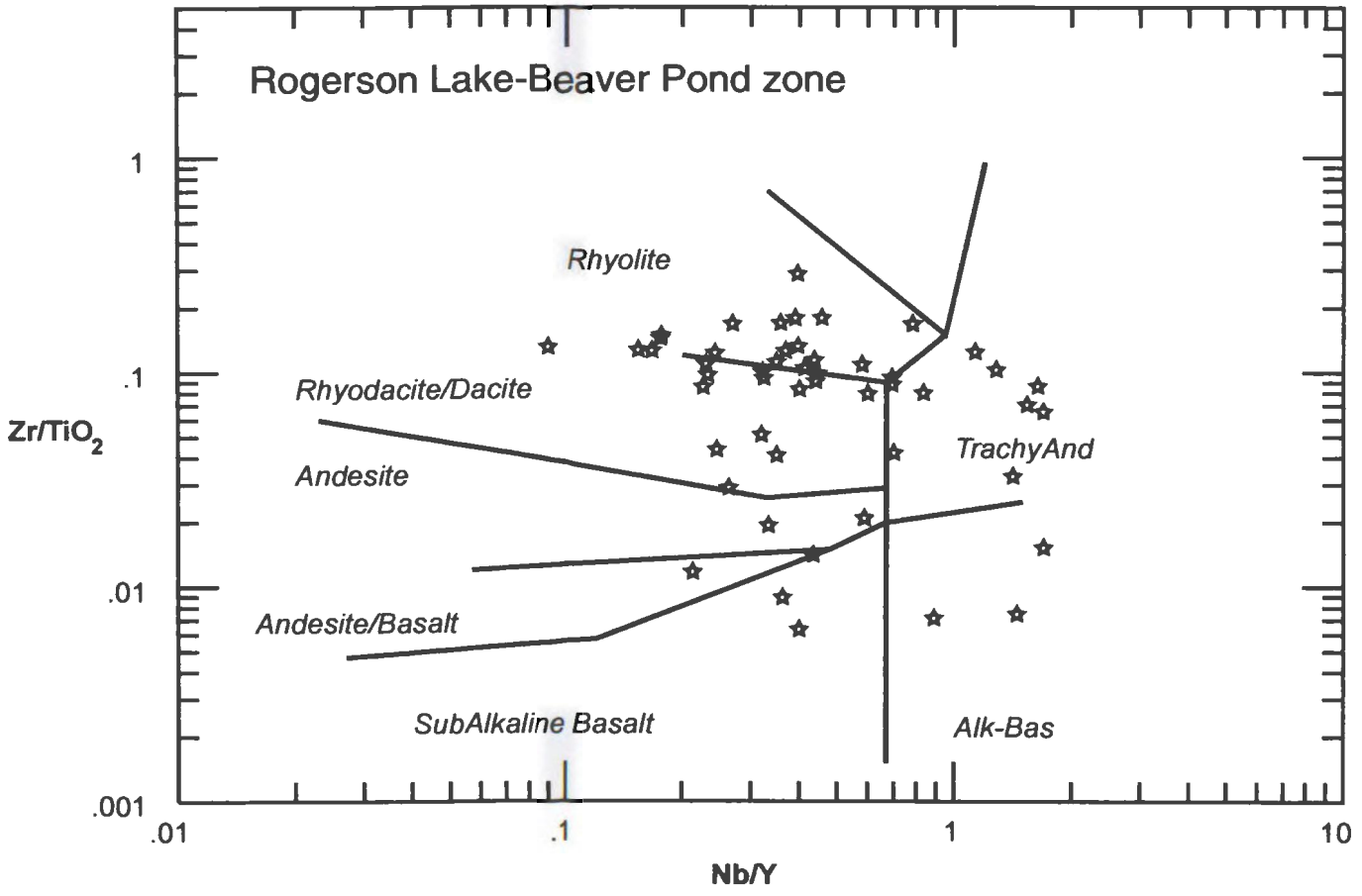

Figure 4.2(e) *Nb/Y vs. Zr/Ti discrimination diagram for identifying rock type (Winchester and Floyd, 1977).*

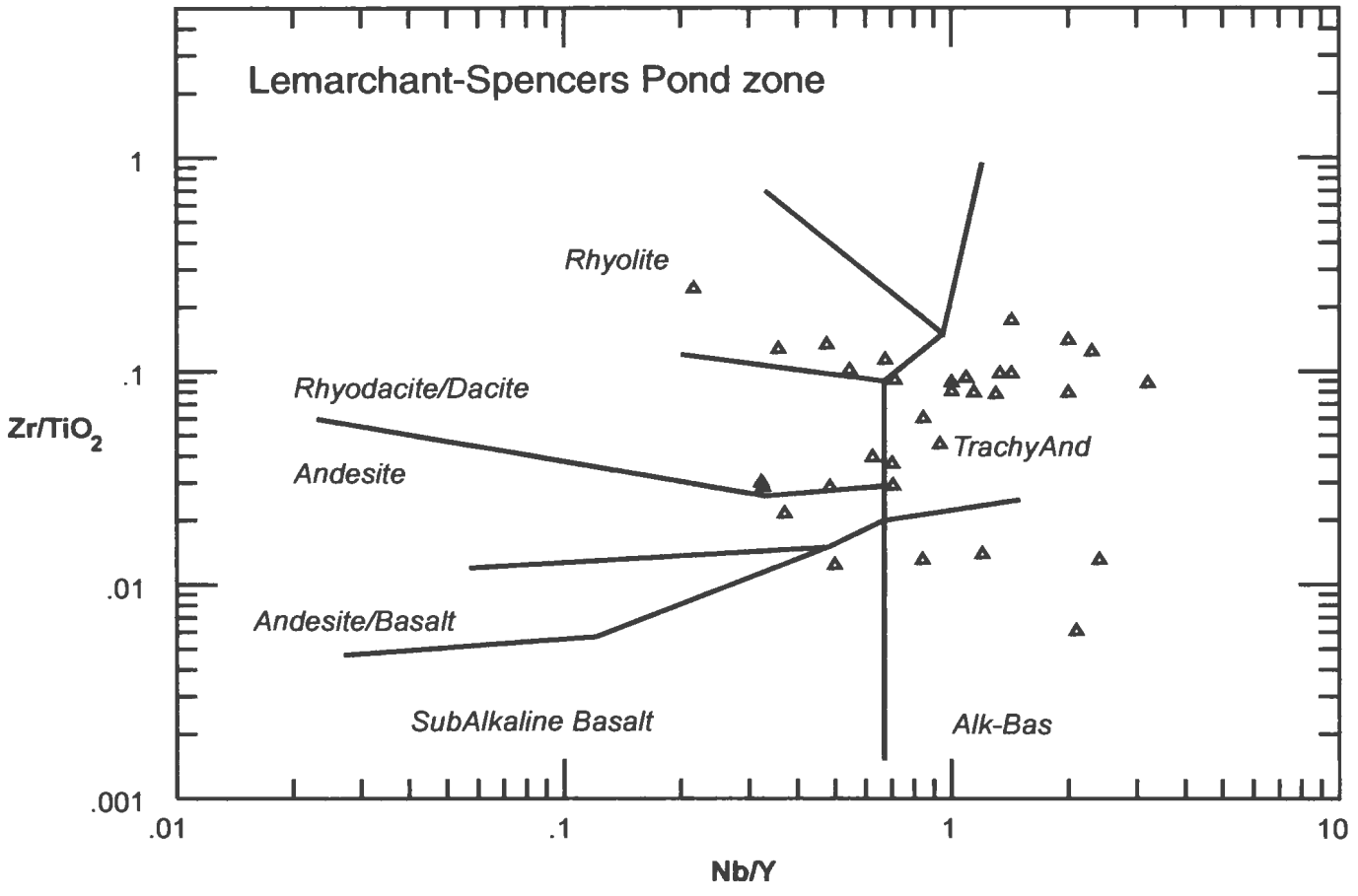

Figure 4.2(f) *Nb/Y vs. Zr/Ti discrimination diagram for identifying rock type (Winchester and Floyd, 1977).*

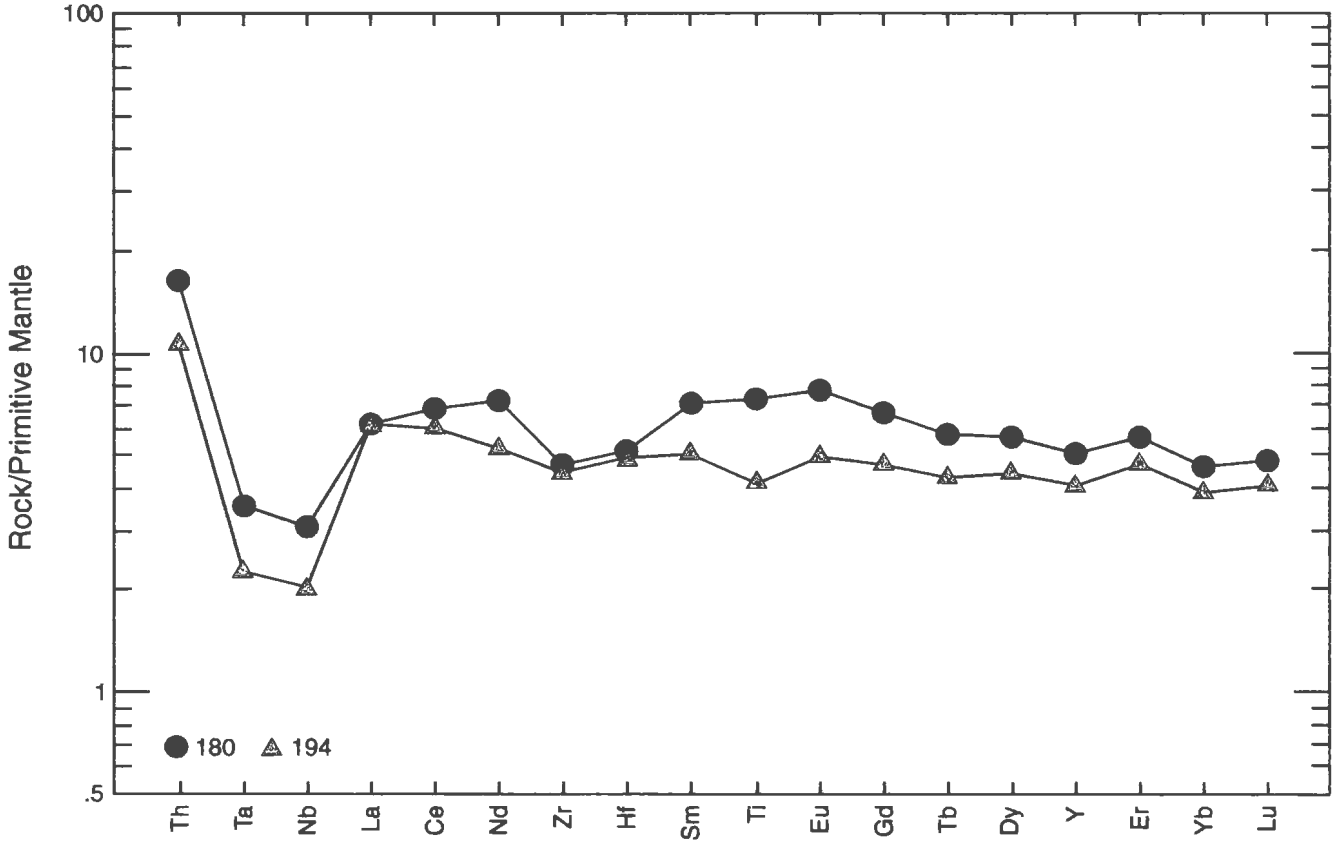

Figure 4.3 *Primitive mantle normalized-extended rare-earth-element plots of mafic volcanic rocks of the Lake Ambrose Formation in the Duck Pond zone.*

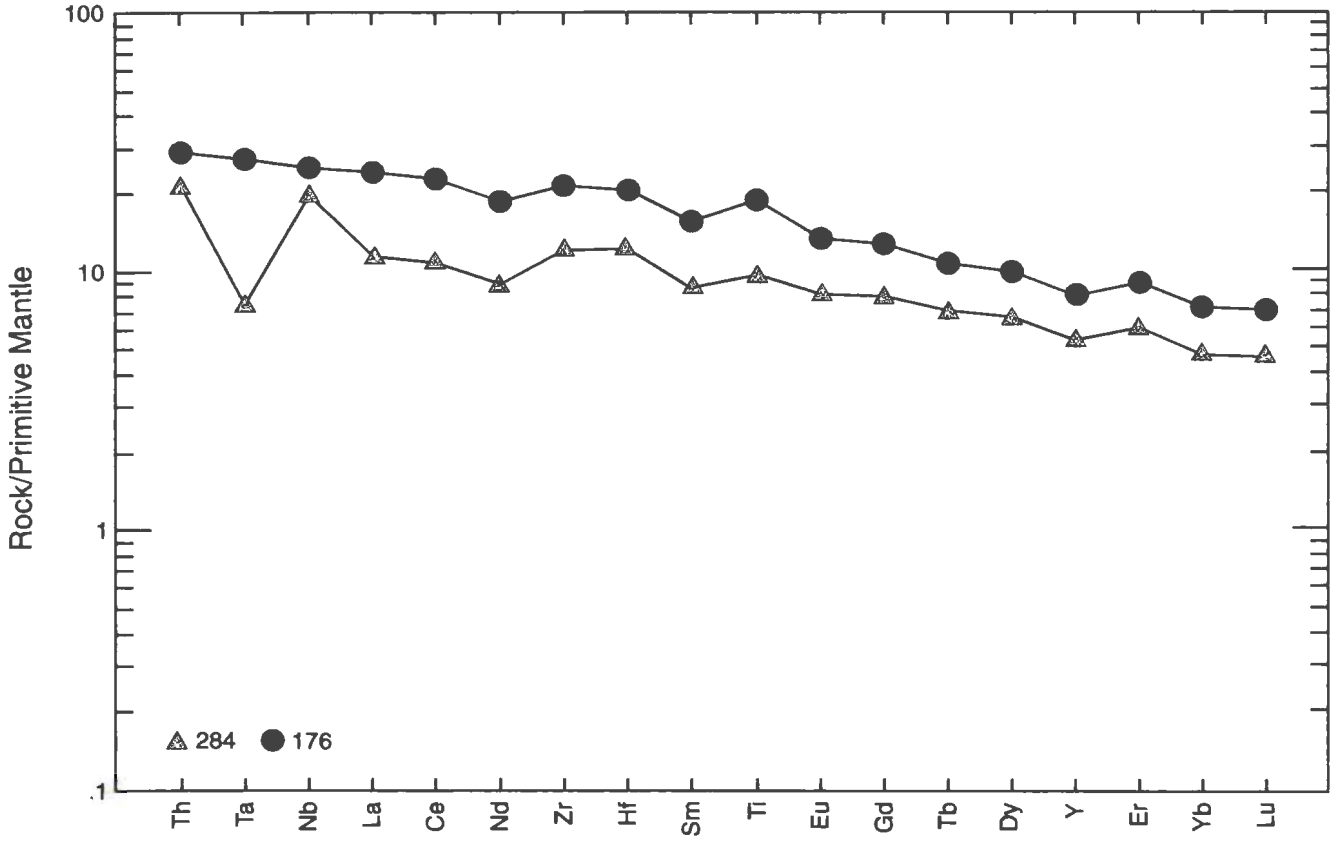

Figure 4.4 *Primitive mantle normalized-extended rare-earth-element plots of mafic intrusive rocks of the Harpoon gabbro from the Duck Pond zone.*

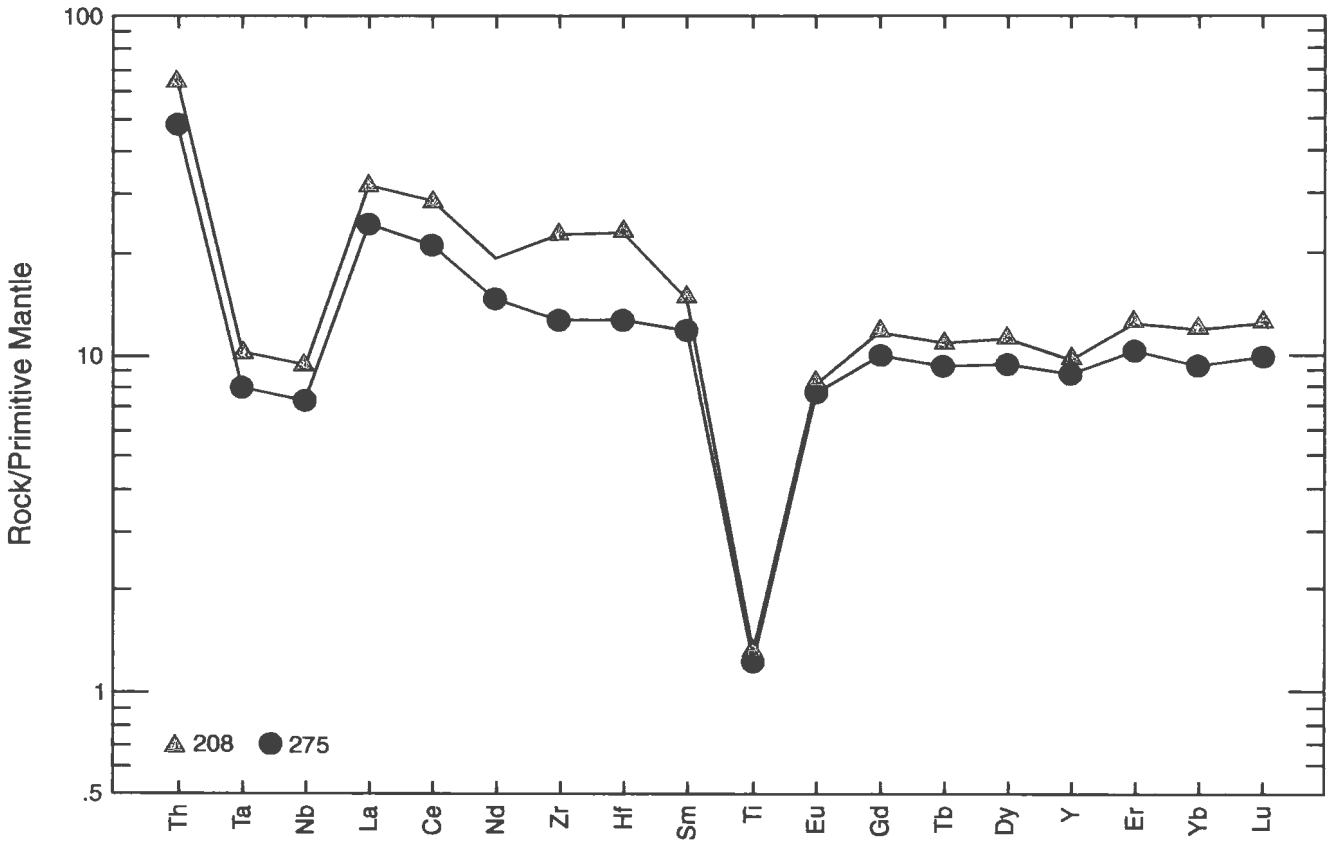

Figure 4.5 *Primitive mantle normalized-extended rare-earth-element plots of felsic Duck Pond hangingwall rocks.*

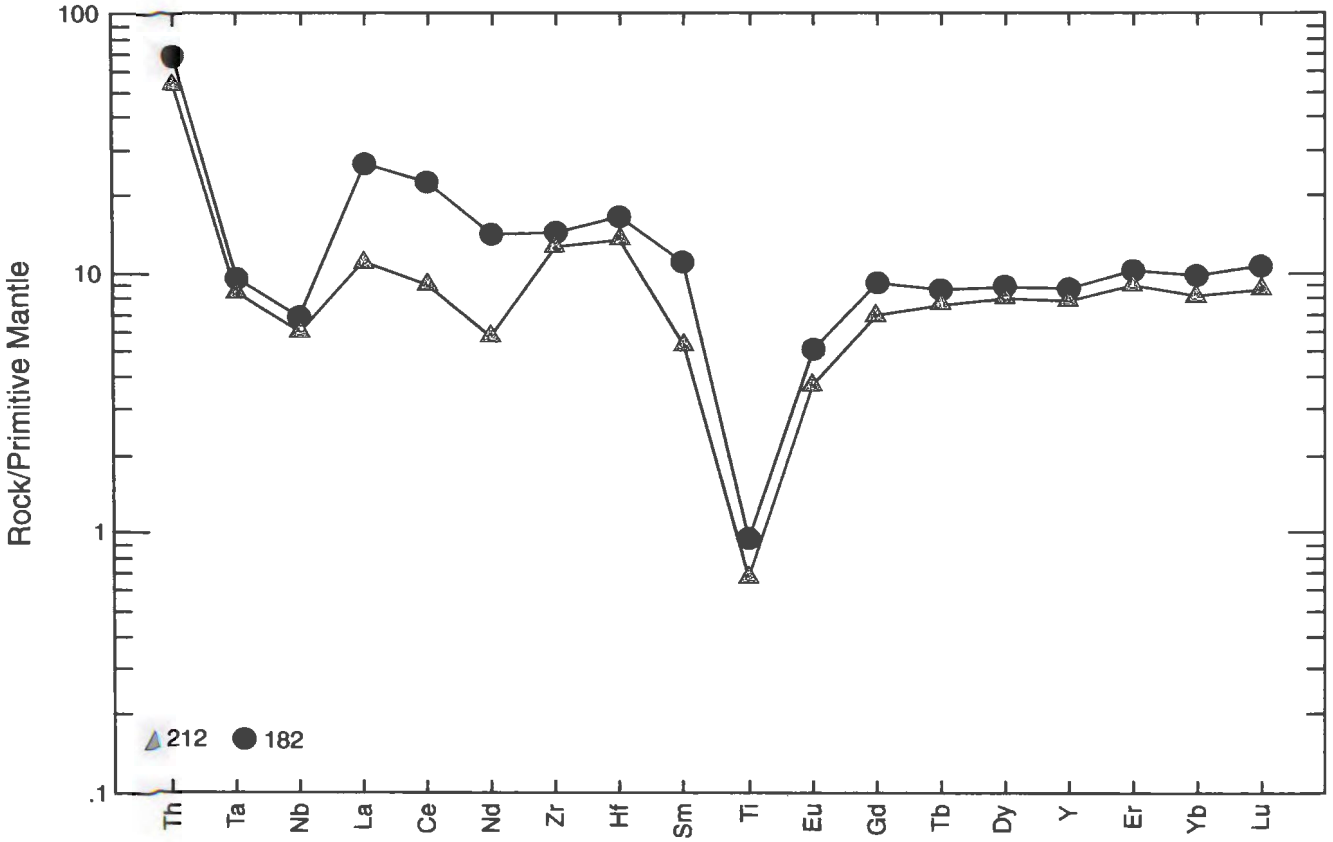

Figure 4.6 *Primitive mantle normalized-extended rare-earth-element plots of porphyritic rhyolite from the Duck Pond zone.*

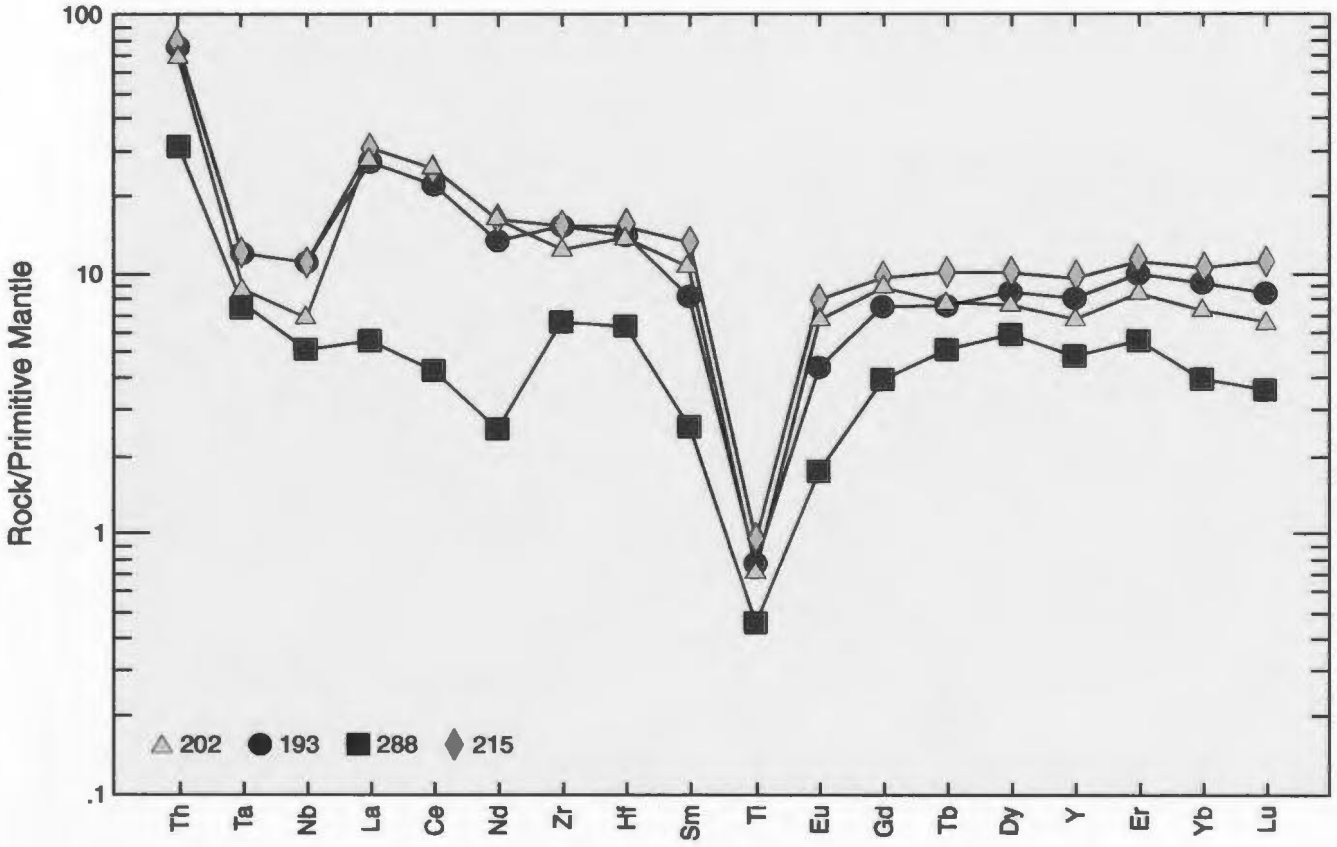

Figure 4.7 *Primitive mantle normalized-extended rare-earth-element plots of felsic Duck Pond footwall rocks.*

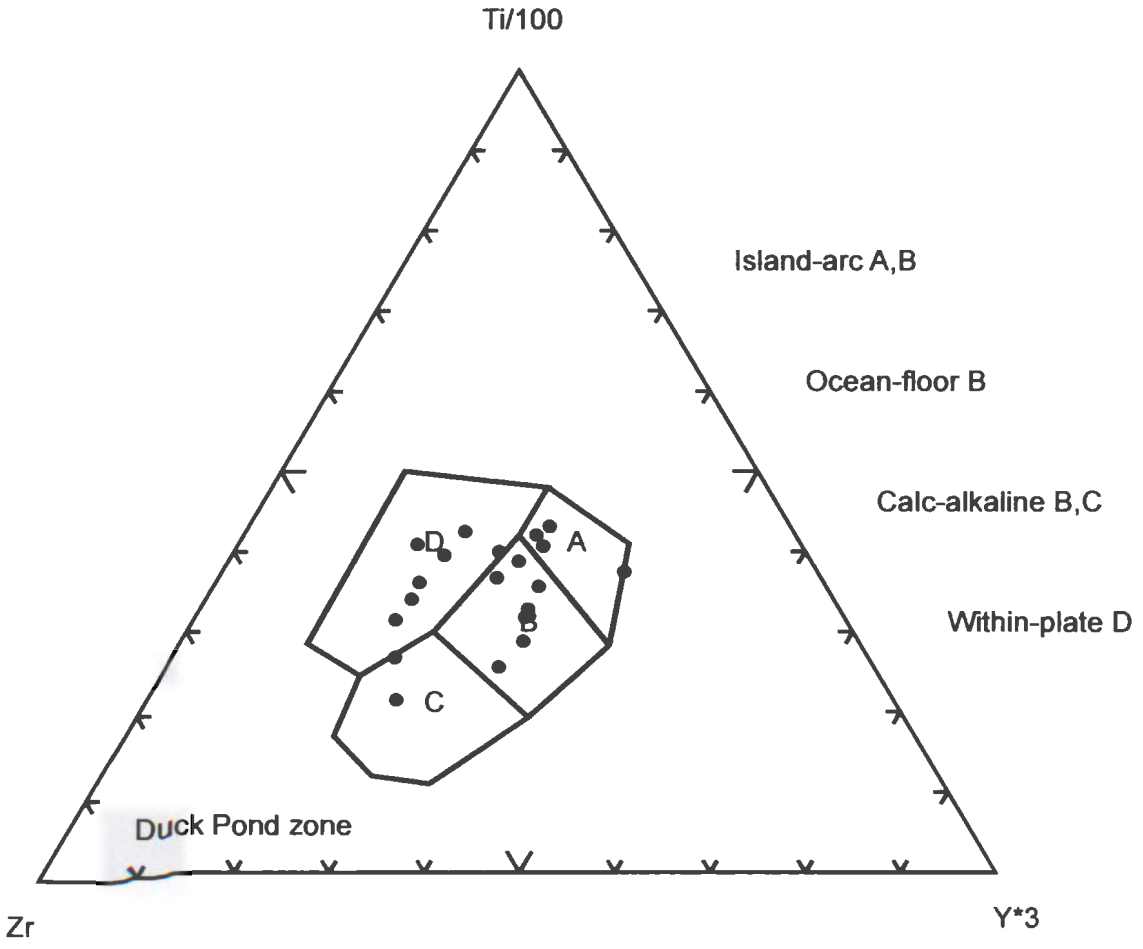

Figure 4.8(a) *Ti-Zr-Y diagram (Pearce and Cann, 1973) of mafic volcanic rocks in the Duck Pond zone.*

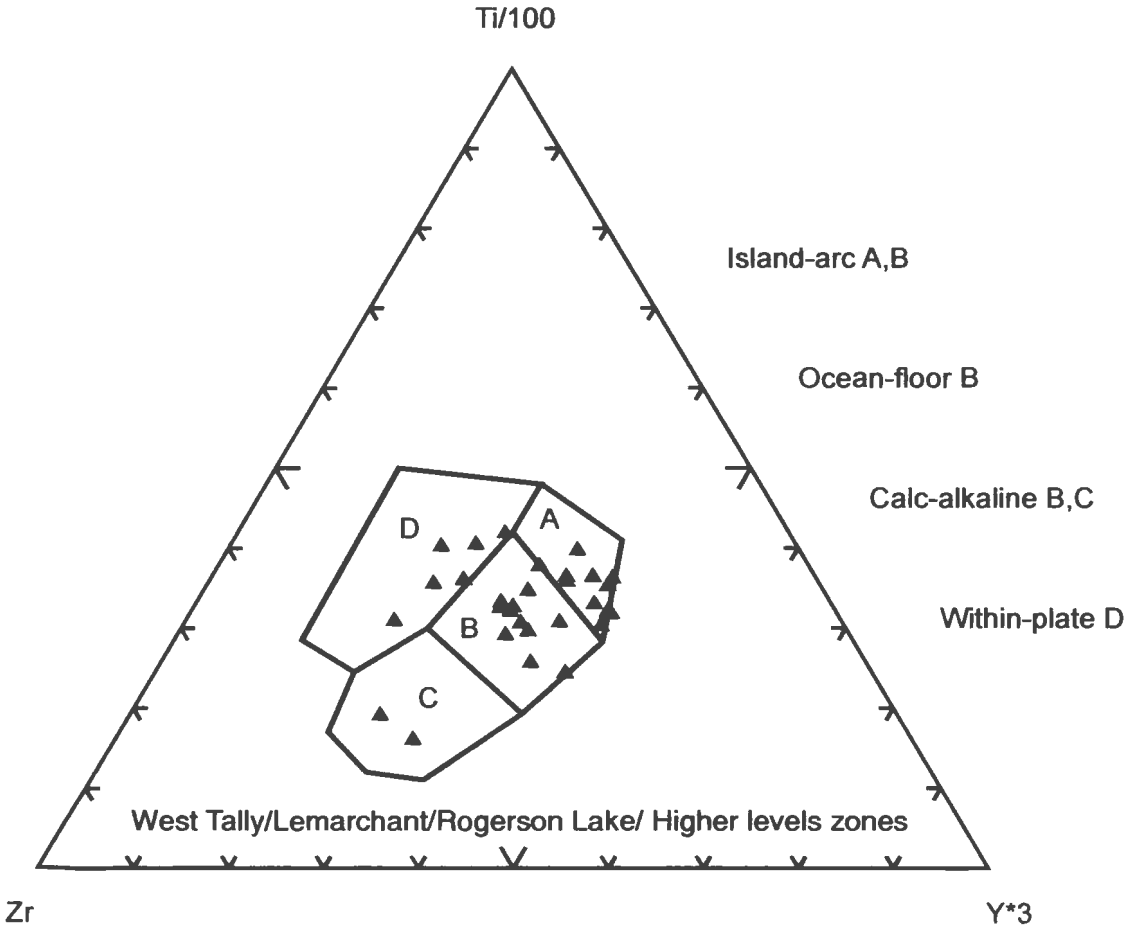

Figure 4.8(b) *Ti-Zr-Y diagram (Pearce and Cann, 1973) of mafic volcanic rocks in the Duck Pond zone.*

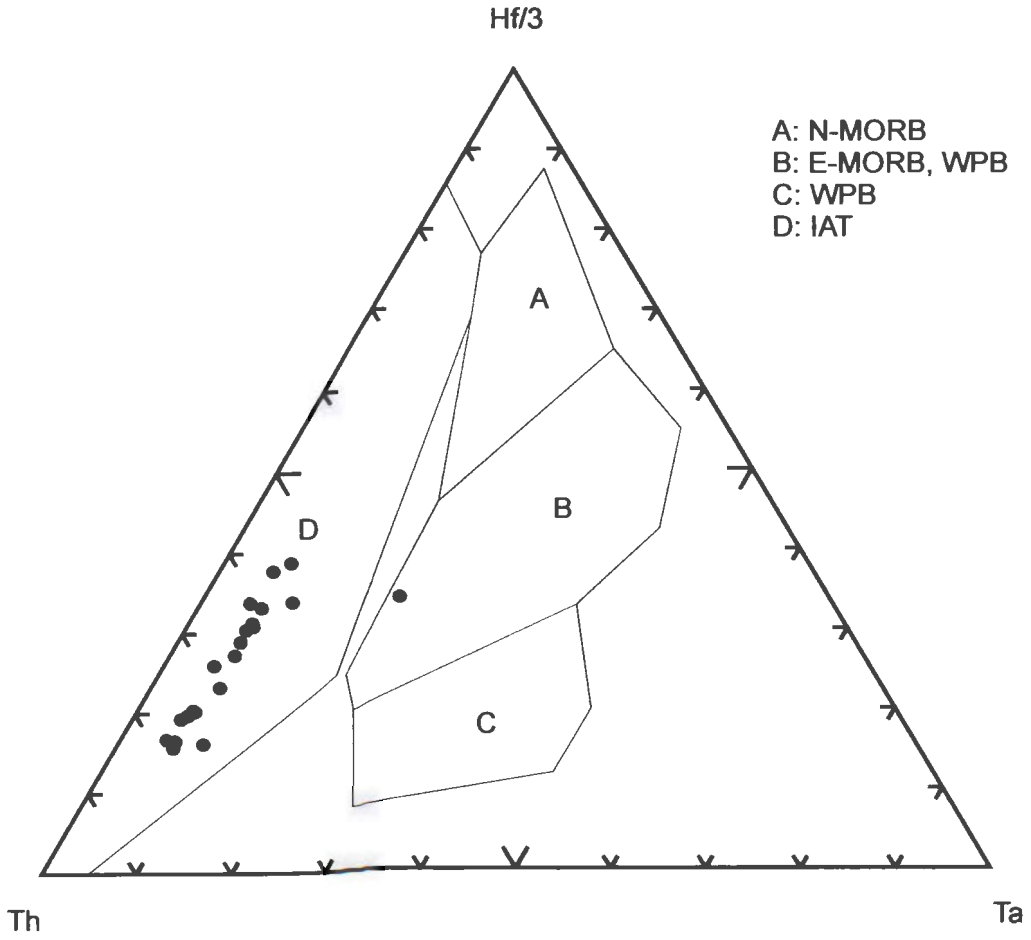

Figure 4.9 *Th-Hf-Ta diagram for mafic rocks in the Tally Pond Group.*

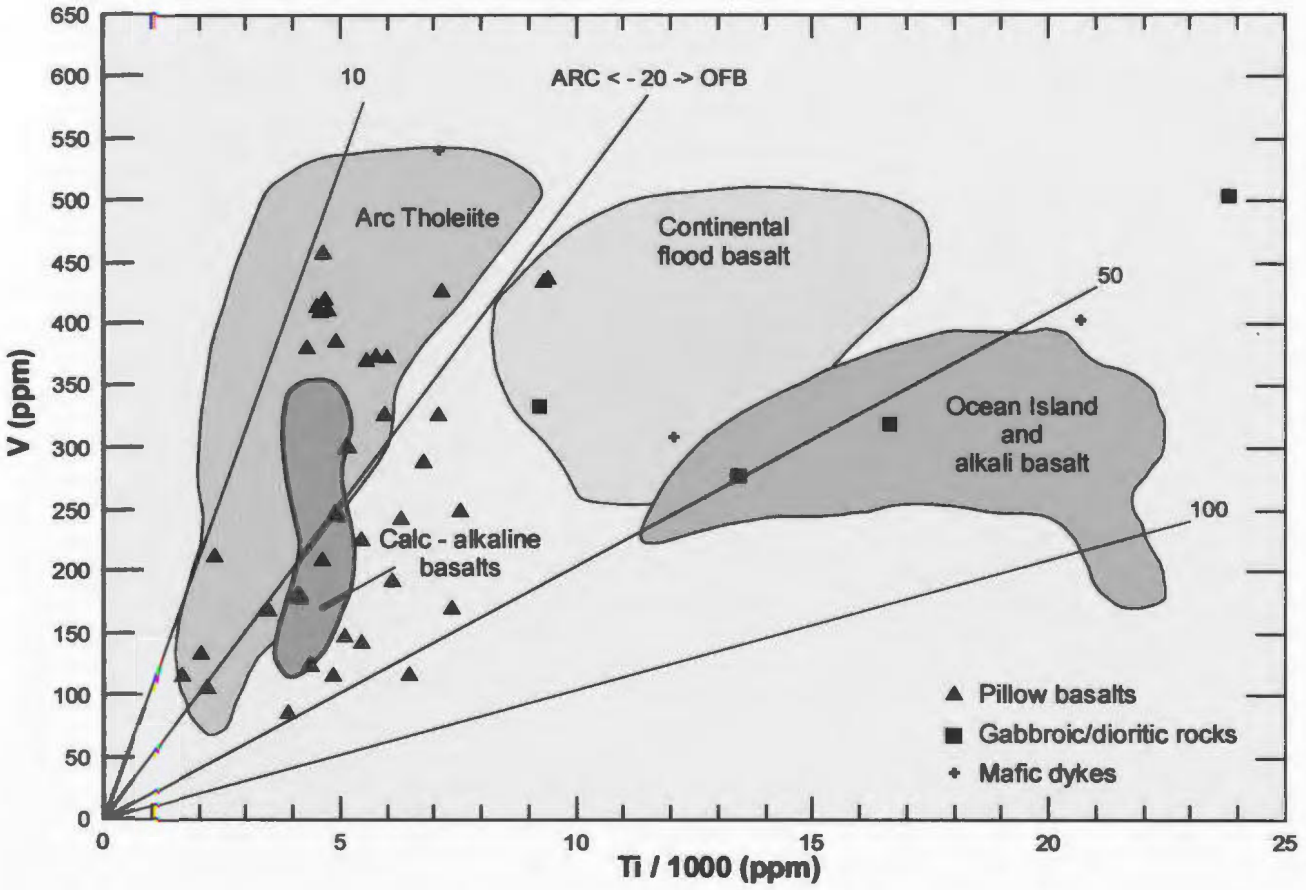

Figure 4.10 *Ti vs. V (Shervais, 1982) diagram for mafic rocks in the Tally Pond Group.*

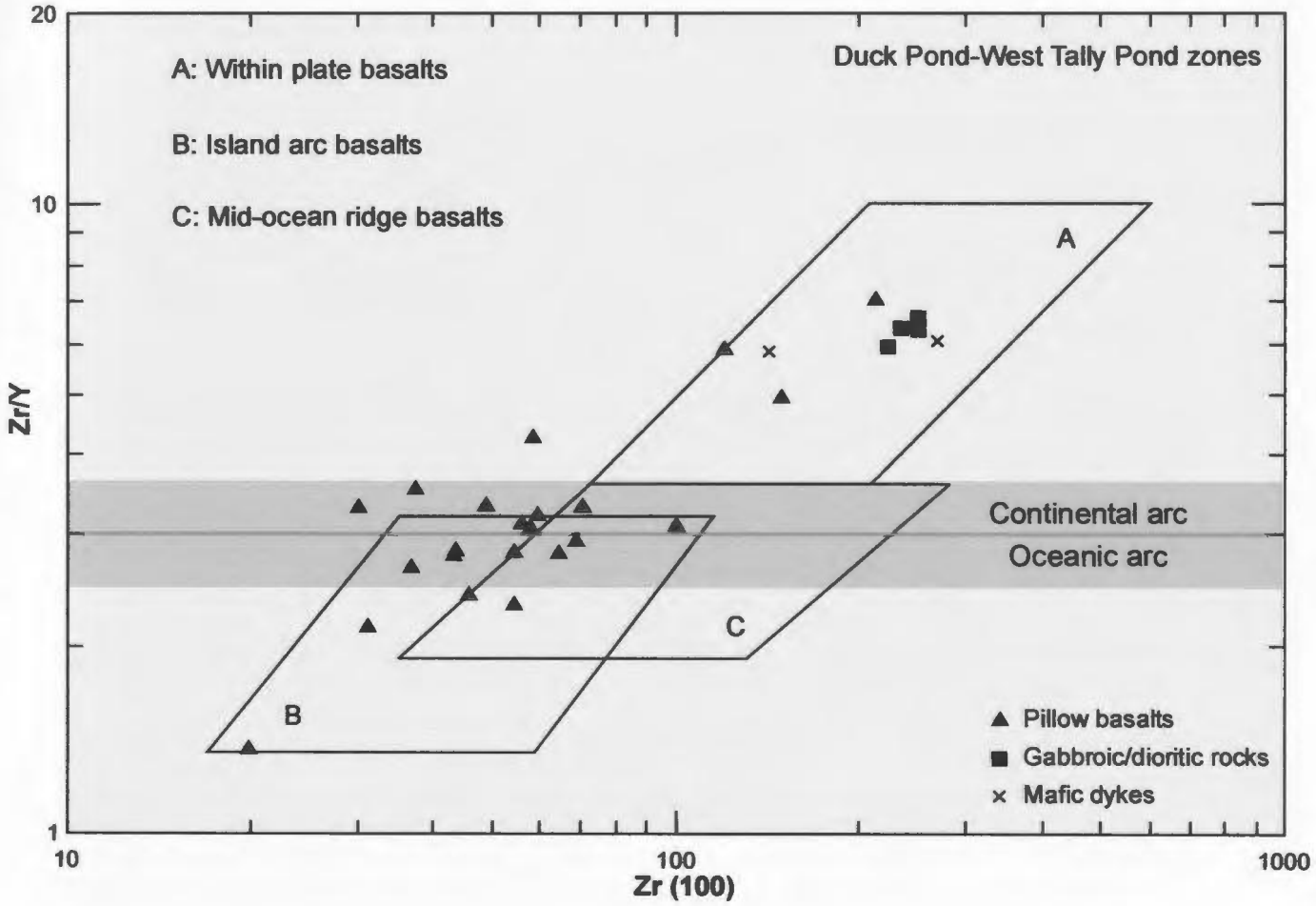

Figure 4.11(a) *Zr vs. Zr/Y (Pearce and Norry, 1979; Pearce, 1983) diagram for mafic rocks in the Tally Pond Group.*

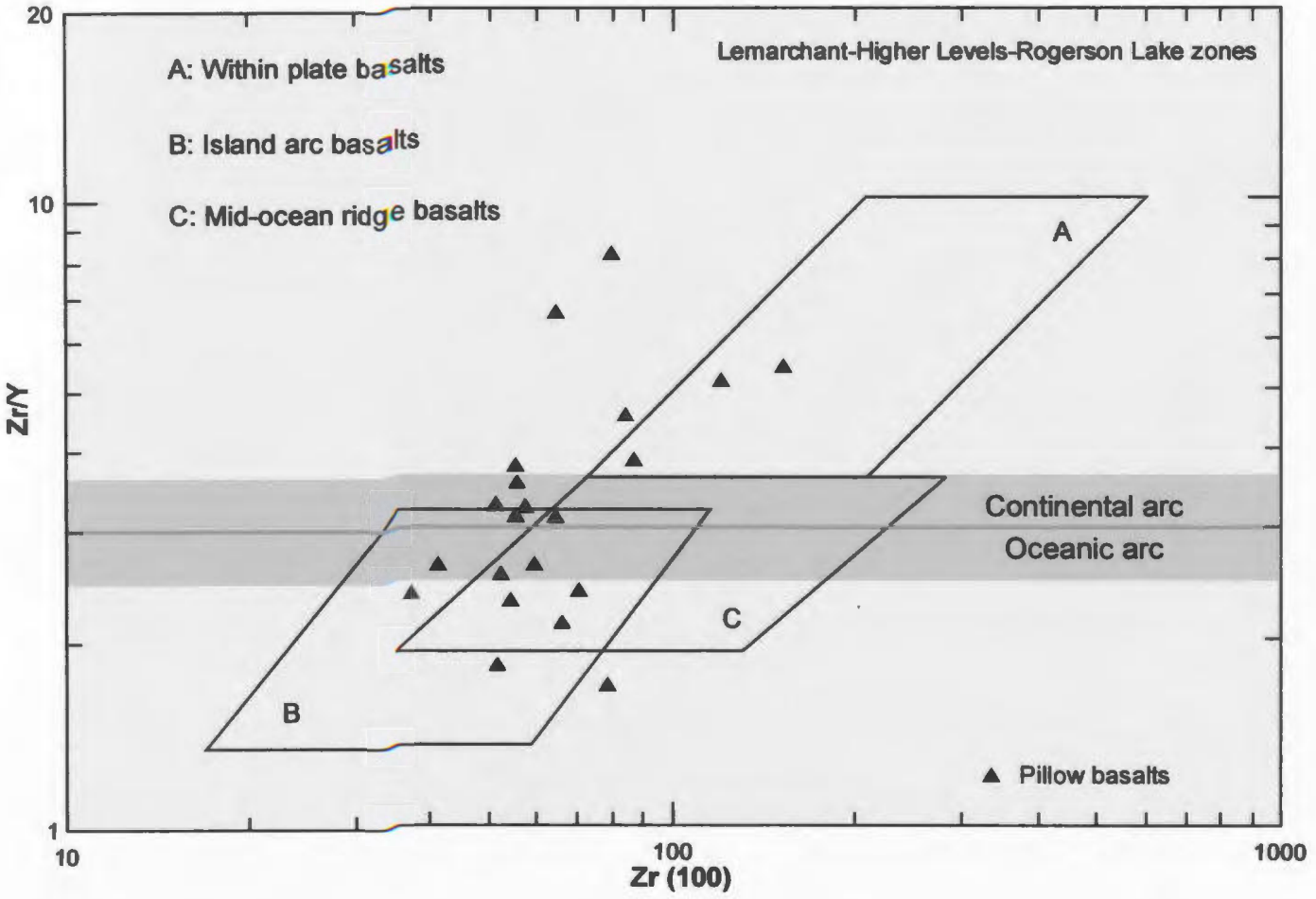

Figure 4.11(b) *Zr vs. Zr/Y (Pearce and Norry, 1979; Pearce, 1983) diagram for mafic rocks in the Tally Pond Group.*

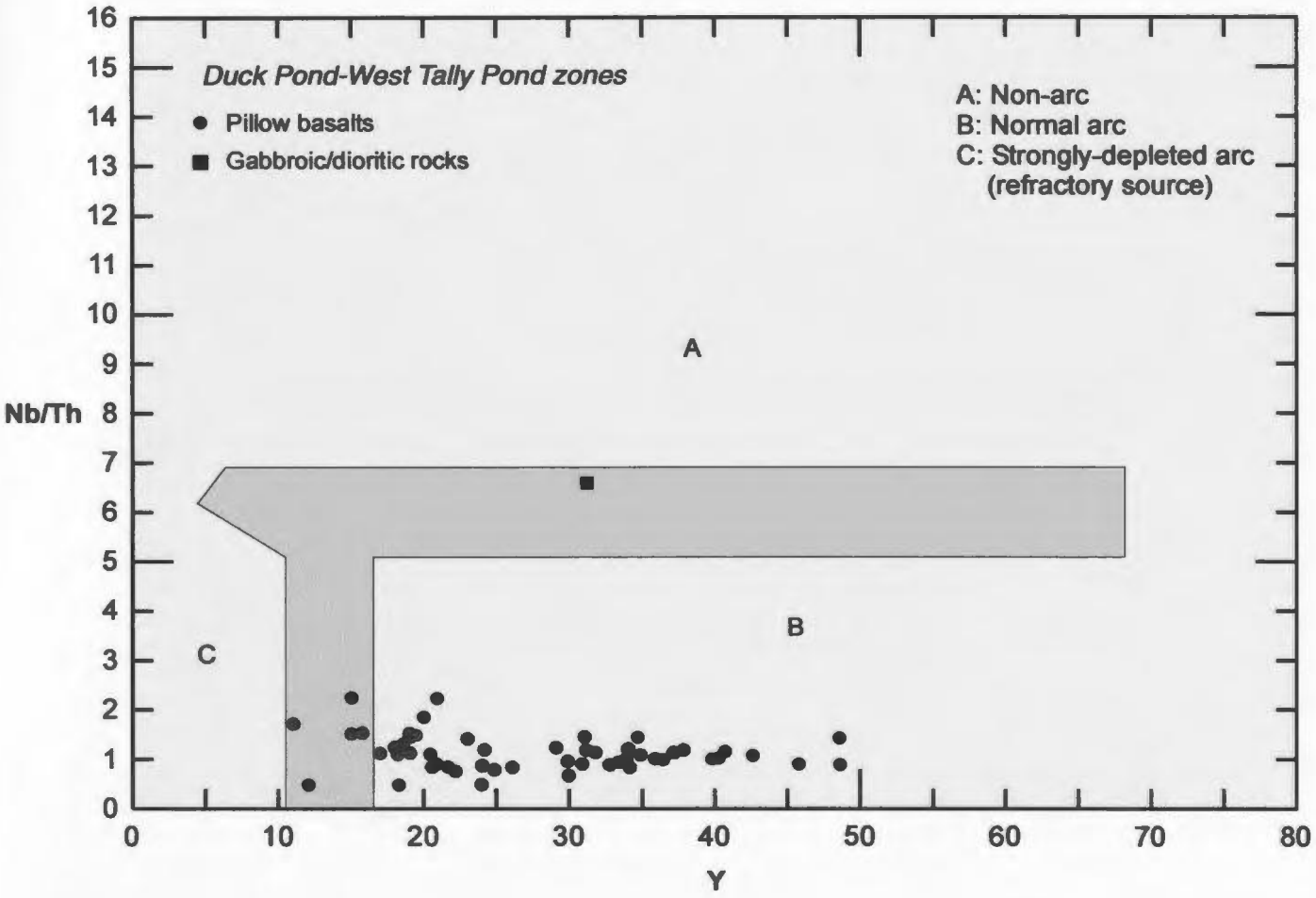

Figure 4.12 *Y vs. Nb/Th plot for mafic rocks of the Duck Pond and West Tally Pond zones in the Tally Pond Group.*

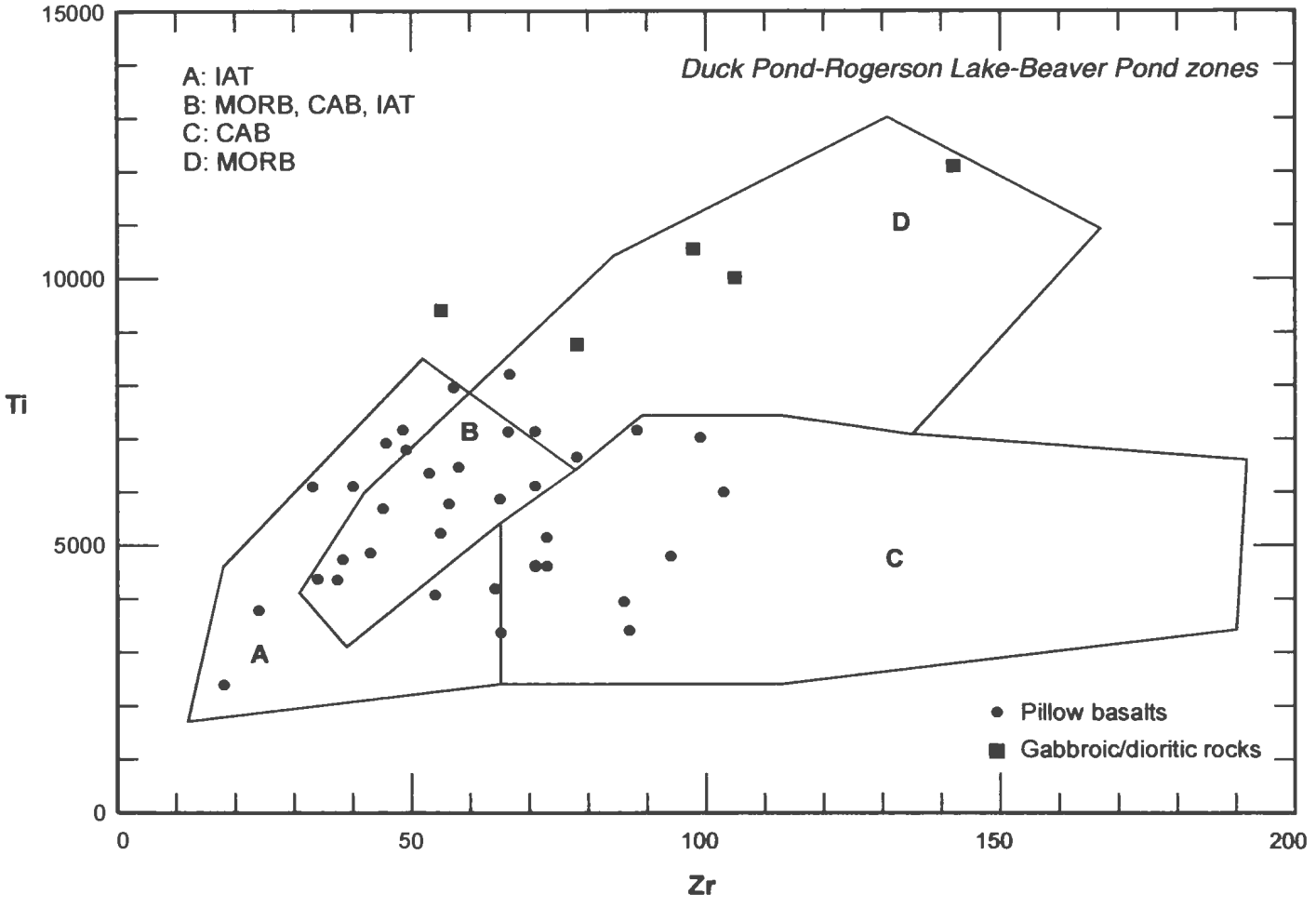

Figure 4.13(a) *Bivariate Zr vs Ti plot (Pearce and Cann, 1973) for mafic rocks in the Tally Pond Group.*

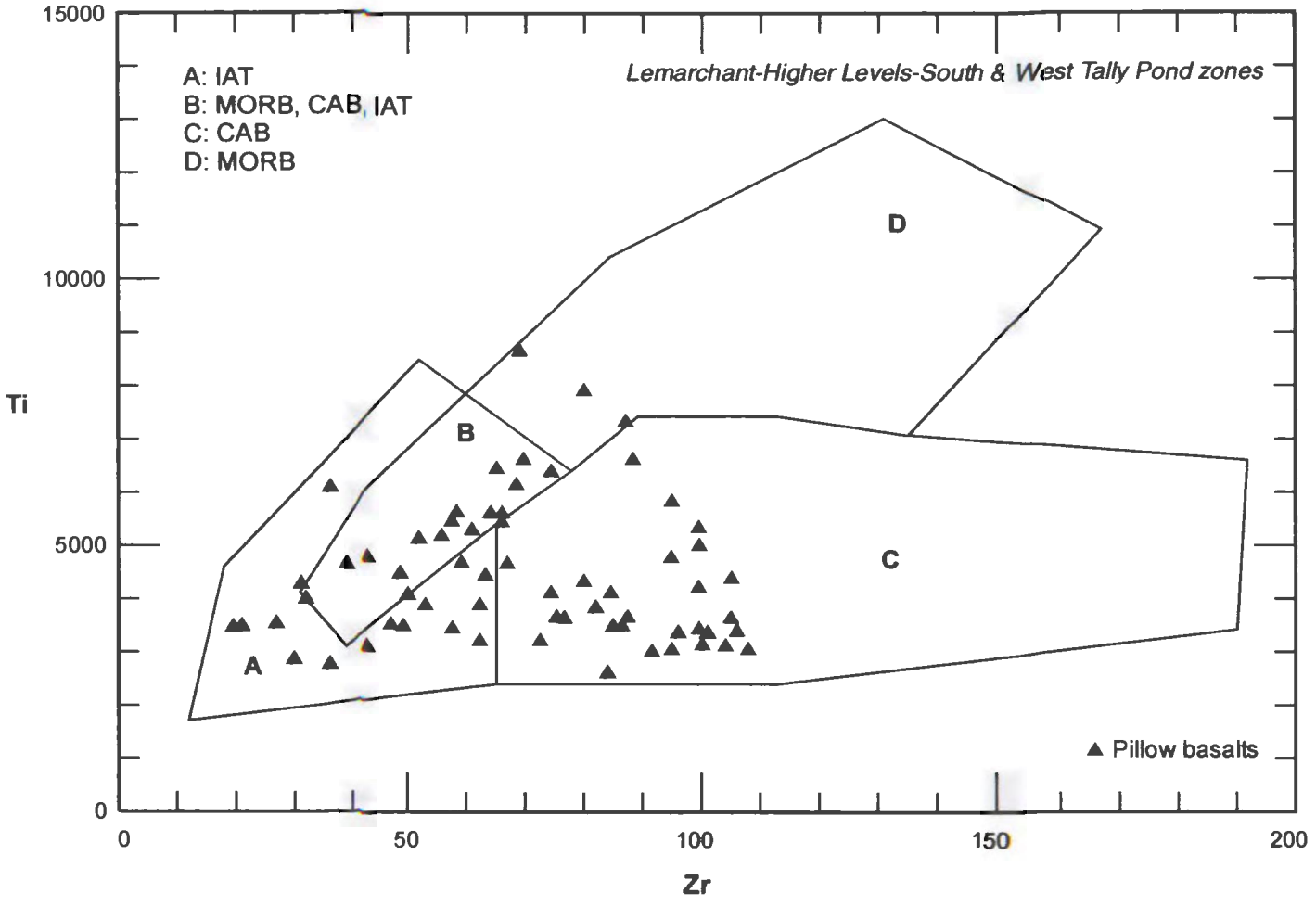

Figure 4.13(b) *Bivariate Zr vs Ti plot (Pearce and Cann, 1973) for mafic rocks in the Tally Pond Group.*

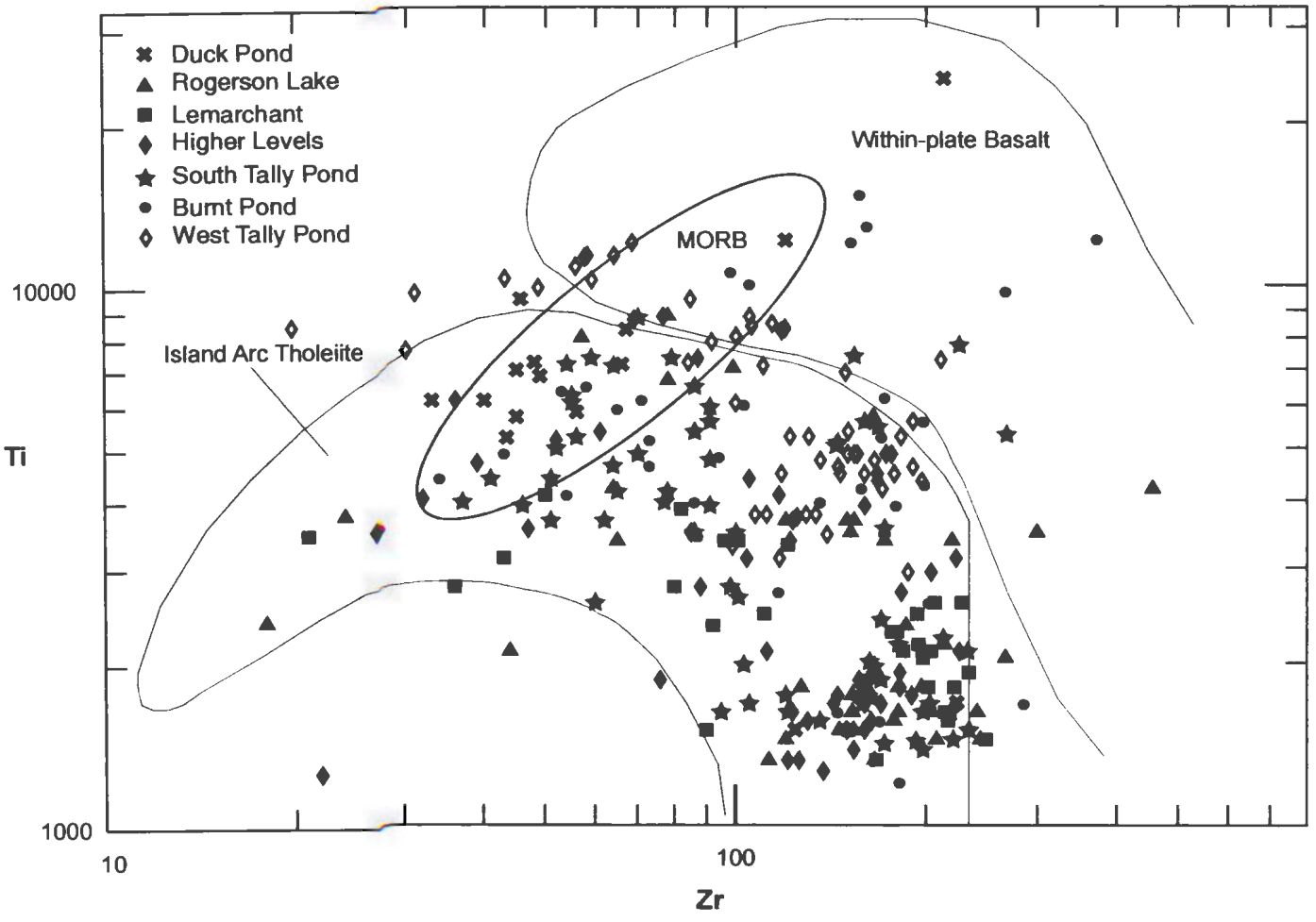

Figure 4.14 *Bivariate logarithm plot of Zr vs Ti (Pearce, 1982) for mafic rocks in the Tally Pond Group.*

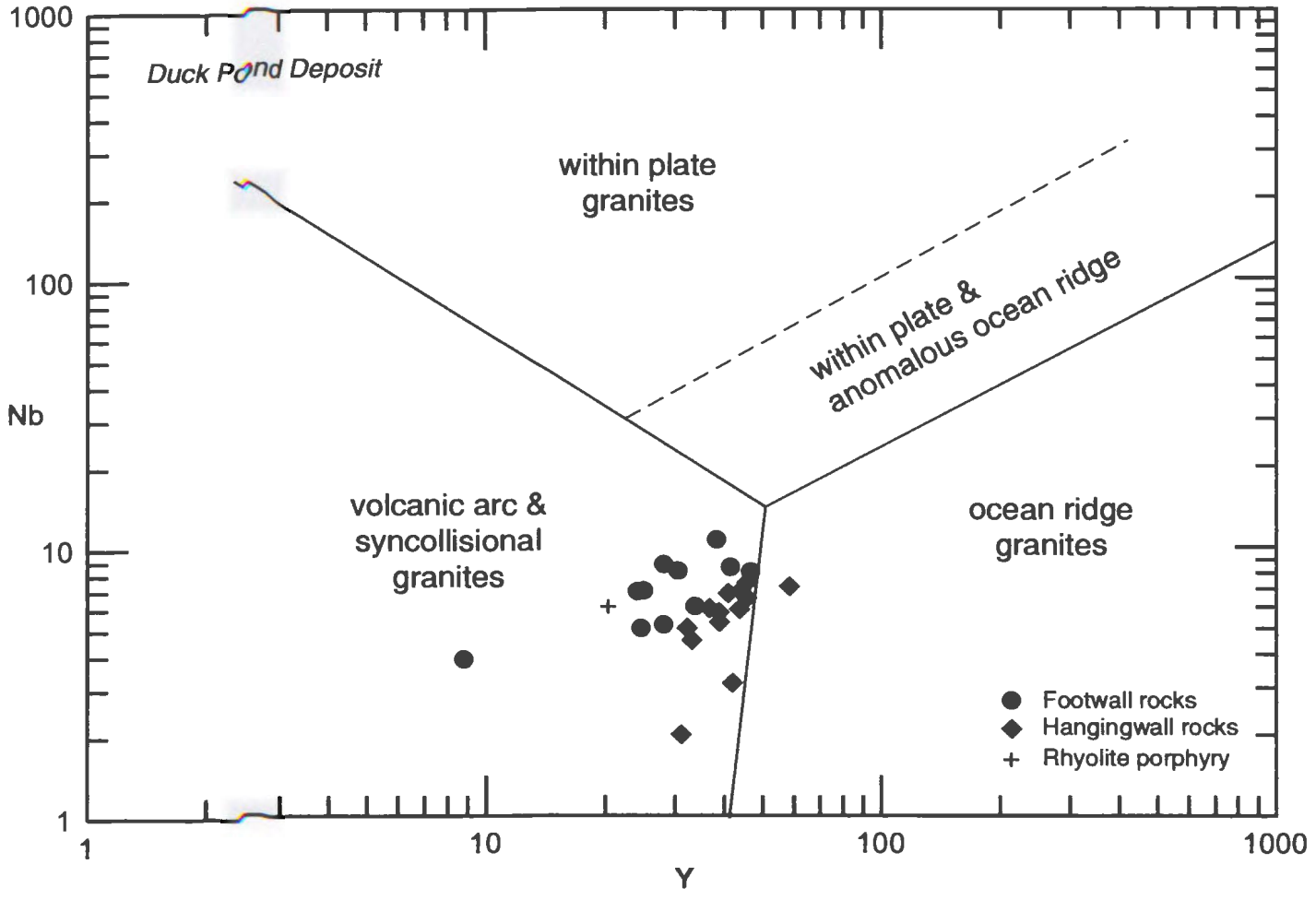

Figure 4.15(a) *Bivariate logarithm plot of Y vs Nb for felsic volcanic rocks in the Tally Pond Group.*

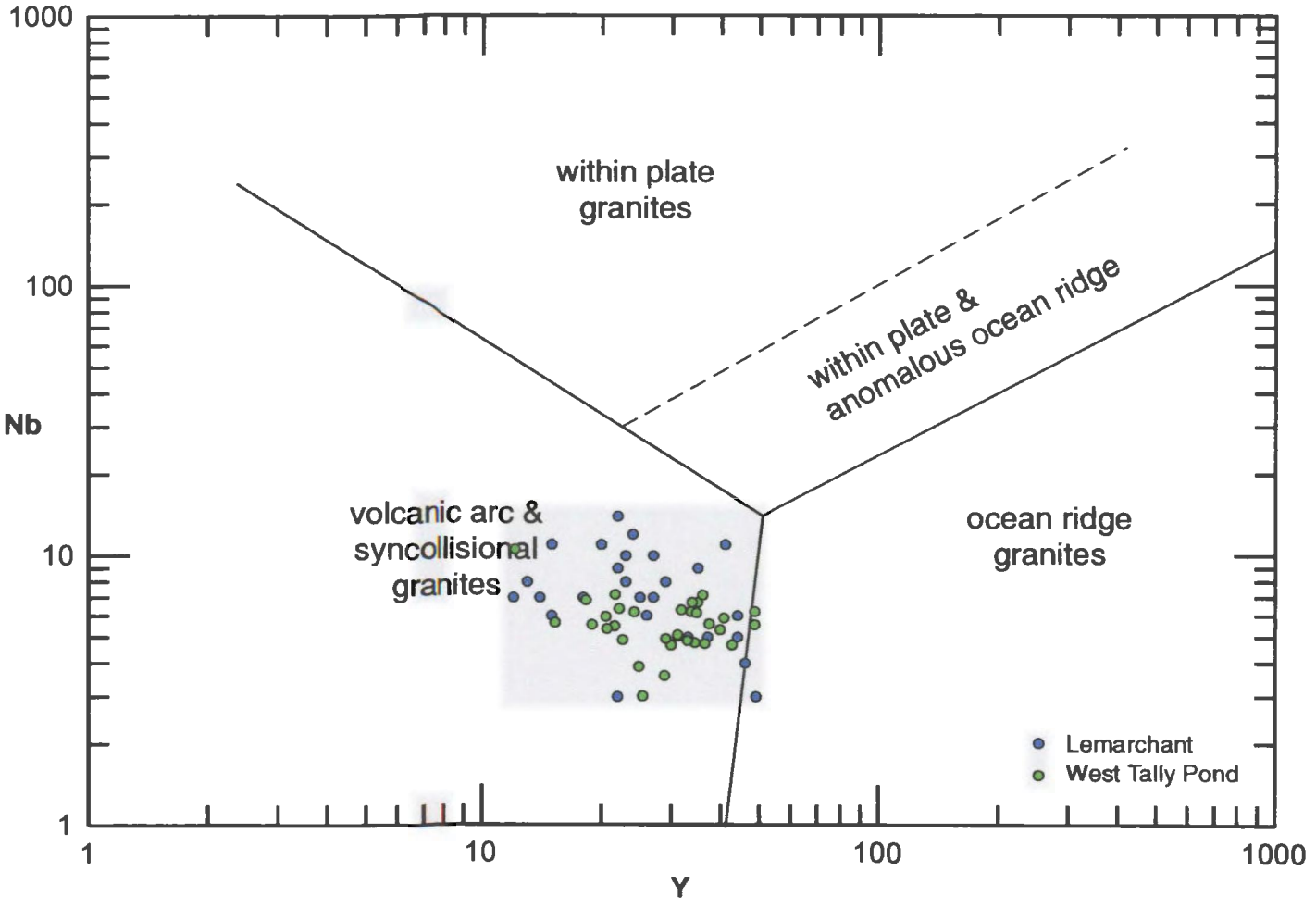

Figure 4.15(b) *Bivariate logarithm plot of Y vs Nb for felsic volcanic rocks in the Tally Pond Group.*

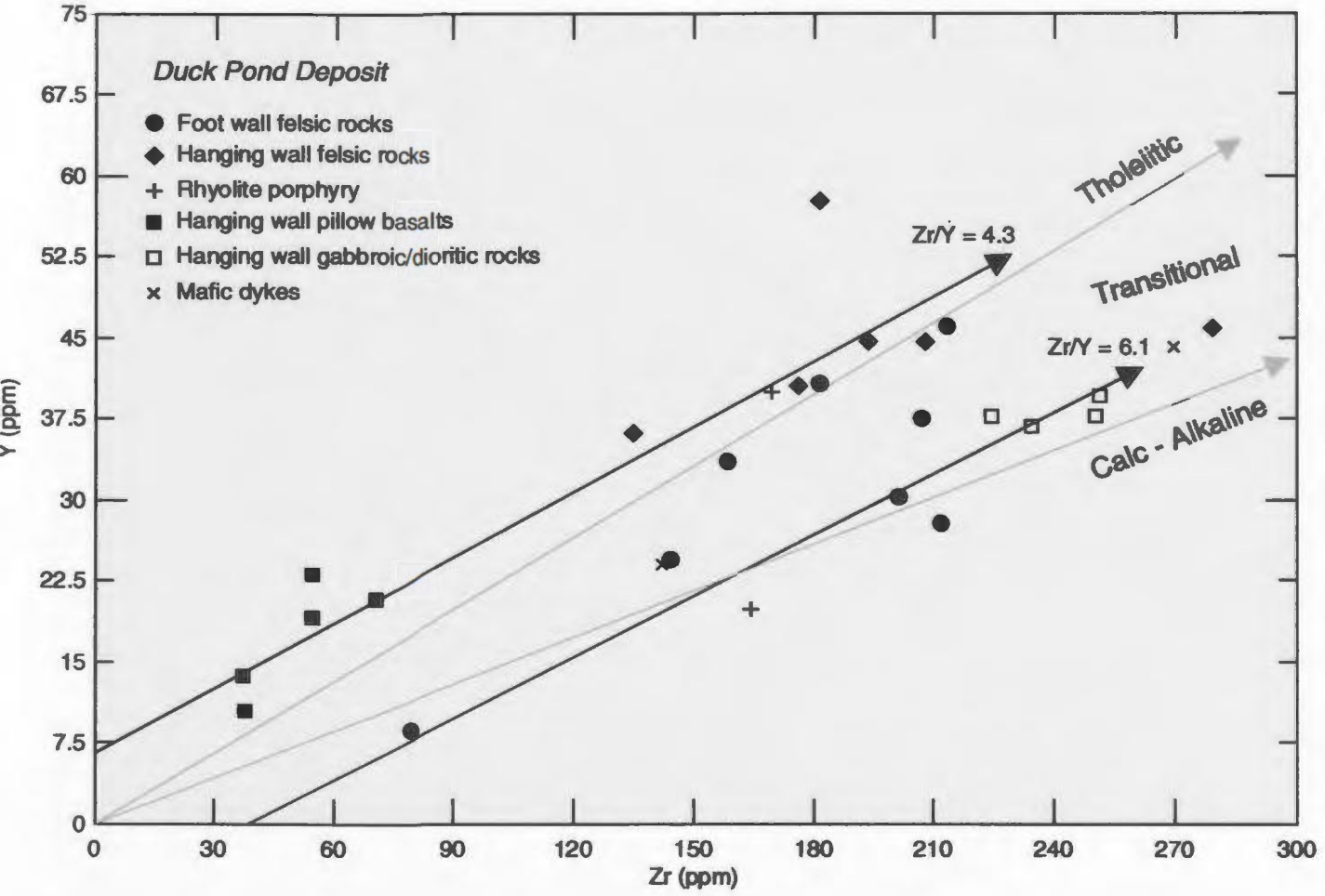

Figure 4.16(a) *Zr vs Y diagram for mafic and felsic volcanic rocks in the Tally Pond Group.*

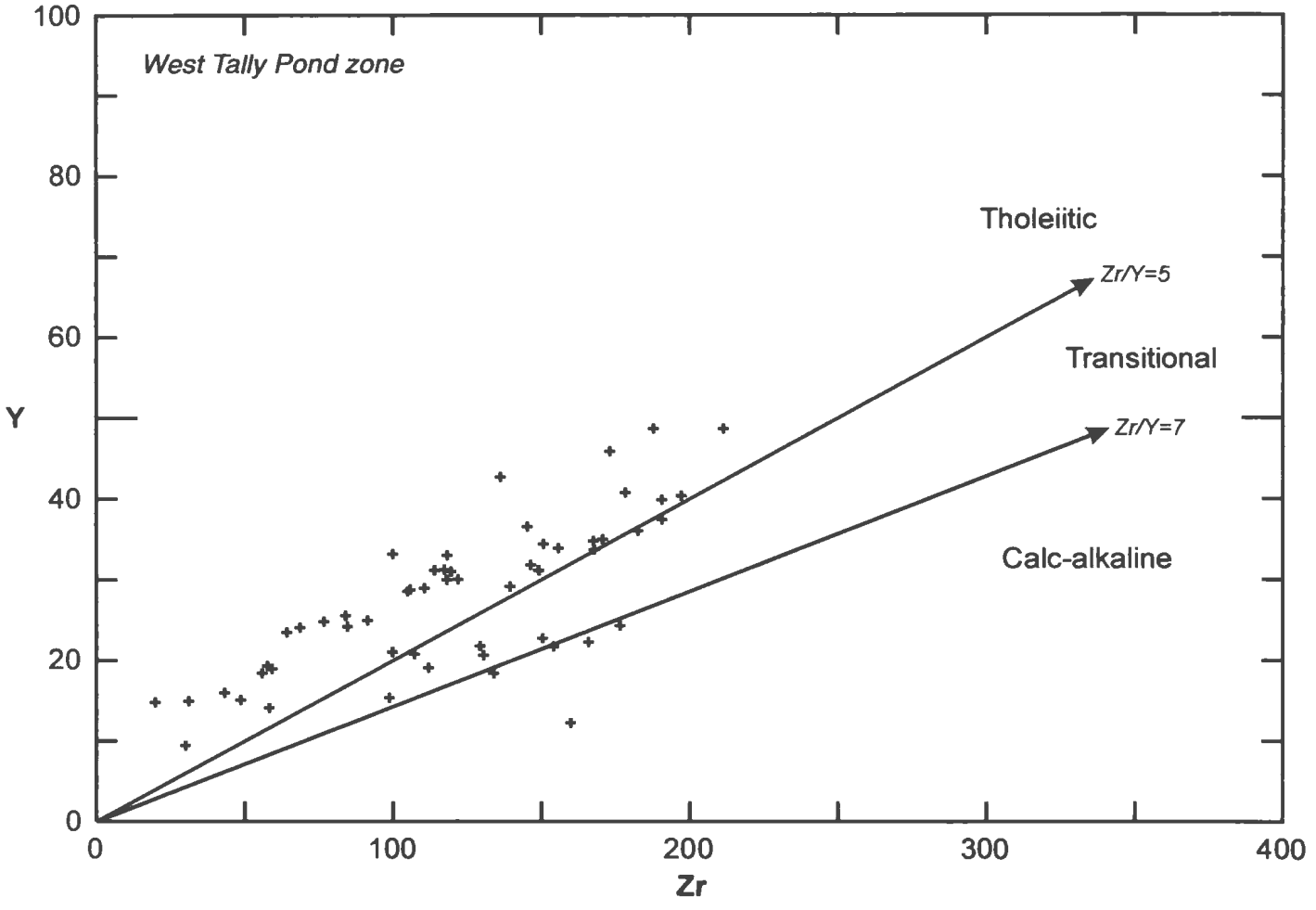

Figure 4.16(b) *Zr vs Y diagram for mafic and felsic volcanic rocks in the Tally Pond Group.*

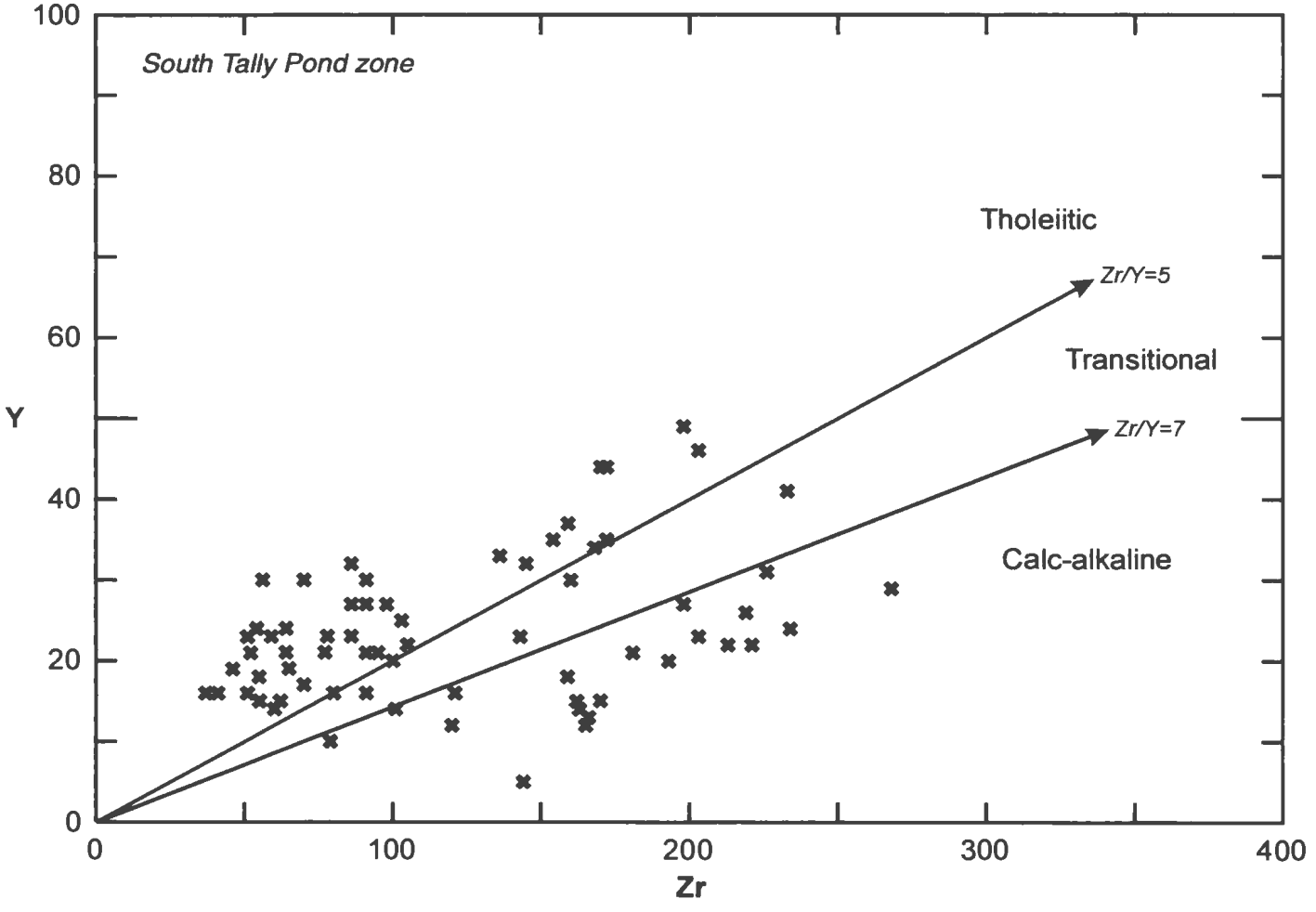

Figure 4.16(c) *Zr vs Y diagram for mafic and felsic volcanic rocks in the Tally Pond Group.*

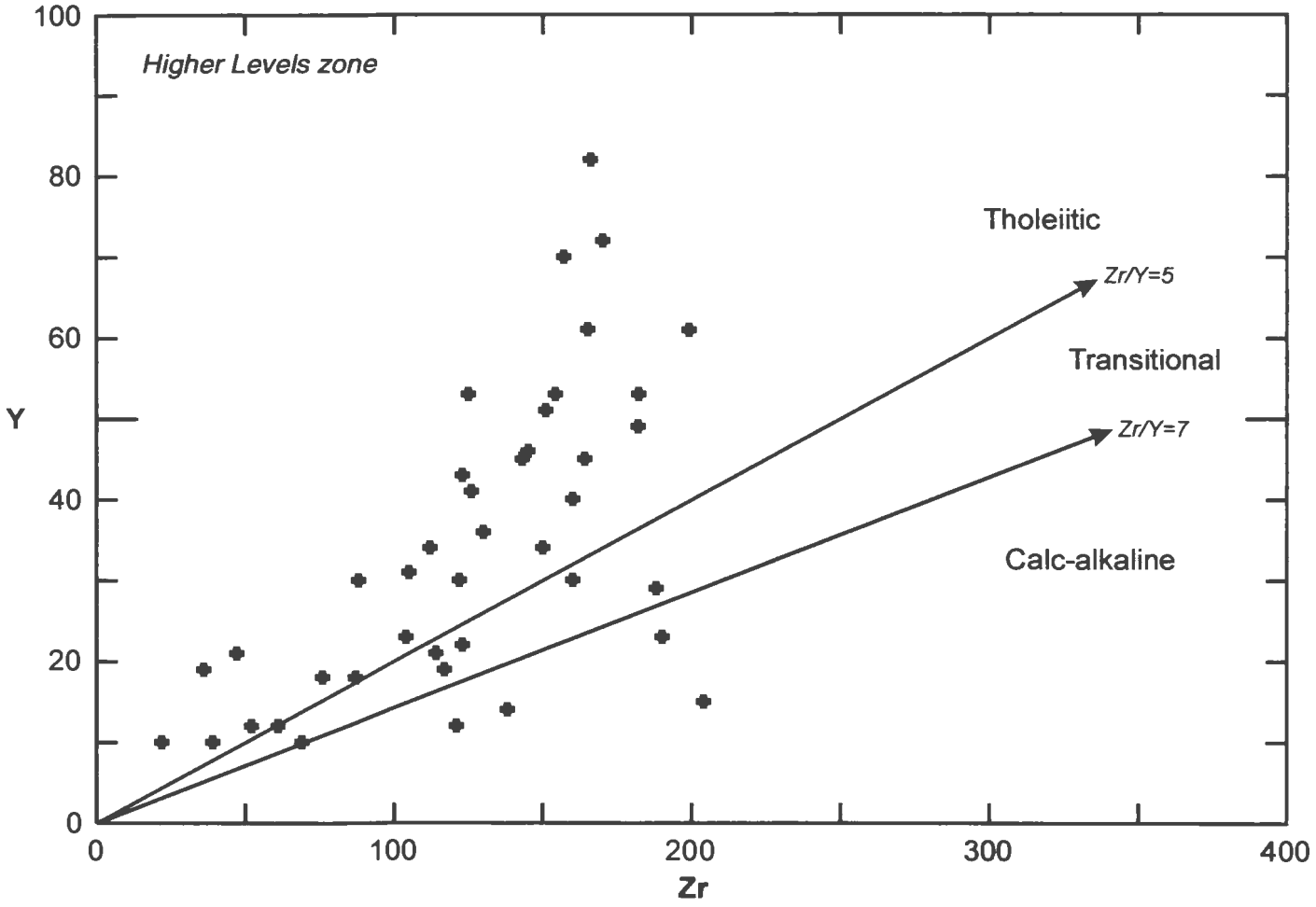

Figure 4.16(d) *Zr vs Y diagram for mafic and felsic volcanic rocks in the Tally Pond Group.*

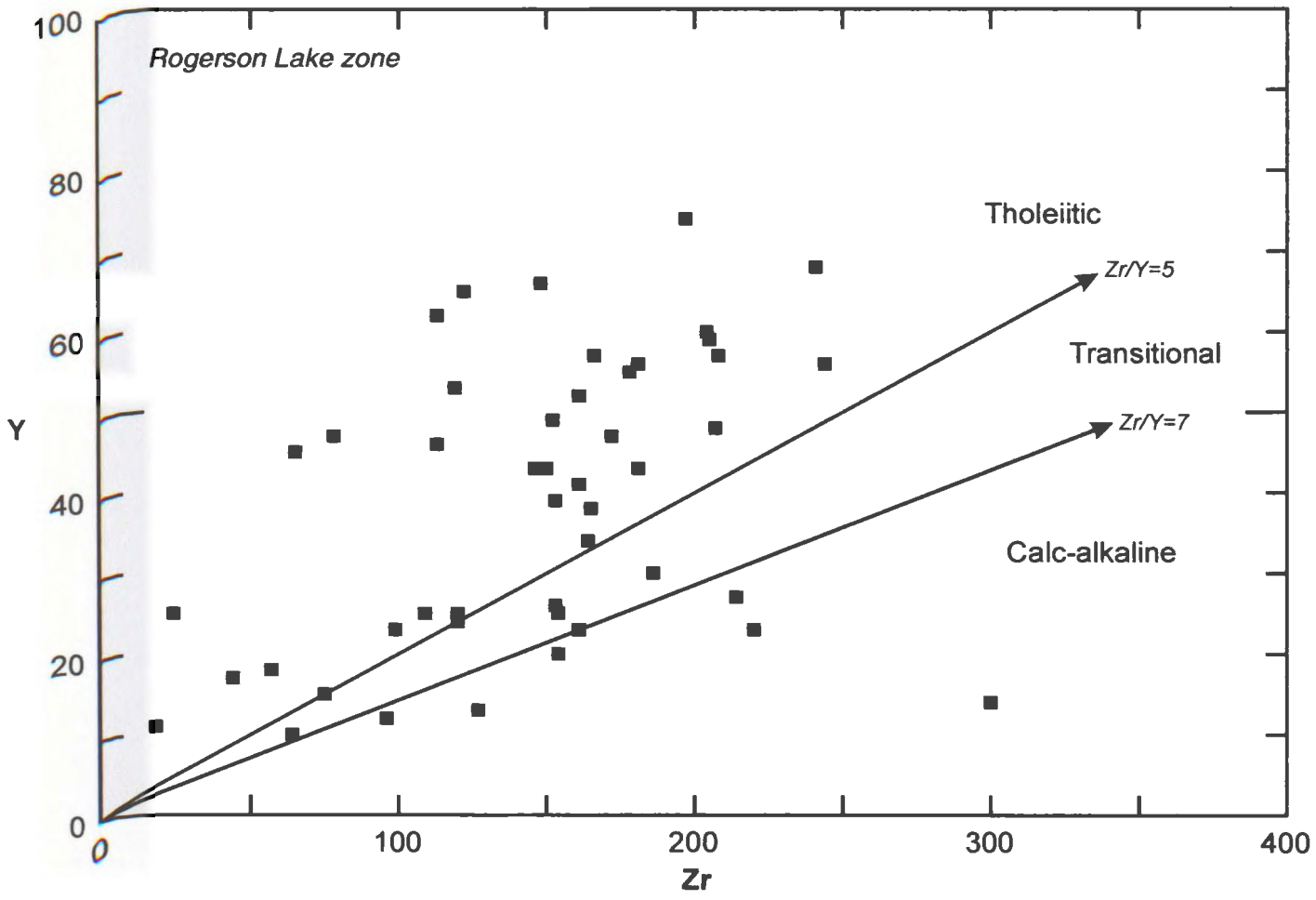

Figure 4.16(e) *Zr vs Y diagram for mafic and felsic volcanic rocks in the Tally Pond Group.*

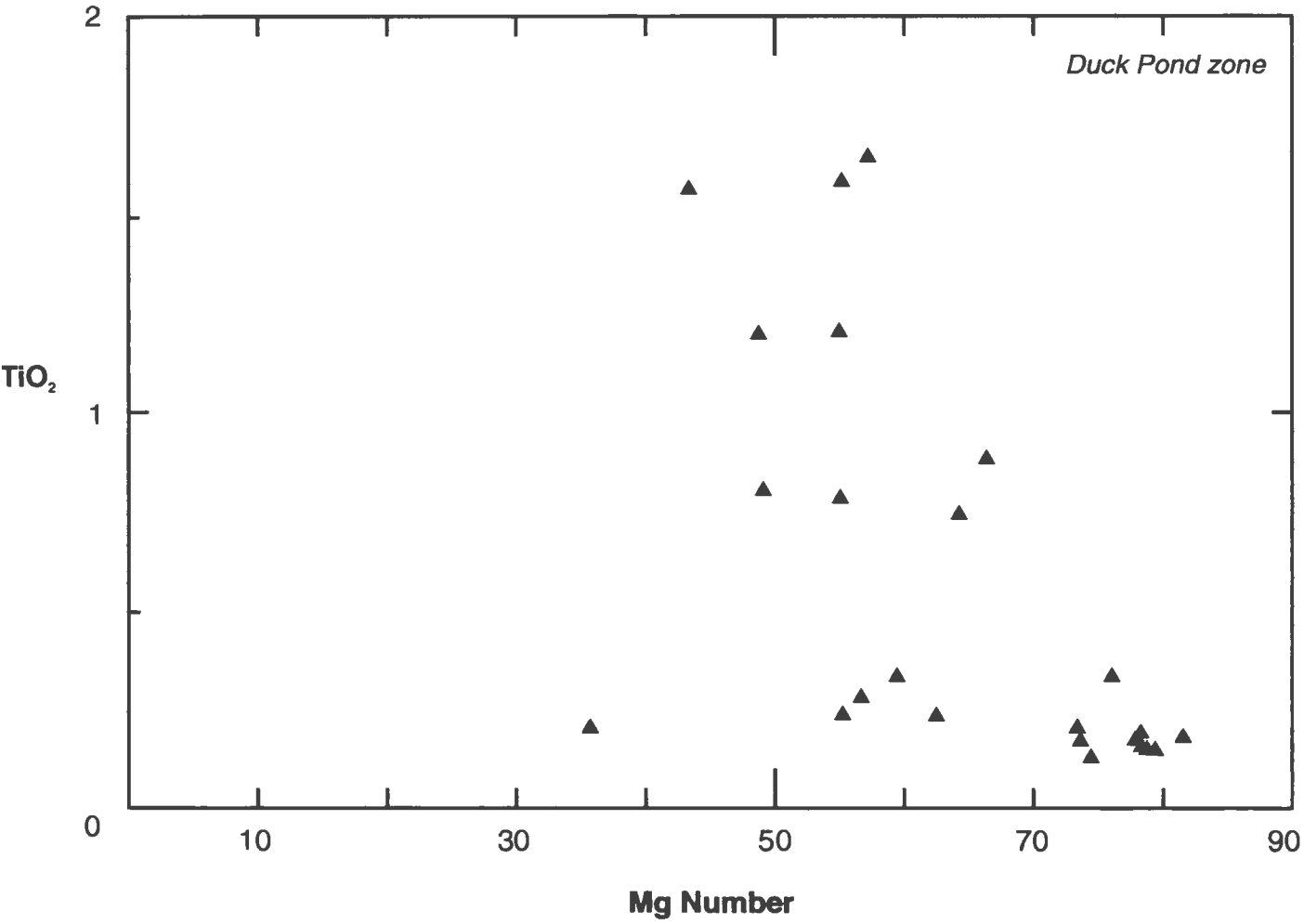

Figure 4.17(a) *Mg# vs TiO_2 for mafic volcanic rocks in the Tally Pond Group.*

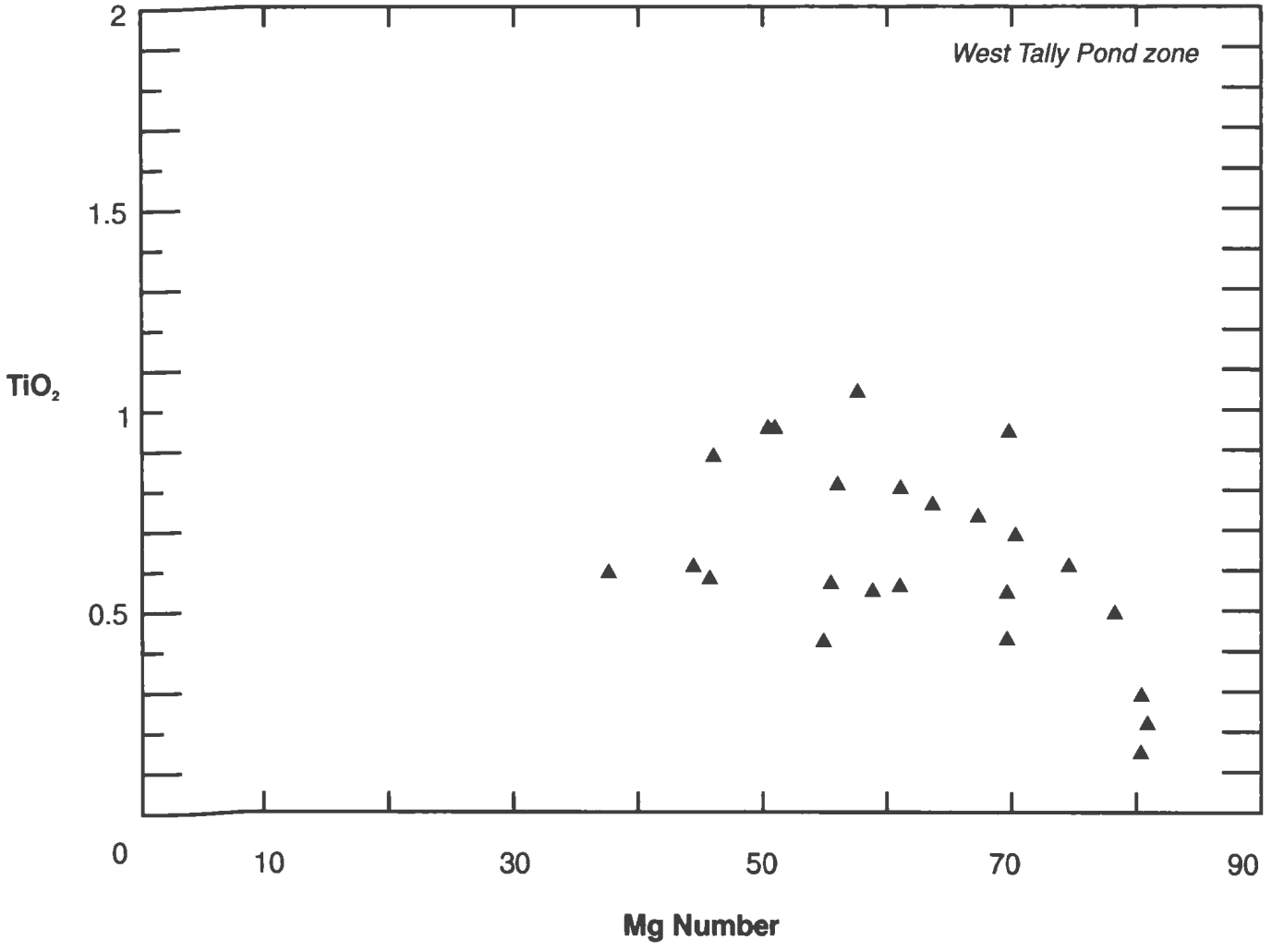

Figure 4.17(b) *Mg# vs TiO_2 for mafic volcanic rocks in the Tally Pond Group.*

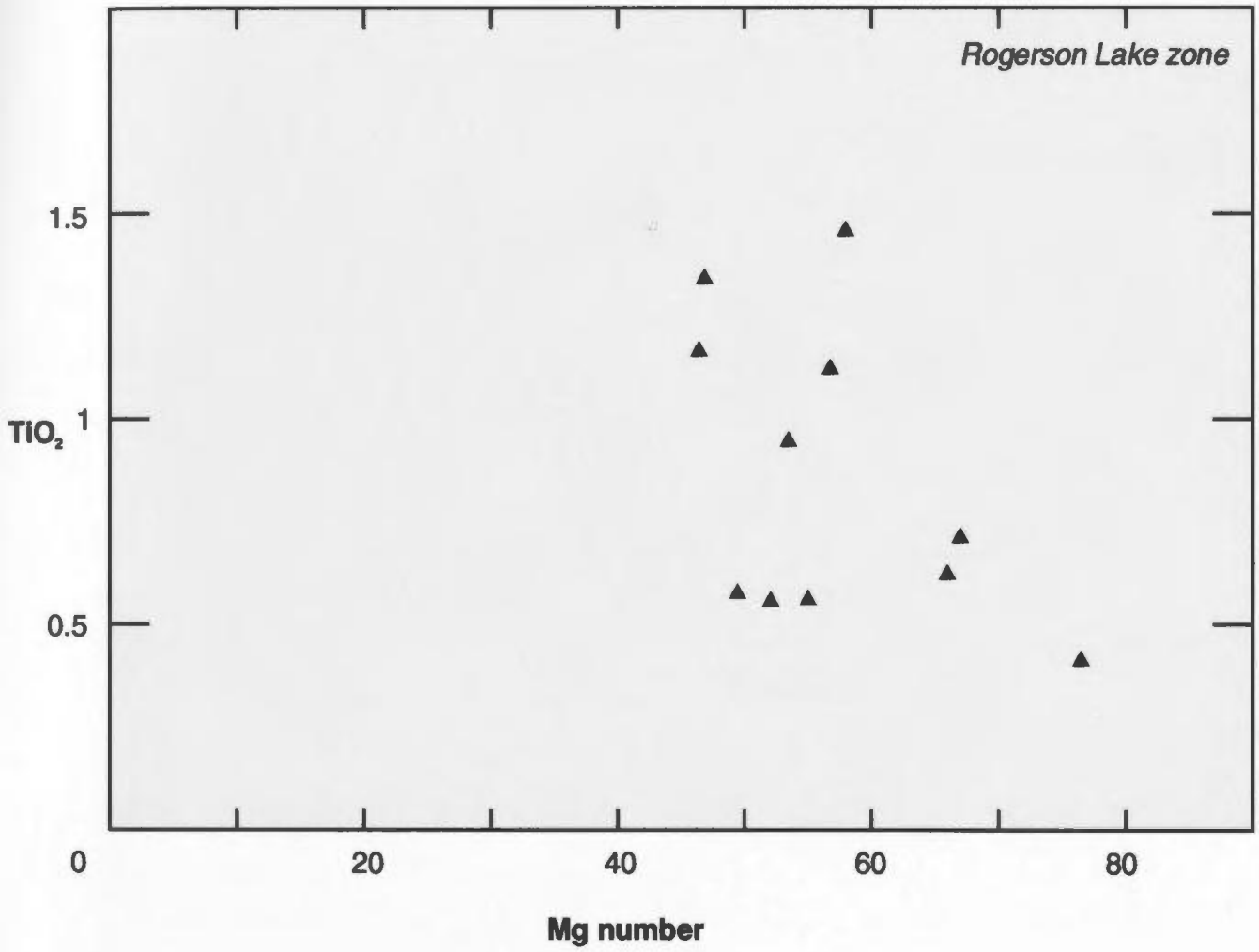

Figure 4.17(c) *Mg# vs TiO_2 for mafic volcanic rocks in the Tally Pond Group.*

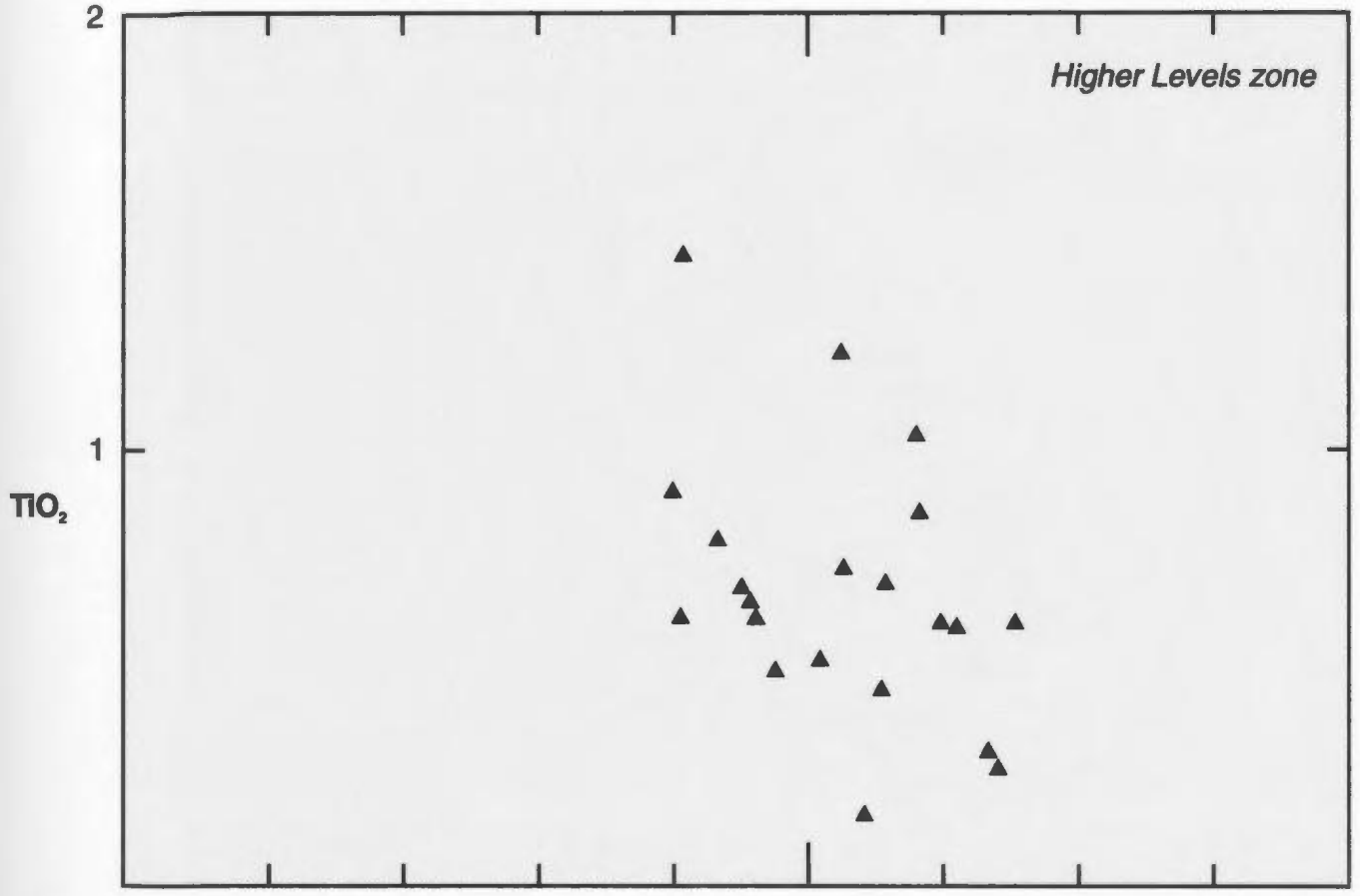

Figure 4.17(d) *Mg# vs TiO_2 for mafic volcanic rocks in the Tally Pond Group.*

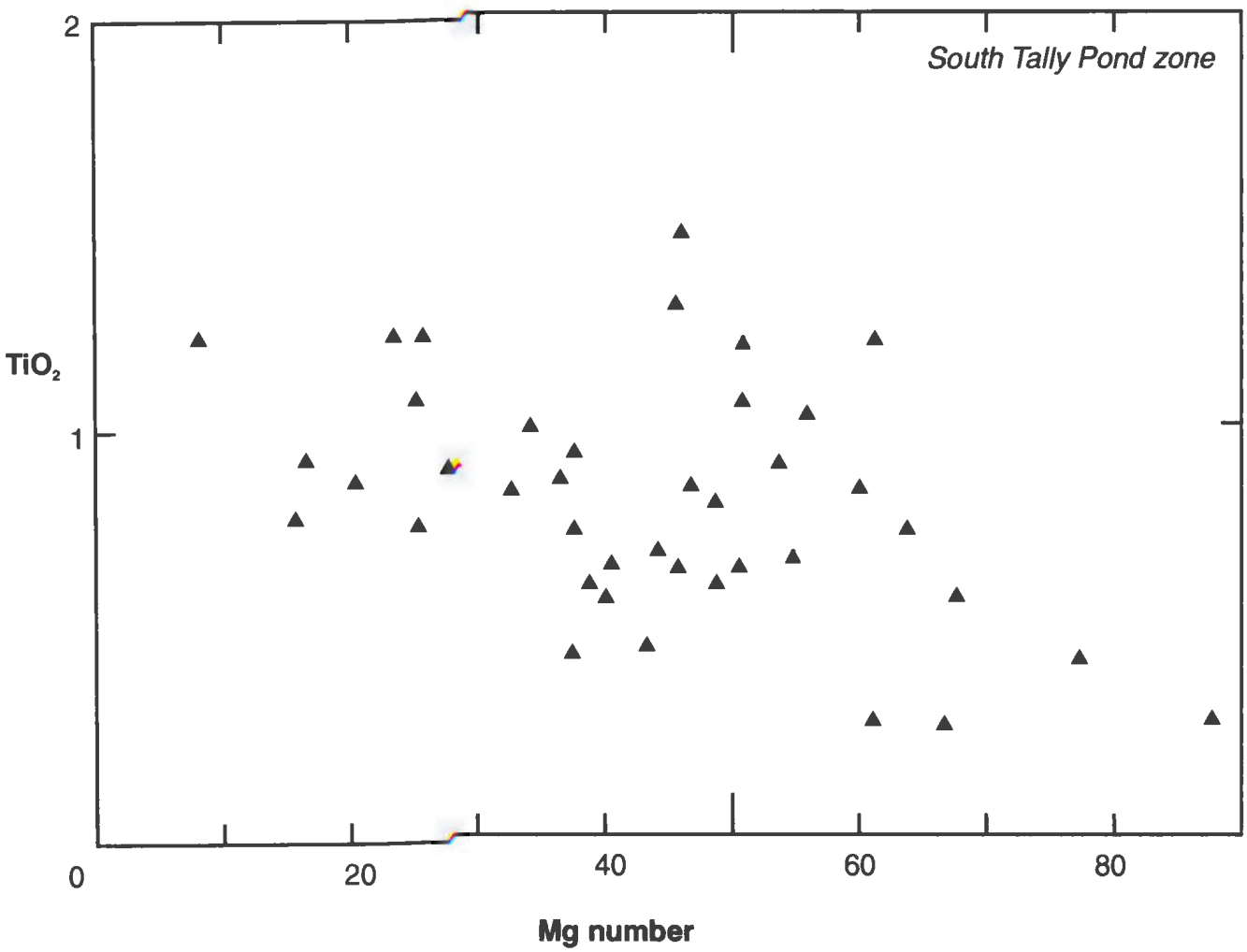

Figure 4.17(e) *Mg# vs TiO_2 for mafic volcanic rocks in the Tally Pond Group.*

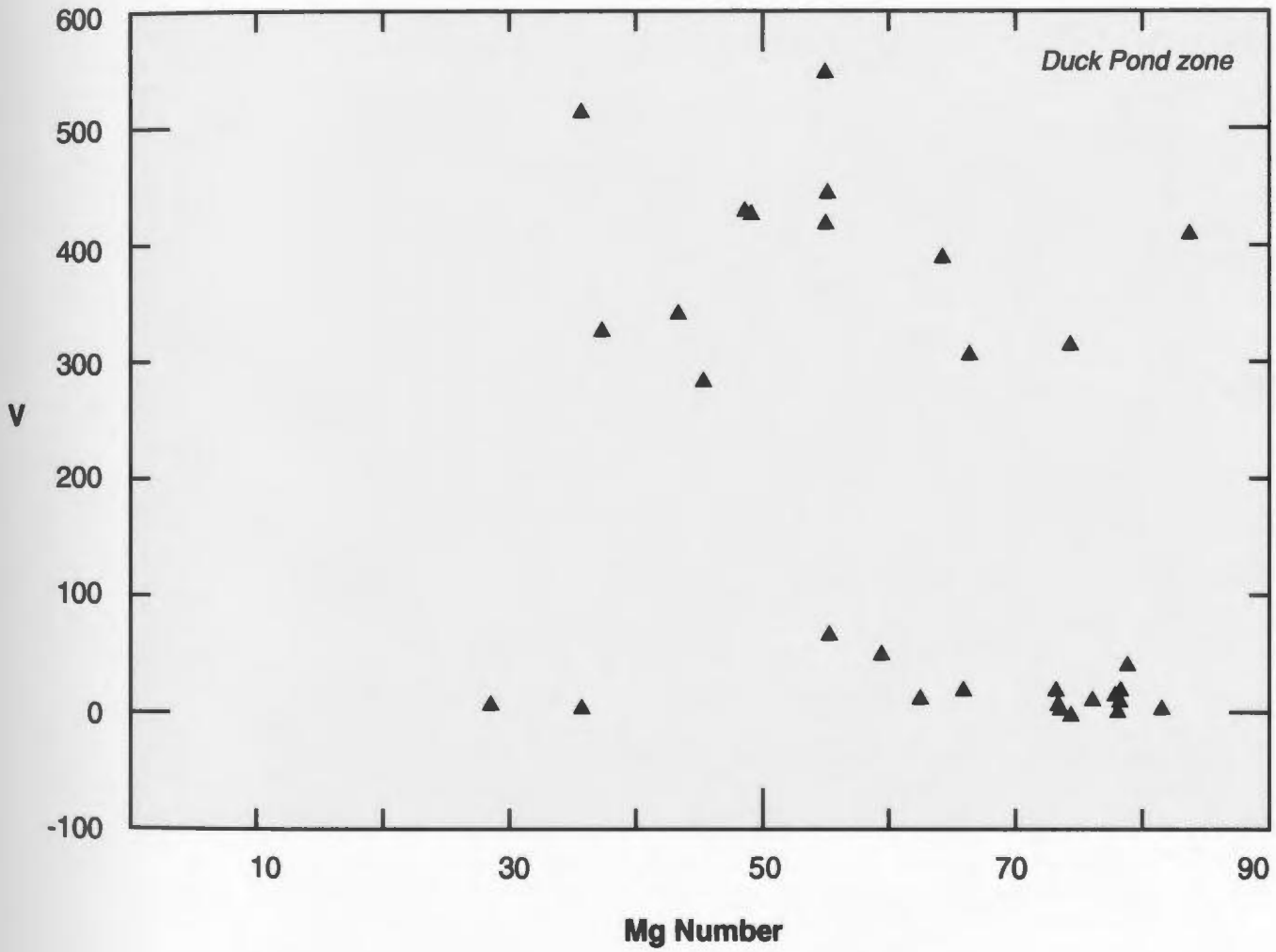

Figure 4.18(a) *Mg# vs V for mafic and intermediate volcanic rocks in the Tally Pond Group.*

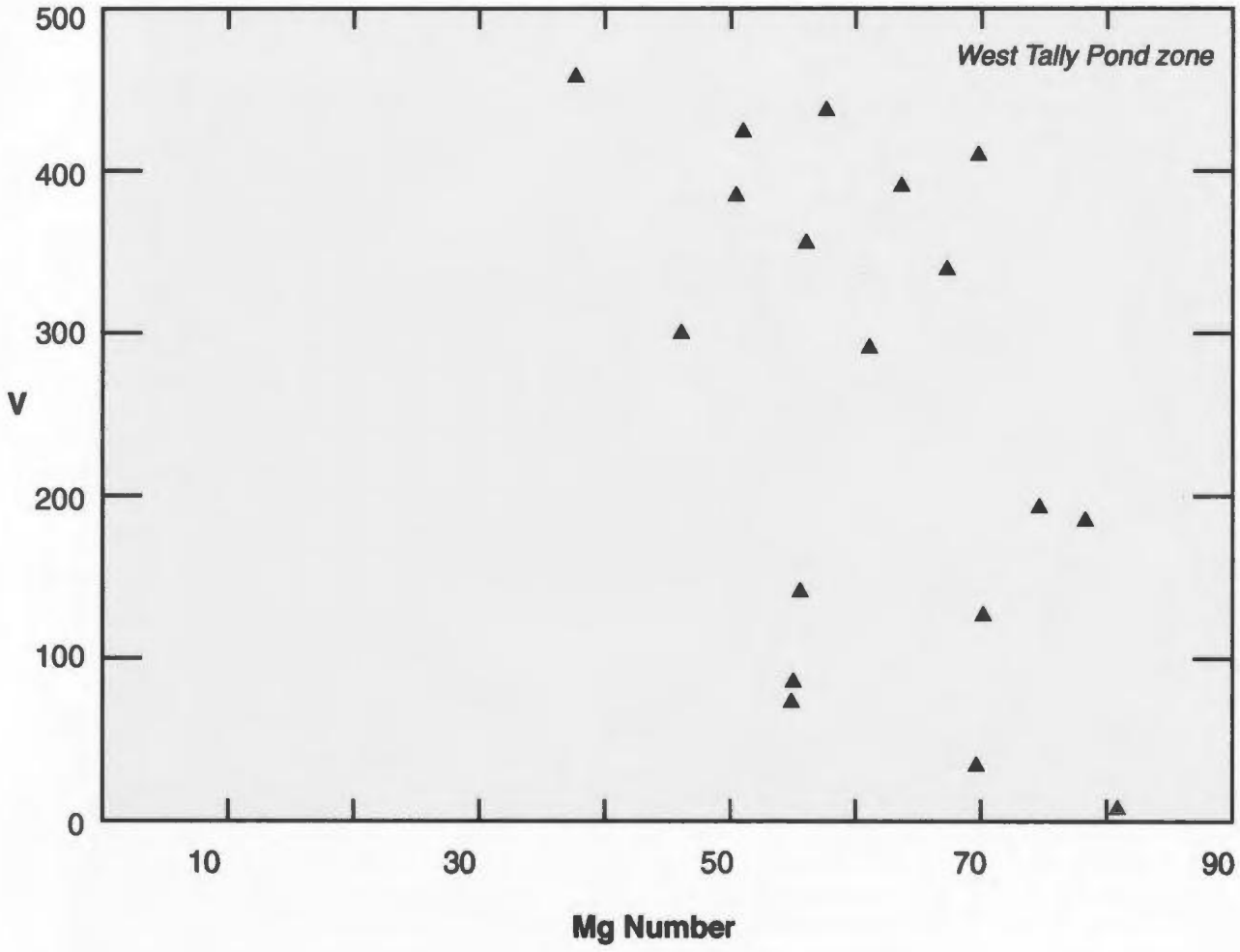

Figure 4.18(b) *Mg# vs V for mafic and intermediate volcanic rocks in the Tally Pond Group.*

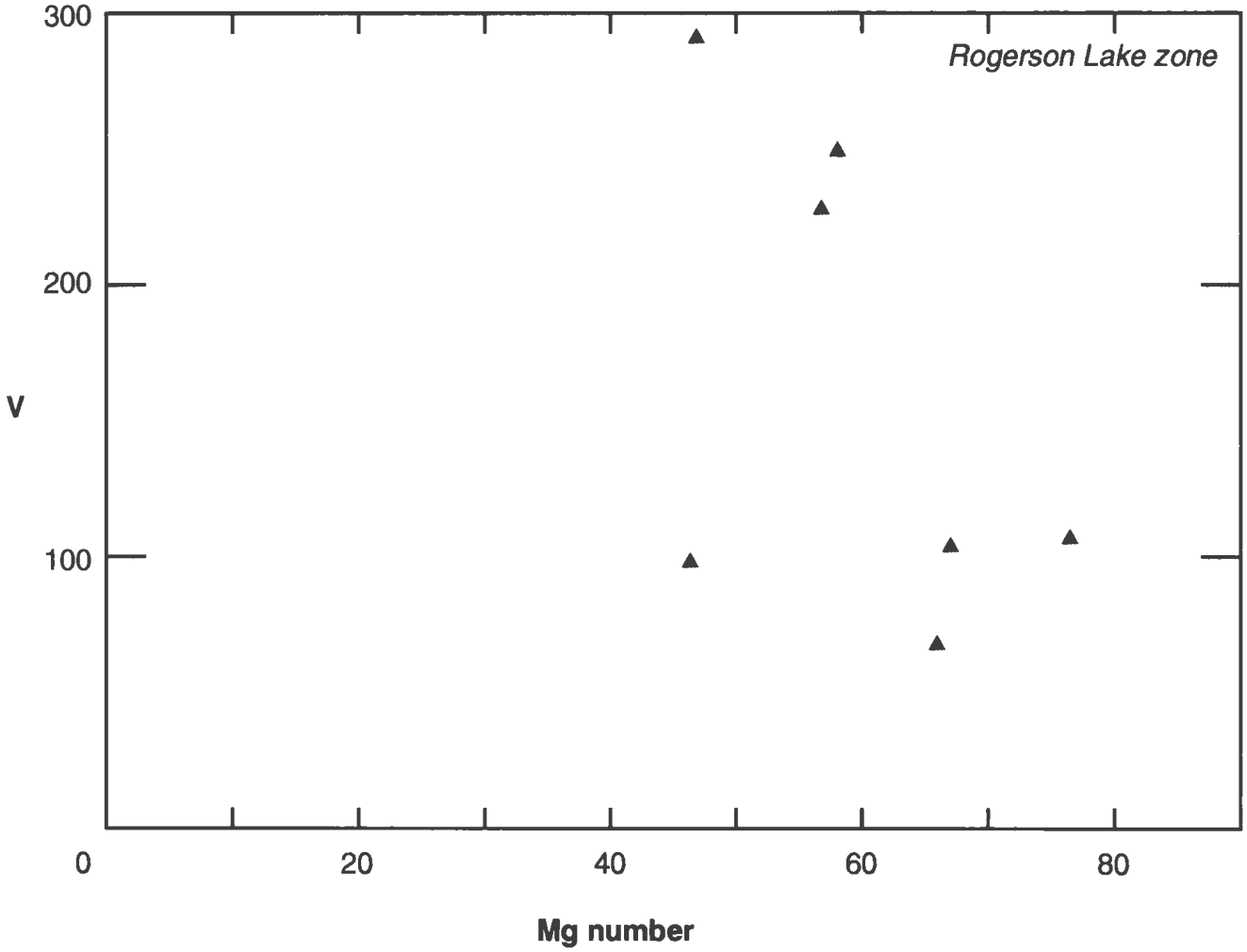

Figure 4.18(c) *Mg# vs V for mafic and intermediate volcanic rocks in the Tally Pond Group.*

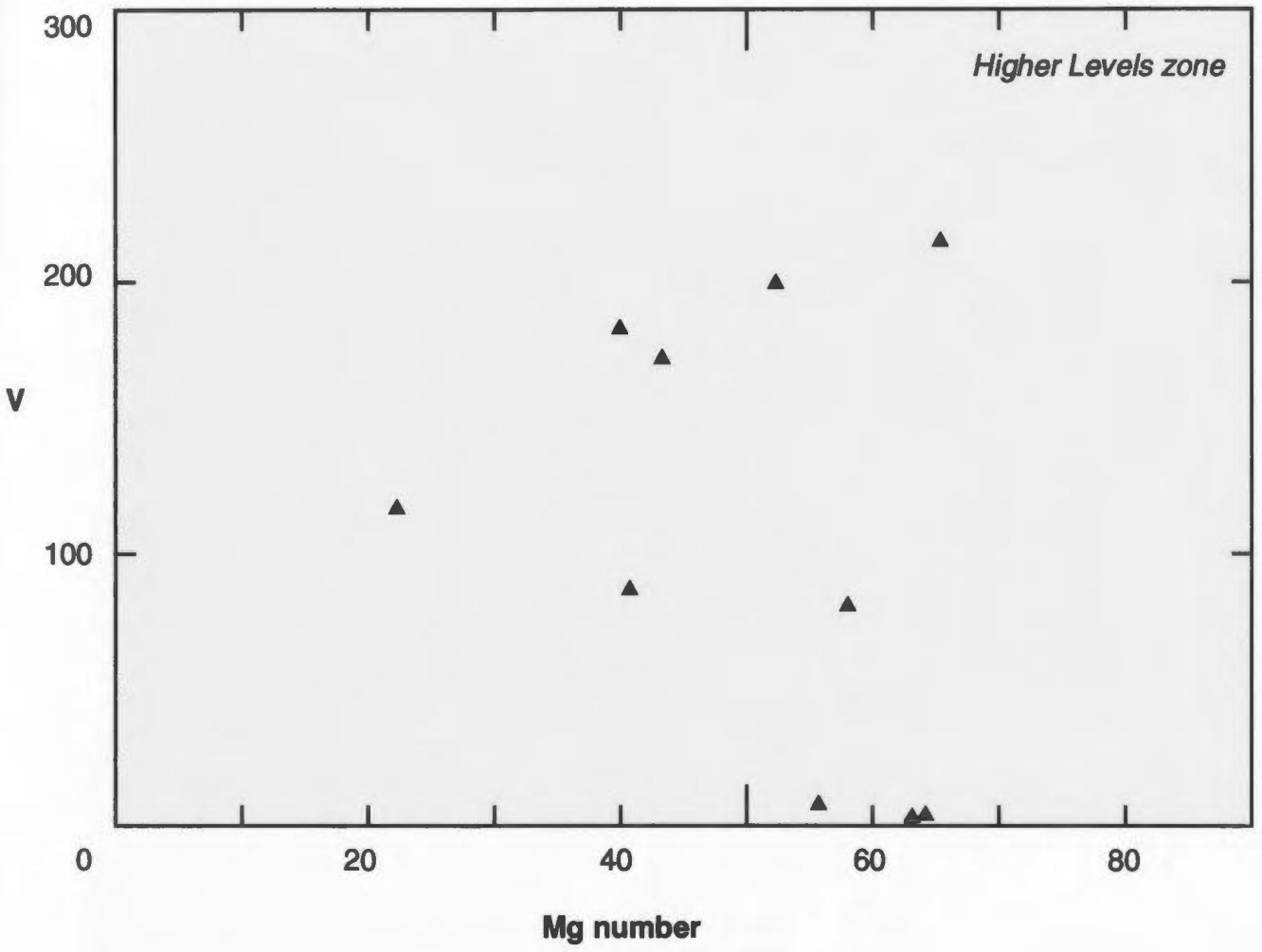

Figure 4.18(d) *Mg# vs V for mafic and intermediate volcanic rocks in the Tally Pond Group.*

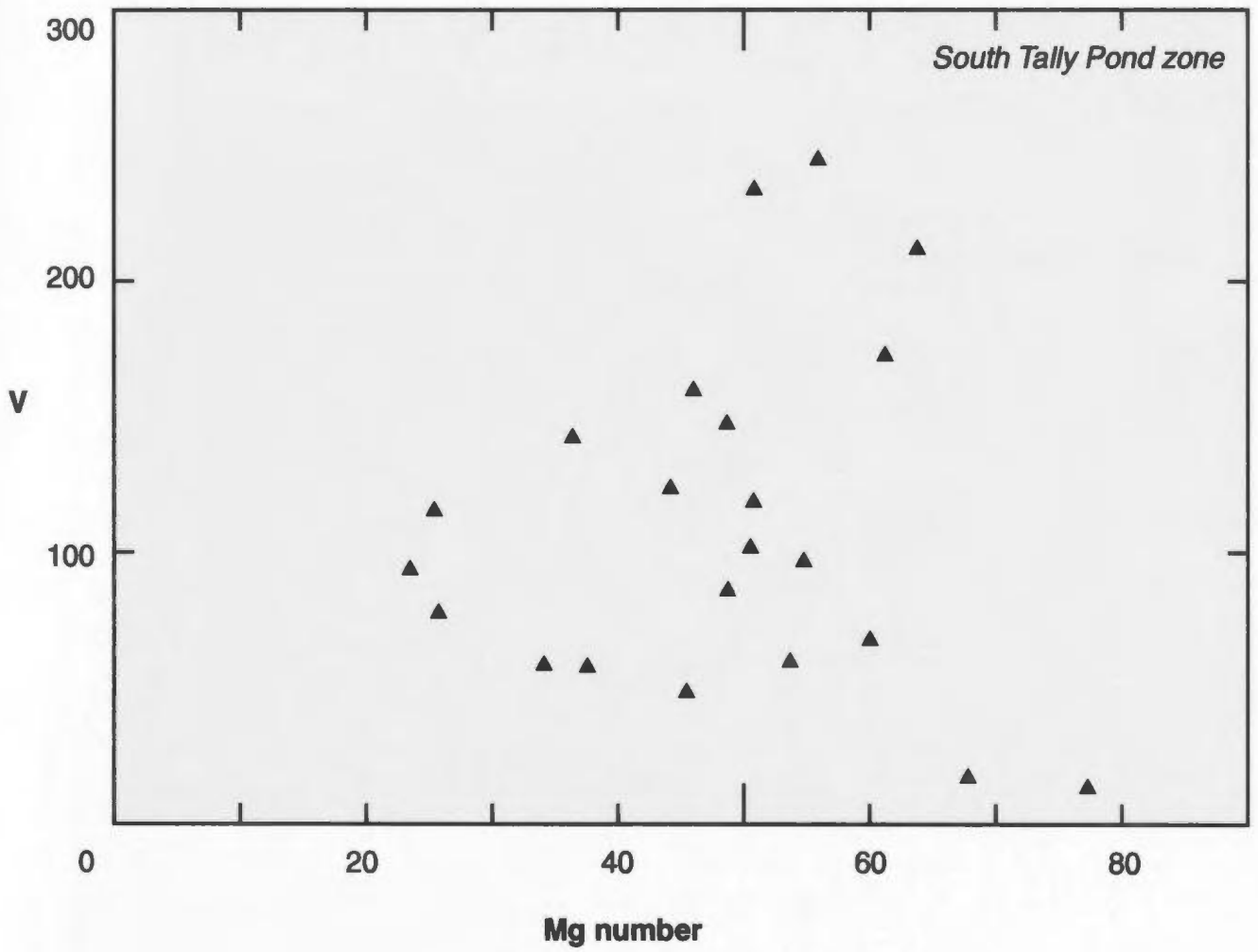

Figure 4.18(e) *Mg# vs V for mafic and intermediate volcanic rocks in the Tally Pond Group.*

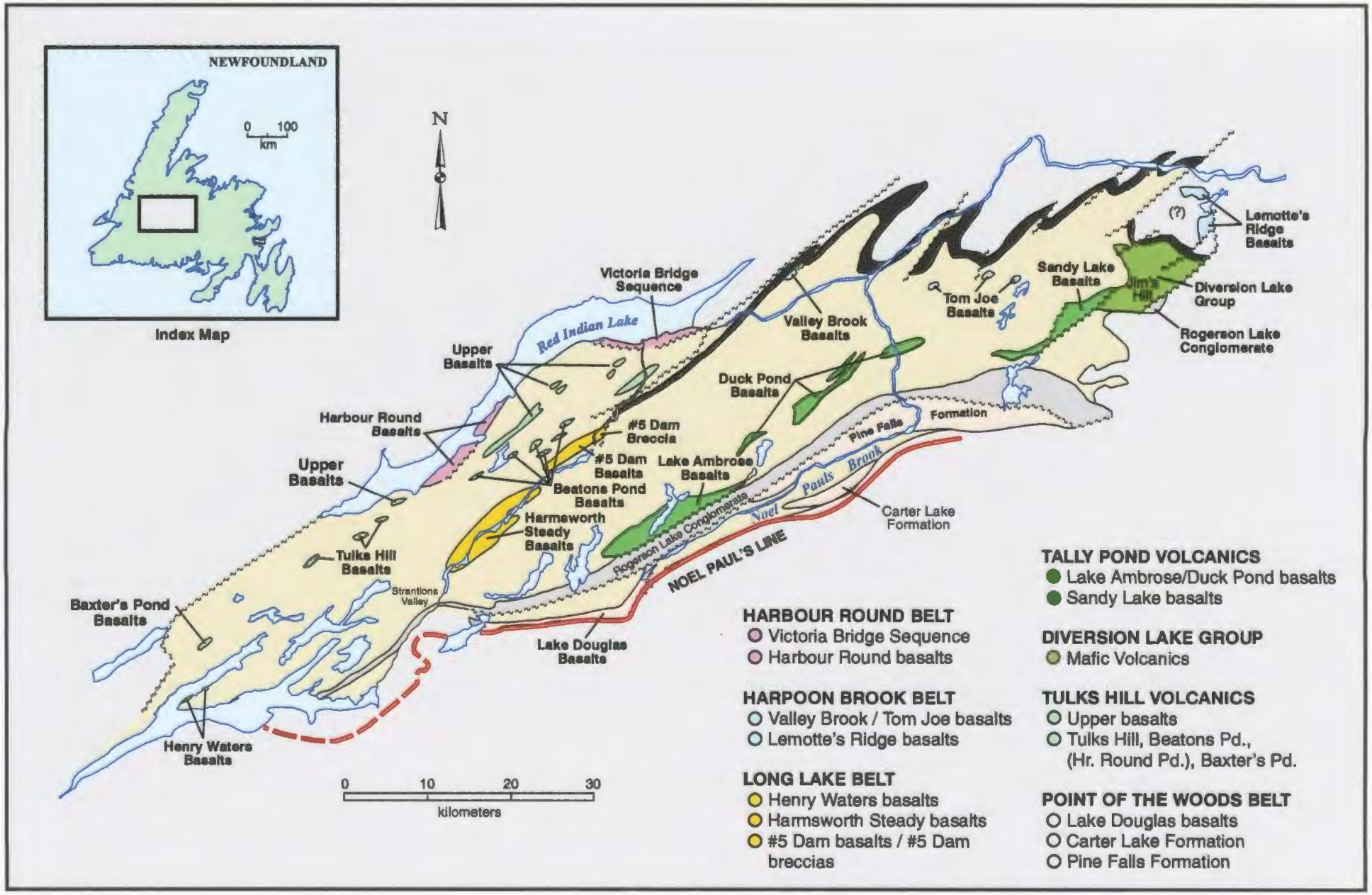

Figure 4.19 *Distribution of major mafic volcanic rock units within the Victoria Lake Supergroup. From Evans and Kean (2002).*

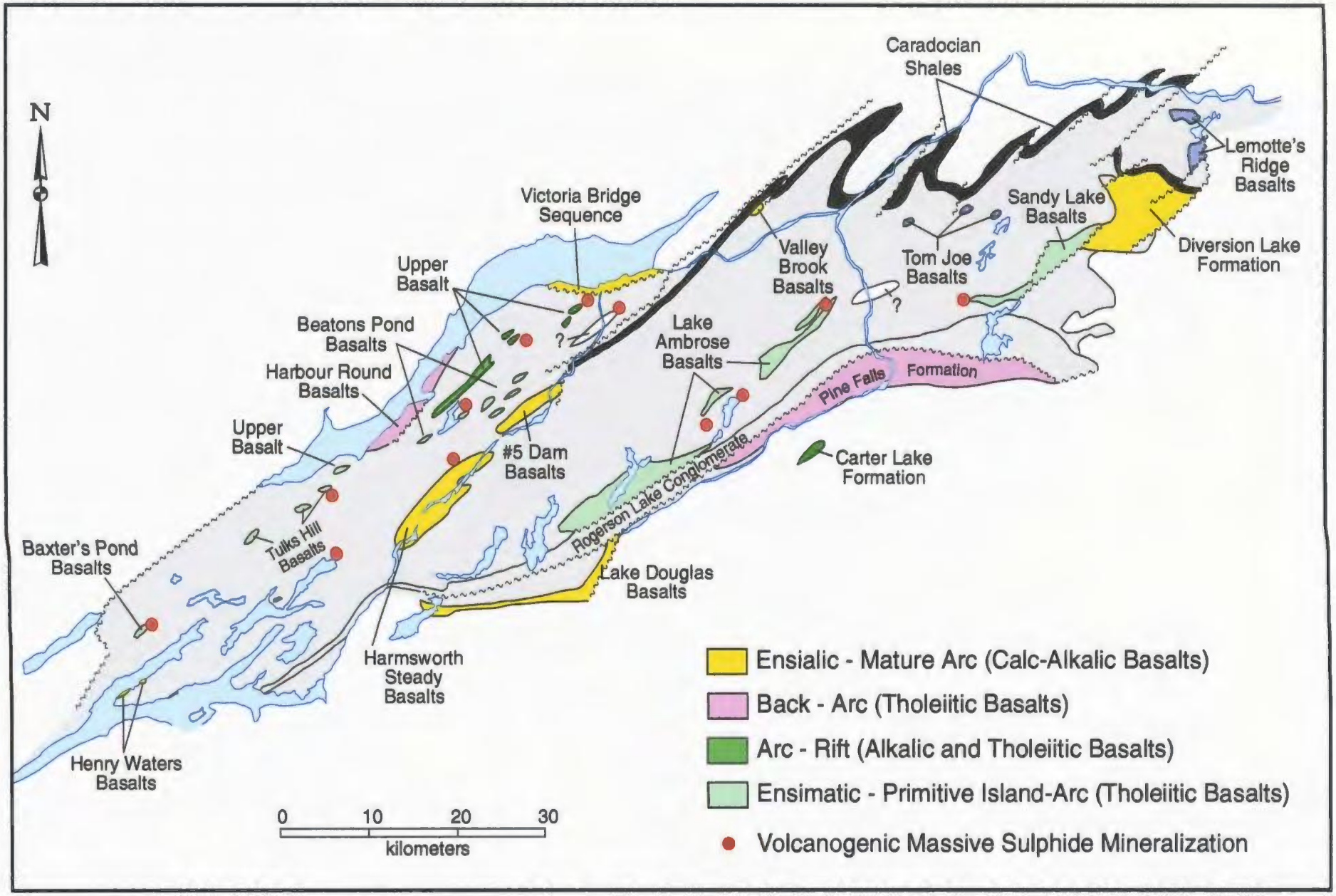

Figure 4.20 *Geographic distribution of the different geochemical groups of basalts. From Evans and Kean (2002).*

CHAPTER 5

HYDROTHERMAL ALTERATION GEOCHEMISTRY

5.1 Preamble

Hydrothermal alteration systems associated with volcanic massive sulphide deposits are one of the most extensively studied attributes of these deposit types. The basic hydrothermal alteration process consists of sub-seafloor circulation of seawater convectively driven primarily by magmatic heat sources, and the reaction of the heated seawater with permeable rocks of the crust and/or upper mantle. The alteration of the host rocks to VMS deposits can provide insights into how the hydrothermal system works as well as documenting the structural, mineralogical, metallogical and geochemical setting of the deposit.

Alteration mineral assemblages and associated chemical changes occur in two distinct zones (Figure 5.1) beneath VMS deposits (Franklin *et al.*, 1981; Franklin, 1995):

1. Alteration pipes occur immediately below the massive sulphide zone where a complex interaction occurs between the immediate substrata to the deposit and both hydrothermal fluids and advecting seawater.
2. Lower, semiconformable alteration zones occur as laterally extensive regions several hundred metres or more below the massive sulphide

deposit and are interpreted to represent the reservoir zone (Hodgson and Lydon, 1977) where the metals and sulphur were leached prior to their ascent and discharge onto the seafloor.

For this study, the chemistry of the alteration minerals sericite, chlorite and carbonate from the Duck Pond Deposit was analyzed using a Cameca SX-50 electron microprobe with SAMx software at the Department of Earth Sciences, Memorial University of Newfoundland. Details of the analytical techniques and procedures are given in Appendix C. Criterion for sample selection were based on the need to have a large spatial distribution throughout the alteration zones and to sample the differing types of hydrothermal alteration. The compositions of the alteration minerals present can vary based on the temperature, pressure, pH, oxidation state, and fluid and host rock compositions during ore deposition and formation. Consequently, these conditions can be estimated by analyzing the chemical composition of the various alteration minerals that are present.

5.2 Alteration zones of the Duck Pond Deposit

All rock sequences of the Tally Pond Group have been subjected to lower greenschist facies regional metamorphism. However, zones of weak to intense hydrothermal alteration are associated with the numerous volcanogenic massive sulphide occurrences throughout the group. Several varieties of hydrothermal alteration related to the Duck Pond deposit are present and best developed in the mineralized block of the deposit.

Felsic volcanic rocks in the footwall of the Duck Pond deposit have undergone extensive silicification, chloritization, and sericitization with areas of local carbonatization (Plate 5.1). Texturally, alteration consists of angular, brecciated cm-scale fragments surrounded by a fine-grained siliceous matrix (Plate 5.2). The fragments typically exhibit a jig-saw puzzle texture indicating in-situ origin of brecciation. The cores of the fragments are locally grey and less altered suggesting that silicification proceeded from the outer rims of the fragments inwards. The nature and amount of silica indicate that the rocks have undergone widespread permeation by hydrothermal fluids. Extensive zones, on the order of several tens to hundreds of metres, of the footwall are pervasively silicified but are not brecciated. Locally portions of the altered footwall consist of up to 75 per cent fine-to medium-grained pyrite. Base metals are typically absent; however, minor amounts chalcopyrite and sphalerite are present in millimetre to centimetre scale quartz veins. The pervasive alteration is interpreted to represent the source area for the metals that now form the massive sulphide lenses, which were leached from the felsic host rocks and subsequently transported to the site of deposition (Squires *et al.*, 2001).

Feeder pipe alteration consists of zones in which 25 to 100 per cent intense chlorite alteration (Plate 5.3) of the footwall rhyolites occurs as numerous 100 m thick tabular vertical zones that have very sharp contacts with the surrounding lithologies. The alteration consists of stringers of massive black chlorite developed along fractures in the host rhyolite. The intensity of the chlorite alteration is proportional to the distance from both the pipe centre and massive sulphide lens. Sulphide minerals, dominantly pyrite and minor chalcopyrite, are present in zones of greater than 50 per cent chlorite. The sulphide

content increases to amounts greater than 75 per cent in the chlorite pipes that immediately underlie the deposit (Plate 5.4). These intense chlorite alteration zones are interpreted to be the focusing conduits which developed along steep, synvolcanic faults that served as the transport mechanism for the upwelling metalliferous brine solutions that were convectively driven to the overlying exhalative horizon (Squires *et al.*, 1990).

As the intense chlorite alteration zones approach the massive sulphide lenses they form a zone of unusual carbonate alteration termed 'chaotic carbonate' (Squires *et al.*, 2001). This zone is characterized by millimetre-scale randomly oriented white carbonate veinlets and spheres that cross-cut and are hosted by a fine-grained black chlorite matrix (Plate 5.5). This alteration envelopes the Upper Duck lens of the Duck Pond deposit and varies from 75 m thick in the footwall to 25 m thick in the hanging-wall. The chaotic carbonate alteration has been interpreted (Squires *et al.*, 2001) to have formed by replacement processes within the shallowest part of the volcano-sedimentary sequence. This interpretation suggests that the Duck Pond deposit formed as an epigenetic sulphide body within the tuffaceous ash unit in the hanging-wall, as the carbonate would have been destroyed if the deposit formed on the seafloor and was exposed directly to seawater. An alternate interpretation, and the one favored here, is that the massive sulphide mineralization is syngenetic and formed synchronously with the adjacent volcanic rocks, whereas the carbonate alteration is a later epigenetic feature that formed after deposition of the massive sulphides.

5.3 Carbonate

5.3.1 Samples

Electron microprobe analysis was conducted on 17 carbonate samples from the Duck Pond deposit. Seven samples were from the intensely altered chlorite feeder zone; five were from the mineralized chaotic carbonate zone with greater than 50 per cent chlorite; four were from the unmineralized chaotic carbonate zone with less than 50 per cent chlorite; and one sample was from an altered rhyolite sample from the hanging-wall of the deposit.

5.3.2 Results

The microprobe analyses indicate that dolomite is the dominant carbonate species present in the Duck Pond deposit with samples from each of the different zones showing compositional diversities (Figure 5.2; Table C.1). The seven carbonate samples from the chlorite feeder pipe consist of approximately 50 per cent Ca, 40 per cent Mg and 10 per cent Fe. Five of the seven samples lie in the compositional range of ferroan dolomite, while two samples have Mg/Fe ratios of less than 4 thus would be classified as ankerite. The term ankerite is used here for material with Mg:Fe $\leq$ 4:1. The five samples from the mineralized chaotic carbonate zone contain the same Ca amount, are slightly more (3-5 per cent) Mg-rich and contain approximately 5 per cent Fe. These carbonates are also dolomite. The most Fe-depleted carbonates from the Duck Pond deposit are the four samples from the unmineralized chaotic carbonate zone. These samples are classified as dolomite since they consist of equal amounts of Ca and Mg (~50 per cent) and contain less than one per cent Fe. The one carbonate sample from the felsic volcanic rocks of the hanging-wall is the most Fe-rich carbonate mineral. It consists of roughly 47 per cent Ca, 38 per cent Mg and 15 per cent Fe. The increase in Fe content compared to the dolomite

samples and a Mg/Fe ratio of 2.5 means that the carbonate in the altered rhyolite is ankerite.

5.4 Chlorite

5.4.1 Samples

The nine chlorite analyses include four analyses of two samples from the host felsic volcanic rocks of the hanging-wall of the Duck Pond Deposit; four analyses of two samples from the chlorite dominated portion of the mineralized chaotic carbonate zone; and one analysis of chlorites from the intensely altered chlorite feeder pipes directly beneath the Duck Pond deposit.

5.4.2 Results

Chlorites from the Duck Pond deposit span an extensive range in compositions (Figure 5.3; Table C.2) based on sample location throughout the deposit. In the chaotic carbonate alteration zone, Fe/(Fe+Mg) ratios are in the range of 0.07 and 0.09 and atomic Si is restricted to between 5.6 and 6.0. These samples consist of a Mg-rich chlorite and are therefore classified as *chlinochlore*, based on the classification scheme of Hey (1954). Chlorite from the chlorite feeder zone contain greater concentrations of atomic Si (7-7.5) and have an Fe/(Fe+Mg) ratio of 0.3 and is therefore classified as *diabanite*. The greatest diversity in chlorite compositions is in the chlorite samples hosted by the altered rhyolite rocks of the hanging-wall to the Duck Pond deposit. Fe/(Fe+Mg) ratios for all the samples range from 0.39 to 0.41; there is, however, a larger disparity in atomic Si contents. Two analyses with the lowest atomic Si concentration, approximately 5.4, are

more Fe-rich and lie in the *ripiodolite* field; a further two analyses have atomic Si values of 5.8 and 6.0, are more Mg-rich and are classified as *pycnochlorite*.

Chlorite compositions are plotted on a tetrahedron using the components Mg, Fe, Si and Al. The tetrahedron is projected as a series of ternary diagrams (Figure 5.4) in order to plot a three dimensional object on a two dimensional page. Chlorites from the chaotic carbonate alteration zones are the least diverse samples from the Duck Pond deposit. Fe/Mg and Si/Al ratios are consistent and have a limited range in composition. These chlorites have the lowest Fe/Mg ratios and contents. The altered rhyolite chlorites have higher Fe/Mg ratios and are more Fe-rich and Mg-poor than the chaotic carbonate samples. They have fairly consistent Si/Al ratios, but Mg/Al ratios are more variable. The single chlorite feeder pipe analysis is a Si- and Mg-rich, Fe-poor chlorite that partially overlaps the Fe-deficient chaotic carbonate chlorites. This sample contains a distinctly high Al content which is interpreted to result from sericite contamination. The high K_2O content confirms this interpretation as there is no K present in chlorite.

5.5 Sericite

5.5.1 Samples

In total, 19 sericite analyses were performed using the electron microprobe and include four analyses of two samples from intensely altered chlorite feeder pipes; another six analyses of three samples from the altered rhyolite hanging-wall rocks; five analyses of two samples from the chlorite-rich mineralized chaotic carbonate zone; and four analyses of two samples from the unmineralized chaotic carbonate zone.

5.5.2 Results

The term sericite is a general term used to describe a fine-grained member of the mica group which may be muscovite, paragonite or illite. The data (Figure 5.5; Table C.3) from the various areas of the Duck Pond deposit suggest that muscovite is the only sericite (or mica) type in the Duck Pond deposit. Fe+Mg contents are below 10 per cent for all samples except for one sericite from the altered rhyolite which has a value of approximately 12 per cent. Si/Al ratios range from 1.13 to 1.24 for sericite from the mineralized chaotic carbonate zone and altered rhyolite to an average value of 1.44 for sericite from the altered chlorite feeder pipes and unmineralized chaotic carbonate zones. The higher Si/Al ratios move the composition of these sericite from pure muscovite towards a phengitic composition. Nonetheless the Si/Al ratios are too low for these sericites to be phengite as pure phengite requires a Si/Al ratio of greater than three and also displays a substitution of Mg and Fe for Al with increasing Si contents (Deer *et al.*, 1992).

In most of the samples from the Duck Pond deposit there is an inverse proportionality between Al and Mg. All of the sericites are depleted in Fe and Al substitutes for Mg with constant Fe concentrations.

5.6 Discussion

Chemical compositions of the alteration minerals chlorite, sericite and carbonate are quite variable in the samples analyzed from the Duck Pond deposit. Chlorites from the Duck Pond deposit contain a broad range of Fe/(Fe+Mg) ratios and atomic Si concentrations. Those from the chaotic carbonate alteration zone have a restricted Si

content and have Fe/(Fe+Mg) ratios typical of high Mg chlorites. Chlorites from the feeder pipe to the Duck Pond deposit contain the highest atomic Si amounts and have intermediate Fe and Mg contents. The most ferroan-rich chlorites are those from the altered rhyolite rocks of the hanging-wall to the Duck Pond deposit. The Fe content of the chlorites is inversely proportional, and the Mg content is proportional to the distance from the massive sulphide lenses. Chlorite results from the hydrothermal alteration of pyroxenes, amphiboles and biotite in igneous rocks and as such the composition of the chlorite is often related to that of the original igneous material. The difference in Fe and Mg ratios in the Duck Pond chlorites is attributed to the differences in the source of Fe and Mg, namely the host volcanic rocks and seawater, respectively. Chlorites more distal have undergone alteration at lower water/rock ratios and reflect the higher Fe/(Fe+Mg) ratios of relatively unaltered volcanic rocks. Whereas magnesian-rich chlorites that are geographically closer to the sulphide deposit have experienced significantly higher water/rock ratios than those of the distal zones and are considered to result from the interaction of cold seawater with hot hydrothermal fluids.

Sericites from the Duck Pond deposit are all classified as muscovite with little variation in composition. However, as a whole, the sericites are all depleted in Fe and contain varying amounts of Mg and Al that substitute for Fe in octahedral sites.

Carbonates from the Duck Pond deposit are dominantly dolomite with small compositional variations between the samples from the different alteration zones. Dolomites from the alteration feeder pipes contain roughly equal amounts of Ca and Mg and are characterized by low Fe contents. Some carbonates from the feeder pipe and altered host rhyolites have lower Mg/Fe ratios and have the composition of ankerite.

The variation in Fe and Mg contents in alteration zones associated with VMS deposits is well documented. These deposits commonly show variations in the Mg/Fe ratio when compared to the proximity to the site of hydrothermal discharge. Ferroan chlorites occur in the core of stockwork feeder zones in mafic footwall rocks of Cu-Zn deposits in the Archean Abitibi belt (Doucet *et al.*, 1998). Whereas younger deposits tend to be dominated by magnesian chlorites in their alteration feeder core. The chlorites and carbonates in the feeder pipe and especially the chaotic carbonate zones are extremely Fe-depleted indicating that the hydrothermal fluids that formed the Duck Pond deposit were Mg-rich and Fe-depleted. Similar magnesian chlorites are reported from VMS deposits in the Kuroko district of Japan (Hattori and Sakai, 1979; Urabe *et al.*, 1983) and Buchans (Henley and Thornley, 1981; Winter, 2000).

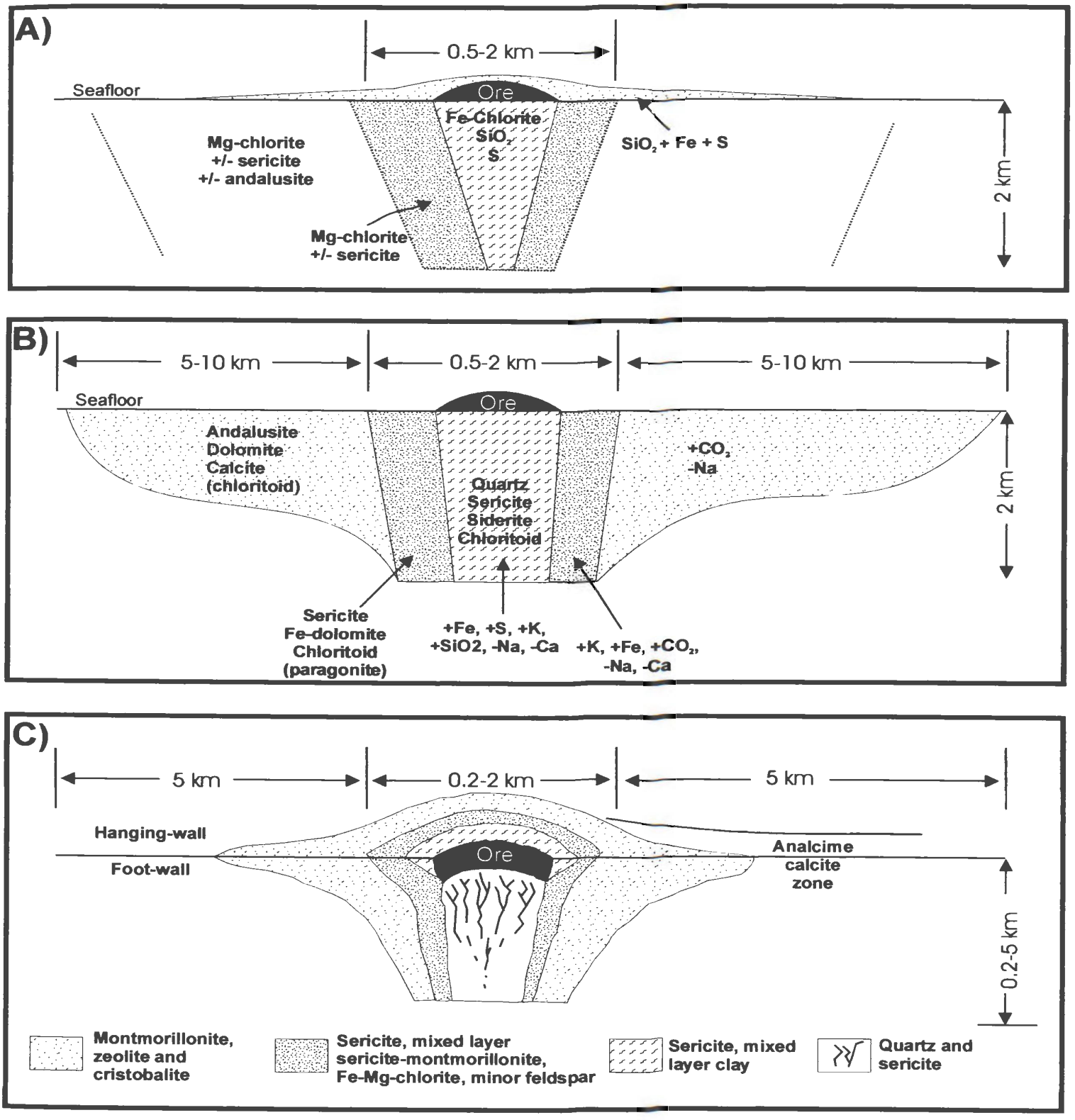

Figure 5.1 *Idealized hydrothermal alteration models for various styles of VMS deposits (after Franklin, 1993). Cu-Zn VMS deposits illustrated in A) Noranda/Cyprus-type (deep water) and B) Mattabi-type (shallow water). C) Zn-Pb-Cu or Kuroko-type.*

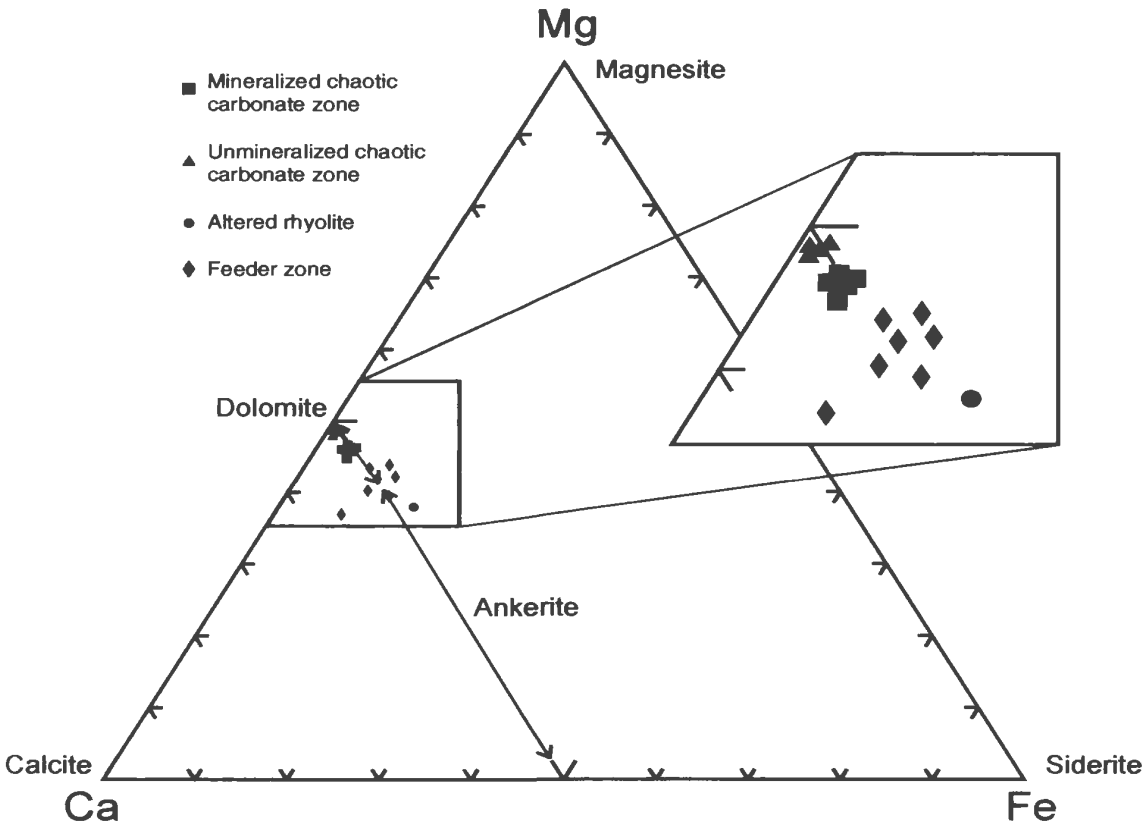

Figure 5.2 *Carbonate compositional ternary diagram based on ideal cationic formulas.*

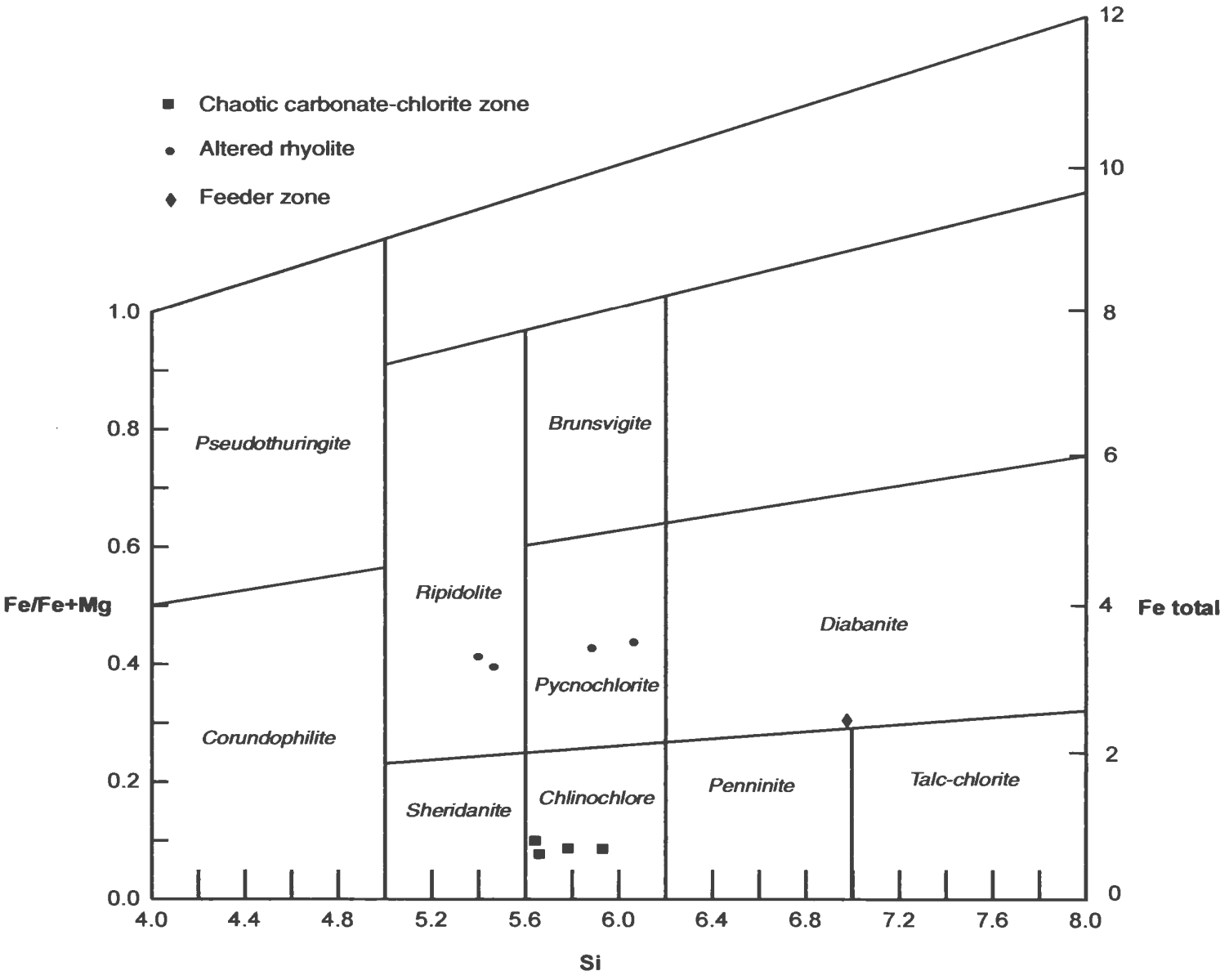

Figure 5.3 *Chlorite compositional diagram, utilizing the classification of Hey (1954).*

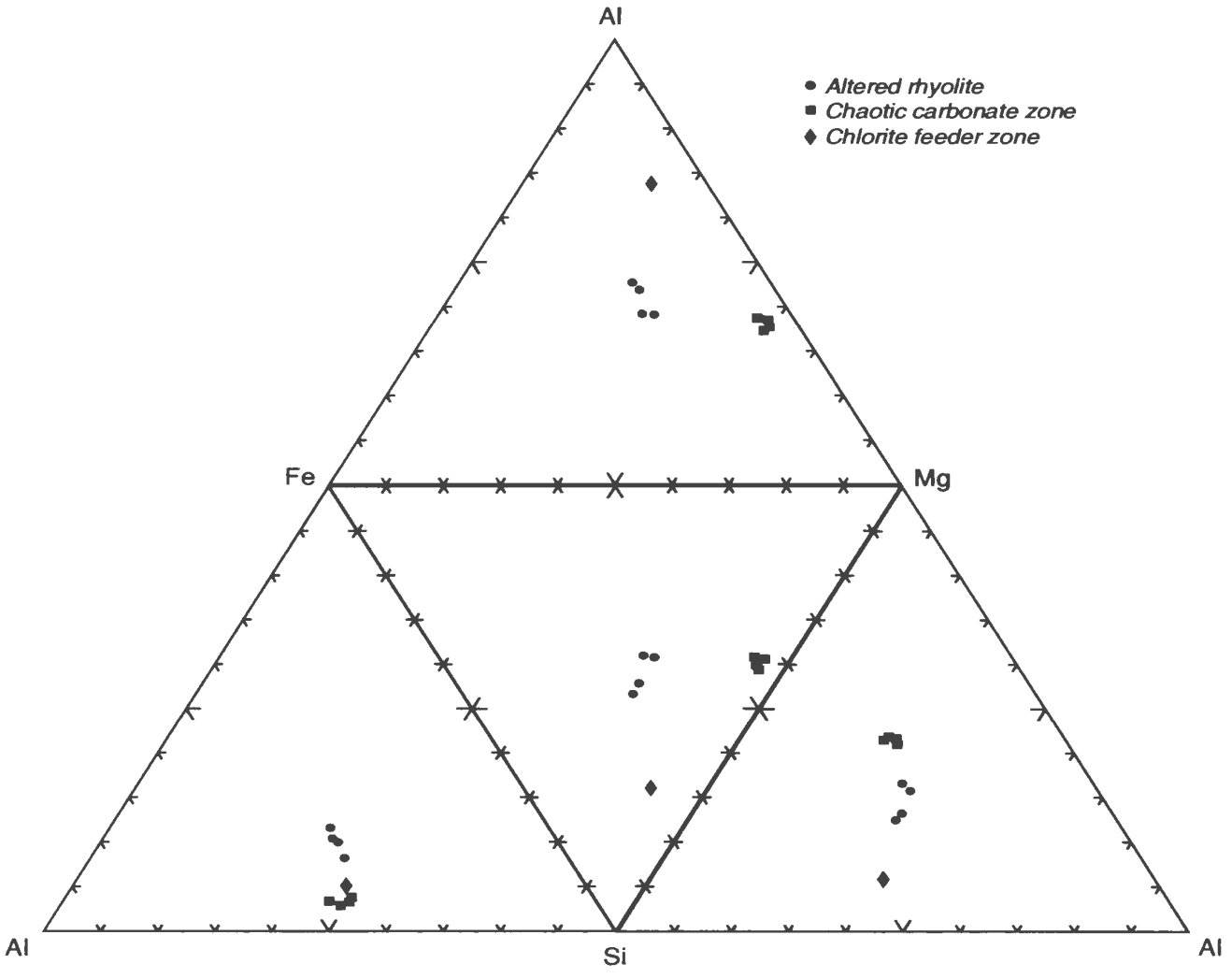

Figure 5.4 *Plot of chlorite composition on a two-dimensional tetrahedron.*

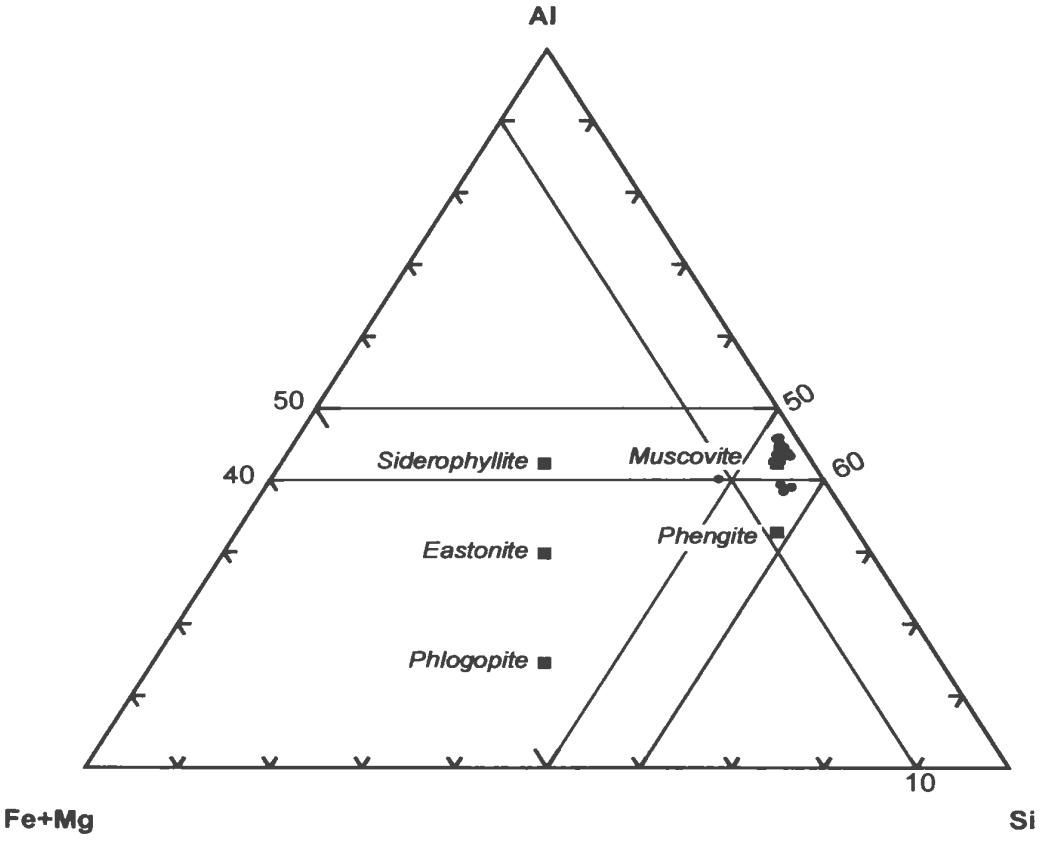

Figure 5.5 *Ternary compositional diagram for mica cations. Fields after Deer* et al. *(1992).*

Plate 5.1 *Variably altered felsic volcanic rocks from the Duck Pond deposit. Carbonate alteration (top), sericite (middle), and chlorite (bottom).*

Plate 5.2 *Carbonate and sericite altered felsic breccia consisting of rhyolite fragments in a silicic-carbonate matrix.*

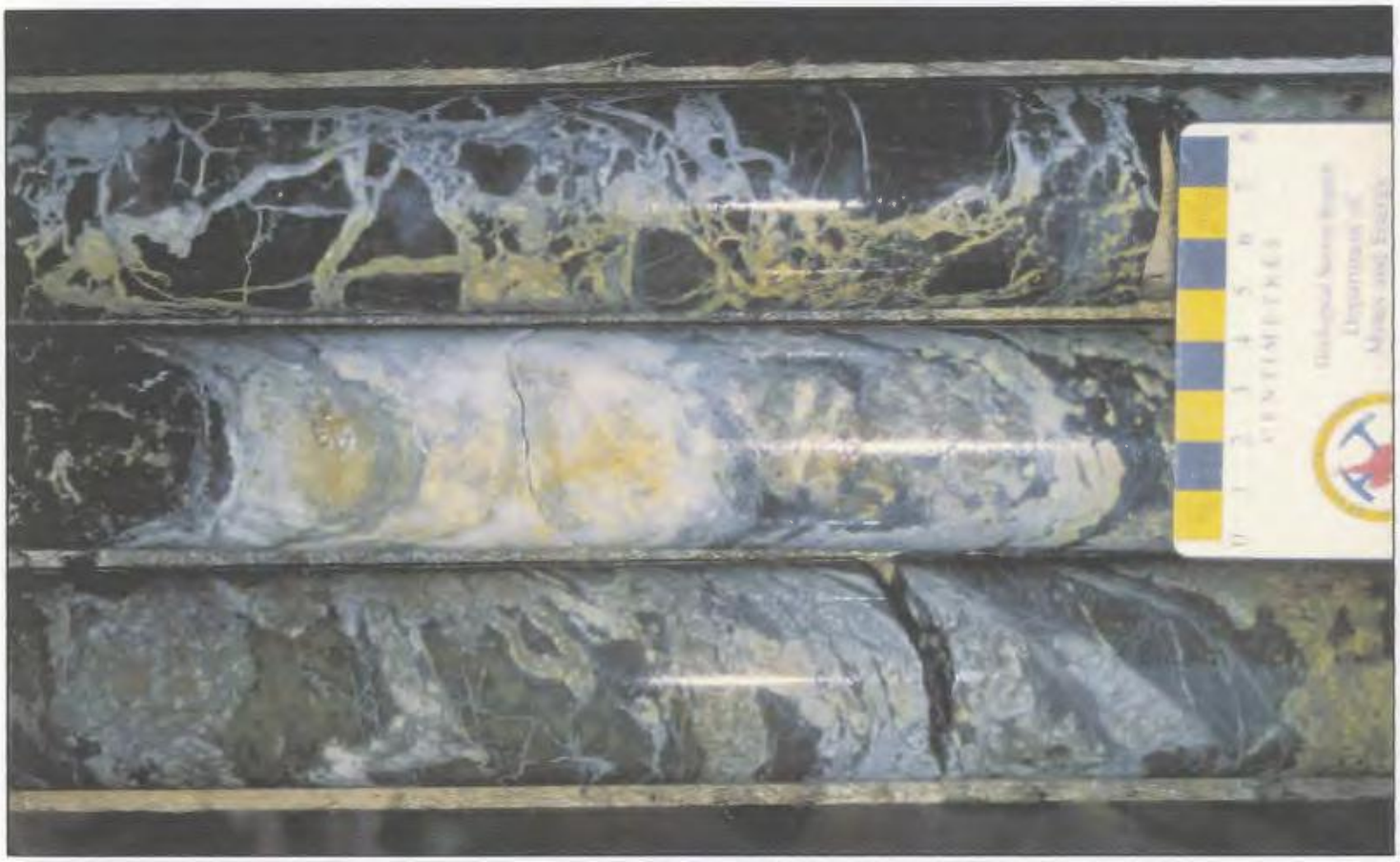

Plate 5.3 *Intense chlorite and chaotic carbonate altered rhyolite from the Mineralized block beneath the Duck Pond deposit.*

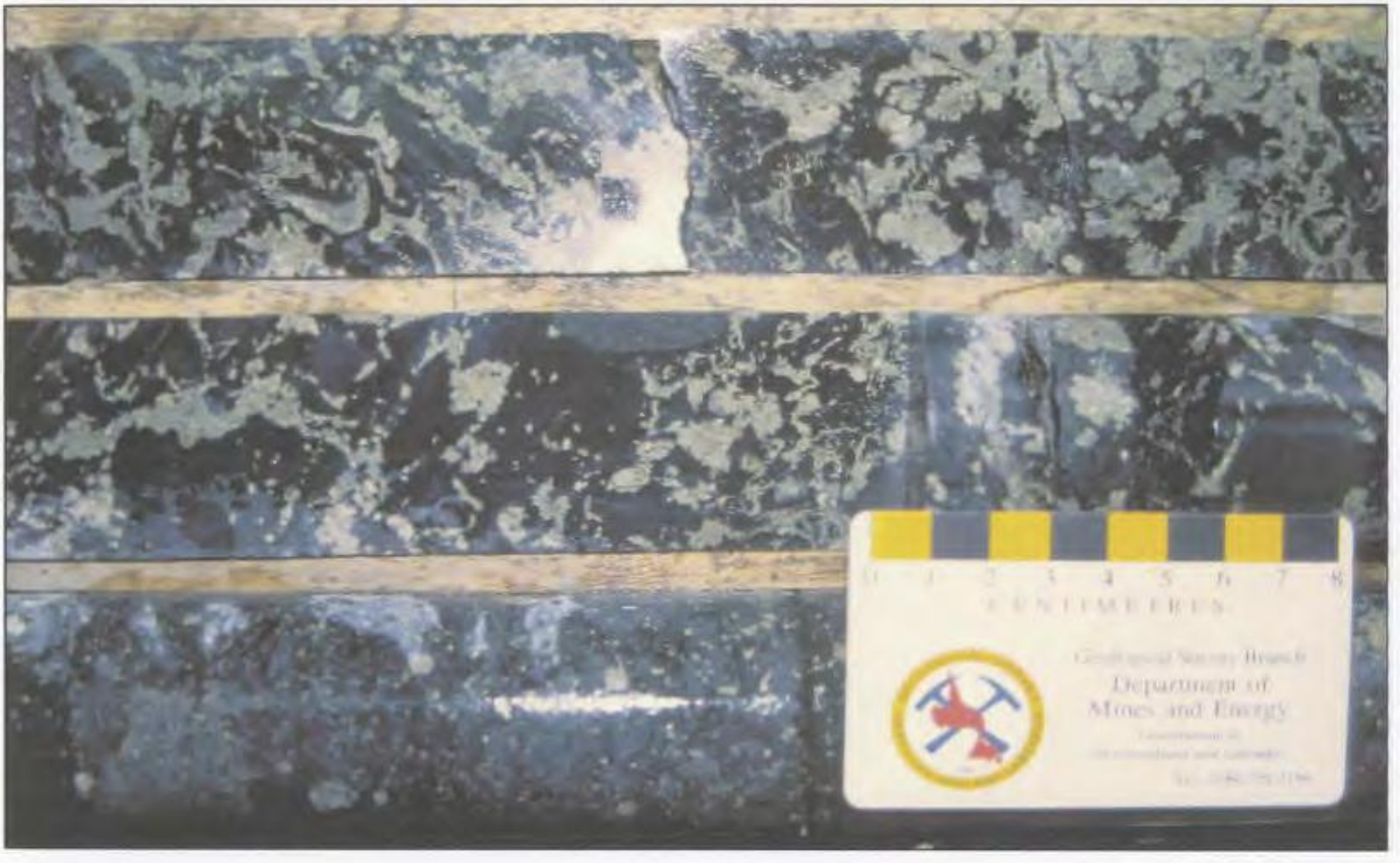

Plate 5.4 *Coarse-grained pyrite in chlorite feeder pipe located adjacent to the Upper Duck lens.*

Plate 5.5 *Chaotic carbonate alteration developed in the massive sulphide of the Upper Duck lens of the Duck Pond deposit.*

CHAPTER 6

RADIOGENIC ISOTOPE GEOCHEMISTRY AND GEOCHRONOLOGY

6.1 Preamble

Radiogenic isotope data are important for the study of geochronology, igneous petrogenesis, magma contamination, crust-mantle interactions, mineral deposit sources, and can be readily applied to field based studies of volcanogenic massive sulphide deposits. There are two primary types of information available from radiogenic isotopic studies, age determination and isotopic source tracing and both are used to establish relationships between lithological units and mineral deposits or internal histories of these systems themselves. Radiogenic isotopes can also be used to delineate the sources of certain components within the systems in terms of likely source reservoirs (Faure, 1986; Heaman and Parrish, 1991; Richards and Noble, 1998). In areas such as the Red Indian Lake region of central Newfoundland, igneous units and their basement rocks are present from opposing sides of Iapetus. Temporal and spatial contrasts exist between both basement and overlying rocks from both sides of the Red Indian Line and these contrasts should therefore be present within the radiogenic isotopic signatures of the rock units.

This chapter first discuses the systematics of the U-Pb radioactive decay system, followed by its applicability to geochronology in the Tally Pond Group. U-Pb data are presented for primary igneous zircons from volcanic and intrusive sequences in the Tally Pond Group and detrital zircon data are given for overlying sedimentary sequences. Secondly, the uses of Pb isotopes in igneous petrogenetical source tracing are demonstrated as Pb isotope data for galena separates from the Duck Pond and Boundary deposits of the Tally Pond Group are presented in an attempt to determine the potential source areas of the sulphide mineralization and to compare to other VMS deposits throughout the Dunnage Zone.

6.2 Uranium-Thorium-Lead Isotope Systematics

Lead is widely distributed throughout the Earth and occurs as four naturally occurring isotopes, of which three, ^{206}Pb (24.10 %), ^{207}Pb (22.10 %), and ^{208}Pb (52.40 %), are the stable end-products of complex decay schemes from parent isotopes ^{238}U (99.2745 %), ^{235}U (0.7200 %), and ^{232}Th (100 %), respectively. The fourth isotope, ^{204}Pb (1.40 %), is non-radiogenic (i.e. not increased by the radioactive decay of U or Th) and is treated as a stable reference isotope. The half-life of ^{238}U is 4.47 Ga and is comparable with the age of the Earth, whereas that for ^{235}U is 0.704 Ga and is much shorter, so that almost all of the primordial ^{235}U in the Earth has now decayed to ^{207}Pb (Dickin, 1995). The ^{232}Th half-life is 14.01 Ga and is similar to the age of the universe. These extremely long half-lifes are a valuable tool because U, Th and Pb isotopes can therefore be applied over a broad range of geological time

The relationship between time and initial and present-day Pb isotopic composition for the U-Th-Pb systems can be expressed in three equations (Faure, 1986):

$$^{206}Pb/^{204}Pb = [^{206}Pb/^{204}Pb]_{initial} + [^{238}U/^{204}Pb] (e^{\lambda_{238}t} - 1)$$

where $\lambda_{238} = (1.55125)*10^{-10}\ a^{-1}$; *half-life = 4.468 Ga*

$$^{207}Pb/^{204}Pb = [^{207}Pb/^{204}Pb]_{initial} + [^{235}U/^{204}Pb] (e^{\lambda_{235}t} - 1)$$

where $\lambda_{235} = (9.8485)*10^{-10}\ a^{-1}$; *half-life = 0.704 Ga*

$$^{208}Pb/^{204}Pb = [^{208}Pb/^{204}Pb]_{initial} + [^{232}Th/^{204}Pb] (e^{\lambda_{232}t} - 1)$$

where $\lambda_{232} = (4.9475)*10^{-11}\ a^{-1}$; *half-life = 14.01 Ga*

If the concentrations of U, Th, and Pb isotopes are measured and initial Pb concentrations are either small enough to be ignored or can otherwise be adequately accounted for, the equations can be solved for *t*, in the form:

$$t_{206} = [1/\lambda_{238}]*\ln \{[(^{206}Pb/^{204}Pb) - (^{206}Pb/^{204}Pb)_{initial} / (^{238}U/^{204}Pb)] + 1\}$$

The equations for ^{207}Pb and ^{208}Pb are solved similarly, resulting in three independent chronometers that are based on three separate decay series. These equations can be then used to verify if the material being dated has remained isotopically closed with respect to U, Th, and Pb because closed (i.e. concordant) systems should give the same date for all three chronometers. If the system has remained closed, the correct values used for the initial Pb isotope ratios, the decay constants of U and Th known accurately, the isotopic composition of U is normal, and all analytical results are accurate, the three dates will be concordant and represent the age of the sample being dated (Faure, 1986).

U-Th-Pb data are usually presented on a plot of $^{207}Pb/^{235}U$ vs $^{206}Pb/^{238}U$, called the concordia plot, in order to provide a visual basis for assessing concordancy. The

concordia curve is contoured in time units and defines the locus of concordant ages for both ^{238}U and ^{235}U decay and is used in the interpretation of samples that have not remained isotopically closed, or discordant (Richards and Noble, 1998). If a U-Pb analysis plots directly on the curve it is said to be concordant and the data record the time at which the sample became isotopically closed, i.e. the time of igneous crystallization. Nevertheless, analyses commonly plot off the concordia curve and are said to be discordant. Discordant analyses can result from a number of factors such as loss of Pb as well as gain or loss of U, and mixtures of old and newer sectors in mineral crystals (Heaman and Parrish, 1991; Dickin, 1995). These factors may result from an episode of metamorphism, continuous diffusion of Pb, or loss of microcapillary water and chemical weathering near the Earth's surface (Richards and Noble, 1998). However, with careful evaluation, important information can still be obtained from discordant data. In many situations, the $^{207}Pb/^{235}U$ and $^{206}Pb/^{238}U$ ratios of samples whose U and Pb concentrations have been altered form linear or sublinear arrays, which are said to define a discordia. The upper and lower intercepts with the concordia curve are usually significant in terms of the times of original crystallization and subsequent isotopic system disturbance, respectively.

In selecting a material suitable for U-Pb geochronology a number of factors must be considered: 1) the material should have high U contents and minimal amounts of common Pb at the time of formation; 2) the material being analyzed must be able to be correlated with the geological process to be dated; 3) the material must be resistant to isotopic exchange after formation; and 4) the material should be relatively common and easily recoverable (Faure, 1986; Heaman and Parrish, 1991; Richards and Noble, 1998;

Dickin, 1995). Whole rocks rarely satisfy these requirements and therefore minerals are most frequently utilized (Richards and Noble, 1998). The most useful minerals and commonly analyzed minerals in U-Pb geochronology are zircon ($ZrSiO_4$), titanite ($CaTi[SiO_3]$), monazite ($CePO_4$) and baddeleyite (ZrO_2). Zircon has become the most widely utilized accessory mineral for geochronology because it crystallizes from a wide range of magma compositions and can also grow during metamorphism. Zircon is also a mainstay for geochronological determinations due to its extremely high U/Pb ratio at the time of formation and the ability of the zircon crystal to retain the daughter products of U and Th radioactive decay. Zircon survives in the crust almost indefinitely (Mezger and Krögstad, 1997) and therefore is easily recoverable for geochronology.

Age information can also be obtained from Pb isotopes in samples that do not have high U/Pb or Th/Pb ratios. In these samples, the isotopic variations reflect the decay of background levels of U or Th, which contribute to the bulk composition of Pb in the system. In comparison to minerals that have high U/Pb or Th/Pb ratios, the observed variations in Pb isotopic ratios are small, but this method has the advantage of being able to study the bulk evolution of Pb in the system, rather than just within a single mineral (Faure, 1986; Gariépy and Dupré, 1991; Richards and Noble, 1998).

Based on the assumption that at the time of formation of the Earth, or shortly thereafter, the Earth was isotopically and chemically homogeneous, various models for the isotopic evolution of Pb in the Earth have been proposed (Holmes, 1946; Houtermans, 1946; Stacey and Kramers, 1975; Cumming and Richards, 1975). The increase of radiogenic Pb isotopes (^{206}Pb, ^{207}Pb, ^{208}Pb) relative to ^{204}Pb over time was modeled using various parameters and tested against the compositions of Pb from

stratiform orebodies of known age. The model proposed by Holmes and Houtermans (1946) consisted of only a single stage of Pb isotope evolution throughout Earth history, whereas the more refined models of Cumming and Richards (1975) and Stacey and Kramers (1975) involved a second stage or continuous process of chemical fractionation of U and Th from Pb, reflecting segregation of the continental crust (Gariépy and Dupré, 1991; Richards and Noble, 1998). These models can be illustrated on a plot of $^{206}Pb/^{204}Pb$ vs $^{207}Pb/^{204}Pb$ as Pb isotopic growth curves. The shape of the growth curve is determined by the ^{238}U and ^{235}U decay constants and its trajectory by the $^{238}U/^{204}Pb$ ratio or 'μ' value of the Pb source.

Model Pb-Pb ages can be obtained from a wide range of rock types from granites to basalts to Pb-bearing ore deposits. These model ages yield reliable dates in samples with a simple crystallization history; however, there are considerable problems in interpreting model ages in systems where the Pb isotopes have been disturbed. This results from the differences in mobility and geochemistry of U and Pb and from the diversity of possible lead isotope constants because of the heterogeneity in concentrations of U, Th, and Pb and the variability of U/Pb and Th/Pb ratios in crustal source rocks (Faure, 1986; Gariépy and Dupré, 1991). It must be noted that model ages are simply a measure of the length of time a sample has been separated from the reservoir from which it was originally derived. The significance of model ages must therefore be evaluated with considerable skeptism as often they have no geochronological significance. Consequently, for this study the isotopic data from Pb-rich minerals are taken at face value and chiefly used as an isotopic tracer for the source of Pb to distinguish between the various reservoirs (e.g. mantle, lower crust or upper crust).

6.3 U-Pb Geochronology - Thermal Ionization-Mass Spectrometry

6.3.1 Introduction

Previous attempts to constrain the age of magmatism in the Tally Pond Group were hampered by the scarcity of outcrop and the lack of geologically significant dateable units. The volcanic sequences of the Tally Pond Group are also notorious for being devoid of zircon, therefore a previous attempt (Dunning *et al.*, 1991) at dating the Tally Pond Group utilized porphyritic felsic rocks that were interpreted as hybabyssal intrusions. Two 513 ± 2 Ma ages were obtained by Dunning *et al.* (1991), however, these data were interpreted to provided a minimum age for the Tally Pond Group and did not constrain the main episode of volcanism or the age of volcanogenic massive sulphide mineralization.

In order to rectify the shortfalls of previous geochronological attempts and the regional tectonic and metallogenic significance of determining the age of volcanism and timing of mineralization in the Tally Pond Group, U-Pb zircon geochronology was conducted on a sample of felsic quartz crystal tuff from the Boundary Brook Formation and from a sample of the Harpoon Gabbro that intrudes the Tally Pond Group. The purpose of this has six separate objectives: 1) to determine the age of the main episode of magmatism in the Tally Pond Group; 2) to constrain the age of volcanogenic massive sulphide mineralization of the Boundary and Duck Pond deposits; 3) to determine the relationship between the felsic volcanic rocks and felsic 'intrusive' rocks of the Tally Pond Group; 4) to determine the age of the mafic rocks that intrude the Tally Pond Group; 5) to resolve the temporal and spatial relationships between the Tally Pond Group

and the various tectonic elements of the Victoria Lake Supergroup; and 6) to compare the age of the Tally Pond Group to other Cambrian volcanic sequences throughout the Appalachian Orogen.

With these objectives in mind, three samples were collected from drillcore in the Tally Pond area surrounding the Duck Pond and Boundary deposits. In selecting samples appropriate for geochronology, the zirconium content as defined by XRF analyses was first used as a tool to discriminate between felsic volcanic sequences that might contain zircon. Of the samples that contained moderate to high concentrations of zirconium, two rhyolite flows from Duck Pond drillcore were selected for geochronology; one sample from the hangingwall and one from the footwall. However, both of these samples contained no zircon and were discarded. A third sample (JP-01-GC1) of a quartz crystal tuff (Plate 6.1), obtained from drillcore in the immediate hangingwall of the Boundary deposit, yielded numerous zircons and was dated by U-Pb zircon thermal ionization mass spectrometry at the Geological Survey of Canada in Ottawa, Ontario. In addition, one sample of the Harpoon Gabbro was selected from a coarse-grained outcrop at the top of Harpoon Hill (Plate 3.17) and submitted for geochronology. Ages were calculated using Isoplot ver. 2.21 (Ludwig, 1992) and represent a weighted average $^{207}Pb/^{206}Pb$ age for samples. The ages were calculated using the ^{238}U ($1.55125*10^{-10}$ a^{-1}) and ^{235}U ($9.8485*10^{-10}$ a^{-1}) decay constants and the present day $^{238}U/^{235}U$ ratio of 137.88 determined by Jaffey *et al.* (1971). The error ellipses shown on the figures and all age uncertainties are reported at 2σ. A complete description of analytical techniques is given in appendix D.

6.3.2 TIMS U-Pb Results

6.3.2.1 Quartz Crystal Tuff

The quartz crystal ash tuff sample from the Boundary deposit yielded numerous zircons which were separated into three fractions: 1) colourless, euhedral, stubby prisms (Plate 6.2); 2) small, colourless, well faceted crystal tips (Plate 6.3); and 3) clear to pale brown zircon fragments with numerous inclusions (Plate 6.4). All of the zircons contain numerous internal and surficial fractures with growth zoning evident in several grains; there are however, no visible cores. All three fractions have varying uranium contents (Table D.1), from small amounts in fraction 1 (89 ppm) to more moderate amounts in fraction 3 (132 ppm) and fraction 2 (231 ppm). All three fractions were strongly abraded to remove the outer surfaces which are typically enriched in uranium due to Pb loss (Plates 6.5, 6.6, 6.7). Two fractions (1 and 2) overlap Concordia (Figure 6.1), with similar $^{207}Pb/^{206}Pb$ ages of 510 and 509 Ma respectively. The third fraction (3) lies slightly beneath concordia and gives a $^{207}Pb/^{206}Pb$ age of 514 Ma, which could reflect slight Pb-loss or incomplete zircon dissolution. With more weight given to the more precise analyses (fractions 1 and 2) an age of 509 ± 1 Ma has been assigned to this sample.

6.3.2.2 Harpoon Gabbro

The gabbro sample from the summit of Harpoon Hill contains numerous zircon grains which were separated into six fractions ranging from nine grains (Z2) to 100 grains (Z1) Plates 6.8, 6.9, 6.10). All fractions were strongly abraded to remove the outer surfaces which are typically enriched in uranium due to Pb loss (Plates 6.11, 6.12, 6.13).

The U-Pb results for all six fractions display some scatter and are less than 5% discordant. Three fractions (Z2, Z3, and Z4) comprise stubby, well faceted clear prisms that overlap concordia (Figure 6.2) with similar $^{207}Pb/^{206}Pb$ ages of 467 and 462 Ma. Fraction Z5 is reversely discordant, plots above the concordia curve and is considered to result from the incomplete zircon dissolution; consequently this date is unreliable. A small set of stubby, well faceted, diamagnetic prisms with minor inclusions comprise fraction Z6. This analysis plots below concordia and has a $^{207}Pb/^{206}Pb$ age of 503 Ma. This analysis most likely results from the presence of minor inherited zircon coupled with secondary Pb-loss. Fraction Z1 lies on concordia and gives a $^{207}Pb/^{206}Pb$ age of 469 Ma, which might result from a possible mixture of zircon from fractions Z5 and/or Z6 and fractions Z2, Z3, and/or Z4. An alternate interpretation, and the one favored here, is that the older age reflects an older (~470 Ma) inherited zircon component in this fraction. With more weight given to the more precise analyses (Z2, Z3 and Z4) a date of 465 ± 1 Ma is interpreted as the age of zircon crystallization and igneous emplacement.

6.3.3 TIMS U-Pb Discussion

The U-Pb data for the quartz crystal tuff indicate that the volcanic succession of the Boundary Brook Formation is confined to an age of 509 ±1 Ma. This data coupled with field relationships, confirm that the main episode of felsic volcanism in the Tally Pond Group is Middle Cambrian. The 509 Ma age also indicates that the quartz-feldspar porphyritic rocks dated by Dunning *et al.* (1991) as 513 ± 2 Ma are older than the Boundary Brook Formation volcanic rocks which they were interpreted to intrude. Therefore, these porphyritic rocks are not intrusions. Based on similar trace and rare earth

element geochemical compositions and equivalent Middle Cambrian ages, it is proposed that the quartz-feldspar porphyritic rocks are essentially comagmatic with the adjacent Boundary Brook Formation felsic volcanic rocks. However, the possibility exists that the quartz-feldspar porphyritic rocks may represent several phases that span several million years in age. Field relationships in drillcore from the Duck Pond deposit define quartz-feldspar porphyritic rocks cross-cutting flow banding and textures in the volcanic rocks and contain chilled margins. Nonetheless, the 4 Ma age disparity (1 Ma within uncertainties) between the porphyritic rhyodacite and quartz crystal tuff is interpreted to be due to the porphyritic nature of the rhyodacite.

Extrusion temperatures for most rhyolitic lavas are between 800 and 1000°C (Hall, 1996) which is similar to the U-closure temperature of zircon (Richards and Noble, 1998). However, at depth, increased pressure allows H_2O to dissolve in the magma, which in turn causes a significant lowering of the melting temperature by several hundred degrees (Philpotts, 1990; Hall, 1996). This increase in pressure and dissolved H_2O has little or no effect on zircon solubility (Harrison and Watson, 1983). Once the rhyolitic magma has cooled to below the closure temperature of zircon (ca. 800°C), zircon will crystallize and the isotopic 'clock' will be set. In time, as the magma rises in the crust and erupts, the decrease in pressure is proportional to the decrease in H_2O solubility and both these factors will cause an increase in the melting temperature and in so doing effectively causing the residual magma to crystallize.

The 509 Ma age for the Tally Pond Group indicates that the group is separate, at least temporally, from adjacent rocks of the Tulks Hill assemblage. U-Pb age dating from the Tulks Hill assemblage indicates that this assemblage is Late Cambrian, 503 Ma (van

Staal, personal communication) and 498 +6/-4 Ma, to Tremadocian 495 ±2 Ma (Evans *et al.*, 1990). However, a similar Middle Cambrian age of 505 Ma was obtained from a felsic volcanic rock of the Long Lake assemblage (van Staal, personal communication).

The 465 Ma age for the Harpoon Gabbro indicates that the mafic intrusions in the Tally Pond Group are Ordovician and therefore much older than previously thought, as they were considered to be Silurian-Devonian (Kean and Jayasinghe, 1980; Kean, 1985; Kean and Evans, 1988; Evans and Kean, 2002). This 465 Ma age represents the youngest magmatism recognized in the Tally Pond Group and is comparable to similar Arenig-Llanvirn ages from the Red Indian Lake area; 464 and 468 Ma for the Harbour Round assemblage (Rogers and van Staal, 2002; Zagorevski *et al.*, 2003) and 462 +4/-2 Ma from the Sutherlands Pond assemblage (McNicoll, personal communication). The Harbour Round and Sutherlands Pond assemblages, however, are considered to lie west of the Red Indian Line and as such are part of the Peri-Laurentian Notre Dame Subzone, and therefore are not related to the Harpoon Gabbro.

The intrusion of the Harpoon gabbro in the Tally Pond group is temporally equivalent to magmatism in the Hermitage Flexure in southwestern Newfoundland. Similar middle-Ordovician magmatic events are reported for the Bay du Nord group (466 ± 3 Ma; Dunning *et al.*, 1990), the Margaree orthogneiss (465 ± 3 Ma; Valverde-Vaquero *et al.*, 2000), and Bay d-Espoir groups (468 ± 2 Ma; Colman-Sadd *et al.*, 1992). In the northeastern Exploits Subzone, the gabbro is also coeval, within limits of analytical error, with Early and Mid-Ordovician arc volcanic and intrusive rocks in the Wild Bight and Exploits groups. Late Arenig volcanism and hypabyssal intrusions are well documented in the Lawrence Head Formation of the Exploits Group and show no geochemical

characteristics of a subduction zone. These rocks comprise enriched tholeiitic and alkalic basalt are interpreted to represent a 470-468 Ma volcanic and seafloor intrusive event related to arc rifting and back-arc basin formation (O'Brien *et al.*, 1997). The 463.7 ± 2 Ma Thwart Island Gabbro (O'Brien *et al.*, 1997) were intruded during the late stages of this back arc basin. Similar geochemical and stratigraphic relationships are present in the Wild Bight Group. Volcanic arc magmatism with calc-alkaline affinities and isotopic evidence for minor crustal contamination are interpreted to have formed in a 472 Ma volcanic arc along the Gondwanan margin (MacLachlan and Dunning, 1998). Gabbro sills from the Wild Bight Group have been dated at 471 ± 4 Ma and 472 + 2/-9 Ma (MacLachlan and Dunning, 1998), have enriched tholeiitic to alkaline geochemical signatures and represent subsequent rifting of this arc and formation of a marginal back arc basin (Swinden *et al.*, 1990). The involvement of peri-Gondwana continental crust material during magmatism in the Exploits Subzone is clearly present as far back as the Arenig. The presence of inherited Precambrian zircons in the 474 +6/-3 Ma Partridgeberry Hills granite (Colman-Sadd *et al.*, 1992) confirms this premise.

The 509 Ma and 513 Ma ages from the Tally Pond Group correlate with other Cambrian volcanic sequences in the Appalachian Orogen. The New River Belt (Johnson and McLeod, 1996) in southern New Brunswick consists of a faulted zone of Precambrian granitoid rocks, the Ragged Falls pluton, and volcanic and sedimentary rocks of Cambrian to Silurian age. One particular unit in the New River Belt, the Mosquito Lake Road volcanics comprises a conformable sequence of rhyolite flows, felsic crystal tuffs interbedded with feldspathic wacke, siltstone and mafic volcanic rocks that grade laterally into epiclastic rocks. The Mosquito Lake Road volcanics and Ragged

Falls pluton are unconformably overlain by Silurian quartz-pebble conglomerate of the Matthews Lake Formation.

Rhyolite within the Mosquito Lake Road sequence yielded zircons that produced an age of 515 +3/-2 Ma (Johnson and McLeod, 1996). This age, along with 555 ±2 Ma and 555 ±10 Ma ages for the Ragged Falls pluton (Currie and Hunt, 1991), correlates with ages for felsic volcanism in the Tally Pond Group and with the 563 ±2 Ma and 565 +4/-3 Ma ages for the Valentine Lake and Crippleback Lake quartz monzonites, respectively.

The Tally Pond Group is very similar in age, lithology, and metallogeny to the Harborside-Blue Hill belt in Maine. U-Pb zircon ages of 509 ±5 Ma and 502 ±2 Ma are reported for rhyolite from the Harborside volcanics (Ruitenberg *et al.*, 1993). However, there is evidence of zircon inheritance and discriminating between the differing ages is complex. The Harborside belt also hosts the Harborside Mine and Leach deposit, volcanogenic massive sulphide deposits hosted by felsic pyroclastic rocks, rhyolite breccia and hyaloclastites. The deposits contain over 725 750 tonnes that average 5.5 % Zn, 1.25 % Cu, 0.5 % Pb and 17.1 g/t Ag and approximately 90 000 tonnes that contains 8 % combined Cu and Zn, respectively (Ruitenberg *et al.*, op. cit.).

The age and trace element characteristics of the Harpoon Gabbro suggest that this intrusion and the temporally equivalent components of the Wild Bight and Exploits groups represent different parts of the same Late Arenig to Llanvirn arc system. This arc, termed the Victoria arc in Newfoundland, can be correlated with the Mid-Ordovician part of the New Brunswick Popelogan Arc. The Popelogan Arc is characterized by ensialic arc plutonic-volcanic complexes that were emplaced during the Arenig (479-474 Ma) in

central and northern New Brunswick and adjacent Maine (van Staal *et al.*, 1996). Mid-Ordovician felsic volcanic rocks in Newfoundland and New Brunswick are considered to represent the early phases of ensialic magmatism generated during the rifting of the Popelogan arc, which produced the Exploits back-arc basin (van Staal and Williams, 1991). The hiatus of approximately 15 Ma between volcanism in the Tulks Hill sequence and intrusion of the Harpoon Gabbro is interpreted to correspond to the collision, exhumation and obduction of the Penobscot (Mid-Cambrian-Late Tremadoc) arc volcanic rocks (Chapter 8).

6.4 U-Pb Geochronology - Laser Ablation Microprobe-Inductively Coupled Plasma-Mass Spectrometry

6.4.1 Introduction

The analysis of heavy mineral fractions, particularly zircons, in clastic sedimentary rocks is an important method for investigating the sedimentological history of clastic rocks and can be used to fingerprint their sediment sources and depositional histories. Zircon is a common accessory mineral in most rocks and is an often studied component of detrital assemblages because it is extremely resistant to chemical weathering and physical breakdown during transport. The range and frequency of the U-Pb ages measured on detrital zircon populations therefore yields information relating to the ages of crustal elements in the source region and the clastic transport pathway. This becomes especially important in sedimentary sequences that lack individual biostratigraphic marker beds, distinct stratigraphic horizons and dateable cross-cutting intrusions. Geochronological data from the Rogerson Lake Conglomerate in central Newfoundland were obtained in order to determine the maximum deposition age and

sediment provenance of the conglomerate.

6.4.2 Detrital Zircon Samples

Two 10 kg samples of the Rogerson Lake Conglomerate (Plate 6.14) were collected for detrital zircon analysis. This sample was subsequently reduced to approximately 3-4 kg by selecting unweathered portions of rock that are representative of the unit. One sample was from a pebble conglomerate that outcrops on the Burgeo Road and another sample was collected from the type area at the south shore of Rogerson Lake.

The Rogerson Lake sample (71) consisted of a single zircon population (31 zircons) comprised of grains that were clear and slightly red to colourless with euhedral to subhedral shapes (Plate 6.15). The sample from the Burgeo Highway (72) contained two zircon populations containing approximately 40 grains each, zircons that are euhedral, clear and colorless, and grains that are slightly rounded, clear and slightly reddish in colour (Plate 6.16). Some of the zircon grains from each of the two samples contain internal cracks and fissures in addition to zircon rims and cores (Plate 6.17). The zircons were mounted with epoxy in 2.5 cm diameter grain mounts and polished to expose even surfaces at the cores of the grains for analysis. The aim was to analyze at least 50-60 grains per sample because analysis of 60 grains provides a 95 % probability of finding any population that comprises 5 % of the total (Dodson *et al.*, 1988). In order to avoid the influence of highly precise analyses, 2σ errors were used to determine whether the scatter in a given group is consistent with the internal errors, although uncertainties reported in tables and figures are given at $\pm 1\sigma$. A complete description of the analytical techniques used for LAM-ICP-MS geochronology is listed in appendix D.

6.4.3 LAM-ICP-MS U-Pb Results

Sample 71 – South shore of Rogerson Lake. U-Pb data for detrital zircons from the Rogerson Lake Conglomerate from Rogerson Lake are listed in Table E.1 and plotted on a concordia diagram in Figure 6.3. The 31 grains analyzed from the sample are split into two groups that area well separated in frequency and age. The data (Figure 6.4) show one major cluster of 30 analyses (*a1-a13* and *a15-a31*) that produced $^{206}Pb/^{238}U$ ages between 407 and 552 Ma. These zircons varied from 1 to almost 80 % discordant and show a concentration of ages at ca. 495 Ma, representing a dominantly Paleozoic zircon source. Although comprising only one grain (*a14*) that is 23% discordant, a minor Late Mesoproterozoic component is recognized with a $^{206}Pb/^{238}U$ age of 994 Ma and a $^{207}Pb/^{235}U$ age of 972 Ma. The majority of analyses plot either on concordia or slightly above concordia; the negative discordance is due to either a high common Pb contamination or to incorrect correction for U-Pb fractionation.

Sample 72 – Burgeo Road. A total of 80 single detrital zircon grains analyzed from the Burgeo Road sample include both zircon populations of clear, colourless zircons and clear, red zircons. The data (Table E.2) show that no age differences are apparent between detrital zircons of different colour or morphology. The distribution of data points in the concordia diagram on Figure 6.5 suggests that the ages of the sample have five maxima. The majority of the zircons (70 grains) have $^{206}Pb/^{238}U$ ages between 419 and 530 Ma that vary between 1-80 % discordant. These data (Figure 6.6) show a strong concentration of ages at ca. 500 Ma with a minor concentration of ages in the 450-480 Ma range. The second cluster of ages is represented by analyses *a1*, *a2* and *a28* with

$^{206}Pb/^{238}U$ ages of 759, 698 and 723 Ma, respectively that are between 6-15 % discordant and bracket the age of the source at ca. 725 Ma.

The presence of Neoproterozoic and Late Mesoproterozoic components is indicated by the cluster of zircon analyses at ages of 890 and 1030 Ma. Zircons *a18*, *a43* and *a66* are between 4-20% discordant and have ages between 838 and 915 Ma. Two analyses (*a23* and *a31*) produced ages of 1079 and 1016 Ma that are 27 and 9 % discordant, respectively. Middle Mesoproterozoic ages of 1240 and 1480 Ma are represented by three analyses (*a38*, *a40* and *a68*). Zircon *a68* has a $^{206}Pb/^{238}U$ age of 1244 Ma and a $^{207}Pb/^{235}U$ age of 1233 Ma; the analysis lies close to concordia and is 7% discordant. Analyses *a38* and *a40* produced $^{206}Pb/^{238}U$ ages of 1469 and 1487 Ma and $^{207}Pb/^{235}U$ ages of 1481 and 1514 Ma, respectively. These ages are 2 and 8 % percent discordant and indicate the age of the zircon component is approximately 1480 Ma.

6.4.4 Discussion

The new data from the two samples of the Rogerson Lake Conglomerate indicate that the age spectra in these rocks are dominated by Paleozoic zircons with minor Mesoproterozoic input. Both conglomerate samples contain over 80 % zircons that have Paleozoic ages of between 419 and 552 Ma; however the majority of these grains have an age in the 490-540 Ma range. These ages correspond well with the ages of Exploits arc/backarc volcanic sequences and basement rocks in the Victoria Lake Supergroup that are unconformably beneath the Rogerson Lake Conglomerate. Zircons derived from two rhyolite samples of the Tally Pond Group have yielded U-Pb ages of 509 ± 1 Ma and 513 ± 2 Ma (Dunning *et al.*, 1991) and dating of a sub-volcanic porphyry of the Tulks belt

yielded a Tremadocian age of 498 + 6/-4 Ma (Evans *et al.*, 1990). A coeval quartz monzonite intrusion in the Tulks belt also yielded a Tremadocian age of 495 ± 2 Ma (Evans *et al.*, 1990). Therefore the Exploits arc volcanic sequences of the Victoria Lake Supergroup, the Tally Pond Group and Tulks belt, represent the major component in the sediment source to the Rogerson Lake Conglomerate. The ca. 540-560 Ma ages in the detrital zircon population correlate with the Neoproterozoic Cripplеback Lake and Valentine lake quartz monzonite intrusive suites that nonconformably underlie the Rogerson Lake Conglomerate.

The Rogerson Lake Conglomerate detritus also contains zircon populations that are Ordovician, approximately 440-480 Ma. The source of these grains is most likely the adjacent rocks of the Notre Dame arc; a collection of Arenig to Llanvirn calc-alkaline volcanic rocks intruded by Lower to Upper Ordovician (488-456 Ma) magmatic arc plutons (van Staal *et al.*, 1998), represented by the Dashwoods Subzone. The Dashwoods Subzone is located immediately to the west of the Rogerson Lake conglomerate sample from the Cape Ray Belt at Burgeo Road and consists of medium- to high-grade metamorphic rocks cut by tonalites and granites. Two of these plutons, the Cape Ray Granite and Cape Ray Tonalite have been dated by U-Pb zircon geochronology and yielded ages of 488 ± 3 Ma and 469 ± 2 Ma, respectively (Dube *et al.*, 1996). A deformed volcano-sedimentary rocks sequence, the Windsor Point Group yields a U-Pb zircon age of 453 + 5/-4 Ma and is intruded by a pre-tectonic S-type granite, Windowglass Hill Granite, that is 424 ± 2 Ma (Dube *et al.*, 1996).

The three detrital zircons ages in the ca. 725 Ma range are not correlated with any known rocks in the Laurentian Basement or Notre Dame arc sequences. However, these

ages may be related to the earliest stages of Iapetan rifting along the Laurentian Margin. Wanless *et al.* (1968) reported an igneous crystallization K-Ar age of 761 ± 100 Ma for mafic dykes of the Long Range Dyke swarm and ages between 760 and 702 Ma have been reported for mafic dykes and rhyolites in the central and southern Appalachians (Su *et al.*, 1994; Tollo and Hutson, 1996; Tollo and Aleinkoff, 1992; Goldberg et al., 1986). Late Neoproterozoic rift-related intrusive rocks are present along all the margins of Laurentia (Hoffman, 1989), including the southwestern and northern Canadian Shield (Kamo *et al.*, 1995). One of these events, the Franklin dyke swarm located in Nunavut, has been dated by U-Pb geochronology at 723 Ma (Heaman *et al.*, 1992). This intrusive dyke event may be related to a widespread episode of extension, break-up and rifting along northwestern Laurentia and may in part be linked to a series of protracted or repeated, large-scale intrusive events, including the Long Range dykes, that span over 200 Ma, and document the final breakup of the supercontinent Rodinia.

The possibility also exists that the 725 Ma zircons are Avalonian as similar 700-760 Ma ages are found in the Burin Group (763 ± 2 Ma) and Flemish Cap Granodiorite (751 Ma). However, due to the absence of additional Avalonian ages and the fact that the provenance source indicates a dominantly westward transportation direction of the zircons, an Avalonian source for detritus in the Rogerson Lake Conglomerate is not contemplated.

The Neoproterozoic (890 Ma) and Mesoproterozoic age groups (1030 and 1250 Ma) correspond with rocks of the Grenville Orogen, while the Middle Mesoproterozoic ages (ca. 1500 Ma) are correlated with basement gneisses of the Grenville Orogen (Owen and Erdmer, 1990). These Laurentian rocks contributed a minor quantity of the zircons

which were analyzed in the Rogerson Lake Conglomerate. The Indian Head Inlier of western Newfoundland contains several granitic gneiss units in the 800-900 Ma range. Samples from the Stephenville area contain hornblende and biotite that yielded undisturbed $^{40}Ar/^{39}Ar$ spectra with ages of 880 and 825 Ma, respectively (Dallmeyer, 1978). K-Ar ages obtained from biotite yield ages that correspond with the $^{40}Ar/^{39}Ar$ data. A granitic gneiss unit was dated at 830 ± 42 Ma (Lowden, 1961) and a 900 ± 45 Ma age was obtained from biotite in a pegmatite dyke (Lowden *et al.*, 1963).

A correlative of the Indian Head Inlier, the Long Range Inlier is the largest exposure of basement rocks in the Newfoundland Appalachians and contains similar Mesproterozoic high-grade quartz feldspar gneisses and granites. Basement gneisses of the Long Range Inlier in the area of Western Brook Pond are dated at 1250 Ma (Erdmer, 1986) and 1466 ± 10 Ma (Heaman *et al.*, 2002). However, gneissic basement rocks sampled from the eastern edge of the Long Range Inlier near Cat Arm Road are older and yield early Mesoproterozoic ages of 1530 ± 8 Ma and 1631 ± 2 Ma (Heaman *et al.*, 2002). These rocks are intruded by a magmatic belt of granitoid plutons in the Long Range Inlier and the adjacent Grenville Province in southern Labrador and adjacent Quebec. These large plutons yield U-Pb zircon ages between 1080 and 960 Ma (Gower and Loveridge, 1987; Schärer and Gower, 1988). Ages of 1023 + 7/-5 Ma and 1022 ± 2 Ma are reported from Early-Grenvillian granitoid intrusions of the Lake Michel intrusive suite (Owen and Erdmer, 1990; Heaman *et al.*, 2002) and a 1032 ±1.5 Ma age from the Lomond River granite (Heaman *et al.*, 2002). Late Grenvillian granitoids of the Long Range Inlier include the Horse Chops Granite 993 ± 7 Ma, Cloud River Granite 985 ± 1.6

Ma, Potato Hill Granite 999 ± 4 Ma and Aspey Granite 1006 ±82 Ma (Heaman *et al.*, op. cit.).

Another series of exposed Appalachian basement rocks occur in the Steel Mountain Inlier of southwest Newfoundland. A felsic granulite gneiss of the Disappointment Hill complex yielded an upper intercept U-Pb zircon age 1498 + 9/-8 Ma and a foliated gabbro related to Steel Mountain anorthositic rocks has an upper intercept age of 1254 ± 14 Ma (Currie *et al.*, 1992).

The Proterozoic ages of zircons in the Rogerson Lake Conglomerate therefore cover the same age range within the limits of uncertainty with the previously reported ages for Laurentian rocks of the Grenvillian basement inliers in western Newfoundland. These ages, however, also correspond to the ages of magmatism, deformation and metamorphism in southern Labrador. The 1487 Ma age from zircon in the Rogerson Lake Conglomerate corresponds to the Pinwarian Orogen of the eastern Grenville Province (Gower *et al.*, 1988; Tucker and Gower, 1990). Rocks of Pinwarian age are between 1520 and 1460 Ma, and on the south coast of Labrador three intrusions, the Cape Charles quartz monzonite, St. Peter Bay granite and Wolf Cove quartz monzonite, have U-Pb ages of 1490 ± 5 Ma, 1479 ± 2 Ma and 1472 ± 3 Ma, respectively (Tucker and Gower, 1994).

Late Elsonian (1290 to 1230 Ma) magmatism in the Canadian Shield of Labrador is equivalent to the 1244 Ma age from the Rogerson Lake Conglomerate. The Mealy dykes form an east-northeast trending swarm of gabbroic and diabase intrusions in the eastern Grenville Province and the time of emplacement is fixed by a zircon age of 1250 ± 2 Ma (Hamilton and Emslie, 1997). The Seal Lake Group located along the northern

margin of the Grenville Province is a sequence of sedimentary and volcanic rocks and the age of these rocks is constrained by a 1250 + 14/-7 Ma zircon age from gabbro sills (Romer *et al.*, 1995). The Late Elsonian age from the Rogerson Lake Conglomerate also correlates with the Strange Lake peralkaline complex in northern Labrador. It consists of exotic-bearing granitoid rocks that contain an abundant and varied collection of rare-metal-bearing minerals that yielded a concordant zircon age of 1240 ± 2 Ma (Miller *et al.*, 1997).

The various Late Mesoproterozoic ages (1079 to 994 Ma) in the Rogerson Lake Conglomerate are equivalent to Grenvillian orogenesis in Labrador that occurred between 1080 and 985 Ma (Gower and Krogh, 2002). Tectonothermal activity throughout the Lake Melville terrane of the Grenville province is demonstrated by zircon ages of 1080 ± 2 Ma for deformed pegmatitic metagabbro and 1079 ± 6 Ma from the Southwest Brook granite (Schärer and Gower, 1988), and by metamorphic monazite ages of 1078 ± 2 Ma from granitic veins of the Rexon's Cove intrusion and 1077 ± 3 Ma from the Alexis Bay gneiss. The Romaine River monzogranite, located along the southern edge of the eastern Grenville Province, yielded an age of 1079 +17/-11 Ma, but it is unclear as to whether the zircons are igneous or metamorphic (Loveridge, 1986).

The 1016, 1001, and 994 Ma ages correspond to numerous igneous events thorough the Grenville Province. Granitic magmatism in the Hart Jaune terrane is represented by zircon ages of 1017 ± 2, 1015 ± 2, and 1007 ± 2 Ma, while metamorphism is documented by titanite ages of 1006 ± 5, 1006 ± 2, 1004 ± 4, 997 ± 3, and 991 ± 5 Ma from various amphibolite, dioritic and mangerite units (Indares *et al.*, 1998; Cox *et al.*,

1998). Monazite ages of 1011 ± 3 Ma and 992 ± 2 Ma from granitic veins further constrain the metamorphism in the Hart Jaune terrane (Gower and Krogh, 2002).

Grenvillian metamorphism in the Pinware terrane of Labrador was initiated around the same time as that in the Long Range Inlier in Newfoundland. The Lodge quartz monzodiorite gneiss contains metamorphic zircons dated at 1019 ± 14 Ma that are interpreted to represent the onset of metamorphism (Tucker and Gower, 1994; Wasteneys *et al.*, 1997). The continuation of metamorphism in the Pinware terrane is exhibited by zircon dates of 1009 ± 10 Ma from the St. Paul's River quartz monzonite, 1000 ± 2 Ma from the St. Peter Bay mafic dyke and monazite dates of 982 ± 5 Ma and 979 ± 20 Ma from the Cat Pond quartz monzonite and L'Anse-au-Loup volcanics, respectively (Tucker and Gower, 1994; Wasteneys *et al.*, 1997; Gower and Krogh, 2002). Additional ages of 1016 to 1003 Ma are reported for rocks in the Cape Caribou River allochthon and Mealy Mountains terrane and dates of 1001 to 989 Ma were obtained from the Lac Joseph, Wilson Lake, Molson Lake and Churchill Falls terranes (Connelly and Heaman, 1993; Corrigan *et al.*, 1997). For further information on Grenville Province geochronology the reader is forwarded to the papers of Gower and Tucker (1994), Connelly and Heaman (1993); James *et al.* (2000) and Gower and Krogh (2002). Although the ages of zircon in the Rogerson Lake Conglomerate correlate with those of the Grenville Province of Labrador, the probability that the zircons in the conglomerate were derived from the Grenvillian basement rocks of insular Newfoundland is greater.

The absence of zircons in the 680-620 Ma range in the Rogerson Lake Conglomerate is attributed to the presence of a Silurian seaway separating the Gander margin and Avalonia from the Notre Dame, Victoria and Exploits arc terranes that were

accreted to Laurentia. The presence of the Dog Bay Line at the Silurian edge of Laurentia and its recognition as a Silurian seaway suture zone implies that the Dog Bay Line marks the location of such a seaway (Williams, 1993; Williams *et al.*, 1993). Northwest of the Dog Bay Line, in the present Exploits Subzone, Silurian rocks of the Badger and Botwood groups were deposited on Ordovician rocks already accreted to Laurentia. Whereas, southeast of the line, the Silurian rocks were deposited on Ordovician rocks that were amalgamated with the continental Gander Zone. A residual seaway, termed the Exploits seaway (Williams *et al.*, 1993; van Staal *et al.*, 1998), is inferred to separate these opposing landmasses and may represent the terminal Iapetus suture in Newfoundland.

McNicoll and van Staal (2001) reported U-Pb SHRIMP data for zircons from syntectonic sediments in the Badger Belt along the Red Indian Line. Coarse-grained sandstones samples from the base and top of the Badger Group were dominated by Late Cambrian to Ordovician zircons with the amount of Grenville-aged zircons decreasing towards the top of the group. The Rogerson Lake Conglomerate and similar Botwood Belt rocks overlie the Badger Group and contain an even smaller proportion of Grenvillian detrital zircons. The decrease in contribution of Laurentian zircons from the base of the Badger Group stratigraphically upwards to the Rogerson Lake Conglomerate is attributed to the Early to Middle Ordovician collision induced uplift of the Notre Dame arc that progressively diminished the input of Laurentian basement.

6.5 Lead Isotope Geochemistry

6.5.1 Introduction

Lead isotopes are a powerful tool for studying mantle and crustal evolution. Lead is widely distributed throughout the Earth not only occurs as the radiogenic daughter of U and Th but it also forms its own minerals from which U and Th are excluded. The isotopic composition of Pb varies from the highly radiogenic Pb in very old, U and Th bearing minerals to the common Pb in galena and other minerals that have low U/Pb and Th/Pb ratios (Faure, 1986; Gariépy and Dupré, 1991; Richards and Noble, 1998). Since major sulphide minerals generally contain abundant Pb and very low contents of U and Th, they are ideal candidates for Pb isotope analysis. Galena (PbS) is a frequent component of ore deposits and thus allows the study of volcanogenic massive sulphide deposits by the isotopic composition of Pb in galena and other common Pb minerals.

Lead is a trace element in all types of rocks and its isotopic composition in different varieties of rocks contains a record of the chemical environments in which the Pb resided. These environments include the mantle, upper and lower crust, or Pb ores, and each has distinct U/Pb and Th/Pb ratios that affect the isotopic evolution of Pb (Gariépy and Dupré, 1991; Dickin, 1995). These ratios are modified by magma generation and fractionation, by hydrothermal and metamorphic processes, and by weathering. Therefore the isotopic compositions of Pb in rocks and ore deposits display intricate patterns of variation that reflect their geological histories (Faure, 1986; Heaman and Parrish, 1991; Richards and Noble, 1998).

A total of 15 galena separates from the Tally Pond Group were analyzed for their lead isotope ratios. Galena was collected from the shallow and deep sections of the Upper Duck lens of the Duck Pond deposit, the North Zone of the Boundary deposit, the South Moose Pond zone, and the Lemarchant prospect. Analyses were carried out at the

GEOTOP Laboratory, Université du Québec á Montréal (UQAM). Data are reported as $^{206}Pb/^{204}Pb$, $^{207}Pb/^{204}Pb$, $^{208}Pb/^{204}Pb$ and $^{207}Pb/^{206}Pb$ with an analytical uncertainty of 0.04% amu^{-1} at the 1σ level. Full analytical techniques are given in appendix F.

6.5.2 Results

The lead isotope data for the Tally Pond Group are listed in Table F.1 and shown in Figure 6.7. The mantle, orogene, lower crust and upper crust growth curves of Zartman and Doe's (1981) plumbotectonics model are shown for reference. μ values were calculated according to Stacey and Kramers (1975) model using Isoplot ver. 2.06 (Ludwig, 1999).

The data indicate that all samples from the Tally Pond Group show a very small variation in the $^{206}Pb/^{204}Pb$ ratio bound on the lower end by the Lemarchant prospect and the high end by the samples from the deep sections of the Upper Duck lens. The $^{207}Pb/^{204}Pb$ ratios are highly variable, define linear trends and indicate that the lead isotopes for the Tally Pond Group can be classified as three groups: 1) a primitive group represented by galena from the Lemarchant prospect; 2) a slightly more radiogenic group that includes the stratigraphically higher levels (<350m) of the Upper Duck lens and South Moose zones; and 3) a relatively radiogenic group that represents the stratigraphically deep sections (>400 m) of the Upper Duck lens.

Group 1 samples from the Lemarchant prospect are the least radiogenic. Variations within the group are mainly exhibited in the $^{206}Pb/^{204}Pb$ ratios (18.098-18.138), while the $^{207}Pb/^{204}Pb$ ratios (15.555-15.584) and $^{208}Pb/^{204}Pb$ ratios (37.762-37.821) define a small interval. This group plots on $^{206}Pb/^{204}Pb$ versus $^{207}Pb/^{204}Pb$

diagram between the Zartman and Doe (1981) growth curves for the orogene and mantle, with a bias towards to more radiogenic orogene curve. On the $^{206}Pb/^{204}Pb$ versus $^{208}Pb/^{204}Pb$ diagram, the Lemarchant prospect samples lie between the orogene and upper crust growth curves and similar to the $^{206}Pb/^{204}Pb$ versus $^{207}Pb/^{204}Pb$ ratios, plot nearer and sub-parallel to, the orogene growth curve.

Group 2 samples from the Duck Pond and Boundary deposits and South Moose Pond zones define a group that is slightly more radiogenic that the Lemarchant prospect (group 1) samples. The data form a narrow cluster with $^{206}Pb/^{204}Pb$ ratios vary between 18.144 and 18.189, $^{207}Pb/^{204}Pb$ ratios between 15.548 and 15.599, and $^{208}Pb/^{204}Pb$ ratios between 37.754 and 37.892. In the $^{206}Pb/^{204}Pb$ versus $^{207}Pb/^{204}Pb$ diagram, the data plot in a trend that when extrapolated through the least radiogenic end intersects the growth curve for the mantle. This line also trends towards more radiogenic compositions and approaches the orogene growth curve. On a $^{206}Pb/^{204}Pb$ versus $^{208}Pb/^{204}Pb$ diagram, the data define a linear trend that plots sub-parallel to the orogene and upper crust curves.

Group 3 samples from the stratigraphically deeper sections of the Upper Duck lens of the Duck Pond Deposit define a group that is the most radiogenic when compared to other samples from the Tally Pond Group. The three samples constitute a group with a large variation in isotopic ratios. $^{206}Pb/^{204}Pb$ ratios vary between 18.209 and 18.311, $^{207}Pb/^{204}Pb$ ratios between 15.641 and 15.783, and $^{208}Pb/^{204}Pb$ ratios between 38.081 and 38.950. On a plot of $^{206}Pb/^{204}Pb$ versus $^{207}Pb/^{204}Pb$ the group defines a linear trend that primarily lies in the radiogenic compositions zone above the upper crust growth curve and intersects this curve at a steep angle. In the $^{206}Pb/^{204}Pb$ versus $^{208}Pb/^{204}Pb$ diagram (Figure 6.8), the group lies above the orogene growth curve and define a linear array that

at the least radiogenic end originates near this curve and trends towards more radiogenic compositions.

Model ages for the sulphide occurrences have been calculated according to the Stacey and Kramers (1975) model, using the $^{206}Pb/^{204}Pb$ and $^{207}Pb/^{204}Pb$ ratios and are listed in Table F.1. The model ages for the 14 analyses from the Tally Pond Group range from a high of 589 Ma to a low of 295 Ma. Six samples from the top section of the Upper Duck lens, two samples from the South Moose Pond zone, two samples from the Lemarchant prospect, and one sample from the Boundary Deposit yield model ages that range from 299 Ma to 323 Ma, which are significantly younger than the model ages for the three samples from the deep section of the Upper Duck lens, calculated at 396, 425 and 589 Ma. These dates are not considered to be particularly meaningful due to the linear distribution of data.

The Pb isotope data were regressed using the algorithm of York (1969) with equal weights and zero error correlations assigned to each point. Linear regression of the $^{207}Pb/^{204}Pb$ versus $^{206}Pb/^{204}Pb$ data produces a line with a slope of 0.95 ± 0.20 at 2σ, which is much steeper than Phanerozoic Pb growth curves for the mantle and crust. The mean square of weighted deviates (MSWD) value is a measure of the observed scatter of the points (from the best fit line) to the expected scatter (from the assigned errors and error correlations. The MSWD value of 177 for the Tally Pond Group samples indicates a significantly poor fit to the line, this is due to the data points for the Lemarchant prospect and the deep sections of the Upper Duck lens.

6.5.3 Discussion

The Pb isotope data for the 15 samples from the Tally Pond Group define a linear trend which supports the hypothesis that the different VMS occurrences throughout the Tally Pond Group are genetically related to each other. There are a couple of possibilities that might be responsible for producing the linear trend in the data and the examination of these process can therefore shed light on the nature of the mineralizing event(s). Since the differences in Pb isotope compositions between mineralized occurrences is a function of the variable nature of the source rock Pb reservoirs that are tapped during mineralization, and the age differences between the occurrences, the two possibilities that could produce a linear trend are: 1) the data define a mixing line, or 2) the data define a secondary isochron.

If the linear trend is an isochron it is implied that all of the Pb in the samples originally had a homogenous isotopic composition when it was segregated from its source reservoir and that all the Pb samples were separated from this region at the same time. The differences in the Pb composition are due to the Pb subsequently residing in various environments having diverse U/Pb and Th/Pb ratios. The age of this isochron should therefore indicate the time at which the homogenous Pb was separated from its source reservoir. The isochron for the Tally Pond Group samples was calculated at 5163 ± 290 Ma. This age is older than the age of primordial Pb and older than the accepted age of the Earth at 4.57 Ga. Further evidence against interpreting the linear trend as an isochron is provided by the age of the host rock units. The 14 samples are associated with felsic volcanic rocks of the Boundary Brook Formation of the Tally Pond Group which has been dated at 509 ±1 Ma. The age of the Pb in the Tally Pond samples is constrained by this age and therefore the observed variations in Pb isotopic compositions between the

various VMS occurrences probably reflect differences in source regions of the Pb rather than age differences. Finally, the poor fit of the data to the least-squares regression line suggests that the present Pb composition does not result from simple Pb growth from a homogeneous source reservoir. This is because higher values in the MSWD indicate either an underestimation of the analytical error, or in this case, that the scatter in the data is due to geological processes and not to analytical factors. Each of these statements suggests that the linear trend in the Tally Pond Group data does not represent an isochron and that the Pb isotopic composition of the samples is the result of growth in at least two or more source areas with different U/Pb and Th/Pb ratios. Thus, the alternative interpretation, is that the linear trend lacks any precise geochronological significance, and instead, represents a mixing line between different Pb reservoirs which evolved from distinct long-lived environments. This alternative seems more probable as the model ages obtained by applying the model of Stacey and Kramers (1975) are unrealistic.

If the linear trend is considered a mixing line, then the Pb isotope compositions can be explained in terms of variable mixtures of two end-member sources or reservoirs. The least radiogenic end members, the Lemarchant prospect, Upper Duck lens of the Duck Pond deposit, South Moose Pond zone and Boundary Deposit, would closely approach the composition of the least radiogenic source region. The cluster in isotopic compositions between the four occurrences suggests that they are from the same source and not are the product of mixture, which indicates that the Pb isotope compositions of the Lemarchant prospect, Upper Duck lens of the Duck Pond deposit, South Moose Pond zone and Boundary Deposit predominantly reflect the average composition of the immediate volcanic host rocks during mineralization. This interpretation seems

reasonable as the $^{206}Pb/^{204}Pb$ and $^{207}Pb/^{204}Pb$ ratios for these occurrences lie just below the orogene growth curve of Zartman and Doe (1981). This is an average Pb growth curve that suggests a rather uniform U/Pb and Th/Pb source, generated by the homogenizing processes of sedimentation, volcanism, plutonism, metamorphism and rapid erosion. The most obvious manifestation of the orogenic environment is in geologically active island and continental arcs, such as the Tally Pond Group. In these systems come great quantities of tholeiitic basalt and pelagic sediments of the oceanic crust, clastic and chemical detritus of the adjacent continental crust and the lower crust and mantle wedge material that constitute the region above the subduction zones. The Pb isotopic composition of such an arc system should therefore reflect the proportions of its contributing components (Doe and Zartman, 1981). The Tally Pond Group is one such island arc system, and the Pb isotopic composition of the Lemarchant prospect, Upper Duck lens of the Duck Pond deposit, South Moose Pond zone and Boundary Deposit indicate a more radiogenic composition than a mantle source and that there is a considerable contribution of Pb from a radiogenic source reservoir, considered to be the upper continental crust.

However, the possibility of a minor mantle component in these Pb isotopic compositions cannot be ruled out. These occurrences plot in a linear trend that when extrapolated from the least radiogenic end intercepts the mantle growth curve. The bulk uranogenic Pb composition of contemporaneous mantle is significantly less radiogenic than the Pb in the Tally Pond galenas, however; a minor amount of mantle Pb contributed to the samples would lower their $^{207}Pb/^{204}Pb$ ratio and cause them to plot slightly below the Orogene growth curve. There is also the possibility of a lower crust Pb contribution,

but the $^{208}Pb/^{204}Pb$ isotopic ratios in the Tally Pond Group galena samples indicate a major contribution from a considerably more uranogenic Pb-rich environment rather than the thorogenic Pb-rich environment that is normally postulated for the lower crust (Gariépy and Dupré, 1991; Dickin, 1995).

The Pb isotope signature in the more radiogenic stratigraphically deeper section and shallow section of the Upper Duck lens is less constrained and may be related to a couple of different factors. Lead in the deeper sections of the Upper Duck lens is more radiogenic than the apparently stratigraphically higher levels of the Upper Duck lens suggesting derivation from a source with higher U/Pb ratios, i.e. the upper crust. Such a scenario may indicate that the entire deposit has been structurally inverted since its time of formation. This scenario seems unlikely as sulphide-bearing debris flow beds are fining upwards sequences, and the large chlorite alteration feeder pipes are presently located beneath the massive sulphide bodies.

However, the more radiogenic composition of the Pb in galenas from the deep section of the Upper Duck lens is accompanied by an increase in the amount of sedimentary rock sequences in the immediate host rocks. This correlation implies that the increasingly radiogenic composition reflects a change from more abundant felsic volcanic rock components higher in the stratigraphic sequence to black shale dominated sequences in the lower stratigraphic units. Consequently, the Pb isotopic composition of galena from the deep section of the Upper Duck lens most likely reflects the average Pb composition of the immediate clastic sedimentary host rocks during mineralization. The black shales in the sedimentary sequence are interpreted to be the source of the highly radiogenic values, because pelagic black shales are derived in part from continental material with

high U/Pb and Th/Pb, and are often enriched in ^{207}Pb and ^{208}Pb with respect to mid-ocean ridge basalts (Kesler *et al.*, 1994; Dickin, 1995). The high μ values (>10) from the Deep Upper Duck lens further support this interpretation.

Stacey and Kramers' (1975) model ages calculated from the $^{207}Pb/^{204}Pb$ and $^{206}Pb/^{204}Pb$ data for the Tally Pond Group should be used with caution, as these ages are only accurate if both U and Pb remained closed to external disturbance during radioactive decay in the source material and were then separated into the ore deposit. These rigid conditions are seldom realized in nature and one must assume that the U and Pb isotopes have been disturbed. All of the model ages (except sample 342 at 589 Ma) are much younger than the minimum age of the Tally Pond Group, which has been precisely determined by U-Pb zircon geochronology as 509 ± 1 Ma. These model ages suggest that the U and/or Pb in the source materials were disturbed and mixed at one or possibly many times before the Pb was segregated into the ore. The anomalously old 589 Ma model age may be in part due to a remobilization from an earlier Pb accumulation, i.e. the Pb in the black shale sequence, combined with a mixture of various Pb source reservoirs.

Previous workers (Swinden, 1987; Hall *et al.*, 1998; Williams *et al.*, 1988; Evans, 1996) have suggested that the lead isotopic signatures in volcanogenic massive sulphide deposits of the Notre Dame Subzone contrast with those of the Exploits Subzone. Analysis of the lead isotope data (Table F.2) from other deposits in the Victoria Lake Supergroup and elsewhere in the Newfoundland Dunnage Zone (Figure 6.9) indicate that such a contrast does exist in the lead isotopic signatures between the two subzones. The Skidder, Connel, Clementine, Buchans, and Mary March deposits (Cumming and Krstic, 1987; Winter 2000), located in the Notre Dame Subzone, display a larger variation in the

$^{206}Pb/^{204}Pb$ ratio than the $^{207}Pb/^{204}Pb$ ratio and are the most primitive in terms of their U/Pb evolution. Other deposits from the Notre Dame Subzone, the Lochinvar, Oil Islands, Seal Bay, York Harbour, Catchers Pond, Bull Road, Pilleys Island and Shamrock occurrences, lie in the same field as those of the Buchans area, with the Pilleys Island sample being the most primitive. The one exception are the two galena samples from the Ming Mine which are more radiogenic than Notre Dame Subzone Pb deposits and plot in the field of the Exploits Subzone.

Samples from the Exploits subzone include the 15 samples collected for this study, the Boundary and Burnt Pond occurrences from Swinden and Thorpe (1984), all of the Tally Pond group, and the Tulks East, Tulks Hill, and Victoria Mine prospect from elsewhere in the Victoria Lake Supergroup (Swinden and Thorpe, 1984; Cumming and Krstic, 1987). The lead isotope signatures of each of these deposits are much more radiogenic than those of the Notre Dame Subzone and have larger variations in the $^{207}Pb/^{204}Pb$ ratio than the $^{206}Pb/^{204}Pb$ ratio; this is opposite to that of the Notre Dame Subzone and indicates that the material from each subzone was derived from sources with different U/Pb ratios. The Strickland, Facheux Bay and Barasway de Cerf deposits (Swinden and Thorpe, 1984), located in the southwest Exploits Subzone, contain high $^{207}Pb/^{204}Pb$-$^{206}Pb/^{204}Pb$ ratios and are among the most radiogenic and lie in the field defined by the Exploits Subzone. Galena from the Handcamp occurrence has the same $^{206}Pb/^{204}Pb$ ratio as deposits in the Exploits Subzone, however, the $^{207}Pb/^{204}Pb$ ratio is slightly less indicating that the Handcamp occurrence is less radiogenic than the deposits in the Victoria Lake Supergroup.

The Neoproterozoic Winter Hill deposit from the Avalon Zone is included in this study for comparative purposes. Five samples from the deposit (Sears and Wilton, 1996) have significantly lower $^{206}Pb/^{204}Pb$ and $^{207}Pb/^{204}Pb$ ratios and are much older than VMS deposits in the Dunnage Zone. The lead isotopes are more radiogenic than those of the Notre Dame Subzone, and suggest that the Gondwanan continental crust contained a higher $^{238}U/^{204}Pb$ ratio, or μ value, than the Laurentian crust.

Lead isotope ratios for volcanogenic massive sulphide deposits in the Newfoundland Dunnage Zone indicate that there are two general groups of deposits. A primitive group, which consists of the Buchans, Skidder, Mary March, Connel, Pilleys Island, Lochinvar, and York Harbour deposits of the Notre Dame Subzone and a relatively more radiogenic group comprising the deposits of the Victoria Lake Supergroup and the Facheux Bay, Barasway de Cerf, Strickland and Handcamp occurrences of the Exploits Subzone. The variations in these lead isotope ratios suggest that the deposits of the Exploits subzone contain a greater influence of U/Pb-rich material while galena from the Notre Dame Subzone overlaps the mantle growth curve and evolved in a U/Pb-poor environment.

Previous studies (Cumming and Krstic, 1987; Winter, 2000) have shown that there is a consistency in the lead isotope ratios of all data from the Buchans area and that these deposits evolved in a region of relatively low U/Pb. This feature is also a characteristic of lead deposits in the Grenville Province (Farquhar and Fletcher, 1980) and suggests that the Buchans deposits and other galena occurrences in the Notre Dame Subzone evolved under the influence of Laurentian continental crust.

The lead isotope data from the Victoria Lake Supergroup and other deposits indicate that the Exploits Subzone evolved in a region of higher U/Pb relative to the Notre Dame Subzone. The Exploits Subzone appears to have been influenced not by the Laurentian crust but rather by Gondwanan continental crust. This hypothesis seems rational as data from the Avalon Zone, namely the Winter Hill deposit, indicate that the Avalonian continental margin of peri-Gondwana consists of a considerable amount of crustal material that evolved with a relatively high U/Pb ratio.

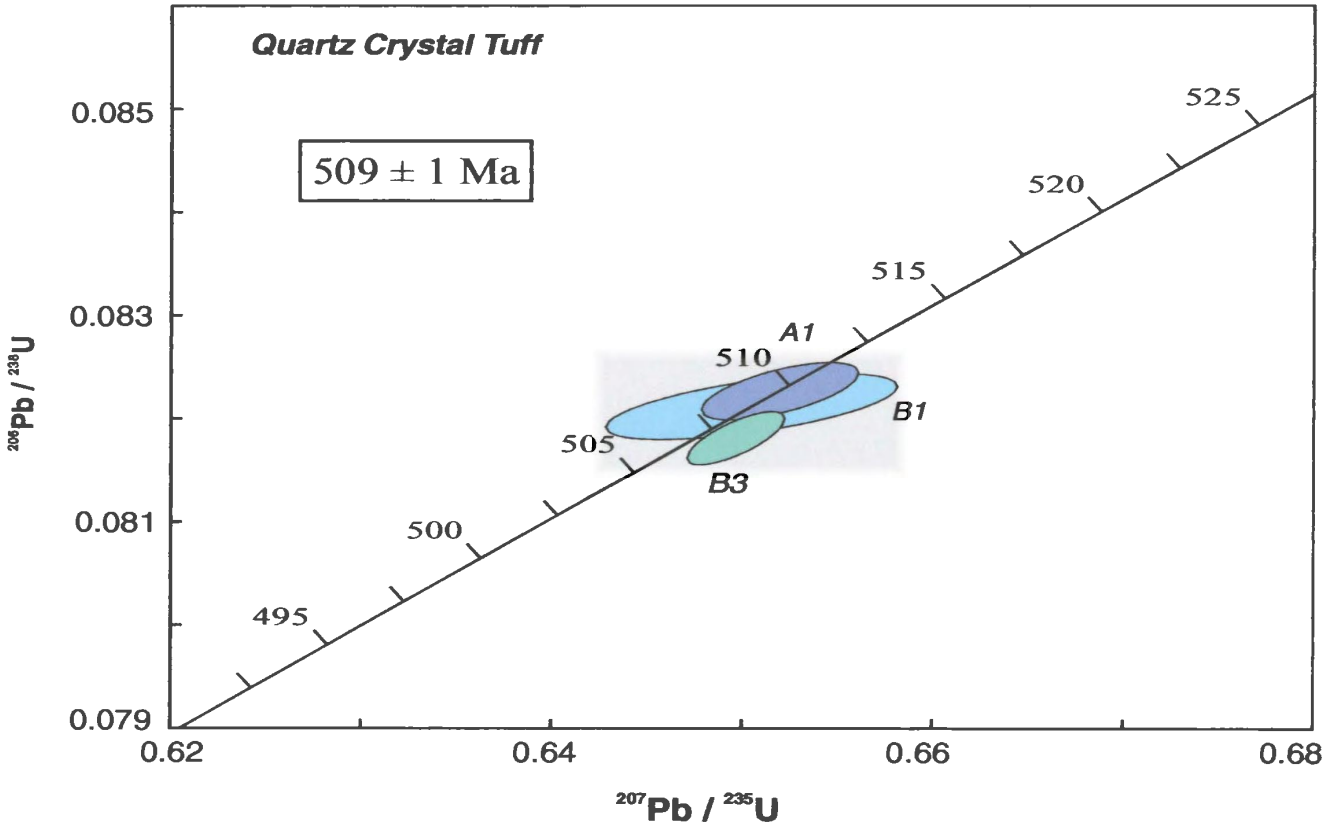

Figure 6.1 *Concordia diagram for felsic tuff (JP-01-GC1) from the Tally Pond Group.*

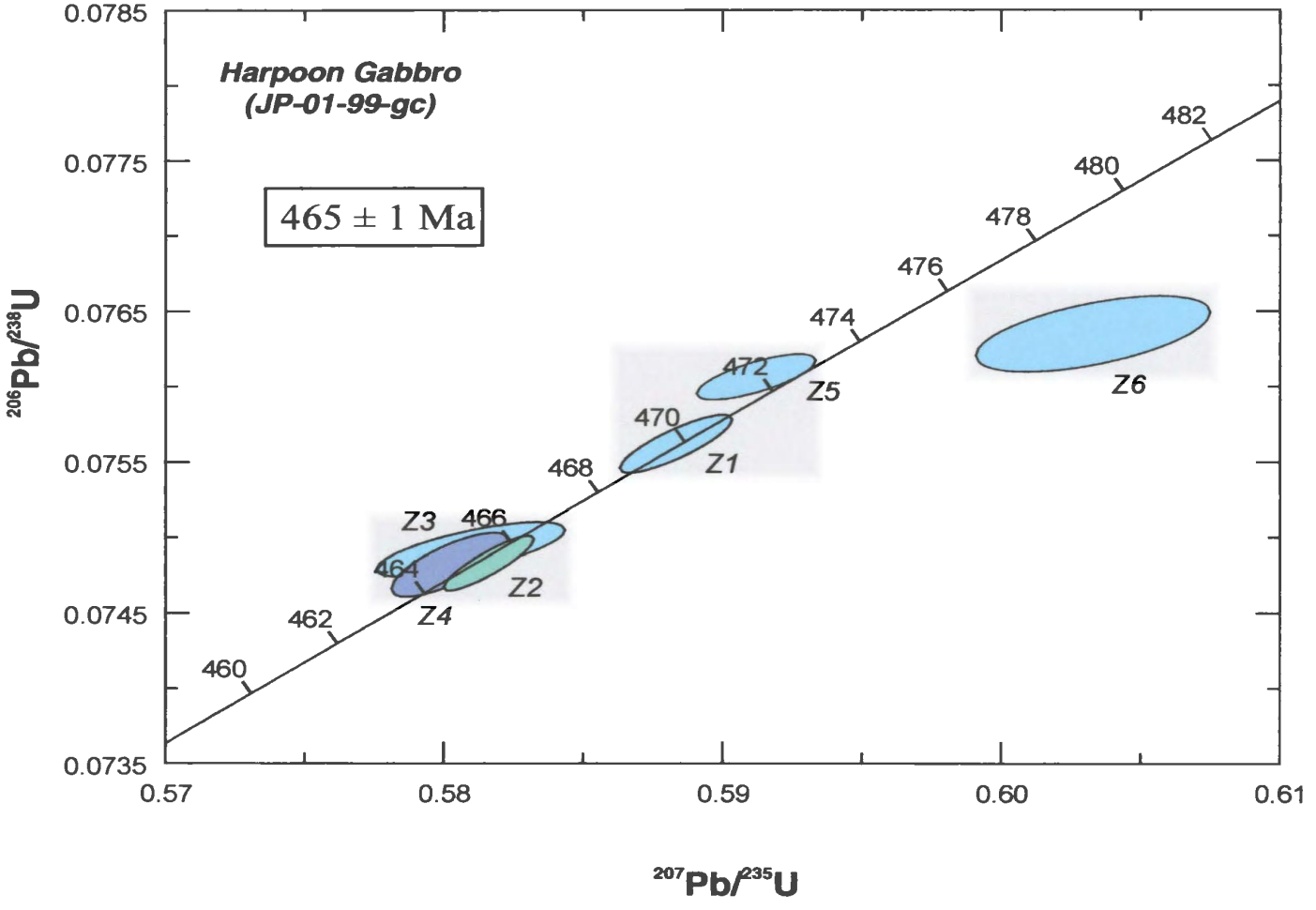

Figure 6.2 *Concordia diagram for Harpoon Gabbro from the summit of Harpoon Hill.*

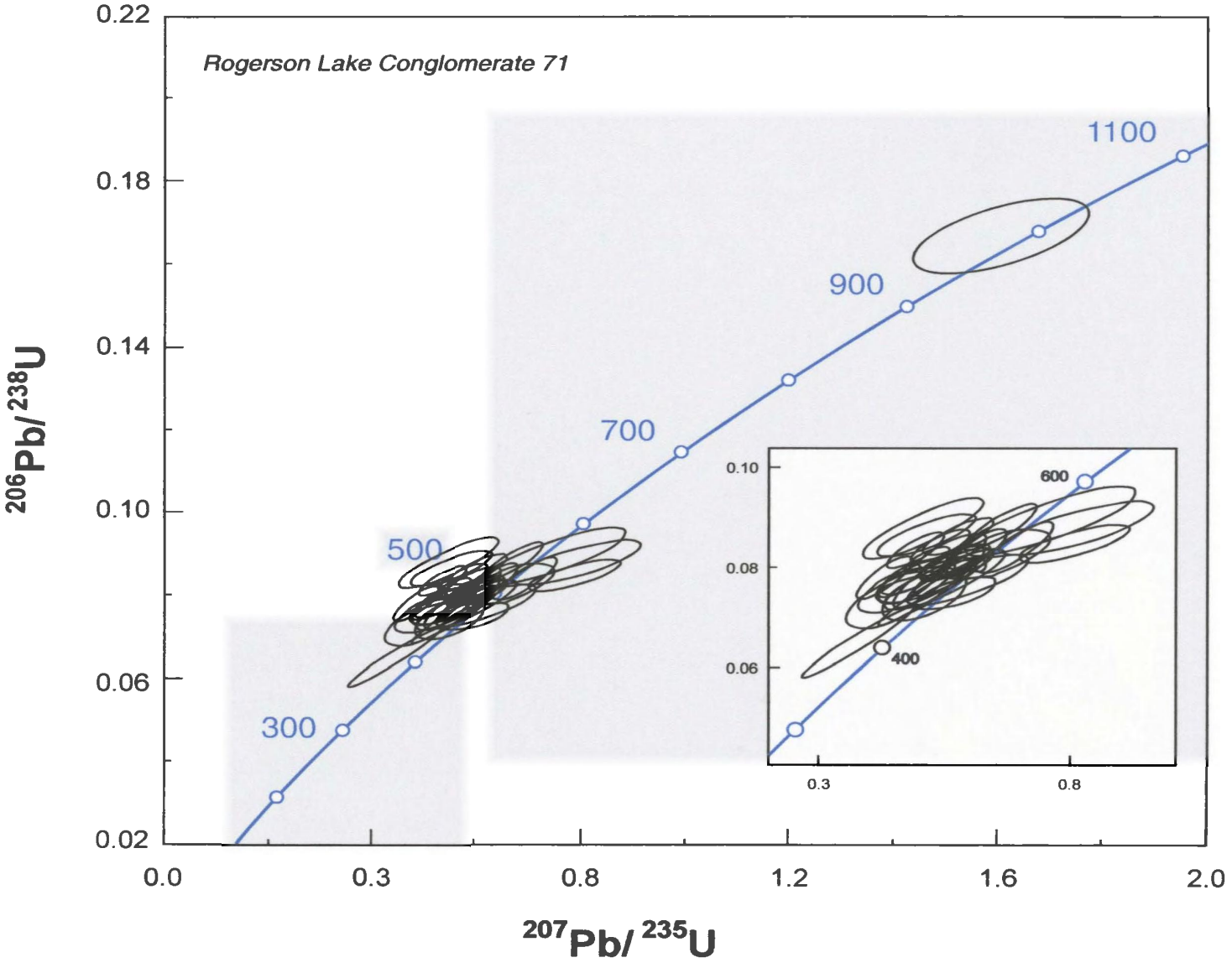

Figure 6.3 *Concordia diagram showing data points measured on detrital zircons from the Rogerson Lake Conglomerate (71) at Rogerson Lake. The inset shows a detailed condordia plot for the ca. 500 Ma range.*

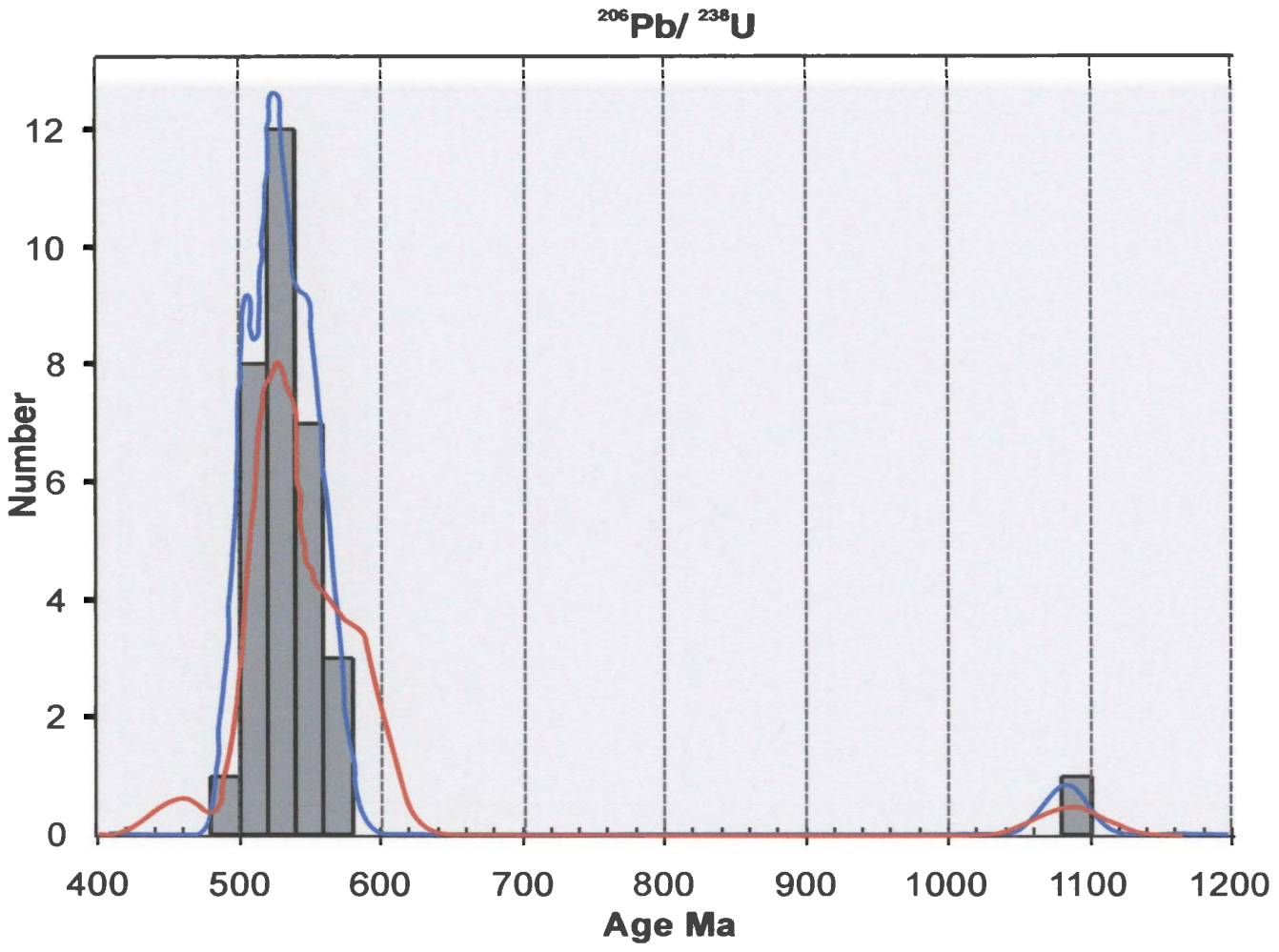

Figure 6.4 *Cummulative probability plot of $^{206}Pb/^{238}U$ ages of detrital zircons from the Rogerson Lake Conglomerate (71) at Rogerson Lake. The blue line represents all zircon analyses; the red line represents those zircons that are 90% or greater concordant.*

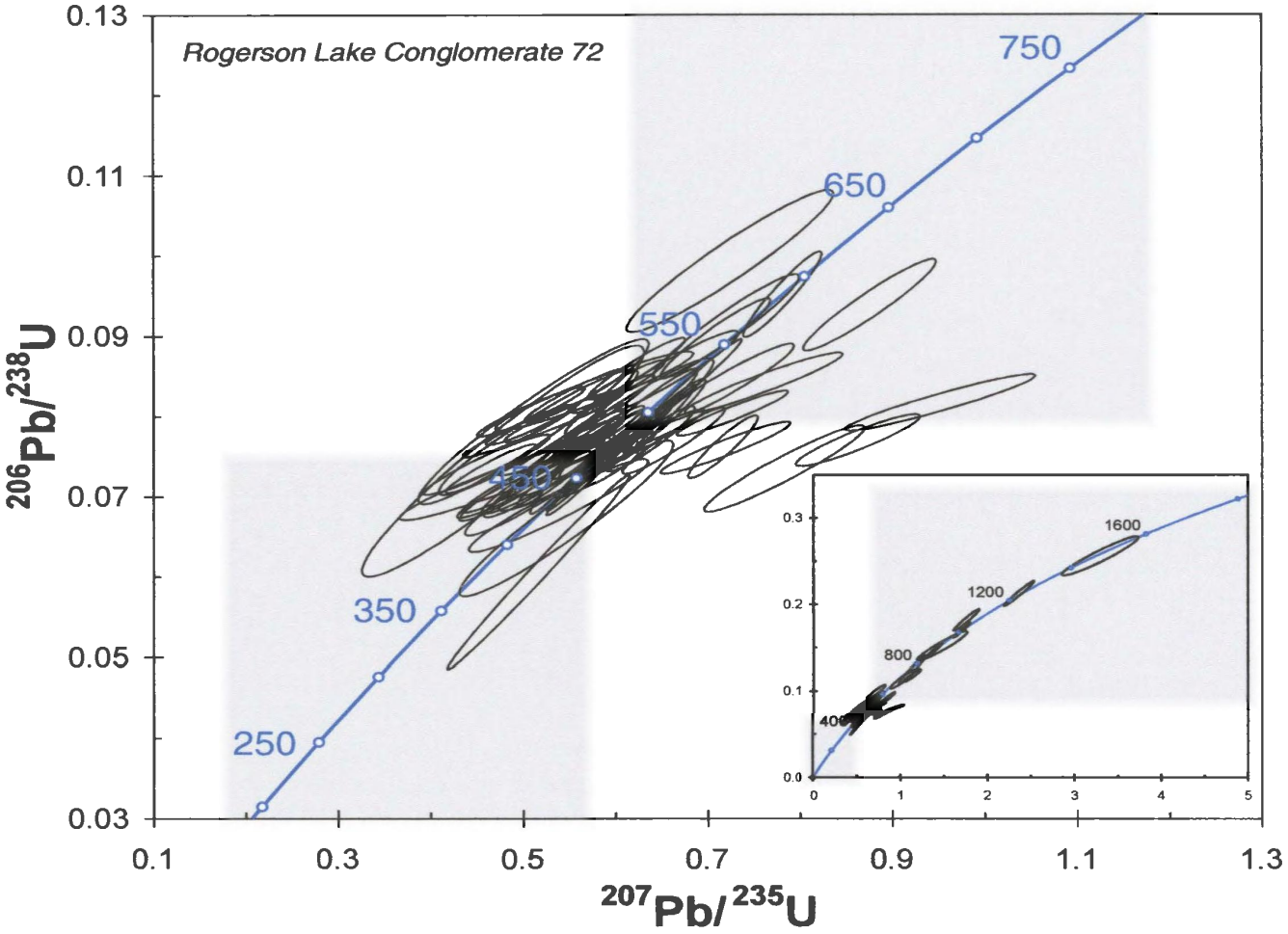

Figure 6.5 *Concordia diagram for detrital zircons from the Rogerson Lake Conglomerate (72) at Burgeo Road for the ca. 500 Ma range. The inset displays a concordia plot for the whole range.*

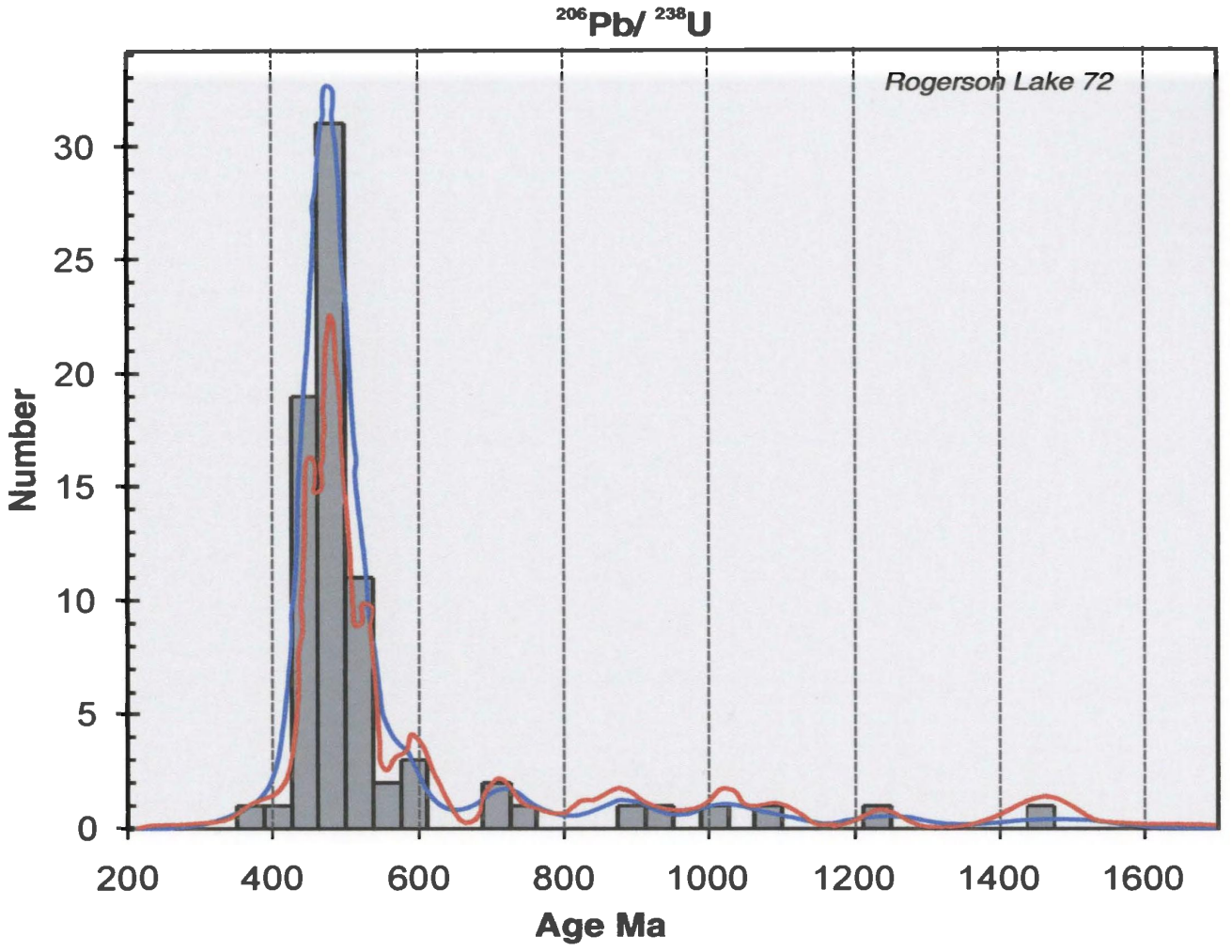

Figure 6.6 *Cummulative probability plot of $^{206}Pb/^{238}U$ ages of detrital zircons from the Rogerson Lake Conglomerate (72) at Burgeo Road. The blue line represents all zircon analyses; the red line represents those zircons that are 90% or greater concordant.*

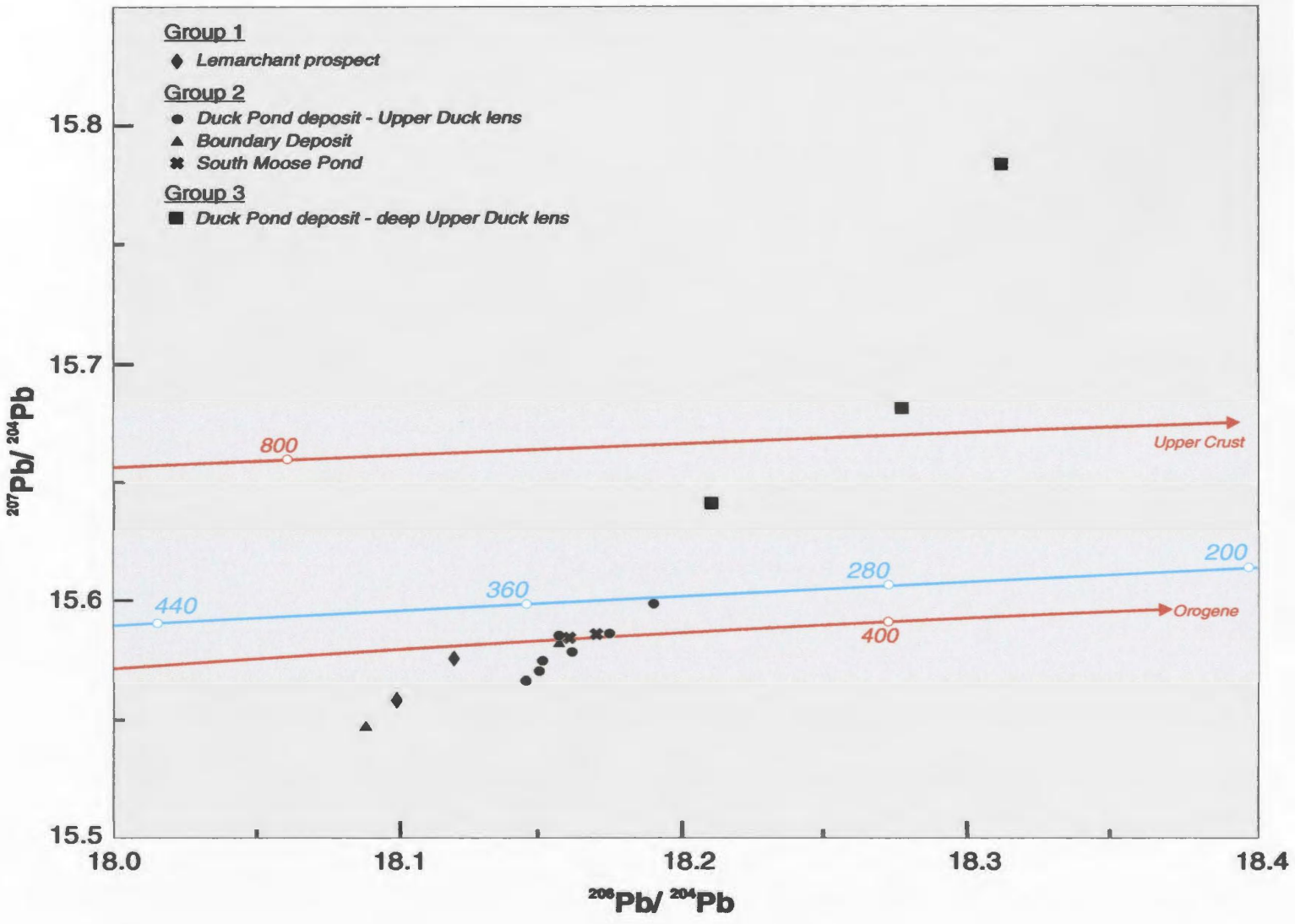

Figure 6.7 *$^{206}Pb/^{204}Pb$ vs. $^{207}Pb/^{204}Pb$ data for galena in the Tally Pond Group. The solid blue line is Stacy and Kramers' (1975) average crust growth curve. The solid red lines are Zartman and Doe's (1981) growth curves; ages in Ma.*

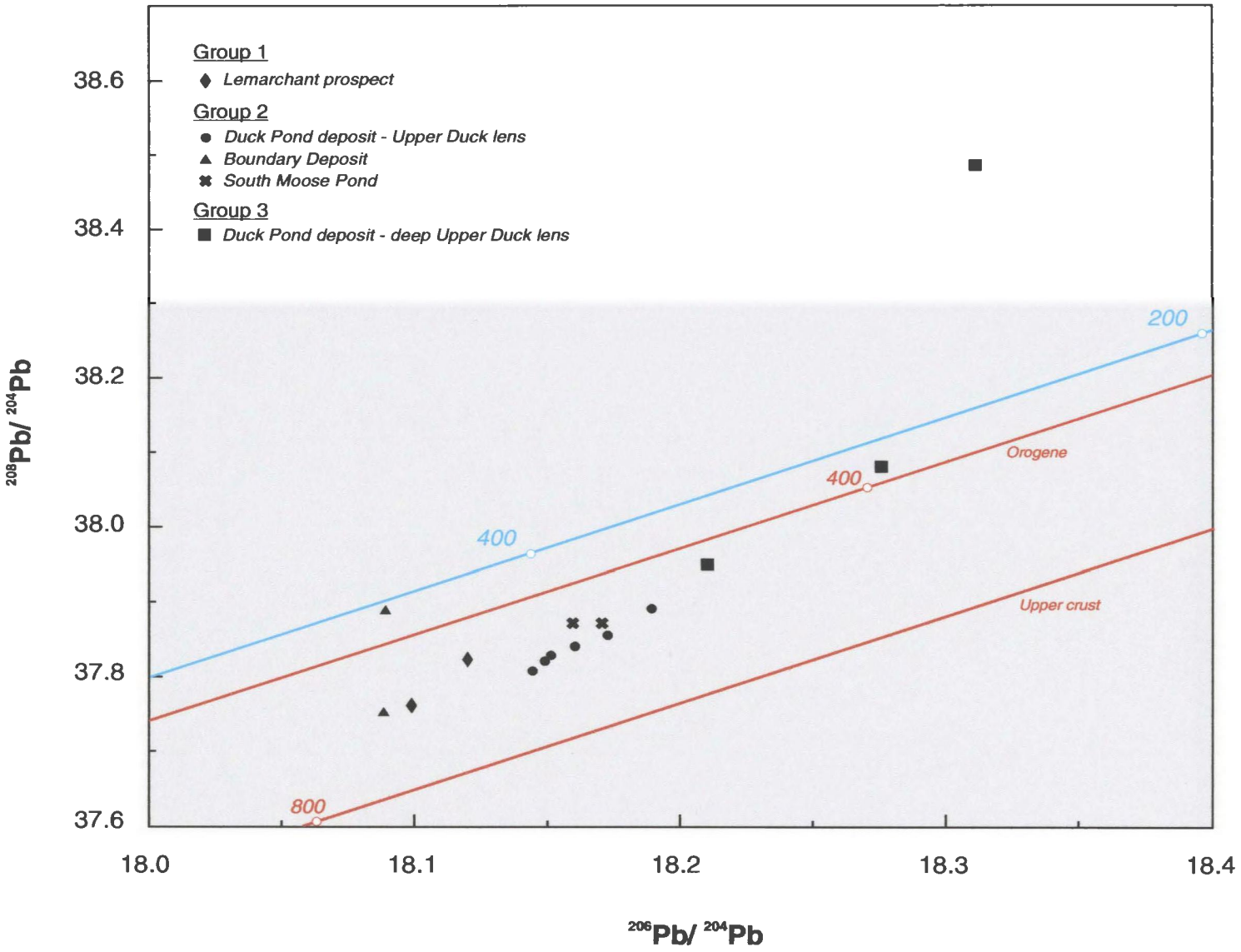

Figure 6.8 *$^{206}Pb/^{204}Pb$ vs. $^{208}Pb/^{204}Pb$ data for galena in the Tally Pond Group. The solid blue line is Stacey and Kramers' (1975) average crust growth curve. The solid red lines are Zartman and Doe's (1981) growth curves; ages in Ma.*

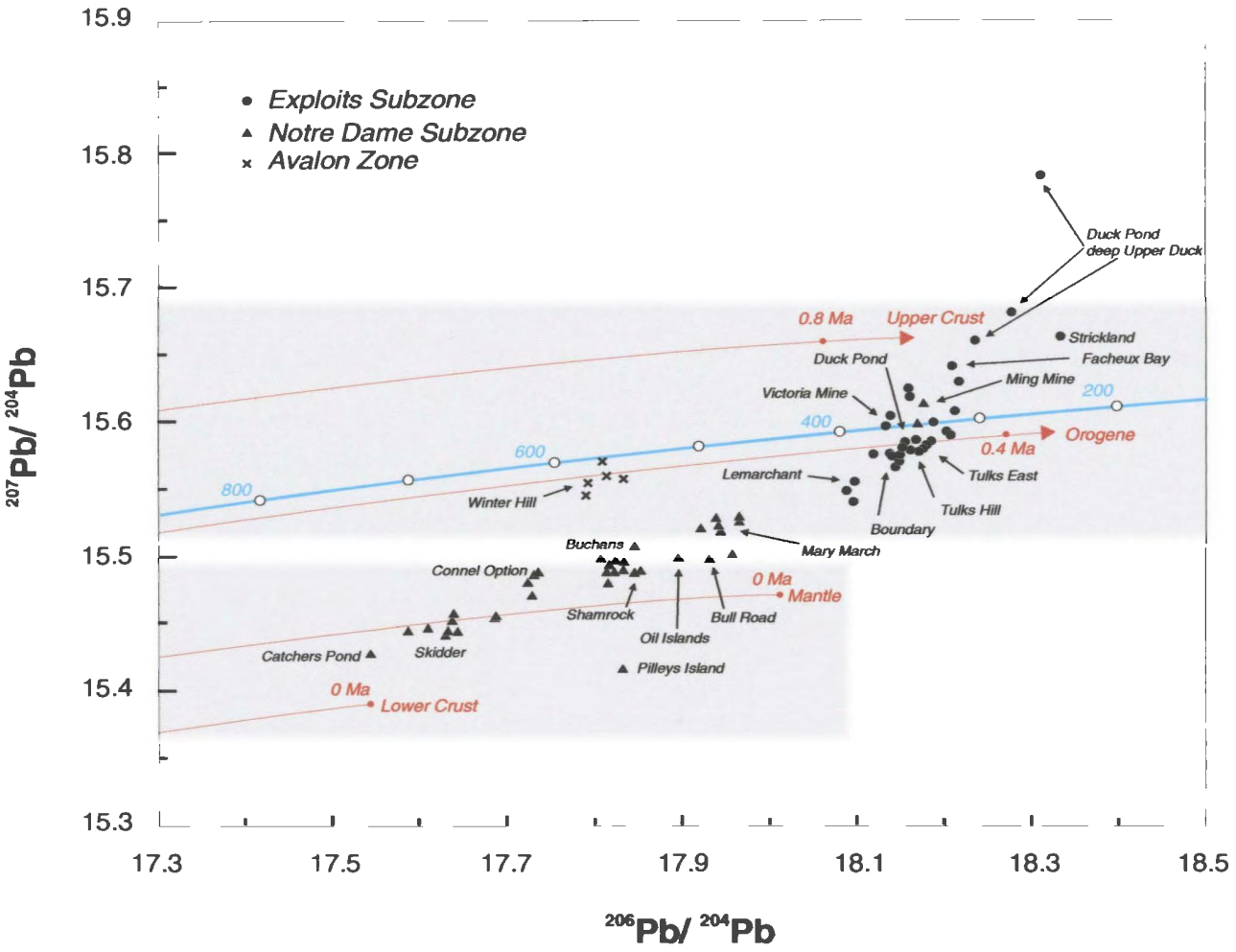

Figure 6.9 *$^{206}Pb/^{204}Pb$ vs. $^{207}Pb/^{204}Pb$ data for galena in the Newfoundland Dunnage Zone. The solid blue line is Stacy and Kramers' (1975) average crust growth curve. The solid red lines are Zartman and Doe's (1981) growth curves; ages in Ma.*

Plate 6.1 *Quartz-crystal tuff from the hanging wall of the Boundary deposit. This sample was dated at 509 +/- 1 Ma.*

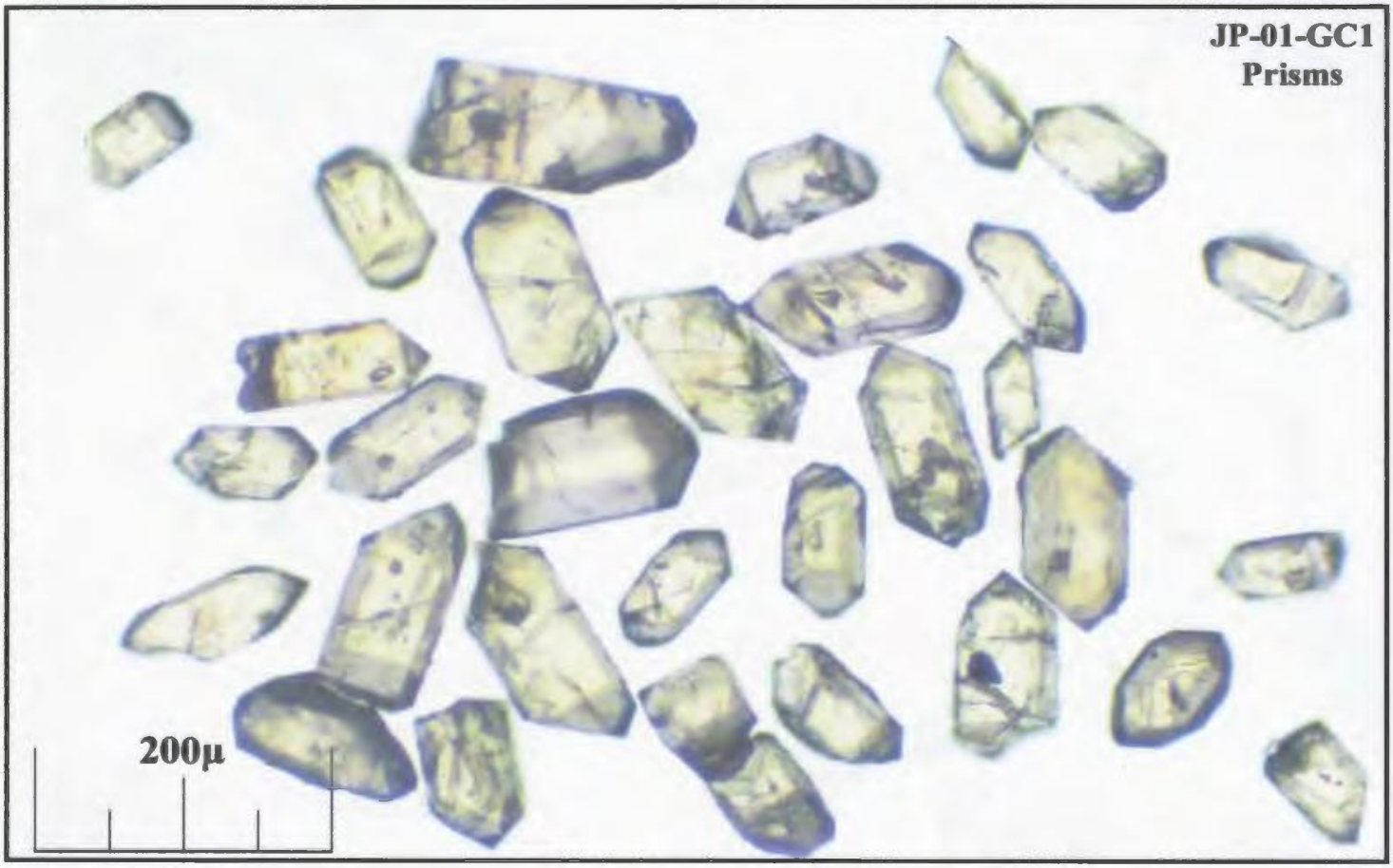

Plate 6.2 *Photomicrograph of fraction 1: unabraded zircon prisms.*

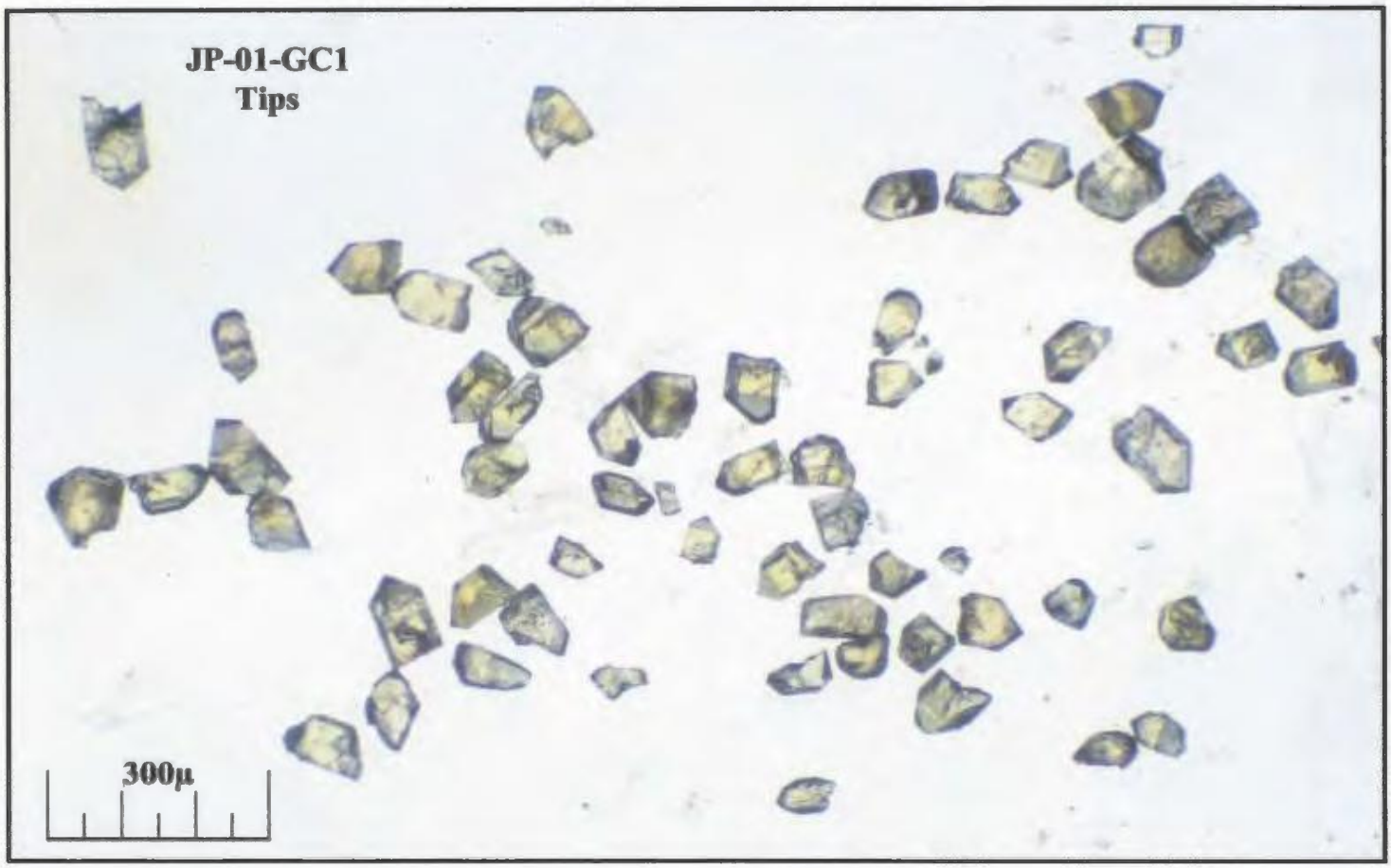

Plate 6.3 *Photomicrograph of fraction 2: unabraded zircon tips.*

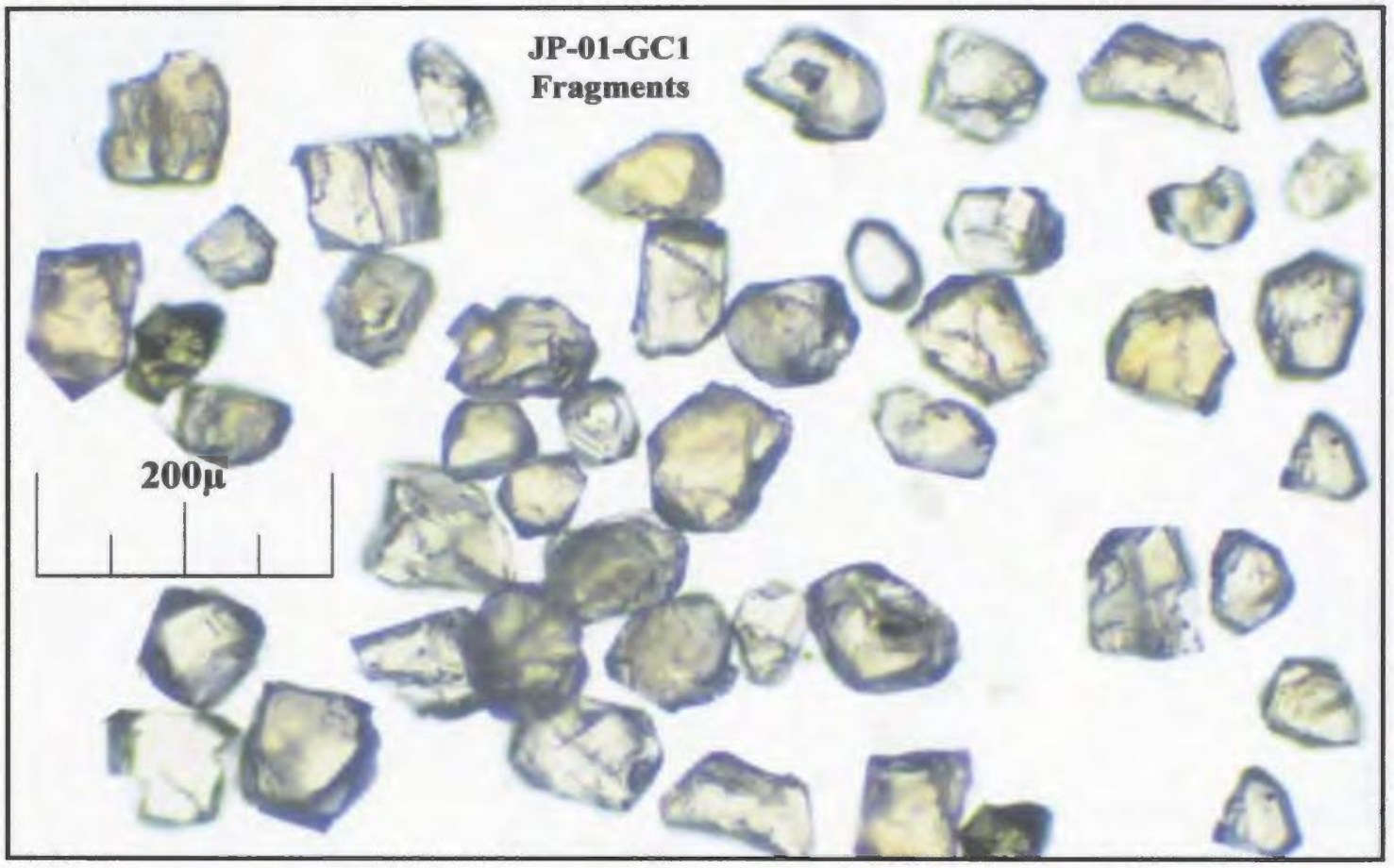

Plate 6.4 *Photomicrograph of fraction 3: unabraded zircon fragments.*

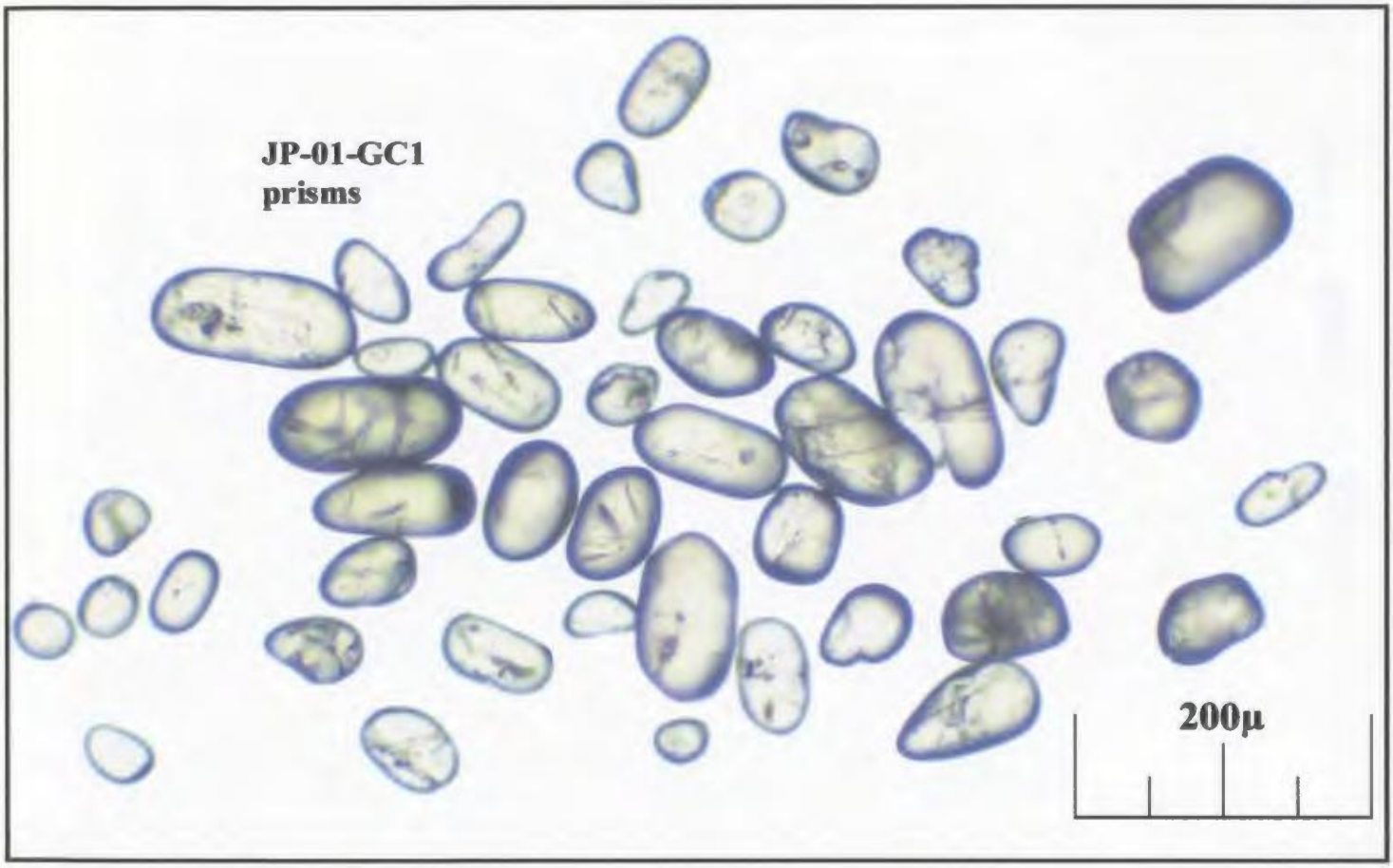

Plate 6.5 *Photomicrograph of fraction 1: abraded zircon prisms.*

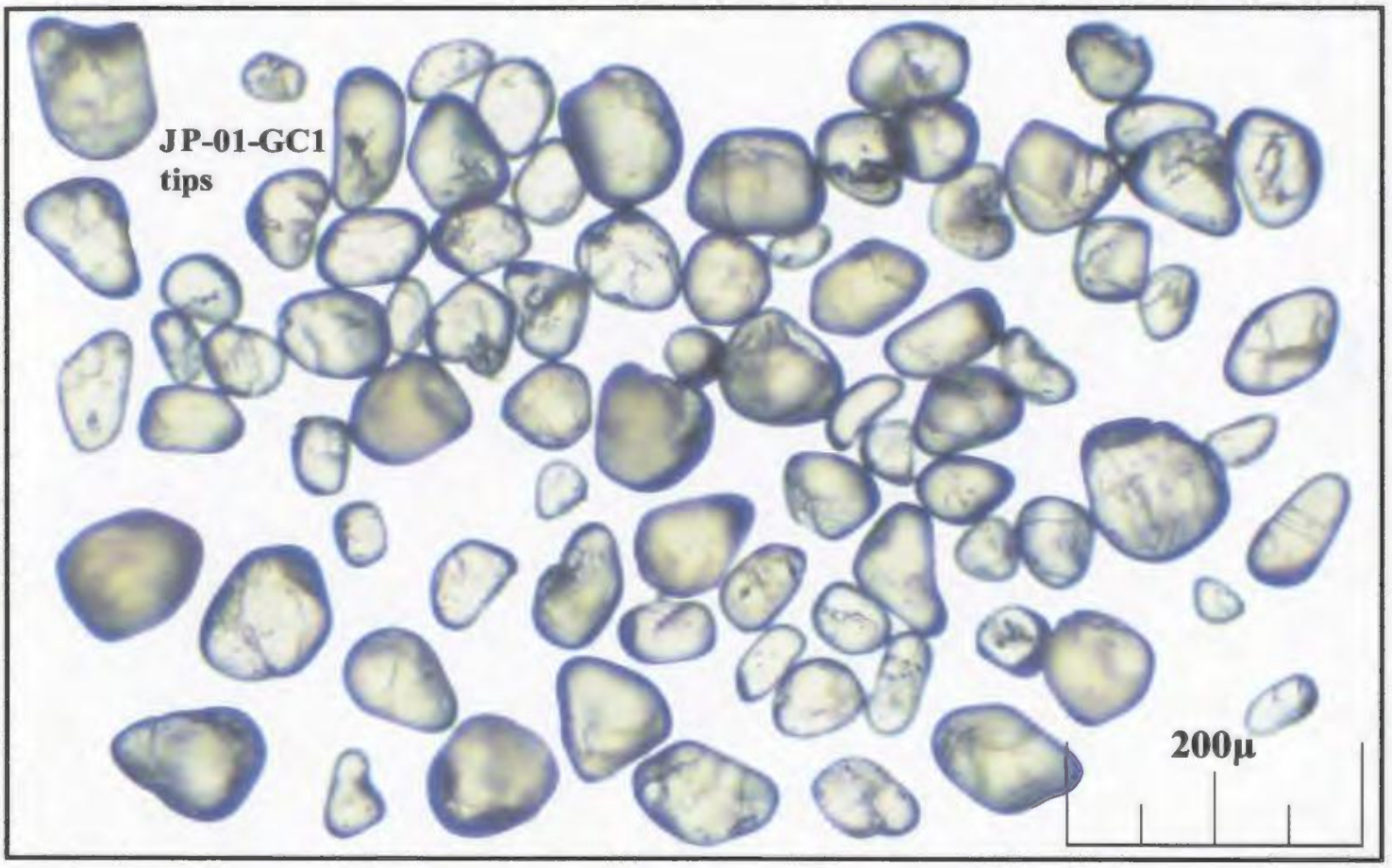

Plate 6.6 *Photomicrograph of fraction 2: abraded zircon tips.*

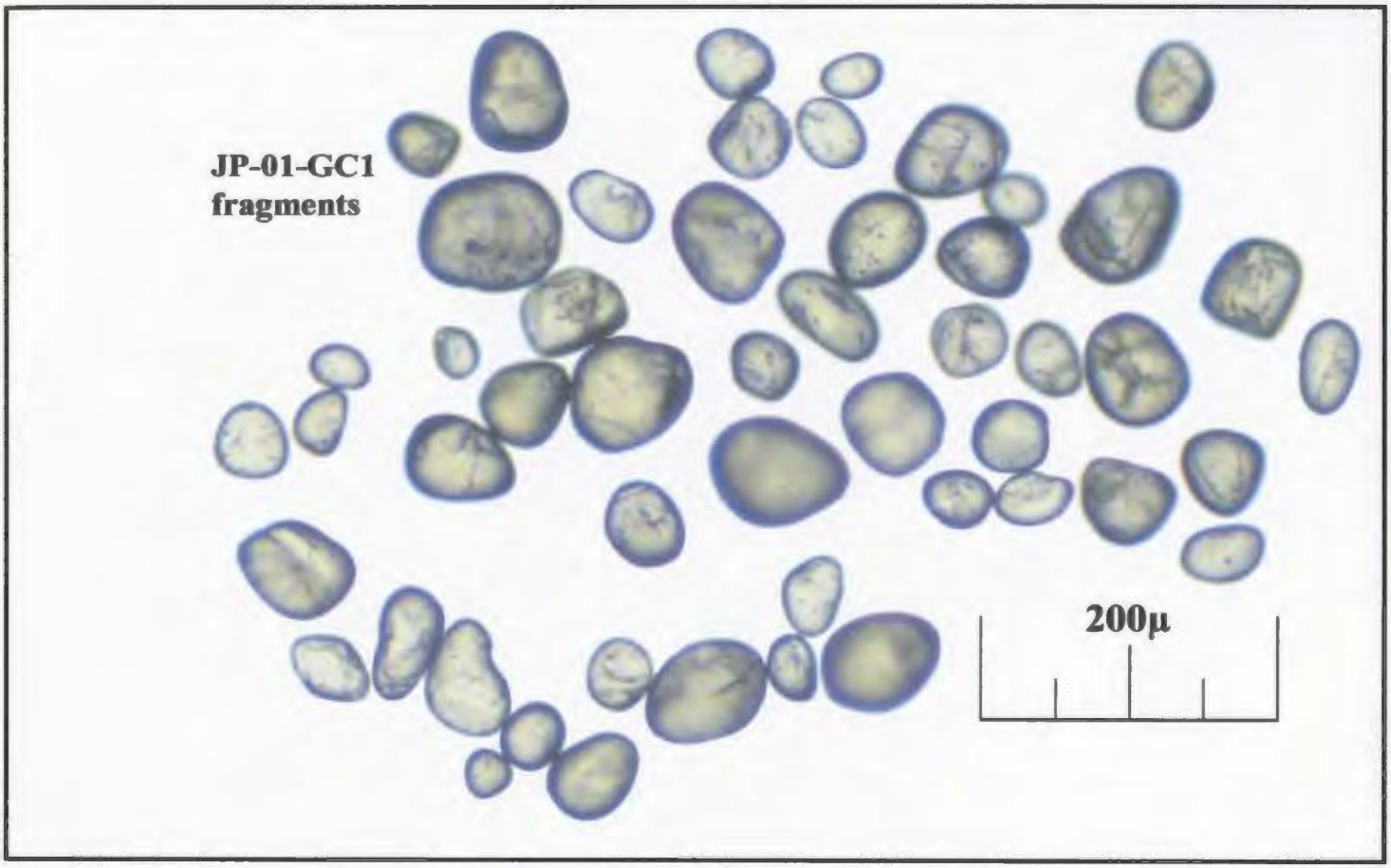

Plate 6.7 *Photomicrograph of fraction 3: abraded zircon fragments.*

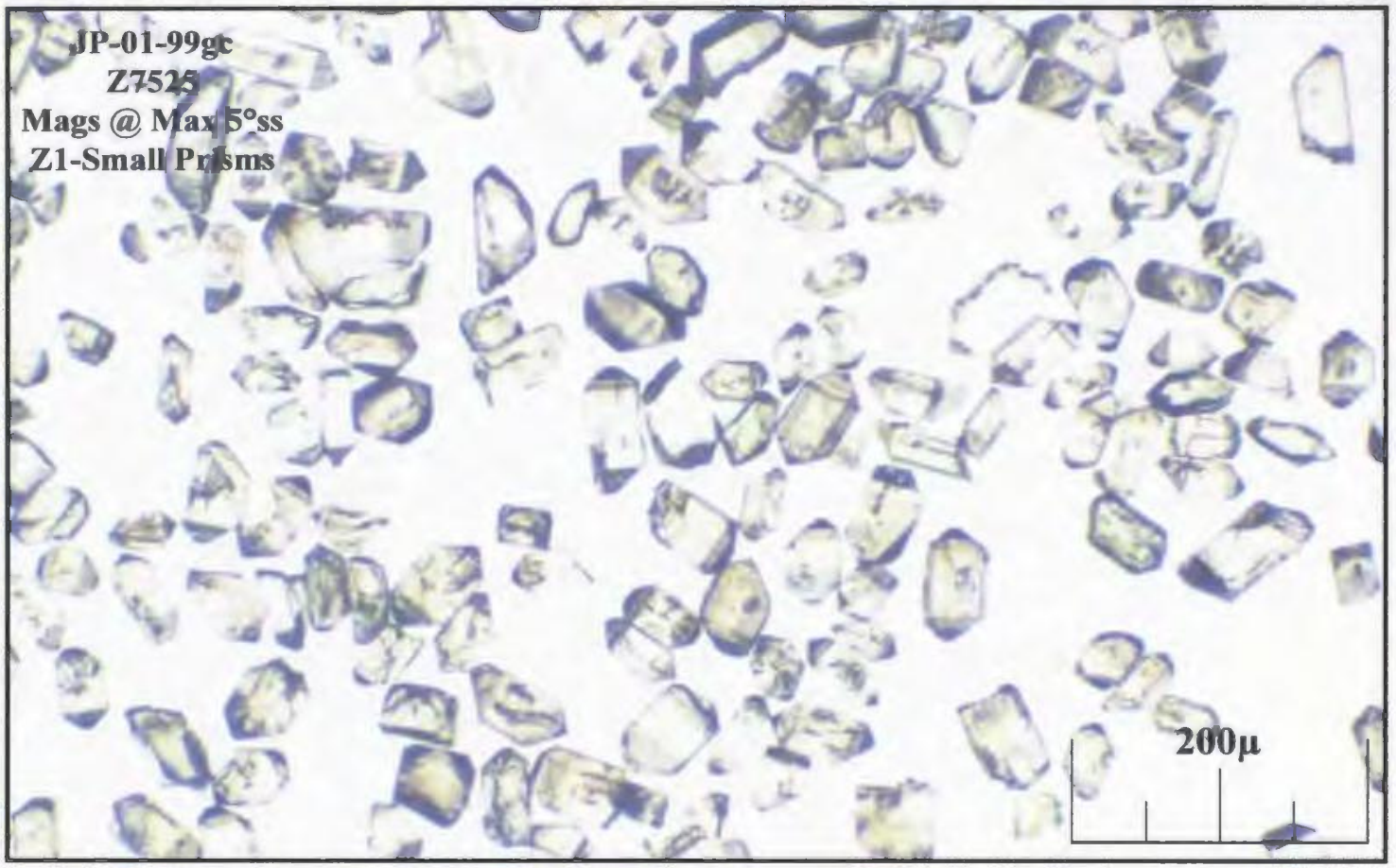

Plate 6.8 *Photomicrograph of Harpoon Gabbro fraction 1: unabraded zircon prisms.*

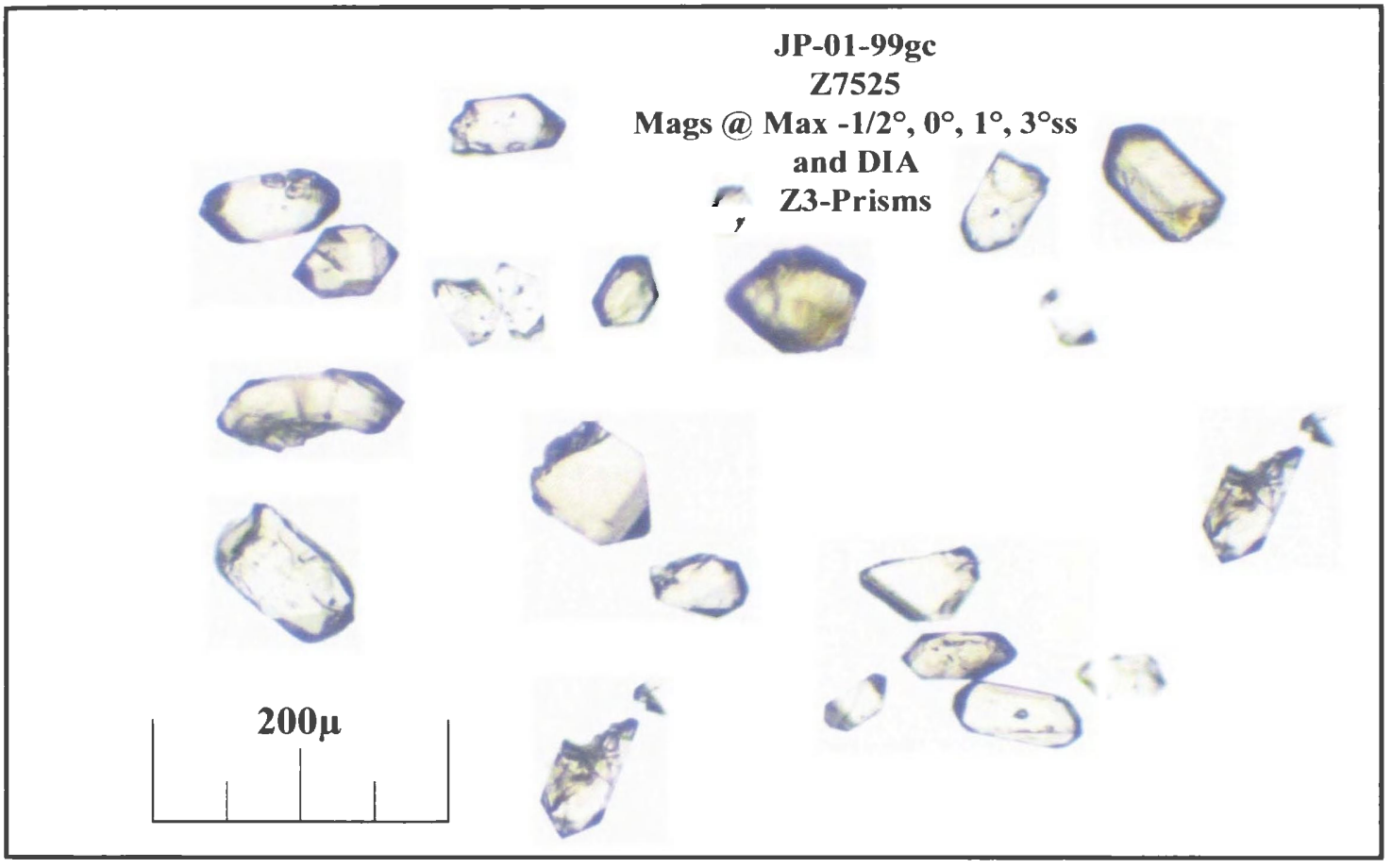

Plate 6.9 *Photomicrograph of Harpoon Gabbro fraction 2: unabraded zircon diamagnetic stubby prisms.*

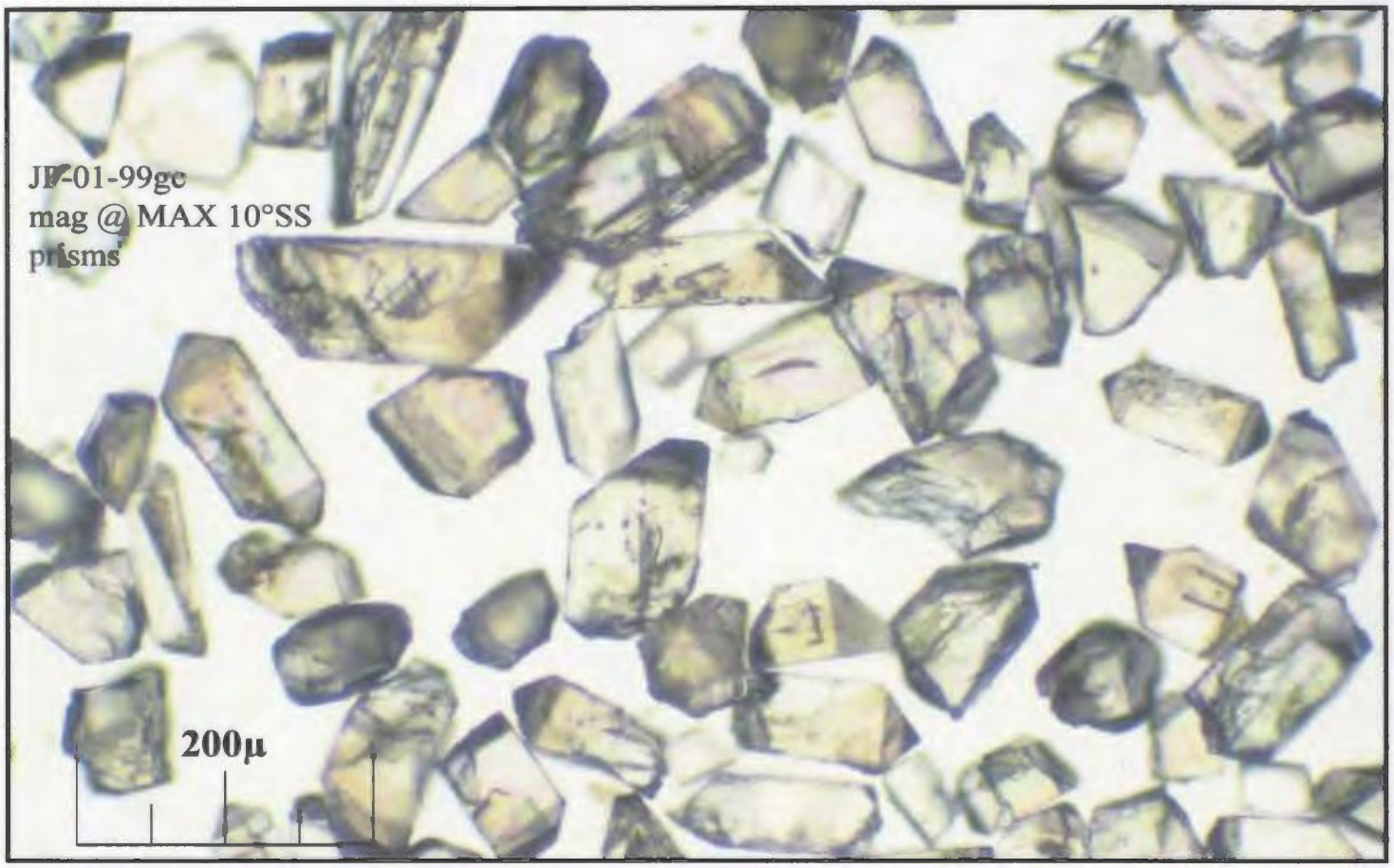

Plate 6.10 *Photomicrograph of Harpoon Gabbro fractions 3 and 4: unabraded zircon stubby prisms.*

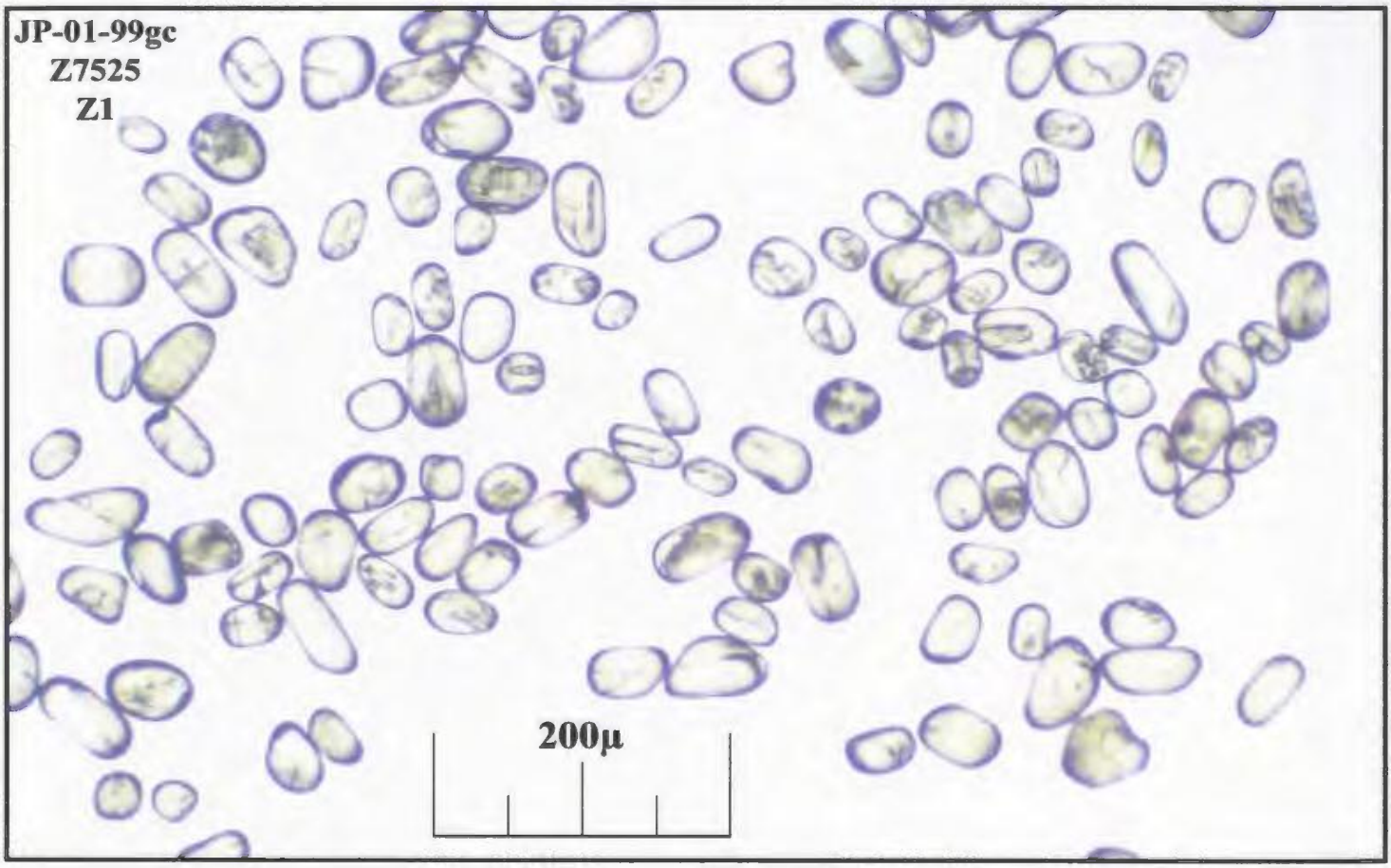

Plate 6.11 *Photomicrograph of Harpoon Gabbro fraction 1: abraded zircon prisms.*

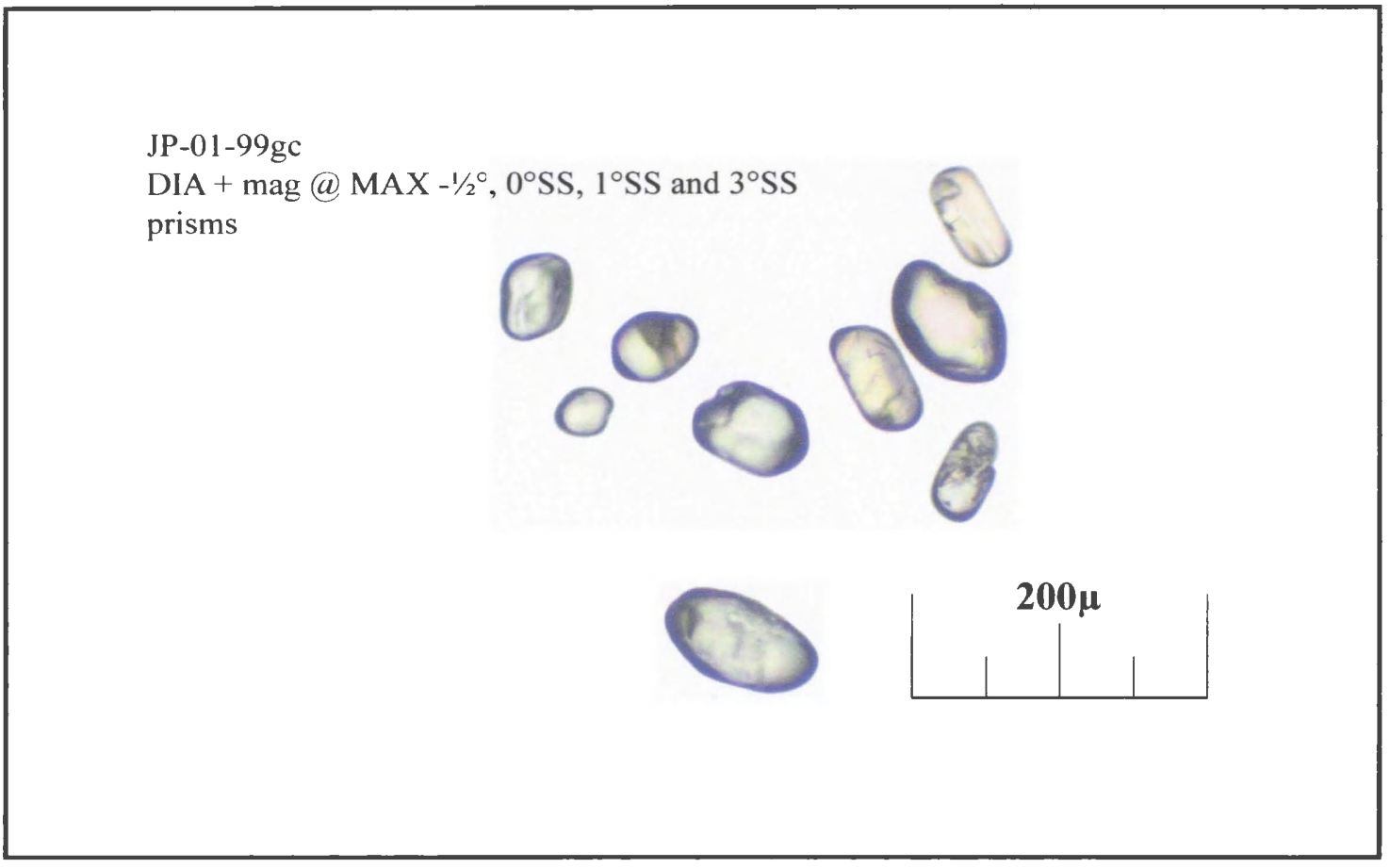

Plate 6.12 *Photomicrograph of Harpoon Gabbro fraction 2: abraded diamagnetic zircon prisms.*

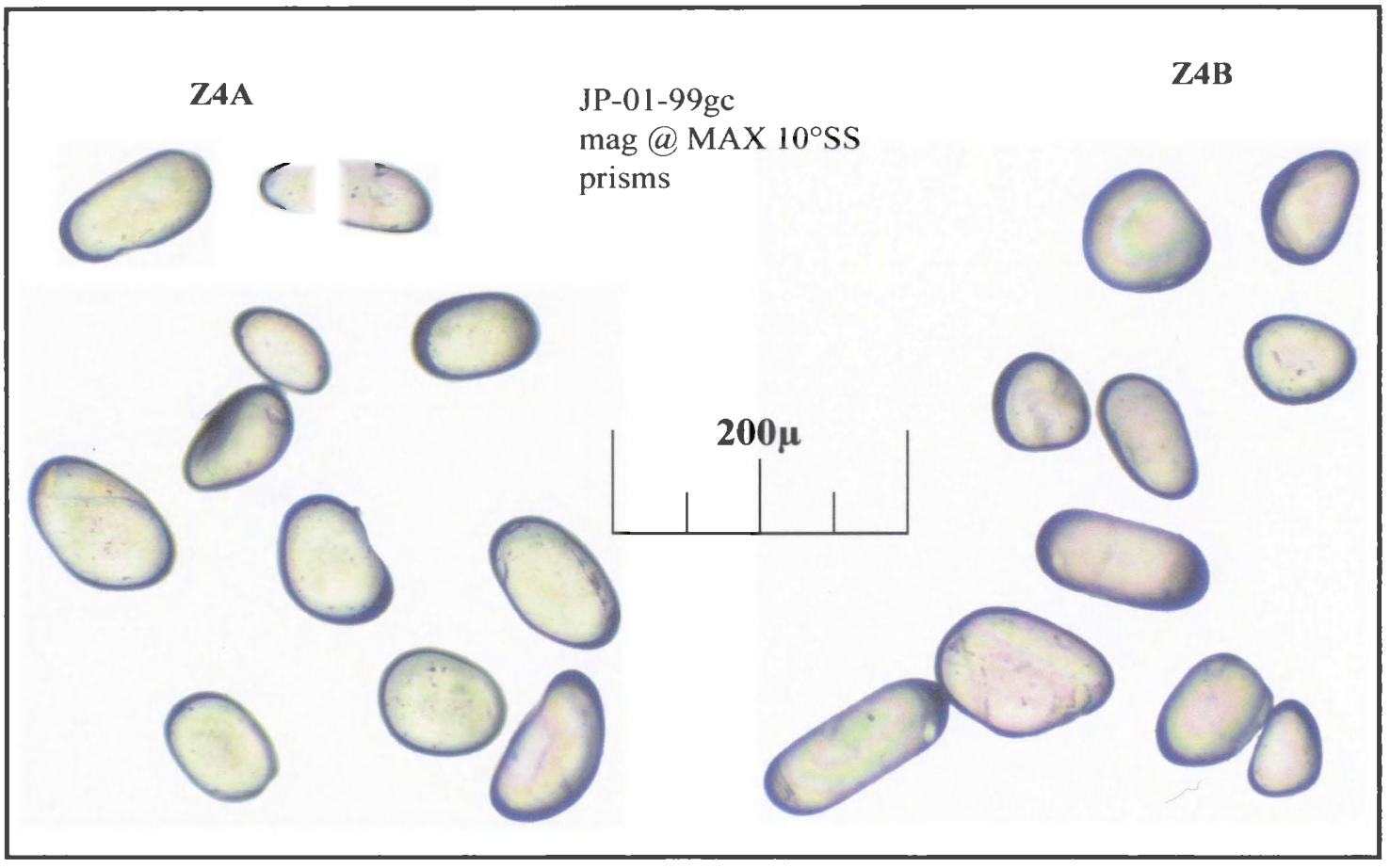

Plate 6.13 *Photomicrograph of Harpoon Gabbro fractions 3 and 4: abraded zircon stubby prisms.*

Plate 6.14 *Polymictic Rogerson Lake Conglomerate selected for detrital zircon analysis.*

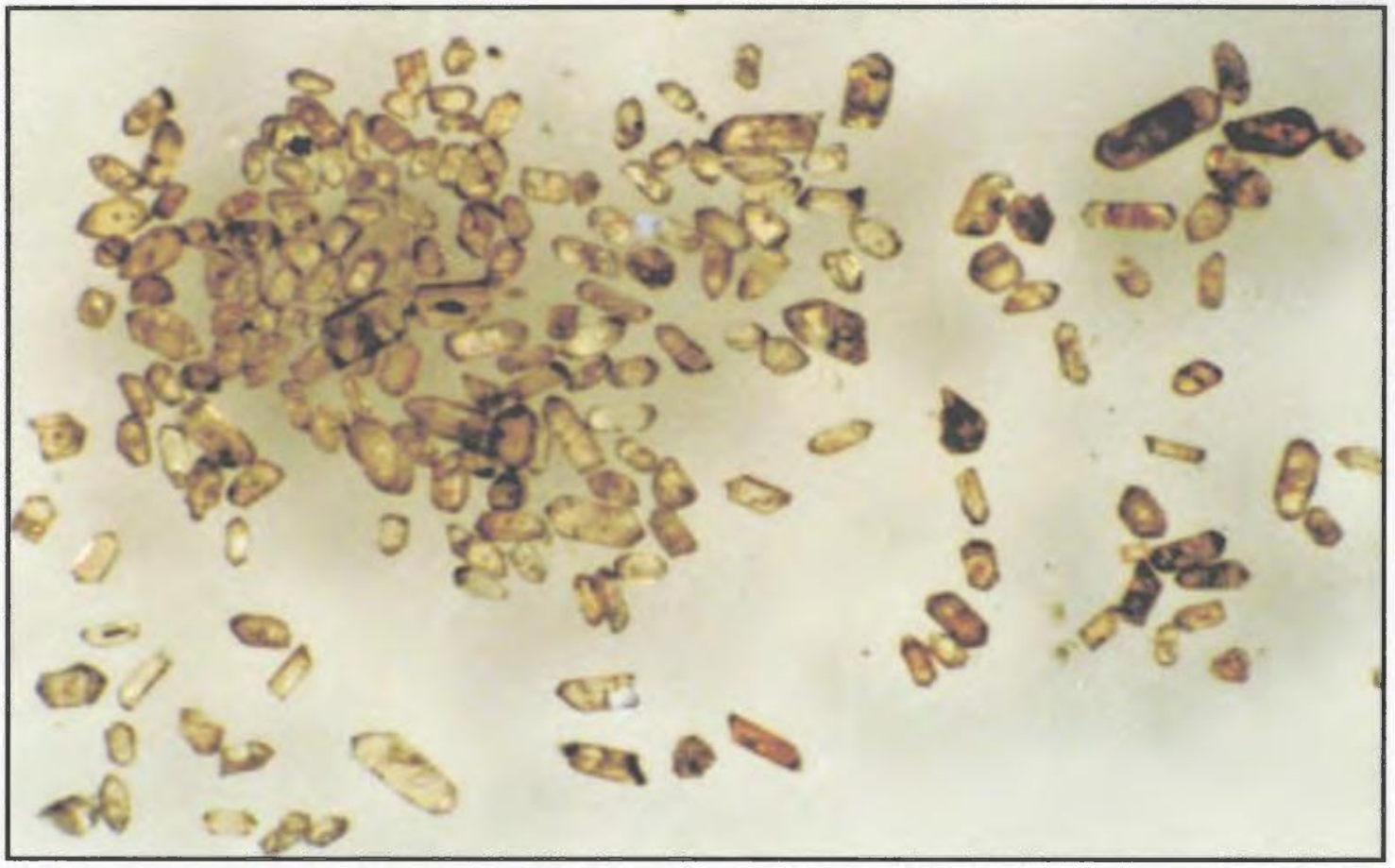

Plate 6.15 *Photomicrograph of single detrital zircon population from sample 71.*

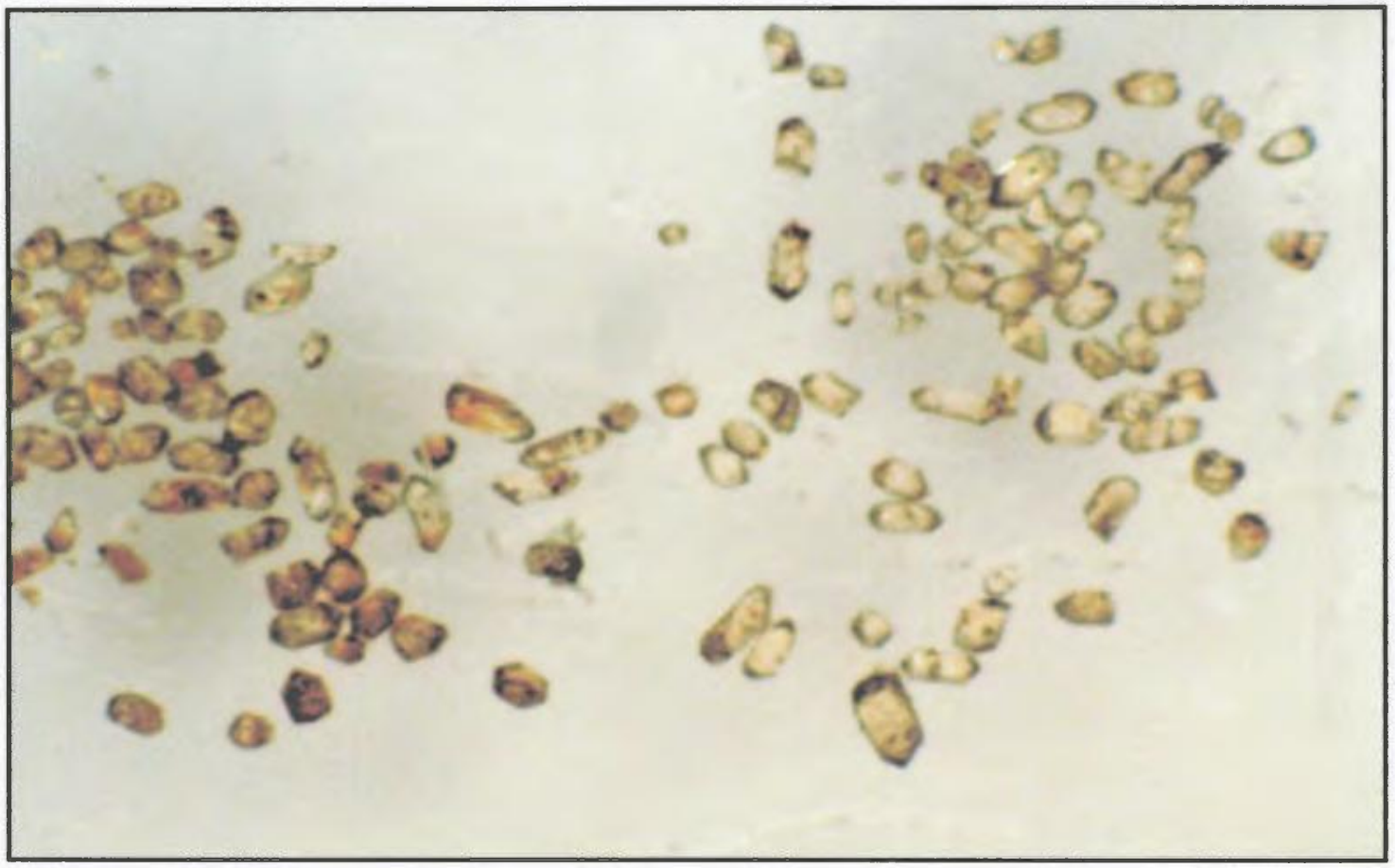

Plate 6.16 *Photomicrograph of detrital zircons from sample 72, Burgeo Road. Note the two separate zircon populations based on colour.*

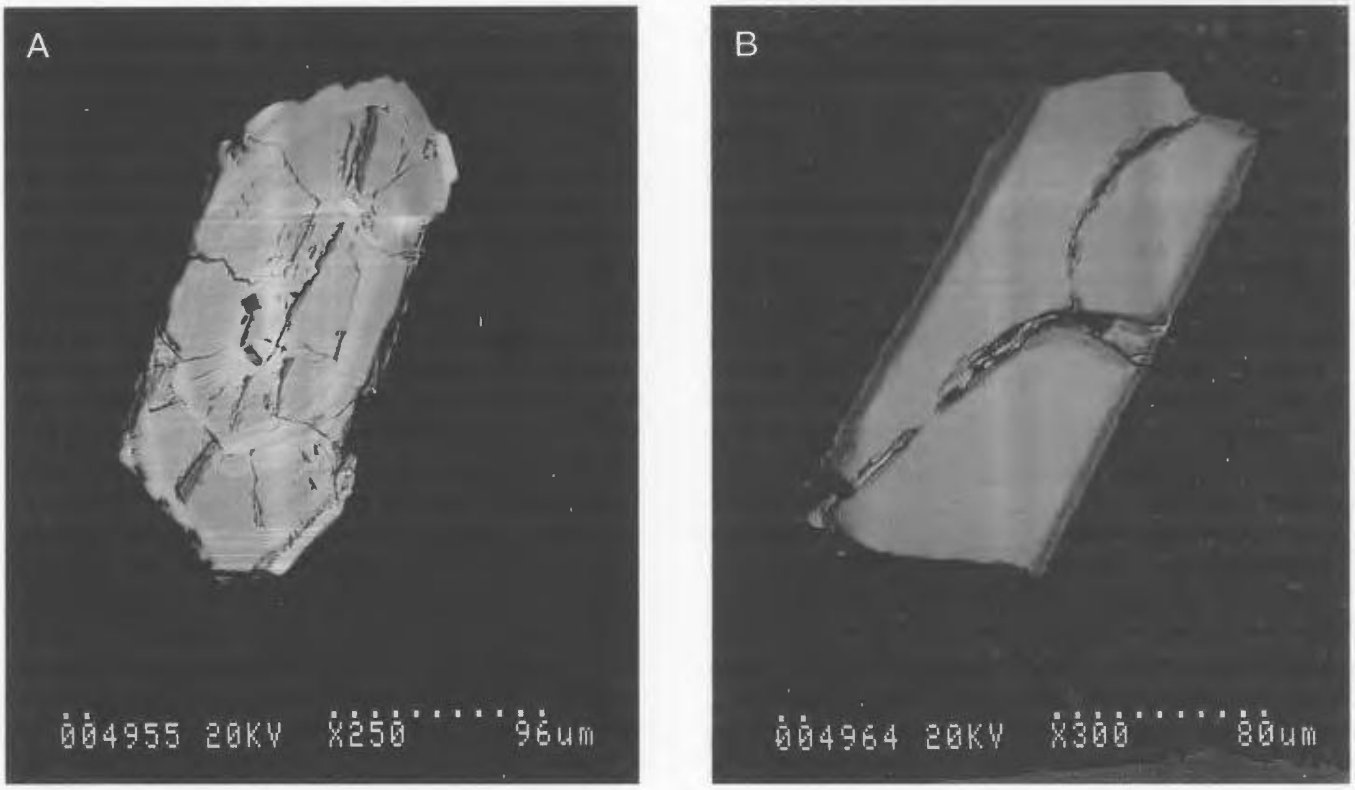

Plate 6.17 *Scanning electron micrograph of detrital zircons of the Rogerson Lake Conglomerate showing: a) complex rim and core zoning; and b) internal cracks and fissures.*

CHAPTER 7

SULPHUR ISOTOPE GEOCHEMISTRY

7.1 Preamble

Sulphur isotope data are an integral tool in refining geological models for the formation of volcanogenic massive sulphide deposits. Of all the light stable isotope systems (O, C, H, and S) commonly used in the study of VMS deposits, the greatest amount of data, undoubtedly exists for sulphur (Campbell and Larson, 1998; Huston, 1999). Sulphur isotope geochemistry has many uses in ore deposit research including: 1) determination of the origin of sulphur; 2) calculation of the paleotemperature of formation of fluids and sulphides; 3) the resulting degree of equilibrium obtained; and 4) constraints on the mechanism of ore deposition (Campbell and Larson, 1998; Faure, 1986). The major goal of S-isotope analysis in this study is to delineate the source of sulphur within the Tally Pond Group volcanogenic sulphide occurrences, specifically, whether the sulphur is of primary magmatic origin, or has been derived from an external source (i.e. seawater sulphate or biogenic sources).

7.2 Sulphur Isotope Systematics

Sulphur is widely distributed in the Earth's lithosphere, biosphere, hydrosphere, and atmosphere. Sulphur has four naturally occurring isotopes including ^{32}S (95.02 %), ^{33}S (0.75 %), ^{34}S (4.21 %) and ^{36}S (0.0017 %) (Hoefs, 1980, 1987; Rollinson, 1993). The ratio between the two most abundant isotopes, $^{34}S/^{32}S$, is used in S-isotope studies and is expressed in parts per thousand (per mil) relative to the reference troilite (FeS) standard from the iron meteorite Canon Diablo whose $^{34}S/^{32}S$ ratio is 0.0450045. The isotopic composition is expressed in terms of $\delta^{34}S$, which is defined as:

$$\delta^{34}S = [(^{34}S/^{32}S_{sample}/^{34}S/^{32}S_{CDT})-1]*1000$$

where $^{34}S/^{32}S_{sample}$ and $^{34}S/^{32}S_{CDT}$ are the $^{34}S/^{32}S$ ratios from the sample and Canon Diablo Troilite, respectively. The Canon Diablo Troilite is used as the standard because it is believed to represent the composition of the bulk undifferentiated Earth (Ohmoto and Rye, 1979). Therefore, the $\delta^{34}S$ value of a given sample of terrestrial sulphur can be considered as a measure of the change that has occurred in its isotopic composition since derivation from its primary source reservoir.

$\delta^{34}S$ values are subdivided into two major groups: 1) those with $\delta^{34}S > 0$ contain higher amounts of the ^{34}S isotope and are considered to be isotopically heavy; and 2) those with $\delta^{34}S < 0$, containing lesser ^{34}S and relatively more ^{32}S and are considered isotopically light (Ohmoto, 1972; Rye and Ohmoto, 1974; Hoefs, 1980). The subdivsions between the isotopically light and heavy groups are controlled by the naturally occurring relative fractionation of ^{34}S and ^{32}S. This fractionation in stable isotopes is related to mass and is caused by two main processes:1) kinetic isotope fractionation, such as reduction of sulphate ions to hydrogen sulphide by anaerobic bacteria which results in the

enrichment of ^{32}S in the sulphide (Taylor, 1974; Ohmoto and Rye, 1979); and 2) various equilibrium fractionation and isotopic exchange reactions between sulphur-bearing ions, molecules, and solids through which ^{34}S is generally concentrated in the compounds that have the highest oxidation state of S or the greatest bond strength (Faure, 1986).

Naturally occurring sulphur occurs as oxidized sulphate in the oceans and in evaporite rocks (Figure 7.1) and as native sulphur in the cap rocks of salt domes and in the rocks of various volcanic regions. Sulphur also occurs in the reduced form as sulphide in metallic mineral deposits (Figure 7.2) associated with igneous, metamorphic, and sedimentary rocks and in the gaseous state as H_2S and SO_2 (Kyser, 1986; 1990). There are three isotopically distinct reservoirs of sulphur: 1) mantle-derived sulphur with $\delta^{34}S$ values in the range 0 ± 3 ‰ (Chaussidon and Lorand, 1990); 2) seawater sulphur with $\delta^{34}S$ today of about +20 ‰, although this value has varied in the past from a low of +10.5 ‰ in the Permian to a high of +31.0 ‰ at the base of the Cambrian (Claypool *et al.*, 1980); and 3) strongly reduced (sedimentary) sulphur with large negative $\delta^{34}S$ values (Rollinson ,1993).

Although the distinction between reservoirs is useful in determining the source reservoir of the sulphur, it is clear that $\delta^{34}S$ values do not indicate a single or unique source of the sulphur due to the extensive possible overlap of $\delta^{34}S$ values. However, primary sulphides in mantle derived rocks can be assumed to inherit the $\delta^{34}S$ characteristics of their parental mantle melt and mantle source region, and usually lie in the range 0 ± 3 ‰ (Ohmoto and Rye, 1979). Any values in mantle derived rocks that fall outside this range are probably due to the inheritance of a partial S-isotopic signature from an external source, or result from S-isotope heterogeneities in the mantle source

reservoir (Kyser, 1986, 1990; Chaussidon *et al.*, 1987; 1989). It must be realized, however, that due to changes in pH, the fugacity of oxygen (Faure *et al.*, 1984), and mantle metasomatism due to crustal fluids and sediments, variations in the $\delta^{34}S$ ratios of mantle derived sulphides can exist.

7.3 Results

A total of 39 sulphide separates from the Tally Pond Group were analyzed on a Finnigan MAT 252 IR-MS at Memorial University of Newfoundland for their sulphur isotope compositions including 31 pyrite samples, six chalcopyrite/sphalerite samples, and one sample each of galena and sphalerite. The samples were collected mainly from drillcore and consist of 18 samples from the Upper block and Upper Duck sulphide lens of the Duck Pond deposit, 12 samples from the North, South and Southeast zones of the Boundary deposit, five samples from the South Moose Pond zone, two from the North Moose Pond zone and one sample each from East Pond and the Lemarchant prospect. These samples were derived from a variety of rock types including massive sulphide, mafic and felsic volcanic rocks, alteration pipes and zones, and sedimentary rocks. The results are presented in Figure 7.3 and Table G.1.

Five samples of pyrite were collected from variably altered mafic volcanic and intrusive rocks at the South Moose Pond zone and Duck Pond deposit that have $\delta^{34}S$ values between -3.8 ‰ and +8.5 ‰, with an average of +2.8 ‰. Three altered mafic volcanic rocks from the South Moose Pond zone have $\delta^{34}S$ values of -0.2 ‰, +5.7 ‰, and +8.5 ‰, whereas a sample of a mafic volcanic flow from the Upper block of the Duck Pond deposit has a $\delta^{34}S$ value of -3.9 ‰. The $\delta^{34}S$ value obtained from pyrite in a

mafic intrusion in the Upper block is slightly heavier than the corresponding ratios in the volcanic rocks and has a $\delta^{34}S$ value of +3.7 ‰.

Sulphur isotope ratios from the Mineralized block of the Duck Pond deposit range from +5.8 ‰ to +13.7 ‰, with an average value of +7.3 ‰. Six samples of pyrite and chalcopyrite from the massive sulphide lenses (Plate 7.1) have $\delta^{34}S$ values that have a mean value of + 8.7 ‰ and vary from +6.3 ‰ to 11.2 ‰. Seven samples of variably altered rhyolite and the intense chlorite altered feeder zones contain pyrite that have $\delta^{34}S$ values in the range of +5.8 ‰ to +13.7 ‰, with an average value of +8.7 ‰. One sample of a sulphide debris flow (Plate 7.2) located near the Upper Duck lens contains pyrite with a $\delta^{34}S$ value +7.0 ‰.

Two samples from East Pond and the Lemarchant prospect have similar $\delta^{34}S$ values as those from the Mineralized block of the Duck Pond deposit. A single sphalerite sample from a felsic breccia at East Pond has a $\delta^{34}S$ value of +6.7 ‰, while galena from an altered felsic volcanic rock in the Lemarchant prospect returned a $\delta^{34}S$ value of +6.6 ‰. A similar, although slightly higher $\delta^{34}S$ value of +8.2 ‰ was obtained for pyrite in a felsic dyke from the South Moose Pond zone.

The 12 samples from the Boundary deposit were collected from host felsic volcanic rocks, the massive sulphide lenses and from alteration zones surrounding the deposit. Six samples were taken from the North zone and three samples each from the South zone and Southeast zone and contain sulphur with $\delta^{34}S$ values that are slightly higher than those from the Duck Pond deposit with $\delta^{34}S$ values ranging from a low of +6.5 ‰ to a high of +13.0 ‰, with a mean of +10.6 ‰. Five samples of massive sulphide were analyzed from the Boundary deposit and include two pyrite/chalcopyrite/sphalerite

samples from the North zone, two pyrite samples from the South zone, and one pyrite sample from the Southeast zone. Collectively these five samples have homogenous $\delta^{34}S$ values in the range of +10.0 ‰ to +11.8 ‰. Three samples of pyrite from the intensely altered chlorite feeder zones contain $\delta^{34}S$ values that are somewhat isotopically heavier than those of the massive sulphide lenses. Two pyrite samples from the North zone returned $\delta^{34}S$ values of +11.3 ‰ and +12.4 ‰, whereas a single sample from the South zone has a $\delta^{34}S$ value of +13.0 ‰.

Three pyrite samples hosted by mineralized felsic lapilli tuff (Plate 7.3) from the Boundary deposit are slightly isotopically lighter than those from the massive sulphide lenses and alteration feeder zones. Two pyrite/chalcopyrite/sphalerite samples from the North zone have $\delta^{34}S$ values of +8.8 ‰ and +10.7 ‰, and a single pyrite sample from the Southeast zone contains a $\delta^{34}S$ value of +10.0 ‰. The remaining sample from the Boundary deposit is a laminated pyrite and sediment sample (Plate 7.4) from the Southeast zone and is isotopically the lightest sample that was analyzed from the Boundary deposit with a $\delta^{34}S$ value of +6.5 ‰.

The lightest $\delta^{34}S$ values from the samples analyzed from the Tally Pond Group consist of four samples, two from the Duck Pond deposit and two from the North Moose Pond zone. Two pyrite samples were collected from graphitic sedimentary shales (Plate 7.5) in the Upper block of the Duck Pond deposit and have $\delta^{34}S$ values of -13.7 ‰ and -17.4 ‰. The two $\delta^{34}S$ values of -8.7 ‰ and -7.1 ‰ were obtained from pyrite samples in the North Moose Pond zone and were collected from a graphitic argillite and felsic agglomerate rhyolite, respectively.

7.4 Discussion

Sulphur isotope data for the Tally Pond Group in the area surrounding the Duck Pond and Boundary deposits are characterized by a wide range of $\delta^{34}S$ values, representing sulphur from a variety of potential sources.

The sulphur isotope ratio from one sample of a mafic volcanic rock of the South Moose zone fall within the range (-3 to +3 ‰) of igneous rocks with a mantle origin and two additional mafic intrusive and volcanic samples lie slightly outside the normal accepted magmatic sulphide a $\delta^{34}S$ range. These data suggest that the sulphides in this mafic volcanic rock may have been derived from reduced sulphur from a deep-seated magmatic source. The variations in $\delta^{34}S$ values from the typical mantle derived range however, suggest that other factor may be involved and a true mantle derived source cannot be verified. The degassing of mafic lavas can deplete the melt in the oxidized SO_2 species, which can cause lower $\delta^{34}S$ values due to the loss of ^{34}S with SO_2 gases (Kyser, 1989, 1990). On the other hand, increases in the $\delta^{34}S$ value can be caused by high oxygen fugacities in the melt which can cause oxidation of the sulphide species to SO_2 gas, which when trapped in the melt will increase $\delta^{34}S$ values due to preferential enrichment of ^{34}S in the gas (Ripley, 1983). In addition, conditions such as mantle S-isotope heterogeneity and potential mantle metasomatism due to crustal and meteoric fluids and other lithologies (e.g. sedimentary and other volcanic units) (Chaussidon *et al.*, 1987, 1989) can cause variations in the $\delta^{34}S$ values depending on the sulphur isotopic nature of the metasomatic material.

The $\delta^{34}S$ values from the felsic volcanic rocks, alteration zones and massive sulphide bodies from the Duck Pond, East Pond and Lemarchant prospect are marginally

heavier than $\delta^{34}S$ values for the mafic volcanic and intrusive rocks. The $\delta^{34}S$ values from the Duck Pond deposit (+5.70 ‰ - +13.72 ‰) lie well above the typical mantle derived realm and are too heavy to be derived from a purely magmatic source. The most probable source of fluids and sulphur in the Duck Pond deposit is reduced seawater sulphate as the $\delta^{34}S$ values show a shift towards the seawater sulphate value. The present day seawater sulphate $\delta^{34}S$ value is around +22 ‰. However, this value has changed through time and has varied from a low of +10 ‰ in the Triassic, to a high of over +30 ‰ during the Neoproterozoic (Figure 7.1). The minimum age of the Duck Pond and Boundary deposits has been constrained by the U-Pb age of 509 ± 2 Ma (Chapter 6) from a crystal tuff unit located stratigraphically above the Boundary deposit. The reported $\delta^{34}S$ range of seawater sulphate during the Middle Cambrian is between +26 ‰ and +32 ‰.

One mechanism for the partial to complete inorganic reduction of seawater sulphate is the precipitation of seawater sulphate as anhydrite at low temperatures of around 150°C due to retrograde anhydrite solubility and calcium increase due to fluid/rock reactions (Ohmoto *et al.*, 1983). These reactions occur in a high-temperature reaction zone (Figure 7.4) near the magma chamber where the heated, evolved-seawater fluid becomes reducing, acidic, MgO- and SO_4-depleted, metal-rich, and strongly enriched in H_2S due to a combination of hydrolysis of rock sulphides and sulphate reduction by reaction with ferrous minerals (e.g. olivine, pyroxene, magnetite) that are present in basalts (Ohmoto, 1986). This method removes most of the original sulphate in the fluid, but a small amount remains in solution at equilibrium with the precipitated anhydrite (Shanks *et al.*, 1981, 1988; Shanks, 2001). At temperatures of between 250° and 400°C, the fractionation of sulphur isotopes between aqueous sulphate and sulphide

is 18-25 ‰ lower than coeval seawater (Huston, 1999). Therefore the initial sulphide produced by reduction would have a $\delta^{34}S$ value of 18-25 ‰ lower than coeval seawater.

$\delta^{34}S$ values from the Boundary deposit fall within the same range as those of the Duck Pond deposit, East Pond and Lemarchant prospect. However, there is a slight variability between sulphide separates collected from the host rock, feeder zones and massive sulphide bodies. The samples from the altered feeder zones beneath the deposit are the isotopically heaviest, while the samples from the massive sulphide lenses are slightly lighter, and the $\delta^{34}S$ values from samples within the surrounding felsic volcanic host rocks are scarcely even lighter. The highest $\delta^{34}S$ values from the feeder zones are interpreted to be due to reduction of seawater sulphate in the circulating fluids around the deposit. This is the same mechanism responsible for the heavy $\delta^{34}S$ values in the Duck Pond deposit, East Pond and Lemarchant prospects. The isotopically lightest $\delta^{34}S$ values from the adjacent felsic volcanic host rocks is attributable to leaching of sulphur from the hydrothermal cell and/or the direct incorporation of magmatic sulphur. This would result in a decrease in the $\delta^{34}S$ values of the ore fluids produced by inorganic sulphate reduction by approximately 0 - 5 ‰.

The intermediate $\delta^{34}S$ values from the massive sulphide lenses possibly result from the mixing of inorganic seawater sulphate coupled with more intense leaching of volcanic rock sulphur due to the increased residence time of the fluid in the hydrothermal cell. Alternatively, the intermediate $\delta^{34}S$ values might be due to a decrease in temperature from the feeder zone upward towards the top of the massive sulphide lens or to the oxidation of aqueous H_2S during mixing with seawater at the top of the massive sulphide lens. Both of these hypotheses are constrained by the slow kinetics of redox reactions

between oxidized and reduced sulphur species (Ohmoto and Lasga, 1982), which moderate sulphate reduction in peripheral low temperature zones.

The lightest $\delta^{34}S$ values from the Tally Pond Group are from three samples of graphitic argillite from the Duck Pond and Boundary deposits and the North Moose Pond zone, and one sample of felsic agglomerate from North Moose Pond. The values for these occurrences are highly negative (-7.1 ‰ to -17.4 ‰) and lie well below the normal mantle derived or inorganic sulphate reduction regions. Thermochemical reduction of this sulphate requires a large fractionation of around 40 ‰ which is much higher than the generally accepted value of 18 ‰ to 24 ‰ (Ohmoto and Rye, 1979; Ohmoto, *et al.*, 1983, 1986). Therefore, these extremely low $\delta^{34}S$ values could only result from biogenetic fractionation, which is consequently the most important cause for variations in the isotopic composition of sulphur in nature. Anaerobic bacteria such as *Descufovibrio desulfuricans* (Ohmoto, 1986) live in sediment deposited in the oceans at low (i.e. below 50°C) temperatures. These bacteria use oxygen from sulphate ions, instead of O_2, to metabolize organic compounds and excrete H_2S which is enriched in ^{32}S relative to the sulphate (Ohmoto, 1983, 1986; Canfield, 2001). In most sediments, H_2S (or HS^-, depending on pH) reacts with iron to form pyrite early in the diagenetic process when the sediments are within one metre of the seawater-surface interface (Berner, 1980).

This H_2S+Fe reaction is strongly dependent on whether the system is open or closed. In an open system such as a large body of seawater there is an infinite reservoir of seawater sulphate where the rate of sulphate supply is greater than the rate of sulphate reduction. Sulphate reducing bacteria operating in these waters will produce H_2S that is extremely depleted in ^{34}S while the $\delta^{34}S$ in seawater will remain effectively unchanged

(Rollinson, 1993; Huston, 1999). Fractionations as large as 48 ‰ have been reported for modern intertidal sediments in open systems (Chambers, 1982).

The two sulphur samples from a debris flow flanking the Duck Pond deposit and from laminated sulphide/sedimentary sequences in the Boundary deposit have positive $\delta^{34}S$ values of +7.0 ‰ and +6.5 ‰, respectively. These samples were initially interpreted in the field to be sedimentary sulphides, however, the heavy $\delta^{34}S$ values indicate that these samples could not have formed as a result of biogenic fractionation. The sulphides have $\delta^{34}S$ values similar to those from the massive sulphide bodies of the Duck Pond and Boundary deposits. These sulphide samples are now interpreted to have originally formed as part of the massive sulphide lens, where they were subsequently eroded, deposited and lithified in the adjoining sedimentary sequence.

The recognition of diverse $\delta^{34}S$ values from different sulphide samples throughout the Tally Pond Group is a vital tool in the interpretation of the genesis of the volcanogenic massive sulphide deposits. The analyses of S-isotope ratios in the sulphides indicate that seawater modified, magmatic S-sources dominate throughout the Tally Pond Group. These same data not only suggest a possible source of sulphur that formed the sulphide but can also discriminate between sulphides formed in purely sedimentary environments from those which originally formed as part of a massive sulphide lens and were subsequently brecciated and deposited in sediment.

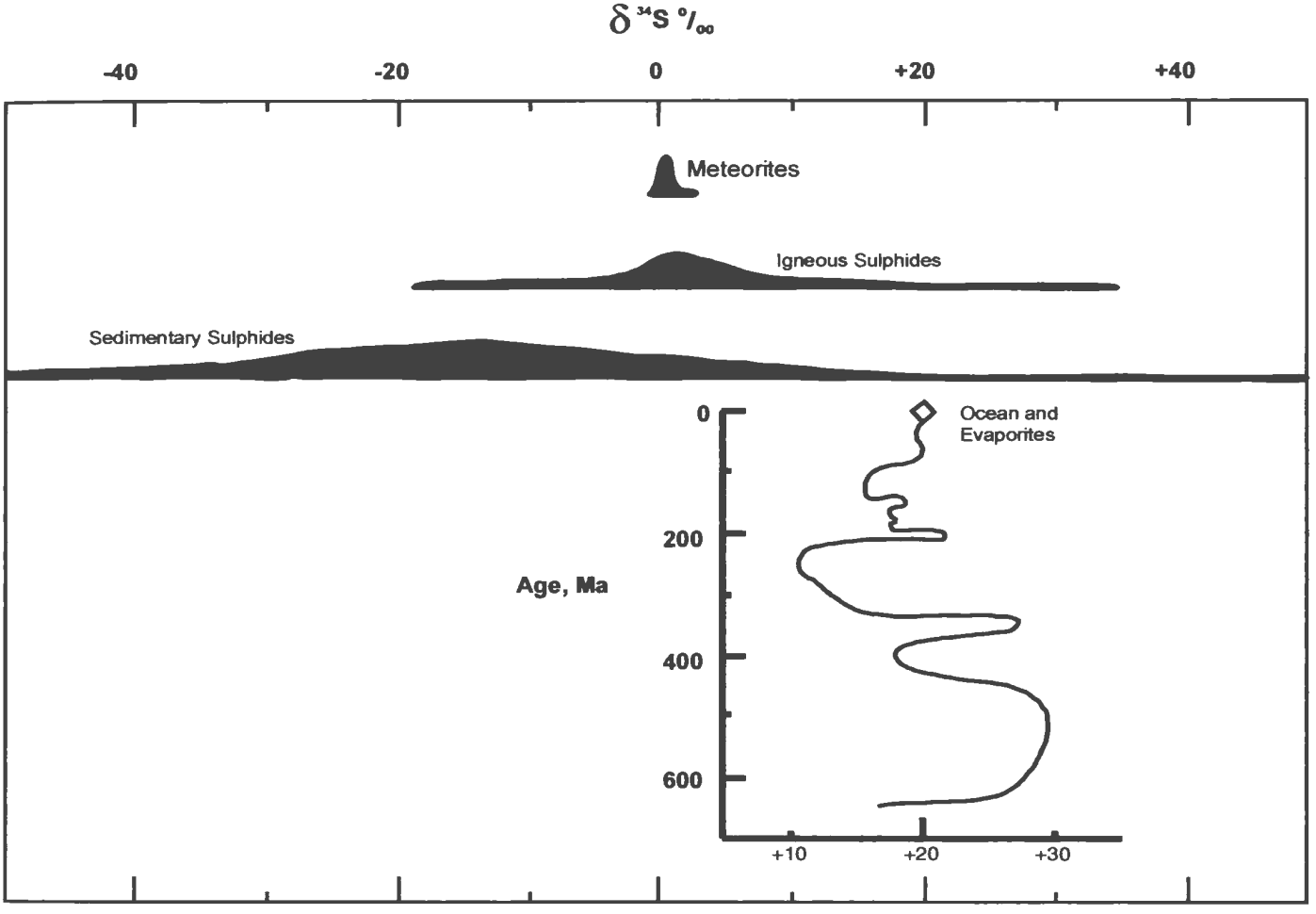

Figure 7.1 *The distribution of Sulphur isotope values for common large earth reservoirs.*

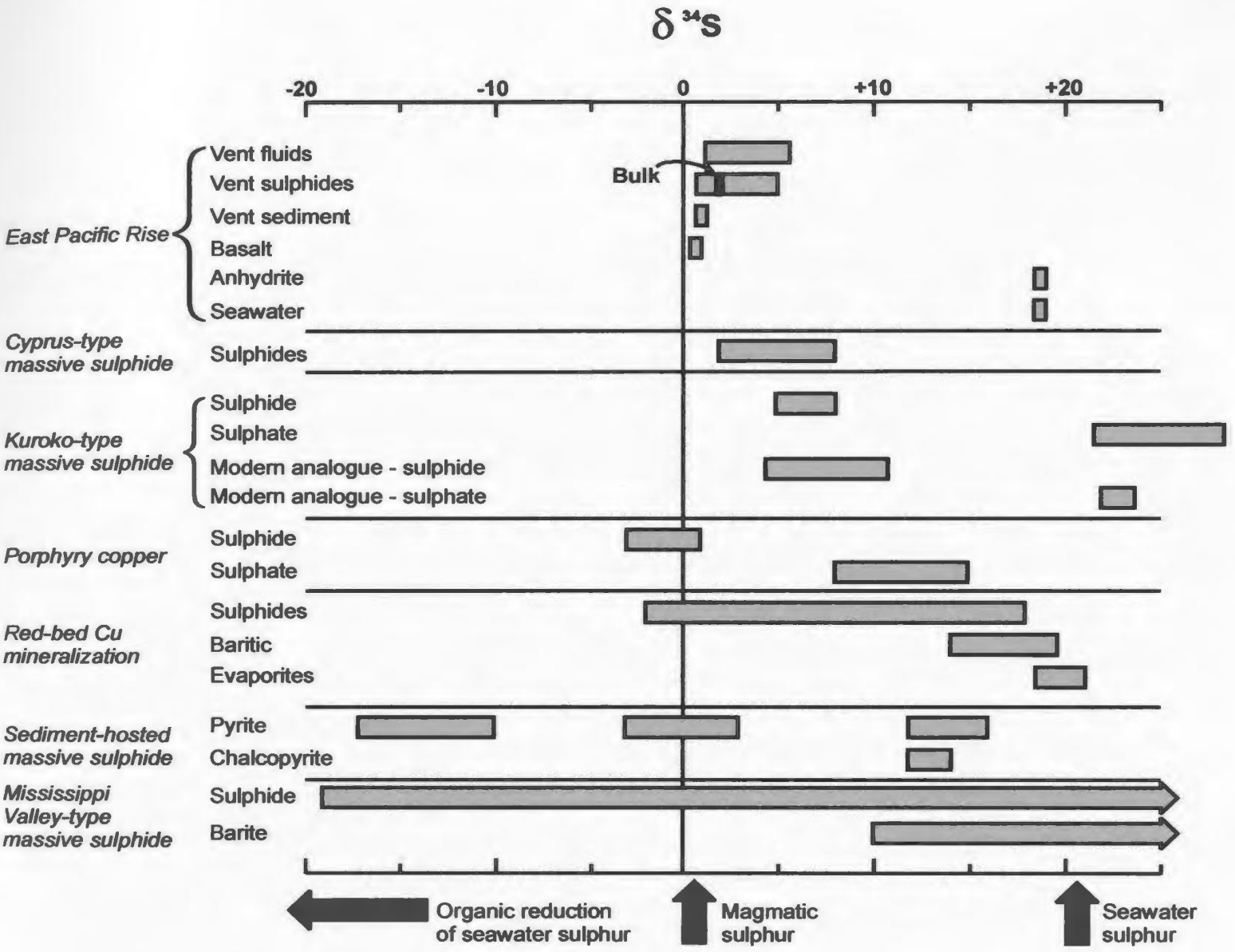

Figure 7.2 *Sulphur isotope values for various natural occurring sulphur minerals.*

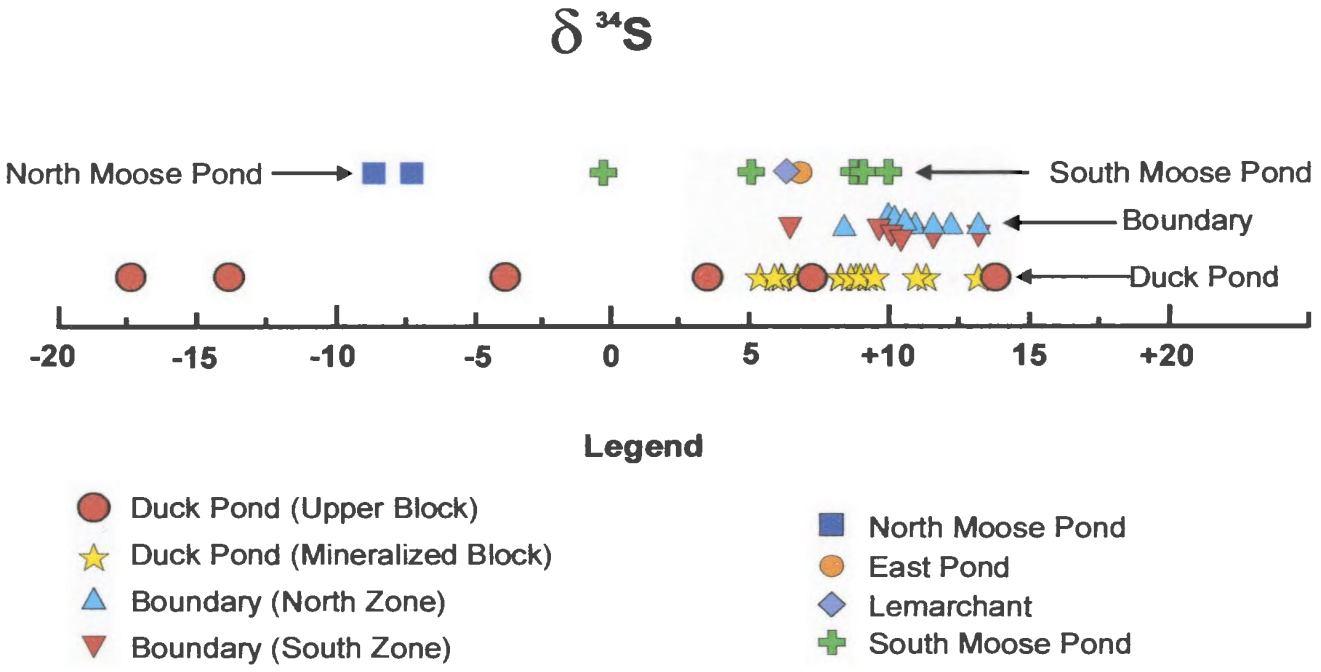

Figure 7.3 *Sulphur isotope compositions of sulphide separates from the Tally Pond Group.*

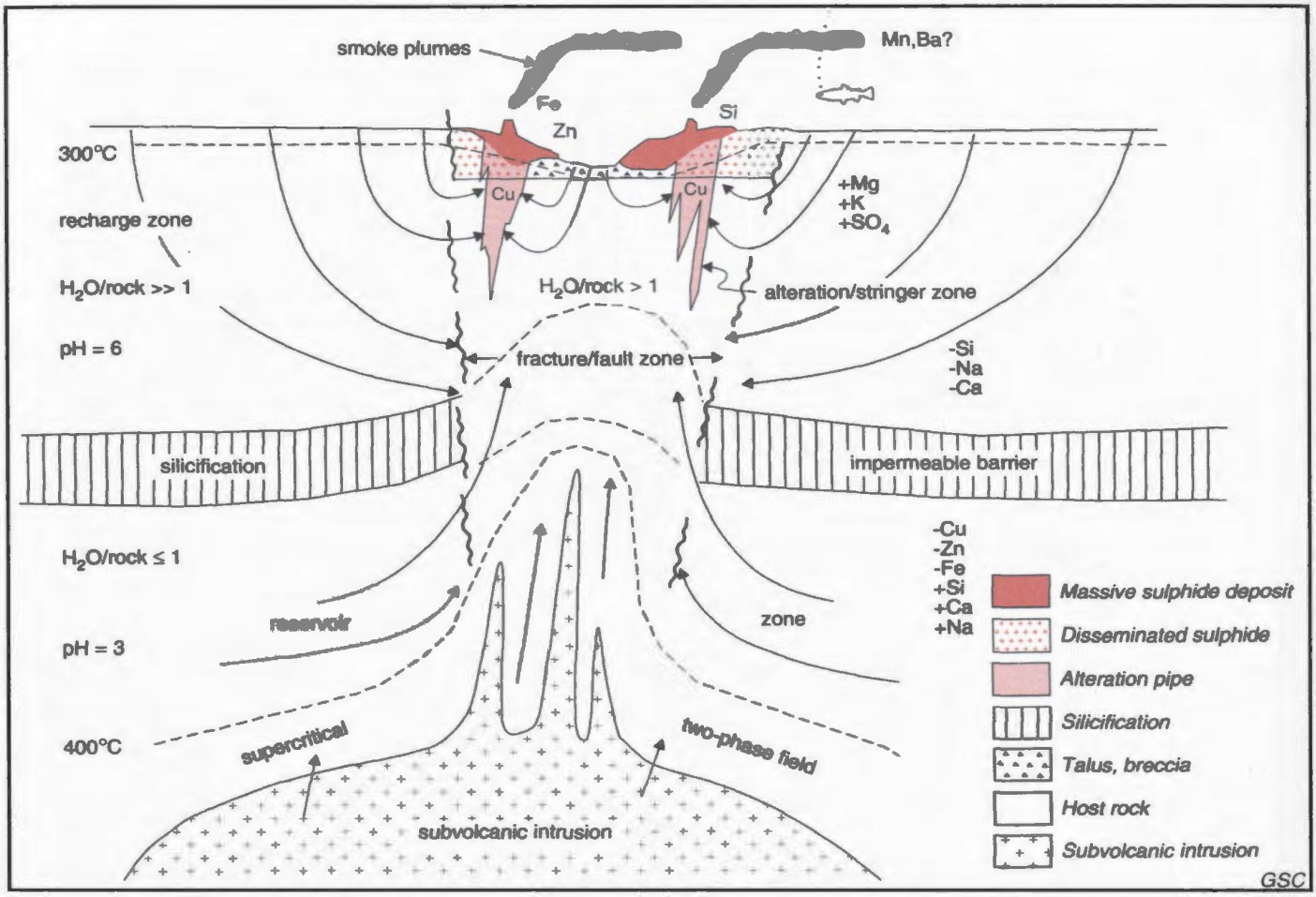

Figure 7.4 *Model of VMS-producing hydrothermal system, perpendicular to the fracture system which controls hydrothermal discharge. Modified from Franklin (1995).*

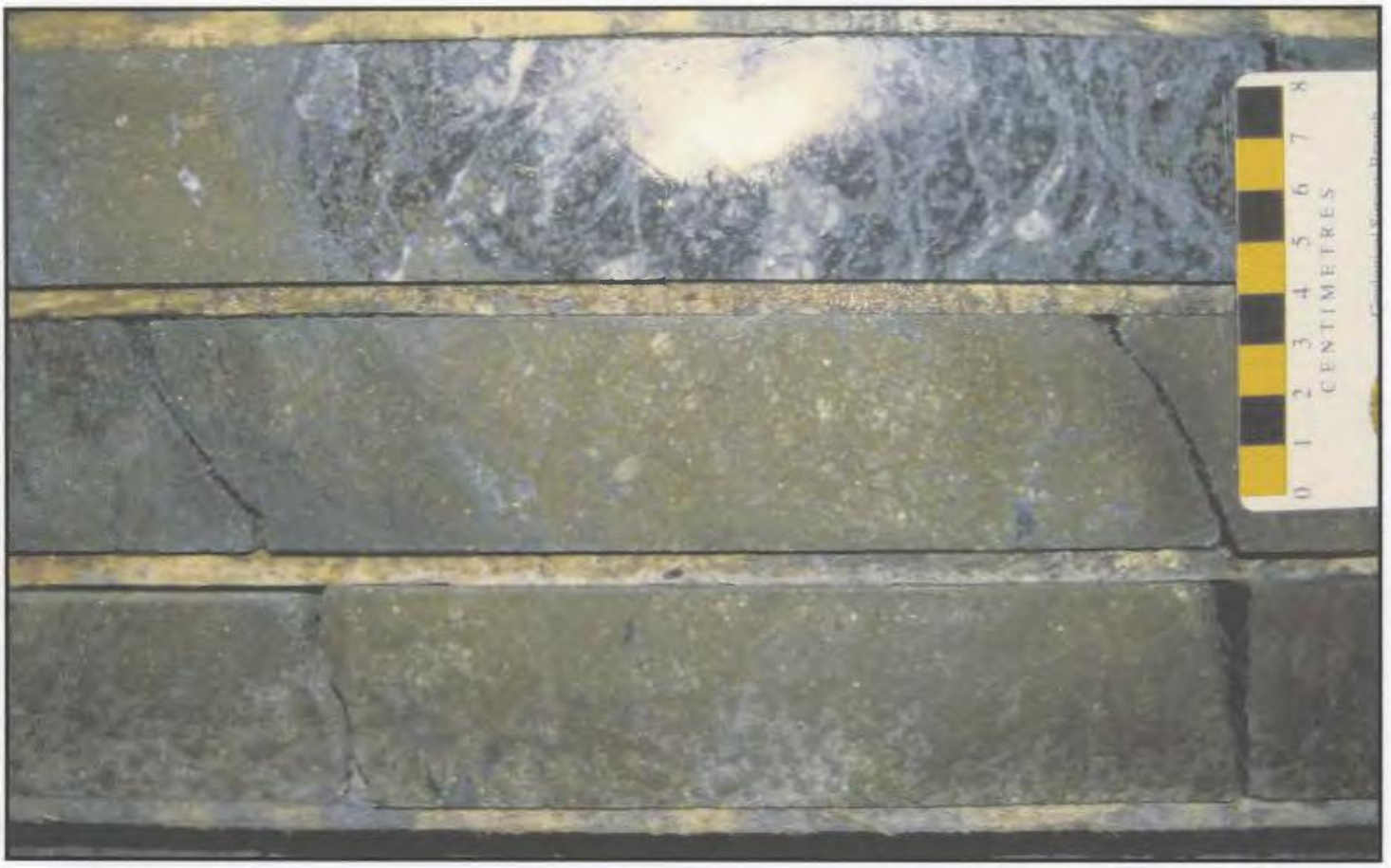

Plate 7.1 *Massive pyrite from the Upper Duck lens, Duck Pond deposit.*

Plate 7.2 *Sedimentary debris flow containing dominantly felsic volcanic fragments with lesser fragments of massive sulphide.*

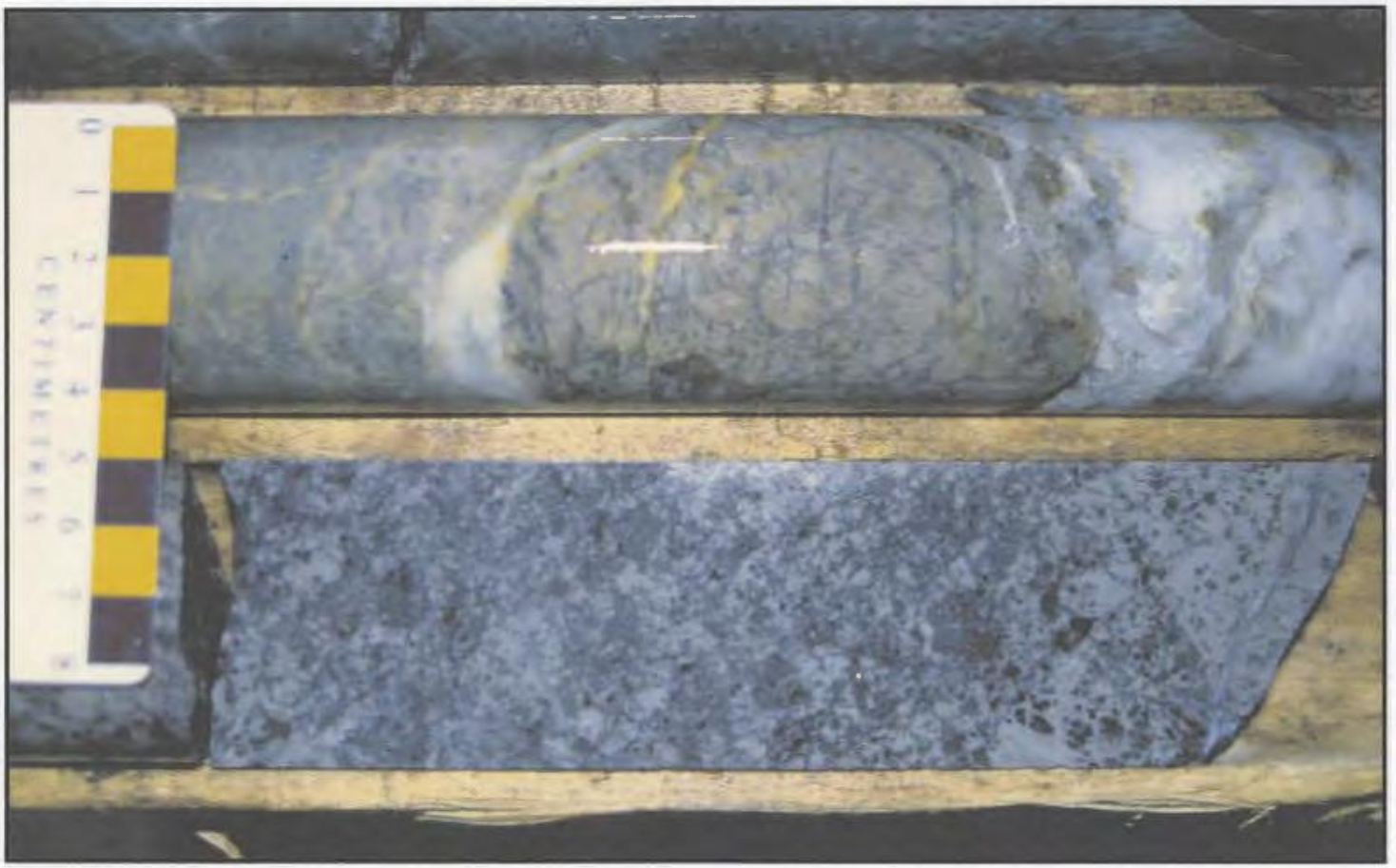

Plate 7.3 *Felsic lapilli tuff from the hangingwall of the Boundary deposit.*

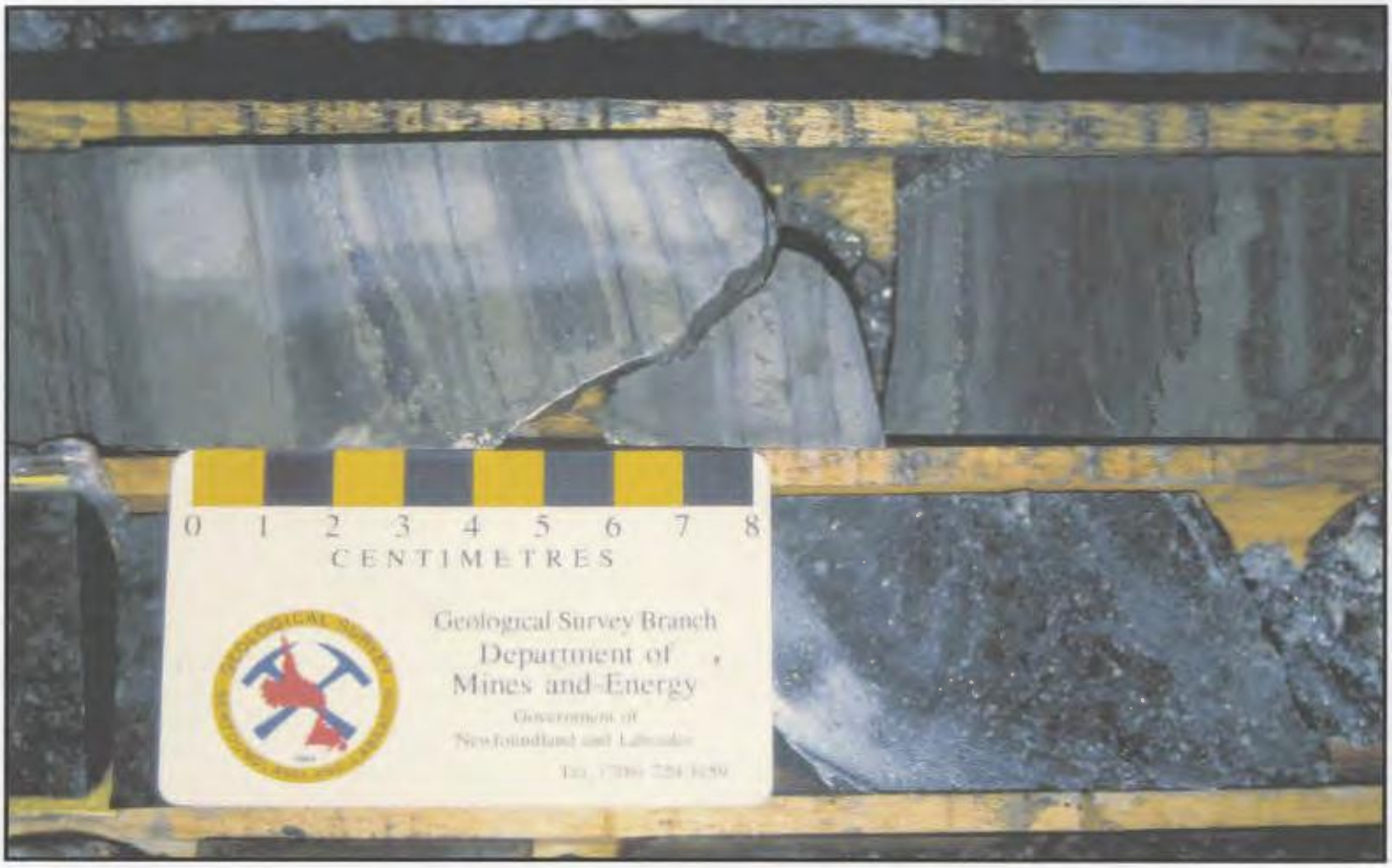

Plate 7.4 *Laminated pyrite and sediment from the Southeast Zone of the Boundary deposit.*

Plate 7.5 *Graphitic sedimentary shales (top) from the Upper block of the Duck Pond deposit. Note the felsic rhyolite breccia (middle) and altered felsic volcanic rocks (bottom) adjacent to the shales.*

CHAPTER 8

SUMMARY AND CONCLUSIONS

8.1 Preamble

This thesis presents the results of an integrated geological, geochemical, geochronological and radiogenic and stable isotopic study of the Cambro-Ordovician rocks and mineral deposits in the Tally Pond Group. Detailed mapping (1:50 000) in the Tally Pond area, combined with major and trace element geochemical, and Pb and S isotope analyses of rocks, and U-Pb geochronology have proven to be powerful tools for defining volcanic stratigraphy, linking volcanic and plutonic events, determining crustal source reservoirs for magmas, and providing absolute time constraints on magmatism and mineralization. The end result is presentation of a detailed picture of the changing magmatic and paleotectonic history of the Tally Pond Group.

8.2 Principal Results

This work presents a collection of precise and internally consistent geochemical and isotopic data set for a carefully chosen and prepared representative set of rock samples. It has shown that the Tally Pond Group is composite in nature and comprises a mixed volcanic assemblage dominated by felsic pyroclastic volcanic rocks with minor

mafic flow and intrusions. Geochronology and geochemistry indicate that the Tally Pond Group is temporally and genetically distinct from other arc volcanic sequences in the Exploits Subzone of the Dunnage Zone.

The felsic volcanic rocks are felsic breccia, lapilli tuffs, quartz porphyry, crystal tuff, and flow banded rhyolite, rhyodacite, and rhyolite breccia. The breccias contain angular felsic volcanic fragments within a tuffaceous matrix. Tuffisitic gas breccias are present which consist of flow-aligned clasts in an aphanitic siliceous matrix. The lapilli tuff consists of dacite and rhyolite clasts, locally flow banded, in a fine-grained to locally vitric tuffaceous matrix. The rhyolite generally comprises a thick sequence of massive to locally flow banded, aphyric to quartz and/or feldspar porphyritic flows; these are mostly rhyolitic, but locally grade into dacitic compositions. The felsic volcanic rocks display a volcanic arc signature due to their high Y/Nb ratios. These rocks are variably LREE-enriched island arc volcanic rocks that are mainly tholeiitic in nature with some of the samples having transitional to slight calc-alkaline affinities.

The mafic volcanic rocks consist dominantly of fine- to medium-grained, both massive and pillowed amygdaloidal basalt. Interpillow material is common throughout the formation and consists of mafic tuff, green chert and minor graphitic shale. Mafic breccias are present and consist of mafic volcanic rock fragments that are intimately associated with pillow basalts. Locally, minor hyaloclastite is present. The basaltic rocks consistently exhibit an arc signature based on their Zr–Zr/Y ratios and high V contents relative to Ti. They are depleted arc tholeiites with moderate LREE enrichments. The felsic volcanic rocks do not appear to define a fractionation trend with the mafic varieties based on their Zr/Y ratios and REE concentrations. REE patterns for the felsic volcanic

rocks do not parallel those of the mafic rocks and the overall trace element abundances of the mafic volcanic rocks are less than those of the felsic rocks.

All rock sequences of the Tally Pond Group have been subjected to lower greenschist facies regional metamorphism. The metamorphism is interpreted to be related to accretion and burial of the sequence and from sub-seafloor hydrothermal activity, involving low water/rock ratios and temperatures of less than 300°C. However, zones of weak to intense hydrothermal alteration, interpreted as feeder pipe alteration zones, are associated with the numerous volcanogenic massive sulphide occurrences throughout the group. Felsic volcanic rocks in the footwall of the Duck Pond deposit have undergone extensive silicification, chloritization, and sericitization with areas of local carbonatization. Sericites from the Duck Pond deposit are all classified as muscovite with little variation in composition. Chlorites from the Duck Pond deposit contain a broad range of Fe/(Fe+Mg) ratios and atomic Si concentrations, whereas carbonates from the Duck Pond deposit are dominantly dolomite with only small compositional variations between the samples from the different alteration zones.

Geochronology of a felsic tuff brackets the age of volcanism in the Tally Pond Group between 513 and 509 Ma. This age also indicates that mineralization in the Boundary deposit occurred during this same Mid-Cambrian time span. The 509 Ma age for the Tally Pond Group indicates that the group is separate, at least temporally, from adjacent rocks of the Late Cambrian to Tremadocian Tulks Hill assemblage. A 465 Ma age for the Harpoon Gabbro indicates that the mafic intrusions in the Tally Pond Group are Ordovician and therefore much older than the Silurian-Devonian age as previously contemplated (Kean and Jayasinghe, 1980; Kean, 1985; Kean and Evans, 1988; Evans

and Kean, 2002). The age and trace element characteristics of the Harpoon Gabbro suggest that this intrusion can be correlated with the temporally equivalent components of the Wild Bight and Exploits groups and with the Mid-Ordovician part of the New Brunswick Popelogan Arc (van Staal, 1994).

The zircon age ranges obtained by LAM-ICP-MS provide new insights into the depositional history of the Rogerson Lake Conglomerate. This Silurian sedimentary sequence dominantly consists of detritus derived from the underlying Late Cambrian to Early Ordovician arc volcanic sequences of the Victoria Lake Supergroup. The conglomerate also yielded a smaller proportion of Ordovician (480-440 Ma) zircons which in all probability were derived from the calc-alkaline volcanic rocks and associated magmatic arc plutons of the adjacent Notre Dame arc. The presence of a small number of ca. 725 Ma zircons may be attributed to input from igneous intrusions associated with the earliest stages of Iapetan rifting on the Laurentian margin.

The Rogerson Lake Conglomerate also contains a minor zircon population derived from Proterozoic Laurentian basement rocks. High-grade quartz feldspar basement gneisses and younger granite plutons within Grenville inliers have yielded U-Pb zircon ages ranging from ca. 900 to 1500 Ma (Heaman *et al.*, 2002). The high proportion of Paleozoic zircons relative to Proterozoic grains is presumably the result of Middle Ordovician exhumation of the Notre Dame arc and its subsequent collision and accretion to Laurentia.

The sulphur isotope ratios derived from the mafic volcanic and intrusive rocks of the Duck Pond deposit typically fall outside the range of mafic igneous rocks with a mantle origin and suggest that the sulphides in these rocks were not derived from reduced

sulphur from a deep-seated magmatic source. The $\delta^{34}S$ values in the Tally Pond Group are marginally heavier than $\delta^{34}S$ values for typical mantle derived sulphur, implying that the sulphur was derived from a non-magmatic source. The most probable source of fluids and sulphur is reduced seawater sulphate as the $\delta^{34}S$ values show a shift towards the heavier seawater sulphate value. The lightest $\delta^{34}S$ values are from graphitic argillite from the Duck Pond and Boundary deposits. The values for these occurrences are highly negative and lie well below the normal mantle-derived or inorganic sulphate reduction regions and result from biogenetic fractionation of seawater sulphate. Sulphur isotopes are invaluable in deciphering source areas of massive sulphide accumulation in sedimentary debris flows. Analyses of sulphur isotopes indicate the source of the sulphide and can distinguish massive sulphide debris flow that contain purely sedimentary sulphide fragments from those that contain sulphide clasts that were eroded from a pre-existing massive sulphide body.

The Pb isotope data from the Tally Pond Group define a linear trend which indicates that the different VMS occurrences throughout the Tally Pond Group are genetically related. The linear trend lacks any precise geochronological significance because the model ages obtained are unrealistic and, consequently, represents a mixing line between different Pb reservoirs which evolved from distinct long-lived environments. The lead isotope data from the Victoria Lake Supergroup and other deposits indicate that the Exploits Subzone evolved in a region of higher U/Pb relative to the Notre Dame Subzone. The Exploits Subzone appears to have been influenced not by the Laurentian crust but rather by Gondwanan continental crust.

8.3 Regional Tectonic Implications

The recognition and definition of the Tally Pond Group as a temporally and spatially separate unit in the Victoria Lake Supergroup as proposed in this thesis requires modification of the existing tectonomagmatic models for the evolution of the Victoria Lake Supergroup and Exploits Subzone. The geochemical, isotopic and geochronological data allow a consistent interpretation of the nature of the source regions and temporal history of the various Tally Pond Group elements. Due to inherent depositional gaps in the stratigraphic sequence and tectonism and erosion of the rock record these data do not provide direct evidence for the geological and paleotectonic history recorded by the Tally Pond Group. In order to present an acceptable analogue for the Tally Pond Group, comparisons between the Victoria Lake Supergroup and those in modern settings must be utilized.

A reasonable analogue for the Tally Pond Group in a modern tectonic setting should have the following as a minimum requirement; an early period of island arc volcanism with a geochemical signature of subduction, followed by partial obduction of this arc, and finally a transition to back-arc basin activity and magmatism that does not have an arc geochemical signature. Stratigraphic successions such as this are not common in the modern record due to the fact that most back-arc basins, and remnant arcs, subside rapidly as the newly formed crust cools, and therefore most modern analogues subsequently lie in deep ocean water. Elements of such a succession have been recorded, however, in the Japanese Islands (Kimura *et al.*, 1991; Hashimoto, 1991) and in the Taupo volcanic zone of northern New Zealand, which is the on-land extension of the Tonga/Fiji arc (Graham *et al.*, 1995; Spörli, 1989). In both cases, a transition from

continental island-arc volcanism to back-arc basin development is observed. Early volcanism is characterized by tholeiitic basalt which progressed to calc-alkaline andesites and Low K-rhyolites. Subsequent extension and thinning of the island-arc led to the initiation of seafloor spreading which propagated into the thinned crustal region and formed a new oceanic region behind the active arc. Rocks developed in the back-arc basin in the Pacific Ocean generally represent melting of mantle sources with no subduction slab component. Isotopic and geochemical data suggest that the sources are dominantly ocean-island basalt with a slighter MORB-like component (Gill, 1981). Geological, geochemical, isotopic and geochronological results presented in this thesis, in conjunction with modern tectonic settings where similar relationships exist, indicate that the Tally Pond Group stratigraphic succession records the transition from microcontinental island arc to back arc environments.

The oldest magmatic rocks in the Exploits Subzone are the two late Neoproterozoic (ca. 563 Ma) quartz monzonite plutons (Figure 8.1). These rocks are interpreted to represent island arc plutons that formed in a Neoproterozoic peri-Gondwanan island arc (van Staal *et al.*, 2002). U-Pb studies indicate that these plutons experienced an early Cambrian metamorphism (Evans *et al.*, 1990). Recognition of these Neoproterozoic plutons in Newfoundland as volcanic arc granites suggest a period of island arc magmatism on the peri-Gondwanan margin that may not be Iapetan related. The formation of the Iapetan ocean basin is constrained by the ca. 570 Ma separation of Laurentia from the west Gondwanan cratons to produce a wide Iapetus ocean by 550 Ma (Cawood *et al.*, 2001). The early Cambrian (ca. 540-535 Ma) rift-drift transition on the Laurentian margin therefore represents rifting of the Dashwoods microcontinent from

Laurentia into an already open Iapetus Ocean (Waldron and van Staal, 2001). The Neoproterozoic plutons are interpreted to form the basement to Ganderia because their age, nature of plutonism and metamorphism are typical of Gander basement rocks exposed elsewhere throughout the Appalachians (O'Brien *et al.*, 1996; Barr and White, 1996).

Formation of a primitive island arc outboard of the Gondwanan margin by westward subduction had begun by the Mid-Cambrian (Figure 8.1). This is represented by the main period of volcanism in the Tally Pond Group and is constrained by U-Pb ages of 513 and 509 Ma. Lithogeochemistry and isotopic data suggest that the mafic and felsic volcanic rocks were subduction zone related and formed in an ensimatic island arc setting. The abundant amounts of rhyolite in the Tally Pond Group probably indicate that the arc formed under the partial influence of continental crust or the presence of a well thickened arc-crust. Similar tholeiitic volcanic assemblages have been documented in modern arc environments (e.g. Tongan arc, Vallier *et al.*, 1990) and in other ancient arc settings elsewhere in Newfoundland (Swinden *et al.*, 1990; 1997; MacLachlan and Dunning, 1998). However, the base of the Tally Pond Group is not exposed and the ca. 60 Ma span between the ca. 570 Ma opening of Iapetus (Cawood *et al.*, 2001) and volcanism in the Tally Pond Group suggests that there might be an extensive history of island arc magmatism prior to deposition of the Tally Pond Group that is not preserved or alternatively, not exposed in central Newfoundland.

Given that the top of the Tally Pond Group is absent, a relationship between the group and its original Cambro-Ordovician stratigraphic cover is not present in Newfoundland. However, the Tally Pond Group correlates with other Cambrian volcanic

sequences in the Appalachian Orogen, namely the New River Belt (Johnson and McLeod, 1996), where these critical relationships are present. In southern New Brunswick, the Lower Cambrian volcanic rocks of the New River Belt are unconformably overlain by Ordovician arenite-shale sequence (van Staal *et al.*, 2002), typical of Gander-type rocks in Newfoundland, thereby providing a stratigraphic links between the Mid to Lower Cambrian volcanic sequences of the Tally Pond Group and Ganderia.

By ca. 500 Ma termination of westward obduction and partial obduction of the Tally Pond volcanic arc had begun. Initiation of eastward subduction beneath the Gondwanan margin and formation of a volcanic arc commenced soon afterward and is represented by the Upper Cambrian to lower Tremadoc island arc tholeiitic rocks of the Tulks Hill assemblage; the age of volcanism is constrained at 498 and 495 Ma (Evans *et al.*, 1990). All of the Lower Cambrian and Tremadoc arc volcanic rocks of the Exploits Subzone are interpreted to represent a single south-east facing, ensimatic arc-back-arc complex termed the Penobscot Arc (van Staal, 1994). The age of the Penobscot arc rocks partial overlaps with the formation of Tremadoc ophiolites in the Exploits Subzone. The Gander River Complex (O'Neill, 1991) and Pipestone Pond Complex (494 Ma, Dunning and Krogh, 1985) probably formed in a back-arc basin that developed contemporaneously with the Penobscot island arc (Jenner and Swinden, 1993; van Staal *et al.*, 1998).

The hiatus of approximately 10 Ma between (ca. 485-475 Ma) volcanism in the Penobscot and Victoria arcs is interpreted to result from the interaction of the Gondwanan margin and a subduction zone. The difficulty in subducting buoyant continental crust therefore caused termination of this westward subduction. This interval also corresponds with the period of obduction of the Penobscot age ophiolites on the

Gander Zone in Newfoundland. Unconformities, stitching plutons and tightly-dated movement zones constrain this event to the late Tremadoc-early Arenig (Williams and Piasecki, 1990; van Staal and Williams, 1991; Colman-Sadd *et al.*, 1992; Dunning *et al.*, 1993).

Renewed arc-related volcanism (Victoria arc of van Staal *et al.*, 1998) at approximately 475 Ma is well documented in the Wild Bight and Exploits group (MacLachlan and Dunning, 1998; O'Brien *et al.*, 1997). This period indicates the formation of a new subduction zone dipping east beneath the composite Gondwanan margin, consisting of the Gander Zone continental rocks and its overlying obducted Penobscot ophiolites (Figure 8.2). Rifting and migration of this arc formed a margin basin termed the Exploits back-arc basin in Newfoundland and the Arenig-Llanvirn Popelogan Arc-Tetagouche complex in New Brunswick (van Staal *et al.*, 1998). No Mid-Ordovician ophiolites have been recognized in central Newfoundland; however, similar age ocean floor basalts are found in parts of the Exploits Subzone (Swinden, 1987). The 465 Ma Harpoon Gabbro that intrudes the Tally Pond Group and Tom Joe Basalts of the Victoria Lake Supergroup are probably equivalent to these rocks and possibly formed in the Exploits back-arc basin. Both rock sequences exhibit MORB-like geochemical signatures with no evidence of influence from a subducting slab.

By the Caradoc, the Popelogan-Victoria Arc had accreted to the arc/back-arc complexes of the Notre Dame Subzone (Figure 8.3). This active Laurentian margin was separated from the Gander margin by the Exploits back-arc basin which was the site of deep water sedimentary deposition, represented by a regionally extensive black shale

sequence that extends throughout and is typical of the Exploits Subzone. This black shale unit conformably overlies the volcanic rocks of the Victoria Lake Supergroup.

Closure of the Exploits Basin took place by westward subduction during the late Ordovician and Lower Silurian. During the Silurian the last remnants of Iapetus had disappeared and the Gander margin had been juxtaposed with the Laurentian margin. This terminal Iapetus suture (Dog Bay Line) records the transition from marine to terrigenous sedimentation in the Exploits Subzone (Williams *et al.*, 1993; Pollock *et al.*, 2003). Silurian sub aerial terrigenous sedimentary sequences (Botwood Belt) of the Exploits Subzone unconformably overlie the volcanic, intrusive and sedimentary rocks of the Tally Pond Group, Victoria Lake Supergroup, and Crippleback Lake quartz monzonite.

The Neoproterozoic and early Cambrian rocks of the Tally Pond group are more akin to rocks of the Brookville and Bras d'Or terranes in New Brunswick and Nova Scotia than similar sequences in the Dunnage Zone of Newfoundland. Neoproterozoic plutonic rocks in the Brookville and Bras d'Or terranes are interpreted to have been produced in a ca. 565-555 Ma subduction zone along the peri-Gondwanan continental margin. The presence of ca. 510 Ma plutons (White and Barr, 1996) in the Brookville terrane indicates a tectonomagmatic event that correlates with island arc-volcanism in the Exploits Subzone; however, the data do not indicate whether the former represents a prolonged and continuous tectonomagmatic event between 550-500 Ma or two separate and distinct Neoproterozoic and early Cambrian events (White and Barr, 1996).

Previous workers (Barr and White, 1996; van Staal *et al.*, 1996) have demonstrated that the Brookville and Bras d'Or terranes represent the eastern margin of

the Central Mobile Belt of the Appalachians; in essence the Gander Zone. The age and tectonothermal nature of these sequences indicate that these rocks did not experience a similar Neoproterozoic to Early Paleozoic history to, and hence do not constitute part of, the Avalon Zone (*sensu stricto*). Correlation of the Tally Pond Group with the Brookville and Bras d'Or terranes imply that all of these sequences formed along the peri-Gondwanan margin of Iapetus (Barr and White, 1996). The Silurian Rogerson Lake Conglomerate that unconformably overlies the Tally Pond Group indicates that these terranes were accreted to Laurentia by Late Ordovician-Early Silurian.

8.4 Significance of This Work

The work presented in this thesis has important implications for mineral exploration in the Tally Pond Group, and has shown that the major massive sulphide occurrences are typically hosted by a quartz-phyric felsic volcanic sequence. The extensive hydrothermal alteration zones that surround the known VMS occurrences in the Tally Pond Group extend for several hundred metres around the deposits. Therefore locating these zones is a useful tool in finding unknown VMS deposits as they can aid in selecting volcanic successions with and environment favourable for hosting massive sulphide deposits and can assist in targeting specific areas for more detailed exploration.

U-Pb geochronology has shown that volcanism occurred during the Mid-Cambrian and that mineralization occurred syngenetically with the surrounding volcanic rocks. It has also demonstrated that the mafic intrusive magmatism in the Tally Pond Group is Mid-Ordovician, and therefore coeval with similar magmatism in other areas of the Exploits Subzone. New lithogeochemical and isotopic data combined with new

interpretations of structural and stratigraphic relationships in the Tally Pond Group has led to a new interpretation of the regional geology of the Tally Pond Group and its particular setting within the Victoria Lake Supergroup. A new map has been produced to demonstrate the nature of these relationships and a tectonic model attempts to portray the Precambrian to Ordovician paleotectonic history of the Exploits Subzone of the Newfoundland Dunnage Zone.

8.5 Outstanding Problems and Directions for Future Study

Having reviewed the principal results of this thesis and possible geological paleotectonic evolution of the Tally Pond Group, I conclude with a summary of some of the problems that remain unresolved and possible suggestions for future work in the Tally Pond area of Central Newfoundland.

The nature of the internal stratigraphy of the Tally Pond Group remains equivocal. The volcanic rocks comprise sequences of mafic volcanism interspersed with several felsic volcanic episodes. The exact relationship between these rock units is uncertain and careful U-Pb geochronology may help resolve the stratigraphic position of these rocks. There is still considerable uncertainty about the nature of the original stratigraphic base of the Tally Pond Group. An original contact between the Tally Pond Group and its substrate has not been identified and is inferred based on correlation with surrounding units. The nature of this relationship is important, because I cannot preclude the presence of Precambrian volcanic rocks in central Newfoundland. Stratigraphic and structural relationships in the northeast part of the Tally Pond Group suggest that Precambrian volcanic rocks may be present in the Sandy Lake sequence adjacent to the

Crippleback Lake quartz monzonite pluton. Careful field mapping coupled with whole-rock lithogeochemical analyses and U-Pb geochronology may locate and confirm or refute the presence of such rocks.

The nature of influence by continentally derived sediments and continental lithosphere on the volcanic rocks of the Tally Pond Group remains unclear at present. Precambrian inheritance has not been identified in zircons from the Tally Pond Group and therefore Nd-isotopic studies of the volcanic rocks should aid in determining the possible influence of Ganderian and/or Avalonian continental crust. The clastic sedimentary rocks that are located between the Tally Pond Group and Tulks Hill assemblage were not studied in detail. Future research could focus on categorizing and potentially subdividing these rocks.

The gabbroic intrusions in the Tally Pond Group may possibly host auriferous quartz veins. Although no auriferous veins were found in the course of this study, similar gabbroic intrusions elsewhere in the Exploits Subzone are known to contain abundant gold-bearing mesothermal quartz veins (Evans, 1996). Volcanogenic massive sulphide deposits within the Tally Pond Group remain a significant exploration target with excellent potential for further discoveries. Extensive areas remain that have only had preliminary reconnaissance exploration.

The results presented in this thesis have answered many of the fundamental geological problems that exist in the Tally Pond area. These same results, however, have generated more questions about the detailed geology than were originally contemplated during the initiation of this study. I hope that this work provides a capable foundation for future workers who strive to solve the myriad of present or some unforeseeable problems.

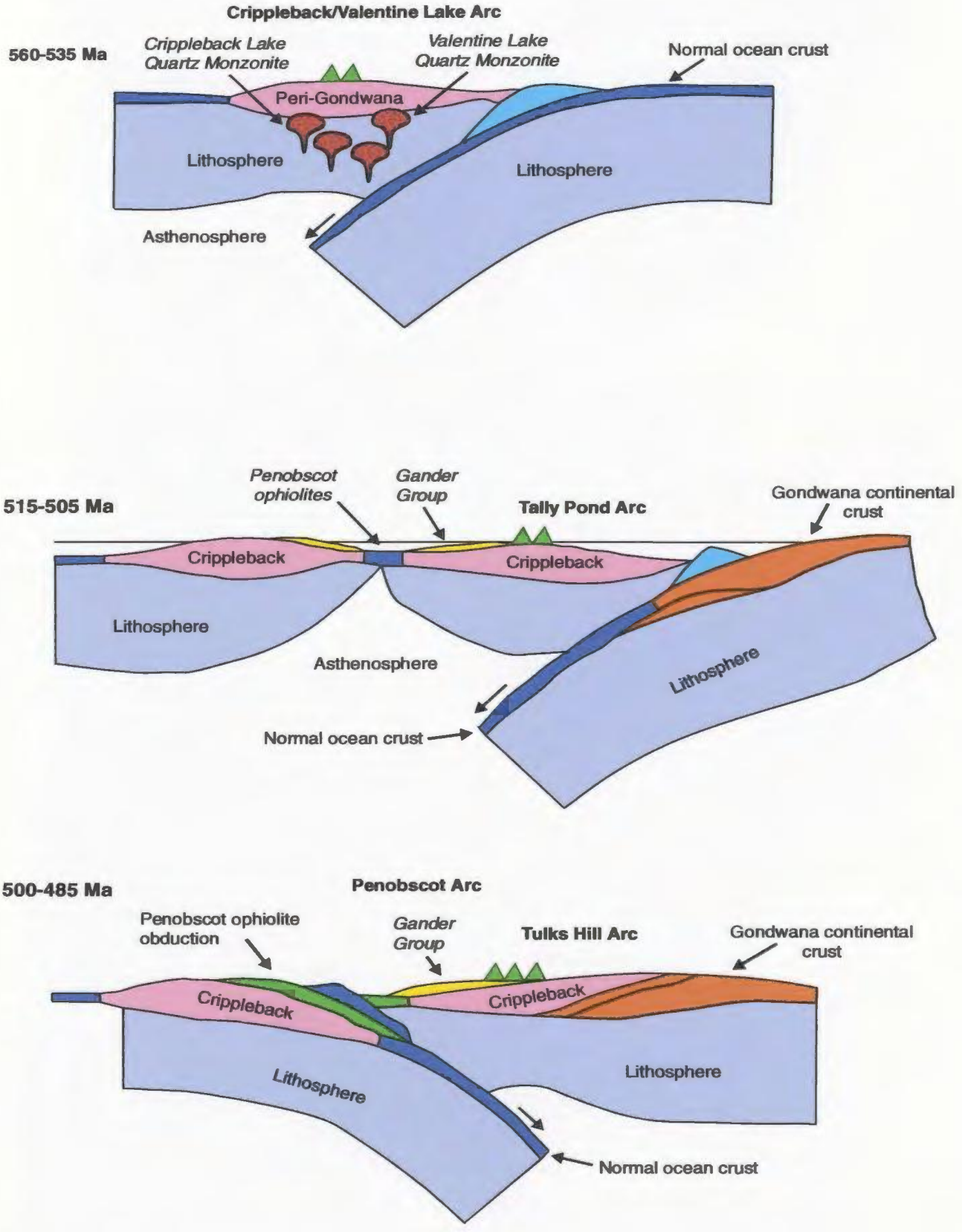

Figure 8.1 *Neoproterozoic to Tremadoc paleotectonic evolution of the Gondwanan margin of Iapetus. Modified from van Staal* et al. *(1998) and from C.R. van Staal and N.Rogers (pers. com.).*

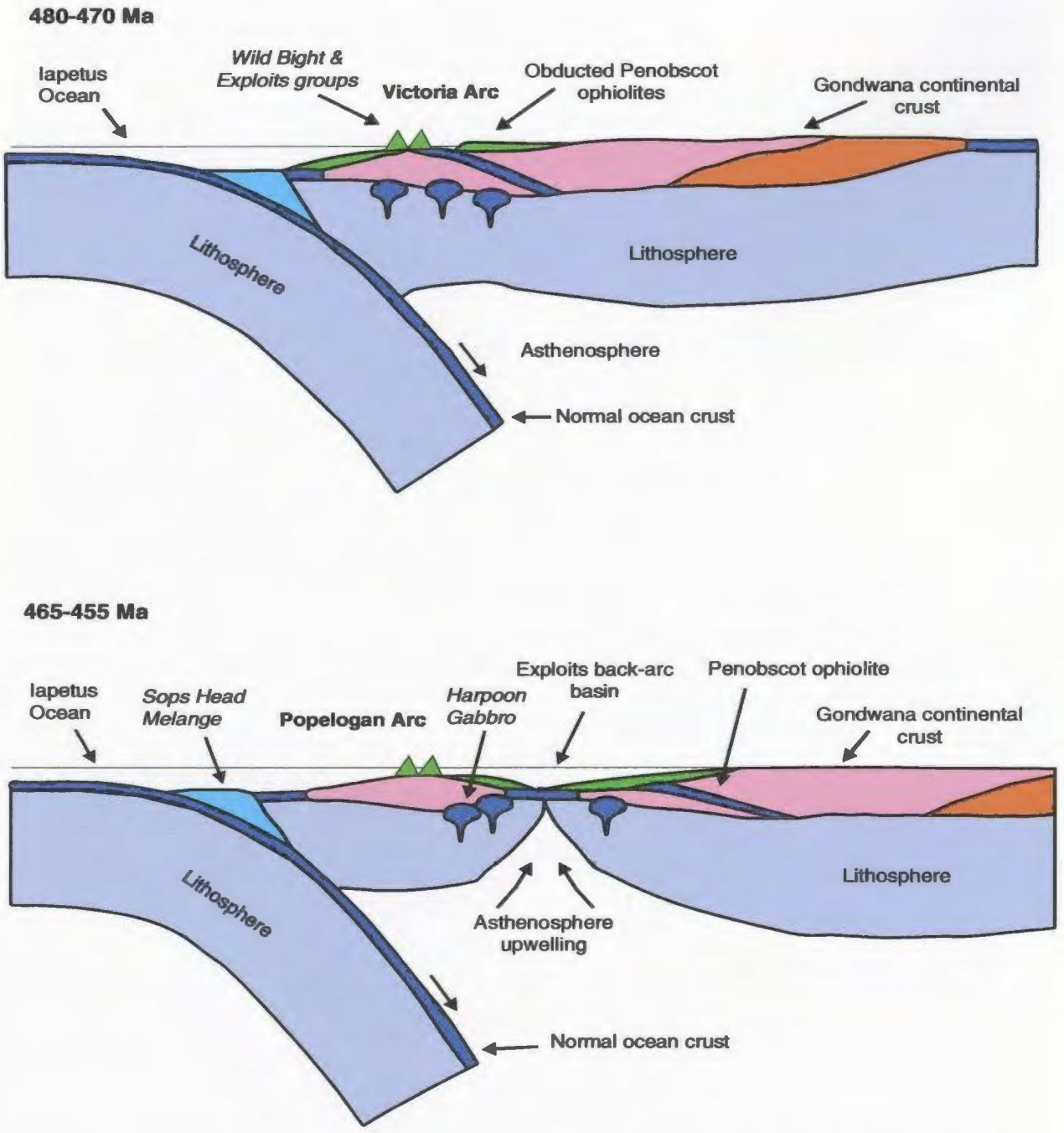

Figure 8.2 *Ordovician (Arenig to Caradoc) paleotectonic evolution of the Gondwanan margin of Iapetus. Modified from van Staal* et al. *(1998) and from C.R. van Staal and N.Rogers (pers. com.).*

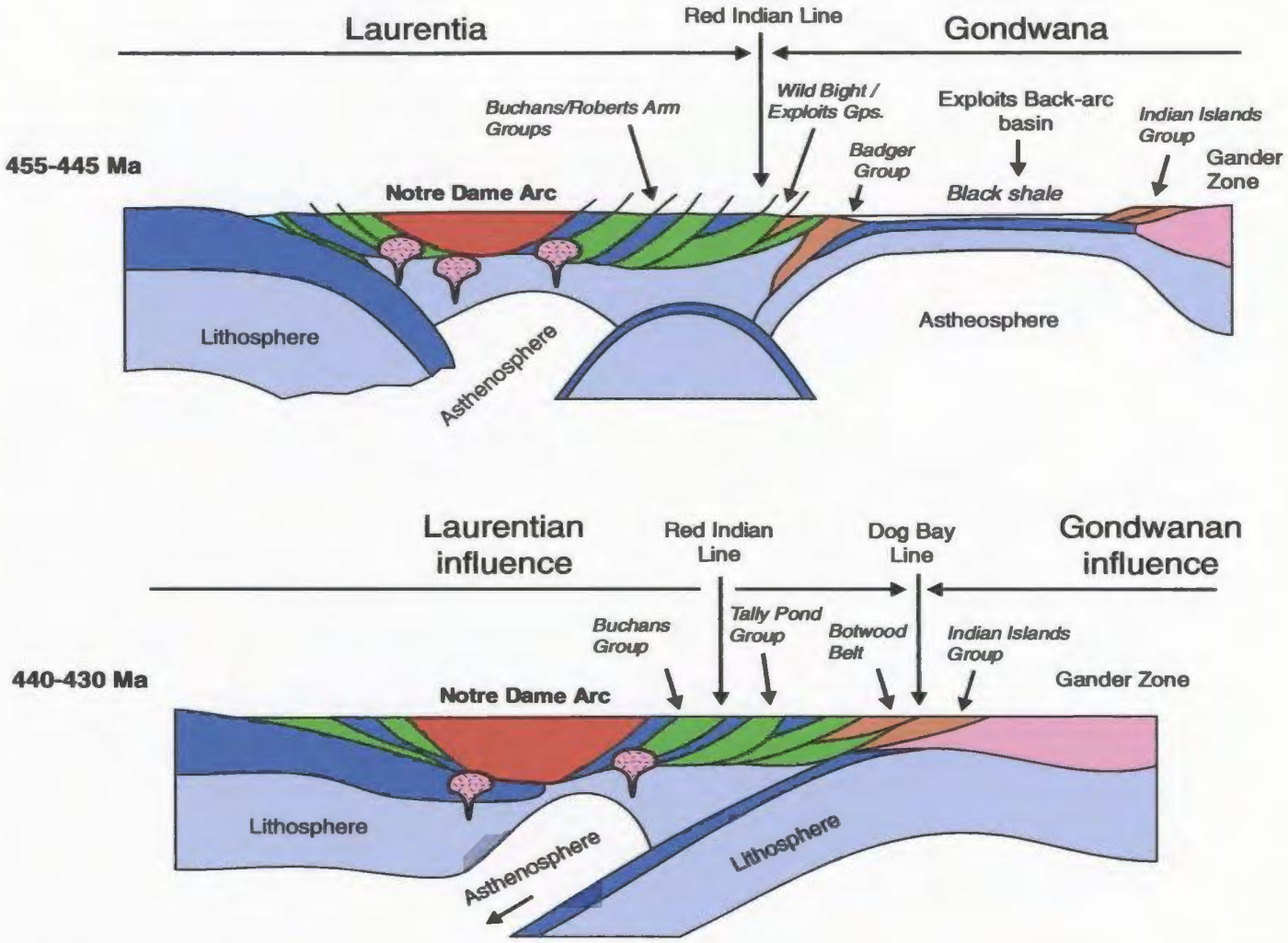

Figure 8.3 *Late Ordovician to Early Silurian paleotectonic evolution of the Laurentian and Gondwanan margin of Iapetus. Modified from van Staal* et al. *(1998) and from C.R. van Staal and N. Rogers (pers. com.).*

REFERENCES

Alt, J.C. and Emmermann, R.
1985: Geochemistry of hydrothermally altered basalts: Deep Sea Drilling Project Hole 504B, Leg 83. In Initial Reports of the Deep Sea Drilling Project, vol. 83. U.S. Government printing Office, Washington, p. 249-262.

Barr, S.M. and White, C.E.
1996: Contrasts in the late Precambrian-early Paleozoic tectonothermal history between Avalon composite terrane sensu stricto and other possible peri-Gondwanan terranes in southern New Brunswick and Cape Breton Island, Canada. *In* Avalonian and related Peri-Gondwanan Terranes of the Circum-North Atlantic, (ed.) R.D. Nance and M.D. Thompson, Geological Society of America Special Paper 304. p. 95-108.

Barrett, T.J. and MacLean, W.H.
1994: Chemostratigraphy and hydrothermal alteration in exploration for VHMS deposits in greenstones and younger volcanic rocks. In Alteration and alteration processes associated with ore-forming systems. Edited by D.R. Lentz. Geological Association of Canada, Short Course Notes, vol. 11, pages 433-467.
1999: Volcanic sequences, lithogeochemistry and hydrothermal alteration in some bimodal volcanic-associated massive sulphide systems. *In* Volcanic-Associated Massive Sulfide Deposits: Processes and Examples in Modern and Ancient Settings, (ed.) C.T. Barrie and M.D. Hannington, Reviews in Economic Geology, Society of Economic Geologists, vol. 8, p. 101-127.

Berner, R.A.
1980: Early diagenesis; a theoretical approach. Princeton Univ. Press, Princeton, NJ, United States, 237 p.

Bird, J.M. and Dewey, J.F.
1970: Lithospheric plate-continental margin tectonics and the evolution of the Appalachian Orogen; Geological Society of America, Bulletin, v. 84, p. 3917-3928.

Bischoff, J.L. and Dickson, F.W.
1975: Seawater-basalt interaction at 25°C and 500 bars: implications for origin of sea-floor heavy metal deposits and regulation of seawater chemistry. Earth and Planetary Science Letters, vol. 25, p. 385-397.

Boyce, W.D., Ash, J.S., O'Neill, P. and Knight, I.
1988: Ordovician biostratigraphic studies in the Central Mobile Belt and their implications for Newfoundland tectonics. In Current Research, Newfoundland Department of Mines and Energy, Mineral Development Division, Report 88-1, p. 177-182.

Brown, N.E.
1952: Geology of the Buchans Junction area, Newfoundland. Unpublished M.Sc. thesis, McGill University, Montreal, 88 pages.

Campbell, A.R. and Larson, P.B.
1998: Introduction to stable isotope applications in hydrothermal systems. In Techniques in hydrothermal ore deposits geology, Reviews in Economic Geology, vol.10, p. 173-192.

Canfield, D.E.
2001: Isotope fractionation by natural populations of sulfate-reducing bacteria. Geochimica et Cosmochimica Acta, vol.65, no.7, p. 1117-1124.

Cann, J.R.
1971: Major element variations in ocean-floor basalts. Philosophical Transactions of the Royal Society of London, vol. A268, p. 495-505.

Cawood, P.A., McCausland, P.J., and Dunning, G.R.
2001: Opening Iapetus: Constraints from the Laurentian margin in Newfoundland. Geological Society of America Bulletin, vol. 113, p. 443-453.

Chambers, L.A.
1982: Sulfur isotope study of a modern intertidal environment, and the interpretation of ancient sulfides. Geochimica et Cosmochimica Acta, vol.46, no.5, p. 721-728.

Chaussidon, M. and Lorand, J.P.
1990: Sulphur isotope composition of orogenic spinel lherzolite massifs from Ariege (north-eastern Pyrenees, France); an ion microprobe study. Geochimica et Cosmochimica Acta, vol. 54, no.10, p. 2835-2846.

Chaussidon, M., Albarede, F. and Sheppard, S.M.F.
1987: Sulphur isotope heterogeneity in the mantle from ion microprobe measurements of sulphide inclusions in diamonds. Nature, vol.330, no.6145, p. 242-244.
1989: Sulphur isotope variations in the mantle from ion microprobe analyses of micro-sulphide inclusions. Earth and Planetary Science Letters, vol.92, no.2, p. 144-156.

Chorlton, L.B., Williams, H. and Wilton, D.H.C.
1995: Cape Ray Belt; *In* Chapter 4 of geology of the Appalachian-Caledonian Orogen in Canada and Greenland, ed. by Williams, H. Geological Survey of Canada, Geology of Canada, no. 6, p. 397-403.

Claypool, G.E., Leventhal, J.S. and Goldhaber, M.B.
1980: Geochemical effects of early diagenesis of organic matter, sulfur, and trace elements in Devonian black shales, Appalachian Basin. AAPG Bulletin, vol. 64, no.5, p. 692.

Coish, R.A.
1977: Ocean floor metamorphism in the Betts Cove ophiolites, Newfoundland. Contributions to Mineralogy and Petrology, vol. 60, p. 255-270.

Collins, C.
1992: Report on 1991 assessment work over concession lands within the boundary of the Noranda-BP Resources Ltd., Tally pond joint venture (A.N.D. Charter, Reid lot 229, 231, 234, &235), NTS 12A/7, 9, 10. Newfoundland and Labrador Geological Survey, Assessment File 12A/0630, Noranda Exploration Company Ltd., 835 p.

Colman-Sadd, S.P. and Swinden, H.S.
1984: A tectonic window in central Newfoundland? Geological evidence that the Appalachian Dunnage Zone may be allochthonous; Canadian Journal of Earth Sciences, v. 21, p. 1349-1367.

Colman-Sadd, S.P., Hayes, J.P., and Knight, I.
1990: Geology of the Island of Newfoundland; Geological Survey Branch, Newfoundland Department of Mines and Energy, Map 90-01, scale 1: 1 000 000.

Colman-Sadd, S.P., Dunning, G.R., and Dec, T.
1992: Dunnage-Gander relationships and Ordovician orogeny in central Newfoundland: A sediment provenance and U/Pb age study; American Journal of Science, v. 292, p. 317-355.

Connelly, J.N. and Heaman, L.M.
1993: U-Pb geochronological constraints on the tectonic evolution of the Grenville Province, western Labrador. Precambrian Research, vol.63, no.1-2, p. 123-142.

Corrigan, D., Rivers, T. and Dunning, G.R.
1997: Preliminary report on the evolution of the allochthon boundary thrust in eastern Labrador; Mechin River to Goose Bay. Eastern Canadian Shield Onshore-Offshore Transect (ECSOOT), Lithoprobe Report, vol.61, p. 45-56.

Cox, R.A., Dunning, G.R. and Indares, A.
1998: Petrology and U-Pb geochronology of mafic, high-pressure, metamorphic coronites from the Tshenukutish Domain, eastern Grenville Province. Precambrian Research, vol.90, no.1-2, p. 59-83.

Cumming, G.L. and Krstic, D.
1987: Detailed lead isotope study of Buchans and related ores. In Buchans Geology, Newfoundland. Edited by R.V. Kirkham, GeologicalSurvey of Canada, Paper 86-24, p. 227-233.

Cumming, G.L. and Richards, J.R.
1975: Ore lead isotope ratios in a continuously changing Earth. Earth and Planetary Science Letters, vol.28, no.2, p. 155-171.

Currie, K.L., van Breeman, O., Hunt, P.A. and van Berkel, J.T.
1992: The age of high-grade gneisses south of Grand Lake, Newfoundland. Atlantic Geology, vol. 28, no. 2, p. 153-161.

Currie, K.L., and Hunt, P.A.
1991: Latest Precambrian igneous activity near Saint John, New Brunswick. Radiogenic age and isotopic studies, Report 4 Paper - Geological Survey of Canada, Report: 90-02, p. 11-17.

Dallmeyer, R.D.
1978: $^{40}Ar/^{39}Ar$ incremental release ages of hornblendeand biotite from Grenville basement rocks within the Indian Head Range Complex, southwest Newfoundland: their bearing on late Proterozoic-Early Paleozoic thermal history. Canadian Journal of Earth Sciences, vol. 15, p. 1374-1379.

Dean, P.F.
1978: The volcanic stratigraphy and metallogeny of Notre Dame Bay, Newfoundland. Memorial University of Newfoundland, geology Report 7.

Deer, W.A., Howie, R.A., Zussman, J.
1992: An introduction to the rock-forming minerals, Longman Scientific Technical, Harlow, United Kingdom, 696 p.

Dewey, J.F.
1969: Evolution of the Appalachian/Caledonian Orogen; Nature, v. 222, p. 124-129.

Dewey, J.F. and Bird, J.M.
1971: Origin and Emplacement of the ophiolite suite: Appalachian Ophiolites in Newfoundland; Journal of Geophysical Research, v. 76, p. 3179-3206.

Dickin, A.P.
1995: Radiogenic Isotope Geology. Cambridge University Press, 490 p.

Dimmel, P.
1986: A case history of the discovery and geophysical and geochemical signatures of the Burnt Pond sulphide prospects, Noel Paul's Brook, central Newfoundland, NTS 12A/9. Unpublished B.Sc. thesis, University of New Brunswick, 56 p.

Dodson, M.H., Compston, W., Williams, I.S. and Wilson, J.F.
1988: A search for ancient detrital zircons in Zimbabwean sediments. Journal of the Geological Society of London, vol.145, Part 6, p. 977-983.

Doucet, P., Mueller, W. and Chartrand, F.
1998: Alteration and ore mineral characteristics of the Archean Coniagas massive sulfide deposit, Abitibi Belt, Quebec. Canadian Journal of Earth Sciences, vol.35, no.6, p. 620-636

Dube, B., Dunning, G.R., Lauziere, K. and Roddick, J.C.
1996: New insights into the Appalachian Orogen from geology and geochronology along the Cape Ray fault zone, southwest Newfoundland. Geological Society of America Bulletin, vol. 108, p. 101-116.

Dudas, F.O.
1992: Petrogenetic evaluation of trace element discrimination diagrams. In Basement Tectonics 8, (ed.) M.J. Bartholomew, D.W. Hyndman, D.W. Mogk and R. Mason, Kluwer, Dordrecht, p. 93-127.

Dunning, G.R. and Krogh, T.E.
1985: Geochronology of ophiolites of the Newfoundland Appalachians. Canadian Journal of Earth Sciences, vol.22, no.11, p. 1659-1670.

Dunning, G.R., Kean, B.F., Thurlow, J.G. and Swinden, H.S.
1987: Geochronology of the Buchans, Roberts Arm and Victoria Lake groups and Mansfield Cove Complex, Newfoundland. Canadian Journal of Earth Sciences, vol. 24, p. 1175-1184.

Dunning, G.R., Swinden, H.S., Kean, B.F., Evans, D.T.W. and Jenner, G.A.
1991: A Cambrian island arc in Iapetus: geochronology and geochemistry of the Lake Ambrose Volcanic Belt, Newfoundland Appalachians. Geological Magazine, vol. 128, pages 1-17.

Dunning, G.R., O'Brien, S.J., O'Brien, B.H., Holdsworth, R.E. and Tucker, R.D.
1993: Chronology of Pan-African, Penobscot and Salinic shear zones on the Gondwanan margin, Northern Appalachians. Abstracts with Programs - Geological Society of America, vol.25, no.6, p. 421-422.

Ellis, A.J.
1968: Natural hydrothermal systems and experimental hot water-rock interaction: reactions with NaCl solutions and trace metal extraction. Geochimica et Cosmchimica Acta, vol. 12, p. 1356-1363.

Erdmer, P.
1986: Geology of the long Range Inlier in Sandy Lake map area (12H) western Newfoundland. Geological Survey of Canada, Open file 1310.

Evans, D.T.W.

1986: The geology, geochemistry, alteration and sulphide petrology of the Lower Ordovician Jacks pond pyritic volcanogenic massive sulphide prospects, central Newfoundland. Unpublished B.Sc.(Hons.) thesis, Memorial University of Newfoundland, St. John's, Newfoundland, 209 pages.

1996: Epigenetic gold occurrences, eastern and central Dunnage Zone, Newfoundland. Department of Mines and Energy, Geological Survey, Mineral Resource Report 9, 135 pages.

Evans, D.T.W. and Wilson, M.R.

1994: Epigenetic gold occurrences in the eastern Dunnage Zone, Newfoundland: preliminary stable isotope results. In Current Research. Newfoundland Department of Mines and Energy, Geological Survey, Report 94-1, pages 211-223.

Evans, D.T.W. and Wilton, D.H.C.

1995: Midas Pond gold prospect, Victoria Lake Group, central Newfoundland: a shear hosted quartz vein system. In Current Research. Newfoundland Department of Mines and Energy, Geological Survey, Report 95-1, pages 139-144.

Evans, D.T.W. and Kean, B.F.

1987: Gold and massive sulphide mineralization in the Tulks Hill volcanics, Victoria lake Group, central Newfoundland. In Current Research. Newfoundland Department of Mines and Energy, Mineral Development Division, Report 87-1, pages 103-111.

2002: paleotectonic setting of the Victoria Lake Supergroup and adjoining sequences, central Newfoundland. Newfoundland Department of Mines and Energy, Geological Survey Open File, NFLD/2790, 79 pages.

Evans, D.T.W., Kean, B.F. and Dunning, G.R.

1990: Geological studies, Victoria Lake Group, central Newfoundland. In Current Research. Newfoundland Department of Mines and Energy, Geological Survey Branch, Report 90-1, pages 131-144.

Farquhar, R.M. and Fletcher, I.R.

1980: Ore-lead isotopes and Grenville plate tectonics. In The Continental Crust and its Mineral Deposits. Edited by D.W. Strangway. Geological Association of Canada, Special Paper 20, p. 771-788.

Faure, G.

1986: Principles of Isotope Geology. John Wiley & Sons, New York, NY, 589 p.

Faure, G., Hoels, J. and Mensing, T.M.
1984: Effect of oxygen fugacity on sulphur isotope compositions and magmatic concentrations in the Kirkpatrick basalt, Mount Falla, Queen Alexandra Range, Antarctica. Isotope Geoscience, vol. 2, p. 301-311.

Franklin, J.M.
1995: Volcanic-associated massive sulphide base metals. In Geology of Canadian Mineral Deposit Types, (ed.) Eckstrand, O R; Sinclair, W D; Thorpe, R I, Geological Survey of Canada, Canada, p. 158-183.

Franklin, J.M., Sangster, D.M. and Lydon, J.W.
1981: Volcanic-associated massive sulfide deposits. In Economic geology; Seventy-fifth anniversary volume; 1905-1980, p. 485-627.

Gariépy, C. and Dupré, B
1991: Pb isotopes and crust-mantle evolution. In Applications of radiogenic isotope systems to problems in geology; short course handbook, MAC Short Course Handbook, vol.19, p. 194-221.

Gieseman, A., Jäger, H.J., Norman, A.L., Krouse, H.R. and Brand, W.A.
1994: Online sulphur-isotope analysis using an elemental analyzer coupled to a mass spectrometer. Analytical Chemistry, vol. 66, p. 2816-2819

Gill, J.B.
1981: Orogenic andesites and plate tectonics. Springer-Verlag, Berlin, Heidelberg, New York, 385 p.

Goldberg, S. A., Butler, J.R. and Fullagar, P.D.
1986: The Bakersville dike swarm: Geochronology and petrogenesis of Late Proterozoic basaltic magmatism in the southern Appalachian Blue Ridge. American Journal of Science, vol. 286, p. 403 - 430

Govindaraju, K.
1989: 1989 compilation of working values and sample description for 272 geostandards. Geostandards Newsletter, vol.13, 113 p.

Gower, C.F. and Krogh, T.E.
2002: A U-Pb geochronological review of the Proterozoic history of the eastern Grenville Province. Canadian Journal of Earth Sciences, vol.39, no.5, p. 795-829.

Gower, C.F. and Loveridge, W.D.
1987:Grenvillian plutonism in the eastern Grenville Province. *In* Ragiogenic Age and Isotope Studies: Report 1: Geological Survey of Canada, Paper 87-2, p. 55-58.

Gower, C.F., Van Nostrand, T. and Smyth, J.
1988: Geology of the St. Lewis River map region, Grenville Province, eastern Labrador. In Current Research. Newfoundland Department of Mines and Energy, Mineral Development Division, Report 88-1, pages 59-73.

Graham, I.J.,Cole, J.W., Briggs, R.M., Gamble, J.A. and Smith, I.E.M.
1995: Petrology and petrogenesis of volcanic rocks from the Taupo volcanic zone; a review. Journal of Volcanology and Geothermal Research, vol.68, no.1-3, p. 59-87.

Hall, A.

1996: Igneous Petology. Longman Group Ltd., Harlow, UK, 551 p.

Hall, J., Marille, F. and Dehler, S.

1998: Geoophysical studies of the structure of the Appalachian orogen in the Atlantic borderlands of Canada. Canadian journal of Earth Sciences, volume 35, pages 1205-1221.

Hamilton, M.A. and Emslie, R.F.
1997: Mealy dykes, Labrador: U-Pb baddeleyite age and implications for the eastern Grenville Province. GAC-MAC, Program with abstracts, vol. 22, p. A62.

Hanson, G.N.
1978: The application of trace elements to the petrogenesis of igneous rocks of granitic composition. Earth and Planetary Science Letters, vol.38, no.1, p. 26-43.

Harrsion, T.M. and Watson, E.W.
1983: Kinetics of zircon dissolution and zirconium diffusion in granitic melts of variable water content. Contributions to Mineralogy and Petrology, vol.84, no.1, p. 66-72.

Hashimoto, M.
1991: Geology of Japan. Developments in Earth and Planetary Sciences, Terra Scientific Publishing Company, Tokyo, 249 p.

Hattori, K. and Sakai, H.
1979: D/H ratios, origins, and evolution of the ore-forming fluids for the Neogene veins and kuroko deposits of Japan. Economic Geology and the Bulletin of the Society of Economic Geologists, vol.74, no.3, p. 535-555.

Heaman, L.M. and Parrish, R.
1991; U-Pb geochronology of accessory minerals. In Applications of radiogenic isotope systems to problems in geology; short course handbook, MAC Short Course Handbook, vol.19, p. 59-102.

Heaman, L.M., LeCheminant, A.N. and Rainbird, R.H.
1992: Nature and timing of Franklin igneous events, Canada: Implications for a Late Porterozoic mantle plume and the breakup of Laurentia. Earth and Planetary Science Letters, vol. 109, p. 117-131.

Heaman, L.M., Erdmer, P. and Owen, J.V.
2002: U-Pb geochronologic constraints on the crustal evolution of the Long Range Inlier, Newfoundland. Canadian Journal of Earth Sciences, vol.39, no.5, p. 845-865.

Henley, R.W. and Thornley, P.
1981: Low grade metamorphism and the geothermal environment of massive sulphide ore formation, Buchans, Newfoundland. In The Buchans orebodies; fifty years of geology and mining, Special Paper - Geological Association of Canada, no.22, p. 205-228.

Hey, M.H.
1954: A new review of the chlorites. Mineralogical Magazine, vol.30, no.224, p. 277-292

Hibbard, J.P., and Williams, H.
1979: The regional setting of the Dunnage Mélange in the Newfoundland Appalachians; American Journal of Science, v. 279, p. 993-1021.

Hodgson, C.J. and Lydon, J.W.
1977: Geological setting of volcanogenic massive sulphide deposits and active hydrothermal systems; some implications for exploration. CIM Bulletin, vol.70, no.786, p.95-106.

Hoefs, J.
1980: Stable isotope geochemistry. Springer-Verlag, Berlin, Federal Republic of Germany (DEU), 208 p.
1987: Stable isotope geochemistry. Minerals and Rocks, vol. 9, 241 p.

Hoffman, P. F.
1988: United plates of America, The birth of a craton: Early Proterozoic assembly and growth of Laurentia. Annual Reviews of Earth and Planetary Sciences, vol. 16, p. 543-603.
1989: Precambrian geology and tectonic history of North America. *In* The Geology of North America-An Overview, eds. A.W Bally and A.R. Palmer, Geological Society of America, The Geology of North America, v. 1A.

Holmes, A.
1946: An estimated age of the Earth. Nature, vol. 157, p. 680-684.

Houtermans, F.G.

1946: Dis Isotopen-Haufigkeiten im naturlichen Blei und dasAalter des Urans. Naturwissenschaften, vol. 33, p. 185-187.

Howley, J.P.

1917: Report of Progress for the year 1888—Survey across country by way of Bay d'est River, Noel Paul's and the Exploits. Geological Survey of Newfoundland, St. John's.

Humphris, S.E. and Thompson, G.

1978: Hydrothermal alteration of oceanic basalts by seawater. Geochimica et Cosmchimica Acta, vol. 42, p. 107-125.

Huston, D.L.

1999: Stable isotopes and their significance for understanding the genesis of volcanic-hosted massive sulphide deposits: A review. In Volcanic-Associated Massive Sulfide Deposits: Processes and Examples in Modern and Ancient Settings, (ed.) C.T. Barrie and M.D. Hannington, Reviews in Economic Geology, Society of Economic Geologists, vol. 8, p. 157-176.

Indares, A., Dunning, G.R. and Cox, R.

1998: Crust-mantle interactions and the role of extension in a Grenvillian continental collision setting; Manicouagan imbricate zone, Canada. Abstracts with Programs - Geological Society of America, vol.30, no.7, p. 394.

James, D.T., Kamo, S. and Krogh, T.E.

2000: Preliminary U-Pb geochronological data from the Mealy Mountains Terrane, Grenville Province, southern Labrador. In Current Research Report, Newfoundland Department of Mines and Energy, Report: 2000-1, pp.169-178.

Jenner, G.A.

1996: Trace element geochemistry of igneous rocks: geochemical nomenclature and analytical geochemistry. In Trace Element geochemistry of Volcanic Rocks: Application For Massive Sulphide Exploration. Edited by D.A. Wyman. Geological Association of Canada, Short Course Notes, vol. 12, p. 51-77.

Jenner, G.A. and Swinden, H.S.

1993: The Pipestone Pond Complex, central Newfoundland; complex magmatism in an eastern Dunnage Zone ophiolites. Canadian Journal of Earth Sciences, vol. 30, no.3, p. 434-448.

Jenner, G.A., Longerich, H.P., Jackson, S.E., and Fryer, B.F.

1990: ICP-MS a powerful tool for high precision trace-element analysis in Earth Sciences: evidence from analysis of selected U.S.G.S. reference samples. Chemical Geology, vol. 33, p. 133-148.

Johnson, S.C. and McLeod, M.J.

1996: The New River Belt; a unique segment along the western margin of the Avalon composite terrane, southern New Brunswick, Canada. In Avalonian and related peri-Gondwanan terranes of the Circum-North Atlantic, Special Paper - Geological Society of America, vol.304, p.149-164.

Kamo, S.L., Krogh, T.E. and Kumarapeli, P.S.

1995: Age of the Grenville dyke swarm, Ontario-Quebec: implications for the timing of Iapetan rifting. Canadian Journal of Earth Sciences, vol. 32, p. 273-280.

Kay, M.

1976: Dunnage Mélange and subduction of the Protoacadic Ocean, northeast Newfoundland; Geological Society of America, Special Paper 175, 49 p.

Kay, M. and Colbert, E.H.

1965: Stratigraphy and Life History. John Wiley and Sons Inc., New York, 736 p.

Kean, B.F.

1977: Geology of the Victoria Lake map area (12A/6), Newfoundland. Newfoundland Department of Mines and Energy, Mineral Development Division, report 77-4, 11 pages.

1979: Star Lake map area, Newfoundland. Newfoundland Department of Mines and Energy, Mineral Development Division, Map 79-1.

1985: Metallogeny of the Tally Pond volcanics, Victoria Lake Group, central Newfoundland. In Current Research. Newfoundland Department of Mines and Energy, Mineral Development Division, Report 85-1, pages 89-93.

Kean, B.F. and Evans, D.T.W.

1988: Regional Metallogeny of the Victoria Lake Group, central Newfoundland, In Current Research. Newfoundland Department of Mines and Energy, Mineral Development Division, Report 88-1, pages 319-330.

Kean, B.F. and Jayasinghe, N.R.

1980: Geology of the Lake Ambrose (12A/10)-Noel Paul's Brook (12A/9) map area, central Newfoundland. Newfoundland Department of Mines and Energy, Mineral Development Division, Report 80-02, 29 pages.

1982: Geology of the Badger map area (12A/16), Newfoundland. Newfoundland Department of Mines and Energy, Mineral Development Division, Report 81-2, 37 pages.

Kennedy, M.J.

1979: The continuation of the Canadisn Appalachians into the Caledonides of Ireland and Britian. In The Caledonides of the British Isles-Reviewed, (ed.) A.L. Harris, C.H. Holland, and B.E.Leake, Geological Society of London, p. 33-64.

Kesler, S.E., Cumming, G.L., Krstic, D. and Appold, M.S.

1994: Lead isotope geochemistry of Mississippi valley-type deposits of the Southern Appalachians. Economic Geology and the Bulletin of the Society of Economic Geologists, vol. 89, no.2, p. 307-321.

Ketchum, J.W.F., Jackson, S.E., Culshaw, N.G. and Barr, S.M.

2001: Depositional and tectonic setting of the Paleoproterozoic Lower Aillik Group, Makkovik Province, Canada: evolution of a passive margin-foredeep sequence based on petrochemistry and U-Pb (TIMS and LAM-ICP-MS) geochronology. Precambrian Research, vol. 105, p. 331-356.

Kimura, T., Hayami, I. and Yoshida, S.

1991: Geology of Japan. Univ. Tokyo Press, Tokyo, Japan, 287 p.

Kosler, J., Tubrett, M. and Sylvester, P.

2001: Application of Laser Ablation ICP-MS to U-Th-Pb dating of monazite. The Journal of Geostandards and Geoanalysis, vol. 25, no. 2.

Kosler, J., Fonneland, H., Sylvester, P., Tubrett, M. and Pederson, R.B.

2002: U-Pb dating of detrital zircons for sediment provenance studies – a comparison of laser ablation ICP-MS and SIMS techniques. Chemical Geology, vol. 182, pages 605-618.

Krogh, T.E.

1973: A low-contamination method for hydrothermal decomposition of zircon and extraction of U and Pb for isotopic age determinations. Geochimica et Cosmochimica Acta, vol.37, no.3, p. 485-494.

1982: Improved accuracy of U-Pb ages by the creation of more concordant systems using an air abrasion technique. Geochimica et Cosmchimica Acta, vol. 46, p. 637-649.

Kyser, T. K.

1986: Stable isotope variations in the mantle. Reviews in Mineralogy, vol.16, p. 141-164.

1990: Stable isotopes in the continental lithospheric mantle. Oxford Monographs on Geology and Geophysics, vol.16, p. 127-156.

Longerich, H.P.

1995: Analysis of pressed pellets of geological samples using wavelength-dispersive X-ray fluorescence spectrometry. X-ray Spectrometry, vol. 24, p. 123-136.

Longerich, H.P., Jenner, G.A., Fryer, B.J. and Jackson, S.E.

1990: Inductively coupled plasma-mass spectrometric analysis of geological samples: A critical evaluation based on case studies. Chemical Geology, vol. 83, p. 105-118.

Loveridge, W.D.

1986: U-Pb ages on zircon from rocks of the Lac de Morhiban map area, Quebec. In Current Research, part A. Geological Survey of Canada, Paper 86-1A, p. 523-530.

Lowden, J.A.

1961: Age determinations by the Geological Survey of Canada: Report 1, isotopic ages. Geological Survey of Canada, Paper 60-17, 51 p.

Lowden, J.A., Stockwell, C.H., Tipper, H.W. and Wanlesss, R.K.

1963: Age determinations and geological studies (including isotopic ages- Report 3). Geological Survey of Canada, Paper 62-17, 140 p.

Ludwig, K.R.

1999: Using Isoplot/Ex, Version 2.01: a geochronological toolkit for Microsoft Excel. Berkeley Geochronology Center Special Publication No. 1a, 47 p.

MacLachlan, K. and Dunning, G.R.

1998a: U-Pb ages and tectonomagmatic relationships of Early Ordovician low-Ti tholeiite, boninites and related plutonic rocks in central Newfoundland, Canada. Contributions to Mineralogy and petrology, vol. 133, p. 235-258.

1998b: U-Pb ages and tectonomagmatic evolution of middle Ordovician volcanic rocks of the Wild Bight Group, Newfoundland Applachians. Canadian Journal of Earth Sciences, vol. 39, p. 998-1017.

MacLachlan, K., O'Brien, B.H. and Dunning, G.R.

2001: Redefinition of the Wild Bight Group, Newfoundland: implications for models of island-arc evolution in the Exploits Subzone. Canadian Journal of Earth Sciences, vol. 38, p. 889-907.

MacLean, W.H. and Barrett, T.J.

1993: Lithogeochemical techniques using immobile elements: Journal of geochemical Exploration, vol. 48, p. 109-133.

McNicoll, V.J. and van Staal, C.R.

2001: Accretionary history of the Northern Appalachians: SHRIMP study of Ordovician-Silurian syntectonic sediments in the Canadian Appalachians. Geological Association of Canada, Abstracts with programs, vol. 26, p. 100.

Meschede, M.

1986: A method of discriminating between different types of mid-ocean ridge basalts and continental tholeiites with the Nb-Zr-Y diagram. Chemical Geology, vol. 56, p. 207-218.

Mezger, K and Krögstad, E.J.

1997: Interpretation of discordant U-Pb zircon ages; an evaluation. Journal of Metamorphic Geology, vol.15, no.1, p. 127-140.

Miller, R.R., Heaman, L.M. and Birkett, T.C.

1995: U-Pb zircon age of the Strange Lake peralkaline complex: implications for Mesoproterozoic peralkaline magmatism in north-central Labrador. Precambrian Research, vol. 81, p. 67-82.

Miyashiro, A.

1974: Volcanic rock series in island arcs and active continental margins. American Journal of Science, vol. 274, p. 321-355.

Moore, P.J.

2003: Stratigraphic implications for mineralization: Preliminary findings of a metallogenic investigation of the Tally Pond volcanics, central Newfoundland. In Current Research. Newfoundland Department of Mines and Energy, Geological Survey, Report 2003-01, p. 241-257.

Moritz, R. and Malo, M.

1996: Lead isotope signatures on Devonian Acadian structurally controlled mineral occurrences in the Gaspe Peninsula, Quebec Appalachians: constrains on source rocks. Economic Geology, volume 91, pages 1145-1150.

Mottl, M.J.

1983: Metabasalts, axial hot springs and the structure of hydrothermal alteration of basalt by seawater-I. Experimental results for major and minor components of seawater. Geochimica et Cosmchimica Acta, vol. 42, p. 1103-1115.

Mottl, M.J. and Seyfried, W.E.

1980: Sub-seafloor hydrothermal systems: Rock- vs. seawater-dominated, In Seafloor Spreading Centers: Hydrothermal Systems, (ed.) P.A. Rona and R.P. Lowell. Dowden, Hutchinson and Ross Inc., Stroudsburg, Pennsylvania, p. 869-884.

Mullins, J.

1961: Geology of the Noel Paul's Brook area, central Newfoundland. Unpublished M.Sc. thesis, Memorial University of Newfoundland, 96 pages.

Murray, A.H.

1872: Survey of Exploits River and Red Indian Lake. Geological Survey of Newfoundland, Report for 1871.

O'Brien, B.H.

1992: Internal and external relationships of the South Lake Igneous Complex, north-central Newfoundland (NTS 2E/5,6): Ordovician and later tectonism in the Exploits Subzone? Newfoundland Department of Mines and Energy, Geological Survey Branch, Report 93-1,p. 279-291.

O'Brien, B.H., Swinden, H.S., Dunning, G.R., Williams, S.H., and O'Brien, F.H.C.

1997: A peri-Gondwanan arc-back arc complex in Iapetus: Early-Mid Ordovician evolution of the Exploits Group, Newfoundland; American Journal of Science, v. 297, p. 220-272.

O'Brien, S.J., O'Brien, B.H., Dunning, G.R. and Tucker, R.D.

1996: Late Neoproterozoic evolution of Avalonian and associated peri-Gondwanan rocks of the Newfoundland Appalachians. *In*: Avalonian and Related Terranes of the Circum-North Atlantic. *Edited by* M.D. Thompson and R.D. Nance. Geological Society of America, Special Paper 304, pages 9-28

Ohmoto, H.

1972: Systematics of Sulfur and Carbon Isotopes in Hydrothermal Ore Deposits. Economic Geology and the Bulletin of the Society of Economic Geologists, vol.67, no.5, p. 551-578.

1986: Stable isotope geochemistry of ore deposits. Reviews in Mineralogy, vol.16, p. 491-559.

Ohmoto, H. and Rye, R.O.

1979: Isotopes of sulfur and carbon. In Geochemistry of hydrothermal ore deposits, John Wiley & Sons, New York, NY, p. 509-567.

Ohmoto, H., Mizukami, M., Drummond, S.E., Eldridge, C.S., Pisutha-Arnond, V. and Lenagh, T.C.

1983: Chemical processes of Kuroko formation. Economic Geology Monographs, vol.5, p. 570-604.

O'Neill, P.P.

1991: Geology of the Weir's Pond area, Newfoundland (NTS 2E/1). Newfoundland Department of Mines, Mineral Development Division, Report 91-3,164 p.

O'Neill, P.P and Blackwood, F.

1989: A proposal for revised stratigraphic nomenclature of the Gander and Davidsville groups and the Gander River Ultrabasic Belt of northeastern

Newfoundland. In Current Research, Newfoundland Department of Mines, Mineral Development Division, Report 89-1, p. 165-176.

Owen, J.V. and Erdmer, P.

1990: Middle Proterozoic geology of the Long Range Inlier, Newfoundland: Regional significance and tectonic implications. *In* Middle Proterozoic Laurentia-Baltica, eds. C.F. Gower, T. Rivers and B. Ryan, Geological Association of Canada, Special Paper 38, p. 215-231.

Parrish, R.R., Roddick, J.C., Loveridge, W.D., Sullivan, R.W.

1987: Uranium-lead analytical techniques at the geochronology laboratory, Geological Survey of Canada. Radiogenic age and isotopic studies. Report 1, Geological Survey of Canada Paper 87-2, 3-7.

Pearce, J.A.

1982: Trace element characteristics of lavas from destructive plate boundaries. In Andesites, (ed.) Thorpe, R.S., John Wiley and Sons, p. 535-547.

1987: An expert system for the tectonic characterisation of ancient volcanic rocks. Journal of Volcanological and Geothermal Research, vol. 44, p. 189-229.

Pearce, J.A. and Cann, J.R.

1971: Ophiolite origin investigated by a discriminant analysis using Ti, Zr, and Y. Earth and Planetary Science Letters, vol. 19, p. 290-300.

1973: Tectonic setting of basic volcanic rocks using trace element analysis. Earth and Planetary Science Letters, volume 19, pages 290-300.

Pearce, J.A. and Norry, M.J.

1979: Petrogenetic implications of Ti, Zr, Y, and Nb variations in volcanic rocks. Contributions to Mineralogy and Petrology, volume 69, pages 33-47.

Pearce, J.A. and Peate, D.W.

1995: Tectonic implications of the composition of volcanic arc magmas: Annual Review of Earth and Planetary Sciences, vol. 23, p. 251-285.

Pearce, J.A., Harris, N.B.W. and Tindle, A.G.

1984: Trace element discrimination diagrams for the tectonic interpretation of granitic rocks. Journal of Petrology, volume 25, pages 956-983.

Philpotts, A.R.

1990: Principles of Igneous and Metamorphic Geology. Prentice Hall, New Jersey, 498 p.

Pollock, J.C. and Wilton, D.H.C.

2001: Metallogenic studies of the Tally Pond belt, Victoria Lake Group: Trace-element geochemistry and lead-isotope data from the exploits Subzone, Newfoundland. In Current Research. Newfoundland Department of Mines and Energy, Geological Survey, Report 2001-01, p. 247-266.

Pollock, J.C., Wilton, D.H.C. and van Staal, C.R.

2002: Geological studies and definition of the Tally Pond Group, Victoria Lake Supergroup, Exploits Subzone, Newfoundland Appalachians. In Current Research. Newfoundland Department of Mines and Energy, Geological Survey, Report 2002-01, p. 155-167.

Pollock, J.C., Wilton, D.H.C., van Staal, C.R. and Tubrett. M.N.

2002: Laser ablation ICP-MS geochronology and provenance of detrital zircons from the Rogerson Lake Conglomerate, Botwood Belt, Newfoundland. In Current Research. Newfoundland Department of Mines and Energy, Geological Survey, Report 2002-01, p. 168-183.

Pollock, J.C., Morrissey, K., Wilton, D.H.C. and Tubrett, M.N.

2003: Laser Ablation U-Th-Pb geochronology of detrital zircons from the Botwood and Indian Islands belts: Accretionary tectonic evolution of the northeast Exploits Subzone, Dunnage Zone, Newfoundland Appalachians. Geological Society of America, Northeastern Section Annual Meeting, Abstracts vol. 38.

Potts, P.J.

1987: A handbook of silicate rock analysis. Chapman & Hall, New York, NY, 622 p.

Richards, J.P. and Noble, S.R.

1998: Application of radiogenic isotope systems to the timing and origin of hydrothermal processes. In Techniques in hydrothermal ore deposits geology, Reviews in Economic Geology, vol.10, p. 195-233.

Ripley, E.M.

1983: Sulfide mineralogy and sulfur isotope geochemistry of layered sills in the Deer Lake Complex, Minnesota. Mineralium Deposita, vol.18, no.1, p. 3-15.

Roddick, J.C.

1987: Generalized numerical error analysis with applications to geochronology and thermodynamics. Geochimica et Cosmchimica Acta 51, 2129-2135.

Rogers, N. and van Staal, C.R.

2002: Toward a Victoria Lake Supergroup: A provisional stratigraphic revision of the Red Indian to Victoria Lake area, central Newfoundland. In Current Research. Newfoundland Department of Mines and Energy, Geological Survey, Report 2002-01, p. 185-195.

Rollinson, H.
1993: Using geochemical data: evaluation, presentation, interpretation: Longman, Harlow, 352 p.

Romer, R.L., Schaerer, U., Wardle, R.J. and Wilton, D.H.C.
1995: U-Pb age of the Seal Lake Group, Labrador; relationship to Mesoproterozoic extension-related magmatism of Laurasia. Canadian Journal of Earth Sciences, vol.32, no.9, p. 1401-1410.

Ruitenberg, A.A., McLeod, M.J. and Krogh, T.E.
1993: Comparative metallogeny of Ordovician volcanic and sedimentary rocks in the Annidale-Shannon (New Brunswick) and Harborside-Blue Hill (Maine) areas; implications of new U-Pb age dates, Exploration and Mining Geology, vol.2, no.4, p. 355-365.

Rye, R.O. and Ohmoto, H.
1974: Sulfur and Carbon Isotopes and Ore Genesis: A Review. In Stable Isotopes as Applied to Problems of Ore Deposits, Economic Geology and the Bulletin of the Society of Economic Geologists, vol.69, no.6, p. 947-953.

Saunders, A.D., Tarney, J., Marsh, N.G. and Wood, D.A.
1980: Ophiolites as ocean crust of marginal basin crust: a geochemical approach. In Ophiolites, Proceeding of the International Ophiolite Symposium, Cyprus, (ed.) A. Panayioutou, p. 261-272.

Schärer, U. and Gower, C.F.
1988: Crustal Evolution in eastern Labrador: constraints from precise U-Pb ages. Precambrian Research, vol. 38, p. 405-421.

Schuchert, C.
1923: Sites and natures of North American geosynclines. Geological Society of America Bulletin, v. 34, p. 151-229.

Schuchert, C. and Dunbar, C.O.
1934: Stratigraphy of western Newfoundland. Geological Society of America, Memoir 1, 123 p.

Sears, W.A. and Wilton, D.H.C.
1996: Base metal massive sulfide deposits at the Winter Hill and Franchman Head prospects, Avalon Zone, Newfoundland. Exploration and Mining Geology, vol. 5, no. 3, pages 181-195.

Seyfried, W.E., Mottl, M.J. and Bischoff, J.L.

1978: Seawater-basalt ratio effects on the chemistry and mineralogy of spillites from the ocean floor. Nature, vol. 275, no. 5677, p. 211-213.

Shanks, W.C.

2001: Stable isotopes in seafloor hydrothermal systems; vent fluids, hydrothermal deposits, hydrothermal alteration, and microbial processes. Reviews in Mineralogy and Geochemistry, vol. 43, p. 469-525.

Shanks, W.C. and Slack, J.F.

1988: Comparative studies of metal and sulfur sources in modern and ancient besshi-type massive sulfide deposits. V. M. Goldschmidt conference; program and abstracts, p. 73.

Shanks, W.C., Bischoff, J.L. and Rosenbauer, R.J.

1981: Seawater sulfate reduction and sulfur isotope fractionation in basaltic systems; interaction of seawater with fayalite and magnetite at 200-350 degrees C. Geochimica et Cosmochimica Acta, vol.45, no.11, p. 1977-1995.

Shervais, J.W.

1982: Ti-V plots and the petrogenesis of modern and ophiolitic lavas. Earth and Planetary Science Letters, volume 59, pages 101-118.

Snelgrove, A.K.

1928: The geology of the Central Mineral Belt of Newfoundland. Canadian Mining and Metallurgical Bulletin, no. 197, p. 1057-1127.

Spörli, K.B.

1989: Tectonic framework of Northland, New Zealand. In Geology of Northland, accretion, allochthons and arcs at the edge of the New Zealand micro-continent. The Royal Society of New Zealand, Bulletin 26, p.3-14.

Squires, G.C., Brace, T.D. and Hussey, A.M.

2000: Duck Pond project: Geological and geotechnical summary. Unpublished internal report for Thundermin Resources Inc, 21 pages

2001: Newfoundland's polymetallic Duck Pond deposit: Earliest Iapetan VMS Mineralization, formed within a sub-seafloor, carbonate-rich alteration system. North Atlantic Minerals Symposium, Extended abstracts volume, p .160-162.

Squires, G.C., MacKenzie, A.C. and MacInnis, D.

1990: Geology and genesis of the Duck Pond volcanogenic massive sulphide deposit. *In* Metallogenic framework of base and precious metal deposits, central and western Newfoundland. *Edited by* H.S. Swinden, D.T.W. Evans and B.F. Kean. Eighth IAGOD Symposium Field Trip Guidebook. Geological Survey of Canada, Open File 2156, pages 56-64.

Stacey, J.S. and Kramers, J.D.
1975: Approximation of terrestrial lead isotope evolution by a two-stage model. Earth and Planetary Science Letters, vol. 26, pages 207-221.

Swinden, H.S.
1987: Ordovician volcanism and mineralization in the Wild bight Group, central Newfoundland: a geological, petrological, geochemical and isotopic study. Unpublished Ph.D. thesis, Memorial University of Newfoundland, St. John's, 452 pages.

Swinden, H.S., Jenner, G.A., Kean, B.F. and Evans, D.T.W.
1989: Volcanic rock geochemistry as a guide for massive sulphide exploration in central Newfoundland. In Current Research. Newfoundland Department of Mines, Geological Survey Branch, Report 89-1, pages 201-219.

Swinden, H.S., Jenner, G.A., Fryer, B.J. Hertogen, J. and Roddick, J.C.
1990: Petrogenesis and paleotectonic history of the Wild Bight Group, an Ordovician rifted island arc in central Newfoundland. Contributions to Mineralogy and petrology, vol. 105, p. 219-241.

Swinden, H.S. and Thorpe, R.I.
1984: Variations in style of volcanism and massive sulfide deposition in Early to Middle Ordovician Island arc sequences of the Newfoundland Central Mobile Belt. Economic Geology, volume 79, pages 1596-1619.

Swinden, H.S., Jenner, G.A. and Szybinski, Z.A.
1997: Magmatic and tectonic evolution of the Cambrian-Ordovician Laurentian margin of Iapetus: Geochemical and isotopic constraints from the Notre Dame subzone, Newfoundland. In The Nature of Magmatism in the Appalachian Orogen, Geological Society of America, Memoir 191.

Su, Q., Goldberg, S.A. and Fullagar, P.D.
1994: Precise U-Pb zircon ages of Neoproterozoic plutons in the southern Appalachian Blue Ridge and their implications for the initial rifting of Laurentia: Precambrian Research, vol. 68, p. 81-95.

Sun, S.S.
1982: Chemical composition and origin of the earth's primitive mantle. Geochimica et Cosmchimica Acta, vol. 46, p. 179-192.

Taylor, H.P.
1974: The Application of Oxygen and Hydrogen Isotope Studies to Problems of Hydrothermal Alteration and Ore Deposition. Economic Geology and the Bulletin of the Society of Economic Geologists, vol.69, no.6, p. 843-883.

Thurlow, J.G. and Swanson, E.A.
1981: Geology and ore deposits of the Buchans area, central Newfoundland. In The Buchans Orebodies: Fifty years of geology and mining, edited by E.A. Swanson, D.F. Strong and J.G. Thurlow, Geological Association of Canada, Special Paper 22, pages 113-142.

Tollo, R.P. and Aleinikoff, J.N.
1996: Petrology and U-Pb geochronology of the Robertson River Igneous Suite, Blue Ridge Province, Virginia: evidence for multistage magmatism associated with an early episode of Laurentian rifting. American Journal of Science, vol. 296, p. 1045-1090.

Tollo, R.P. and Hutson, F.E.
1996: 700 Ma age for the Mechum River Formation, Blue Ridge province, Virginia: a unique time constraint on pre-Iapetan rifting of Laurentia. Geology, vol. 24, p. 59-62.

Tucker, R.D. and Gower, C.F.
1990: Salient features of the Pinware Terrane, Grenville Province, eastern Labrador. Program with Abstracts - Geological Association of Canada; Mineralogical Association of Canada; Canadian Geophysical Union, Joint Annual Meeting, vol.15, p. 133.
1994: A U-Pb geochronological framework for the Pinware Terrane, Grenville Province, Southeast Labrador. Journal of Geology, vol.102, no.1, p. 67-78.

Twenhofel, W.H. and MacClintock, P.
1940: Surfaces of Newfoundland. Geological Society of America Bulletin, vol. 51, p. 1665-1728.

Urabe, T., Scott, S.D. and Hattori, K.
1983: A comparison of footwall-rock alteration and geothermal systems beneath some Japanese and Canadian volcanogenic massive sulfide deposits. In The kuroko and related volcanic massive sulfide deposits, Economic Geology Monographs, vol.5, p. 345-364.

Vallier, T.L., Jenner, G.A., Frey, F.A., Gill, J.B., Davis, A.S., Volpe, A.M., Hawkins, J.W., Morris, J.D., Cawood, P.A., Morton, J.L., Scholl, D.W., Rautenschlein, M., White, W.M., Williams, R.W., Stevenson, A.J. and White, L.D.
1991: Subalkaline andesite from Valu Fa Ridge, a back-arc spreading center in southern Lau Basin; petrogenesis, comparative chemistry, and tectonic implications. Chemical Geology, vol.91, no.3, p. 227-256.

van Staal, C.R.
1994: Brunswick subduction complex in the Canadian Appalachians; record of the Late Ordovician to Late Silurian collision between Laurentia and the

Gander margin of Avalon. Tectonics, vol.13, no.4, p. 946-962.

van Staal, C.R. and Williams, H.
1991: Dunnage Zone-Gander Zone relationships in the Canadian Appalachians. Abstracts with Programs - Geological Society of America, GSA Northeastern Section, 26th annual meeting, vol.23, no.1, pp.143

van Staal, C.R., Sullivan, R.W. and Whelan, J.
1996: Provenance and tectonic history of the Gander Margin in the Caledonian/Appalachian Orogen: implications for the orogin and assembly of Avalonia. In Avalonian and related peri-Gondwanan terranes of the Circum-North Atlantic, Special Paper - Geological Society of America, vol.304, pp.347-367.

van Staal, C.R., Dewey, J.F., Mac Niocaill, C. and McKerrow, W.S.
1998: The Cambrian-Silurian tectonic evolution of the northern Appalachians and British Caledonides: history of a complex, west and southwest Pacific-type segment of Iapetus. *In* Lyell: the Past is the Key to the Present. *Edited by* D.J. Blundell and A.C. Scott. Geological Society, London, Special Publication, 143, p. 199-242.

van Staal, C.R., Barr, S., Fyffe, L.R., McNicoll, V., Pollock, J., Reusch, D., Thomas, M., Valverde-Vaquero, P. and Whalen, J.B.
2002: Ganderia - An Important Gondwanan terrane in the Northern Appalachians. Geological Society of America, Northeastern Section Annual Meeting, Abstracts with programs, vol. 37.

Wanless, R.K., Stevens, R.D., Lachance, G.R. and Edmonds, C.M.
1968: Age determinations and geological studies: K-Ar isotopic ages, Report 8. Geological Survey of Canada, Paper 67-2A, 141 pages.

Wasteneys, H.A., Kamo, S.L., Moser, D., Krogh, T.E., Gower, C.F. and Owen, J.V.
1997: U-Pb geochronological constraints on the geological evolution of the Pinware Terrane and adjacent areas, Grenville Province, Southeast Labrador, Canada. Precambrian Research, vol.81, no.1-2, p. 101-128.

Williams, H.
1964: The Appalachians in northeastern Newfoundland: a two-sided symmetrical system; American Journal of Science, v. 262, p. 1137-1158.
1970: Red Indian Lake (east half), Newfoundland. Geological Survey of Canada, Map 1196A.
1976: Tectonic stratigraphic subdivision of the Appalachian Orogen (abstract); *in* Abstracts with Programs; Geological Society of America, v. 8, no. 2, p. 300.

1978: Tectonic-lithofacies map of the Appalachian Orogen; Memorial University of Newfoundland, St. John's, Newfoundland, Map No. 1, scale 1:1 000 000; Map No 1a, scale 1: 2 000 000.
1979: Appalachian Orogen in Canada; Canadian Journal of Earth Sciences, Tuzo Wilson volume, v. 16, p. 792-807.
1984: Miogeoclines and suspect terranes of the Caledonian-Appalachian Orogen: tectonic patterns in the north Atlantic region; Canadian Journal of Earth Sciences, v. 21, p. 887-901.
1993: Stratigraphy and structure of the Botwood Belt and definition of the Dog Bay Line in northeastern Newfoundland; in Current Research, Part D; Geological Survey of Canada, Paper 93-1D, p. 19-27.
1995: Geology of the Appalachian-Caledonian Orogen in Canada and Greenland. Geological Survey of Canada, Geology of Canada, no. 6, p. 142-166 (also Geological Society of America, The Geology of North America, v. F-1).

Williams, H, and Hatcher, R.D.
1982: Suspect terranes and accretionary history of the Appalachian Orogen; Geology, v. 10, p. 530-536.
1983: Appalachian suspect terranes; *in* Contributions to the Tectonics and Geophysics of Mountain Chains, (eds.) R.D. Hatcher, H. Williams, and I. Zietz; Geological Society of America, Memoir 158, p. 35-53.

Williams, H. and Hibbard, J.P.
1976: The Dunnage Mélange, Newfoundland; *in* Report of Activities, Part A; Geological Survey of Canada, Paper 76-1A, p. 183-185.

Williams, H. and Piasecki, M.
1990: The Cold Spring Melange and a possible model for Dunnage-Gander Zone interaction in central Newfoundland. Canadian Journal of Earth Sciences, vol. 27, no.8, p. 1126-1134.

Williams, H. and St-Julien, P.
1982: The Baie Verte-Brompton Line: continent ocean interface in the Northern Applachians. In Major Structural Zones and Faults of the Northern Applachians, (ed.) P. St-Julien and J. Beland, Geological Association of Canada, Special Paper 11, p. 181-261.

Williams, H., Colman-Sadd, S.P. and Swinden, H.S.
1988: Tectono-Stratigraphic subdivisons of central Newfoundland. In Current Research, Part B. Geological Survey of Canada, Paper 88-1B, pages 91-98.

Williams, H., Currie, K.L. and Piasecki, M.A.J.
1993: The Dog Bay Line; a major Silurian tectonic boundary in Northeast Newfoundland. Canadian Journal of Earth Sciences, vol.30, no.12, p. 2481-2494.

Williams, H., Dehler, S.A., Grant, A.C. and Oakey, G.N.
1999: Tectonics of Atlantic Canada. Geoscience Canada, vol. 26, no. 2, p. 51-70.

Winchester, J.A. and Floyd, P.A.
1977: Geochemical discrimination of different magma series and their differentiation products using immobile elements. Chemical Geology, volume 20, pages 325-343.

Winter, L.S.
2000: Derivation of base-line geochemistry, petrography, and isotopic data for the host rocks to the Lucky Strike deposit and comparison with data from other alteration zones, Buchans mining camp, Newfoundland. Unpublished M.Sc. thesis, Memorial University of Newfoundland, St. John's, Newfoundland, 270 pages.

Wood, D.A., Joron, J.L. and Treuil, M.
1979: A re-appraisal of the use of trace elements to classify and discriminate between magma series erupted in different tectonic settings. Earth and planetary Science Letters, volume 45, pages 326-336.

York, D.
1969: Least squares fitting of a straight line with correlated errors. Earth and Planetary Science Letters 5, 320-324.

Zagorevski, A, Rogers, N. and van Staal, C.R.
2003: Tectonostratigraphic relationships in the Lloyds River and Tulks Brook region of central Newfoundland: A geological link between Red Indian and King George IV lakes. In Current Research. Newfoundland Department of Mines and Energy, Geological Survey, Report 2003-1, pages 167-178.

Zartman, R.E. and Doe, B.R.
1981: Plumbotectonics; the model. Tectonophysics, vol.75, no.1-2, p. 135-162.

APPENDIX A

A.1 Sampling procedure

This study primarily involved bulk sampling of drillcore from the Tally Pond area, supplemented by samples selected from surface units during field mapping. The purpose of this sampling procedure was to provide an adequate spatial representation of the surface geology and to expand this dataset in areas of deficient surface outcrops by sampling diamond drill-holes.

Sufficient material (e.g. 15-40 cm in diameter) was sampled to allow for lithogeochemical and petrologic analysis. Samples were cut with a diamond tipped saw to remove weathered edges in order to obtain material for chemistry, with small blocks kept for thin sections and hand specimen. Samples of similar lithologic character (i.e. mafic, felsic, sulphides) were crushed in groups to minimize intergroup contamination between samples.

All samples were crushed in a steel jaw crusher to reduce the samples to ~ 1 cm size rock chips, and these were then placed in a tungsten carbide bowl-puck mill and ground for ~ 2-3 minutes to reduce the sample to a very fine powder (200 mesh/74 μ). The jaw crusher was extensively cleaned between each sample, and silica sand was periodically powdered in the bowl-puck mill in addition to the normal cleaning between

samples to account for any potential cross contamination between samples. These powders were used in all of the whole rock geochemical techniques (e.g. XRF and ICP-MS). Processing occurred at the Department of Earth Sciences, Memorial University of Newfoundland and at the Department of Mines and Energy Laboratories, St. John's, Newfoundland.

Thin sections from the Tally Pond Group were produced at the Department of Earth Sciences, Memorial University of Newfoundland. A representative selection of rock types was selected for thin section and polished thin sections were produced for mineralized samples and electron microprobe analyses.

A.2 X-Ray Fluorescence (XRF) analysis

Selected major and trace element analysis were carried out at Memorial University of Newfoundland, Department of Earth Sciences, X-Ray Fluorescence laboratory using a Fisons/ARL model 8420 + sequential wavelength-dispersive X-Ray spectrometer. Analyses were from pressed pellets which were prepared following the method of Longerich (1995) as follows:

1) 5.00 grams of rock powder and 0.70 grams of BRP-5933 bakelite phenolic powder resin were placed in a glass jar with two stainless steel ball bearings and homogenized for ~10 minutes, or till well mixed.

2) the mixture was then placed in a pellet press and pressed for 5 seconds at a pressure of 20 tonnes.

3) the pressed pellets were then placed in an oven and baked for 15 minutes at 200°C.

Data collection was carried out via an automated computer system attached to the XRF. In addition to the pressed pellets obtained from the samples being analyzed for the purpose of this thesis, four quality control reference materials (AGV-1, DNC-1, JG-1, and BCR-1) as well as five internal standards were analyzed (DTS-1, United States Geological Survey (USGS) reference material; BHVO-1, USGS reference; SY-2 and SY-3, syenite from the Canadian Certified Reference Materials Project and PACS-1, National Research Council of Canada reference material). Published values for the reference materials used are published in Potts *et al.* (1992), Jenner *et al.* (1990), and Longerich *et al.* (1990).

Analysis for 30 elements were conducted via this method consisting of: quantitative elements (P, S, Cl, K, Ca, Sc, Ti, V, Cr, Mn, Fe, Ni, Cu, Zn, Ga, As, Rb, Sr, Y, Zr, Nb, Ba, Ce, Pb, Th, and U) and semi-quantitative (Na, Mg, Al, Si). The limits of detection vary depending upon the elemental group being considered; details of calibration, matrix corrections, precision and accuracy are all described in detail in Longerich (1995). As quoted by Longerich (1995), limits of detection range from 120 ppm for Na_2O and MgO to less than 20 ppm for MnO, K_2O, and CaO; with detection limits for trace elements, in brackets, as: Sc (6), V (6), Cr (7), Ni (5), Cu (4), Zn (3), Rb (0.7), Sr (1.2), Y(0.7), Zr (1.2), Nb (0.7), Ba (23), and Pb (4).

A.3 Precision and accuracy

Precision and accuracy associated with the XRF analysis are based upon five replicate analyses on standard DNC-1 between September 2000 and November 2002. Precision is typically excellent (0-3 % RSD) for all major oxides. Precision for trace

element data was excellent (0-3 % RSD) with the exceptions of S, Sc, Ba, Rb, and Nb (Table A.1). Many of these elements with higher RSD's have very low concentrations in this standard; thereby explaining the lower precision. The long term precision varies from 2 (Rb, Sr) to 5 % (Ba, Nb, Zr, Y) RSD at the 1σ level. The limit of detection varies for each element and ranges from 0.6 ppm for Nb and Y, 0.7 ppm for Rb, 1.1 ppm for Sr and Zr, and 21 ppm for Ba (Longerich, 1995).

Accuracy is typically considered excellent (Table A.1) (RD's from 0-3 %) with the exception of P_2O_5, $A1_2O_3$, S, and Zr. Again, low concentrations of these elements explain the poor statistical results. Although the elements Na, Al, Mg, and Si are typically considered to be semi-quantitative (Longerich, 1995), they were found to have good accuracy and precision and are considered useful for the purposes in this study. The major element data (Tables A2-A.8) reported is the analytical total and do not always total 100 %, thereby reflecting the semi-quantitative nature of the pressed-pellet powder data. The data for all samples, however, were recalculated to 100 % anhydrous for interpretation.

Table A.1 *Precision and accuracy for standard DNC-1 calculated from 5 XRF determinations over the period October 2000 to June 2002.*

Element	Mean values	RSD %	Quoted MUN values	RD %
ppm rock	(n=5)			
Na2O	0.02	1.44	1.94	1.05
MgO	0.10	0.71	0.10	2.07
Al2O3	0.19	0.54	0.18	6.67
SiO2	0.44	0.62	0.44	0.30
P2O5	0.00	3.06	0.00	6.65
K2O	0.00	1.94	0.00	0.56
CaO	0.11	0.76	0.11	0.46
TiO2	0.00	0.67	0.00	0.15
MnO	0.00	2.04	0.00	-2.19
Fe2O3T	0.10	0.34	0.10	-1.05
S	1198	4.82	1032	16.15
Sc	29	15.10	31	-4.85
V	144	3.19	148	-2.63
Cr	299	1.80	307	-2.74
Ba	108	9.40	115	-5.92
Ni	238	1.50	252	-5.55
Cu	83	2.06	87	-4.59
Ga	14.5	3.75	14	4.13
Rb	3.57	4.84	3.4	5.14
Sr	143	0.77	142	0.72
Y	15.4	6.57	16	-2.83
Zr	38.2	3.24	36	6.33
Nb	1.93	17.17	2	1.51

All major element oxide reorted as weight percent (%) and trace elements reported to ppm.
Quoted MUN values are long term averages of Longerich (1995)

RSD is relative standard deviation
RD is relative difference to the standard value

Table A.2 *Pressed pellet X-ray fluorescence (XRF) data for the volcanic and intrusive rock of the Tally Pond Group, Duck Pond area.*

	Sample	JP-00-127	JP-00-202	JP-00-176	JP-00-177	JP-00-178	JP-00-180	JP-00-182	JP-00-185	JP-00-188	JP-00-193	JP-00-194	JP-00-195
SiO2	wt%	75.5	68.1	46.1	72.8	66.9	46.3	70.5	61.5	45.5	77.8	46.8	46.1
TiO2	wt%	0.21	0.2	4.02	0.17	0.23	1.57	0.19	0.15	0.79	0.15	0.87	2.81
Al2O3	wt%	15.5	18.8	12.2	15.3	17.6	15.7	16.9	22.3	18.6	13.2	15.4	12.2
Fe2O3	wt%	0.13	0.19	3.24	0.4	0.69	2.7	0.36	1.5	1.83	0.07	1.88	2.94
FeO	wt%	0.65	0.99	16.5	2.06	3.53	13.8	1.86	7.67	9.34	0.34	9.58	15
MnO	wt%	0.03	0.08	0.25	0.02	0.06	0.24	0.03	0	0.3	0.01	0.17	0.24
MgO	wt%	0.83	1.78	6.06	2.56	3.88	11.2	4.4	1.15	5.94	0.36	12.5	5.88
CaO	wt%	1.3	4.08	8.17	0.32	0.36	4.23	0.24	0.07	13.2	0.63	8.03	10.4
Na2O	wt%	3.5	1.24	2.49	4.66	3.14	3.66	2.23	0.35	0.32	7.33	2.66	2.56
K2O	wt%	2.27	4.5	0.64	1.69	3.62	0.21	3.3	5.37	4.05	0.15	2.01	1.47
P2O5	wt%	0.02	0.02	0.31	0.01	0.03	0.43	0.01	0.01	0.04	0.01	0.07	0.41
Total		100	100	100	100	100	100	100	100	100	100	100	100
Sc	ppm			50.4	19.5	24.6	51.8	11.7	18.5	48.5	30	32.3	31.6
V	ppm		18.6	509		12.3	440	9.43		422		302	322
Rb	ppm	30.3	63.5	19.3	25.3	57.1	2.49	50.2	70	48.8	1.84	30.1	52.3
Ba	ppm	987	2180	182	444	448	0	2130	1330	706		879	225
Sr	ppm	61.9	89.6	254	63.8	60.8	112	16.1	18.8	297	86.4	237	342
Nb	ppm	8.5	6.8	20.4	6.49	7.4	3.16	8.38	7.99	2.18	10.2	2.11	20.9
Zr	ppm	212	144	237	194	208	54.6	169	202	37.5	207	54.5	253
Y	ppm	28	24.5	37.3	44.9	44.9	23.3	40	30.5	10.6	37.7	19.3	38.2
Th	ppm	6.21			7.71	6.88		5.77	8.17		8.23		
Ce	ppm												
Ga	ppm	15	17.6	24.4	15.7	23.6	26.5	14.2	21.6	18.1	7.4	15.7	26.1
Cr	ppm	28.3	16.3			14.9	58.2		14.3	15.6		303	
Ni	ppm								523			103	
Cu	ppm			73.1			20.4		15.2	58.2		38.9	53.2
Pb	ppm			10					84.6	11			
Zn	ppm			130	29.6	56.9	72.7	15.7		348		33.2	92.5
S	ppm	1060	3770	1690	55.4	3320	1180	345	62200	11000	1010	138	2850
As	ppm		40.1	37.1			24.2		150	74.4			
U	ppm												
Cl	ppm	89.1	175	65.2			63				67.8		90.4
Mg #		65.9	73.2	35.7	65.2	62.5	55.1	78.2	18.6	49.1	61.6	66.4	37.3

All elements are recalulated to 100 % anhydrous.

Table A.2 *Pressed pellet X-ray fluorescence (XRF) data for the volcanic and intrusive rock of the Tally Pond Group, Duck Pond area.*

		JP-00-199	JP-00-202	JP-00-207	JP-00-208	JP-00-209	JP-00-210	JP-00-212	JP-00-215	JP-00-275	JP-00-276	JP-00-277	JP-00-279
SiO2	wt%	79.6	71.6	72.8	68.4	49.5	47.8	71.8	74.6	73.4	47.8	47.4	74.7
TiO2	wt%	0.13	0.14	0.18	0.28	0.77	1.55	0.14	0.19	0.25	0.73	2.27	0.15
Al2O3	wt%	13.3	16.8	16.3	15.4	16.1	13.4	19.9	15.9	13.5	14.1	13.4	14.1
Fe2O3	wt%	0.16	0.44	0.37	0.57	2.2	2.89	0.35	0.34	0.51	1.57	2.69	0.21
FeO	wt%	0.81	2.26	1.88	2.92	11.2	14.7	1.79	1.74	2.62	8	13.7	1.08
MnO	wt%	0.04	0.01	0.04	0.05	0.22	0.3	0	0.06	0.12	0.21	0.23	0.05
MgO	wt%	1.03	5.56	1.49	2.51	9.06	7.44	1.25	0.4	1.47	9.49	7.51	0.4
CaO	wt%	1.23	0.07	1.73	2.15	5.27	7.74	0.09	0.51	2.57	13.1	8.59	2.03
Na2O	wt%	1	1.31	2.45	7.08	4.88	3.22	0.75	2.24	4.05	3.93	2.77	4.67
K2O	wt%	2.74	1.79	2.73	0.61	0.66	0.77	3.89	3.99	1.48	0.96	0.96	2.56
P2O5	wt%	0.02	0.01	0.02	0.05	0.05	0.18	0	0.02	0.02	0.06	0.37	0.02
Total		100	100	100	100	100	100	100	100	100	100	100	100
Sc	ppm	14.4	20.8	14	13.8	60.3	42.1	15.4			48.8		24.1
V	ppm	18.9	40.4	8.35	16.1	414	337				385	279	
Rb	ppm	32.3	28.3	38.4	7.15	6.5	9.63	59.7	58.5	24.2	9.37	11.3	24.3
Ba	ppm	360	889	1280	170	158	382	1470	1020	217	688	425	560
Sr	ppm	27	69.8	42.4	94.4	73.9	338	24.4	40	303	258	444	58.4
Nb	ppm	5.95	6.02	8.3	8.06	3.88	18.9	5.98	8.03	6.8		18.4	7.12
Zr	ppm	135	159	182	280	70.8	226	164	213	177	37	253	182
Y	ppm	36.4	33.6	40.9	46	21.1	38.2	20	46.2	40.6	13.8	40.2	57.8
Th	ppm	5.96	4.56	7.45	8.34			7.28	7.84		7.13	8.77	
Ce	ppm												
Ga	ppm	12.3	16.1	13.8	20.6	18.9	23.8	17.9	18.6	15	10.2	20.9	14.4
Cr	ppm	10.9				203	34.9		16	31.1	453	42.1	
Ni	ppm					84.1	29				96.9	32.9	
Cu	ppm					66.2	70.8	4.6		7.24	52.6	96.3	
Pb	ppm	45.6				9.33							
Zn	ppm		9.22	28.8	31.3	117	82.4		32.4	33.2	16.6	87.3	
S	ppm	1290	13800	5470	73.2	2220	944	13200	370	981	949	239	128
As	ppm	27.1	76.3	42.4		70		52.4	39.6		42.6		
U	ppm					5.16							
Cl	ppm											82.8	
Mg #		65.9	78.8	54.7	56.6	55	43.3	51.4	25.9	46	64.2	45.3	35.8

All elements are recalulated to 100 % anhydrous.

Table A.2 *Pressed pellet X-ray fluorescence (XRF) data for the volcanic and intrusive rock of the Tally Pond Group, Duck Pond area.*

		JP-00-284	JP-00-288	JP-00-201	JP-00-106	JP-00-73	JP-00-123	JP-00-05	JP-00-94	JP-00-62	JP-00-158	JP-00-72	JP-00-88
SiO2	wt%	39.8	79.4	51.1	52.1	45	77	75.4	45.7	73.4	72.3	45.8	69.3
TiO2	wt%	2.02	0.09	3.46	0.32	0.23	0.14	0.17	0.19	0.16	0.12	0.19	0.13
Al2O3	wt%	25.6	9.41	19.6	31.5	16.7	13.8	11.1	23	15.6	13.8	15	16
Fe2O3	wt%	0.74	0.63	0.9	0.44	2.28	0.32	0.38	3.19	0.39	1.62	2.49	0.71
FeO	wt%	3.79	3.21	4.6	2.24	11.6	1.65	1.92	16.3	1.98	8.24	12.7	3.64
MnO	wt%	0.22	0.03	0.12	0.03	0.19	0.07	0.07	0.3	0.08	0	0.19	0.18
MgO	wt%	7.24	2.53	15.6	4.7	23	3.91	1.06	5.97	4.63	0.71	23	6.99
CaO	wt%	15.2	2.58	1.46	0.02	0.22	0.08	4.66	0.14	0.1	0.02	0.27	0.06
Na2O	wt%	3.67	0.54	0.82	0.21	0.34	0.17	5.11	2.25	0.19	0.02	0.18	0.33
K2O	wt%	1.64	1.55	2.15	8.48	0.47	2.87	0.04	2.99	3.43	3.22	0.12	2.64
P2O5	wt%	0.16		0.26	0.01	0.03	0.05	0.04	0.01	0.01	0.01	0.07	0.01
Total		100	100	100	100	100	100	100	100	100	100	100	100
Sc	ppm	39.9		58.6	21.9	23.2	14.9	12.4	2.91	11.4	14.5	19.3	13.5
V	ppm	310	20.5	405	5.7	0.32	20.2	7.82	1.4	0.71	0.97	2.02	2.2
Rb	ppm	25.9	24.2	41.3	156	6.94	51.5	0.1	43.7	54.4	48.7	1.7	39.2
Ba	ppm	2740	1930	1690	3950	164	1530	26.4	1440	586	628	43.4	1960
Sr	ppm	325	26.1	58.3	9.66	12.5	5.67	142	76.4	4.4	3.39	5	8.55
Nb	ppm	14.1	3.96	24.8	12.3	9.62	4.96	5.92	8.52	5.71	5.35	8.6	6.03
Zr	ppm	142	79.2	270	386	254	143	169	217	151	129	229	144
Y	ppm	24.2	8.68	44.4	98	53.4	31.7	44.1	56.6	38.2	39.3	55.8	34.1
Th	ppm	7.38	21.2		8.71	6.75	2.44	3.11	14.2	4.3	15.6	7.24	2.64
Ce	ppm				74.8	29.3	4.5	35.2	60.5	49.1	21.5	17.5	25.6
Ga	ppm	21.3	14.9	25.8	66.4	23.7	13.7	10.4	29.8	12.7	7.27	24.7	17.8
Cr	ppm	193	43.9		9	1.6	1.8	31.3	2	5.1	2.97	0.65	1.1
Ni	ppm	16.5	<10	<10	<10	<10	<10	<10	<10	<10	<10	<10	<10
Cu	ppm		2220		10.9	17.1	81	0.11	2770	93.2	8370	73.4	0.79
Pb	ppm		3110		27.1	14	120	30	23	221	12.5	34	30
Zn	ppm	41.1	2320	99.4	49.5	120	312	16	184	114	141	181	43.9
S	ppm	326	33000	678	651	406	4610	734	66900	8110	84700	3710	4500
As	ppm	124	174	35.6	2.57	0.01	18.6	0.6	112	48.7	211	13.9	18.3
U	ppm				4.67	3.8	0.53	2.16	3.17	1.05	5.64	5.52	1.09
Cl	ppm				10.4	52.7	51.7	55.8	49.7	107	-13	54.7	181
Mg #		74.3	54.4	83.7	76.1	74.9	78.2	45.5	35.7	78	11.6	73.4	74.4

All elements are recalulated to 100 % anhydrous.

Table A.2 *Pressed pellet X-ray fluorescence (XRF) data for the volcanic and intrusive rock of the Tally Pond Group, Duck Pond area.*

		JP-00-64	JP-00-113	JP-00-97	JP-00-127	JP-00-108	JP-00-120	JP-00-30	JP-00-06	JP-00-156	JP-00-27	JP-00-04	JP-00-07
SiO2	wt%	70.8	60.2	76	71.8	68.9	53	72.7	66.6	78.6	53.8	51.1	45.3
TiO2	wt%	0.17	0.18	0.16	0.12	0.12	0.16	0.24	0.33	0.12	1.2	1.19	33.6
Al2O3	wt%	18.6	16.1	16.2	15.3	10.9	12.7	9.61	14.9	14.6	14.9	14.4	10.2
Fe2O3	wt%	0.37	0.98	0.45	1.21	1.94	1.88	0.64	0.78	0.41	2.08	2.3	0.56
FeO	wt%	1.88	5.01	2.27	6.17	9.89	9.57	3.27	3.97	2.11	10.6	11.7	2.85
MnO	wt%	0.1	0.34	0.01	0.02	0.14	0.27	0.12	0.14	0	0.28	0.29	0.05
MgO	wt%	3.46	14.6	1.13	1.5	6.92	22.2	2.67	3.84	0.78	6.62	9.44	0.75
CaO	wt%	0.09	0.04	0.04	0.03	0.03	0.03	6.56	3.45	0.03	5.93	4.61	1.58
Na2O	wt%	0.23	0.15	0.34	0.21	0	0.2	3.94	4.22	0.2	3.9	4.74	5
K2O	wt%	4.23	2.42	3.34	3.63	1.23	0.07	0.18	1.72	3.22	0.57	0.11	0.09
P2O5	wt%	0.01	0.02	0.01	0.01	0.01	0.01	0.07	0.05	0	0.15	0.11	0.1
Total		100	100	100	100	100	100	100	100	100	100	100	100
Sc	ppm	20	15.5	13.5	8.32	14.6	10.8	15.8	18.6	15	42.3	52.3	25.2
V	ppm	2.5	2.87	5.59	0.38	5.4	9.63	65.8	49.1	1.8	428	543	1.73
Rb	ppm	70.8	44.5	51.8	54.5	19.2	1.14	1.88	38.2	48.9	9.59	1.64	1.27
Ba	ppm	709	1760	1650	1180	476	62.9	78	365	997	408	151	34.4
Sr	ppm	4.93	3.19	9	3.14	1.36	1.62	88.7	55.7	5.64	111	209	44.6
Nb	ppm	6.86	6.46	5.84	4.96	5.08	7.1	3.12	2.01	4.48	3.76	3.47	2.86
Zr	ppm	183	191	155	138	136	171	156	90.3	143	87.6	70.9	102
Y	ppm	43.6	45.5	38.4	25.3	28.3	37.4	42.3	31.4	33	30.3	25.3	32.2
Th	ppm	4.9	5.95	4.34	6.58	5.67	10	0.51	0.3	5.52	1.76	2.03	2.19
Ce	ppm	50.2	50	19	6.7	35.6	48.9	4.2	13	29.8	34.8	2	15.7
Ga	ppm	16.1	22.8	14	12	14.1	40.3	9.26	18.4	13.8	18.4	23.8	15.1
Cr	ppm	4.05	26.8	1.9	1.11	0.54	1.6	39.4	5.17	2.93	8.38	3.5	0.81
Ni	ppm	<10	<10	<10	<10	<10	<10	<10	<10	<10	<10	<10	<10
Cu	ppm	86	33.2	1580	421	7530	134	33.1	2.23	194	11	38.4	1.3
Pb	ppm	8.13	36.2	30	14	8.7	138	35	33	19	27	31	33
Zn	ppm	3.36	176	4.6	3100	117	3780	10	27.9	1960	50.9	74.6	9.6
S	ppm	7880	3160	15900	51000	27900	21400	2190	271	18700	4410	1860	423
As	ppm	140	8.41	6.72	70.7	74.4	119	0.9	10.4	100	55.9	12.6	10.7
U	ppm	4.01	3.22	3.86	3.77	2.39	3.77	2.7	0	0.55	0.47	1.46	3.05
Cl	ppm	45.6	21.8	32.3	20.7	64.1	69.7	92.6	38.3	20.1	13.2	35.9	32.5
Mg #		73.6	81.6	43	26.9	51.4	77.8	55.3	59.5	35.9	48.6	55	28.5

All elements are recalulated to 100 % anhydrous.

Table A.3 *Major and trace element data for the mafic volcanic rocks of the Duck Pond area .*

	Sample	1542501	154502	1542511	1542512	1543029	1543281	1543282	1543283	1543322
SiO2	wt %	58.6	49.2	54.7	37.6	58.7	51.2	54.2	48.6	53.5
TiO2	wt %	1.16	1.13	1.2	1.02	1.19	1.02	0.97	0.95	1.38
Al2O3	wt %	17	16.6	16.5	13.2	15.4	17.4	19.2	18.1	20.7
FeO	wt %	9.56	12.4	10.8	9.21	10.5	9.64	10.9	11.8	9.45
MnO	wt %	0.07	0.25	0.18	0.22	0.12	0.24	0.08	0.2	0.07
MgO	wt %	2.87	8.76	5.79	8.88	5.99	9.68	5.87	9.59	8.32
CaO	wt %	3.87	6.09	6.93	27.2	3.48	4.94	2.42	5.71	0.42
Na2O	wt %	5.47	3.41	3.46	2.08	4.64	2.88	4.99	4.18	5.76
K2O	wt %	1.23	1.92	0.04	0.56	0.11	2.88	1.17	0.85	0.11
P2O5	wt %	0.17	0.19	0.31	0.12	0	0.13	0.11	0.07	0.31
LOI	wt %	2.05	4.42	4.98	15.6	4.98	7.17	6.06	4.62	4.48
Total		102	104	105	116	105	107	106	105	104
Sc	ppm	35	26	25	44	31	44	44	41	35
V	ppm	375	372	375	248	328	388	459	416	328
Rb	ppm	19	14	0	2	6	16	21	8	2
Cs	ppm	2.3	0.16	0.03	0.07	0.07	0.26	0.72	0.55	0.3
Ba	ppm	63	181	41	228	38	498	414	221	38
Sr	ppm	194	218	667	215	55	103	98	194	33
Li	ppm	23.1	19	0	0	10.6	24.4	29.8	36.4	42.9
Ta	ppm	0.15	0.11	0.13	0.11	0.12	0.09	0.14	0.09	0.13
Nb	ppm	2	1.8	1.9	1.5	2	1.1	2.2	1.2	2.2
Hf	ppm	1.47	1.61	1.54	1.43	2.3	1.77	1.94	1.18	2.11
Zr	ppm	45	49	48	33	66	40	56	45	67
Y	ppm	17	20	19	23	19	18	11	15	15
Th	ppm	1.78	0.97	1.24	1.06	1.38	0.88	1.28	0.79	0.98
U	ppm	1.86	0.36	0.47	0.39	0.59	0.8	1.84	0.75	0.73
La	ppm	7.25	6.06	7.06	5.62	5.67	2.58	9.07	3.53	4.62
Ce	ppm	18.3	15.6	17.3	13.1	15	7.81	21.1	8.75	12.4
Pr	ppm	2.56	2.16	2.28	1.85	2.1	1.28	2.82	1.24	1.95
Nd	ppm	11.9	10.2	11	8.92	10.2	6.59	12.1	6.08	10.7
Sm	ppm	3.16	2.89	2.9	2.89	3.29	2.21	3.13	1.69	3.21
Eu	ppm	1.09	1.02	0.96	0.83	1.31	0.82	0.9	0.6	0.97
Gd	ppm	4.12	3.65	3.57	3.69	3.79	2.94	3.26	2.47	3.74
Tb	ppm	0.6	0.57	0.5	0.6	0.52	0.43	0.33	0.38	0.46
Dy	ppm	3.9	3.91	3.72	4.51	3.9	3.41	2.19	2.88	3.33
Ho	ppm	0.76	0.81	0.79	0.93	0.84	0.7	0.48	0.59	0.8
Er	ppm	2.39	2.33	2.22	2.72	2.28	2.11	1.23	1.73	2.46
Tm	ppm	0.26	0.35	0.31	0.38	0.3	0.33	0.19	0.28	0.28
Yb	ppm	1.58	2.36	2.08	2.46	2.22	1.9	1.44	1.78	1.88
Lu	ppm	0.28	0.35	0.31	0.34	0.3	0.27	0.17	0.27	0.27
Mg#		31.9	55.8	48.8	63.2	50.5	64.2	48.9	59.3	61.1

Total is analytical total. All elements recalculated to 100 % anhydrous

Table A.4 *Pressed pellet X-ray fluorescence (XRF) data for the volcanic rocks of the Higher Levels area.*

Sample	171723	171724	171725	171726	171727	171728	171729	171730	171731	171732	171733	171734	171735
SiO2	72.3	54	73.6	78.7	70	76.7	48	59.8	73.3	37.7	68.5	73.2	82.4
TiO2	0.23	0.89	0.28	0.19	0.32	0.25	0.78	1.22	0.26	0.86	0.27	0.29	0.15
Al2O3	12.1	14.8	11.9	11.8	14	12.6	13.6	15.2	12.6	15.4	12.9	14.6	10.6
Fe2O3	2.7	11.9	2.05	2.51	4.1	1.82	10.9	9.13	5.4	9.55	3.29	1.84	0.52
MgO	0.5	3.99	0.46	0.61	1.57	0.5	4.19	5.07	0.75	6.74	2.96	0.52	0.31
MnO	0.15	0.21	0.13	0.04	0.09	0.03	0.17	0.08	0.02	0.24	0.1	0.04	0.03
CaO	3.08	4.21	3.14	0.36	1.74	0.02	10.1	1.24	0.11	10.1	2.42	1.32	0.48
K2O	1.34	0.78	1.63	2.31	1.1	6.1	0.45	0.28	3.17	0.72	1.21	2.57	1.82
Na2O	4.18	2.77	3.79	1.82	4.4	0.01	0.81	3.58	0.58	2.33	4.01	2.92	2.24
P2O5	0.05	0.21	0.06	0.04	0.06	0.05	0.14	0.21	0.05	0.11	0.05	0.05	0.03
LOI	3.2	6.25	3.25	1.75	2.75	1.6	11.3	4.05	3.9	16.5	4.8	2.75	1.55
Total	99.8	100	100	100	100	99.7	100	99.9	100	100	101	100	100
Sc	1.7	12.6	1.6	0.5	2.7	0.5	18.7	16.4	0.5	14.4	0.9	0.5	0.5
V	2	181	3	2	10	2	170	200	5	82	4	2	2
Rb	32	10	24	39	13	111	10	10	50	10	17	35	30
Ba	293	144	217	445	300	1510	106	153	2490	485	652	680	500
Sr	225	74	134	37	198	10	85	28	21	279	76	63	28
Ta	1	2	1	1	2	1	3	3	3	4	3	1	1
Nb	11	21	15	14	23	33	19	13	16	10	19	12	23
Zr	154	61	170	199	166	150	39	87	130	52	123	145	114
Y	53	12	72	61	82	34	10	18	36	12	22	46	21
La	15.7	6.9	14.9	13.5	14.1	18.1	5.6	7.8	6.2	4.2	4.4	19.5	14.8
Cu	3.8	90.9	12.6	3.4	9.6	2.6	34	2.6	14.8	15.2	1.6	22	2.3
Pb	12	2	2	6	8	2	2	2	22	2	5	21	9
Zn	47.7	90.5	21	45.4	94.2	29.1	71.4	80.6	16.1	67.9	92.1	68.8	115
Ag	0.1	0.3	0.1	0.1	0.1	0.1	0.1	0.1	0.5	0.1	0.1	0.1	0.1
Hg	10	7	5	10	6	5	5	5	52	5	9	7	14
As	3	3	4	3	3	8	3	3	165	41	3	11	3
Ni	1	7	1	2	4	1	32	10	3	35	1	2	1
Cr	81	28	85	76	92	72	43	36	81	25	40	27	44
UTMX	523600	523500	523425	523300	523225	523400	523700	523175	523075	523070	523000	523450	523250
UTMY	5377020	5376875	5376800	5376775	5376800	5378150	5376325	5376250	5375875	5375875	5375750	5375350	5375250

Total is analytical total. All elements recalculated to 100 % anhydrous

Table A.4 *Pressed pellet X-ray fluorescence (XRF) data for the volcanic rocks of the Higher Levels area.*

Sample	171736	171737	169110	169111	169112	182564	182565	182566	182567	182568	182569	182570	182571
SiO2	69.4	76.1	69.5	64.4	83.4	67	65.7	66.6	78.1	64.5	64	73.5	69
TiO2	0.62	0.35	0.21	0.49	0.22	0.65	0.73	0.61	0.28	0.52	0.46	0.56	0.31
Al2O3	15.4	12.3	12	16	9.39	14.6	17.5	16.2	11	12.6	14.8	12.5	15.5
Fe2O3	3.79	1.44	5.43	5.73	0.77	5.25	3.19	4.39	3.32	5.62	4.09	3.61	1.77
MgO	1.3	0.66	1.48	2.62	0.06	2.21	1.8	1.89	0.4	1.23	0.92	0.68	1.54
MnO	0.06	0.04	0.1	0.06	0.02	0.09	0.1	0.1	0.02	0.16	0.15	0.07	0.08
CaO	0.26	1.41	1.79	1.7	0.12	1.42	0.36	0.47	0.26	4.5	4.08	0.95	1.95
K2O	0.7	0.68	3.11	2.75	0.04	3.17	6.55	0.51	3.24	2.66	1.41	2.23	3.92
Na2O	6.77	4.44	2	2.2	5.5	1.64	0.9	7.32	0.77	1.59	4.69	2.39	1.04
P2O5	0.15	0.08	0.04	0.1	0.04	0.17	0.15	0.17	0.07	0.17	0.1	0.18	0.07
LOI	1.55	2.4	4.23	4.39	0.77	3.7	2.8	1.3	2.3	6.1	5.8	2.4	4.55
Total	100	99.9	99.9	100	100	99.9	99.8	99.6	99.8	99.7	101	99.1	99.7
Sc	2.1	0.9				1.7	1.2	5.3	0.5	2.1	1.8	1.4	0.7
V	5	2				3	2	8	2	4	2	3	2
Rb	10	10	61	72	15	47	123	10	37	24	21	37	57
Ba	576	260	452	404	142	1220	3780	476	1670	568	396	525	1090
Sr	134	85				66	14	113	10	61	89	67	105
Ta	1	3				1	1	1	1	1	1	1	1
Nb	10	12	2	2	2	19	18	13	16	10	10	15	10
Zr	125	112	138	204	121	105	123	143	104	88	122	76	151
Y	53	34	14	15	12	31	43	45	23	30	30	18	51
La	17.6	16.8				13.7	11.7	12.9	9.4	15.7	21.7	19.9	21
Cu	1.6	2.5	7	11	3	2.9	6.2	2.2	5.7	2.3	49.3	3.5	3.5
Pb	2	3	2	12	5	2	11	2	9	4	4	2	9
Zn	108	14.4	153	176	12	109	104	111	29.9	105	133	84.7	111
Ag	0.1	0.1				0.2	0.4	0.1	2.1	0.2	0.3	0.1	0.1
Hg	5	5	43	41	18	5	23	5	39	9	17	5	7
As	3	3	37	3	37	3	57	3	73	3	3	3	3
Ni	1	1				1	1	1	2	1	1	1	1
Cr	29	35	10	10	11	40	92	44	93	40	66	85	49
UTMX	522650	523625	523175	522940	523250	522900	522690	522650	523120	523230	522880	522950	523170
UTMY	5375300	5375300	5377950	5377490	5377575	5374420	5374900	5375300	5374950	5374890	5374670	5374600	5375450

Total is analytical total. All elements recalculated to 100 % anhydrous

Table A.4 *Pressed pellet X-ray fluorescence (XRF) data for the volcanic rocks of the Higher Levels area.*

Sample	182572	182573	182575	182576	182577	182586	182587	182588
SiO2	75.7	73.3	41.7	48.2	47.7	75.5	75	69.6
TiO2	0.18	0.22	0.68	1.02	0.59	0.21	0.29	0.26
Al2O3	10.9	12.6	15.6	14.8	13.7	13.5	12.4	13.3
Fe2O3	4.05	2.65	8.72	10.8	8.18	1.65	2.57	2.36
MgO	1.55	0.53	5.54	7.53	7.78	0.24	0.9	1.04
MnO	0.07	0.05	0.18	0.16	0.11	0.05	0.06	0.11
CaO	0.66	1.32	10.6	4.65	6.58	0.58	0.86	3.17
K2O	0.78	0.45	1.6	0.12	0.2	1.86	0.32	0.28
Na2O	3.42	5.93	1.8	2.51	1.92	4.85	6.39	6.87
P2O5	0.05	0.06	0.09	0.13	0.08	0.06	0.07	0.11
LOI	2.95	2.1	13.3	9.85	12.9	1.45	1.1	2.9
Total	100	99.2	99.8	99.8	99.7	100	100	100
Sc	1.3	1.4	10.4	25	22.7	0.5	2.5	2.5
V	2	6	79	213	117	2	4	13
Rb	10	10	22	10	24	55	18	13
Ba	397	265	317	131	128	547	164	207
Sr	73	68	101	153	146	71	119	107
Ta	1	1	1	1	1	1	1	1
Nb	16	10	10	11	10	28	13	14
Zr	126	117	36	47	22	190	164	188
Y	41	19	19	21	10	23	45	29
La	19.3	9.1	6.3	7.9	4.2	26.3	7	34
Cu	4.9	116	84.1	9.5	113	5.4	4.5	9.1
Pb	2	18	2	2	2	29	2	2
Zn	73.5	116	65	69.7	46	6.2	13.6	27.3
Ag	0.2	0.3	0.4	0.2	0.2	0.1	0.1	0.1
Hg	5	11	5	5	5	5	5	5
As	3	12	46	4	58	3	3	3
Ni	3	7	68	18	47	1	2	1
Cr	91	10	18	43	65	62	56	67
UTMX	523330	523450	524070	524190	524090	525200	524330	524680
UTMY	5375430	5375430	5375970	5375850	5375550	5378250	5379440	5379760

Total is analytical total. All elements recalculated to 100 % anhydrous

Table A.4 *Pressed pellet X-ray fluorescence (XRF) data for the volcanic rocks of the Higher Levels area.*

Sample	133231	133232	133233	115323	115321	115322	171716	171717	171718	171719	171720	171721	171722
SiO2	50.1	41.6	66.7	61.2	67.7	43	76.7	75.3	78.6	56	74.3	72.7	72.2
TiO2	0.58	0.59	0.35	0.52	0.45	0.67	0.25	0.31	0.32	1.44	0.28	0.3	0.32
Al2O3	15.2	17.9	15.2	17.8	14.4	16.9	12.1	10	11.6	18.6	11.8	13.7	13.5
Fe2O3	9.04	5.97	3	5.31	4.1	9.44	1.89	4.69	1.4	7.59	3.56	3.97	1.78
MgO	7.13	4.48	1.09	2.76	2.58	3.9	0.41	1.82	0.21	2.63	1.44	1.83	0.75
MnO	0.09	0.16	0.08	0.06	0.05	0.14	0.06	0.07	0.03	0.11	0.08	0.08	0.09
CaO	3.21	8.62	1.84	1.25	1.26	7.14	1.27	1.47	0.24	2.44	1.04	0.68	2.27
K2O	0.76	3.93	1.42	1.81	0.92	3.47	1.5	0.28	0.3	3.25	1.07	1.74	0.29
Na2O	3.39	1.03	5.14	4.48	4.73	1.3	4.52	3.82	6.41	1.22	3.4	2.82	6.91
P2O5	0.11	0.08	0.06	0.11	0.11	0.12	0.05	0.06	0.06	0.04	0.05	0.06	0.06
LOI	9.54	15.6	4.7	3.93	3	9.54	1.55	2.3	0.65	5.3	2.5	2.45	2.15
Total	99.2	100	99.6	99.2	99.3	95.6	100	100	99.8	98.6	99.5	100	100
Sc							0.5	4	1.6	6.7	1.3	1.3	2.2
V							2	4	2	87	4	3	2
Rb	24	72	39	60	27	80	35	11	10	75	22	28	13
Ba	358	431	299	377	271	286	298	120	130	401	222	318	113
Sr							101	62	170	75	131	117	174
Ta							4	2	1	3	4	1	3
Nb	1	1	2	2	1	1	16	10	22	10	13	10	19
Zr	85	27	226	223	183	32	160	157	165	69	160	182	182
Y							40	70	61	10	30	53	49
La							14.3	9.3	10.1	6.4	9.4	11	11
Cu	63.4	104	2	46.5	9.2	77.1	3.9	4.7	5	46.9	4.6	3.9	4.1
Pb	6	2	2	2	2	5	2	2	2	3	10	11	8
Zn	95.6	68.2	58.6	44.8	87.7	57.9	43.3	137	35.2	73.2	72.6	86	32.8
Ag							0.1	0.1	0.1	0.1	0.2	0.1	0.1
Hg	13	11	9	3	3	10	10	6	8	6	8	7	6
As	21	54	3	8	9	25	3	3	3	3	41	3	3
Ni							2	1	2	1	4	1	2
Cr	27	17	18	23	23	12	93	12	15	26	77	69	10
UTMX	523025	523025	523025	523000	523000	523000	522900	522800	523075	523050	523175	523325	523300
UTMY	5377300	5377300	5377300	5377450	5377430	5377420	5378230	5378100	5377950	5377850	5377450	5377400	5377350

Total is analytical total. All elements recalculated to 100 % anhydrous

Table A.5 *Major and trace element data for the volcanic rocks of the Lemarchant-Spencer's Pond area.*

Sample	171715	171701	171702	171703	171704	171705	171706	171707	171708	171709	171710	171711	171712
SiO2	69.20	53.80	76.90	83.30	81.00	69.20	70.80	68.80	71.40	73.50	72.10	75.60	76.00
TiO2	0.38	0.68	0.46	0.30	0.25	0.52	0.43	0.39	0.41	0.35	0.43	0.27	0.30
Al2O3	15.30	18.40	10.90	9.27	11.40	13.90	18.10	14.80	16.80	15.10	15.90	14.70	15.00
Fe2O3	3.73	9.00	5.04	1.47	0.79	5.14	2.10	3.84	2.58	3.26	3.24	2.44	1.91
MgO	0.73	3.27	0.61	0.46	0.34	2.98	0.25	2.05	0.40	0.49	0.46	0.32	0.32
MnO	0.16	0.12	0.08	0.03	0.07	0.12	0.01	0.06	0.03	0.08	0.04	0.09	0.03
CaO	2.40	2.77	0.46	0.49	0.36	0.57	0.02	2.97	0.15	0.09	0.21	0.03	0.05
K2O	3.46	2.98	1.50	1.65	2.88	0.99	4.81	2.07	4.53	3.86	4.35	3.90	3.93
Na2O	0.49	2.72	0.41	0.15	0.70	3.67	0.26	1.98	0.18	0.17	0.17	0.14	0.18
P2O5	0.14	0.27	0.13	0.05	0.10	0.16	0.05	0.09	0.16	0.11	0.17	0.04	0.05
LOI	3.95	5.82	2.65	1.80	1.85	2.70	3.10	2.70	3.05	3.00	3.15	2.60	2.55
Total	99.94	99.83	99.14	98.97	99.74	99.95	99.93	99.75	99.69	100.01	100.22	100.13	100.32
Sc	0.6	2.8	2.2	0.5	0.5	3.4	0.5	1.0	0.5	0.5	0.5	0.5	0.5
V	9	54	25	3	2	60	5	16	5	6	5	3	3
Rb	119	56	33	46	40	25	170	46	171	131	176	135	132
Ba	1430	1130	381	407	2360	449	1040	503	702	857	760	992	986
Sr	52	83	46	10	10	68	24	280	34	35	17	17	32
Ta	2	1	1	2	1	3	1	2	4	2	1	1	1
Nb	16	10	16	29	27	12	22	10	20	20	10	10	23
Zr	180	50	36	202	90	43	228	92	194	204	207	215	222
Y	14	20	19	43	32	10	22	16	10	14	10	21	10
La	24.9	16.8	5.5	11.9	12.6	7.3	24.2	7.2	21.2	20.7	21.3	24.7	25.2
Cu	4.7	8.2	3200.0	11.7	9.5	7.6	10.1	10.2	6.9	9.5	41.0	9.1	9.0
Pb	2	2	2	2	18	2	27	2	16	5	5	2	11
Zn	91.9	69.7	53.9	19.6	27.0	84.9	7.1	55.0	29.3	51.4	49.3	37.1	34.4
Ag	0.3	0.1	0.5	0.1	0.1	0.1	0.1	0.1	0.1	0.1	0.1	0.1	0.1
Hg	6	5	40	6	7	9	11	7	41	9	8	18	17
As	3	3	4	3	3	3	9	3	3	3	5	3	3
Co	5	17	11	2	1	13	1	6	3	5	4	4	2
Ni	2	5	13	2	2	9	1	1	2	1	1	3	1
Cr	81.00	55.00	15.00	14.00	99.00	12.00	68.00	78.00	78.00	92.00	97.00	80.00	85.00
UTMX	518670	520000	520100	520200	519760	519240	520400	520300	520500	520530	520940	521050	521110
UTMY	5372670	5371800	5372060	5372320	5372650	5372890	5372380	5372550	5372420	5372390	5372700	5372600	5372580

Total is analytical total. All elements recalculated to 100 % anhydrous

Table A.5 *Pressed pellet X-ray fluorescence (XRF) data for the volcanic rocks of the Lemarchant-Spencer's Pond area.*

Sample	171713	171714	182540	182541	182542	182543	182544	182545	182546	182547	182548	182549	182550
SiO2	72.90	74.80	73.60	71.20	48.10	55.20	68.30	71.70	70.40	69.20	77.20	68.00	76.00
TiO2	0.32	0.38	0.34	0.36	0.58	0.18	0.56	0.41	0.55	0.64	0.14	0.46	0.24
Al2O3	16.20	14.10	15.20	16.10	19.30	6.72	16.90	16.10	16.50	16.30	12.00	13.30	13.20
Fe2O3	2.05	3.03	2.94	3.61	9.40	7.59	4.72	3.96	3.09	3.31	1.45	4.28	1.77
MgO	0.42	0.20	0.43	0.55	4.97	3.72	0.28	0.85	0.53	0.77	0.71	0.41	0.81
MnO	0.02	0.01	0.02	0.12	0.19	0.39	0.02	0.06	0.04	0.07	0.03	0.17	0.04
CaO	0.08	0.12	0.31	0.33	5.51	10.20	0.29	0.66	0.67	1.59	0.65	3.50	0.29
K2O	4.47	3.75	4.36	4.38	0.42	1.59	3.48	2.52	2.41	3.65	0.05	2.24	4.49
Na2O	0.15	0.29	0.26	0.36	4.99	0.28	1.05	1.00	3.48	1.81	6.75	2.88	0.68
P2O5	0.04	0.11	0.14	0.15	0.13	0.12	0.14	0.24	0.12	0.21	0.04	0.16	0.04
LOI	2.70	3.00	2.45	2.75	5.50	12.40	4.10	2.55	2.35	2.75	0.60	2.80	1.60
Total	99.35	99.79	100.05	99.91	99.09	98.39	99.84	100.05	100.14	100.30	99.62	98.20	99.16
Sc	0.5	0.5	0.5	0.6	7.1	1.8	0.9	1.0	1.2	1.6	4.0	1.3	0.5
V	3	5	5	5	135	15	4	7	6	5	11	3	2
Rb	162	132	187	166	30	41	114	67	38	93	10	56	152
Ba	941	992	1200	791	214	424	1170	1070	2060	2310	174	536	1550
Sr	21	22	10	34	356	33	33	36	100	51	135	55	10
Ta	1	1	2	1	1	1	1	1	1	1	1	1	1
Nb	435	13	16	10	21	24	16	14	19	10	11	12	30
Zr	234	177	198	195	21	14	96	111	121	82	204	80	249
Y	17	10	12	14	10	10	33	15	27	27	51	17	21
La	30.6	18.2	31.9	24.3	5.2	5.0	8.1	23.0	14.1	10.4	12.4	8.1	35.6
Cu	4.2	11.3	5.9	7.4	145.0	24.5	22.5	4.1	8.2	7.9	4.1	5.1	2.7
Pb	4	8	5	5	2	39	22	2	7	9	2	4	14
Zn	24.4	5.5	29.8	76.0	71.2	151.0	25.7	40.9	73.6	37.0	4.6	58.7	5.6
Ag	0.1	0.1	0.1	0.3	0.3	0.6	0.4	0.1	0.3	1.0	0.1	0.2	0.1
Hg	5	11	5	5	5	24	52	5	11	5	5	7	5
As	3	3	25	3	3	3	4	3	13	66	3	3	3
Co	1	6	1	3	28	14	8	4	3	6	6	2	1
Ni	1	2	1	2	14	9	1	9	1	1	2	1	1
Cr	87.00	12.00	10.00	98.00	51.00	61.00	86.00	80.00	87.00	39.00	11.00	59.00	53.00
UTMX	521180	518980				522800	522640	522220					521590
UTMY	5372620	5372750				5373500	5373250	5372920					5376200

Total is analytical total. All elements recalculated to 100 % anhydrous

Table A.5 *Pressed pellet X-ray fluorescence (XRF) data for the volcanic rocks of the Lemarchant-Spencer's Pond area.*

Sample	182551	182552	182556	182562	182563	182593	182594
SiO2	69.00	77.60	80.40	73.30	71.80	72.00	76.30
TiO2	0.25	0.22	0.09	0.56	0.56	0.35	0.26
Al2O3	12.00	12.30	5.65	13.30	13.50	15.20	14.10
Fe2O3	2.71	1.63	4.98	2.75	3.19	4.20	2.12
MgO	1.14	0.26	1.15	0.50	0.38	0.36	0.38
MnO	0.11	0.04	0.17	0.05	0.06	0.04	0.04
CaO	4.23	1.04	2.04	1.33	1.42	0.27	0.21
K2O	0.40	2.72	0.79	0.05	1.29	3.88	4.02
Na2O	5.82	2.20	0.61	7.49	5.38	0.60	0.28
P2O5	0.07	0.06	0.06	0.14	0.15	0.14	0.06
LOI	3.95	1.65	3.50	0.95	2.35	3.10	2.60
Total	99.68	99.72	99.44	100.42	100.08	100.14	100.37
Sc	2.5	0.6	0.5	6.7	1.9	0.5	0.5
V	7	2	7	8	5	4	2
Rb	10	73	14	10	33	131	144
Ba	181	634	492	125	710	1850	998
Sr	145	90	55	110	91	53	24
Ta	1	1	1	1	1	1	1
Nb	24	15	12	15	10	32	24
Zr	151	167	50	96	101	184	217
Y	44	42	11	46	31	10	12
La	11.7	12.3	7.8	12.1	13.9	23.9	34.4
Cu	3.8	6.3	824.0	4.8	2.9	28.1	2.9
Pb	2	23	18	2	2	23	16
Zn	8.3	24.9	142.0	44.7	27.5	38.6	33.9
Ag	0.1	0.1	1.2	0.1	0.1	2.5	0.1
Hg	5	11	6	5	5	9	5
As	3	9	16	3	3	11	3
Co	5	1	8	2	5	8	1
Ni	1	1	4	2	1	2	1
Cr	62.00	11.00	21.00	14.00	96.00	30.00	27.00
UTMX	521480	521470	522880	522600	522520	523440	
UTMY	5376130	5375770	5373950	5374560	5374520	5374360	

Total is analytical total. All elements recalculated to 100 % anhydrous

Table A.6 *Pressed pellet X-ray fluorescence (XRF) data for the volcanic rocks of the Rogerson Lake Beaver Pond area.*

Sample	171738	171739	171740	171741	171742	171743	171744	171745	171746	171747	171748	171749	171750
SiO2	74.50	61.20	77.10	75.10	81.60	62.70	76.30	74.50	59.00	56.40	48.30	78.80	79.40
TiO2	0.20	0.34	0.16	0.18	0.20	1.17	0.24	0.36	1.46	0.95	1.33	0.15	0.16
Al2O3	12.60	22.40	12.00	12.60	10.70	14.50	13.50	13.70	14.50	19.80	14.30	10.60	10.20
Fe2O3	3.44	3.12	3.05	3.43	1.49	6.53	2.46	2.53	7.56	6.96	10.70	2.35	2.68
MgO	3.00	2.26	1.19	0.55	0.81	2.85	0.37	1.35	5.27	4.05	4.75	0.60	0.76
MnO	0.05	0.04	0.05	0.07	0.05	0.13	0.03	0.03	0.24	0.13	0.19	0.11	0.09
CaO	0.23	0.12	0.47	0.70	0.09	3.07	0.05	0.19	1.30	0.50	7.74	0.21	0.68
K2O	1.30	3.75	1.57	1.75	1.65	1.28	2.51	1.08	0.07	1.55	0.04	0.21	0.63
Na2O	2.53	3.52	2.54	3.93	1.51	3.22	2.68	4.71	4.93	6.12	4.05	5.83	4.54
P2O5	0.03	0.04	0.02	0.04	0.03	0.14	0.04	0.05	0.19	0.35	0.19	0.03	0.03
LOI	2.35	3.10	2.00	1.90	1.75	4.50	1.80	1.75	3.60	3.45	7.95	1.00	1.15
Total	100.23	99.89	100.15	100.25	99.88	100.09	99.98	100.25	98.12	100.26	99.54	99.89	100.32
Sc	2.2	1.5	1.0	1.4	0.5	6.3	0.8	1.0	18.5	2.8	26.2	1.6	1.7
V	4	2	2	2	2	98	2	3	249	41	289	2	3
Rb	25	58	21	20	28	25	55	21	10	25	10	10	16
Ba	374	1480	429	223	772	965	1280	457	124	789	66	597	344
Sr	119	83	43	26	46	107	17	40	53	67	96	123	89
Ta	5	1	1	1	1	1	2	1	3	2	3	1	3
Nb	16	10	14	19	11	10	20	12	17	10	16	21	10
Zr	148	267	161	113	109	99	244	214	78	165	57	119	122
Y	66	112	52	46	25	23	56	27	47	38	18	53	65
La	5.6	17.1	7.6	8.4	7.9	6.4	18.2	19.5	4.0	11.1	7.7	7.4	6.2
Cu	3.2	2.9	1.5	1.5	2.0	27.5	1.1	1.6	6.8	13.9	8.9	24.3	12.8
Pb	2	2	2	2	7	2	2	2	4	2	2	15	5
Zn	88.0	102.0	54.3	66.4	36.9	54.1	44.4	33.7	178.0	102.0	110.0	51.0	119.0
Ag	0.2	0.1	0.1	0.1	0.1	0.1	0.1	0.1	0.1	0.1	0.1	0.1	0.1
Hg	9	10	5	5	5	5	5	5	5	14	5	16	38
As	3	3	3	3	3	8	3	3	11	3	3	3	3
Ni	1	1	1	1	1	9	1	1	4	1	4	1	1
Cr	31.00	12.00	28.00	35.00	28.00	22.00	30.00	37.00	17.00	13.00	10.00	57.00	72.00
UTMX	523540	523640	522940	522620	522780	522830	522890	522800	521970	521120	520680	520480	520420
UTMY	5380950	5380850	5380525	5379970	5380350	5380280	5380670	5380910	5380370	5380040	5379730	5379400	5379340

Total' is analytical total. All elements recalculated to 100 % anhydrous

Table A.6 *Pressed pellet X-ray fluorescence (XRF) data for the volcanic rocks of the Rogerson Lake Beaver Pond area.*

Sample	171751	171752	171753	171754	171755	171756	171757	171758	171759	182553	182554	182555	182557
SiO2	75.40	76.50	54.80	70.30	60.20	74.60	74.10	65.70	77.80	78.00	68.80	75.20	76.00
TiO2	0.19	0.27	1.11	0.56	0.63	0.30	0.29	0.35	0.27	0.12	0.30	0.20	0.25
Al2O3	12.00	12.30	17.00	12.90	14.70	13.10	12.80	14.00	13.30	11.70	13.00	13.30	12.80
Fe2O3	3.11	2.22	10.20	4.33	8.12	2.40	1.55	6.22	1.60	1.46	4.86	1.52	3.50
MgO	2.03	1.11	6.75	2.68	2.34	1.10	0.72	2.35	0.60	0.75	2.88	0.69	0.20
MnO	0.07	0.04	0.18	0.15	0.24	0.10	0.07	0.07	0.02	0.04	0.08	0.04	0.09
CaO	0.11	0.10	0.26	1.34	4.30	1.06	0.48	2.29	0.03	0.97	3.25	1.51	1.36
K2O	1.09	0.10	0.06	1.81	2.11	2.37	5.70	1.58	2.75	0.34	0.06	0.17	1.40
Na2O	3.98	6.61	4.42	2.52	2.48	2.25	3.03	2.64	1.85	5.52	4.44	6.96	1.49
P2O5	0.03	0.05	0.15	0.13	0.14	0.06	0.08	0.07	0.03	0.04	0.06	0.06	0.06
LOI	1.85	1.00	5.10	3.45	5.10	2.60	0.90	3.65	1.90	0.95	2.35	0.75	2.80
Total	99.86	100.30	100.03	100.17	100.36	99.94	99.72	98.92	100.15	99.89	100.08	100.40	99.95
Sc	0.8	4.6	20.4	2.4	6.2	0.5	1.3	3.8	0.5	2.1	4.6	1.3	1.5
V	2	5	226	7	23	4	5	23	2	2	24	12	2
Rb	39	10	10	19	28	52	57	22	38	14	10	10	28
Ba	569	137	138	259	298	413	2080	377	950	204	102	251	561
Sr	56	47	99	40	77	34	43	73	29	147	190	170	282
Ta	2	1	5	2	2	1	1	3	1	1	1	1	1
Nb	27	10	10	15	10	20	11	10	12	19	18	10	10
Zr	205	204	78	65	24	127	164	44	241	207	181	96	146
Y	59	60	47	45	25	13	34	17	68	48	56	12	43
La	12.1	14.8	5.1	4.7	3.8	9.6	11.8	2.7	8.2	4.8	5.5	8.5	18.7
Cu	3.6	1.1	207.0	7.7	1.8	2.3	69.8	173.0	6.2	4.2	2.1	3.8	4.5
Pb	2	2	2	2	2	3	100	2	2	2	2	2	2
Zn	29.1	13.2	701.0	71.8	101.0	44.4	294.0	34.4	7.9	9.1	17.5	5.7	22.0
Ag	0.1	0.1	0.2	0.1	0.1	0.1	0.2	0.1	0.1	0.1	0.1	0.1	0.2
Hg	6	5	32	6	6	5	59	15	11	5	5	5	5
As	3	3	3	3	3	3	3	3	3	3	3	3	3
Ni	1	1	5	1	1	1	1	1	9	2	51	2	2
Cr	57.00	45.00	14.00	37.00	15.00	35.00	85.00	31.00	48.00	14.00	17.00	11.00	80.00
UTMX	520250	520750	521850	525070	525400	521460	521060	524410	523300	518750	518610	518590	525200
UTMY	5379030	5379100	5380280	5381980	5382175	5380430	5377360	5381120	5379950	5374800	5374670	5374560	5375230

Total' is analytical total. All elements recalculated to 100 % anhydrous

Table A.6 *Pressed pellet X-ray fluorescence (XRF) data for the volcanic rocks of the Rogerson Lake Beaver Pond area.*

Sample	182558	182561	182580	182581	182582	182583	182584	182585	182589	182590	182591	182592	182595
SiO2	70.10	63.50	80.00	71.30	68.50	78.20	77.70	73.30	69.50	64.80	75.00	69.00	48.30
TiO2	0.39	0.61	0.10	0.26	0.61	0.15	0.22	0.16	0.30	0.56	0.29	0.70	0.40
Al2O3	15.70	17.30	11.10	13.30	14.80	11.50	13.50	11.30	14.70	15.30	13.20	12.40	13.50
Fe2O3	4.91	6.57	0.78	3.28	4.91	1.55	0.68	2.26	4.46	6.07	2.20	8.41	8.36
MgO	0.30	0.98	0.18	0.65	1.45	0.30	0.09	1.01	2.59	3.32	0.35	1.09	13.70
MnO	0.04	0.09	0.02	0.08	0.08	0.04	0.03	0.15	0.08	0.11	0.05	0.22	0.30
CaO	0.29	1.62	0.36	2.22	0.58	0.30	0.27	2.55	0.65	1.88	0.55	0.29	4.87
K2O	3.81	2.65	0.73	1.65	0.16	0.22	1.70	1.76	1.88	1.97	3.88	2.13	0.34
Na2O	1.15	3.11	5.92	4.72	7.05	6.66	4.41	3.90	3.12	2.31	3.24	2.24	0.93
P2O5	0.13	0.24	0.04	0.07	0.19	0.04	0.06	0.04	0.12	0.14	0.07	0.13	0.05
LOI	3.45	3.55	0.65	2.70	1.90	1.00	1.45	3.50	2.70	3.80	1.40	3.35	9.25
Total	100.27	100.22	99.88	100.23	100.23	99.96	100.11	99.93	100.10	100.26	100.23	99.96	100.00
Sc	1.0	3.6	0.5	1.1	11.7	2.2	1.2	0.6	2.2	3.6	0.5	2.6	24.0
V	6	22	2	2	19	3	2	2	11	3	2	8	105
Rb	120	83	28	32	16	13	31	32	56	47	53	57	10
Ba	2100	1370	534	478	178	395	259	454	466	344	759	1240	176
Sr	81	131	86	98	104	62	41	79	101	127	88	45	52
Ta	1	1	1	1	1	1	1	1	1	1	1	1	2
Nb	18	14	17	24	15	16	14	18	17	15	18	40	16
Zr	186	154	75	178	150	161	113	161	197	172	153	456	18
Y	30	20	15	55	43	41	62	23	74	47	26	69	11
La	20.9	33.2	12.4	14.4	13.8	9.9	8.8	10.0	18.0	7.6	14.0	31.5	3.4
Cu	15.6	147.0	3.9	72.5	1.8	5.7	4.2	4.6	1.9	0.9	0.7	9.4	97.2
Pb	11	3	2	2	2	2	2	8	7	2	2	5	2
Zn	41.9	141.0	0.5	26.6	69.5	8.7	6.1	52.6	119.0	121.0	16.1	119.0	31.0
Ag	2.4	0.2	0.1	0.1	0.1	0.1	0.1	0.2	0.1	0.2	0.1	0.2	0.4
Hg	30	5	5	5	5	5	5	14	9	5	5	5	5
As	3	3	3	3	3	3	3	4	3	3	3	3	115
Ni	3	16	1	1	1	1	1	1	1	1	1	9	233
Cr	11.00	12.00	53.00	29.00	40.00	67.00	48.00	36.00	21.00	25.00	37.00	38.00	73.00
UTMX	525470	525500	522700	523070	523255	523140		522840					
UTMY	5375340	5375300	5379080	5379340	5379595	5379590		5378560					

Total' is analytical total. All elements recalculated to 100 % anhydrous

Table A.6 *Major and trace element data for the volcanic rocks of the Rogerson Lake Beaver Pond area.*

Sample	182596	182597	182598	182599	182600	143813	143814	143815	143816	143817	143818
SiO2	77.90	46.10	75.80	72.60	69.30	76.90	74.50	62.00	75.10	78.70	50.50
TiO2	0.25	0.61	0.22	0.24	0.58	0.24	0.27	0.58	0.27	0.56	0.70
Al2O3	11.10	15.00	12.70	13.60	14.90	9.64	11.20	16.30	12.40	9.42	15.60
Fe2O3	1.48	7.62	1.79	3.06	4.11	4.57	4.49	4.83	2.53	4.92	8.91
MgO	0.40	7.44	0.16	0.47	1.31	2.19	1.32	2.38	0.32	0.25	9.12
MnO	0.09	0.22	0.04	0.07	0.09	0.14	0.11	0.09	0.05	0.05	0.21
CaO	1.03	6.32	0.43	0.38	0.72	1.27	1.97	2.30	0.31	0.24	5.10
K2O	0.90	1.14	0.54	3.95	1.05	1.12	2.00	4.58	2.90	1.90	0.69
Na2O	5.64	4.14	7.07	4.66	6.83	2.39	2.31	3.89	5.12	1.34	4.39
P2O5	0.07	0.11	0.05	0.06	0.16	0.08	0.08	0.18	0.06	0.09	0.11
LOI	1.15	11.50	0.95	1.10	1.25	1.75	2.12	1.85	0.75	2.35	3.85
Total	100.01	100.20	99.75	100.19	100.30	100.29	100.37	98.98	99.81	99.82	99.18
Sc	1.0	9.2	1.1	2.0	3.6	1.3	1.7	3.0	2.2	1.5	4.4
V	2	66	2	3	6	5	3	37	4	6	102
Rb	22	23	10	41	10	20	46	81	20	60	10
Ba	630	523	291	898	397	286	326	2040	932	2280	420
Sr	98	137	70	50	102	95	311	210	52	69	137
Ta	1	1	1	1	1	1	1	1	1	1	1
Nb	32	34	21	10	12	10	27	23	15	39	17
Zr	154	120	166	208	152	120	153	300	181	220	64
Y	25	24	57	57	49	25	39	14	43	23	10
La	19.7	5.6	9.7	16.8	20.1	5.0	6.8	25.6	18.0	18.6	6.1
Cu	12.2	49.4	25.4	2.7	1.3	4.7	6.8	40.6	7.6	34.5	61.5
Pb	7	2	6	26	2	5	2	8	2	4	2
Zn	70.6	73.9	25.5	56.7	68.3	101.0	63.8	32.7	22.5	56.1	57.7
Ag	0.1	0.3	0.1	0.1	0.2	0.1	0.1	0.1	0.1	0.1	0.1
Hg	12	5	5	5	9	5	5	5	5	8	5
As	3	15	37	3	3	3	3	3	3	35	3
Ni	3	66	1	1	1	1	2	7	1	24	110
Cr	75.00	16.00	56.00	48.00	41.00	55.00	13.00	13.00	10.00	13.00	30.00

Total' is analytical total. All elements recalculated to 100 % anhydrous

Table A.7 *Major and trace element data for the volcanic rocks of the South Tally Pond area.*

Sample	STP.01	STP.02	STP.03	STP.04	STP.05	STP.06	STP.07	ST.01-01
SiO2	75.3	76.7	75.6	77.5	77.1	75.1	75.8	68
Al2O3	14.2	13.4	14.1	13.7	12.8	15.2	13.1	18.1
CaO	0.11	0.12	0.13	0.08	0.15	0.08	0.13	0.17
MgO	0.22	0.36	0.31	0.29	0.3	0.21	0.33	0.59
Na2O	0.35	0.35	0.3	0.32	0.35	0.36	0.41	0.76
K2O	4.05	3.77	4.11	3.9	3.6	4.44	3.49	2.76
Fe2O3	2.53	2.48	2.42	1.58	2.8	1.71	3.41	4.57
MnO	0.01	0.01	0.01	0.01	0.01	0.01	0.04	0.12
TiO2	0.34	0.31	0.33	0.24	0.24	0.24	0.29	0.88
P2O5	0.09	0.1	0.11	0.03	0.09	0.04	0.1	0.15
Cr2O3	0.01	0.01	0.01	0.01	0.01	0.01	0.02	0.01
LOI	2.9	2.45	2.5	2.45	2.65	2.5	2.9	2.88
Total	100	100	99.9	100	100	99.9	100	99
Sc	0	0	0	0	0	0	0	2.5
V	3.39	3.59	2.67	1	2.18	1.11	3.08	14
Rb	148	138	158	137	127	154	113	0
Ba	823	721	909	758	705	625	634	806
Sr	25	24	23	24	25	27	23	5
Ta	0	0	0	0	0	0	0	5
Nb	7	7	8	11	9	14	6	8
Zr	163	165	166	193	172	221	162	268
Y	14	12	13	20	35	22	15	29
La	11.9	14.9	18.1	21.7	14.1	29.2	11.7	27
Ce	22.6	29.7	29.3	42	27.2	59.2	19.3	0
Au	5	11	8	5	13	5	5	2.5
Fe	1.17	1.08	1	0.66	1.43	0.48	2.05	1.85
P	0.05	0.05	0.06	0.02	0.06	0.02	0.06	
Hg	1	1	1	1	1	1	1	
Mg	0.06	0.12	0.1	0.11	0.1	0.04	0.13	0.2
As	10	7.16	70.5	7.51	11	5	36.6	10
Na	0.14	0.15	0.12	0.11	0.12	0.14	0.17	0.14
Mo	2.25	1	2.37	1.21	9.58	1.18	1.8	0.5
Al	0.56	0.62	0.55	0.57	0.61	0.57	0.68	1.66
Be	0.5	0.5	0.5	0.5	0.5	0.5	0.5	
Ca	0.03	0.03	0.04	0.01	0.05	0.01	0.04	0.11
Zn	19.6	33.6	18.4	22.7	17.8	11.7	35.6	31
Cu	24.6	13.7	6.75	5.92	8.58	5.59	10.4	2
Sb	5	5	5	5	5	5	5	2.5
Ag	0.2	0.2	0.2	0.2	0.2	0.2	0.2	0.1
Pb	5.54	6.28	4.47	2	9.02	2	5.13	1
Bi	2.02	2.74	2	2.2	7.9	5.14	4.78	2.5
Ti	2010	1880	1970	1430	1410	1440	1730	5280
Cd	0.59	1.21	0.8	0.5	0.5	0.5	1.23	0.1
Co	3.14	1.83	4.17	2.79	11	2.04	7.07	3
Ni	1.24	2	1.99	1.73	2.83	1.94	3.16	6
W	10	10	10	10	10	10	10	10
K	33600	31300	34100	32400	29900	36900	29000	22900
Mn	76.4	47.2	52.6	47	89.7	56.1	295	334
Cr	75.2	86	72.3	51.5	43.9	44.9	83.8	44

Total is analytical total. All elements recalculated to 100 % anhydrous

Table A.7 *Pressed pellet X-ray fluorescence (XRF) data for the volcanic rocks of the South Tally Pond area.*

Sample	ST.01-02	ST.01-03	ST.01-04	ST.01-05	ST.01-06	ST.01-07	ST.01-08
SiO2	65.3	75.6	68.9	62.4	61.3	63.7	65.5
Al2O3	18.2	14.5	16	18.7	19.7	20.7	18.3
CaO	0.26	0.02	0.33	0.17	0.5	0.09	0.29
MgO	0.93	0.27	0.17	0.39	0.77	0.81	0.28
Na2O	0.91	0.15	1.14	1.06	0.9	0.41	0.66
K2O	3.29	4.19	3.12	2.38	2.81	1.44	3.59
Fe2O3	5.45	1.73	4.36	8.5	8.21	8.1	5.89
MnO	0.04	0.01	0.02	0.08	0.15	0.18	0.07
TiO2	1.08	0.27	0.59	1.23	0.79	0.93	0.69
P2O5	0.21	0.05	0.17	0.16	0.31	0.09	0.25
Cr2O3	0.01	0.01	0.01	0.02	0.01	0.01	0.01
LOI	3.34	2.18	4.22	4.27	3.66	2.97	3.77
Total	99.1	99	99	99.4	99.1	99.4	99.3
Sc	2.5	2.5	2.5	2.5	2.5	2.5	2.5
V	39	2	4	27	28	29	20
Rb	0	0	0	0	0	0	0
Ba	587	612	776	831	721	352	958
Sr	6	0.5	5	4	8	3	5
Ta	5	5	5	5	5	5	5
Nb	4	6	5	5	5	4	4
Zr	86	219	172	154	91	91	65
Y	32	26	44	35	27	21	19
La	6	33	6	3	8	0.5	3
Ce	0	0	0	0	0	0	0
Au	8	8	7	30	2.5	2.5	102
Fe	3.41	0.77	3.06	3.86	4	1.57	3.29
P							
Hg							
Mg	0.44	0.03	0.03	0.1	0.31	0.1	0.06
As	2.5	10	2.5	23	2.5	2.5	6
Na	0.16	0.01	0.16	0.17	0.17	0.11	0.14
Mo	0.5	1	3	2	0.5	0.5	2
Al	2	0.54	0.63	1.45	2.47	2	1.36
Be							
Ca	0.17	0.02	0.21	0.1	0.3	0.04	0.19
Zn	65	24	39	40	74	23	41
Cu	114	4	29	27	45	0.5	22
Sb	2.5	2.5	2.5	2.5	2.5	2.5	2.5
Ag	0.1	0.1	0.4	0.4	0.2	0.1	0.6
Pb	3	34	22	6	3	1	20
Bi	2.5	2.5	2.5	2.5	2.5	2.5	2.5
Ti	6470	1620	3540	7370	4740	5580	4140
Cd	0.1	0.1	0.8	0.1	0.1	0.1	0.1
Co	15	1	11	31	17	5	16
Ni	7	1	5	13	7	5	9
W	10	10	10	10	10	10	10
K	27300	34800	25900	19800	23300	12000	29800
Mn	186	89	176	176	731	312	309
Cr	37	27	37	43	46	44	46

Total' is analytical total. All elements recalculated to 100 % anhydrous

Table A.8 *Major and trace element data for the volcanic rocks of the West Tally Pond area*

Sample		NF2763	NF2764	NF2765	NF2766	NF2767	NF2768	NF2769	NF2770	NF2771	NF2772	NF2773	NF2774
SiO2	wt%	40.3	44.6	40.6	75.5	47.5	71.7	68.8	73.7	44.3	44.7	46.7	41.4
TiO2	wt%	1.62	1.67	1.76	0.28	2.14	0.27	0.43	0.26	1.06	0.86	0.98	1.08
Al2O3	wt%	14.6	13.9	13.5	11.3	14.9	14.7	13.6	12.5	16.0	14.2	15.7	14.8
Fe2O3T	wt%	8.18	11.80	10.70	2.10	12.20	2.09	4.33	2.62	11.80	10.30	10.50	11.20
MnO	wt%	0.13	0.12	0.14	0.03	0.19	0.08	0.14	0.09	0.19	0.18	0.13	0.13
MgO	wt%	2.93	3.92	6.08	0.54	3.77	0.67	1.99	0.96	3.22	7.93	7.74	9.38
Na2O	wt%	2.48	2.73	2.50	1.12	1.12	1.10	1.99	2.33	1.53	3.20	3.70	3.32
K2O	wt%	1.95	2.00	1.06	7.54	2.04	2.81	1.81	2.26	1.75	0.30	0.57	0.34
P2O5	wt%	0.27	0.23	0.24	0.05	0.37	0.05	0.08	0.05	0.15	0.14	0.12	0.23
CaO	wt%	11.30	7.31	8.60	0.46	5.25	2.63	2.42	2.23	8.20	5.61	3.75	5.68
Cr203	wt%	0.02	0.03	0.02		0.01	<0.01	<0.01	<0.01	<0.01	<0.01	<0.01	<0.01
LOI		14.8	11.8	14.6	1.00	10.2	3.93	3.93	2.77	10.8	10.8	8.54	10.9
total		98.7	100.2	99.9	100.1	99.8	100.1	99.6	99.9	99.1	98.3	98.5	98.5
Ni	ppm	52	94	111	<10	111	<10	<10	<10	19	19	20	36
Cu	ppm	35	54	65	<10	72	<10	<10	<10	29	63	55	87
Zn	ppm	101	97	81	95	119	84	99	75	93	85	126	102
Rb	ppm	56	70	31	104	44	56	37	41	33	18	17	18
Sr	ppm	228	138	164	<10	189	218	165	76	166	89	61	124
Y	ppm	26	31	<10	120	30	48	54	45	13	16	23	<10
Zr	ppm	267	105	98	286	161	145	202	169	53	73	65	58
Nb	ppm	65	28	20	43	32	<10	20	<10	15	20	<10	16
Ba	ppm	538	400	243	911	348	366	311	368	413	300	214	272

Total' is analytical total. All elements recalculated to 100 % anhydrous

Table A.8 *Pressed pellet X-ray fluorescence (XRF) data for the volcanic rocks of the West Tally Pond area*

Sample		NF2751	NF2752	NF2753	NF2754	NF2755	NF2756	NF2757	NF2758	NF2759	NF2760	NF2761	NF2762
SiO2	wt%	43.5	45.9	41.6	58.8	59.9	62.8	62.6	61.2	53.2	54.0	40.2	48.7
TiO2	wt%	0.80	1.00	2.45	0.66	1.03	0.65	0.71	0.70	0.93	0.87	2.00	2.03
Al2O3	wt%	12.6	16.5	13.6	12.3	14.7	12.7	13.5	13.7	15.9	14.7	17.9	15.7
Fe2O3T	wt%	8.16	8.30	14.20	5.64	7.30	5.35	5.88	5.86	8.03	7.64	14.10	13.50
MnO	wt%	0.15	0.17	0.22	0.17	0.15	0.17	0.18	0.20	0.36	0.31	0.25	0.11
MgO	wt%	4.93	3.43	5.15	2.75	2.97	2.69	2.36	2.58	3.64	3.61	4.00	2.23
Na2O	wt%	1.52	1.58	1.16	3.33	4.17	4.12	4.78	4.32	1.82	1.95	2.00	2.48
K2O	wt%	1.60	2.12	0.65	0.85	1.23	0.72	0.91	1.00	2.92	2.74	2.05	2.20
P2O5	wt%	0.16	0.21	0.28	0.11	0.15	0.09	0.11	0.11	0.20	0.21	0.23	0.36
CaO	wt%	10.20	7.83	7.28	5.87	3.37	5.59	3.89	4.92	3.98	4.66	5.85	3.91
Cr203	wt%	0.05	<0.01	<0.01	<0.01	<0.01	<0.01	<0.01	0.01	0.01	<0.01	<0.01	<0.01
LOI		15.8	12.5	13.3	9.54	4.39	5.31	4.16	5.47	8.39	9.31	10.1	8.7
total		99.7	99.7	100.0	100.1	99.5	100.3	99.2	100.2	99.5	100.1	98.8	100.1
Ni	ppm	149	45	<10	16	21	19	20	17	43	35	16	12
Cu	ppm	12	107	40	<10	20	40	58	<10	<10	29	59	42
Zn	ppm	84	89	129	79	111	81	82	85	90	102	131	81
Rb	ppm	62	63	21	27	34	22	27	18	96	94	64	60
Sr	ppm	259	258	172	229	147	140	169	164	95	130	175	
Y	ppm	10	<10	31	38	49	20	29	45	28	20	23	42
Zr	ppm	94	103	157	136	172	179	199	158	198	170	152	372
Nb	ppm	16	15	30	26	<10	20	16	<10	29	20	25	31
Ba	ppm	231	307	142	311	457	228	570	480	445	367	424	525

Total' is analytical total. All elements recalculated to 100 % anhydrous

APPENDIX B

B.1 Inductively Coupled Plasma-Mass Spectrometry

Inductively coupled plasma mass spectrometry (ICP-MS) was used for quantitative determinations of the lanthanides (or REE), Y and Th and data was also collected for Ba, Hf, Nb, and Zr. The samples were analyzed at the Department of Earth Sciences, Memorial University, using a Hewlett Packard model 4500+ ICP-MS. Data acquisition is via manufacturer software whereas data reduction and concentration calculations are carried out using an in house written spreadsheet program.

The mafic and felsic volcanic samples were prepared using a sodium peroxide (Na_2O_2) sinter dissolution (Longerich *et al.*, 1990). This is because the HF-HNO_3 acid dissolution method may not dissolve some acid resistant mineral phases (e.g. zircon, spinel, fluorite, titanite, garnet). The advantage of this sintering technique is that it is successful in dissolving resistant REE-bearing accessory phases, and has low blanks for REE, Th, and the high-field strength elements (HFSE). The internal check of Zr analyzed by XRF and ICP-MS indicates that there are no dissolution problems with the Na_2O_2 sinter method.

Elemental masses analyzed via this method consist of ^{89}Y, ^{90}Zr, ^{93}Nb, ^{137}Ba, ^{139}La, ^{140}Ce, ^{141}Pr, ^{145}Nd, ^{147}Sm, ^{151}Eu, ^{157}Gd, ^{159}Tb, ^{160}Gd, ^{163}Dy, ^{165}Ho, ^{167}Er, ^{169}Tm, ^{173}Yb, ^{175}Lu, ^{177}Hf, ^{181}Ta, ^{232}Th.

The Na_2O_2 sinter method has the ability to run up the samples, standards, blanks, and duplicates in one data run. Addition of spikes to samples serve as the method of internal standardization, and external standards are used to calibrate most elements. The sample analysis as well as the standard analysis must be background corrected and corrected for a number of variables such as matrix factors, drift factors, etc. Full details pertaining to the relevant procedures associated with this technique are given in Longerich *et al.* (1990) and Jenner *et al.* (1990).

Average detection limits observed during this study for the analysed elements consisted of: 0.1 - 0.3 ppm for Rb, Sr, Zr, Ba, and Ta; 0.094, 0.071 and 0.052 ppm for Pb, Li, and Cs respectively; from 0.03 - 0.05 ppm for Mo, Sm, Nd and Eu; from 0.1 - 0.3 for Y, La, , Ce, Pr, Gd, Dy, Er, Tm, Yb, Lu, Hf, Bi, and U; and below 0.01 ppm for Nb, Tb, Ho, Ta, and Th.

B.2 Precision and accuracy

The precision and accuracy of analysis were determined through the use of standards basalt BR-688 and gabbro MRG-1, which were run four times during the collection of the data and presented in Table B.1. Precision for most elements was observed as mostly excellent (0-3 % RSD) with some elements having good (3-7 % RSD) precision; whereas the accuracy of all major elements was good (3-7 % RD) with some of the trace elements having excellent precision (0-3 % RSD).

The long term precision for the Na_2O_2 method varies from 4 to 6% RSD for the REE, Zr, Y, Th and Ba, to 10% RSD for Nb and Hf. The limits of detection for this method are at the sub-parts per million level for the REE and Th, and are higher for Nb and Hf (0.25 ppm), Y (0.3 ppm), Ba (1 ppm) and Zr (3ppm) (Longerich *et al.*, 1990).

Table B.1 *Precision and accuracy for ICP-MS analysis of standards BR-688 and MRG-1.*

Element	BR-688 *quoted value*	BR-688 *Mean*	SD	RSD %	RD %	MRG-1 *quoted value*	MRG-1 *Mean*	SD	RSD %	RD %
Y	17.81	16.30	0.76	5.00	-8.48	11.50	10.90	0.30	3.00	-5.22
Zr	59.15	59.40	3.33	6.00	0.42	107.00	105.00	1.42	1.00	-1.87
Nb	4.87	4.71	0.32	7.00	-3.29	22.30	22.10	0.89	4.00	-0.90
Ba	163.33	158.00	2.50	2.00	-3.26	49.40	46.50	1.57	3.00	-5.87
La	4.98	4.72	0.14	3.00	-5.22	8.83	8.36	0.23	3.00	-5.32
Ce	11.55	11.00	0.29	3.00	-4.76	25.80	24.30	0.81	3.00	-5.81
Pr	1.65	1.57	0.04	3.00	-4.85	3.71	3.51	0.10	3.00	-5.39
Nd	8.03	7.61	0.22	3.00	-5.23	17.60	17.10	0.26	2.00	-2.84
Sm	2.30	2.21	0.05	2.00	-3.91	4.34	4.33	0.04	1.00	-0.23
Eu	0.94	0.90	0.02	3.00	-4.26	1.38	1.39	0.01	0.00	0.72
Gd 160	2.88	2.72	0.09	3.00	-5.56	3.97	3.96	0.02	1.00	-0.25
Tb	0.48	0.45	0.02	4.00	-6.25	0.52	0.53	0.00	1.00	1.92
Dy	3.21	3.00	0.13	4.00	-6.54	3.00	2.84	0.08	3.00	-5.33
Ho	0.70	0.68	0.01	2.00	-2.86	0.49	0.49	0.00	1.00	0.00
Er	2.10	2.15	0.02	1.00	2.38	1.16	1.25	0.05	4.00	7.76
Tm	0.30	0.29	0.01	2.00	-3.33	0.14	0.14	0.00	1.00	0.00
Yb	2.00	1.85	0.08	5.00	-7.50	0.79	0.79	0.01	1.00	0.00
Lu	0.30	0.28	0.02	6.00	-6.67	0.11	0.11	0.00	2.00	0.00
Hf	1.54	1.64	0.05	3.00	6.49	3.89	4.17	0.14	3.00	7.20
Ta	0.18	0.28	0.05	18.00	55.56	0.74	0.87	0.07	8.00	17.57
Th	0.33	0.39	0.03	9.00	18.18	0.82	0.77	0.03	4.00	-6.10

SD is the standard deviation
RSD is relative standard deviation
RD is relative difference to the standard value
Quoted values from Govindaraju (1989) and from from long term MUN averages

Table B.2 *Na2O2 sinter data for the Tally Pond Group rocks.*

Sample		DP-99-202	JP-00-193	JP-00-288	JP-00-215	JP-00-208	JP-00-275	JP-00-284	JP-00-176
Ba	ppm	1340	41.1	1300	739	132	172	1400	168
Ta	ppm	0.38	0.52	0.33	0.52	0.44	0.34	0.33	1.19
Nb	ppm	4.46	7.23	3.34	7.06	6.14	4.79	4.07	16.6
Hf	ppm	3.85	3.95	1.78	4.34	6.48	3.55	3.45	5.8
Zr	ppm	123	150	63.6	151	224	124	120	213
Y	ppm	26.1	31.2	18.7	37.5	37.9	34	21.1	31.3
Th	ppm	6	6.55	2.75	6.77	5.71	4.28	1.92	2.57
La	ppm	19.3	17.1	3.45	19.3	20	15.3	7.3	15.5
Ce	ppm	40.6	34.7	6.72	40.7	45.7	33.6	17.2	37.2
Pr	ppm	4.79	4.03	0.76	4.84	5.68	4.2	2.35	5.05
Nd	ppm	19.6	16.2	3.1	20	23.6	17.8	10.9	23
Sm	ppm	4.28	3.29	1.04	5.26	5.89	4.71	3.48	6.22
Eu	ppm	0.99	0.66	0.26	1.18	1.23	1.17	1.23	2.03
Gd	ppm	4.75	3.99	2.09	5.9	6.22	5.31	4.28	6.73
Tb	ppm	0.76	0.75	0.51	1	1.08	0.92	0.7	1.06
Dy	ppm	5.07	5.6	3.87	6.67	7.37	6.21	4.39	6.53
Ho	ppm	1.11	1.3	0.81	1.46	1.57	1.35	0.87	1.3
Er	ppm	3.65	4.37	2.37	4.84	5.33	4.42	2.62	3.88
Tm	ppm	0.51	0.62	0.3	0.69	0.78	0.62	0.35	0.51
Yb	ppm	3.21	4.09	1.74	4.65	5.21	4.1	2.1	3.16
Lu	ppm	0.43	0.55	0.24	0.73	0.81	0.65	0.31	0.47
La/Yb		6.02	4.19	1.99	4.15	3.84	3.74	3.48	4.92
Zr/Y		4.71	4.82	3.4	4.04	5.91	3.65	5.7	6.82

Table B.2 *Na2O2 sinter data for the Tally Pond Group rocks.*

Sample		JP-00-212	JP-00-182	JP-00-194	JP-00-180	JP-00-182'	JP-00-212'	DP-99-202*
Ba	ppm	1340	41.1	1300	739	132	172	1400
Ta	ppm	0.38	0.52	0.33	0.52	0.44	0.34	0.33
Nb	ppm	4.46	7.23	3.34	7.06	6.14	4.79	4.07
Hf	ppm	3.85	3.95	1.78	4.34	6.48	3.55	3.45
Zr	ppm	123	150	63.6	151	224	124	120
Y	ppm	26.1	31.2	18.7	37.5	37.9	34	21.1
Th	ppm	6	6.55	2.75	6.77	5.71	4.28	1.92
La	ppm	19.3	17.1	3.45	19.3	20	15.3	7.3
Ce	ppm	40.6	34.7	6.72	40.7	45.7	33.6	17.2
Pr	ppm	4.79	4.03	0.76	4.84	5.68	4.2	2.35
Nd	ppm	19.6	16.2	3.1	20	23.6	17.8	10.9
Sm	ppm	4.28	3.29	1.04	5.26	5.89	4.71	3.48
Eu	ppm	0.99	0.66	0.26	1.18	1.23	1.17	1.23
Gd	ppm	4.75	3.99	2.09	5.9	6.22	5.31	4.28
Tb	ppm	0.76	0.75	0.51	1	1.08	0.92	0.7
Dy	ppm	5.07	5.6	3.87	6.67	7.37	6.21	4.39
Ho	ppm	1.11	1.3	0.81	1.46	1.57	1.35	0.87
Er	ppm	3.65	4.37	2.37	4.84	5.33	4.42	2.62
Tm	ppm	0.51	0.62	0.3	0.69	0.78	0.62	0.35
Yb	ppm	3.21	4.09	1.74	4.65	5.21	4.1	2.1
Lu	ppm	0.43	0.55	0.24	0.73	0.81	0.65	0.31
La/Yb		6.02	4.19	1.99	4.15	3.84	3.74	3.48
Zr/Y		4.71	4.82	3.4	4.04	5.91	3.65	5.7

APPENDIX C

C.1 Electron Microprobe

Mineral analyses were conducted using a Camera SX50 electron microprobe with automation SamX –Xmas software for combined wavelength-dispersion (Cameca) and energy-dispersive (Oxford Link) analyses at the Department of Earth Sciences, Memorial University of Newfoundland. The beam current was set at 20 nA with a 15 kV accelerating potential using count times of 100 s. Analyses for Al, Si, K, Ca, Ti and Mn were done in energy-dispersive (ED) mode whereas wave-dispersive (WD) mode was used for analyses of Na, Mg, and Fe. Analyses were conducted on carbonate, chlorite and sericite.

C-2 Precision and Accuracy

In order to determine the precision and accuracy of analyses, the Kakanui Hornblende was analyzed several times in conjunction with each successive analysis and used as the standard for precision and instrument calibration. The analyses indicate that the data vary from good with RSD less than 7 % to excellent with RSD less than 3 %. Calibration standard deviations are generally less than 1.0 wt %, thereby giving a measure of analytical accuracy.

Table C.1 *Carbonate compositions from the Duck Pond Deposit*

Label	JP-00-CC1	JP-00-CC2	JP-00-CC3	JP-00-CC4	JP-00-CC5	JP-00-AR1
Na2O	0.25	0.22	0.2	0.29	0.26	0.21
MgO	22.5	20.5	21.6	22.9	22.1	17.5
Al2O3	0	0	0	0	0	0
SiO2	0.16	0.26	1	0.24	0.19	0.2
K2O	0	0.01	0.05	0.01	0.02	0.07
CaO	34.5	32.5	32.4	34.1	32.6	30.2
TiO2	0.04	0	0	0	0.04	0
MnO	0.87	1.03	1.22	0.74	0.51	0.08
FeO	2.57	3.32	3.27	2.97	3.63	12.1
Total	60.9	57.8	59.7	61.3	59.3	60.3
Beam current	20.11	20.09	20.09	20.07	20.04	20.11
Number of Ions based on 6 O						
Na	0.04	0.04	0.03	0.04	0.04	0.03
Mg	2.72	2.62	2.67	2.75	2.74	2.26
Ca	3	3	2.87	2.94	2.91	2.81
Mn	0.06	0.07	0.09	0.05	0.04	0.01
Fe	0.17	0.24	0.23	0.2	0.25	0.88
O	6	6	6.03	6	6	6
Total	12	12	12	12	12	12
Mg/Fe	15.6	11	11.8	13.8	10.8	2.58

Note: Carbon excluded from cation calculations
CC samples from mineralized chaotic carbonate zone
AR samples from altered rhyolite
CA samples from unmineralized chaotic carbonate zone
ST samples from chlorite feeder zone

Table C.1 *Carbonate compositions from the Duck Pond Deposit*

Label	JP-00-CA1	JP-00-CA2	JP-00-CA3	JP-00-CA4	JP-00-ST1	JP-00-ST2
Na2O	0.28	0.2	0.38	0.28	0.19	0.27
MgO	23	22.6	23.9	23.3	21	15
Al2O3	0	0	0	0	0	0
SiO2	0.14	0.16	0.21	0.16	0.21	0.19
K2O	0.03	0.01	0.05	0	0.03	0.08
CaO	33.3	33.1	33.8	34.3	31.2	31.4
TiO2	0.09	-0.1	0.04	0	0.03	0.03
MnO	0.36	0.09	0.2	0.13	1.32	3.15
FeO	1.02	0.58	1.22	0.82	7.75	5.33
Total	58.1	56.6	59.8	58.9	61.5	55.4
Beam current	20.46	20.03	20.11	20.16	20.04	20.1
Number of Ions based on 6 O						
Na	0.05	0.03	0.06	0.05	0.03	0.05
Mg	2.87	2.89	2.89	2.86	2.58	2.1
Ca	2.98	3.03	2.94	3.03	2.76	3.16
Mn	0.03	0.01	0.01	0.01	0.09	0.25
Fe	0.07	0.04	0.08	0.06	0.53	0.42
O	5.99	6	5.99	6	6.01	5.99
Total	12	12	12	12	12	12
Mg/Fe	40.2	69.2	34.8	50.6	4.83	5.02

Note: Carbon excluded from cation calculations
CC samples from mineralized chaotic carbonate zone
AR samples from altered rhyolite
CA samples from unmineralized chaotic carbonate zone
ST samples from chlorite feeder zone

Table C.1 *Carbonate compositions from the Duck Pond Deposit*

Label	JP-00-ST3	JP-00-ST4	JP-00-ST5	JP-00-ST6	JP-00-ST7
Na2O	0.29	0.35	0.24	0.28	0.28
MgO	18.5	17.8	19.3	20.8	19.6
Al2O3	0	0.43	0	0	0
SiO2	0.21	4.79	0.14	0.15	0.28
K2O	0.03	0.2	0.07	0.04	0.12
CaO	32	30.3	31.4	32.8	30.3
TiO2	0	0	0	0.06	0
MnO	1.04	0.6	1.26	3.01	0.67
FeO	7.01	8.64	7.03	6.24	8.73
Total	59	63.2	59.4	63.2	60
Beam curr	20.11	20.06	20.04	20.11	20.09
Number of Ions based on 6 O					
Na	0.05	0.05	0.04	0.04	0.05
Mg	2.38	2.12	2.46	2.49	2.48
Ca	2.97	2.59	2.89	2.83	2.77
Mn	0.08	0.04	0.09	0.21	0.05
Fe	0.51	0.58	0.5	0.42	0.62
O	6	6.18	5.99	5.99	6
Total	12	12	12	12	12
Mg/Fe	4.7	3.68	4.88	5.94	3.99

Note: Carbon excluded from cation calculations
CC samples from mineralized chaotic carbonate zone
AR samples from altered rhyolite
CA samples from unmineralized chaotic carbonate zone
ST samples from chlorite feeder zone

Table C.2 *Chlorite Compositions from the Duck Pond Deposit.*

Sample	JP-00-CC1	JP-00-CC2	JP-00-CC3	JP-00-CC4	JP-00-AR1	JP-00-AR2
Na2O	0.23	0.31	0.24	0.34	0.26	0.27
MgO	28	28	28.1	29.1	17.6	16.7
Al2O3	20.9	20.7	23.6	21.9	23	22.6
SiO2	30.4	29.4	29.8	30.5	27	25.9
K2O	0.01	0.01	0.02	0	0.12	0.07
CaO	0.08	0.05	0.04	0.12	0	0.03
TiO2	0.07	0	0.09	0.09	0.03	0
MnO	0.08	0.09	0.05	0.05	0	0.05
FeO	4.66	4.98	5.51	4.91	20.5	21
Total	84.2	83.5	87.2	86.8	88.5	86.5
Beam current	20.11	20.11	20.07	20.07	20.09	20.09
Number of Ions based on 28 O						
Na	0.09	0.12	0.09	0.13	0.1	0.11
Mg	8.13	8.25	7.92	8.23	5.3	5.18
Al	4.8	4.83	5.26	4.89	5.49	5.54
Si	5.93	5.81	5.64	5.78	5.47	5.4
K	0	0	0.01	0	0.03	0.02
Ca	0.02	0.01	0.01	0.02	0	0.01
Ti	0.01	0	0.01	0.01	0	0
Mn	0.01	0.01	0.01	0.01	0	0.01
Fe	0.76	0.82	0.87	0.78	3.47	3.65
O	28	28	28	28	28	28
Total	47.7	47.8	47.8	47.8	47.9	47.9
Fe/Fe+Mg	0.09	0.09	0.10	0.09	0.40	0.41

Note: CC samples from mineralized chaotic carbonate zone
AR samples from altered rhyolite
CA samples from unmineralized chaotic carbonate zone
ST samples from chlorite feeder zone

Table C.2 *Chlorite Compositions from the Duck Pond Deposit.*

Sample	JP-00-CC5	JP-00-AR3	JP-00-ST2	JP-00-AR3	JP-00-AR4	JP-00-ST1
Na2O	0.23	0.87	0.26	0.34	0.43	1.7
MgO	31.4	6.3	12.8	13.3	13.9	8.36
Al2O3	25	28.7	0.1	24.6	24.2	31.4
SiO2	32.2	39.3	26.8	30.5	29.1	38.1
K2O	0.03	2.39	0.04	1.03	1.25	1.79
CaO	0.07	0.07	22.1	0.02	0	0.17
TiO2	0	0.15	0	0.11	0.06	0.23
MnO	0	0.03	0.43	0.03	0.04	0
FeO	4.63	17.4	4.52	18.5	18.6	6.46
Total	93.5	95.1	66.9	88.3	87.5	88.2
Beam current	20.04	20.07	20.07	20.11	20.09	20.08
Number of Ions based on 28 O						
Na	0.08	0.3	0.14	0.13	0.17	0.6
Mg	8.2	1.69	5.31	3.95	4.19	2.28
Al	5.17	6.08	0	5.77	5.77	6.78
Si	5.66	7.06	7.45	6.06	5.88	6.97
K	0.01	0.55	0.01	0.26	0.32	0.42
Ca	0.01	0.01	6.58	0	0	0.03
Ti	0	0.02	0	0.02	0.01	0.03
Mn	0	0	0.1	0	0.01	0
Fe	0.68	2.61	1.05	3.07	3.14	0.99
O	28	28	28	28	28	28
Total	47.8	46.3	48.6	47.2	47.5	46.1
Fe/Fe+Mg	0.08	0.61	0.17	0.44	0.43	0.30

Note: CC samples from mineralized chaotic carbonate zone
AR samples from altered rhyolite
CA samples from unmineralized chaotic carbonate zone
ST samples from chlorite feeder zone

Table C.3 *Sericite compositions from the Duck Pond deposit.*

Sample	JP-00-CC1s	JP-00-CC2s	JP-00-CC3s	JP-00-CC4s	JP-00-CC5s	JP-00-AR1s	JP-00-AR2s
Na2O	0.77	0.58	0.49	0.28	0.41	0.48	0.7
MgO	1.47	1.72	1.49	2.57	1.43	1.71	0.98
Al2O3	36	37	36.3	35.7	36.4	36.2	36
SiO2	50	51.8	51.5	52.5	51.4	51.7	49.4
K2O	6.6	6.62	6.47	6.02	6	6.25	5.86
CaO	0.04	0.03	0	0.03	0.09	0.06	0.18
TiO2	0.25	0.2	0.23	0.18	0.38	0.19	0.15
MnO	0	0	0.04	0.1	0.02	0.05	0.1
FeO	0.31	0.08	0.21	0.44	0.24	0.89	0.72
Total	95.4	97.9	96.6	97.7	96.2	97.4	94
Beam current	20.05	20.1	20.07	20.08	20.08	20.07	20.07
Number of Ions based on 28 O							
Na	0.24	0.18	0.15	0.09	0.13	0.15	0.22
Mg	0.36	0.41	0.36	0.61	0.34	0.41	0.24
Al	6.93	6.91	6.86	6.67	6.89	6.81	7.02
Si	8.16	8.21	8.26	8.31	8.26	8.26	8.16
K	1.38	1.34	1.33	1.22	1.23	1.27	1.24
Ca	0.01	0.01	0	0	0.01	0.01	0.03
Ti	0.03	0.02	0.03	0.02	0.05	0.02	0.02
Mn	0	0	0.01	0.02	0	0.01	0.01
Fe	0.04	0.01	0	0.1	0.03	0.1	0.1
O	28	28	28	28	28	28	28
Fe/(Fe+Mg)	0.11	0.03	0.07	0.09	0.09	0.22	0.29

Note: CC samples from mineralized chaotic carbonate zone
AR samples from altered rhyolite
CA samples from unmineralized chaotic carbonate zone
ST samples from chlorite feeder zone

Table C.3 *Sericite compositions from the Duck Pond deposit.*

Sample	JP-00-AR3s	JP-00-AR4s	JP-00-AR5s	JP-00-AR6s	JP-00-CA1s	JP-00-CA2s	JP-00-CA3s
Na2O	0.74	0.32	0.22	0.53	0.08	0.21	0.13
MgO	0.96	1.41	1.64	2.92	3.17	2.11	1.9
Al2O3	34.5	34.8	36.1	31.6	31.9	34.4	35.7
SiO2	51.2	50.3	52.5	44.9	53.1	51.3	52.5
K2O	5.96	6.35	6.34	5.05	5.94	6.08	6.42
CaO	0	0.1	0.06	0.25	0.05	0.03	0.07
TiO2	0.27	0.16	0.3	0.17	0.46	0.32	0.57
MnO	0.08	0.1	0	0.02	0	0	0.1
FeO	0.52	0.67	0.84	7.38	0.15	0.11	0.33
Total	94.1	94	98	92.9	94.6	94.5	97.4
Beam current	20.1	20.07	20.1	20.1	20.07	20.05	20.13
Number of Ions based on 28 O							
Na	0.24	0.1	0.07	0.18	0.03	0.07	0.04
Mg	0.24	0.35	0.39	0.76	0.77	0.52	0.45
Al	6.69	6.78	6.75	6.5	6.13	6.63	6.68
Si	8.42	8.31	8.32	7.83	8.65	8.39	8.35
K	1.25	1.34	1.28	1.12	1.24	1.27	1.3
Ca	0	0.01	0.01	0.05	0.01	0	0.01
Ti	0.03	0.02	0	0	0.06	0.04	0.07
Mn	0.01	0.01	0	0	0	0	0.01
Fe	0.07	0.1	0.11	1.1	0	0.02	0
O	28	28	28	28	28	28	28
Fe/(Fe+Mg)	0.23	0.21	0.22	0.59	0.03	0.03	0.09

Note: CC samples from mineralized chaotic carbonate zone
AR samples from altered rhyolite
CA samples from unmineralized chaotic carbonate zone
ST samples from chlorite feeder zone

Table C.3 *Sericite compositions from the Duck Pond deposit.*

Sample	JP-00-CA4s	JP-00-ST1S	JP-00-ST2s	JP-00-ST3s	JP-00-ST4s
Na2O	0.24	0.93	1.83	0.75	0.9
MgO	3.42	1.01	1.25	1.49	1.11
Al2O3	32.3	33.9	39	36.4	37.2
SiO2	55.8	49.2	52	52.1	49.7
K2O	5.68	6.08	4.44	5.69	6.15
CaO	0.02	0.07	0.1	0.01	0.04
TiO2	0.38	0.43	0.38	0.44	0.39
MnO	0.03	0.06	0.02	0.05	0.1
FeO	0.05	0.4	0.49	0.39	0.17
Total	97.8	91.9	99.5	97.2	95.4
Beam curre	20.1	19.98	20.02	20.08	20.12
Number of Ions based on 28 O					
Na	0.07	0.31	0.55	0.23	0.28
Mg	0.8	0.25	0.29	0.35	0.27
Al	5.98	6.75	7.12	6.83	7.13
Si	8.77	8.32	8.07	8.28	8.08
K	1.14	1.31	0.88	1.15	1.28
Ca	0	0.01	0.02	0	0.01
Ti	0.05	0.05	0.04	0.05	0.05
Mn	0	0.01	0	0.01	0.01
Fe	0	0.1	0.06	0.05	0.02
O	28	28	28	28	28
Fe/(Fe+Mg)	0.01	0.18	0.18	0.13	0.08

Note: CC samples from mineralized chaotic carbonate zone
AR samples from altered rhyolite
CA samples from unmineralized chaotic carbonate zone
ST samples from chlorite feeder zone

APPENDIX D

D.1 TI-MS U-Pb Geochronology

Geochronological samples for U-Pb thermal ionization mass spectrometry (TI-MS) were analyzed in the geochronology laboratory at the Geological Survey of Canada. Details regarding analytical methods and procedures are outlined in Parrish *et al.* (1987). Heavy mineral concentrates were prepared by standard crushing, grinding, Wilfley table, and heavy liquid techniques. Mineral separates were sorted by magnetic susceptibility using a Frantz™ isodynamic separator. Multigrain zircon fractions analyzed were very strongly air abraded following the method of Krogh (1982). Treatment of analytical errors follows Roddick (1987). U-Pb analytical results are presented in Tables D.1 and D.2, where errors on the ages are reported at the 2σ level, and displayed in the concordia plots (Figure 6.1; 6.2).

Table D.1 *U-Pb TIMS analytical data for the Tally Pond Group*

JP-01-GC1: Quartz crystal tuff, Tally Pond Group (UTM zone 21, 541103E - 5389364N)

Fraction[1]	Description[2]	Wt. (µg)	U ppm	Pb[3] ppm	$^{206}Pb/^{204}Pb$[4]	Pb[5] pg	$^{208}Pb/^{206}Pb$	Isotopic Ratios[6] $^{207}Pb/^{235}U$	±1SE Abs	$^{206}Pb/^{238}U$	±1SE Abs	Corr.[7] Coeff.	$^{207}Pb/^{206}Pb$	±1SE Abs	Ages (Ma)[8] $^{206}Pb/^{238}U$	±2SE	$^{207}Pb/^{235}U$	±2SE	$^{207}Pb/^{206}Pb$	±2SE
A1 (32)	Co,Clr,nln,Eu,St	16	89	8	741	10	0.162	0.65198	0.00205	0.08227	0.00014	0.641	0.05748	0.00014	509.7	1.6	509.7	2.5	509.8	10.7
B1 (31)	Co,Clr,rln,Eu,Tips	29	231	20	318	115	0.164	0.64787	0.00415	0.08215	0.00018	0.671	0.05720	0.00030	509.0	2.1	507.2	5.1	499.1	22.7
B2 (43)	Co,Clr,nln,Eu,Tips	17	132	11	1817	6	0.166	0.64967	0.00128	0.08182	0.00013	0.743	0.05759	0.00008	507.0	1.5	508.3	1.6	514.2	5.8

Notes:

[1] All fractions comprised of zircon which were abraded following the method of Krogh (1982). Number in brackets refer to number of grains in analysis.

[2]Zircon descriptions: Co=Colourless, Clr=Clear, fln=Few Inclusions, nln=Numerous Inclusions, rln=Rare Inclusions, Eu=Euhedral, St=Stubby Prism, Tips=Tips.

[3]Radiogenic Pb

[4]Measured ratio, corrected for spike and fractionation

[5]Total common Pb in analysis corrected for fractionation and spike

[6]Corrected for blank Pb and U and common Pb, errors quoted are 1 sigma absolute; procedural blank values for this study ranged from 0.1- 0.6 pg for U and 3-5 pg for Pb; Pb blank isotopic composition is based on the analysis of procedural blanks; corrections for common Pb were made using Stacey-Kramers compositions;

[7]Correlation Coefficient

[8]Corrected for blank and common Pb, errors quoted are 2 sigma in Ma

Table D.2 *U-Pb TIMS Analytical data for Harpoon Gabbro (UTM Zone 21 E 528198, N 5381717).*

								Isotopic Ratios[6]							Ages (Ma)[8]					
Fraction[1]	Description[2]	Wt. (μg)	U (ppm)	Pb^{3} ppm	$^{206}Pb/^{204}Pb$	Pb^{5} pg	$^{208}Pb/^{206}Pb$	$^{207}Pb/^{235}U$	±1SE Abs	$^{206}Pb/^{238}U$	±1SE Abs	Corr.[7] Coeff.	$^{207}Pb/^{206}Pb$	±1SE Abs	$^{206}Pb/^{238}U$	±2SE	$^{207}Pb/^{235}U$	±2SE	$^{207}Pb/^{206}Pb$	±2SE
Z1 (150)	Co,Clr,nIn,Eu,St	23	681	66	3592	2	0.439	0.58833	0.00100	0.07562	0.00010	0.838	0.05642	0.00005	469.9	1.2	469.8	1.3	469.1	4.1
Z2 (75)	Co,Clr,nIn,Eu,St	43	912	88	32134	6	0.401	0.59750	0.00169	0.07683	0.00021	0.989	0.05640	0.00002	477.2	2.5	475.6	2.1	468.3	1.9
Z3A (9)	Co,Clr,fIn,Eu,St	6	141	12	932	4	0.196	0.60328	0.00210	0.07635	0.00012	0.571	0.05731	0.00017	474.3	1.5	479.3	2.7	503.3	12.6
Z4A (11)	Co,Clr,Eu,St	10	955	90	7688	6	0.402	0.58159	0.00081	0.07483	0.00009	0.884	0.05637	0.00004	465.2	1.1	465.5	1.0	467.0	2.9
Z4B (10)	Co,Clr,Eu,St	12	995	92	8979	6	0.383	0.58020	0.00105	0.07482	0.00011	0.752	0.05624	0.00007	465.2	1.3	464.6	1.3	461.8	5.3
Z4C (5)	Co,Clr,Eu,St	7	837	80	2235	5	0.404	0.59119	0.00106	0.07606	0.00008	0.726	0.05638	0.00007	472.5	0.9	471.6	1.4	467.2	5.6
Z4D (7)	Co,Clr,Eu,St	5	834	79	663	31	0.416	0.58095	0.00168	0.07492	0.00009	0.713	0.05624	0.00012	465.7	1.1	465.1	2.2	461.7	9.8

Notes:

[1] All fractions comprised of zircon which were abraded following the method of Krogh (1982). Number in brackets refer to number of grains in analysis.

[2]Zircon descriptions: Co=Colourless, Clr=Clear, fIn=Few Inclusions, nIn=Numerous Inclusions, rIn=Rare Inclusions, Eu=Euhedral, St=Stubby Prism, Tips=Tips.

[3]Radiogenic Pb

[4]Measured ratio, corrected for spike and fractionation

[5]Total common Pb in analysis corrected for fractionation and spike

[6]Corrected for blank Pb and U and common Pb, errors quoted are 1 sigma absolute; procedural blank values for this study ranged from 0.1- 0.6 pg for U and 3-5 pg for Pb; Pb blank isotopic composition is based on the analysis of procedural blanks; corrections for common Pb were made using Stacey-Kramers compositions;

[7]Correlation Coefficient

[8]Corrected for blank and common Pb, errors quoted are 2 sigma in Ma

APPENDIX E

E.1 LAM-ICP-MS Geochronology

Zircons were extracted at Memorial University of Newfoundland using conventional mineral separation techniques (crushing, Wilfley table, heavy liquids) from the least magnetic split obtained with a Frantz isodynamic separator. The zircons were then hand-picked in alcohol under a binocular microscope. Approximately 150 zircons were selected and then separated into populations based on morphology and colour.

The U-Pb method followed that described by Kosler *et al.* (2002). Laser Ablation Microprobe-Inductively Coupled Plasma-Mass Spectrometry (LAM-ICP-MS) analyses were performed in the Department of Earth Sciences at Memorial University of Newfoundland using a VG PlasmaQuad 2 S+ mass spectrometer coupled to an in-house custom-built Q switched Nd:YAG ultraviolet laser operating with a wavelength of 266 nm. Zircons were ablated using a laser repetition rate of 10Hz and a laser energy of 0.8 mJ/pulse. The beam was focused 100 μm above the sample surface and reduced to a diameter of 10 μm by masking the beam with a white Teflon® attenuator. The sample cell was mounted on a computer driven motorised stage on the microscope. The stage was moved beneath the stationary laser to produce a variable size (20-40 μm) laser line pit in the sample. The depth of the pit varied from ca 10 to 50 μm depending on line length and

ablation time.

Using He as a carrier gas, the ablated sample material was transported from the sample cell to the plasma by acid washed plastic tubing via the mixing chamber at the rear of the plasma torch. The mass spectrometer measured the U/Pb and Pb isotopic ratios in detrital zircons as well as a Tl/Bi/Np tracer solution that was nebulised simultaneously with the laser ablated solid sample. The tracer solution contained natural Tl ($^{205}Tl/^{203}Ti$=2.3871), ^{209}Bi and ^{237}Np at concentrations of 10.6 ppb for each isotope.

Typical acquisitions consisted of ca. 60 s measurements of the He gas blank and tracer solution signals just before the start of ablation. The U and Pb zircon ablation signal, along with the continuing Tl/Bi/Np solution signal were acquired for another 180 –200 s. External standards were periodically measured using the 295 ±1 Ma (Ketchum *et al.*, 2001) pegmatitic gem zircon standard (02123) to monitor the precision and accuracy of our measurements. The data were acquired in time resolved-peak jumping-pulse counting mode with 1 point measured per peak using commercial PQVision v. 4.30 software. In total masses 201 (flyback), 203 (Tl), 204 (Pb), 205 (Tl), 206 (Pb), 207 (Pb), 209 (Bi), 237 (Np) and 238 (U) were measured. Oxides of Np ($^{237}Np^{16}O$ = 254) and U ($^{238}U^{16}O$ = 254) were also monitored to correct for minor changes in the solution over the coarse of the analysis. Quadrupole settling time was 1 ms for all masses and the dwell time was 8.3 ms for all masses except for mass 207 where it was 24.9 ms. Over the 240 seconds of measurement approximately 1600 data acquisition cycles (sweeps) were collected.

E.2 Data Reduction

The raw data were collected for electron multiplier dead time (20ns) and downloaded to a PC for processing using an in-house spreadsheet utility program to integrate signals from each sequential set of ten sweeps. $^{207}Pb/^{206}Pb$, $^{208}Pb/^{206}Pb$, $^{206}Pb/^{238}U$ and $^{207}Pb/^{235}U$ were calculated for each reading using a natural $^{238}U/^{235}U$ ratio of 137.88. Signal intervals for the background and ablation were selected for each sample and matched with similar intervals for the standards. The calculated isotopic ratios were then corrected for gas blank and the small contribution of Pb and U from the tracer solution. This was typically less than 100 and 300 cps on masses 206 and 238, respectively. Using ^{233}U in the tracer solution allowed for a real-time instrument mass bias correction with the $^{205}Tl/^{233}U$ value measured while the sample was ablated; this technique is largely independent of matrix effects that can variably influence measured isotopic ratios and hence the resulting ages. The amount of common Pb present in zircons analysed in this study was insignificant relative to the content of radiogenic Pb and accordingly, no common Pb correction was applied to the data.

Accuracy and reproducibility of U-Pb analysis in the Memorial University laboratory are routinely monitored by measurements of natural in-house zircon standards of known TIMS U-Pb age. The average mass bias corrected $^{206}Pb/^{238}U$ value for the zircon standard 02123 (N = 58), taken over the 3 days of this study, was 0.041767. This value, expressed at the 95% confidence interval, is in excellent agreement with the accepted value of 0.046818 (Ketchum *et al.*, 2001). Final ages and concordia diagrams were produced using the Isoplot/Ex macro (Ludwig, 1999) in conjunction with the LAMdate Excel spreadsheet program (Kosler *et al.*, 2002).

Table E.1 *Laser ablation U-Pb data and calculated ages for detrital zircons from the Rogerson Lake Conglomerate at Rogerson Lake (Sample 71).*

	CONCORDIA COLUMNS							2 s %	2 s %	2 s %	AGES Ma						
analysis	207/235	7/5 err	206/238	6/8 err	Rho	207/206	7/6 err	207/235	206/238	207/206	7/5 age	1 sigma	6/8 age	1sigma	7/6 age	1 sigma	% Concordant
1	0.5533	0.0641	0.0866	0.0035	0.0131	0.0617	0.0018	23.19	8.08	5.85	447.2	41.9	535.3	20.7	663.0	62.7	119.71
2	0.7905	0.0717	0.0850	0.0031	0.0101	0.0766	0.0023	18.14	7.22	5.96	591.5	40.7	525.7	18.2	1110.9	59.5	88.88
3	0.5361	0.0371	0.0835	0.0029	0.0111	0.0578	0.0014	13.84	6.96	4.83	435.8	24.5	517.2	17.3	522.5	53.0	118.66
4	0.5280	0.0417	0.0775	0.0022	0.0114	0.0643	0.0016	15.79	5.73	4.91	430.5	27.7	481.1	13.3	749.9	51.8	111.76
5	0.6039	0.0466	0.0864	0.0031	0.0101	0.0652	0.0016	15.43	7.10	4.85	479.7	29.5	534.1	18.2	782.4	51.0	111.34
6	0.5769	0.0243	0.0767	0.0019	0.0059	0.0574	0.0008	8.44	4.92	2.72	462.4	15.7	476.6	11.3	506.6	29.9	103.06
7	0.7509	0.1118	0.0895	0.0056	0.0143	0.0860	0.0035	29.77	12.57	8.15	568.8	64.8	552.6	33.3	1337.9	78.8	97.16
8	0.4984	0.0349	0.0769	0.0024	0.0099	0.0547	0.0011	14.00	6.29	4.05	410.6	23.6	477.3	14.5	401.5	45.4	116.25
9	0.6095	0.0308	0.0792	0.0026	0.0072	0.0566	0.0010	10.11	6.61	3.46	483.2	19.4	491.6	15.6	475.2	38.3	101.72
10	0.5139	0.0580	0.0749	0.0031	0.0208	0.0597	0.0026	22.59	8.19	8.75	421.1	38.9	465.5	18.4	593.6	94.8	110.53
11	0.6297	0.0380	0.0832	0.0024	0.0091	0.0585	0.0013	12.08	5.73	4.52	495.9	23.7	515.2	14.2	549.8	49.4	103.89
12	0.6150	0.0334	0.0785	0.0030	0.0063	0.0583	0.0009	10.85	7.62	3.07	486.7	21.0	487.1	17.9	542.6	33.6	100.09
13	0.6004	0.0363	0.0800	0.0034	0.0119	0.0562	0.0016	12.08	8.52	5.70	477.5	23.0	495.8	20.3	458.6	63.2	103.85
14	1.6061	0.1367	0.1667	0.0075	0.0129	0.0844	0.0053	17.03	8.95	12.52	972.6	53.3	994.0	41.2	1301.2	121.6	102.20
15	0.5033	0.0640	0.0737	0.0046	0.0332	0.0625	0.0043	25.42	12.50	13.76	413.9	43.2	458.2	27.6	691.3	146.8	110.69
16	0.6717	0.0466	0.0883	0.0037	0.0093	0.0613	0.0015	13.87	8.32	4.85	521.8	28.3	545.5	21.7	651.1	52.0	104.55
17	0.7935	0.1001	0.0881	0.0043	0.0133	0.1017	0.0040	25.23	9.82	7.90	593.2	56.7	544.2	25.6	1654.9	73.2	91.75
18	0.5339	0.0394	0.0779	0.0029	0.0111	0.0581	0.0014	14.77	7.38	4.83	434.4	26.1	483.8	17.2	531.8	52.9	111.38
19	0.5540	0.0296	0.0818	0.0021	0.0093	0.0554	0.0012	10.69	5.22	4.18	447.6	19.3	506.6	12.7	429.8	46.6	113.19
20	0.5481	0.0785	0.0880	0.0050	0.0156	0.0617	0.0021	28.65	11.38	6.90	443.8	51.5	543.8	29.7	664.7	73.9	122.55
21	0.6981	0.0465	0.0842	0.0042	0.0105	0.0585	0.0017	13.32	9.89	5.65	537.7	27.8	521.1	24.8	549.9	61.6	96.91
22	0.5343	0.0492	0.0772	0.0029	0.0134	0.0731	0.0021	18.43	7.61	5.82	434.7	32.6	479.4	17.6	1017.1	58.9	110.28
23	0.4447	0.0738	0.0652	0.0059	0.0113	0.0591	0.0012	33.18	18.23	4.21	373.5	51.9	407.2	36.0	572.4	45.8	109.02
24	0.4867	0.0371	0.0780	0.0035	0.0154	0.0517	0.0016	15.25	8.86	6.21	402.6	25.3	484.5	20.7	270.3	71.2	120.32
25	0.5781	0.0356	0.0745	0.0023	0.0072	0.0619	0.0010	12.31	6.30	3.33	463.2	22.9	463.3	14.1	671.6	35.6	100.01
26	0.6654	0.0703	0.0828	0.0041	0.0221	0.0737	0.0042	21.12	9.95	11.45	517.9	42.8	512.9	24.5	1032.0	115.7	99.03
27	0.6195	0.0796	0.0777	0.0042	0.0164	0.0746	0.0030	25.69	10.71	8.02	489.5	49.9	482.4	24.9	1056.7	80.7	98.54
28	0.5487	0.0547	0.0743	0.0040	0.0360	0.0659	0.0053	19.93	10.65	16.02	444.1	35.8	462.1	23.7	802.6	167.7	104.04
29	0.6024	0.0497	0.0752	0.0027	0.0179	0.0636	0.0027	16.51	7.18	8.59	478.7	31.5	467.3	16.2	729.3	91.0	97.62
30	0.6211	0.0396	0.0803	0.0033	0.0066	0.0577	0.0009	12.74	8.24	3.26	490.5	24.8	497.6	19.7	517.7	35.7	101.45
31	0.5145	0.0321	0.0758	0.0025	0.0187	0.0530	0.0021	12.46	6.67	7.89	421.5	21.5	471.3	15.2	330.2	89.4	111.82
32	0.5905	0.0298	0.0789	0.0024	0.0082	0.0584	0.0011	10.11	6.07	3.85	471.2	19.0	489.5	14.3	544.2	42.1	103.89

Table E.1 *Laser ablation U-Pb data and calculated ages for detrital zircons from the Rogerson Lake Conglomerate at Rogerson Lake (Sample 71).*

	CONCORDIA COLUMNS							2 s %	2 s %	2 s %	AGES Ma						
analysis	207/235	7/5 err	206/238	6/8 err	Rho	207/206	7/6 err	207/235	206/238	207/206	7/5 age	1 sigma	6/8 age	1sigma	7/6 age	1 sigma	% Concordant
1	0.5533	0.0641	0.0866	0.0035	0.0131	0.0617	0.0018	23.19	8.08	5.85	447.2	41.9	535.3	20.7	663.0	62.7	119.71
2	0.7905	0.0717	0.0850	0.0031	0.0101	0.0766	0.0023	18.14	7.22	5.96	591.5	40.7	525.7	18.2	1110.9	59.5	88.88
3	0.5361	0.0371	0.0835	0.0029	0.0111	0.0578	0.0014	13.84	6.96	4.83	435.8	24.5	517.2	17.3	522.5	53.0	118.66
4	0.5280	0.0417	0.0775	0.0022	0.0114	0.0643	0.0016	15.79	5.73	4.91	430.5	27.7	481.1	13.3	749.9	51.8	111.76
5	0.6039	0.0466	0.0864	0.0031	0.0101	0.0652	0.0016	15.43	7.10	4.85	479.7	29.5	534.1	18.2	782.4	51.0	111.34
6	0.5769	0.0243	0.0767	0.0019	0.0059	0.0574	0.0008	8.44	4.92	2.72	462.4	15.7	476.6	11.3	506.6	29.9	103.06
7	0.7509	0.1118	0.0895	0.0056	0.0143	0.0860	0.0035	29.77	12.57	8.15	568.8	64.8	552.6	33.3	1337.9	78.8	97.16
8	0.4984	0.0349	0.0769	0.0024	0.0099	0.0547	0.0011	14.00	6.29	4.05	410.6	23.6	477.3	14.5	401.5	45.4	116.25
9	0.6095	0.0308	0.0792	0.0026	0.0072	0.0566	0.0010	10.11	6.61	3.46	483.2	19.4	491.6	15.6	475.2	38.3	101.72
10	0.5139	0.0580	0.0749	0.0031	0.0208	0.0597	0.0026	22.59	8.19	8.75	421.1	38.9	465.5	18.4	593.6	94.8	110.53
11	0.6297	0.0380	0.0832	0.0024	0.0091	0.0585	0.0013	12.08	5.73	4.52	495.9	23.7	515.2	14.2	549.8	49.4	103.89
12	0.6150	0.0334	0.0785	0.0030	0.0063	0.0583	0.0009	10.85	7.62	3.07	486.7	21.0	487.1	17.9	542.6	33.6	100.09
13	0.6004	0.0363	0.0800	0.0034	0.0119	0.0562	0.0016	12.08	8.52	5.70	477.5	23.0	495.8	20.3	458.6	63.2	103.85
14	1.6061	0.1367	0.1667	0.0075	0.0129	0.0844	0.0053	17.03	8.95	12.52	972.6	53.3	994.0	41.2	1301.2	121.6	102.20
15	0.5033	0.0640	0.0737	0.0046	0.0332	0.0625	0.0043	25.42	12.50	13.76	413.9	43.2	458.2	27.6	691.3	146.8	110.69
16	0.6717	0.0466	0.0883	0.0037	0.0093	0.0613	0.0015	13.87	8.32	4.85	521.8	28.3	545.5	21.7	651.1	52.0	104.55
17	0.7935	0.1001	0.0881	0.0043	0.0133	0.1017	0.0040	25.23	9.82	7.90	593.2	56.7	544.2	25.6	1654.9	73.2	91.75
18	0.5339	0.0394	0.0779	0.0029	0.0111	0.0581	0.0014	14.77	7.38	4.83	434.4	26.1	483.8	17.2	531.8	52.9	111.38
19	0.5540	0.0296	0.0818	0.0021	0.0093	0.0554	0.0012	10.69	5.22	4.18	447.6	19.3	506.6	12.7	429.8	46.6	113.19
20	0.5481	0.0785	0.0880	0.0050	0.0156	0.0617	0.0021	28.65	11.38	6.90	443.8	51.5	543.8	29.7	664.7	73.9	122.55
21	0.6981	0.0465	0.0842	0.0042	0.0105	0.0585	0.0017	13.32	9.89	5.65	537.7	27.8	521.1	24.8	549.9	61.6	96.91
22	0.5343	0.0492	0.0772	0.0029	0.0134	0.0731	0.0021	18.43	7.61	5.82	434.7	32.6	479.4	17.6	1017.1	58.9	110.28
23	0.4447	0.0738	0.0652	0.0059	0.0113	0.0591	0.0012	33.18	18.23	4.21	373.5	51.9	407.2	36.0	572.4	45.8	109.02
24	0.4867	0.0371	0.0780	0.0035	0.0154	0.0517	0.0016	15.25	8.86	6.21	402.6	25.3	484.5	20.7	270.3	71.2	120.32
25	0.5781	0.0356	0.0745	0.0023	0.0072	0.0619	0.0010	12.31	6.30	3.33	463.2	22.9	463.3	14.1	671.6	35.6	100.01
26	0.6654	0.0703	0.0828	0.0041	0.0221	0.0737	0.0042	21.12	9.95	11.45	517.9	42.8	512.9	24.5	1032.0	115.7	99.03
27	0.6195	0.0796	0.0777	0.0042	0.0164	0.0746	0.0030	25.69	10.71	8.02	489.5	49.9	482.4	24.9	1056.7	80.7	98.54
28	0.5487	0.0547	0.0743	0.0040	0.0360	0.0659	0.0053	19.93	10.65	16.02	444.1	35.8	462.1	23.7	802.6	167.7	104.04
29	0.6024	0.0497	0.0752	0.0027	0.0179	0.0636	0.0027	16.51	7.18	8.59	478.7	31.5	467.3	16.2	729.3	91.0	97.62
30	0.6211	0.0396	0.0803	0.0033	0.0066	0.0577	0.0009	12.74	8.24	3.26	490.5	24.8	497.6	19.7	517.7	35.7	101.45
31	0.5145	0.0321	0.0758	0.0025	0.0187	0.0530	0.0021	12.46	6.67	7.89	421.5	21.5	471.3	15.2	330.2	89.4	111.82
32	0.5905	0.0298	0.0789	0.0024	0.0082	0.0584	0.0011	10.11	6.07	3.85	471.2	19.0	489.5	14.3	544.2	42.1	103.89

Table E.2 *Laser ablation U-Pb data and calculated ages for detrital zircons from the Rogerson Lake Conglomerate at Burgeo Road (Sample 72).*

	Concordia Colums							2 sigma	2 sigma	2 sigma	Ages Ma						
Analysis	207/235	7/5 err	206/238	6/8 err	Rho	207/206	7/6 err	207/235	206/238	207/206	207/235	1 sigma	206/238	1sigma	207/206	1 sigma	% Concordant
1	1.1447	0.1027	0.1250	0.0109	0.9754	0.0688	0.0014	17.94	17.49	3.95	774.7	48.6	759.3	62.6	891.3	40.8	98.01
2	1.0330	0.0948	0.1144	0.0071	0.9542	0.0642	0.0012	18.35	12.38	3.88	720.4	47.3	698.2	41.0	748.1	41.0	96.92
3	0.7613	0.0565	0.0843	0.0025	0.8006	0.0777	0.0017	14.85	5.92	4.43	574.7	32.6	521.5	14.8	1140.2	44.0	90.74
4	0.8628	0.0447	0.0771	0.0022	0.7089	0.0705	0.0020	10.35	5.62	5.59	631.6	24.3	478.7	13.0	942.1	57.3	75.79
5	0.6093	0.0222	0.0757	0.0016	0.8999	0.0591	0.0006	7.29	4.15	2.01	483.1	14.0	470.3	9.4	570.8	21.9	97.35
6	0.6565	0.0511	0.0854	0.0035	0.8128	0.0618	0.0018	15.57	8.18	5.86	512.5	31.3	528.4	20.8	667.0	62.8	103.11
7	0.5166	0.0654	0.0607	0.0080	0.9926	0.0596	0.0010	25.32	26.47	3.23	422.8	43.8	379.7	48.8	590.8	35.0	89.79
8	0.5729	0.0267	0.0786	0.0021	0.8675	0.0558	0.0008	9.32	5.25	3.01	459.9	17.2	487.6	12.3	444.9	33.5	106.03
9	0.6075	0.0270	0.0770	0.0017	0.7264	0.0584	0.0012	8.90	4.49	4.24	482.0	17.1	478.4	10.3	544.0	46.4	99.24
10	0.5220	0.0323	0.0750	0.0016	0.8334	0.0545	0.0007	12.37	4.15	2.75	426.5	21.5	465.9	9.3	393.5	30.8	109.25
11	0.6550	0.0286	0.0804	0.0029	0.9250	0.0578	0.0009	8.74	7.24	2.98	511.5	17.6	498.3	17.4	520.5	32.7	97.42
12	0.5774	0.0245	0.0739	0.0022	0.9038	0.0561	0.0008	8.47	6.06	2.87	462.8	15.7	459.4	13.4	458.1	31.8	99.27
13	0.6381	0.0319	0.0773	0.0027	0.8557	0.0598	0.0013	10.01	6.99	4.23	501.1	19.8	479.7	16.2	596.0	45.8	95.73
14	0.5943	0.0321	0.0816	0.0025	0.9466	0.0569	0.0006	10.79	6.05	2.06	473.6	20.4	505.6	14.7	486.5	22.7	106.76
15	0.6126	0.0235	0.0767	0.0024	0.9089	0.0565	0.0008	7.68	6.38	2.93	485.2	14.8	476.7	14.7	473.0	32.4	98.24
16	0.6472	0.0273	0.0793	0.0031	0.9830	0.0577	0.0004	8.44	7.89	1.47	506.8	16.8	492.2	18.7	518.5	16.2	97.13
17	0.5841	0.0392	0.0744	0.0041	0.9689	0.0539	0.0008	13.43	11.03	2.82	467.1	25.1	462.4	24.6	367.6	31.7	98.99
18	1.3917	0.0670	0.1467	0.0060	0.9693	0.0668	0.0007	9.63	8.19	2.08	885.4	28.5	882.7	33.8	833.0	21.7	99.69
19	0.7089	0.0395	0.0898	0.0033	0.9251	0.0572	0.0009	11.13	7.29	2.99	544.1	23.4	554.3	19.4	501.0	32.9	101.89
20	0.6364	0.0354	0.0812	0.0032	0.9433	0.0614	0.0008	11.12	7.81	2.75	500.0	22.0	503.5	18.9	653.3	29.5	100.69
21	0.7832	0.0578	0.0736	0.0036	0.9735	0.0755	0.0009	14.75	9.74	2.29	587.3	32.9	457.5	21.5	1080.8	23.0	77.90
22	0.5560	0.0362	0.0826	0.0022	0.7783	0.0620	0.0013	13.04	5.34	4.31	448.9	23.6	511.9	13.1	673.8	46.1	114.03
23	1.7686	0.0988	0.1824	0.0083	0.9462	0.0673	0.0010	11.17	9.10	3.11	1034.0	36.2	1079.8	45.2	845.8	32.4	104.43
24	0.6252	0.0250	0.0786	0.0021	0.9389	0.0563	0.0006	8.00	5.34	1.96	493.1	15.6	487.8	12.5	464.1	21.7	98.94
25	0.5838	0.0299	0.0764	0.0028	0.9582	0.0554	0.0006	10.25	7.24	2.16	466.9	19.2	474.6	16.6	426.6	24.1	101.65
26	0.7817	0.0281	0.0953	0.0035	0.9524	0.0606	0.0007	7.18	7.38	2.36	586.5	16.0	586.6	20.7	624.2	25.5	100.02
27	0.5826	0.0351	0.0766	0.0029	0.9308	0.0555	0.0008	12.07	7.65	3.01	466.2	22.6	475.7	17.5	434.3	33.5	102.05
28	1.1473	0.0659	0.1187	0.0048	0.9653	0.0671	0.0007	11.48	8.06	2.18	776.0	31.1	723.3	27.6	841.2	22.7	93.21
29	0.7168	0.0252	0.0763	0.0026	0.9385	0.0603	0.0008	7.02	6.83	2.51	548.8	14.9	473.9	15.6	615.3	27.1	86.35
30	0.8759	0.0475	0.0940	0.0038	0.9590	0.0634	0.0007	10.84	8.00	2.36	638.7	25.7	578.9	22.2	722.0	25.1	90.63
31	1.7175	0.0658	0.1707	0.0059	0.9754	0.0699	0.0006	7.66	6.97	1.58	1015.1	24.6	1016.1	32.7	925.4	16.2	100.10
32	0.5988	0.0714	0.0787	0.0057	0.9797	0.0587	0.0009	23.85	14.47	2.96	476.4	45.3	488.2	34.0	554.5	32.3	102.47
33	1.0334	0.1046	0.0975	0.0057	0.8264	0.1024	0.0041	20.25	11.68	7.96	720.6	52.2	599.5	33.4	1668.4	73.6	83.20
34	1.6469	0.1701	0.1680	0.0157	0.9818	0.0703	0.0013	20.66	18.64	3.61	988.4	65.3	1001.2	86.4	937.8	37.0	101.30
35	0.6231	0.0351	0.0860	0.0025	0.8630	0.0584	0.0010	11.28	5.92	3.47	491.8	22.0	531.9	15.1	545.0	37.9	108.16
36	0.7248	0.0741	0.0994	0.0058	0.9077	0.0604	0.0016	20.44	11.71	5.41	553.5	43.6	610.8	34.1	619.2	58.4	110.36
37	0.7203	0.0525	0.0912	0.0043	0.9466	0.0601	0.0010	14.57	9.44	3.21	550.8	31.0	562.8	25.4	606.4	34.8	102.17
38	3.4427	0.1799	0.2595	0.0128	0.9772	0.0948	0.0010	10.45	9.90	2.15	1514.2	41.1	1487.0	65.8	1523.6	20.3	98.21
39	0.5351	0.0244	0.0751	0.0018	0.8435	0.0593	0.0009	9.10	4.70	2.99	435.2	16.1	466.7	10.6	577.4	32.5	107.22
40	3.3023	0.2905	0.2560	0.0149	0.9608	0.0988	0.0017	17.59	11.68	3.37	1481.6	68.6	1469.4	76.7	1601.1	31.4	99.17

Table E.2 *Laser ablation U-Pb data and calculated ages for detrital zircons from the Rogerson Lake Conglomerate at Burgeo Road (Sample 72).*

	Concordia Colums							2 sigma	2 sigma	2 sigma	Ages Ma						
Analysis	207/235	7/5 err	206/238	6/8 err	Rho	207/206	7/6 err	207/235	206/238	207/206	207/235	1 sigma	206/238	1sigma	207/206	1 sigma	% Concordant
41	0.7207	0.0485	0.0842	0.0033	0.9317	0.0680	0.0010	13.47	7.74	3.02	551.1	28.6	521.0	19.4	867.4	31.3	94.54
42	0.9516	0.0684	0.0818	0.0023	0.6992	0.0782	0.0023	14.37	5.71	5.84	678.9	35.6	507.0	13.9	1151.7	58.0	74.67
43	1.2001	0.1042	0.1390	0.0073	0.8935	0.0682	0.0018	17.37	10.52	5.29	800.6	48.1	838.9	41.4	875.9	54.7	104.78
44	0.5218	0.0426	0.0723	0.0032	0.9413	0.0563	0.0009	16.35	8.95	3.21	426.4	28.5	449.9	19.5	466.2	35.6	105.52
45	0.5086	0.0387	0.0806	0.0020	0.7680	0.0582	0.0012	15.21	5.05	4.21	417.5	26.0	499.9	12.2	538.5	46.1	119.73
46	0.5573	0.0215	0.0710	0.0022	0.9506	0.0561	0.0006	7.73	6.27	2.05	449.8	14.1	442.1	13.4	455.7	22.7	98.30
47	0.5115	0.0828	0.0794	0.0068	0.9760	0.0553	0.0011	32.36	17.16	3.83	419.5	55.6	492.4	40.7	424.5	42.7	117.39
48	0.5490	0.0499	0.0726	0.0029	0.8834	0.0563	0.0012	18.17	7.99	4.24	444.3	32.7	451.8	17.4	463.1	47.0	101.69
49	0.5450	0.0429	0.0801	0.0021	0.7701	0.0626	0.0014	15.76	5.35	4.43	441.7	28.2	496.9	12.8	693.9	47.2	112.49
50	0.5510	0.0291	0.0734	0.0037	0.9698	0.0534	0.0007	10.55	10.08	2.54	445.6	19.0	456.8	22.2	345.8	28.7	102.50
51	0.6037	0.0335	0.0838	0.0022	0.8354	0.0629	0.0011	11.09	5.25	3.46	479.6	21.2	518.6	13.1	703.5	36.8	108.13
52	0.5776	0.0711	0.0832	0.0033	0.8482	0.0689	0.0017	24.61	7.82	4.88	462.9	45.7	515.4	19.4	895.4	50.4	111.34
53	0.6889	0.0324	0.0848	0.0032	0.9554	0.0592	0.0007	9.40	7.59	2.35	532.1	19.5	525.0	19.1	576.1	25.5	98.66
54	0.4922	0.0409	0.0712	0.0028	0.9466	0.0589	0.0008	16.62	7.80	2.65	406.4	27.8	443.1	16.7	564.1	28.9	109.03
55	0.4138	0.0401	0.0723	0.0028	0.8726	0.0546	0.0012	19.36	7.76	4.35	351.6	28.8	450.0	16.9	397.4	48.7	127.97
56	0.4858	0.0382	0.0707	0.0022	0.7823	0.0604	0.0015	15.72	6.26	4.99	402.1	26.1	440.3	13.3	618.0	53.8	109.50
57	0.5867	0.0300	0.0782	0.0021	0.8652	0.0642	0.0010	10.21	5.43	3.14	468.8	19.2	485.3	12.7	748.3	33.2	103.52
58	0.4812	0.0759	0.0722	0.0034	0.8981	0.0614	0.0014	31.53	9.43	4.62	398.9	52.0	449.5	20.5	652.7	49.6	112.70
59	0.4650	0.0323	0.0735	0.0020	0.8710	0.0549	0.0009	13.91	5.57	3.14	387.7	22.4	457.3	12.3	408.5	35.1	117.94
60	0.5791	0.0300	0.0727	0.0019	0.7999	0.0598	0.0012	10.35	5.19	3.89	463.9	19.3	452.3	11.3	594.6	42.2	97.50
61	0.5175	0.0534	0.0710	0.0038	0.9575	0.0584	0.0010	20.65	10.84	3.26	423.5	35.7	441.9	23.1	545.8	35.7	104.36
62	0.4929	0.0385	0.0780	0.0020	0.7928	0.0595	0.0012	15.64	5.25	4.04	406.9	26.2	484.0	12.2	584.1	43.8	118.95
63	0.6276	0.0220	0.0789	0.0016	0.8510	0.0589	0.0008	7.00	4.15	2.56	494.6	13.7	489.3	9.8	564.8	27.9	98.93
64	0.5330	0.0263	0.0722	0.0023	0.9540	0.0560	0.0005	9.88	6.24	1.96	433.8	17.4	449.5	13.5	452.9	21.8	103.60
65	0.6084	0.0129	0.0765	0.0012	0.9249	0.0574	0.0004	4.25	3.19	1.31	482.6	8.2	475.3	7.3	505.3	14.4	98.50
66	1.4917	0.1924	0.1525	0.0113	0.9676	0.0778	0.0015	25.79	14.79	3.86	927.0	78.4	915.1	63.1	1140.7	38.3	98.71
67	0.5167	0.0715	0.0781	0.0052	0.9285	0.0514	0.0014	27.68	13.33	5.33	422.9	47.9	484.6	31.1	258.2	61.3	114.57
68	2.3701	0.1155	0.2129	0.0096	0.9756	0.0787	0.0008	9.75	9.00	2.03	1233.6	34.8	1244.2	50.9	1164.8	20.1	100.85
69	0.5382	0.0643	0.0689	0.0038	0.9551	0.0662	0.0011	23.88	11.15	3.46	437.2	42.4	429.6	23.2	813.0	36.2	98.25
70	0.3891	0.0627	0.0755	0.0030	0.8368	0.0564	0.0014	32.23	7.82	5.11	333.7	45.8	469.2	17.7	467.5	56.6	140.62
71	0.4912	0.0380	0.0716	0.0024	0.8942	0.0592	0.0010	15.49	6.62	3.31	405.7	25.9	445.5	14.2	575.1	36.0	109.82
72	0.7269	0.0402	0.0805	0.0019	0.7988	0.0650	0.0011	11.06	4.66	3.51	554.7	23.6	498.9	11.2	774.5	36.9	89.93
73	0.6471	0.0331	0.0783	0.0018	0.8725	0.0670	0.0009	10.23	4.55	2.55	506.7	20.4	485.8	10.6	837.1	26.5	95.88
74	0.7195	0.0468	0.0761	0.0022	0.7856	0.0666	0.0015	13.01	5.69	4.48	550.4	27.6	473.1	13.0	825.7	46.7	85.96
75	0.5270	0.0475	0.0729	0.0033	0.9672	0.0565	0.0007	18.03	9.10	2.39	429.8	31.6	453.5	19.9	473.5	26.4	105.51
76	0.5077	0.0317	0.0790	0.0017	0.7118	0.0612	0.0013	12.50	4.23	4.17	416.9	21.4	490.2	10.0	646.9	44.8	117.57
77	0.4785	0.1011	0.0745	0.0095	0.9882	0.0514	0.0010	42.27	25.59	3.97	397.0	69.5	463.0	57.2	258.9	45.6	116.61
78	0.4606	0.0454	0.0740	0.0025	0.8856	0.0602	0.0011	19.73	6.78	3.55	384.7	31.6	460.2	15.0	612.4	38.4	119.65
79	0.6634	0.0369	0.0770	0.0027	0.9126	0.0616	0.0010	11.14	7.13	3.19	516.7	22.5	478.3	16.4	661.2	34.2	92.58
80	0.5500	0.0394	0.0764	0.0023	0.8841	0.0572	0.0009	14.32	6.05	3.20	445.0	25.8	474.6	13.8	499.9	35.2	106.65
81	0.5466	0.0766	0.0673	0.0064	0.9779	0.0611	0.0012	28.01	19.07	4.07	442.7	50.3	419.9	38.8	643.0	43.8	94.84

APPENDIX F

F.1 Lead Isotope Geochemistry

A total of 15 galena separates from the Tally Pond belt were analyzed for their lead isotope ratios. Galena was collected from the shallow and deep sections of the Upper Duck lens of the Duck Pond deposit, the North Zone of the Boundary deposit, the South Moose Pond zone, and the Lemarchant prospect. Analyses were carried out using multi-collector ICP-MS at the GEOTOP Laboratory, Université du Québec á Montréal (UQAM).

Hand-picked grains of galena were placed in pre-cleaned polypropylene bottles, and leached with 6N HCl for several days. A small aliquot of this solution (<<0.1 ml) was then diluted with ~0.6 ml of a 2% HNO_3 solution spiked with the NBS 997 Thallium standard (2.5ppb). Pb isotope compositions of the samples were measured on an IsoProbe multicollector-ICP-MS. Samples were aspirated (~50 microlitres/min.) into the ICP torch using an ARIDUS® microconcentric nebuliser. Simultaneous measurement of all the Pb and Tl isotopes, and ^{202}Hg ion signal was achieved by using 7 Faraday collectors. The $^{205}Tl/^{203}Tl$ ratio was measured in order to correct for instrumental mass bias (exponential law; $^{203}Tl/^{205}Tl$=0.418638). Prior to sample introduction, collector baselines were measured with the line of sight valve closed (50 seconds) followed by an "on-peak-zero" baseline measurement (i.e. gas and acid blank) also for 50 seconds. Upon sample introduction, data

acquisition consisted of 2 half-mass unit baseline measurements and 1 block of 50 scans (10 seconds integration each) for isotope ratio analysis. Hg interferences were monitored and corrected using ^{202}Hg, however, the latter is negligible in all cases.

At the beginning of each analytical session, a 25 ppb solution of the NBS981 Pb standard, which was also spiked with the NBS 997 Tl standard (1.25ppb), was analyzed. Each analysis of the standard consumes approximately 12.5 ng of total Pb. Repeated measurement (n=40) of this standard solution over the period of Dec. 1999-present yields the following mean values and associated (2σ) standard deviations: $^{206}Pb/^{204}Pb=16.938\pm0.016$, $^{207}Pb/^{204}Pb=15.492\pm0.018$, $^{208}Pb/^{204}Pb=36.702\pm0.052$, $^{207}Pb/^{206}Pb=0.91462\pm0.00049$, $^{208}Pb/^{206}Pb=2.1668\pm0.0017$. The associated standard deviations correspond to external reproducibilities in the order of 0.04% amu^{-1} (per atomic mass unit).

Table F.1 *Lead isotope ratios for 15 samples from the Tally Pond Group.*

Sample	Deposit	206Pb/204Pb	%error	207Pb/204Pb	%error	208Pb/204Pb	%error	207Pb/206Pb	%error	208Pb/206Pb	%error	Model Age	μ
												Ma	
JP-00-03	Lemarchant	18.098	0.005	15.555	0.0065	37.762	0.0112	0.8595	0.0031	2.0866	0.0031	305	9.557
JP-00-34	South Moose Pond	18.159	0.005	15.584	0.0065	37.872	0.0112	0.8582	0.0031	2.0855	0.0031	319	9.67
JP-00-65	Boundary	18.088	0.005	15.585	0.0065	37.888	0.0112	0.85837	0.0031	2.08664	0.0031	323	9.675
JP-00-78	Boundary	18.088	0.005	15.548	0.0065	37.754	0.0112	0.85946	0.0031	2.08709	0.0031	298	9.528
JP-00-44	South Moose Pond	18.17	0.005	15.586	0.0065	37.872	0.0112	0.8577	0.0031	2.0842	0.0031	314	9.676
JP-00-90	Lemarchant	18.119	0.005	15.576	0.0065	37.821	0.0112	0.8597	0.0031	2.0874	0.0031	332	9.645
JP-00-322	Upper Duck	18.16	0.005	15.579	0.0065	37.84	0.0112	0.8578	0.0031	2.0834	0.0031	307	9.647
JP-00-336	Upper Duck	18.189	0.005	15.599	0.0065	37.892	0.0112	0.8576	0.0031	2.0832	0.0031	327	9.729
JP-00-337	Upper Duck	18.144	0.005	15.567	0.0065	37.809	0.0112	0.8579	0.0031	2.0838	0.0031	295	9.598
JP-00-338	Upper Duck	18.172	0.005	15.586	0.0065	37.858	0.0112	0.8577	0.0031	2.0834	0.0031	313	9.675
JP-00-339	Upper Duck	18.149	0.005	15.571	0.0065	37.822	0.0112	0.8579	0.0031	2.0839	0.0031	299	9.614
JP-00-340	Upper Duck	18.15	0.005	15.575	0.0065	37.829	0.0112	0.8582	0.0031	2.0844	0.0031	307	9.632
JP-00-341	Lower-Upper Duck	18.276	0.005	15.681	0.0065	38.081	0.0112	0.8579	0.0031	2.0834	0.0031	425	10.07
JP-00-342	Lower-Upper Duck	18.311	0.005	15.783	0.0065	38.484	0.0112	0.8614	0.0031	2.1014	0.0031	589	10.53
JP-00-343	Lower-Upper Duck	18.209	0.005	15.641	0.0065	37.95	0.0112	0.8577	0.0031	2.0834	0.0031	396	9.912

Table F.2 *Lead isotope ratios for various volcanogenic massive sulphide occurrences in the Newfoundland Dunnage Zone.*

Sample	Deposit	206Pb/204Pb	207Pb/204Pb	208Pb/204Pb	207Pb/206Pb	208Pb/206Pb	Model Age	μ	*Reference*
JP-00-03	Lemarchant	18.098	15.555	37.762	0.860	2.087	305	9.557	*Pollock and Wilton (2001)*
JP-00-90	Lemarchant	18.119	15.576	37.821	0.860	2.087	332	9.645	*Pollock and Wilton (2001)*
JP-00-34	South Moose Pond	18.159	15.584	37.872	0.858	2.086	319	9.670	*Pollock and Wilton (2001)*
JP-00-44	South Moose Pond	18.170	15.586	37.872	0.858	2.084	314	9.676	*Pollock and Wilton (2001)*
JP-00-65	Boundary	18.156	15.585	37.888	0.858	2.087	323	9.675	*Pollock and Wilton (2001)*
JP-00-322	Upper Duck	18.160	15.579	37.840	0.858	2.083	307	9.647	*Pollock and Wilton (2001)*
JP-00-336	Upper Duck	18.189	15.599	37.892	0.858	2.083	327	9.729	*Pollock and Wilton (2001)*
JP-00-337	Upper Duck	18.144	15.567	37.809	0.858	2.084	295	9.598	*Pollock and Wilton (2001)*
JP-00-338	Upper Duck	18.172	15.586	37.858	0.858	2.083	313	9.675	*Pollock and Wilton (2001)*
JP-00-339	Upper Duck	18.149	15.571	37.822	0.858	2.084	299	9.614	*Pollock and Wilton (2001)*
JP-00-340	Upper Duck	18.150	15.575	37.829	0.858	2.084	307	9.632	*Pollock and Wilton (2001)*
JP-00-341	Deep Upper Duck	18.276	15.681	38.081	0.858	2.083	425	10.070	*Pollock and Wilton (2001)*
JP-00-342	Deep Upper Duck	18.311	15.783	38.484	0.861	2.101	589	10.530	*Pollock and Wilton (2001)*
JP-00-343	Deep Upper Duck	18.209	15.641	37.950	0.858	2.083	396	9.912	*Pollock and Wilton (2001)*
TQ 80-85	Victoria	18.161	15.619	38.112	0.860	2.099	388	9.826	*Swinden and Thorpe (1984)*
TQ-80-85	Victoria	18.159	15.624	38.102	0.860	2.098	399	9.849	*Swinden and Thorpe (1984)*
TQ 82-1	Tulks Hill	18.144	15.571	37.957	0.858	2.092	303	9.616	*Swinden and Thorpe (1984)*
TQ 81-50	Tulks Hill	18.142	15.575	37.955	0.859	2.092	313	9.634	*Swinden and Thorpe (1984)*
TQ 81-54	Burnt Pond	18.138	15.576	37.862	0.859	2.087	319	9.640	*Swinden and Thorpe (1984)*
TQ 83-29	Tally Pond (Boundary)	18.156	15.583	37.902	0.858	2.088	318	9.666	*Swinden and Thorpe (1984)*
SP 2999	Ming	18.175	15.613	38.066	0.859	2.094	365	9.795	*Swinden and Thorpe (1984)*
SP 3033	Ming	18.169	15.598	38.025	0.858	2.093	340	9.730	*Swinden and Thorpe (1984)*
TQ 83-30	Seal Bay	18.212	15.608	38.112	0.857	2.093	328	9.763	*Swinden and Thorpe (1984)*
TQ 80-83	Barasway de Cerf	18.235	15.660	38.142	0.859	2.092	414	9.990	*Swinden and Thorpe (1984)*
TQ 80-84	Strickland	18.333	15.663	38.209	0.854	2.084	348	9.760	*Swinden and Thorpe (1984)*
TQ 83-1	Facheux Bay	18.217	15.630	38.096	0.858	2.091	368	9.860	*Swinden and Thorpe (1984)*
TQ 81-52	Shamrock	17.844	15.488	37.599	0.868	2.107	362	9.326	*Swinden and Thorpe (1984)*
TQ 81-51	Oil Islands	17.894	15.499	37.616	0.866	2.102	346	9.361	*Swinden and Thorpe (1984)*
TQ 91-53	Catchers Pond	17.544	15.428	37.495	0.879	2.137	473	9.142	*Swinden and Thorpe (1984)*
TQ 71-63	York Harbour	17.851	15.489	37.465	0.868	2.099	358	9.328	*Swinden and Thorpe (1984)*
TQ 72-78	Pilleys Island	17.922	15.522	37.591	0.866	2.097	372	9.457	*Swinden and Thorpe (1984)*
TQ 72-62	Pilleys Island	17.937	15.529	37.613	0.866	2.097	375	9.484	*Swinden and Thorpe (1984)*
Winter 01	Buchans	17.826	15.494	37.611	0.869	2.110	388	9.358	*Swinden and Thorpe (1984)*
Winter 02	Airport Zone	17.806	15.498	37.550	0.871	2.109	412	9.382	*Winter (2000)*
Winter 03	Woodmans Brook Zone	17.610	15.447	37.494	0.877	2.129	460	9.208	*Winter (2000)*
Winter 04	Sandfill Prospect	17.845	15.508	37.597	0.869	2.107	403	9.416	*Winter (2000)*
Winter 05	Middle Branch Zone	17.815	15.480	37.569	0.869	2.109	368	9.298	*Winter (2000)*

Table F.2 *Lead isotope ratios for various volcanogenic massive sulphide occurrences in the Newfoundland Dunnage Zone.*

Sample	Deposit	06Pb/204P	07Pb/204P	08Pb/204P	07Pb/206P	08Pb/206P	Model Age	μ	*Reference*
Winter 06	Powerhouse Zone	17.727	15.471	37.429	1.146	2.111	418	9.283	*Winter (2000)*
Winter 07	Middle Branch East	17.958	15.502	37.627	1.159	2.095	302	9.357	*Winter (2000)*
W-97-18	Pilleys Island	17.831	15.417		0.865		217	9.013	*Wilton (Unpublished data)*
W-97-19	Bull Road	17.931	15.498		0.864		315	9.347	*Wilton (Unpublished data)*
65768.00	Lochinvar	17.594	15.456		0.878		491	9.255	*Wilton (Unpublished data)*
Wilton 1	Daniel's Pond	18.167	15.578		0.857		300	9.641	*Wilton (Unpublished data)*
Wilton 2	West Tulks	18.226	15.584		0.855		268	9.652	*Wilton (Unpublished data)*
OI-93-1	Oil Islands	17.934	15.526		0.866		371	9.471	*Wilton (Unpublished data)*
OI-93-3	Oil Islands	17.873	15.514		0.868		393	9.435	*Wilton (Unpublished data)*
W-95-38	Handcamp	18.096	15.540		0.859		275	9.490	*Wilton (Unpublished data)*
CK-1	Buchans- McLean	17.829	15.492	37.620	0.869	2.110	382	9.348	*Cumming and Krstic (1987)*
CK-2	Buchans- McLean	17.823	15.490	37.612	0.869	2.110	382	9.341	*Cumming and Krstic (1987)*
CK-3	Buchans- McLean	17.823	15.488	37.612	0.869	2.110	378	9.332	*Cumming and Krstic (1987)*
CK-4	Buchans- McLean Extension	17.821	15.488	37.606	0.869	2.110	380	9.332	*Cumming and Krstic (1987)*
CK-5	Buchans- McLean Extension	17.820	15.490	37.621	0.869	2.111	385	9.342	*Cumming and Krstic (1987)*
CK-6	Buchans- McLean Extension #4	17.832	15.496	37.628	0.869	2.110	388	9.365	*Cumming and Krstic (1987)*
CK-7	Buchans- Old Buchans	17.818	15.496	37.654	0.870	2.113	399	9.369	*Cumming and Krstic (1987)*
CK-8	Buchans- Oriental	17.827	15.490	37.626	0.869	2.111	379	9.340	*Cumming and Krstic (1987)*
CK-9	Buchans- Oriental #1 East	17.823	15.491	37.610	0.869	2.110	384	9.345	*Cumming and Krstic (1987)*
CK-10	Buchans- Oriental #1 West	17.825	15.497	37.632	0.869	2.111	395	9.372	*Cumming and Krstic (1987)*
CK-11	Buchans- Lucky Strike Main	17.832	15.496	37.634	0.869	2.110	388	9.365	*Cumming and Krstic (1987)*
CK-12	Buchans- Lucky Strike Main	17.829	15.493	37.619	0.869	2.110	384	9.352	*Cumming and Krstic (1987)*
CK-13	Buchans- Lucky Strike North	17.826	15.492	37.617	0.869	2.110	384	9.349	*Cumming and Krstic (1987)*
CK-14	Buchans- Lucky Strike North	17.815	15.489	37.606	0.869	2.111	386	9.338	*Cumming and Krstic (1987)*
CK-15	Buchans- Engineer Zone	17.833	15.495	37.624	0.869	2.110	385	9.360	*Cumming and Krstic (1987)*
CK-16	Clementine	17.828	15.491	37.613	0.869	2.110	380	9.344	*Cumming and Krstic (1987)*
CK-17	Connel Option	17.735	15.488	37.560	0.873	2.118	447	9.358	*Cumming and Krstic (1987)*
CK-18	Connel Option	17.731	15.486	37.543	0.873	2.117	446	9.350	*Cumming and Krstic (1987)*
CK-19	Connel Option	17.732	15.486	37.543	0.873	2.117	445	9.349	*Cumming and Krstic (1987)*
CK-20	Mary March	17.723	15.480	37.543	0.873	2.118	440	9.325	*Cumming and Krstic (1987)*
CK-21	Mary March	17.965	15.527	37.662	0.864	2.096	349	9.467	*Cumming and Krstic (1987)*
CK-22	Mary March	17.965	15.529	37.677	0.864	2.097	353	9.476	*Cumming and Krstic (1987)*
CK-23	Mary March	17.943	15.519	37.634	0.865	2.097	349	9.437	*Cumming and Krstic (1987)*
CK-24	Mary March	17.941	15.523	37.635	0.865	2.098	359	9.456	*Cumming and Krstic (1987)*
CK-25	Skidder	17.639	15.457	37.458	0.876	2.124	458	9.245	*Cumming and Krstic (1987)*
CK-26	Skidder	17.586	15.445	37.498	0.878	2.132	475	9.207	*Cumming and Krstic (1987)*
CK-27	Skidder	17.629	15.442	37.463	0.876	2.125	434	9.180	*Cumming and Krstic (1987)*

Table F.2 *Lead isotope ratios for various volcanogenic massive sulphide occurrences in the Newfoundland Dunnage Zone.*

Sample	Deposit	06Pb/204P	07Pb/204P	08Pb/204P	07Pb/206P	08Pb/206P	Model Age	μ	*Reference*
CK-28	Skidder	17.634	15.445	37.461	0.876	2.124	437	9.192	*Cumming and Krstic (1987)*
CK-29	Skidder	17.644	15.445	37.464	0.875	2.123	429	9.189	*Cumming and Krstic (1987)*
CK-30	Skidder	17.638	15.452	37.491	0.876	2.126	448	9.223	*Cumming and Krstic (1987)*
CK-31	Skidder	17.684	15.455	37.492	0.874	2.120	418	9.223	*Cumming and Krstic (1987)*
CK-32	Skidder	17.685	15.455	37.481	0.874	2.119	417	9.222	*Cumming and Krstic (1987)*
CK-33	Tulks Hill	18.144	15.571	37.957	0.858	2.092	303	9.616	*Cumming and Krstic (1987)*
CK-34	Tulks Hill	18.142	15.575	37.955	0.859	2.092	313	9.634	*Cumming and Krstic (1987)*
CK-35	Tulks East	18.203	15.591	37.997	0.857	2.087	300	9.689	*Cumming and Krstic (1987)*
CK-36	Tulks East	18.204	15.590	37.998	0.856	2.087	297	9.684	*Cumming and Krstic (1987)*
CK-37	Tulks East	18.180	15.584	37.963	0.857	2.088	303	9.664	*Cumming and Krstic (1987)*
CK-38	Tulks East	18.173	15.578	37.958	0.857	2.089	296	9.639	*Cumming and Krstic (1987)*
CK-39	Tulks East	18.177	15.581	37.967	0.857	2.089	299	9.652	*Cumming and Krstic (1987)*
CK-40	Tulks East	18.186	15.586	37.995	0.857	2.089	302	9.671	*Cumming and Krstic (1987)*
CK-41	Victoria	18.139	15.604	38.060	0.860	2.098	374	9.765	*Cumming and Krstic (1987)*
CK-42	Victoria	18.134	15.597	38.045	0.860	2.098	364	9.735	*Cumming and Krstic (1987)*

APPENDIX G

G.1 Sulphur Isotope Geochemistry

Sulphur isotopes were performed at the Department of Earth Sciences, Memorial University of Newfoundland and conducted on SO_2 gas extractions from single crystals of sulphide material. Single crystals of pyrite, chalcopyrite, galena and sphalerite were hand-picked from hand samples and drill-core and crushed in a ceramic mortar and pestal assembly. The sulphide powder (4-9 mg) were weighed and mixed with V_2O_5. The resultant mixture was crushed and transferred to high purity tin capsules. The samples are then loaded onto a Carlo Erba Automatic Gas Chromatographic Elemental Analyzer carousel and the sample details are entered into an auto run file in the machine. The machine's auto-run is then started which sequentially drops each sample into a combustion region of the elemental analyzer.

The samples were combusted at 1000°C on a cryogenic separation line to remove SO_2 gas following the method of Rafter (1965). Extracted SO_2 gas was analyzed for $^{34}S/^{32}S$ ratios on a Finnigan MAT 252 isotope ratio mass spectrometer (IR-MS) followed by data processing using a personal computer. Sulphur dioxide gas samples are run on the mass spectrometer against internal standards, (ie. Mun-Py). Full details regarding analytical procedures associated with this process are given in Giesemann *et al.* (1994).

Calibration standards (NBS-123, NBS-127, and NZ1) were run during the course of the analysis resulting in calibration standard deviations in the range of ±0.3 ‰, thereby giving a measure of analytical accuracy.

Table G.1 *Sulphur isotope values for the Tally Pond Group.*

	Sample number	Drill hole	Depth (m)	Location	Host rock	Mineral	$\delta^{34}S$ VCDT
1	JP-00-02	n/a	outcrop	East Pond	felsic breccia	sphalerite	6.67
2	JP-00-03	LM-91-01	99.7	Lemarchant	altered felsic volcanic	galena	6.59
3	JP-00-11	NM-00-02	199.25	North Moose Pond	felsic agglomerate rhyolite	pyrite	- 7.12
4	JP-00-12	NM-00-02	199.85	North Moose Pond	graphitic argillite	pyrite	- 8.69
5	JP-00-18	TH-00-01	187.8	South Moose Pond 'Thunder'	rhyolite dyke	pyrite	8.20
6	JP-00-35	SM-97-07	98.8	South Moose Pond	altered mafic volcanic	pyrite	8.47
7	JP-00-39	SM-97-08	123.3	South Moose Pond	chloritized mafic volcanic	pyrite	- 0.23
8	JP-00-46	SM-97-05	28	South Moose Pond	altered mafic volcanic	pyrite	5.70
9	JP-00-50	SM-97-05	138.5	South Moose Pond	massive sulphide	chalcopyrite/sphalerite	9.98
10	JP-00-63	BD-99-105	20	Boundary Deposit - North Zone	massive sulphide	pyrite	11.70
11	JP-00-65	BD-99-104	17.3	Boundary Deposit - North Zone	mineralized felsic lapilli tuff	pyrite/sphalerite/galena	8.83
12	JP-00-69	BD-99-108	29.2	Boundary Deposit - North Zone	carbonatized/chloritized feeder pipe	pyrite	11.29
13	JP-00-75	BD-99-108	38.4	Boundary Deposit - North Zone	mineralized lapilli tuff	pyrite/chalcopyrite	10.73
14	JP-00-78	BD-112	8.7	Boundary Deposit - North Zone	massive sulphide	pyrite/sphalerite/chalcopyrite	10.64
15	JP-00-83	BD-99-113	26.57	Boundary Deposit - North Zone	intensely chloritized feeder	pyrite	12.44
16	JP-00-107	BD-99-126	20.4	Boundary Deposit - South East Zone	felsic tuff	pyrite	9.97
17	JP-00-114	BD-99-170	15.65	Boundary Deposit - South East Zone	laminated sulphide and sediment	pyrite	6.46
18	JP-00-124	BD-99-159	6.4	Boundary Deposit - South East Zone	massive sulphide	pyrite	10.04
19	JP-00-130	BD-99-120	11.9	Boundary Deposit - South Zone	massive sulphide	pyrite	10.68
20	JP-00-152	BD-99-163	24.1	Boundary Deposit - South Zone	chlorite feeder	pyrite	13.02
21	JP-00-157	BD-99-122	11.7	Boundary Deposit - South Zone	massive sulphide	pyrite	11.38
22	JP-00-179	DP-88-142	208.6	Duck Pond - Upper Block	graphitic sediment	pyrite	- 13.74
23	JP-00-184	DP-88-142	404.3	Duck Pond - Upper Block	rhyolite	pyrite/chalcopyrite	13.72
24	JP-00-191	DP-88-142A	779.6	Duck Pond - Lower Duck lens	massive sulphide	pyrite/chalcopyrite	7.83
25	JP-00-195	DP-87-116	126.7	Duck Pond - Upper Block	diorite intrusion	pyrite	3.71
26	JP-00-213	DP-87-139	330.65	Duck Pond - Upper Duck lens	rhyolite	pyrite	9.03
27	JP-00-221	DP-88-145	273	Duck Pond - Upper Block	graphitic sediment	pyrite	- 17.41
28	JP-00-243	DP-88-185	282.2	Duck Pond - Upper Block	mafic flows	pyrite	- 3.85
29	JP-00-245	DP-88-185	412.6	Duck Pond - Upper Duck lens	massive sulphide	pyrite	8.41
30	JP-00-283	DP-99-209	202.9	Duck Pond - Upper Duck lens	mineralized rhyolite	pyrite	7.38
31	JP-00-287	DP-99-209	253	Duck Pond - Upper Duck lens	massive sulphide	pyrite	11.19
32	JP-00-295	DP-00-218	94	Duck Pond - Upper Block	massive pyrite	pyrite	7.44
33	JP-00-301	DP-00-218	264.2	Duck Pond - Upper Duck lens	intensely altered rhyolite	pyrite	6.85
34	JP-00-313	DP-88-168	182.4	Duck Pond - Upper Duck lens	chlorite feeder stringer zone	pyrite	5.79
35	JP-00-317	DP-88-168	229.7	Duck Pond - Upper Duck lens	sulphide debris flow	pyrite	7.04
36	JP-00-323	DP-88-168	276.1	Duck Pond - Upper Duck lens	silicifed zone	pyrite	9.21
37	JP-00-324	DP-88-168	364.8	Duck Pond - Upper Duck lens	chlorite alteration pipe	pyrite	8.54
38	JP-00-342	DP-99-213	375.6	Duck Pond - Deep Upper Duck lens	massive sulphide	pyrite	11.01
39	JP-00-343	DP-99-219	337	Duck Pond - Deep Upper Duck lens	massive sulphide	pyrite	6.33